



**Scuola Universitaria Superiore IUSS Pavia**

**Targeting Nrf2 and NF- $\kappa$ B signaling pathways to counteract  
degenerative processes by new molecular entities**

A Thesis Submitted in Fulfilment of the Requirements  
for the Degree of Doctor of Philosophy in

**BIOMOLECULAR SCIENCES AND BIOTHECNOLOGY**

Obtained in the framework of the Doctoral Programme in  
Biomolecular Sciences and Biothecnology

by

**Francesca Fagiani**

Supervisors: Prof. Stefano Govoni

Prof. Cristina Lanni

February, 2021

XXXIII Cycle



Alla mia famiglia, le mie radici  
A Marco, le mie ali



## TABLE OF CONTENTS

<b>PREFACE</b> .....	<b>p. 1</b>
<b>CHAPTER I.</b> Dysregulation of the intracellular machinery in Alzheimer's Disease and neurodegenerative disorders .....	<b>p. 5</b>
<b>PART 1.</b> Beta-amyloid short- and long-term synaptic entanglement .....	<b>p. 7</b>
<b>PART 2.</b> Amyloid- $\beta$ and synaptic vesicle dynamics: a cacophonous orchestra .....	<b>p. 55</b>
<b>PART 3.</b> Merging memantine and ferulic acid to probe connections between NMDA receptors, oxidative stress and amyloid- $\beta$ peptide in Alzheimer's disease .....	<b>p. 79</b>
<b>PART 4.</b> Targeting dementias through cancer kinases inhibition .....	<b>p. 105</b>
<b>PART 5.</b> The peptidyl-prolyl isomerase Pin1 in neuronal signalling: at the crossroad between cell death and survival .....	<b>p. 127</b>
<b>CHAPTER II.</b> Targeting Nrf2 and NF- $\kappa$ B signaling pathways to counteract oxidative stress and inflammation .....	<b>p. 151</b>
<b>PART 1.</b> Modulation of Keap1/Nrf2/ARE signaling pathway by curcuma- and garlic-derived hybrids .....	<b>p. 153</b>
<b>PART 2.</b> Targeting cytokine release through the differential modulation of Nrf2 and NF- $\kappa$ B pathways by electrophilic/non-electrophilic compounds .....	<b>p. 175</b>
<b>CHAPTER III.</b> Study of gene environment interactions contributing to autism spectrum disorders .....	<b>p. 205</b>
<b>PART 1.</b> Gene environment interactions in developmental neurotoxicity - a case study of synergy between chlorpyrifos and CHD8 knockout in human BrainSpheres... ..	<b>p. 207</b>
<b>CHAPTER IV.</b> The COVID-19 pandemic outbreak: a critical discussion of the major pharmacological challenges .....	<b>p. 257</b>
<b>PART 1.</b> Immune response in COVID-19: addressing a pharmacological challenge by targeting pathways triggered by SARS-CoV-2 .....	<b>p. 259</b>
<b>PART 2.</b> Molecular features of IGHV3-53-encoded antibodies elicited by SARS-CoV-2 .....	<b>p. 287</b>

**CHAPTER V. Other collaborative activities ..... p. 293**

**LIST OF PUBLICATIONS ..... p. 299**

---

## PREFACE

During the PhD course, I carried out the research activity at the Department of Drug Sciences of the University of Pavia, Pharmacology Section.

As described in Chapter I, my research activity has been mainly focused on the study of the dysregulation of the intracellular machinery within the context of Alzheimer's Disease (AD). In particular, I analysed the different mechanisms through which  $\beta$ -amyloid ( $A\beta$ ) influences synaptic activity (*Lanni et al, 2019*), specifically focusing on  $A\beta$  interaction with key synaptic proteins regulating the neurotransmitter release machinery (*Fagiani et al, 2019*). Notably, defects in the fine-tuning of synaptic vesicle cycle by  $A\beta$  and deregulation of key molecules and kinases, which orchestrate synaptic vesicle availability, have been hypothesized to alter synaptic homeostasis, possibly contributing to synaptic loss and cognitive decline.

Moreover, within the context of AD, in collaboration with the group of pharmaceutical chemist of the University of Bologna, led by Prof. Michela Rosini, we tested a set of compounds and found promising tools for investigating NMDAR-mediated neurotoxic events involving  $A\beta$  burden and oxidative damage, by applying a multifunctional approach conjugating the anti-AD drug memantine to ferulic acid, known to protect the brain from  $A\beta$  neurotoxicity and neuronal death (*Rosini et al, 2019*). In particular, we investigated the effects of these compounds on cell viability, their scavenging activity against reactive oxygen species (ROS) production, as well as their ability to activate intracellular cytoprotective pathways in human neuroblastoma SH-SY5Y cells (*Rosini et al, 2019*).

As reported in Chapter II, the main research project was based on the study of Nrf2 (NF-E2-related factor 2) intracellular signaling pathway as a pharmacological target. Nrf2, a member of the Cap'n'collar (CNC) transcription factor family, is a pivotal redox-sensitive transcription factor that coordinates a multifaceted response to various forms of stress and to inflammatory processes, thereby maintaining a homeostatic intracellular environment. The anti-inflammatory potential of Nrf2 has been related to the crosstalk with the transcription factor NF- $\kappa$ B (nuclear factor kappa B), a pivotal mediator of inflammatory responses and of multiple aspects of innate and adaptive immune functions. However, the underlying molecular basis has not been completely identified. In collaboration with the group of Prof. Michela Rosini of the University of Bologna, we synthesized and tested a set of molecules carrying (pro)electrophilic features responsible for the activation of the Nrf2 pathway (*Serafini et al, 2020*). In particular, the chemical structure of such molecules combines two pharmacophoric moieties, such as diallyl sulfide (i.e. the mercaptan moiety

of garlic-derived organosulfur compounds), and the hydroxycinnamoyl group (i.e. a typical chemical moieties of polyphenols, including curcumin) (*Serafini et al, 2020*). First, we investigated the ability of compounds to induce a structure-dependent activation of Nrf2 pathway, in comparison with two reference molecules with antioxidant and anti-inflammatory properties, i.e. curcumin and dimethyl fumarate, a drug approved for the treatment of relapsing-remitting multiple sclerosis (*Serafini et al, 2020*).

Then, we used such compounds as valuable pharmacologic tools to dissect the mechanistic connection between Nrf2 and NF- $\kappa$ B (*Fajiani et al, 2020*). We investigated whether the activation of the Nrf2 pathway by electrophilic/non-electrophilic compounds might affect the secretion of pro-inflammatory cytokines, upon immune stimulation, in a human immortalized monocyte-like cell line (THP-1), as well as in human primary peripheral blood mononuclear cells (*Fajiani et al, 2020*). The capability of compounds to affect the NF- $\kappa$ B pathway was also investigated. We demonstrated that compounds induced a differential modulation of innate immune cytokine release, by differently regulating Nrf2 and NF- $\kappa$ B intracellular signaling pathways (*Fajiani et al, 2020*).

As described in the Chapter III, during the 6-months internship at Johns Hopkins University (Baltimore, Maryland, US), I worked at the Center for Alternatives to Animal Testing, Bloomberg School of Public Health, under the supervision of Prof. Thomas Hartung, MD, PhD, and Lena Smirnova, PhD. During this period, I worked on a project investigating gene environmental interaction contributing to autism spectrum disorder (ASD), characterized by a complex genetic and environmental component. To investigate gene-environment interaction in ASD, we used a human 3D BrainSphere model, an organotypic brain model derived from human induced pluripotent stem cells (iPSC) (*Modafferi et al, 2020*). In particular, we studied the synergistic interaction of two factors, i.e. the pesticide chlorpyrifos (CPF) and the autism risk gene encoding chromodomain helicase DNA binding protein 8 (CHD8). In particular, using human iPSC-derived BrainSpheres with a CRISPR/Cas9-introduced inactivating mutation in the ASD risk gene *CHD8*, exposed to the pesticide CPF and its oxon-metabolite (CPO), we investigated neural differentiation, viability, oxidative stress, neurite outgrowth, the levels of several neurotransmitters and selected metabolites (*Modafferi et al, 2020*). Notably, we demonstrated that CHD8 protein was reduced in CHD8 heterozygous knockout (CHD8<sup>+/-</sup>) BrainSpheres, compared to CHD8<sup>+/+</sup> derived BrainSpheres and due to CPF or CPO treatment. Neurite outgrowth was also perturbed (*Modafferi et al, 2020*). Moreover, we found that several metabolic perturbations that have been observed in patients with ASD were largely reflected in CHD8<sup>+/-</sup> spheroids, such as the reduction in GABA and dopamine



levels, the decrease in choline content, and increase in tryptophan, kynurenic acid, lactic acid, and  $\alpha$ -hydroxyglutaric acid upon treatment with CPF or CPO (Modafferi *et al*, 2020).

As described in Chapter IV, during the coronavirus disease 2019 (COVID-19) pandemic outbreak, we critically discussed in a review article the intracellular signaling pathways altered during viral infections in order to unravel the most relevant molecular cascades implicated in biological processes mediating viral infections and to suggest potential drug repurposing (Catanzaro *et al*, 2020). Then, upon invitation by the editorial board, we critically discussed results presented in *Science* by Yuan *et al*. providing novel insights into the molecular features of neutralizing antibody responses to the severe acute respiratory syndrome coronavirus 2 (see the paper by Fagiani *et al*, 2020).

As described in the Chapter V, I was involved in other research projects covering different research topics, where I contributed with my expertise in basic science and cellular biology.

## REFERENCES

Lanni, C., Fagiani, F., Racchi, M., Preda, S., Pascale, A., Grilli, M., Allegri, N., Govoni, S. [2019] "Beta-amyloid short- and long-term synaptic entanglement", *Pharmacol Res*, Vol. 139, pp. 243-260. doi:10.1016/j.phrs.2018.11.018.

Fagiani, F.\*, Lanni, C.\*, Racchi, M., Pascale, A., Govoni, S. [2019] "Amyloid- $\beta$  and Synaptic Vesicle Dynamics: A Cacophonous Orchestra", *J Alzheimers Dis*, Vol. 72, No. 1, pp. 1-14. doi:10.3233/JAD-190771. \*both authors equally contributed

Rosini, M., Simoni, E., Caporaso, R., Basagni, F., Catanzaro, M., Abu, I.F., Fagiani, F., Fusco, F., Masuzzo, S., Albani, D., Lanni, C., Mellor, I.R., Minarini, A. [2019] "Merging memantine and ferulic acid to probe connections between NMDA receptors, oxidative stress and amyloid- $\beta$  peptide in Alzheimer's disease", *Eur J Med Chem*, Vol. 180, pp. 111-120. doi:10.1016/j.ejmech.2019.07.011

Serafini, M.M.\*, Catanzaro, M.\*, Fagiani, F., Simoni, E., Caporaso, R., Dacrema, M., Romanoni, I., Govoni, S., Racchi, M., Daglia, M., Rosini, M., Lanni, C. [2020] "Modulation of Keap1/Nrf2/ARE Signaling Pathway by Curcuma- and Garlic-Derived Hybrids", *Front Pharmacol*, 10:1597. doi:10.3389/fphar.2019.01597. \*both authors equally contributed

Fagiani, F.\*, Catanzaro, M.\*, Buoso, E., Basagni, F., Di Marino, D., Raniolo, S., Amadio, M., Frost, E.H., Corsini, E., Racchi, M., Fulop, T., Govoni, S., Rosini, M., Lanni, C. [2020] "Targeting cytokine release through the differential modulation of Nrf2 and NF- $\kappa$ B pathways by electrophilic/non-electrophilic compounds", *Front. Pharmacol*, doi: 10.3389/fphar.2020.01256. \*both authors equally contributed

Modafferi, S., Zhong, X., Kleensang, A., Murata, Y., Fagiani, F., Pamies, D., Hogberg, H., Calabrese, V., Lachman, H., Hartung, T., Smirnova, L. [2020] "Synergistic developmental neurotoxicity of chlorpyrifos and CHD8 knockout in human BrainSpheres", under review in *Environmental Health Perspectives*.

Catanzaro, M.\*, Fagiani, F.\*, Racchi, M., Corsini, E., Govoni, S., Lanni, C. [2020] “Immune response in COVID-19: addressing a pharmacological challenge by targeting pathways triggered by SARS-CoV-2”, *Signal Transduct Target Ther*, Vol. 5, No. 1, pp. 84. doi:10.1038/s41392-020-0191-1. \*both authors equally contributed

Fagiani, F.\*, Catanzaro, M.\*, Lanni, C. [2020] “Molecular features of IGHV3-53-encoded antibodies elicited by SARS-CoV-2”, *Signal Transduct Target Ther*, Vol. 5, No. 1, pp. 170. doi:10.1038/s41392-020-00287-4. \*both authors equally contributed

## **CHAPTER I**

---

Dysregulation of the intracellular machinery in Alzheimer's Disease and neurodegenerative disorders



---

## PART 1

The following manuscript was published in *Pharmacological Research* in 2019 as:

### **Beta-amyloid short- and long-term synaptic entanglement**

Cristina Lanni, **Francesca Fagiani**, Marco Racchi, Stefania Preda, Alessia Pascale, Massimo Grilli, Nicola Allegri, Stefano Govoni

#### **Abstract**

Beta-amyloid ( $A\beta$ ) is a peptide that derives from the proteolytic cleavage of the amyloid precursor protein (APP) by several secretases. Since its isolation and sequencing from Alzheimer's disease (AD) brains,  $A\beta$  has been intensively investigated in the context of AD as the main pathogenic marker responsible for neurodegenerative processes. During the last three decades, results from several independent studies have converged to form the so-called amyloid cascade hypothesis of AD and several therapeutic strategies designed to modulate the APP amyloidogenic pathway have been developed. However, none of the clinical trials targeting  $A\beta$  culminated in a significant clinical outcome, thus challenging the concept that targeting  $A\beta$ , at least within the time window so far explored in clinical trials, may have a therapeutic effect. However, besides its presence in AD brains, brain cells produce  $A\beta$ , thus suggesting that, under normal conditions, the peptide may have a role in the regulation of brain functions, which is consistent with its ubiquitous presence and normal synthesis. Taking into account that  $A\beta$  has been found to exhibit a dual role strictly correlated with its concentration (neuromodulatory/neuroprotective vs neurotoxic), we discuss emerging evidence indicating that physiological concentrations of  $A\beta$  peptide modulate synaptic activity. The review examines the physiological effects of  $A\beta$  on acute synaptic activities and the functional interplay existing between  $A\beta$  and different neurotransmitter systems, i.e. cholinergic, glutamatergic, GABAergic, catecholaminergic, serotonergic, and peptidergic. The review also provides an insight into the different mechanisms through which  $A\beta$  affects synaptic activity, focusing in particular on  $A\beta$  interaction with the key synaptic proteins that regulate the neurotransmitter release machinery. These interactions may help to identify or recognize alterations in neurotransmitter activity and correlated behaviors as predictive signs for the development of AD and to understand the limitations of current interventions and the failure so far of amyloid targeted therapies.

**Keywords:** beta-amyloid; acute synaptic activity; neurotransmitter release; SNARE complex; behavioral correlates.



Contents lists available at ScienceDirect

## Pharmacological Research

journal homepage: [www.elsevier.com/locate/yphrs](http://www.elsevier.com/locate/yphrs)

Review

## Beta-amyloid short- and long-term synaptic entanglement

Cristina Lanni<sup>a</sup>, Francesca Fagiani<sup>b</sup>, Marco Racchi<sup>a</sup>, Stefania Preda<sup>a</sup>, Alessia Pascale<sup>a</sup>,  
Massimo Grilli<sup>c</sup>, Nicola Allegri<sup>d</sup>, Stefano Govoni<sup>a,\*</sup><sup>a</sup> Department of Drug Sciences, Pharmacology Section, University of Pavia, Italy<sup>b</sup> Scuola Universitaria Superiore IUSS, Pavia, Italy<sup>c</sup> Pharmacy, Section of Pharmacology and Toxicology, University of Genoa, Italy<sup>d</sup> IRCCS Mondino Foundation, Pavia, Italy

## 1. INTRODUCTION

The soluble aggregates of beta-amyloid (A $\beta$ ) play a crucial role in the onset of Alzheimer's disease (AD) and have been intensively investigated in the neurodegenerative process within the amyloid cascade hypothesis of AD [1]. Based on this hypothesis, an intense research effort has been directed towards the development of novel therapeutic approaches for the treatment of AD, ranging from strategies specifically targeting the levels of A $\beta$  peptides, either by interfering with their production (e.g.  $\beta$ - and  $\gamma$ -secretase inhibitors) or by enhancing their clearance, to immunotherapy (e.g. humanized antibodies against A $\beta$  peptides). However, all Phase III clinical trials for the treatment of AD failed to meet the desired endpoints, mainly due to a lack of efficacy and/or unexpected side effects. Despite the failure of these attempts, the validity of the amyloid cascade hypothesis and the role of A $\beta$  peptides in the progression of the disease cannot be discounted. The ineffectiveness of these approaches may depend on two critical factors: the fact that A $\beta$  may not be an ideal druggable target for all AD patients or the wrong timing of therapeutic intervention, a key factor for the success of AD treatment.

The study of specific biomarkers may be useful to better select and stratify patients for an appropriate therapeutic approach. Furthermore, interventions in the early stage of the disease, before the appearance of the first clinical symptoms, may target still reversible pathological alterations.

This time-window based approach makes it necessary to set up new and effective diagnostic tools to detect AD in its prodromal stage. A detailed comprehension of the physiological role of A $\beta$  peptides and their effects on the aging brain might be a starting point to design

novel and more efficient therapeutic strategies. Data from literature demonstrate that A $\beta$  peptides exhibit a dual role, i.e. neuromodulatory/neuroprotective vs neurotoxic, strictly correlated with their concentration and aggregation state [2,3].

Although the literature defines concentrations of A $\beta$  ranging from picomolar to low nanomolar as physiological, not leading to neurotoxicity, *in vitro* models investigating the effect of synthetic A $\beta$  revealed a great variability in this paradigm. For instance, the issue of extreme supplier-to-supplier and batch-to-batch variability of synthetic peptides is rarely addressed [4]. These limitations, together with the complex dynamic balance existing between A $\beta$  species, contribute to the widespread and controversial literature on A $\beta$ .

The present review examines the effects of exogenous applications of low concentrations of A $\beta$  peptides on the synaptic activity and its functional interplay with different neurotransmitter systems (i.e. cholinergic, glutamatergic, GABAergic, catecholaminergic, serotonergic and peptidergic systems) (Fig. 1). It also explores how A $\beta$ -driven effects may alter neurotransmission over time, possibly contributing to the onset of early neuropsychiatric manifestations such as depression, apathy and psychotic symptoms.

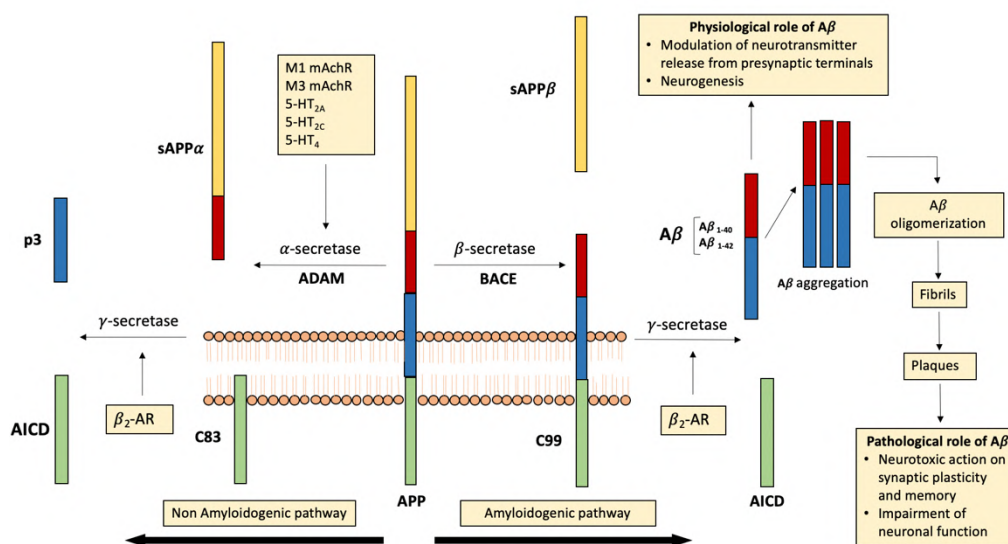


**Fig. 1. APP metabolism.** Schematic representation of the non-amyloidogenic and amyloidogenic pathways and definition of the physiological and pathological roles of A $\beta$  fragments generated. The modulation of different neurotransmission systems may affect A $\beta$  production and concentration. The figure shows the mechanisms underlying this modulation, focusing on the involvement of different receptor subtypes and their targets ( $\alpha$ -,  $\beta$ - or  $\gamma$ -secretase).

## 2. Beta-amyloid acute synaptic activities

### 2.1. Electrophysiology studies

Evidence from the literature shows that A $\beta$  exhibits a dual role that seems to be strictly correlated with its concentration and the age-related cellular environment in the human brain [5]. Low concentrations (picomolar-low nanomolar) of A $\beta$  positively modulate neurotransmission and memory, whereas higher concentrations (high nanomolar-low micromolar) exhibit a neurotoxic and detrimental effect on synaptic plasticity and memory. Furthermore, a regulatory loop has been identified, according to which not only A $\beta$  morphologically and functionally modulates the synapses and synaptic plasticity but also synaptic activity affects A $\beta$  homeostasis [6].

Several *in vitro* [7] and *in vivo* [8] studies have demonstrated that synaptic activity directly regulates the production of A $\beta$  and its release into the extracellular space at the synapses. In the context of amyloid-precursor protein (APP), overexpression in either transgenic (chronic) or virally (acute) driven settings, as well as in the case of endogenous levels of APP, electrophysiological data show that A $\beta$  levels (both A $\beta$  1-40 and the more fibrillogenic A $\beta$  1-42) are significantly modified depending on neuronal electrical activity, whose enhancement promotes A $\beta$  release whereas its reduction has the opposite effect [7,8].

Such results are consistent with the hypothesis that neuronal activity regulates the regional vulnerability to A $\beta$  deposition. Brain areas with high baseline levels of synaptic activity have been found to be more prone to A $\beta$  accumulation [9]. In particular, several studies investigating the impact of neuronal activity on A $\beta$  levels have focused on the default mode network. By using functional magnetic resonance imaging (fMRI) and positron emission tomography (PET) with PIB compound, Buckner *et al.* reported a spatial overlap between the topography of amyloid deposition and the regions of the default mode network (e.g. posterior cingulate and parietal cortex, medial temporal lobe and medial frontal subsystem) [10]. However, not all regions displaying high baseline activity are subject to A $\beta$  accumulation, so the relationship between neuronal activity and A $\beta$  deposition cannot be considered linear. In a further study by Buckner *et al.*, the strong network connectivity rather than elevated baseline activity has been correlated to regional A $\beta$  deposition. Cortical regions (e.g. posterior cingulate, lateral temporal, lateral parietal, and medial/lateral prefrontal cortices) with intense interconnectivity have been found to display high A $\beta$  deposition [11].



Some of these observations have been supported by parallel *in vitro* and *in vivo* studies, linking APP transport, neuronal activity and A $\beta$  metabolism. APP is axonally transported from the entorhinal cortex to the hippocampal formation through the perforant path [12] and alterations of this pathway result in a decreased A $\beta$  deposition within the hippocampus [13]. The brain regions showing the greatest metabolic activity throughout life – and, most likely, the highest levels of neuronal activity – are the most vulnerable to A $\beta$  accumulation and aggregation in AD patients [10]. Further investigations are needed to better understand if prodromal symptoms of neurodegeneration occur under non-pathological conditions or, alternatively, whether they are involved in the control of altered disease-related behaviors.

It has been hypothesized that the modulation of A $\beta$  secretion by neuronal electrical activity may be mediated by BACE ( $\beta$ -site APP-cleaving enzyme) cleavage at  $\beta$ -secretase sites, though it is still unclear whether neuronal activity influences intrinsic BACE activity or the accessibility of APP to BACE [7]. This hypothesis has not been validated, suggesting that altered BACE-dependent activity is not required for the synaptic activity-dependent A $\beta$  increase [8]. Discrepancies of this kind might reflect differences in experimental settings, implying that different time exposure (short or long term) or areas of infusion might impact on the effect of the neuronal activity on BACE cleavage of APP [14]. Furthermore, considerations on the type of synapses involved in this exploratory mechanism should be made. Differences between low- and high-frequency synapses occur, also depending on the fact that neurotransmitter biosynthesis takes place in the synapses or at more distant sites. A further explanation of the discrepancy of BACE activity in regulating A $\beta$  secretion could be that synaptic activity-dependent A $\beta$  alterations, rather than requiring changes in APP processing, are accomplished via a mechanism specifically related to vesicle fusion. According to this hypothesis, Cirrito *et al.* defined a pathway by which synaptic activity drives more APP into the endocytic compartment, leading to an enhanced production and release of A $\beta$  [15], thus proving that the increase in A $\beta$  secretion is linked to a higher presence of APP rather than BACE activity. In particular, it has been suggested that a depolarization of the synaptic terminal might cause calcium influx, leading the synaptic vesicles to fuse with the plasma membrane therefore increasing the amount and rate of endocytosis. Synaptic vesicle membrane recycling via clathrin-mediated endocytosis gives rise to more APP within endosomes, where BACE cleaves APP to release A $\beta$  from the neuron into the brain interstitial fluid [15].

The observation that extracellular A $\beta$  levels are likely to be regulated by synaptic activity suggests that A $\beta$  may be physiologically involved in neuronal processes. Indeed, at physiological levels (pico- molar-low nanomolar range), A $\beta$  plays a pivotal role in synaptic structure-functional plasticity, which is crucial to learning and memory. In line with such

evidence, healthy murine brains treated with a specific A $\beta$  antibody and an siRNA against murine A $\beta$  showed impaired synaptic plasticity and memory [16]. Subsequent addition of human A $\beta$  1-42 rescued these deficits, suggesting that in the healthy brain, physiological A $\beta$  concentrations are necessary for normal synaptic plasticity and memory [16].

Data from studies on APP knock-out (KO) mice with impaired long-term potentiation (LTP) and memory [17] substantiate the involvement of A $\beta$  in hippocampal LTP [2]. In particular, when the A $\beta$  concentration is within the picomolar range, it seems to act as a positive modulator of LTP. The effect of A $\beta$  on LTP has been shown by a dose/response curve, with a postulated biphasic effect of A $\beta$  1-42: low concentrations of A $\beta$  1-42 induced LTP enhancement at the synapses between Schaeffer col- lateral fibers and CA1 neurons, with a maximum effect around 200 pM, whereas higher nanomolar A $\beta$  1-42 impaired LTP, in line with previous investigations [2,7]. This effect was not obtained either with scrambled A $\beta$  1-42, confirming that LTP enhancement is mediated by A $\beta$  1-42, or when the peptide was administered after tetanization, supporting the hypothesis that A $\beta$  is required during the induction phase of synaptic plasticity and memory, but not for plasticity maintenance and memory consolidation [16].

The positive action of A $\beta$  1-42 on synaptic plasticity has been related to an enhancement of neurotransmitter release during high-frequency stimulation, given that post-tetanic potentiation (a form of short-term plasticity based on the increase of glutamate release from presynaptic terminals due to brief periods of high-frequency stimulation) was increased by perfusion with 200 pM A $\beta$  1-42 [2]. However, the N-methyl D-aspartate receptor (NMDAR) and the  $\alpha$ -amino-3-hydroxy-5-methyl-4-isoxazolepropionic acid receptor (AMPA), both implicated in CA-1 LTP, are not involved in A $\beta$ -induced improvement of synaptic function [18]. Low doses of A $\beta$  did not change current-voltage (I/V) relationships in the NMDA and AMPA receptor current ratio, nor did they alter the amplitude of AMPA receptor-mediated excitatory postsynaptic potentials (EPSCs) or their amplitude distribution [2]. Interestingly, A $\beta$  1-42 -induced neuroplasticity has been related to  $\alpha$ 7 nicotinic acetylcholine receptors ( $\alpha$ 7nAChR), since these effects were absent in  $\alpha$ 7nAChR knockout mice and blocked by  $\alpha$ -Bungarotoxin, a selective antagonist of  $\alpha$ 7nAChR [2,16].

These data are consistent with the high-binding affinity of A $\beta$  to  $\alpha$ 7nAChR and the  $\alpha$ 7nAChR-mediated increase in calcium influx in hippocampal synaptosomes upon infusion of picomolar concentrations of A $\beta$  1-42 [19]. The involvement of  $\alpha$ 7nAChR has recently been shown to be essential in presynaptic function modulation by A $\beta$ : low picomolar A $\beta$  1-40 and A $\beta$  1-42 increased, whereas endogenous A $\beta$  depletion or application of

low micromolar concentrations led to a decrease in the synaptic strength [20], according to data suggesting previous hormetic regulation of neurotransmission by A $\beta$  [2]. These A $\beta$ -induced modulations, in addition to requiring functional  $\alpha$ 7nAChR, also involved cyclin-dependent kinase 5 (CDK5) and calcineurin signaling, increasing the recycling rate of the synaptic vesicles and supporting the function of A $\beta$  in the regulation of neurotransmitter release [20]. On the other hand, this suggests that a failure of physiological function in synaptic vesicle recycling might be a prodromal marker of cognitive decline and neurodegeneration.

The depression of excitatory synaptic transmission due to high nanomolar concentrations of A $\beta$ , on the other hand, suggested that A $\beta$  may exert a negative feedback function [7]. Following this negative feedback model, intense neuronal activity increases the production of A $\beta$  from endogenous APP and, consequently, A $\beta$  extracellular levels at and near synapses. In turn, A $\beta$  downregulates synaptic transmission, maintaining neuronal activity within a normal dynamic range [7]. This negative feedback process could also operate as a physiological homeostatic mechanism to limit levels of neuronal activity, which, if unchecked, could lead to excitotoxicity. Pathologically aberrant levels of A $\beta$  would be expected to send this negative feedback regulator into overdrive, suppressing excitatory synaptic activity at the postsynaptic level. However, many questions remain unanswered. It is difficult to assign the neurophysiological effects of A $\beta$  to a specific assembly form (soluble monomers and/or soluble oligomers), because these assemblies are likely to exist in a dynamic equilibrium [21]. A $\beta$  conformations released at synapses are still largely unknown, as is limited our understanding of any age-related change of A $\beta$  species. A $\beta$  conformation following synaptic activity is likely to be a critical factor for the modulation of neurotransmission: nanomolar concentrations of soluble A $\beta$  oligomers, for instance, appear to be much more potent at depressing synaptic transmission than A $\beta$  monomers [22,23]. Given that specific form/s of A $\beta$  1-42 (responsible for the enhancing effects on synaptic plasticity) have not been detailed yet, the interpretation of physiological experiments examining synthetic A $\beta$  1-42 might be problematic. Moreover, two further hydrophobic residues (i.e. alanine and isoleucine) make A $\beta$  1-42 more prone to aggregate than A $\beta$  1-40 isoform (even at low concentrations), which is reported to be the most abundant A $\beta$  monomer under physiological conditions in young mammals [21]. Literature on the characterization of synthetic A $\beta$  profile is quite bewildering as it describes different steps of A $\beta$  nucleation between A $\beta$  1-40 and A $\beta$  1-42 when using synthetic peptides [24].

## **2.2. Neurochemistry studies**

### **2.2.1. Cholinergic system**

Dysfunctional cholinergic transmission is thought to underlie memory impairment and cognitive deficits in AD [25–27]. However, it is still unclear whether this dysfunction is the consequence of the loss of cholinergic neurons and AChRs in the AD brain or a direct effect of molecular interactions of A $\beta$  peptide with AChRs, resulting in a deregulated receptor function. Currently, only few research data explain the putative mechanisms through which physiological A $\beta$  may unbalance the cholinergic system before inducing the loss of cholinergic terminal markers. As several connections between these two key players have been observed, the present review will illustrate the potential interplay linking APP processing, A $\beta$  release and cholinergic receptors before neurodegeneration occurs. A $\beta$  has been reported to interfere with cholinergic neurotransmission by interacting with presynaptic cholinergic receptors function. Notably, both muscarinic and nicotinic receptors are capable of modulating APP processing, diverting its metabolism towards non-amyloidogenic products and promoting the release of the neurotrophic and neuroprotective fragment sAPP $\alpha$  [28].

The activation of specific muscarinic AChRs (mAChRs) M1 and M3 subtypes, mostly distributed in the cerebral cortex and hippocampus, via the stimulation of a downstream signaling pathway involving protein kinase C (PKC), promotes the non-amyloidogenic pathway, concomitantly reducing A $\beta$  production [29]. This evidence is consistent with several studies demonstrating that direct PKC activation by means of phorbol esters and bryostatin-1 promotes the non-amyloidogenic pathway and decreases A $\beta$  release [30].

The reduction of PKC activity has been associated with all major AD neuropathological markers [31] (although PKC subtype coupled with M1-mAChRs stimulation is still uncertain) and the genetic deletion of M1-mAChRs in APPSwe/Ind mice exacerbates A $\beta$  pathological features [32]. In the regulation of APP metabolism,  $\alpha$ 4 $\beta$ 2- and  $\alpha$ 7-nAChRs subtypes are also involved. They are known to boost synaptic plasticity and memory [33] and enhance transmitter release in several brain structures including the hippocampus [34,35], spinal cord dorsal horn [36] and amygdala [37]. Nicotinic agonists, nicotine or epibatidine, decrease secretion and intracellular accumulation of A $\beta$  in human SH-EP1 cells stably transfected with both human  $\alpha$ 4 $\beta$ 2-nAChRs and human APP [38].

Furthermore, nicotine increases the release of sAPP $\alpha$  while decreasing A $\beta$  levels in SH-SY5Y cells that express  $\alpha$ 7-nAChRs, an effect blocked by mecamylamine [39]. A $\beta$  has been reported to induce both activation and inactivation of  $\alpha$ 7-nAChRs, mostly depending upon the peptide concentration, preparation type (monomers vs oligomers) and exposure time [40]. The peptide is also able to interact with  $\alpha$ 4 $\beta$ 2- nAChRs, although its binding affinity for these receptors is 100–5000 times lower than  $\alpha$ 7-nAChRs [41].

Low concentrations (picomolar-low nanomolar) of A $\beta$  activate  $\alpha$ 7-nAChRs, stimulating signal transduction pathways associated with neuroprotection, synaptic plasticity, learning and memory, mainly in the hippocampal and midbrain dopamine areas [3]. Both A $\beta$  1-40 and A $\beta$  1-42 isoforms bind to the  $\alpha$ 7-nAChRs, although A $\beta$  1-40 is more effective in competition binding studies compared to A $\beta$  1-42. Two mechanisms have been hypothesized in the activation of  $\alpha$ 7-nAChRs by low concentrations of A $\beta$ : (1) a direct interaction of A $\beta$  with the nicotinic binding site at presynaptic nerve endings of synaptosomes [19] and (2) an indirect modulation of receptor activity as a result of A $\beta$  binding to membrane lipids [42], such as receptor-associated lipid rafts [43].

Higher concentrations (nanomolar-low micromolar) of A $\beta$  or a prolonged exposure to this peptide induce  $\alpha$ 7-nAChRs desensitization and inactivation, leading to impaired synaptic signaling and neuronal degeneration in response to aversive stimuli. It may be speculated that A $\beta$  physiologically plays a neuromodulatory role on nicotinic receptors, while its accumulation, as occurs in AD, may lead to progressive inactivation of these receptors, thus impairing nicotinic cholinergic transmission. This evidence might suggest that nicotinic agonists are potential agents for AD, although their therapeutic efficacy is limited due to rapid receptor desensitization. However, compounds that block A $\beta$  binding to nAChRs may limit the sensitization aspects. Recently, Sabec et al. reported that nAChRs in the prefrontal cortex exhibit subtype-specific roles in associative memory encoding and retrieval. In particular, homomeric  $\alpha$ 7-nAChRs have been demonstrated to be

essential for both encoding of associative recognition and induction of LTP, whereas  $\alpha$ 4 $\beta$ 2 subtypes are involved in the retrieval of associative memory and LTD [44]. Given that typical AD patients suffer from memory deficits that specifically affect encoding and storage processes,  $\alpha$ 7-nAChRs might play a key role in the onset of these deficits.

While there is relatively abundant literature on the direct interactions between A $\beta$  and nicotinic receptors, no reports have been published so far on the direct effects of the peptide on muscarinic recognition sites. Interestingly, Grilli and collaborators have previously demonstrated that A $\beta$  preferentially inhibits the effect of stimulatory mAChRs, leaving the function of inhibitory subtypes unchanged [45]. However, there is no evidence of a direct interaction of A $\beta$  with these receptors and consequently little is known about any A $\beta$ -induced inhibitory mechanisms. *In vitro* studies demonstrated that A $\beta$  at low concentration counteracts muscarinic receptor-activated DA release from dopaminergic terminals by impairing PKC transduction machinery [46]. One might be led to suppose that the effect of A $\beta$  on these mAChRs may be indirect, including the possibility that A $\beta$  may act on an unknown site downstream the muscarinic signal [47].

Besides the effects of the interaction between A $\beta$  and cholinergic receptors, it might also be interesting to investigate the putative effects on direct neuron-to-neuron signaling at the synaptic level. Such an action would be consistent with the localization of AChRs on presynaptic terminals as well as on postsynaptic elements and would argue in favor of short-term functional effects of the peptide. Indeed, while presynaptic nAChRs generally affect (either positively or negatively) neurotransmitter release from presynaptic terminals, M1 and M3 presynaptic receptors stimulate neurotransmitter release both in dopaminergic terminals [46] and GABAergic terminals [45]. Conversely, M2 receptors inhibit neurotransmitter release in cholinergic terminals at the nucleus accumbens [45]. A $\beta$  has been proved to affect the cholinergic control of neurotransmitter release from synaptic terminals, an event that may occur before neurodegeneration.

A $\beta$ -induced modulation/dysfunction in synaptic transmission involves simultaneously different brain transmitters (DA, GABA, glutamate, aspartate, and glycine) and brain areas (nucleus accumbens, striatum, hippocampus), providing grounds for a multi-transmitter dysregulation hypothesis in the disease. In particular, A $\beta$  1-40 concentrations are capable of modulating the release of several neurotransmitters (DA,  $\gamma$ -aminobutyric acid, aspartate, glutamate), elicited by the stimulation of mAChRs and nAChRs subtypes in different brain areas [2,46,48] (see also **Table 1**).

**Table 1**  
Interactions between beta-amyloid and cholinergic receptors in regulating neurotransmitter release.

Beta-amyloid influence on cholinergic control of neurotransmitter release		Observed effect of beta-amyloid on neurotransmitters	Experimental models/brain area	Reference
<b>Molecular species of A<math>\beta</math></b>	<b>Aggregation status and concentration/ time of exposure</b>			
<b>Dopamine</b> Soluble A $\beta_{1-40}$ and A $\beta_{1-42}$	1:1.0 $\mu$ M/60-80 min (for <i>in vivo</i> experiments); 100 nM/up to 10 min (for <i>in vitro</i> analysis)	- In rat nucleus accumbens, 1 $\mu$ M soluble A $\beta$ completely counteracted the muscarinic receptor-activated DA release in a reversible manner, whereas the overflow of DA elicited by nicotinic receptors activation through ephedrin administration was not altered by A $\beta$ infusion. - The [11 $\beta$ ]DA release evoked by carbachol (30 nM) in accumbens isolated nerve endings is significantly reduced by 100 nM A $\beta$ . Also A $\beta_{1-42}$ (100 nM) significantly reduced the DA release evoked by carbachol to a similar extent. - The extracellular application of A $\beta_{1-42}$ (100 nM) inhibited both nicotinic and muscarinic cholinergic modulation of DA release by acting respectively from outside and inside the nerve endings. - Experiments on isolated nerve endings: - A $\beta$ impaired the muscarinic control of DA release in both nucleus accumbens and caudate putamen; - A $\beta$ affected a specific component of the DA overflow evoked by the non-selective metabotropic glutamate receptors agonist (+)ACPD in caudate putamen	<i>In vivo</i> (brain dialysis) and <i>in vitro</i> (isolated synaptosomes) models, Rat nucleus accumbens	[46]
A $\beta_{1-40}$	100 nM		Synaptosomes/ Rat nucleus accumbens	[62]
A $\beta_{1-40}$ and A $\beta_{1-42}$	10:100 nM/up to 12 min		Synaptosomes/ Caudate-putamen-Nucleus Accumbens	[143]
<b>GABA</b> A $\beta_{1-40}$ and A $\beta_{1-42}$	100 nM/up to 17 min	Experiments on isolated nerve endings: - A $\beta$ inhibited GABA release selectively acting on muscarinic receptor subtypes which stimulate transmitter release (M3 and M5); - A $\beta$ was ineffective on muscarinic receptor subtypes which modulate negatively the stimulated transmitter release (M2 and M4). - Perfusion of 10 $\mu$ M A $\beta$ (microdialysis) inhibited the nicotine-induced release of GABA; - Perfusion of 100 nM A $\beta$ (microdialysis) potentiated the nicotine-evoked GABA overflow; - Experiments on isolated nerve endings: 100 nM A $\beta$ inhibited the nicotine-induced release of GABA; 100 nM A $\beta$ inhibited the release of GABA induced by the $\alpha$ 4 $\beta$ 2 selective agonist 5IA85380.	Synaptosomes/ Rat nucleus accumbens	[45]
Monomers of A $\beta_{1-40}$	100 nM, 1 $\mu$ M, 10 $\mu$ M/40-60 min (for <i>in vivo</i> experiments); 100 pM, 1 nM, 100 nM/up to 10 min (for <i>in vitro</i> analysis)		<i>In vivo</i> (microdialysis) and <i>in vitro</i> (synaptosomes in superfusion) techniques/Hippocampus	[48]
<b>Glycine</b> A $\beta_{1-40}$	10 $\mu$ M/40-60 min (for <i>in vivo</i> experiments); 10 nM, 100 nM/up to 10 min (for <i>in vitro</i> analysis)		<i>In vivo</i> (synaptosomes in superfusion) and <i>in vitro</i> (microdialysis) approaches/Hippocampus	[49]
<b>Aspartate</b> Monomers of A $\beta_{1-40}$	100 nM, 1 $\mu$ M, 10 $\mu$ M/40-60 min (for <i>in vivo</i> experiments); 100 pM, 1 nM, 100 nM/up to 10 min (for <i>in vitro</i> analysis)	- Perfusion of 10 $\mu$ M A $\beta_{1-40}$ (microdialysis) reduced the nicotine-induced Gly overflow and also the Gly overflow induced by the $\alpha$ 7 selective agonist PHA545613; - Experiments on isolated nerve endings: both 10 nM and 100 nM A $\beta$ inhibited the nicotine-induced Gly release; 100 nM A $\beta$ inhibited the release of Gly evoked by the $\alpha$ 7 selective agonist carbachol and by the $\alpha$ 4 $\beta$ 2 selective agonist 5IA85380. - Perfusion of 10 nM and 1 $\mu$ M A $\beta$ (microdialysis) inhibited the nicotine-induced release of aspartate; - Experiments on isolated nerve endings: 100 nM A $\beta$ inhibited the nicotine-induced release of aspartate; 100 nM A $\beta$ inhibited the release of aspartate that was induced by the $\alpha$ 7 selective agonist carbachol; 100 nM A $\beta$ inhibited the release of aspartate induced by the $\alpha$ 4 $\beta$ 2 selective agonist 5IA85380; 100 pM A $\beta$ potentiated the carbachol-induced release of aspartate.	<i>In vivo</i> (microdialysis) and <i>in vitro</i> (synaptosomes in superfusion) techniques/Hippocampus	[48]
<b>Glutamate</b> Monomers of A $\beta_{1-40}$	100 nM, 1 $\mu$ M, 10 $\mu$ M/40-60 min (for <i>in vivo</i> experiments); 100 pM, 1 nM, 100 nM/up to 10 min (for <i>in vitro</i> analysis)	- Perfusion of 10 nM and 1 $\mu$ M A $\beta$ (microdialysis) inhibited the nicotine-induced release of glutamate; - Experiments on isolated nerve endings: 100 nM A $\beta$ inhibited the nicotine-induced release of glutamate; 100 nM A $\beta$ inhibited the release of glutamate induced by the $\alpha$ 7	<i>In vivo</i> (microdialysis) and <i>in vitro</i> (synaptosomes in superfusion) techniques/Hippocampus	[48]
<b>Beta-amyloid influence on cholinergic control of neurotransmitter release</b>				
selective agonist carbachol; 1 nM A $\beta$ potentiated the release of glutamate induced by carbachol; 100 nM A $\beta$ inhibited the release of glutamate induced by the $\alpha$ 4 $\beta$ 2 selective agonist 5IA85380; 100 pM A $\beta$ potentiated the carbachol-induced release of glutamate.				

In the hippocampal region - an early AD target, where the cholinergic pathways are critical for modulation of attention and memory - low A $\beta$  concentrations (100 pM and 1 nM) regulate the nicotine-evoked release of both excitatory (i.e. glutamate and aspartate) and inhibitory aminoacids (i.e. glycine,  $\gamma$  aminobutyric acid) [48,49] (Fig. 2). Higher concentrations of A $\beta$  1-40 (100 nM and 10  $\mu$ M administered *in vitro* and *in vivo*, respectively)

strongly inhibit the nicotine-elicited release of glutamate and aspartate through the impairment of cholinergic modulation mediated by both  $\alpha 7$  and  $\alpha 4\beta 2$  receptors [48].

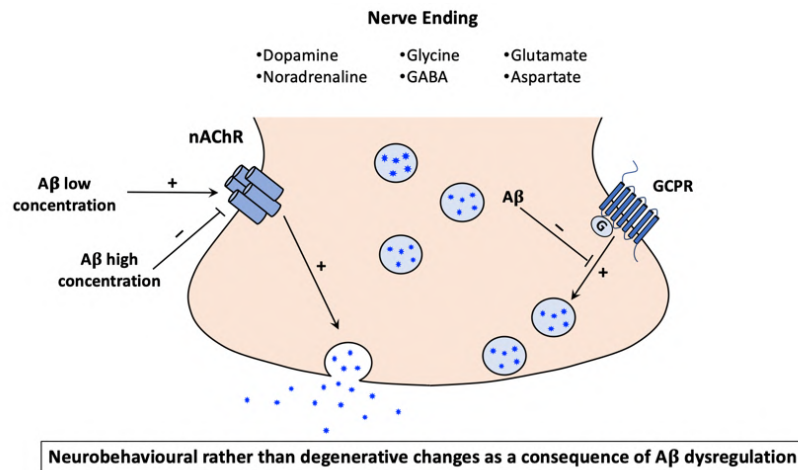


**Fig. 2. Interactions between cholinergic transmission and A $\beta$ .** A $\beta$  can interact with both nicotinic and GPCR transmission, exerting different effects depending on its concentration. In particular, low (picomolar to low nanomolar) A $\beta$  concentrations may directly stimulate nicotinic receptors and also facilitate the nicotinic-induced release of excitatory or inhibitory aminoacid transmitters. High A $\beta$  concentrations have been widely demonstrated to inhibit the nicotinic and GPCR-evoked release of several neurotransmitters.

This effect is in line with that shown in the nucleus accumbens and in the striatum in the case of GABA and dopamine release following muscarinic cholinergic stimuli [45,46]. Hence, it can be hypothesized that an early derangement of A $\beta$  production arguably exceeds the threshold beyond which A $\beta$  loses its ability to co-promote the release of aspartate and glutamate (supposedly linked to an efficient memory trace formation) and, subsequently, gains the ability to inhibit the glutamate and aspartate release mediated by cholinergic receptors, thus impairing memory at this point.

### 2.2.2. Glutamatergic system

Disturbance of excitatory glutamatergic neurotransmission has been linked to several neurodegenerative disorders, including AD [50]. In particular, the exacerbated stimulation of NMDAR is known to mediate excitotoxicity in AD brains, and pyramidal neurons are proposed to be major players in AD-related pathology. Notably, together with acetylcholinesterase inhibitors, the NMDAR noncompetitive antagonist memantine is still an approved choice in the clinical management of AD-type dementia.



Data from the literature strongly support the hypothesis that, in the absence of evident signs of neurotoxicity, A $\beta$  peptides serve a neuromodulatory role on glutamate release, ranging from facilitation to inhibition of stimulated release depending on its concentration.

Recently, Hascup *et al.* investigated the effect of the local application of human monomeric A $\beta$  1-42 on glutamate release in the dentate gyrus, CA3, and CA1 of C57BL/6 J mice [51]. Local exposure to different concentrations of A $\beta$  1-42 (0.01, 0.1, 1, and 10  $\mu$ M) has been found to elicit glutamate release in all hippocampal subfields.

Since the concentration of A $\beta$  1-42 decreases as the distance from the ejection site increases [52], an approximate concentration of A $\beta$  1-42 surrounding MEA (enzyme-based microelectrode array) was calculated. Based on an average distance of 100 microns from the micropipette to the MEA, the concentration of locally-applied A $\beta$  1-42 surrounding the MEA has been approximated to be 1, 10, 100, and 1000 nM (for micropipette concentrations of 0.01, 0.1, 1, and 10  $\mu$ M A $\beta$  1-42, respectively) [51].

The application of 100 nM and 1  $\mu$ M A $\beta$  1-42 significantly increased the average maximal amplitude of glutamate release in the dentate gyrus and CA1, while higher concentrations (10  $\mu$ M) of A $\beta$  1-42 were needed in order to increase glutamate release in the dentate gyrus and CA3 [51]. Glutamate release was completely prevented by coapplication of  $\alpha$ -Bungarotoxin, thus indicating that monomeric A $\beta$  1-42 isoform stimulates glutamate release by acting on  $\alpha$ 7-nAChRs. Complexively, the above presented data are consistent with the hypothesis that low concentrations (pM-nM) of A $\beta$  positively modulate neurotransmitter release by acting on presynaptic  $\alpha$ 7-nAChRs.

Accordingly, *in vivo* (microdialysis technique on freely moving rats) and *in vitro* (isolated nerve endings derived from rat hippocampus) experiments support A $\beta$ -driven modulation of glutamate release [48]. Exposure to low concentrations (100 pM and 1 nM) of A $\beta$  1-40 peptides has been found to potentiate glutamate and aspartate release elicited by the selective stimulation of  $\alpha$ 7-nAChRs, thus suggesting a facilitating effect of low concentrations of A $\beta$  1-40 on the release of these excitatory aminoacids [48].

In contrast, application of higher concentrations (100 nM and 10  $\mu$ M, the two highest concentrations respectively used *in vivo* and *in vitro*) of A $\beta$  1-40 peptide has been reported to strongly reduce glutamate and aspartate release elicited by nicotine, but not to inhibit the release of glutamate and aspartate evoked by a depolarizing stimulus (veratridine). Such evidence suggests that A $\beta$  1-40 at higher concentrations impairs the nicotine-driven

neurotransmitter release by directly binding to nAChRs or by indirectly acting downstream on the cellular transduction machinery [48].

The differences between results reported by Hascup *et al.* and Mura *et al.* (the inhibition of glutamate release by high concentrations of A $\beta$  peptides observed by these latter) may be due to different methodology and tissue preparation, amyloid delivery techniques and peptide choice. Notably, both groups agree that low concentrations of A $\beta$  peptides might increase glutamate release elicited by  $\alpha$ 7-nAChRs stimulation.

### **2.2.3. GABAergic system**

In the past, much research focused on the dysfunctions of the glutamatergic and cholinergic neurotransmitter systems in AD, whereas, the inhibitory component of the excitatory/inhibitory network and, particularly, dysfunction in the GABAergic signaling system was poorly investigated. However, GABAergic transmission plays a key role in modulating neuronal responsiveness and excitability [53], network activity [54,55] as well as the maintenance of the excitatory/inhibitory (E/I) balance in the brain [56], which regulates cortical network function. It is well-established that, at early preclinical stages even before amyloid plaque deposition, soluble physiological A $\beta$  peptides impair synaptic transmission by perturbing excitation/inhibition balance [57], inducing neuronal hyperexcitation. A recent work by Ren and coworkers highlighted that A $\beta$ -driven dysfunction of an excitatory/ inhibitory balance in key brain areas might represent an early pathological mechanism underlying synaptic impairment and cognitive decline in AD [58]. By using whole-cell recordings in acute mouse brain slices, they demonstrated that the application of low concentrations (50 nM) of A $\beta$  1-42 induces hyperexcitability of excitatory pyramidal cells by depressing inhibitory synaptic innervation from fast-spiking interneurons in the anterior cingulate cortex [58], one of the earliest affected areas in AD [59]. Such disruption of GABAergic inhibitory innervation by 50 nM A $\beta$  1-42 has been suggested to depend on the perturbation of GABA release from presynaptic terminals. In particular, the excessive activation of dopamine D1 receptors of fast-spiking interneurons has been found to be the main cause contributing to GABAergic input perturbation and, subsequently, to excitation/inhibition imbalance caused by A $\beta$  1-42 [58]. Accordingly, the SCH23390 D1 receptor antagonist has been found to reverse A $\beta$  1-42 -driven perturbation of GABAergic inhibitory input. Therefore, the D1-dependent impairment of fast-spiking GABAergic inhibitory input is likely to serve a key role in A $\beta$  1-42-induced excitation/inhibition imbalance in anterior cingulate cortex. Similarly, this excessive dopamine innervation of fast-spiking interneurons in anterior cingulate cortex has been suggested to impair excitation/inhibition balance in schizophrenia [60]. A further

contribution to the genesis of psychoses (e.g. schizophrenia and mood disorders with psychotic symptoms) may arise from the impairment of hippocampal GABAergic interneurons and from the subsequent overactivation of neurons that release glutamate into cells located in and projecting from hippocampal CA1 region, in turn impinging upon the dopaminergic control of prefrontal cortex [61]. Therefore, it can be hypothesized that the perturbation of inhibitory synaptic innervation of pyramidal cells may represent the molecular base underlying the onset of early psychotic symptoms, manifestations of cognitive and perceptual dysfunction (e.g. delusions, hallucinations) also occurring in AD.

Moreover, data from literature have demonstrated that A $\beta$  peptides are capable of affecting GABA release from presynaptic terminals in a concentration-dependent manner. In particular, evidence of the dual effect of A $\beta$  on GABA release derives from *in vivo* studies showing that low concentrations of A $\beta$  peptides have a facilitating action on GABA release, whereas higher concentrations reveal an inhibitor effect [48]. Hippocampal perfusion with 100 nM A $\beta$  1-40 (microdialysis) has been found to elicit a nicotine-evoked GABA overflow while 1  $\mu$ M A $\beta$  1-40 proved to be ineffective on GABA release and 10  $\mu$ M A $\beta$  1-40 to inhibit the nicotine-induced release of GABA [48]. This observed dual effect of A $\beta$  1-40 peptides is consistent with the hypothesis that A $\beta$  may serve different biological effects according to the concentration applied, ideally in a continuum from physiology to pathology.

#### **2.2.4. Catecholaminergic system**

As regards the catecholaminergic system, several experimental data have explored the involvement of NE and DA in early AD dysfunctions. The present review mainly focuses on recent insights on A $\beta$  interplay with these two neurotransmitters.

##### **2.2.4.1. Norepinephrine**

The locus coeruleus (LC) plays a critical role in modulating arousal, which is important in regulating consciousness, attention, information processing and promoting behaviors such as motor activity, learning and food intake [62]. Despite its well-established role in a plethora of neurodegenerative and neuropsychiatric diseases involving catecholamine neurotransmitters, the LC-NE system has not been thoroughly investigated in relation to AD. From the prodromal stage of the disease, the central noradrenergic system has been demonstrated to undergo substantial changes. Noradrenergic LC cellular and molecular degeneration is a prominent feature of prodromal disease that contributes to cognitive dysfunction, thus supporting a rational basis for targeting LC neuroprotection as a disease-

modifying strategy [63]. In human *post-mortem* tissues from subjects who died with a clinical diagnosis of no cognitive impairment (NCI), amnesic mild cognitive impairment (aMCI) or mild/moderate AD, stereologic estimates of total LC neurons revealed a 30% loss during the transition from NCI to aMCI, with an additional 25% loss of LC neurons in mild/moderate AD [64]. The observed reduction in the number of noradrenergic LC neurons has been significantly associated with worsening *ante-mortem* global cognitive functions as well as poorer performance on neuropsychological tests of episodic memory, semantic memory, working memory, perceptual speed and visuospatial ability [63]. To examine the cellular and molecular pathogenic processes underlying LC neurodegeneration, single population microarray analysis has been performed, revealing significant reductions in select functional classes of mRNAs regulating mitochondrial respiration, redox homeostasis and structural plasticity in neurons from both aMCI and AD subjects compared to NCI. Specific gene expression levels within these functional classes have also been associated with global cognitive deterioration and neuropathological burden [63]. Noradrenergic receptors have been demonstrated to be mainly involved in the regulation of A $\beta$  production. Although extensive research has demonstrated that various G protein-coupled receptors (GPCRs) may influence APP cleavage by promoting or inhibiting  $\alpha$ -,  $\beta$ -,  $\gamma$ -secretase activity (see review [65]), it has been shown that  $\beta$ 2 and  $\alpha$ 2 adrenergic receptor (ARs) subtypes in the terminal regions of the LC directly affect synaptic transmission and APP processing machinery residing at the synapse, independently of an upsurge in cAMP levels.

The stimulation of  $\beta$ 2ARs has been found to promote A $\beta$  production at noradrenergic synapses. Thathiah *et al.* suggest that  $\beta$ 2ARs modulate A $\beta$  production via its association with  $\beta$ -arrestin2, which physically interacts with the Aph-1a subunit of the  $\gamma$ -secretase complex, leading to an increase in the catalytic activity of  $\gamma$ -secretase complex [66]. It has been demonstrated, for instance, that  $\beta$ -arrestins are expressed to a greater degree in the brain of AD individuals than in aged-matched controls. Conversely, its production has been found to decrease both in the HEK293-APP695 cell line, where Arrb2 (which encodes  $\beta$ -arrestin2) has been silenced, and in 3-month-old APP/PS1 Arrb2<sup>-/-</sup> mice A $\beta$  1-40 and A $\beta$  1-42 [66]. Ni *et al.* proposed another potential mechanism through which  $\beta$ 2AR might associate with  $\gamma$ -secretase, namely, via direct binding to PS1 at the plasma membrane [67]. Indeed, following  $\beta$ 2AR stimulation, clathrin mediated endocytosis of the  $\beta$ 2AR, and the bound to PS1 has been demonstrated. PS1 traffics from the early endosomes to late endosomes and then to lysosomes (LEL), which provide an optimal environment for  $\gamma$ -secretase activity, enhancing its activity and A $\beta$  production [67]. In APP<sub>swe</sub>/PS1DE9 double-transgenic mice, chronic treatment with the  $\beta$ 2AR antagonist ICI 118,551 has been demonstrated to reduce amyloid plaque burden [67].

More recently,  $\alpha 2$ ARs autoreceptors, coupled with Gi/cAMP systems and regulating NE synthesis and release [68], have been shown to promote amyloidogenic APP processing by blocking the interaction between APP and SorLa, a retromer protein that retains APP in the Golgi compartment under normal physiological conditions [69]. This favours APP transport to endosomal compartments, where it may be proteolytically cleaved. Through the activation of  $\beta 2$ AR on microglia cells, NE has also been found to upregulate the insulin-degrading enzyme (IDE), which, acting also on A $\beta$ , supports the role of NE in modulating A $\beta$  levels at the synapse [70]. Since  $\beta 2$  and  $\alpha 2$ ARs are involved in the modulation of A $\beta$  production and clearance, it might be assumed that an aberrant activation of the LC-NE system during prodromal or early stages of AD before degeneration of LC neurons may contribute to increase A $\beta$  production in LC terminal regions through the stimulation of adrenergic receptors [62]. An open question is whether the aberrant activation of LC and subsequent A $\beta$  increase in projection areas of LC trigger the global dysfunction of LC circuitry.

To further investigate the potential interplay between NE and A $\beta$ , other studies have evaluated the effects of acute soluble A $\beta$  injection on noradrenergic neurotransmission (Table 2). In a rat model, a single i.c.v. injection of A $\beta$  1-42 solution (4  $\mu$ M) has been found to induce a significant increase of NE concentrations in the prefrontal cortex, nucleus accumbens and hippocampus, 2 h after administration [71]. The mechanism through which A $\beta$  modulates NE concentrations in these areas has not been fully understood. Morgese *et al.* hypothesized that noradrenergic system activation might be mediated by NO release after NOS induction. The increase in NE concentrations has been associated with higher iNOS mRNA levels and increased NOx concentrations. Furthermore, pharmacological inhibition of the nitrenergic system, 30 min before A $\beta$  injection, has been found to prevent the increase in NE concentrations [71], suggesting that the effects of A $\beta$  on the noradrenergic system could be associated to NO-related actions.

Table 2  
Beta-amyloid induced dysfunctions at the level of synapses of different neurotransmitter.

Molecular species of A $\beta$	Aggregation status and concentration/time of exposure	Observed effect of beta-amyloid on neurotransmitters	Experimental models/ brain areas	Reference
Noradrenergic system Freshly prepared A $\beta$ <sub>1-42</sub>	4 $\mu$ M	- A single i.c.v. injection of A $\beta$ <sub>1-42</sub> solution (4 $\mu$ M) induced a significant increase of NE concentrations in the prefrontal cortex, nucleus accumbens and hippocampus, 2 h after the administration.	Single i.c.v. injection of A $\beta$ <sub>1-42</sub> in rats/prefrontal cortex, nucleus accumbens and hippocampus	[71]
Dopaminergic system Soluble A $\beta$ <sub>1-42</sub>	4 $\mu$ M	- In the prefrontal cortex a single i.c.v. injection of soluble A $\beta$ <sub>1-42</sub> (4 $\mu$ M) induced a marked reduction in extracellular concentrations of basal DA, when measured 2 h and 2 days after peptide administration. - The increase in DA release stimulated by local 100 mM K perfusion was abolished in A $\beta$ <sub>1-42</sub> -injected rats.	Single i.c.v. injection of A $\beta$ <sub>1-42</sub> in rats/prefrontal cortex	[83]
Serotonergic system Soluble A $\beta$ <sub>1-42</sub>	4 $\mu$ M	- Soluble A $\beta$ <sub>1-42</sub> peptide (4 $\mu$ M) has been described to selectively reduce 5-HT content and BDNF expression of either its mRNA or protein in the rat prefrontal cortex.	Injection of A $\beta$ <sub>1-42</sub> in rats/prefrontal cortex	[158]

## 2.2.4.2. Dopamine

The dopaminergic system has been involved in the occurrence of cognitive decline, often being predictive of rapidly progressive forms of AD [72]. The integrative properties of the dopaminergic system are probably associated with direct contribution to cognitive functions at the cortical level, namely in working memory and executive functions. These highly vulnerable functions undergo several changes during the physiological aging process [73] and are severely affected in AD [74]. During aging, in the human caudate putamen, hippocampus and frontal cortex, a reduction has been observed in DA release from its terminals, in D2-subtype receptors and DA transporters, as well as in tyrosine hydroxylase enzyme expression [75]. One of the main correlates of the impairment in DA transmission observed during normal aging is the occurrence of apathy [76], which has been suggested to be a negative prognostic sign in both elderly and AD subjects.

Dopaminergic signals are required for encoding hippocampal memory. In particular, the ventral tegmental area (VTA) and the LC have been described as the primary sources of dopamine acting on dopaminergic receptors in the hippocampus [77]. Nobili *et al.* investigated alterations of the midbrain dopaminergic system in a Tg2576 mouse model of AD.

They found that an apoptotic process occurred only in the VTA, leading to a progressive loss of the dopaminergic neuronal population, while no A $\beta$ -plaque deposition, hyperphosphorylated tau tangles or any signs of neuronal loss in cortical and hippocampal regions was recorded [78]. In the same model, substantia nigra pars compacta dopaminergic neurons were not affected.

Selective VTA dopaminergic neurons degeneration has been seen to result in lower DA outflow both in the hippocampus and nucleus accumbens shell, brain areas primarily implicated in memory and reward, respectively. Accordingly, the progression of dopaminergic cell death has been correlated with impairments in CA1 synaptic plasticity, memory performance and food reward processing, thus suggesting that degeneration of VTA dopaminergic neurons at pre-plaque stages strongly contributes to memory deficits and dysfunction of reward processing observed in Tg2576 mice [78]. To translate these observations into humans, De Marco and Venneri tested the hypothesis that the volume of the VTA nucleus in humans might be associated with cognitive features of AD, finding that VTA size yields a strong association with hippocampal size and memory performance, particularly in healthy adults [79]. In addition, functional connectivity between the VTA and hippocampus has been reported to be significantly associated with both hippocampal size and memory competence, thus demonstrating that diminished dopaminergic VTA activity may be crucial in the earliest pathological features of AD. Moreover, an interplay

between cholinergic and dopaminergic systems seems to play a key role in the modulation of memory processes and, apparently, their impairment is implicated in the development of AD. A link between these two systems has been demonstrated both in the striatum and in the limbic region showing that ACh promotes the activation of dopaminergic nerve terminals by regulating dopamine release [80]. Accordingly, the cholinergic agonist carbachol has been shown to elicit a robust dopamine release from the shell of nucleus accumbens in freely moving adult rats [46]. The carbachol effect seems to be mainly mediated by the stimulation of cholinergic muscarinic receptors, since the increase of dopamine release is inhibited by the muscarinic antagonist atropine and not by the nicotinic antagonist mecamylamine [46].

In rat nucleus accumbens, 1  $\mu$ M soluble A $\beta$  infusion through reverse intracerebral dialysis completely counteracted muscarinic receptor-activated DA release in a reversible manner, whereas the overflow of DA elicited by nicotinic receptor activation through epibatidin administration was not altered by A $\beta$  infusion [46]. However, previous results have shown that both nicotinic and muscarinic receptors are equally potent in stimulating dopamine release [81]. In rat nucleus accumbens synaptosomes, the extracellular application of A $\beta$  1-40 (100 nM) inhibits both nicotinic and muscarinic cholinergic modulation of DA release by acting from outside and inside the nerve endings respectively [82]. In particular, the inhibition of nicotinic-evoked [3H]DA overflow has been related to the interaction of A $\beta$  1-40 with nAChRs through a non-competitive antagonism. On the other hand, the inhibition of muscarinic stimulation of [3H]DA release might be achieved, inside the nerve terminal, through a mechanism which possibly requires the binding of A $\beta$  1-40 to a site downstream the mAChR signal. This latter inhibitory effect has been observed at much lower A $\beta$  1-40 concentrations (1 nM) than those effective in interfering with nicotinic modulation outside the nerve endings (100 nM) [82].

In line with these findings, a single i.c.v. injection of freshly prepared A $\beta$  1-42 (4  $\mu$ M) has been found to induce a marked reduction in extracellular concentrations of basal DA in the prefrontal cortex when measured 2 h and 2 days after peptide administration [83] (**Table 2**). Moreover, the increase in DA release stimulated by local 100 mM K perfusion was abolished in A $\beta$  1-42-injected rats [83]. Overall, these results suggest that acute administration of soluble A $\beta$  at concentrations not producing neuronal death inhibits DA release and may serve as a basis for the functional inter-relationship between acute A $\beta$  dysfunction and the vulnerability of dopaminergic transmission in AD.

### 2.2.5. Serotonergic system

Serotonergic neurotransmission is critically involved in regulating learning processes and memory storage during adulthood and aging. Pathological changes of 5-HT metabolism and/or an imbalance in serotonergic signaling have been associated with the etiology of various pathophysiological conditions in the CNS, including AD [84]. The possible interplay between serotonergic system and A $\beta$  has been suggested by preclinical experimental data and clinical studies showing that the increase in extracellular serotonin is crucial to modulate A $\beta$  concentrations, by reducing its production from APP or interfering with plaque formation. Administration of the antidepressant citalopram, a selective serotonin reuptake inhibitor (SSRI), has been demonstrated to reduce both A $\beta$  1-40 and A $\beta$  1-42 levels in the brain interstitial fluid (ISF) of two- to 3-month-old APP/PS1 transgenic mice [85]. At this age, this mouse model of AD does not yet contain insoluble A $\beta$  deposits. The decrease of A $\beta$  levels occurs almost immediately after drug administration with a significant A $\beta$  reduction starting 12–14 hours after treatment.

As yet, this effect has been evaluated in three different SSRI anti-depressants: citalopram (5 mg/kg and 10 mg/kg), fluoxetine (10 mg/kg) and desvenlafaxine (30 mg/kg) [85]. Similarly, direct infusion of serotonin into mouse hippocampus reduced ISF A $\beta$  levels by 35% over an 8-hour period. Moreover, chronic administration of citalopram over a 4-month period has been found to reduce the appearance of new plaques in the 3-month-old PS1APP transgenic mice both in the cortex and hippocampus, compared to control animals [85]. Chronic treatment (5 months) with paroxetine (5 mg/kg), another SSRI, in 5-month-old 3xTg-AD mice reduced AD-related histopathology (A $\beta$  plaques and NFT) in the cortex and the hippocampus and improved memory performance in the Morris spatial navigation task [86]. This suggests that SSRI, administered prophylactically, might retard the disease process and preserve cognitive function.

The beneficial effects of serotonin on A $\beta$  production and concentrations have also been observed in cognitively healthy individuals. In a double-blind study, the acute administration of citalopram in human healthy volunteers, with no prior history of antidepressant treatment, significantly reduced A $\beta$  concentrations in cerebrospinal fluid (CSF) in the citalopram-treated subjects compared to placebo [87]. This suggests a potential preventive approach for AD through reduced A $\beta$  production. Notably, in AD patients the decrease in A $\beta$  1-42 CSF levels may be due, at least in part, to cerebral deposition of A $\beta$  plaques [88]. However, data on the effect at the end of SSRI treatment are still lacking. Moreover, in a group of patients who had undergone SSRI treatment (mean exposure = 34.5 months) to treat a depressive condition in the five years preceding their enrollment in a positron emission tomography (PET) study with the Pittsburgh Compound B to quantify amyloid binding, lower mean cortical binding potential was observed in comparison with



participants who were not exposed to SSRI [85]. Interestingly, the maximal effective dose of citalopram in lowering A $\beta$  brain concentrations and burden in mice (10 mg/kg) is approximately comparable to a dose (50 mg/day) administered to humans as an antidepressant [87]. Yet, a significant difference was found in the timing of the response to SSRI treatment for depression compared to the effect on A $\beta$  concentration.

SSRI treatment of depression generally takes several weeks before amelioration of symptoms occurs, whereas the reduction in CSF A $\beta$  is a short-term effect requiring just a few hours, thus suggesting that the mechanisms by which SSRIs mediate these two effects are different. These observations indicate that the modulation of serotonergic neurotransmission may affect A $\beta$  concentration, probably by decreasing its production without affecting A $\beta$  clearance. This hypothesis has been investigated by Sheline *et al.* using the incorporation of <sup>13</sup>C6-Leucine labeled A $\beta$  in healthy subjects treated with citalopram as a tracer of newly produced A $\beta$ . The tracer/tracee ratio (<sup>13</sup>C6-Leucine normalized labeled A $\beta$ /unlabeled A $\beta$ ) (ITTR) over 37 h of CSF sampling has been found to overlap in the drug-treated and placebo group, thus suggesting that in both groups the fractional turnover of A $\beta$  was comparable [87] and highlighting the effect on A $\beta$  production. To better understand the mechanism underlying this modulation, several studies have evaluated the involvement of serotonin receptor (5-HTRs) subtypes and their signaling pathways. Among the 15 serotonin receptors expressed in the brain, 5-HT<sub>2A</sub>R, 5-HT<sub>2C</sub>R, 5-HT<sub>4</sub>R, 5-HT<sub>6</sub>R and 5-HT<sub>7</sub>R have been shown to influence APP processing. Fisher *et al.* demonstrated that in APP/PS1 mice a specific group of 5-HTRs coupled to Gs proteins (5-HT<sub>4</sub>R, 5-HT<sub>6</sub>R and 5-HT<sub>7</sub>R) is able to suppress A $\beta$  production. Likewise, serotonin or SSRI via microdialysis, 5-HT<sub>4</sub>R, 5-HT<sub>6</sub>R and 5-HT<sub>7</sub>R agonists significantly reduce ISF A $\beta$  [89]. This effect has been supposed to be mediated by the enhancement of APP non-amyloidogenic processing through the increase of  $\alpha$ -secretase enzymatic activity [90]. In particular, the activation of 5-HT<sub>4</sub>R, 5-HT<sub>6</sub>R and 5-HT<sub>7</sub>R stimulates Gs proteins, which induce adenylate cyclase (AC) to increase cAMP levels, thus leading to PKA activation. Once activated, PKA through the induction of ERK signaling increases the ADAM17 cleavage activity by phosphorylation, thus stimulating the release of sAPP $\alpha$ , whose neurotrophic and neuroprotective actions are widely recognized [91]. Interestingly, ADAM10 contains a similar ERK consensus site, thus suggesting that also this member of the ADAM family may be an ERK substrate [92]. In line with these data, mutations on the putative ERK phosphorylation site block the increase of  $\alpha$ -secretase enzymatic activity [92], as well as the direct inhibition of MEK by a selective inhibitor (PD98059) which decreases sAPP $\alpha$  release *in vitro* [93].

Besides serotonin, a wide range of extracellular signals can stimulate receptors involved in the activation of ERK-dependent pathways. In particular, the possible involvement of TrkB receptors in modulating ISF A $\beta$  levels has been tested *in vivo* [85]. Treatment with brain-derived neurotrophic factor (BDNF) has not been found to modify ISF A $\beta$  levels in mouse hippocampus [85]. However, several studies have investigated the potential interplay between A $\beta$ , 5-HT and BDNF. Preclinical experimental data have shown that A $\beta$  in its soluble form induces detrimental effects on 5-HT transmission and BDNF content, even before plaque formation and neurodegeneration [94]. Indeed, i.c.v. administration of soluble A $\beta$  1-42 peptides (4  $\mu$ M) has been found to produce functional and biochemical deficits able to induce a depressive-like phenotype in rats [95].

The administration of acute fluoxetine has been demonstrated to restore 5-HT and BDNF levels in soluble A $\beta$ -treated rats, thus significantly improving behavioral performance in forced swimming tests (FST) and reverting depressive soluble A $\beta$ -induced phenotype profiles [95]. This observation is also supported by previous evidence showing a specific fluoxetine-associated neuroprotective effect [96,97]. A prevailing hypothesis suggests that the increase in extracellular 5-HT levels, as would occur upon administration of SSRIs, might increase BDNF levels through 5-HT<sub>4</sub>, 5-HT<sub>6</sub>, 5-HT<sub>7</sub> receptor subtypes, which are positively coupled to AC and PKA [98]. Also, an increase in CREB phosphorylation at ser-133 positively regulates the transcription of BDNF [99]. In particular, by activating the PI3K/AKT pathway, low concentrations of A $\beta$  monomers (100 nM) have been found to induce the activation of CREB and the transcription of the BDNF target gene in differentiated neuroblastoma SH-SY5Y cells and in primary rat cortical neurons [99].

Among the different serotonin receptors, data from literature suggest that targeting 5-HT<sub>6</sub>R might represent a promising strategy for the symptomatic treatment of AD. In particular, 5-HT<sub>6</sub>R antagonists have represented a substantial segment of the AD drug development pipeline, with several agents explored with regard to their cognitive enhancing properties and mechanisms [100]. Even if the activation of 5-HT<sub>6</sub>R has been found to direct A $\beta$  metabolism towards non-amyloidogenic processing, thus reducing ISF A $\beta$ , the blockade of 5-HT<sub>6</sub> receptors has been reported to improve cognition, learning and memory in animal models in a wide variety of learning and memory paradigms [101], with a modest side-effect profile. Such pro-cognitive actions may largely rely on enhancements of cholinergic, glutamatergic, noradrenergic and dopaminergic neurotransmission, at least partly modulated by 5-HT<sub>6</sub> receptors [102,103]. Among the developed 5HT<sub>6</sub>R antagonists, idalo-pirdine (LU-AE-58054) exhibited a significant benefit on the Alzheimer's Disease Assessment Scale–Cognitive Subscale (ADAS-Cog) in Phase II [104]. However, in 3 randomized double-blind, placebo-controlled trials, conducted in 2525 patients with mild

to moderate AD, the adjunctive use of idalopirdine with cholinesterase inhibitors did not improve cognitive performance or mitigate cognitive decline as measured by the ADAS-Cog total score, over 6 months of treatment [105]. The failure of idalopirdine to meet the expected outcomes suggests a lack of additive efficacy of this combined therapy in the treatment of AD.

### 2.2.6. Peptidergic system

Neuropeptides are a class of molecules involved in neuron-to-neuron communication. They are found throughout the entire nervous system and act as neurotransmitters, neuromodulators or neurohormones (see review [106]). Inside the nerve cells, neuropeptides are selectively stored within large granular vesicles (LGVs) and commonly coexist in neurons with low-molecular-weight neurotransmitters such as acetylcholine, amino acids and catecholamines. Unlike classical neurotransmitters, neuropeptides have a higher receptor binding affinity and selectivity [106], eliciting their biological effects even when released at lower amounts. The involvement of neuropeptides in brain disorders such as AD was extensively investigated in the nineties, and several studies have currently resumed investigating their role in neurodegeneration (for a review see [107]). This review provides a brief overview about the involvement of some neuropeptides in APP metabolism through their interaction with key enzymes involved in A $\beta$  production and clearance.

Substance P (SP) has been reported to facilitate cognitive functions when directly injected into rat brain regions such as the globus pallidus, central nucleus of amygdala and neostriatum [108] and to play a crucial role not only in memory formation and reinforcement, but also in preventing memory decline during brain aging. SP is negatively modulated in neurodegenerative disorders such as AD [109], even if no direct evidence for a causative role of SP dysregulation in AD has been demonstrated.

The role of SP as a modulator of A $\beta$  generation has been investigated, and it has been found that SP stimulates APP non-amyloidogenic processing without modifying the steady-state level of APP [110]. Through the binding with NK1 receptors, SP has been demonstrated to reduce A $\beta$  levels by promoting  $\alpha$ -secretase-mediated APP cleavage. SP has been seen to specifically increase ADAM9 mRNA and its corresponding protein levels, and to further enhance the amount of the mature form of ADAM10, without modifying its constitutive form [110], thus supporting the previously proposed hypothesis [111] of an upstream activity of ADAM9 on ADAM10 maturation.

A prominent decrease in somatostatin (SST) levels represents another pathological feature of AD. SST has been demonstrated to regulate A $\beta$  metabolism, modulating its proteolytic degradation catalyzed by neprilysin, the major A $\beta$  degrading enzyme regulating the steady-state levels of A $\beta$  1-40 and A $\beta$  1-42. In particular, SST has been shown to significantly increase neprilysin activity in primary murine cortical neuronal cultures, leading to a selective reduction in A $\beta$  1-42 levels in culture media [112]. Moreover, in the hippocampus of SST knockout mice, neprilysin activity has been found to be altered and a corresponding significant increase in A $\beta$  1-42 levels has been observed [112]. Corticotropin releasing hormone (CRH), another neuropeptide with a central role in stress response through its influence on the hypothalamic-pituitary-adrenal axis, has been found to be reduced in CSF, as well as in the frontal and temporal cortex and caudate nucleus of AD patients. Lezoualc'h *et al.* demonstrated that CRH promotes the non-amyloidogenic pathway of APP and subsequently increases the secretion of sAPP $\alpha$  in rat cerebellar neurons, in the human neuroblastoma IMR32 cell line and in mouse hippocampal HT22 cells [113]. CRH-stimulated sAPP $\alpha$ -release is blocked by the nonselective CRH receptor antagonist (CRH9-41) and by the selective CRH-R1 antagonist antalarmin, suggesting that the increase in sAPP $\alpha$  release is mediated by the activation of type 1 CRH receptors. However, the specific mechanism through which CRH increases sAPP $\alpha$  secretion has to be further elucidated.

Significant alterations in opioid peptides in AD postmortem brains have been described. CSF  $\beta$ -endorphin levels have been found to be significantly decreased in AD patients compared to controls [114]. In contrast, increased levels of enkephalins - another class of endogenous opioid peptides modulating functions such as learning, memory, synaptic plasticity and emotional behaviors - have been found in the dentate gyrus of the AD brain compared to controls. Accordingly, in hAPP mice, increased levels of met-enkephalin as well as pre-proenkephalin mRNA levels have been found in neuronal projections from the entorhinal cortex and dentate gyrus, brain regions involved in memory processes and affected in the early stages of AD [115]. The increase of enkephalin levels, secondary to A $\beta$  infusion, have been correlated with A $\beta$ -induced behavioral alterations and memory deficits observed in hAPP mice [115].

Moreover, increased levels of dynorphin A, but no differences in dynorphin B and nociception, have been found in AD postmortem samples (Brodmann area VII) [116]. Opioid receptors have been found to act directly on A $\beta$  production both *in vivo* and *in vitro*. Teng *et al.* discovered that the  $\delta$ -opioid receptor (DOR), a GPCR, promotes the amyloidogenic processing of APP. DOR has been shown to form a complex with BACE1 and  $\gamma$ -secretase, promoting APP amyloidogenic processing and A $\beta$  production [117]. The blockage of DOR retards BACE1 and  $\gamma$ -secretase endocytosis and subsequently A $\beta$

production. Consistently, either knockdown or antagonizing DOR have been seen to reduce A $\beta$  production and to ameliorate A $\beta$  pathology by improving cognitive A $\beta$ -dependent deficits in spatial reference memory in APPSWE/PS1 transgenic mice [117].

### 3. Putative beta-amyloid molecular mechanisms impinging on synaptic activity

Extensive data from the literature demonstrate that synaptic failure precedes cognitive decline in AD [118,119]. However, cellular and molecular events underlying synaptic dysfunction have yet to be fully characterized and understood. This review provides an insight into the different mechanisms through which A $\beta$  affects synaptic activity, focusing on A $\beta$  interaction with key synaptic proteins regulating the neurotransmitter release machinery. Neurotransmitter release is dependent on a tightly coordinated membrane fusion machinery (see review [120]). Exocytosis of synaptic vesicles is mediated by a conserved set of membrane proteins that are commonly known as SNAREs (soluble N-ethylmaleimide-sensitive factor attachment protein [SNAP] receptors) [121]. Several studies have shown that, in neurodegenerative diseases such as AD, membrane fusion machinery is strongly altered [122,123] and the formation of the SNARE complex is substantially reduced in the postmortem brains of AD patients [124–126]. Furthermore, the deletion of the Munc18-1 gene in mice, codifying for the Munc-18 SNARE protein and resulting in a genetic ablation of neurotransmitter release, induces pathological similarities to AD, such as altered Tau phosphorylation, neurofibrillary tangles and accumulation of insoluble protein plaques [127]. A $\beta$  has been found to affect SNARE-mediated exocytosis by directly interacting with different synaptic proteins at presynaptic terminals (**Table 3**).

**Table 3**  
Direct interplay between beta-amyloid and SNARE proteins.

Molecular species of A $\beta$	Aggregation status and concentration/ time of exposure	Observed effect on SNARE proteins	<i>In vitro</i> and <i>in vivo</i> model	Reference
Syntaxin 1a A $\beta$ <sub>1-40</sub> and A $\beta$ <sub>1-42</sub>	Both monomers and oligomers (10 $\mu$ M)	- Oligomeric form of A $\beta$ (10 $\mu$ M) has been found to exert an inhibitory effect on SNARE-mediated exocytosis by binding to the SNARE motif region (SynH3) of Syntaxin 1a, thus specifically inhibiting the fusion step between docking and lipid mixing. - A $\beta$ monomers failed to exhibit any inhibitory effects on SNARE complex formation or membrane fusion, despite their proved capability to bind to SynH3 of Syntaxin 1a.	<i>In vitro</i> single-vesicle content-mixing assay	[128]
Synaptophysin/VAMP complex A $\beta$ <sub>1-42</sub>	Monomers (50 nM/20 min)	- A $\beta$ <sub>42</sub> has been demonstrated to directly compete with VAMP2 for binding Synaptophysin at synaptic contacts, thus preventing the formation of Synaptophysin/VAMP complex and, subsequently, inducing the formation of the fusion pore complex followed by neurotransmitter release. - Electrophysiology recordings in brain slices confirmed that A $\beta$ <sub>42</sub> affects baseline transmission, by preventing the formation of Synaptophysin/VAMP complex. Indeed, in hippocampal slices, the enhancement of single-shock REPSPs by A $\beta$ <sub>42</sub> at synapses further suggest an increased availability of releasable synaptic vesicles.	Primary cultures of CA3-CA1 rat hippocampal neurons	[131]

Recently, Yang *et al.* demonstrated *in vitro* that both A $\beta$  monomers and oligomers are capable of specifically binding to the SNARE motif region (SynH3) of syntaxin 1a [128], which forms a four-helix bundle necessary for membrane fusion [129,130]. However, after binding to the SNARE motif of syntaxin 1a, only the oligomeric form of A $\beta$  (10  $\mu$ M) has been found to exert an inhibitory effect on SNARE-mediated exocytosis, specifically

inhibiting the fusion step between docking and lipid mixing [128]. Otherwise, A $\beta$  monomers failed to exhibit any inhibitory effects on SNARE complex formation or membrane fusion, despite their proven capability to bind to syntaxin 1a.

Another direct interaction between A $\beta$  and synaptic vesicle-associated proteins has been reported by Russel *et al.* [131] In rat hippocampal neurons, the acute application of low concentrations (50 nM) of A $\beta$  1-42 has been followed by its internalization and localization to presynaptic terminals. In these sites, the peptide interacted with synaptophysin, a synaptic vesicle membrane protein binding synaptobrevin/VAMP2 (vesicle-associated membrane protein) and acting as a control protein thus regulating vesicle fusion [132,133]. A $\beta$  1-42 has been demonstrated to directly compete with VAMP2 for binding synaptophysin at synaptic terminals, thus preventing the formation of synaptophysin/VAMP complex and subsequently inducing the formation of the fusion pore complex followed by neurotransmitter release [131]. Electrophysiology recordings in brain slices confirmed that through this mechanism A $\beta$  1-42 affects baseline transmission. Indeed, in hippocampal slices, the enhancement of single shock fEPSPs by A $\beta$  1-42 at synapses further suggests an increased availability of releasable synaptic vesicles [131].

In addition to the direct interaction of A $\beta$  with synaptic vesicle proteins regulating neurotransmitter release, an indirect regulation of the release machinery by A $\beta$  might be hypothesized. Data from the literature demonstrate that post-translational modifications of SNARE proteins by protein kinases may influence synaptic vesicle exocytosis. Activation of PKA has been observed to increase exocytosis and neurotransmitter release by phosphorylating synaptic proteins such as SNAP-25, CSP $\alpha$ , synapsin, snapin and RIM1 (Rab interacting molecule) [134,135]. Activation of PKC has also been found to enhance exocytosis through phosphorylation of SNARE proteins including SNAP-25, Munc-18 and synaptotagmin [136–138]. In particular, a specific phosphorylation site (Ser187) in the SNARE domain of SNAP-25 has been associated with increased exocytosis of synaptic vesicles [139]. Katayama *et al.* demonstrated that phosphorylation-deficient knock-in (KI) mice, in which SNAP-25 Ser187 was replaced with Ala, exhibited an accumulation of synaptic vesicles in enlarged presynaptic terminals and a decreased efficacy of basal synaptic transmission at hippocampal CA1 synapses [140].

Recently, Gao *et al.* found that phosphorylation of SNAP-25 by PKA and PKC differentially regulates exocytosis of synaptic vesicles and noradrenaline (NA) release in PC12 cells by regulating the SNARE complex assembly [141]. Phosphorylation of SNAP-25 at Ser187 by PKC has also been found to enhance Ca<sup>2+</sup>-dependent release of dopamine and acetylcholine in PC12 cells [142]. On the contrary, phosphorylation of SNAP-25 at

Thr138 by PKA has been demonstrated to inhibit assembly of the SNARE complex and subsequently NA secretion in PC12 cells [141], although activation of PKA has been widely demonstrated to enhance  $\text{Ca}^{2+}$ -dependent exocytosis. Taken together these data suggest that phosphorylation of SNARE proteins at specific sites is a key regulatory mechanism through which protein kinases control synaptic vesicle exocytosis and consequently neurotransmitter release.

Given that several data from the literature suggest that  $\text{A}\beta$  might affect protein kinase transduction machinery, it could be assumed that, by interacting with protein kinases,  $\text{A}\beta$  might influence phosphorylation of SNARE and accessory proteins as well as the assembly of the SNARE complex, thus modulating neurotransmitter release from presynaptic terminals. This mechanism could explain the previous results, demonstrating that  $\text{A}\beta$  at low concentrations inhibits the *in vivo* dopamine (DA) release in rat nucleus accumbens and counteracts *in vitro* muscarinic receptor-activated DA release from dopaminergic terminals by impairing PKC transduction machinery [46]. This hypothesis is further supported by *in vitro* results showing that the t-ACPD-induced PKC-mediated release of DA, elicited by presynaptic metabotropic glutamate receptors (mGluRs) located on striatal nerve endings, can be completely antagonized by  $\text{A}\beta$  1-40 [143] (**Fig. 2**). This action has also been demonstrated on signaling cascades downstream mGluRs, where 1  $\mu\text{M}$   $\text{A}\beta$  has been reported to impair mGluRs regulation of GABA transmission by inhibiting PKC transduction machinery in prefrontal cortical neurons [144]. Accordingly, Zhong *et al.* showed that  $\text{A}\beta$  impairs muscarinic regulation of GABA transmission in prefrontal cortex, acting on the transduction machinery downstream muscarinic receptors and inhibiting PKC [145].

In addition to PKC and PKA, several other synaptic proteins implicated in synaptic vesicle release and recycling [146,147] are *in vitro* substrates for various kinases, including the  $\text{Ca}^{2+}$ /calmodulin-dependent protein kinase II (CaMKII), the mitogen-activated kinase (MAPK), c-jun N-terminal kinase (JNK) and CDK5. However, their regulatory role in modulating presynaptic transmission and synaptic plasticity has to be fully elucidated. Ninan and Arancio provided direct evidence that presynaptic activation of CaMKII is necessary for inducing synaptic plasticity in cultured hippocampal neurons [148]. In particular, Watanabe *et al.* suggested that, in the CNS, CaMKII/syntaxin-1 A interaction is essential in recruiting complexin, exerting an inhibitory effect on synaptic vesicle fusion, thus inhibiting synaptic vesicle exocytosis and subsequently neurotransmitter release during repetitive stimulation [149].

The phosphorylation state of CaMKII is critical to the functionality of this kinase and decreased levels of active CaMKII at dendritic arborizations may imply impairment of CaMKII synaptic roles. This includes the regulation of synaptic transmission exerted by phosphorylating presynaptic proteins involved in the release machinery. In the hippocampal dentate gyrus, low concentrations of A $\beta$  1-42 (200 nM) have been found to inhibit CaMKII activity, through a mechanism involving calcineurin (CaN), serving as a regulator for the phosphorylation state of CaMKII. These data are supported by the observation that CaMKII signaling is dysregulated in aged brain [150] and that, specifically in AD brain, phosphorylated (active) forms of CaMKII significantly decrease in immunoblots of the frontal cortex and hippocampus [151]. In human *post-mortem* brain samples from AD patients, an enhanced expression of phosphorylated/active JNK and a positive co-localization with A $\beta$  have also been identified [152]. The mechanism linking A $\beta$  and JNK has demonstrated that oligomeric A $\beta$  1-42 activates JNK, that in turn promotes APP non-amyloidogenic processing, increasing A $\beta$  production [153]. Furthermore, A $\beta$  1-42 activates JNK, leading to neurotransmitter release facilitation at presynaptic terminals by affecting the SNARE complex assembly [154]. Overall, the summarized data suggest that A $\beta$  may both impair and stimulate synaptic functions through an action on kinases affecting the SNARE complex activity. The final effect of A $\beta$  depends on its concentration and aggregation state.

#### **4. Tentative behavioral correlates of the A $\beta$ -induced altered neurotransmission**

##### **4.1. Animal models**

The discovery of gene mutations responsible for familial AD made it possible to reproduce some of the specific well-known hallmarks of AD disorder in transgenic animals, including A $\beta$  accumulation. Mice expressing transgenic APP with mutations like Swedish, Indiana, London, Dutch and Flemish, as well as C-terminal fragments of APP have been found to exhibit relevant alterations in several behavioral tasks, similar to behavioral and psychological symptoms (BPSD) observable in AD patients [155]. On the one hand, these observations suggest that changes in behavioral and psychological symptoms of dementia, such as those reported in AD patients, might be partially reproduced in animal models. Other observations highlight that these animal models are not necessarily predictive. To date, there is a lack of in-depth analysis of the alterations in neurotransmission underlying behavioral changes in AD animal models and further investigations are needed to better characterize soluble A $\beta$ -induced behavioral alterations before plaque deposition. Among the different BPSD observed in AD patients, the depressive phenotype is the best characterized in animal models.



Depressive state is considered a prodromal manifestation of the disease before the appearance of cognitive decline symptoms [156], as well as a relevant risk factor for AD [157]. The effect of soluble A $\beta$  1-42 peptides has been investigated on working memory, motor activity, anxiety- and depression-related behaviors in young adult male rats on 5-HT neurotransmission and neurotrophin, including BDNF and NGF content in various brain regions. I.c.v. administration of the soluble A $\beta$  1-42 peptide appears to induce depressive like-behavior (but not anxiogenic-like phenotype), along with reduced cortical serotonin release and decreased levels of neurotrophines, with no impairment of working memory [157,158]. From a behavioral point of view, soluble A $\beta$ -treated rats exhibited lower exploratory activity, thus suggesting that A $\beta$  might induce motivational deficits before the appearance of cognitive impairments. Moreover, soluble A $\beta$  significantly affected rat behavior during FST by increasing the FST-induced immobility time, thus reflecting a state of behavioral despair or hopelessness [158]. Although obtained in different animal models, these results are consistent with studies reporting that mice overexpressing APPSWE/PS1, at an age characterized by high levels of soluble A $\beta$ , showed an increased duration of immobility in FST [159]. These behavioral alterations induced by soluble A $\beta$  1-42 might be sensitive indicators of early phases of AD and possible risk factors for the development of neuropsychiatric symptoms including depression. Although the mechanism by which soluble A $\beta$  peptide may induce depressive-like behavior has to be fully elucidated, data from the literature suggest that the modulation of 5-HT neurotransmission might be involved [160]. A $\beta$ -induced depressive symptoms might further result in dysfunctions of multiple neurotransmitter systems and in the imbalance of their interactions. Deficits in the dopaminergic system in soluble A $\beta$ -treated rats both in the prefrontal cortex [83] and nucleus accumbens [46] and functional interactions between dopaminergic and 5-HT neuronal systems in the rat prefrontal cortex have been observed. As a possible neuromodulator, soluble A $\beta$  on both the 5-HT and dopaminergic system in the prefrontal cortex might profoundly disrupt the functioning of this area, potentially leading to impairment of mood control. Further investigations are needed to better clarify the molecular mechanism underlying the soluble A $\beta$ -induced depressive phenotype as well as soluble A $\beta$ -induced behavioral alterations mimicking BPSD.

#### **4.2. Tentative clinical correlates**

In AD, the decline of cognitive functions is accompanied by a complex array of neuropsychiatric symptoms (NPS), also known as “non-cognitive” symptoms of AD. They consist of prominent depression, apathy, agitation, anxiety/phobias, delusions, irritability and sleep disturbances, originally labeled as BPSD (see review [161]). A growing body of evidence emphasizes the importance of NPS as prodromal markers of cognitive decline

along the neurodegenerative spectrum. The onset of NPS in MCI patients confers a greater risk of conversion to full-blown dementia compared to MCI patients without NPS [162]. Also, in older adults with normal cognition, the onset of NPS including depression, irritability and agitation has been reported to predict a more rapid cognitive decline compared to subjects without NPS [163], thus suggesting that NPS are prodromal indicators of incipient dementia, measurable even before the onset of MCI. Taragano *et al.* proposed the expression Mild Behavioral Impairment (MBI) syndrome, not only as a diagnostic construct aimed to identify patients with or without cognitive symptoms, who are prone to develop dementia, but also as a counterpart of MCI, being a transitional state between normal aging and dementia [164].

Brain imaging, electrophysiological, neurochemical and neuropathological approaches have been used as tools to improve the understanding of NPS neurobiology, showing that atrophy or dysfunction of NPS-relevant brain regions and their related circuits and networks in AD patients are strictly related to the onset of specific cognitive deficits and NPS.

AD affects several brain regions, including the epicenters of emotions and cognition as well as their extensive and reciprocal neuronal connections, thus contributing to the development of both cognitive and NPS-related manifestations [161]. On the other hand, these behavioural symptoms may likely be associated with disease-related synaptic dysfunction rather than neurodegeneration. The subsequent sections will briefly touch upon mounting evidence related to the most prevalent NPS, including apathy, depression, agitation/aggression and psychosis and their related underlying neuropathological and neurotransmitter alterations in AD patients.

#### **4.2.1. Apathy**

Among the emotional symptoms observed in MCI and AD patients, apathy has been reported to be the most persistent and common NPS [165]. Data on MCI patients and prodromal depressive syndromes suggest that, in prodromal AD, apathy might be linked to dysfunctional affective-emotional processing [166]. This abnormality takes place in the ventromedial prefrontal cortex and in its connections with the amygdala and nucleus accumbens. Consistently, neuropathological progression in AD targets ventromedial parts of the frontal cortex from the early stages of the disease [167]. Evidence from postmortem studies further supports the hypothesis that dopaminergic circuits, linking the basal ganglia with the anterior cingulate and frontal cortices, might be dysfunctional in patients with AD and may account for apathy [72,168].

A reduction in dopamine levels has been observed in the mesolimbic and mesocortical pathways [169], as well as alterations in DA receptor density and localization in apathy-related brain regions in AD patients who experience apathy [170]. In addition, a decrease in blood perfusion to the anterior cingulate [171] and orbitofrontal cortex-areas [172], both innervated by dopaminergic neurons, has been observed. Neuroimaging measures, including magnetic resonance imaging (MRI), single-photon emission CT (SPECT) and F-fluorodeoxyglucose (FDG) positron emission tomography (PET), have revealed correlations between apathy and specific neural networks. An MRI study demonstrated a negative correlation between apathy and grey matter volumes in the anterior cingulate and bilateral frontal cortex [173], whereas FDG-PET investigations reported a correlation between apathy and the left or bitofrontal region [174] and bilateral anterior cingulate region [175].

#### 4.2.2. Depression

Depression is one of the most frequent co-morbid psychiatric disorders in AD, with a prevalence of around 20–50% [176]. The neurobiological and clinical continuum between depression and AD has been suggested by several studies demonstrating that depression might be a relevant risk factor for the development of AD and that the onset of depressive symptoms significantly facilitates the conversion of MCI into AD. Epidemiological evidence and longitudinal studies in MCI and late-life depression (LLD) patients highlighted that depressive disorders represent prodromal manifestations of AD [177]. In addition, studies in earlier-life major depressed (MDD) patients suggested that depression occurring at an early age seems to be an independent risk factor for subsequent AD [178]. However, the neurobiological mechanism underlying this association remains unclear. Depression has been found to share complex pathophysiological routes with dementia. Reduced cortical noradrenergic levels in demented patients with major depression have been observed [179], and a loss of noradrenergic neurons in the LC has been considered an important organic substrate of depression in AD [180]. Furthermore, impaired noradrenergic neurotransmission in the cerebellar cortex might also account for depression in AD [179].

As assessed by PET imaging, a positive correlation between depressive symptoms and cortical amyloid burden has also been observed in the precuneus/posterior cingulate cortex, in cognitively normal subjects with no lifetime history of major depression [181]. This evidence suggests that depressive symptoms might be correlated to A $\beta$  deposition and A $\beta$ -induced synaptic dysfunction during the prodromal phase of the disease.

#### 4.2.3. Agitation and aggression

Agitation and aggression in people with AD range from 48% to 80% [182]. They have been associated with structural and functional abnormalities in frontal and limbic regions involved in emotional regulation and salience, such as the frontal, anterior cingulate and posterior cingulate cortices, amygdala and hippocampus [183]. Neurochemical studies suggest a link between serotonergic alterations and aggression: reduced levels of 5-HT and its metabolites have been measured in the frontal lobes of aggressive AD patients [184] and an inverse correlation has been found between the levels of the main metabolite of 5-HT, hippocampal 5-hydroxyindoleacetic acid (5-HIAA) and agitation scores [179]. Dopaminergic alterations might also lie at the basis of aggression/agitation in AD, since an increased cerebellar dopaminergic turnover has been linked to physically agitated behavior [179]. The observation that dopaminergic turnover correlated with frontal lobe symptoms [179] is potentially indicative of an unbalanced cerebello-thalamic-cortical circuit, since the cerebellum might affect aggressive/agitated behavior in AD by controlling prefrontal circuits [185]. Also, cholinergic modifications are involved in the neurobiology of this specific NPS manifestation, since the treatment with cholinesterase inhibitors significantly improves aggression and agitation in AD patients [167,186].

#### 4.2.4. Psychotic symptoms

Psychosis is common in AD and its major symptoms are delusions, hallucinations and misidentifications. Hallucinations occur less frequently than delusions and are predominantly visual, less commonly auditory and rarely tactile or olfactory [187]. Visual hallucinations in AD patients have been associated with lesions in and atrophy of occipital cortex (visual cortex and association areas), compared to AD patients without visual hallucinations [188]. Delusions have been linked to atrophy of frontal, temporal and limbic regions, including the hippocampus [189]. Derangements in different cerebral circuits have been related to psychosis. A significant reduction in 5-HT levels in the pro-subiculum [190], along with a disruption of the noradrenergic locus coeruleus-thalamus system, have been observed. The latter has been argued to potentially lead to psychotic-like behavior, an assumption that has been partially substantiated by the observation that thalamic MHPG (3-methoxy-4-hydroxyphenylglycol, a major noradrenergic metabolite) levels are inversely correlated with hallucinations in AD [179]. Cholinergic alterations have been linked to psychosis, since treatment with cholinesterase inhibitors, besides the well-established benefits on cognition and global function, reduces psychotic symptoms [186]. Finally, decreased dopaminergic neurotransmission and increased dopaminergic catabolism,

specifically in the amygdala, have recently been suggested to function as a monoaminergic substrate of psychosis in AD.

## 5. Concluding remarks

The reviewed data suggest that A $\beta$  is able to interact with different neurotransmitter release mechanisms in conditions not resulting in neurotoxicity, exerting general effects on neurotransmission. The modulation of neurotransmitter release from presynaptic terminals by A $\beta$  is mediated by its interaction with specific protein kinases, thus influencing the phosphorylation of SNARE and accessory proteins and subsequently the assembly of the SNARE complex. These effects exerted by physiological concentrations of A $\beta$  over time and their derangement in the disease may disturb neurotransmitter activity, thus contributing to the neuropsychiatric manifestations associated with the disease, such as depression, apathy and psychotic symptoms. In this conceptual frame, the tentative behavioral and clinical correlates strongly suggest a relevant interaction between A $\beta$  metabolism alterations, synaptic activity (including but not limited to synaptic loss) and neuropsychiatric manifestations. These mutual interactions may be useful to identify or recognize alterations in neurotransmitter activity as predictive signs for the development of AD and as a target for pharmacological intervention. Moreover, these observations may explain the limitations of current interventions and the failure so far of amyloid targeted therapies, possibly enabling the preservation of A $\beta$  physiological activity while counteracting its deposition.

## REFERENCES

- [1] J. Hardy, The discovery of Alzheimer-causing mutations in the APP gene and the formulation of the “amyloid cascade hypothesis,” *FEBS J.* (2017). doi:10.1111/febs.14004.
- [2] D. Puzzo, L. Privitera, E. Leznik, M. Fa, A. Staniszewski, A. Palmeri, O. Arancio, Picomolar Amyloid- $\beta$  Positively Modulates Synaptic Plasticity and Memory in Hippocampus, *J. Neurosci.* (2008). doi:10.1523/JNEUROSCI.2692-08.2008.
- [3] D. Puzzo, O. Arancio, Amyloid- $\beta$  Peptide: Dr. Jekyll or Mr. Hyde?, *J. Alzheimers. Dis.* (2013). doi:10.3233/JAD-2012-129033.
- [4] M.Y. Suvorina, O.M. Selivanova, E.I. Grigorashvili, A.D. Nikulin, V. V. Marchenkov, A.K. Surin, O. V. Galzitskaya, Studies of Polymorphism of Amyloid- $\beta$ 42 Peptide from Different Suppliers, *J. Alzheimer's Dis.* (2015). doi:10.3233/JAD-150147.
- [5] B. Yankner, L. Duffy, D. Kirschner, Neurotrophic and neurotoxic effects of amyloid beta protein: reversal by tachykinin neuropeptides, *Science.* (1990). doi:10.1126/science.2218531.

- [6] D. Tampellini, Synaptic activity and Alzheimer's disease: A critical update, *Front. Neurosci.* (2015). doi:10.3389/fnins.2015.00423.
- [7] F. Kamenetz, T. Tomita, H. Hsieh, G. Seabrook, D. Borchelt, T. Iwatsubo, S. Sisodia, R. Malinow, APP Processing and Synaptic Function, *Neuron.* (2003). doi:10.1016/S0896-6273(03)00124-7.
- [8] J.R. Cirrito, K.A. Yamada, M.B. Finn, R.S. Sloviter, K.R. Bales, P.C. May, D.D. Schoepp, S.M. Paul, S. Mennerick, D.M. Holtzman, Synaptic activity regulates interstitial fluid amyloid- $\beta$  levels in vivo, *Neuron.* (2005). doi:10.1016/j.neuron.2005.10.028.
- [9] A.W. Bero, P. Yan, J.H. Roh, J.R. Cirrito, F.R. Stewart, M.E. Raichle, J.M. Lee, D.M. Holtzman, Neuronal activity regulates the regional vulnerability to amyloid- $\beta$  2 deposition, *Nat. Neurosci.* (2011). doi:10.1038/nn.2801.
- [10] R.L. Buckner, Molecular, Structural, and Functional Characterization of Alzheimer's Disease: Evidence for a Relationship between Default Activity, Amyloid, and Memory, *J. Neurosci.* (2005). doi:10.1523/JNEUROSCI.2177-05.2005.
- [11] R.L. Buckner, J. Sepulcre, T. Talukdar, F.M. Krienen, H. Liu, T. Hedden, J.R. Andrews-Hanna, R.A. Sperling, K.A. Johnson, Cortical Hubs Revealed by Intrinsic Functional Connectivity: Mapping, Assessment of Stability, and Relation to Alzheimer's Disease, *J. Neurosci.* (2009). doi:10.1523/JNEUROSCI.5062-08.2009.
- [12] J.D. Buxbaum, G. Thinakaran, V. Koliatsos, J. O'Callahan, H.H. Slunt, D.L. Price, S.S. Sisodia, Alzheimer amyloid protein precursor in the rat hippocampus: transport and processing through the perforant path., *J. Neurosci.* (1998). doi:10.1042/BST0350416.
- [13] O. Lazarov, M. Lee, D.A Peterson, S.S. Sisodia, Evidence that synaptically released beta-amyloid accumulates as extracellular deposits in the hippocampus of transgenic mice. Lazarov, Orly Lee, Michael Peterson, Daniel a Sisodia, Sangram S, *J. Neurosci.* (2002). doi:22/22/9785 [pii].
- [14] B.E. Schroeder, E.H. Koo, To think or not to think: Synaptic activity and A $\beta$  release, *Neuron.* (2005). doi:10.1016/j.neuron.2005.12.005.
- [15] J.R. Cirrito, J.E. Kang, J. Lee, F.R. Stewart, D.K. Verges, L.M. Silverio, G. Bu, S. Mennerick, D.M. Holtzman, Endocytosis Is Required for Synaptic Activity-Dependent Release of Amyloid- $\beta$  In Vivo, *Neuron.* (2008). doi:10.1016/j.neuron.2008.02.003.
- [16] D. Puzzo, L. Privitera, M. Fa', A. Staniszewski, G. Hashimoto, F. Aziz, M. Sakurai, E.M. Ribe, C.M. Troy, M. Mercken, S.S. Jung, A. Palmeri, O. Arancio, Endogenous amyloid- $\beta$  is necessary for hippocampal synaptic plasticity and memory, *Ann. Neurol.* (2011). doi:10.1002/ana.22313.
- [17] G.R. Dawson, G.R. Seabrook, H. Zheng, D.W. Smith, S. Graham, G. O'Dowd, B.J. Bowery, S. Boyce, M.E. Trumbauer, H.Y. Chen, L.H.T. Van Der Ploeg, D.J.S. Sirinathsinghji, Age-related cognitive deficits, impaired long-term potentiation and reduction in synaptic marker density in mice lacking the  $\beta$ -amyloid precursor protein, *Neuroscience.* (1999). doi:10.1016/S0306-4522(98)00410-2.
- [18] J. Lisman, S. Raghavachari, A unified model of the presynaptic and postsynaptic changes during LTP at CA1 synapses., *Sci. STKE.* (2006). doi:10.1126/stke.3562006re11.

- [19] J.J. Dougherty, J. Wu, R.A. Nichols, beta-Amyloid Regulation of Presynaptic Nicotinic Receptors in Rat Hippocampus and Neocortex, *J. Neurosci.* (2003). doi:10.1073/pnas.1323226111.
- [20] F.A. Lazarevic V, Fieńko S, Andres-Alonso M, Anni D, Ivanova D, Montenegro-Venegas C, Gundelfinger ED, Cousin MA, Physiological Concentrations of Amyloid Beta Regulate Recycling of Synaptic Vesicles via Alpha7 Acetylcholine Receptor and CDK5/Calcineurin Signaling, *Front Mol Neurosci.* 10:221 (2017).
- [21] L. Mucke, D.J. Selkoe, Neurotoxicity of amyloid  $\beta$ -protein: Synaptic and network dysfunction, *Cold Spring Harb. Perspect. Med.* (2012). doi:10.1101/cshperspect.a006338.
- [22] M. Townsend, G.M. Shankar, T. Mehta, D.M. Walsh, D.J. Selkoe, Effects of secreted oligomers of amyloid  $\beta$ -protein on hippocampal synaptic plasticity: A potent role for trimers, *J. Physiol.* (2006). doi:10.1113/jphysiol.2005.103754.
- [23] C. Holscher, S. Gengler, V.A. Gault, P. Harriott, H.A. Mallot, Soluble beta-amyloid[25-35] reversibly impairs hippocampal synaptic plasticity and spatial learning, *Eur. J. Pharmacol.* (2007). doi:10.1016/j.ejphar.2007.01.040.
- [24] S. Sabella, M. Quaglia, C. Lanni, M. Racchi, S. Govoni, G. Caccialanza, A. Calligaro, V. Belloti, E. De Lorenzi, Capillary electrophoresis studies on the aggregation process of  $\beta$ -amyloid 1-42 and 1-40 peptides, *Electrophoresis.* (2004). doi:10.1002/elps.200406062.
- [25] P. Davies, A.J.F. Maloney, Selective loss of central cholinergic neurons in alzheimer's disease, *Lancet.* (1976). doi:10.1016/S0140-6736(76)91936-X.
- [26] E.K. Perry, B.E. Tomlinson, G. Blessed, K. Bergmann, P.H. Gibson, R.H. Perry, Correlation of cholinergic abnormalities with senile plaques and mental test scores in senile dementia, *Br Med J.* 2(6150):14 (1978).
- [27] P.T. Francis, A.M. Palmer, N.R. Sims, D.M. Bowen, A.N. Davison, M.M. Esiri, D. Neary, J.S. Snowden, G.K. Wilcock, Neurochemical studies of early-onset Alzheimer's disease. Possible influence on treatment, *N.Engl.J.Med.* (1985). doi:10.1056/NEJM198507043130102.
- [28] M. Racchi, M. Sironi, A. Caprera, G. König, S. Govoni, Short- and long-term effect of acetylcholinesterase inhibition on the expression and metabolism of the amyloid precursor protein, *Mol. Psychiatry.* (2001). doi:10.1038/sj.mp.4000878.
- [29] A. Fisher, Cholinergic modulation of amyloid precursor protein processing with emphasis on M1 muscarinic receptor: Perspectives and challenges in treatment of Alzheimer's disease, *J. Neurochem.* (2012). doi:10.1111/j.1471-4159.2011.07507.x.
- [30] M.K. Sun, D.L. Alkon, Bryostatin-1: Pharmacology and therapeutic potential as a CNS drug, *CNS Drug Rev.* (2006). doi:10.1111/j.1527-3458.2006.00001.x.
- [31] D.L. Alkon, M.K. Sun, T.J. Nelson, PKC signaling deficits: a mechanistic hypothesis for the origins of Alzheimer's disease, *Trends Pharmacol. Sci.* (2007). doi:10.1016/j.tips.2006.12.002.
- [32] A.A. Davis, J.J. Fritz, J. Wess, J.J. Lah, A.I. Levey, Deletion of M1 Muscarinic Acetylcholine Receptors Increases Amyloid Pathology *In Vitro* and *In Vivo*, *J. Neurosci.* (2010). doi:10.1523/JNEUROSCI.6393-09.2010.

- [33] D. Ji, R. Lape, J.A. Dani, Timing and location of nicotinic activity enhances or depresses hippocampal synaptic plasticity, *Neuron*. (2001). doi:10.1016/S0896-6273(01)00332-4.
- [34] R. Gray, A.S. Rajan, K.A. Radcliffe, M. Yakehiro, J.A. Dani, Hippocampal synaptic transmission enhanced by low concentrations of nicotine, *Nature*. (1996). doi:10.1038/383713a0.
- [35] K.A. Radcliffe, J.A. Dani, Nicotinic stimulation produces multiple forms of increased glutamatergic synaptic transmission., *J. Neurosci.* (1998).
- [36] J.R. Genzen, D.S. McGehee, Short- and long-term enhancement of excitatory transmission in the spinal cord dorsal horn by nicotinic acetylcholine receptors, *Proc Natl Acad Sci U S A.* (2003). doi:10.1073/pnas.1131709100\n1131709100 [pii].
- [37] R. Girod, N. Barazangi, D. McGehee, L.W. Role, Facilitation of glutamatergic neurotransmission by presynaptic nicotinic acetylcholine receptors, *Neuropharmacology*. (2000). doi:10.1016/S0028-3908(00)00145-3.
- [38] H. Nie, Z. Li, R.J. Lukas, Y. Shen, L. Song, X. Wang, M. Yin, Construction of SH-EP1- $\alpha$ 4 $\beta$ 2-hAPP695 cell line and effects of nicotinic agonists on  $\beta$ -amyloid in the cells, *Cell. Mol. Neurobiol.* (2008). doi:10.1007/s10571-007-9218-1.
- [39] M. Mousavi, E. Hellström-Lindahl, Nicotinic receptor agonists and antagonists increase sAPP $\alpha$  secretion and decrease A $\beta$  levels *in vitro*, *Neurochem. Int.* (2009). doi:10.1016/j.neuint.2008.12.001.
- [40] S. Jürgensen, S.T. Ferreira, Nicotinic receptors, amyloid- $\beta$ , and synaptic failure in Alzheimer's disease, in: *J. Mol. Neurosci.*, 2010. doi:10.1007/s12031-009-9237-0.
- [41] H.Y. Wang, D.H.S. Lee, C.B. Davis, R.P. Shank, Amyloid peptide A $\beta$ 1-42 binds selectively and with picomolar affinity to  $\alpha$ 7 nicotinic acetylcholine receptors, *J. Neurochem.* (2000). doi:10.1046/j.1471-4159.2000.0751155.x.
- [42] D.H. Small, D. Maksel, M.L. Kerr, J. Ng, X. Hou, C. Chu, H. Mehrani, S. Unabia, M.F. Azari, R. Loiacono, M.I. Aguilar, M. Chebib, The beta-amyloid protein of Alzheimer's disease binds to membrane lipids but does not bind to the alpha7 nicotinic acetylcholine receptor, *J Neurochem.* 101:1527–1 (2007).
- [43] G.M. Khan, M. Tong, M. Jhun, K. Arora, R.A. Nichols, Beta-Amyloid activates presynaptic alpha7 nicotinic acetylcholine receptors reconstituted into a model nerve cell system: Involvement of lipid rafts, *Eur J Neurosci.* 31:788–796 (2010).
- [44] M.H. Sabec, S. Wonnacott, E.C. Warburton, Z.I. Bashir, Nicotinic Acetylcholine Receptors Control Encoding and Retrieval of Associative Recognition Memory through Plasticity in the Medial Prefrontal Cortex, *Cell Rep.* (2018). doi:10.1016/j.celrep.2018.03.016.
- [45] M. Grilli, F. Lagomarsino, S. Zappettini, S. Preda, E. Mura, S. Govoni, M. Marchi, Specific inhibitory effect of amyloid- $\beta$  on presynaptic muscarinic receptor subtypes modulating neurotransmitter release in the rat nucleus accumbens, *Neuroscience.* (2010). doi:10.1016/j.neuroscience.2010.01.058.
- [46] S. Preda, S. Govoni, C. Lanni, M. Racchi, E. Mura, M. Grilli, M. Marchi, Acute  $\beta$ -amyloid administration disrupts the cholinergic control of dopamine release in the nucleus accumbens, *Neuropsychopharmacology.* (2008). doi:10.1038/sj.npp.1301485.



- [47] D. V. Janíčková H, Rudajev V, Zimčík P, Jakubík J, Tanila H, El-Fakahany EE, Uncoupling of M1 muscarinic receptor/G-protein interaction by amyloid  $\beta$ (1-42)., *Neuropharmacology*. 67:272-83. (2013).
- [48] E. Mura, S. Zappettini, S. Preda, F. Biundo, C. Lanni, M. Grilli, A. Cavallero, G. Olivero, A. Salamone, S. Govoni, M. Marchi, Dual effect of beta-amyloid on  $\alpha 7$  and  $\alpha 4\beta 2$  nicotinic receptors controlling the release of glutamate, aspartate and GABA in rat hippocampus, *PLoS One*. (2012). doi:10.1371/journal.pone.0029661.
- [49] S. Zappettini, M. Grilli, G. Olivero, E. Mura, S. Preda, S. Govoni, A. Salamone, M. Marchi, *Frontiers: Beta Amyloid Differently Modulate Nicotinic and Muscarinic Receptor Subtypes which Stimulate in vitro and in vivo the Release of Glycine in the Rat Hippocampus*, *Front. Pharmacol*. (2012). doi:10.3389/fphar.2012.00146.
- [50] P.T. Francis, N.R. Sims, A.W. Procter, D.M. Bowen, Cortical Pyramidal Neurone Loss May Cause Glutamatergic Hypoactivity and Cognitive Impairment in Alzheimer's Disease: Investigative and Therapeutic Perspectives, *J. Neurochem*. (1993). doi:10.1111/j.1471-4159.1993.tb13381.x.
- [51] K.N. Hascup, E.R. Hascup, Soluble Amyloid- $\beta$ 42 Stimulates Glutamate Release through Activation of the  $\alpha 7$  Nicotinic Acetylcholine Receptor, *J. Alzheimer's Dis*. (2016). doi:10.3233/JAD-160041.
- [52] C. Nicholson, Diffusion and related transport mechanisms in brain tissue, *Reports Prog. Phys*. (2001). doi:10.1088/0034-4885/64/7/202.
- [53] D.A. McCormick, GABA as an inhibitory neurotransmitter in human cerebral cortex, *J. Neurophysiol*. (1989). doi:10.1152/jn.1989.62.5.1018.
- [54] S.R. Cobb, E.H. Buhl, K. Halasy, O. Paulsen, P. Somogyi, Synchronization of neuronal activity in hippocampus by individual GABAergic interneurons, *Nature*. (1995). doi:10.1038/378075a0.
- [55] J. Szabadics, A. Lorincz, G. Tamás, Beta and gamma frequency synchronization by dendritic gabaergic synapses and gap junctions in a network of cortical interneurons., *J. Neurosci*. (2001). doi:21/15/5824 [pii].
- [56] E.O. Mann, M.M. Kohl, O. Paulsen, Distinct Roles of GABAA and GABAB Receptors in Balancing and Terminating Persistent Cortical Activity, *J. Neurosci*. (2009). doi:10.1523/JNEUROSCI.6162-08.2009.
- [57] M.A. Busche, A. Konnerth, Impairments of neural circuit function in Alzheimer's disease, *Philos. Trans. R. Soc. B Biol. Sci*. (2016). doi:10.1098/rstb.2015.0429.
- [58] C.Z. Ren SQ, Yao W, Yan JZ, Jin C, Yin JJ, Yuan J, Yu S, Amyloid  $\beta$  causes excitation/inhibition imbalance through dopamine receptor 1-dependent disruption of fast-spiking GABAergic input in anterior cingulate cortex., *Sci Rep*. 8(1):302 (2018). doi: 10.1038/s41598-017-18729-5.
- [59] H. Braak, E. Braak, Neuropathological staging of Alzheimer-related changes, *Acta Neuropathol*. (1991). doi:10.1007/BF00308809.
- [60] D.A. Lewis, T. Hashimoto, D.W. Volk, Cortical inhibitory neurons and schizophrenia, *Nat. Rev. Neurosci*. (2005). doi:10.1038/nrn1648.

- [61] J. Lieberman, M. First, Psychotic Disorders, *N Engl J Med.* 379(3):270 (2018). doi:10.1056/NEJMra1801490.
- [62] J.A. Ross, P. McGonigle, E.J. Van Bockstaele, Locus coeruleus, norepinephrine and A $\beta$  peptides in Alzheimer's disease, *Neurobiol. Stress.* (2015). doi:10.1016/j.ynstr.2015.09.002.
- [63] S.C. Kelly, B. He, S.E. Perez, S.D. Ginsberg, E.J. Mufson, S.E. Counts, Locus coeruleus cellular and molecular pathology during the progression of Alzheimer's disease, *Acta Neuropathol. Commun.* (2017). doi:10.1186/s40478-017-0411-2.
- [64] R.S. Wilson, S. Nag, P.A. Boyle, L.P. Hizel, L. Yu, A.S. Buchman, J.A. Schneider, D.A. Bennett, Neural reserve, neuronal density in the locus ceruleus, and cognitive decline, *Neurology.* (2013). doi:10.1212/WNL.0b013e3182897103.
- [65] A. Thathiah, B. De Strooper, The role of G protein-coupled receptors in the pathology of Alzheimer's disease, *Nat. Rev. Neurosci.* (2011). doi:10.1038/nrn2977.
- [66] A. Thathiah, K. Horré, A. Snellinx, E. Vandeweyer, Y. Huang, M. Ciesielska, G. De Kloe, S. Munck, B. De Strooper,  $\beta$ -Arrestin 2 regulates A $\beta$  generation and  $\gamma$ -secretase activity in Alzheimer's disease, *Nat. Med.* (2013). doi:10.1038/nm.3023.
- [67] Y. Ni, X. Zhao, G. Bao, L. Zou, L. Teng, Z. Wang, M. Song, J. Xiong, Y. Bai, G. Pei, Activation of  $\beta$ 2-adrenergic receptor stimulates  $\gamma$ -secretase activity and accelerates amyloid plaque formation, *Nat. Med.* (2006). doi:10.1038/nm1485.
- [68] C.W. Berridge, B.D. Waterhouse, The locus coeruleus-noradrenergic system: Modulation of behavioral state and state-dependent cognitive processes, *Brain Res. Rev.* (2003). doi:10.1016/S0165-0173(03)00143-7.
- [69] Y. Chen, Y. Peng, P. Che, M. Gannon, Y. Liu, L. Li, G. Bu, T. van Groen, K. Jiao, Q. Wang,  $\alpha$ <sub>2A</sub> adrenergic receptor promotes amyloidogenesis through disrupting APP-SorLA interaction, *Proc. Natl. Acad. Sci.* (2014). doi:10.1073/pnas.1409513111.
- [70] Y. Kong, L. Ruan, L. Qian, X. Liu, Y. Le, Norepinephrine Promotes Microglia to Uptake and Degrade Amyloid Peptide through Upregulation of Mouse Formyl Peptide Receptor 2 and Induction of Insulin-Degrading Enzyme, *J. Neurosci.* (2010). doi:10.1523/JNEUROSCI.2985-10.2010.
- [71] M.G. Morgese, M. Colaianna, E. Mhillaj, M. Zotti, S. Schiavone, P. D'Antonio, A. Harkin, V. Gigliucci, P. Campolongo, V. Trezza, A. De Stradis, P. Tucci, V. Cuomo, L. Trabace, Soluble beta amyloid evokes alteration in brain norepinephrine levels: Role of nitric oxide and interleukin-1, *Front. Neurosci.* (2015). doi:10.3389/fnins.2015.00428.
- [72] A. Martorana, G. Koch, Is dopamine involved in Alzheimer's disease?, *Front. Aging Neurosci.* (2014). doi:10.3389/fnagi.2014.00252.
- [73] A.F.T. Arnsten, B.M. Li, Neurobiology of executive functions: Catecholamine influences on prefrontal cortical functions, *Biol. Psychiatry.* (2005). doi:10.1016/j.biopsych.2004.08.019.
- [74] S. Baudic, G.D. Barba, M.C. Thibaudet, A. Smagghe, P. Remy, L. Traykov, Executive function deficits in early Alzheimer's disease and their relations with episodic memory, *Arch. Clin. Neuropsychol.* (2006). doi:10.1016/j.acn.2005.07.002.

- [75] L. Bäckman, U. Lindenberger, S.C. Li, L. Nyberg, Linking cognitive aging to alterations in dopamine neurotransmitter functioning: Recent data and future avenues, *Neurosci. Biobehav. Rev.* (2010). doi:10.1016/j.neubiorev.2009.12.008.
- [76] P.H. Robert, E. Mulin, P. Malléa, R. David, Apathy diagnosis, assessment, and treatment in Alzheimer's disease, *CNS Neurosci. Ther.* (2010). doi:10.1111/j.1755-5949.2009.00132.x.
- [77] M. D'Amelio, L. Serra, M. Bozzali, Ventral Tegmental Area in Prodromal Alzheimer's Disease: Bridging the Gap between Mice and Humans, *J. Alzheimer's Dis.* (2018). doi:10.3233/JAD-180094.
- [78] A. Nobili, E.C. Latagliata, M.T. Viscomi, V. Cavallucci, D. Cutuli, G. Giacobuzzo, P. Krashia, F.R. Rizzo, R. Marino, M. Federici, P. De Bartolo, D. Aversa, M.C. Dell'Acqua, A. Cordella, M. Sancandi, F. Keller, L. Petrosini, S. Puglisi-Allegra, N.B. Mercuri, R. Coccarello, N. Berretta, M. D'Amelio, Dopamine neuronal loss contributes to memory and reward dysfunction in a model of Alzheimer's disease, *Nat. Commun.* (2017). doi:10.1038/ncomms14727.
- [79] M. De Marco, A. Venneri, Volume and connectivity of the ventral tegmental area are linked to neurocognitive signatures of Alzheimer's disease in humans, *J. Alzheimer's Dis.* (2018). doi:10.3233/JAD-171018.
- [80] W. Zhang, M. Yamada, J. Gomeza, A.S. Basile, J. Wess, Multiple Muscarinic Acetylcholine Receptor Subtypes Modulate Striatal Dopamine Release, as Studied with M1-M5 Muscarinic Receptor Knock-Out Mice, *J. Neurosci.* (2002). doi:20026644.
- [81] M. Grilli, M. Parodi, M. Raiteri, M. Marchi, Chronic nicotine differentially affects the function of nicotinic receptor subtypes regulating neurotransmitter release, *J. Neurochem.* (2005). doi:10.1111/j.1471-4159.2005.03126.x.
- [82] G. Olivero, M. Grilli, J. Chen, S. Preda, E. Mura, S. Govoni, M. Marchi, Effects of soluble  $\beta$ -amyloid on the release of neurotransmitters from rat brain synaptosomes, *Front. Aging Neurosci.* (2014). doi:10.3389/fnagi.2014.00166.
- [83] L. Trabace, K.M. Kendrick, S. Castrignanò, M. Colaianna, A. De Giorgi, S. Schiavone, C. Lanni, V. Cuomo, S. Govoni, Soluble amyloid beta1-42 reduces dopamine levels in rat prefrontal cortex: Relationship to nitric oxide, *Neuroscience.* (2007). doi:10.1016/j.neuroscience.2007.04.056.
- [84] M. Butzlaff, E. Ponimaskin, The role of Serotonin Receptors in Alzheimer's disease, *Opera Med Physiol.* (2016). doi:10.1016/S0214-4603(91)75503-4.
- [85] J.R. Cirrito, B.M. Disabato, J.L. Restivo, D.K. Verges, W.D. Goebel, A. Sathyan, D. Hayreh, G. D'Angelo, T. Benzinger, H. Yoon, J. Kim, J.C. Morris, M.A. Mintun, Y.I. Sheline, Serotonin signaling is associated with lower amyloid- $\beta$  levels and plaques in transgenic mice and humans, *Proc. Natl. Acad. Sci.* (2011). doi:10.1073/pnas.1107411108.
- [86] R.L. Nelson, Z. Guo, V.M. Halagappa, M. Pearson, A.J. Gray, Y. Matsuoka, M. Brown, B. Martin, T. Iyun, S. Maudsley, R.F. Clark, M.P. Mattson, Prophylactic treatment with paroxetine ameliorates behavioral deficits and retards the development of amyloid and tau pathologies in 3xTgAD mice, *Exp. Neurol.* (2007). doi:10.1016/j.expneurol.2007.01.037.
- [87] Y.I. Sheline, T. West, K. Yarasheski, R. Swarm, M.S. Jaszec, J.R. Fisher, W.D. Ficker, P. Yan, C. Xiong, C. Frederiksen, M. V. Grzelak, R. Chott, R.J. Bateman, J.C. Morris, M.A. Mintun, J.M.

Lee, J.R. Cirrito, An antidepressant decreases CSF A $\beta$  production in healthy individuals and in transgenic AD mice., *Sci. Transl. Med.* 6, 236re23 (2014).

[88] B. Dubois, H.H. Feldman, C. Jacova, S.T. DeKosky, P. Barberger-Gateau, J. Cummings, A. Delacourte, D. Galasko, S. Gauthier, G. Jicha, K. Meguro, J. O'Brien, F. Pasquier, P. Robert, M. Rossor, S. Salloway, Y. Stern, P.J. Visser, P. Scheltens, Research criteria for the diagnosis of Alzheimer's disease: revising the NINCDS-ADRDA criteria, *Lancet Neurol.* (2007). doi:10.1016/S1474-4422(07)70178-3.

[89] J.R. Fisher, C.E. Wallace, D.L. Tripoli, Y.I. Sheline, J.R. Cirrito, Redundant Gs-coupled serotonin receptors regulate amyloid- $\beta$  metabolism *in vivo*, *Mol. Neurodegener.* (2016). doi:10.1186/s13024-016-0112-5.

[90] G. Hashimoto, M. Sakurai, A.F. Teich, F. Saeed, F. Aziz, O. Arancio, 5-HT<sub>4</sub>receptor stimulation leads to soluble a $\beta$ PP $\alpha$  production through MMP-9 upregulation, *J. Alzheimer's Dis.* (2012). doi:10.3233/JAD-2012-111235.

[91] M. Cochet, R. Donneger, E. Cassier, F. Gaven, S.F. Lichtenthaler, P. Marin, J. Bockaert, A. Dumuis, S. Claeysen, 5-HT<sub>4</sub>receptors constitutively promote the non-amyloidogenic pathway of APP cleavage and interact with ADAM10, *ACS Chem. Neurosci.* (2013). doi:10.1021/cn300095t.

[92] M. Cisse, U. Braun, M. Leitges, A. Fisher, G. Pages, F. Checler, B. Vincent, ERK1-independent  $\alpha$ -secretase cut of  $\beta$ -amyloid precursor protein by M1 muscarinic receptors and PKCs., *Mol. Cell. Neurosci.* (2011). doi:10.1016/j.mcn.2011.04.008.

[93] L.F. Norum JH, Hart K, Ras-dependent ERK activation by the human G(s)-coupled serotonin receptors 5-HT<sub>4</sub>(b) and 5-HT<sub>7</sub>(a), *J Biol Chem.* 278:3098–1 (2003).

[94] D. Moechars, K. Lorent, F. Van Leuven, Premature death in transgenic mice that overexpress a mutant amyloid precursor protein is preceded by severe neurodegeneration and apoptosis, *Neuroscience.* (1999). doi:10.1016/S0306-4522(98)00599-5.

[95] S. Schiavone, P. Tucci, E. Mhillaj, M. Bove, L. Trabace, M.G. Morgese, Antidepressant drugs for beta amyloid-induced depression: A new standpoint?, *Prog. Neuro-Psychopharmacology Biol. Psychiatry.* (2017). doi:10.1016/j.pnpbp.2017.05.004.

[96] F. Caraci, F. Tascetta, S. Merlo, C. Benatti, S.F. Spampinato, A. Munafò, G.M. Leggio, F. Nicoletti, N. Brunello, F. Drago, M.A. Sortino, A. Copani, Fluoxetine prevents A $\beta$ 1-42-induced toxicity via a paracrine signaling mediated by transforming-growth-factor- $\beta$ 1, *Front. Pharmacol.* (2016). doi:10.3389/fphar.2016.00389.

[97] L. Jin, L.F. Gao, D.S. Sun, H. Wu, Q. Wang, D. Ke, H. Lei, J.Z. Wang, G.P. Liu, Long-term Ameliorative Effects of the Antidepressant Fluoxetine Exposure on Cognitive Deficits in 3  $\times$  TgAD Mice, *Mol. Neurobiol.* (2017). doi:10.1007/s12035-016-9952-9.

[98] K. Martinowich, B. Lu, Interaction between BDNF and serotonin: Role in mood disorders, *Neuropsychopharmacology.* (2008). doi:10.1038/sj.npp.1301571.

[99] S. Zimbone, I. Monaco, F. Gianì, G. Pandini, A.G. Copani, M.L. Giuffrida, E. Rizzarelli, Amyloid Beta monomers regulate cyclic adenosine monophosphate response element binding protein functions by activating type-1 insulin-like growth factor receptors in neuronal cells, *Aging Cell.* (2018). doi:10.1111/acel.12684.

- [100] J. Cummings, G. Lee, A. Ritter, K. Zhong, Alzheimer's disease drug development pipeline: 2018, *Alzheimer's Dement. Transl. Res. Clin. Interv.* (2018). doi:10.1016/j.trci.2018.03.009.
- [101] J. Arnt, B. Bang-Andersen, B. Grayson, F.P. Bymaster, M.P. Cohen, N.W. Delapp, B. Giethlen, M. Kreilgaard, D.L. McKinzie, J.C. Neill, D.L. Nelson, S.M. Nielsen, M.N. Poulsen, J.M. Schaus, L.M. Witten, Lu AE58054, a 5-HT<sub>6</sub> antagonist, reverses cognitive impairment induced by subchronic phencyclidine in a novel object recognition test in rats, *Int. J. Neuropsychopharmacol.* (2010). doi:10.1017/S1461145710000659.
- [102] L.A. Dawson, H.Q. Nguyen, P. Li, The 5-HT<sub>6</sub>receptor antagonist SB-271046 selectively enhances excitatory neurotransmission in the rat frontal cortex and hippocampus, *Neuropsychopharmacology.* (2001). doi:10.1016/S0893-133X(01)00265-2.
- [103] A. Mørk, R.V. Russell, I.E.M. de Jong, G. Smagin, Effects of the 5-HT<sub>6</sub>receptor antagonist idalopirdine on extracellular levels of monoamines, glutamate and acetylcholine in the rat medial prefrontal cortex, *Eur. J. Pharmacol.* (2017). doi:10.1016/j.ejphar.2017.02.010.
- [104] Wilkinson D, Windfeld K, E. Colding-Jørgensen, Safety and efficacy of idalopirdine, a 5-HT<sub>6</sub> receptor antagonist, in patients with moderate Alzheimer's disease (LADDER): a randomised, double-blind, placebo-controlled phase 2 trial, *Lancet Neurol.*, (2014), 13(11):109.
- [105] A. Atri, L. Frölich, C. Ballard, P.N. Tariot, J.L. Molinuevo, N. Boneva, K. Windfeld, L.L. Raket, J.L. Cummings, Effect of idalopirdine as adjunct to cholinesterase inhibitors on change in cognition in patients with Alzheimer disease three randomized clinical trials, in: *JAMA - J. Am. Med. Assoc.*, (2018). doi:10.1001/jama.2017.20373.
- [106] A. Merighi, C. Salio, F. Ferrini, L. Lossi, Neuromodulatory function of neuropeptides in the normal CNS, *J. Chem. Neuroanat.* (2011). doi:10.1016/j.jchemneu.2011.02.001.
- [107] D. Van Dam, A. Van Dijk, L. Janssen, P.P. De Deyn, Neuropeptides in Alzheimer's Disease: From Pathophysiological Mechanisms to Therapeutic Opportunities, *Curr. Alzheimer Res.* (2013). doi:10.2174/1567205011310050001.
- [108] L. Liu, M. Shenoy, P.J. Pasricha, Substance P and calcitonin gene related peptide mediate pain in chronic pancreatitis and their expression is driven by nerve growth factor, *J. Pancreas.* (2011).
- [109] C. Severini, C. Petrella, P. Calissano, Substance P and Alzheimer's Disease: Emerging Novel Roles, *Curr. Alzheimer Res.* (2016). doi:10.2174/1567205013666160401114039.
- [110] R. Marolda, M.T. Ciotti, C. Matrone, R. Possenti, P. Calissano, S. Cavallaro, C. Severini, Substance P activates ADAM9 mRNA expression and induces  $\alpha$ -secretase-mediated amyloid precursor protein cleavage, *Neuropharmacology.* (2012). doi:10.1016/j.neuropharm.2011.12.025.
- [111] T. Tousseyn, A. Thathiah, E. Jorissen, T. Raemaekers, U. Konietzko, K. Reiss, E. Maes, A. Snellinx, L. Serneels, O. Nyabi, W. Annaert, P. Saftig, D. Hartmann, B. de Strooper, ADAM10, the rate-limiting protease of regulated intramembrane proteolysis of notch and other proteins, is processed by ADAMS-9, ADAMS-15, and the  $\gamma$ -secretase, *J. Biol. Chem.* (2009). doi:10.1074/jbc.M805894200.
- [112] T. Saito, N. Iwata, S. Tsubuki, Y. Takaki, J. Takano, S.M. Huang, T. Suemoto, M. Higuchi, T.C. Saido, Somatostatin regulates brain amyloid  $\beta$  peptide A $\beta$ 42 through modulation of proteolytic degradation, *Nat. Med.* (2005). doi:10.1038/nm1206.

- [113] F. Lezoualc'h, Corticotropin-Releasing Hormone-Mediated Neuroprotection against Oxidative Stress Is Associated with the Increased Release of Non-amyloidogenic Amyloid Precursor Protein and with the Suppression of Nuclear Factor- $\kappa$ B, *Mol. Endocrinol.* (2000). doi:10.1210/me.14.1.147.
- [114] L.T. Sulkava R, Erkinjuntti T, CSF beta-endorphin and beta-lipotropin in Alzheimer's disease and multi-infarct dementia, *Neurology.* 35(7) (1985) 1057–8.
- [115] W.J. Meilandt, G.-Q. Yu, J. Chin, E.D. Roberson, J.J. Palop, T. Wu, K. Scarce-Levie, L. Mucke, Enkephalin Elevations Contribute to Neuronal and Behavioral Impairments in a Transgenic Mouse Model of Alzheimer's Disease, *J. Neurosci.* (2008). doi:10.1523/JNEUROSCI.0590-08.2008.
- [116] T. Yakovleva, Z. Marinova, A. Kuzmin, N.G. Seidah, V. Haroutunian, L. Terenius, G. Bakalkin, Dysregulation of dynorphins in Alzheimer disease, *Neurobiol. Aging.* (2007). doi:10.1016/j.neurobiolaging.2006.07.002.
- [117] P.G. Teng L, Zhao J, Wang F, Ma L, A GPCR/secretase complex regulates beta- and gamma-secretase specificity for A $\beta$  production and contributes to AD pathogenesis, *Cell Res.* 20(2):138- (2010).
- [118] V. Nimrich, U. Ebert, Is alzheimer's disease a result of presynaptic failure? -Synaptic dysfunctions induced by oligomeric p-amyloid, *Rev. Neurosci.* (2009). doi:10.1515/REVNEURO.2009.20.1.1.
- [119] D.J. Selkoe, Alzheimer's disease is a synaptic failure, *Science* (80-. ). (2002). doi:10.1126/science.1074069.
- [120] T.C. Südhof, J. Rizo, Synaptic vesicle exocytosis, *Cold Spring Harb. Perspect. Biol.* (2011). doi:10.1101/cshperspect.a005637.
- [121] T.C. Südhof, J.E. Rothman, Membrane fusion: Grappling with SNARE and SM proteins, *Science.* (2009). doi:10.1126/science.1161748.
- [122] P. Garcia-Reitböck, O. Anichtchik, A. Bellucci, M. Iovino, C. Ballini, E. Fineberg, B. Ghetti, L. Della Corte, P. Spano, G.K. Tofaris, M. Goedert, M.G. Spillantini, SNARE protein redistribution and synaptic failure in a transgenic mouse model of Parkinson's disease, *Brain.* (2010). doi:10.1093/brain/awq132.
- [123] J. Shen, S.S. Rathore, L. Khandan, J.E. Rothman, SNARE bundle and syntaxin N-peptide constitute a minimal complement for Munc18-1 activation of membrane fusion, *J. Cell Biol.* (2010). doi:10.1083/jcb.201003148.
- [124] M. Sharma, J. Burré, P. Bronk, Y. Zhang, W. Xu, T.C. Südhof, CSP $\alpha$  knockout causes neurodegeneration by impairing SNAP-25 function, *EMBO J.* (2012). doi:10.1038/emboj.2011.467.
- [125] W.G. Honer, A.M. Barr, K. Sawada, A.E. Thornton, M.C. Morris, S.E. Leurgans, J.A. Schneider, D.A. Bennett, Cognitive reserve, presynaptic proteins and dementia in the elderly, *Transl. Psychiatry.* (2012). doi:10.1038/tp.2012.38.
- [126] E.B. Mukaetova-Ladinska, F. Garcia-Siera, J. Hurt, H.J. Gertz, J.H. Xuereb, R. Hills, C. Brayne, F.A. Huppert, E.S. Paykel, M. McGee, R. Jakes, W.G. Honer, C.R. Harrington, C.M. Wischik, Staging of cytoskeletal and  $\beta$ -amyloid changes in human isocortex reveals biphasic synaptic protein

response during progression of Alzheimer's disease, *Am. J. Pathol.* (2000). doi:10.1016/S0002-9440(10)64573-7.

[127] C. Law, M. Schaan Profes, M. Levesque, J.A. Kaltschmidt, M. Verhage, A. Kania, Normal Molecular Specification and Neurodegenerative Disease-Like Death of Spinal Neurons Lacking the SNARE-Associated Synaptic Protein Munc18-1, *J Neurosci.* 13;36(2):5 (2016). doi: 10.1523/JNEUROSCI.1964-15.2016.

[128] Y. Yang, J. Kim, H.Y. Kim, N. Ryoo, S. Lee, Y.S. Kim, H. Rhim, Y.K. Shin, Amyloid- $\beta$  Oligomers May Impair SNARE-Mediated Exocytosis by Direct Binding to Syntaxin 1a, *Cell Rep.* (2015). doi:10.1016/j.celrep.2015.07.044.

[129] M.A. Poirier, W. Xiao, J.C. Macosko, C. Chan, Y.K. Shin, M.K. Bennett, The synaptic SNARE complex is a parallel four-stranded helical bundle, *Nat. Struct. Biol.* (1998). doi:10.1038/1799.

[130] R.B. Sutton, D. Fasshauer, R. Jahn, A.T. Brunger, Crystal structure of a SNARE complex involved in synaptic exocytosis at 2.4 Å resolution, *Nature.* (1998). doi:10.1038/26412.

[131] C.L. Russell, S. Semerdjieva, R.M. Empson, B.M. Austen, P.W. Beesley, P. Alifragis, Amyloid- $\beta$  acts as a regulator of neurotransmitter release disrupting the interaction between synaptophysin and VAMP2, *PLoS One.* (2012). doi:10.1371/journal.pone.0043201.

[132] R.E. Leube, P. Kaiser, A. Seiter, R. Zimbelmann, W.W. Franke, H. Rehm, P. Knaus, P. Prior, H. Betz, H. Reinke, Synaptophysin: molecular organization and mRNA expression as determined from cloned cDNA, *EMBO J.* (1987).

[133] B. Wiedenmann, W.W. Franke, Identification and localization of synaptophysin, an integral membrane glycoprotein of Mr 38,000 characteristic of presynaptic vesicles, *Cell.* (1985). doi:10.1016/S0092-8674(85)80082-9.

[134] G. Lonart, S. Schoch, P.S. Kaeser, C.J. Larkin, T.C. Südhof, D.J. Linden, Phosphorylation of RIM1 $\alpha$  by PKA triggers presynaptic long-term potentiation at cerebellar parallel fiber synapses, *Cell.* (2003). doi:10.1016/S0092-8674(03)00727-X.

[135] J. Boczan, A.G.M. Leenders, Z.H. Sheng, Phosphorylation of Syntaphilin by cAMP-dependent Protein Kinase Modulates Its Interaction with Syntaxin-1 and Annuls Its Inhibitory Effect on Vesicle Exocytosis, *J. Biol. Chem.* (2004). doi:10.1074/jbc.M400496200.

[136] G. Nagy, K. Reim, U. Matti, N. Brose, T. Binz, J. Rettig, E. Neher, J.B. Sørensen, Regulation of Releasable Vesicle Pool Sizes by Protein Kinase A-Dependent Phosphorylation of SNAP-25, *Neuron.* (2004). doi:10.1016/S0896-6273(04)00038-8.

[137] R. Hepp, J.P. Cabaniols, P.A. Roche, Differential phosphorylation of SNAP-25 *in vivo* by protein kinase C and protein kinase A, *FEBS Lett.* (2002). doi:10.1016/S0014-5793(02)03629-3.

[138] J. Fu, A.P. Naren, X. Gao, G.U. Ahmmed, A.B. Malik, Protease-activated receptor-1 activation of endothelial cells induces protein kinase C $\alpha$ -dependent phosphorylation of syntaxin 4 and Munc18c: Role in signaling P-selectin expression, *J. Biol. Chem.* (2005). doi:10.1074/jbc.M410044200.

- [139] Y. Shu, X. Liu, Y. Yang, M. Takahashi, K.D. Gillis, Phosphorylation of SNAP-25 at Ser187 Mediates Enhancement of Exocytosis by a Phorbol Ester in INS-1 Cells, *J. Neurosci.* (2008). doi:10.1523/JNEUROSCI.2352-07.2008.
- [140] N. Katayama, S. Yamamori, M. Fukaya, S. Kobayashi, M. Watanabe, M. Takahashi, T. Manabe, SNAP-25 phosphorylation at Ser187 regulates synaptic facilitation and short-term plasticity in an age-dependent manner, *Sci. Rep.* (2017). doi:10.1038/s41598-017-08237-x.
- [141] J. Gao, M. Hirata, A. Mizokami, J. Zhao, I. Takahashi, H. Takeuchi, M. Hirata, Differential role of SNAP-25 phosphorylation by protein kinases A and C in the regulation of SNARE complex formation and exocytosis in PC12 cells., *Cell. Signal.* (2016). doi:10.1016/j.cellsig.2015.12.014.
- [142] Y. Shimazaki, T.I. Nishiki, A. Omori, M. Sekiguchi, Y. Kamata, S. Kozaki, M. Takahashi, Phosphorylation of 25-kDa synaptosome-associated protein: Possible involvement in protein kinase C-mediated regulation of neurotransmitter release, *J. Biol. Chem.* (1996). doi:10.1074/jbc.271.24.14548.
- [143] E. Mura, S. Preda, S. Govoni, C. Lanni, L. Trabace, M. Grilli, F. Lagomarsino, A. Pittaluga, M. Marchi, Specific neuromodulatory actions of amyloid-beta on dopamine release in rat nucleus accumbens and caudate putamen, *J Alzheimers Dis.* 19(3):1041 (2010). doi:doi: 10.3233/JAD-2010-1299.
- [144] J.P. Tyszkiewicz,  $\beta$ -Amyloid Peptides Impair PKC-Dependent Functions of Metabotropic Glutamate Receptors in Prefrontal Cortical Neurons, *J. Neurophysiol.* (2005). doi:10.1152/jn.00939.2004.
- [145] P. Zhong, Z. Gu, X. Wang, H. Jiang, J. Feng, Z. Yan, Impaired modulation of GABAergic transmission by muscarinic receptors in a mouse transgenic model of Alzheimer's disease, *J.Biol.Chem.* (2003). doi:10.1074/jbc.M302789200.
- [146] P. De Camilli, R. Jahn, Pathways to Regulated Exocytosis in Neurons, *Annu. Rev. Physiol.* (1990). doi:10.1103/PhysRevLett.65.2362.
- [147] K.M. Turner, R.D. Burgoyne, A. Morgan, Protein phosphorylation and the regulation of synaptic membrane traffic, *Trends Neurosci.* (1999). doi:10.1016/S0166-2236(99)01436-8.
- [148] I. Ninan, O. Arancio, Presynaptic CaMKII is necessary for synaptic plasticity in cultured hippocampal neurons, *Neuron.* (2004). doi:10.1016/S0896-6273(04)00143-6.
- [149] Y. Watanabe, N. Katayama, K. Takeuchi, T. Togano, R. Itoh, M. Sato, M. Yamazaki, M. Abe, T. Sato, K. Oda, M. Yokoyama, K. Takao, M. Fukaya, T. Miyakawa, M. Watanabe, K. Sakimura, T. Manabe, M. Igarashia, Point mutation in syntaxin-1A causes abnormal vesicle recycling, behaviors, and short term plasticity, *J. Biol. Chem.* (2013). doi:10.1074/jbc.M113.504050.
- [150] K. Bodhinathan, A. Kumar, T.C. Foster, Intracellular Redox State Alters NMDA Receptor Response during Aging through Ca<sup>2+</sup>/Calmodulin-Dependent Protein Kinase II, *J. Neurosci.* (2010). doi:10.1523/JNEUROSCI.5485-09.2010.
- [151] N. Amada, K. Aihara, R. Ravid, M. Horie, Reduction of NRI and phosphorylated Ca<sup>2+</sup>/calmodulin-dependent protein kinase II levels in Alzheimer's disease, *Neuroreport.* (2005). doi:10.1097/01.wnr.0000185015.44563.5d.



- [152] R. Killick, E.M. Ribe, R. Al-Shawi, B. Malik, C. Hooper, C. Fernandes, R. Dobson, P.M. Nolan, A. Lourdasamy, S. Furney, K. Lin, G. Breen, R. Wroe, A.W.M. To, K. Leroy, M. Causevic, A. Usardi, M. Robinson, W. Noble, R. Williamson, K. Lunnon, S. Kellie, C.H. Reynolds, C. Bazenet, A. Hodges, J.P. Brion, J. Stephenson, J. Paul Simons, S. Lovestone, Clusterin regulates  $\beta$ -amyloid toxicity via Dickkopf-1-driven induction of the wnt-PCP-JNK pathway, *Mol. Psychiatry*. (2014). doi:10.1038/mp.2012.163.
- [153] S.O. Yoon, D.J. Park, J.C. Ryu, H.G. Ozer, C. Tep, Y.J. Shin, T.H. Lim, L. Pastorino, A.J. Kunwar, J.C. Walton, A.H. Nagahara, K.P. Lu, R.J. Nelson, M.H. Tuszynski, K. Huang, JNK3 Perpetuates Metabolic Stress Induced by  $A\beta$  Peptides, *Neuron*. (2012). doi:10.1016/j.neuron.2012.06.024.
- [154] S. Biggi, L. Buccarello, A. Scip, P. Lippiello, N. Tonna, C. Rumio, D. Di Marino, M.C. Miniaci, T. Borsello, Evidence of Presynaptic Localization and Function of the c-Jun N-Terminal Kinase, *Neural Plast.* (2017). doi:10.1155/2017/6468356.
- [155] R. Lalonde, K. Fukuchi, C. Strazielle, APP transgenic mice for modelling behavioural and psychological symptoms of dementia (BPSD), *Neurosci. Biobehav. Rev.* (2012). doi:10.1016/j.neubiorev.2012.02.011.
- [156] M.I. Geerlings, B. Schmand, A.W. Braam, C. Jonker, L.M. Bouter, W. Van Tilburg, Depressive symptoms and risk of Alzheimer's disease in more highly educated older people, *J. Am. Geriatr. Soc.* (2000). doi:10.1111/j.1532-5415.2000.tb04785.x.
- [157] M.G. Morgese, S. Schiavone, L. Trabace, Emerging role of amyloid beta in stress response: Implication for depression and diabetes, *Eur. J. Pharmacol.* (2017). doi:10.1016/j.ejphar.2017.08.031.
- [158] M. Colaianna, P. Tucci, M. Zotti, M. Morgese, S. Schiavone, S. Govoni, V. Cuomo, L. Trabace, Soluble  $\beta$ -amyloid 1-42: A critical player in producing behavioural and biochemical changes evoking depressive-related state?, *Br. J. Pharmacol.* (2010). doi:10.1111/j.1476-5381.2010.00669.x.
- [159] R.S. Filali M, Lalonde R, Cognitive and non-cognitive behaviors in an APP<sup>swe</sup>/PS1 bigenic model of Alzheimer's disease, *Genes Brain Behav.* 8(2):143-8 (2009).
- [160] V. Krishnan, E.J. Nestler, The molecular neurobiology of depression, *Nature*. (2008). doi:10.1038/nature07455.
- [161] D. Van Dam, Y. Vermeiren, A. D. Dekker, P. J.W. Naudé, P. P. De Deyn, Neuropsychiatric Disturbances in Alzheimer's Disease: What Have We Learned from Neuropathological Studies?, *Curr. Alzheimer Res.* (2016). doi:10.2174/1567205013666160502123607.
- [162] P.B. Rosenberg, M.M. Mielke, B.S. Appleby, E.S. Oh, Y.E. Geda, C.G. Lyketsos, The association of neuropsychiatric symptoms in MCI with incident dementia and alzheimer disease, *Am. J. Geriatr. Psychiatry.* (2013). doi:10.1016/j.jagp.2013.01.006.
- [163] N.J. Donovan, R.E. Amariglio, A.S. Zoller, R.K. Rudel, T. Gomez-Isla, D. Blacker, B.T. Hyman, J.J. Locascio, K.A. Johnson, R.A. Sperling, G.A. Marshall, D.M. Rentz, Subjective cognitive concerns and neuropsychiatric predictors of progression to the early clinical stages of Alzheimer disease, *Am. J. Geriatr. Psychiatry.* (2014). doi:10.1016/j.jagp.2014.02.007.

- [164] F.E. Taragano, R.F. Allegri, C. Lyketsos, Mild behavioral impairment A prodromal stage of dementia, *Dement. Neuropsychol.* (2008). doi:10.1590/S1980-57642009DN20400004.
- [165] J. Cummings, Chung JA, Neurobehavioral and neuropsychiatric symptoms in Alzheimer's disease, *Neurol Clin.* 18,829–846 (2000).
- [166] H.C. Guimarães, R. Levy, A.L. Teixeira, R.G. Beato, P. Caramelli, Neurobiology of apathy in Alzheimer's disease, *Arq. Neuropsiquiatr.* (2008). doi:10.1590/S0004-282X2008000300035.
- [167] C.J. Marshall GA, Fairbanks LA, Tekin S, Vinters HV, Neuropathological correlates of apathy in Alzheimer's disease, *Dement Geriatr Cogn Disord.* 21:144–7 (2006).
- [168] R.A. Mitchell, N. Herrmann, K.L. Lanctôt, The Role of Dopamine in Symptoms and Treatment of Apathy in Alzheimer's Disease, *CNS Neurosci. Ther.* (2011). doi:10.1111/j.1755-5949.2010.00161.x.
- [169] D. Storga, K. Vrecko, J.G.D. Birkmayer, G. Reibnegger, Monoaminergic neurotransmitters, their precursors and metabolites in brains of Alzheimer patients, *Neurosci. Lett.* (1996). doi:10.1016/0304-3940(95)12256-7.
- [170] R.A. Sweet, R.L. Hamilton, M.T. Healy, S.R. Wisniewski, R. Henteleff, B.G. Pollock, D.A. Lewis, S.T. DeKosky, Alterations of striatal dopamine receptor binding in Alzheimer disease are associated with Lewy body pathology and antemortem psychosis, *Arch. Neurol.* (2001). doi:10.1001/archneur.58.3.466.
- [171] M. Benoit, I. Dygai, O. Migneco, P.H. Robert, C. Bertogliati, J. Darcourt, J. Benoliel, V. Aubin-Brunet, D. Pringuey, Behavioral and psychological symptoms in Alzheimer's disease. Relation between apathy and regional cerebral perfusion, *Dement. Geriatr. Cogn. Disord.* (1999). doi:10.1159/000017198.
- [172] P.H. Robert, G. Darcourt, M.P. Koulibaly, S. Claret, M. Benoit, R. Garcia, O. Dechaux, J. Darcourt, Lack of initiative and interest in Alzheimer's disease: A single photon emission computed tomography study, *Eur. J. Neurol.* (2006). doi:10.1111/j.1468-1331.2006.01088.x.
- [173] P.D. Bruen, W.J. McGeown, M.F. Shanks, A. Venneri, Neuroanatomical correlates of neuropsychiatric symptoms in Alzheimer's disease, *Brain.* (2008). doi:10.1093/brain/awn151.
- [174] V.A. Holthoff, B. Beuthien-Baumann, E. Kalbe, S. Lüdecke, O. Lenz, G. Zündorf, S. Spirling, K. Schierz, P. Winiecki, S. Sorbi, K. Herholz, Regional cerebral metabolism in early Alzheimer's disease with clinically significant apathy or depression, *Biol. Psychiatry.* (2005). doi:10.1016/j.biopsych.2004.11.035.
- [175] G.A. Marshall, L. Monserratt, D. Harwood, M. Mandelkern, J.L. Cummings, D.L. Sultzer, Positron emission tomography metabolic correlates of apathy in Alzheimer disease, *Arch. Neurol.* (2007). doi:10.1001/archneur.64.7.1015.
- [176] M. Benoit, G. Berrut, J. Doussaint, S. Bakchine, S. Bonin-Guillaume, P. Frémont, T. Gallarda, P. Krolak-Salmon, T. Marquet, C. Mékiès, F. Sellal, S. Schuck, R. David, P. Robert, Apathy and depression in mild Alzheimer's disease: a cross-sectional study using diagnostic criteria, *J Alzheimers Dis.* 31(2):325- (2012). doi:doi: 10.3233/JAD-2012-112003.

- [177] R.J. Mourao, G. Mansur, L.F. Malloy-Diniz, E. Castro Costa, B.S. Diniz, Depressive symptoms increase the risk of progression to dementia in subjects with mild cognitive impairment: systematic review and meta-analysis, *Int. J. Geriatr. Psychiatry*. (2016). doi:10.1002/gps.4406.
- [178] T. Leyhe, C.F. Reynolds, T. Melcher, C. Linnemann, S. Klöppel, K. Blennow, H. Zetterberg, B. Dubois, S. Lista, H. Hampel, A common challenge in older adults: Classification, overlap, and therapy of depression and dementia, *Alzheimer's Dement*. (2017). doi:10.1016/j.jalz.2016.08.007.
- [179] Y. Vermeiren, D. Van Dam, T. Aerts, S. Engelborghs, P.P. De Deyn, Brain region-specific monoaminergic correlates of neuropsychiatric symptoms in Alzheimer's disease, *J. Alzheimers. Dis*. (2014). doi:10.3233/JAD-140309.
- [180] L. Trillo, D. Das, W. Hsieh, B. Medina, S. Moghadam, B. Lin, V. Dang, M.M. Sanchez, Z. De Miguel, J.W. Ashford, A. Salehi, Ascending monoaminergic systems alterations in Alzheimer's disease. Translating basic science into clinical care, *Neurosci. Biobehav. Rev*. (2013). doi:10.1016/j.neubiorev.2013.05.008.
- [181] F. Yasuno, H. Kazui, N. Morita, K. Kajimoto, M. Ihara, A. Taguchi, A. Yamamoto, K. Matsuoka, J. Kosaka, T. Kudo, H. Iida, T. Kishimoto, K. Nagatsuka, High amyloid- $\beta$  deposition related to depressive symptoms in older individuals with normal cognition: a pilot study, *Int. J. Geriatr. Psychiatry*. (2016). doi:10.1002/gps.4409.
- [182] C. Ballard, A. Corbett, Agitation and aggression in people with Alzheimer's disease, *Curr. Opin. Psychiatry*. (2013). doi:10.1097/YCO.0b013e32835f414b.
- [183] L.C. Rosenberg PB, Nowrangi MA, Neuropsychiatric symptoms in Alzheimer's disease: what might be associated brain circuits?, *Mol Asp. Med*. 43–44:25–3 (2015).
- [184] A.M. Palmer, G.C. Stratmann, A.W. Procter, D.M. Bowen, Possible neurotransmitter basis of behavioral changes in alzheimer's disease, *Ann. Neurol*. (1988). doi:10.1002/ana.410230616.
- [185] A. Russo-Neustadt, T.J. Zomorodian, C.W. Cotman, Preserved cerebellar tyrosine hydroxylase-immunoreactive neuronal fibers in a behaviorally aggressive subgroup of Alzheimer's disease patients, *Neuroscience*. (1998). doi:10.1016/S0306-4522(98)00134-1.
- [186] J.L. Cummings, T. McRae, R. Zhang, Effects of donepezil on neuropsychiatric symptoms in patients with dementia and severe behavioral disorders, *Am. J. Geriatr. Psychiatry*. (2006). doi:10.1097/01.JGP.0000221293.91312.d3.
- [187] L.C. Leroy I, Voulgari A, Breitner JC, The epidemiology of psychosis in dementia, *Am J Geriatr Psychiatry*. 11:83–91 (2003).
- [188] S.H. Lin, C.Y. Yu, M.C. Pai, The occipital white matter lesions in Alzheimer's disease patients with visual hallucinations, *Clin. Imaging*. (2006). doi:10.1016/j.clinimag.2006.09.025.
- [189] L. Serra, R. Perri, M. Cercignani, B. Spanò, L. Fadda, C. Marra, G.A. Carlesimo, C. Caltagirone, M. Bozzali, Are the behavioral symptoms of Alzheimer's disease directly associated with neurodegeneration?, *J. Alzheimer's Dis*. (2010). doi:10.3233/JAD-2010-100048.
- [190] G.S. Zubenko, J. Moosy, A.J. Martinez, G. Rao, D. Claassen, J. Rosen, U. Kopp, Neuropathologic and Neurochemical Correlates of Psychosis in Primary Dementia, *Arch. Neurol*. (1991). doi:10.1001/archneur.1991.00530180075020.



---

**PART 2**

The following manuscript was published in *Journal of Alzheimer's Disease* in 2019 as:

**Amyloid- $\beta$  and synaptic vesicle dynamics: a cacophonous orchestra**

**Francesca Fagiani**, Cristina Lanni, Marco Racchi, Alessia Pascale and Stefano Govoni

**Abstract**

It is now more than two decades since amyloid- $\beta$  ( $A\beta$ ), the proteolytic product of the amyloid- $\beta$  protein precursor ( $A\beta$ PP), was first demonstrated to be a normal and soluble product of neuronal metabolism. To date, despite a growing body of evidence suggests its regulatory role on synaptic function, the exact cellular and molecular pathways involved in  $A\beta$ -driven synaptic effects remain elusive. This review provides an overview of the mounting evidence showing  $A\beta$ -mediated effects on presynaptic functions and neurotransmitter release from axon terminals, focusing on its interaction with synaptic vesicle cycle. Indeed,  $A\beta$  peptides have been found to interact with key presynaptic scaffold proteins and kinases affecting the consequential steps of the synaptic vesicle dynamics (e.g., synaptic vesicles exocytosis, endocytosis, and trafficking). Defects in the fine-tuning of synaptic vesicle cycle by  $A\beta$  and deregulation of key molecules and kinases, which orchestrate synaptic vesicle availability, may alter synaptic homeostasis, possibly contributing to synaptic loss and cognitive decline. Elucidating the presynaptic mechanisms by which  $A\beta$  regulate synaptic transmission is fundamental for a deeper comprehension of the biology of presynaptic terminals as well as of  $A\beta$ -driven early synaptic defects occurring in prodromal stage of AD. Moreover, a better understating of  $A\beta$  involvement in cellular signal pathways may allow to set up more effective therapeutic interventions by detecting relevant molecular mechanisms, whose imbalance might ultimately lead to synaptic impairment in AD.

**Keywords:** Amyloid- $\beta$ , intracellular signaling, neurotransmitter release, presynaptic function, SNARE complex, synaptic vesicle cycle.

## Review

# Amyloid- $\beta$ and Synaptic Vesicle Dynamics: A Cacophonous Orchestra

Francesca Fagiani<sup>a,b,1</sup>, Cristina Lanni<sup>a,1</sup>, Marco Racchi<sup>a</sup>, Alessia Pascale<sup>a</sup> and Stefano Govoni<sup>a,\*</sup>

<sup>a</sup>*Department of Drug Sciences, Pharmacology Section, University of Pavia, Italy*

<sup>b</sup>*Scuola Universitaria Superiore IUSS, Pavia, Italy*

Alzheimer's Disease (AD) is a chronic neurodegenerative disorder, whose prominent neuropathological features are the progressive extracellular deposition of amyloid plaques, the intracellular neurofibrillary tangles, and the loss of synapses and neurons [1]. Among the distinctive neuropathological hallmarks of AD, the extent of synaptic loss has been reported as a quantitative neuropathological correlate of memory deficit and cognitive decline observed in AD patients [2]. Such evidence suggests a causal role for dwindling synaptic integrity in the etiology of AD [3] and raises a central question in AD research concerning the role played by synaptic damage. However, the molecular mechanisms underlying such synaptic dysfunction remain largely unknown.

Clinical studies, alongside animal models, have widely demonstrated the importance of amyloid- $\beta$  (A $\beta$ ) [4], a 4-kDa peptide derived from the sequential proteolysis of the amyloid- $\beta$  protein precursor (A $\beta$ PP) by  $\beta$ - and  $\gamma$ -secretase, in the progression of AD. Besides its widely investigated role as the main pathogenic marker responsible for neurodegenerative processes, significant advances have been made over recent years to understand whether A $\beta$  might be an important synaptic regulator affecting age-related synaptic changes. Accordingly, A $\beta$  has been shown to induce several functional and morphological synaptic changes. Intriguingly, these defects in synaptic activity are recognized as one of the earliest events in AD, preceding the deposition of A $\beta$  plaques into the brain [5]. Such evidence has emphasized the need to refocus the experimental approach to A $\beta$ -induced neurotoxicity from frank neurodegeneration to earlier structural and functional perturbations of synaptic homeostasis triggered by A $\beta$  [6]. A great effort has been directed toward evaluating A $\beta$ -driven effects on synaptic activity, in conditions not resulting in neurotoxicity. A highly heterogeneous amount of data, ranging from an A $\beta$ -driven increase in spontaneous synaptic activity [7] to a lack of effect on synaptic transmission [8] or even its depression [9, 10], has been produced. Such contrasting data have been mainly related to crucial factors

affecting the outcome of the experiments, such as the different variants, concentrations, and aggregation forms of A $\beta$  peptides in the different experimental settings [11, 12], as well as to the extreme supplier-to-supplier and batch-to-batch variability of synthetic A $\beta$  peptides [13]. Indeed, A $\beta$  has been demonstrated to exhibit a biphasic action, i.e., neuromodulatory/neuroprotective *versus* neurotoxic, depending on its concentration and aggregation status [14, 15]. Low concentrations (picomolar- low nanomolar) of A $\beta$  peptides positively modulate neurotransmission and memory, whereas, higher concentrations (high nanomolar-low micromolar) exhibit a neurotoxic and detrimental action on synaptic plasticity and memory. In addition, the complex dynamic balance existing between the different species of A $\beta$  (i.e., monomers, oligomers, protofibrils, and fibrils) contribute to the widespread and controversial lit

erature on A $\beta$ -driven synaptic effects [16], further challenging consistent interpretation of the experimental data.

### 1. A $\beta$ as potential modulator of presynaptic activity

Kamenetz and colleagues demonstrated for the first time that, in healthy brain, neuronal activity directly promotes the production and the secretion of A $\beta$  peptides into the extracellular space, and that, in turn, A $\beta$  downregulates excitatory synaptic transmission [9, 10]. This negative feedback loop, wherein neuronal activity promotes A $\beta$  production and A $\beta$  depresses synaptic activity, may provide a physiological homeostatic mechanism preventing the overexcitation of brain circuits [9]. However, in normal brain, extracellular concentrations of endogenous A $\beta$  peptides have been estimated to low picomolar levels, far lower than the concentrations used in the mentioned studies demonstrating A $\beta$ -mediated synaptic depression [10, 15]. This observation prompted extensive research to investigate the impact of lower concentrations of A $\beta$ , which are likely to approximate the endogenous level of the peptide. Several lines of evidence converge to indicate that A $\beta$  peptides at pM concentrations act as a positive endogenous regulator of neurotransmission at presynaptic terminals [14, 15, 17]. Abramov *et al.* demonstrated that the inhibition of extracellular A $\beta$  degradation and the subsequent increase in endogenous levels of A $\beta$  peptides enhanced both the release probability of synaptic vesicles and neuronal activity in rodent hippocampal culture [11]. However, the specific A $\beta$  isoform and conformation responsible for this synaptic effect cannot be identified [11]. These acute effects mediated by the inhibition of A $\beta$  clearance increased spontaneous excitatory postsynaptic currents without affecting inhibitory currents. Such effect was specifically presynaptic and dependent on firing rates, with lower facilitation observed in hippocampal neurons showing higher firing rates [11]. Furthermore, the exposure of rodent neuronal cultures to

picomolar amounts of A $\beta$ 40 monomers and dimers enhanced presynaptic release probability via A $\beta$ PP-A $\beta$ PP interactions at excitatory hippocampal synapses [18]. A $\beta$ 40 monomers and dimers have been found to bind to A $\beta$ PP, increasing the fraction of A $\beta$ PP homodimers at the plasma membrane and inducing activity-dependent A $\beta$ PP-A $\beta$ PP conformational changes [18]. In turn, A $\beta$ PP homodimer activation triggers structural rearrangements within the presynaptic A $\beta$ PP/G0 protein signaling complex, enhancing calcium (Ca<sup>2+</sup>) build-up and, consequently, synaptic vesicle exocytosis and glutamate release [18]. These findings suggest that A $\beta$ PP homodimer may act as a presynaptic A $\beta$ 40 receptor that translates local changes in the extracellular levels of A $\beta$  peptides to modulation of synaptic release probability, maintaining basal neurotransmitter release under physiological conditions. Such a positive modulatory action of endogenous A $\beta$  peptides on synaptic transmission has been further supported indirectly by the observation that mice deficient for A $\beta$ PP [19], PS1 (Presenilin 1) [20], or BACE1 (Beta-site A $\beta$ PP-cleaving enzyme 1) [21] displayed evident defects in synaptic transmission.

According to experimental data suggesting a modulatory action of A $\beta$  peptides on synaptic transmission, Puzzo *et al.* demonstrated that the exposure of hippocampal neurons to high picomolar-low nanomolar concentrations of synthetic A $\beta$ 42 oligomers markedly increased synaptic transmission, whereas higher concentrations (high nanomolar-low micromolar) of A $\beta$ 42 induced the well-established synaptic depression [15]. The facilitator effect of low A $\beta$  concentrations on excitatory transmission did not affect postsynaptic N-methyl-d-aspartate receptors (NMDARs) and  $\alpha$ -amino-3-hydroxy-5-methyl-4-isoxazolepropionic acid receptors (AMPA receptors). This effect was sensitive to  $\alpha$ -bungarotoxin, a selective antagonist of  $\alpha$ 7-nicotinic acetylcholine receptor ( $\alpha$ 7-nAChR), thus implying that functional  $\alpha$ 7-nAChRs are required for A $\beta$ 42-mediated facilitator effect [14, 15]. This observation is consistent with data from literature reporting high-affinity binding of A $\beta$  to  $\alpha$ 7-nAChR [22] and enhanced Ca<sup>2+</sup> build-up through  $\alpha$ 7-nAChR at presynaptic nerve endings of hippocampal synaptosomes upon application of picomolar A $\beta$ 42 [23]. Under normal conditions, picomolar concentrations of A $\beta$ , released by synaptic activity during vesicle exocytosis [10], positively stimulate  $\alpha$ 7-nAChR, whose activation enhances Ca<sup>2+</sup> influx into the presynaptic terminals and neurotransmitter release boosting synaptic plasticity [15]. In line with this hypothesis, blocking or removing  $\alpha$ 7-nAChRs both decreased A $\beta$  secretion and blocked A $\beta$ -induced facilitation [24]. Instead, nanomolar concentrations of A $\beta$  have been found to inactivate  $\alpha$ 7-nAChRs.

Recently, Gulisano *et al.* corroborated such evidence demonstrating that, in rodent CA1 pyramidal neurons, the extracellular administration of 200 pM oligomeric A $\beta$ 42 induced, via  $\alpha$ 7-nAChRs, an increase of miniature EPSCs (excitatory postsynaptic currents)



frequency and a decrease of paired pulse facilitation [17]. Such A $\beta$ 42-induced effects were associated with an enhanced number of docked vesicles at presynaptic terminals, thus indicating that picomolar concentrations of A $\beta$ 42 stimulate neurotransmitter release at presynaptic level [17]. Notably, intracellular application of 6E10, an antibody raised against human A $\beta$ 42, did not hinder the effects induced by extracellular A $\beta$ 42, which were conversely prevented by the extracellular application of 6E10 [17].

Overall, these findings strongly support a potential relationship between concentration of A $\beta$  peptides and synaptic transmission, wherein low concentrations (high picomolar-low nanomolar) of A $\beta$  peptides play a positive modulatory role upon neurotransmission [14, 15], abnormally low levels decrease presynaptic efficacy [19–21] and high concentrations (high nanomolar-low micromolar) induce detrimental effects depressing synaptic transmission, mainly by postsynaptic mechanisms including enhanced internalization or desensitization of postsynaptic glutamate receptors and downstream signaling [9, 25, 26].

Moreover, the time of exposure to A $\beta$ 42 picomolar concentration significantly affects synaptic activity. Koppensteiner *et al.* examined the time course of synaptic changes in mouse hippocampal neurons exposed to picomolar concentration (200 pM) of A $\beta$ 42. They demonstrated that A $\beta$ 42 exerted opposite effects depending also on the time of exposure, with short exposures in the range of minutes enhancing synaptic potentiation in hippocampal cultures and slices and increasing synaptic plasticity as well as memory in mice, and longer exposures lasting several hours decreasing them [27]. In addition, the prolonged exposure to picomolar concentrations of A $\beta$ 42 has been found to induce microstructural changes at the synapse including an increase in the basal frequency of spontaneous neurotransmitter release and in the basal number of functional presynaptic release sites, as well as a redistribution of synaptic proteins such as the vesicle-associated proteins synapsin I and synaptophysin [27].

The clues gained from recent studies in modulation of presynaptic functions by A $\beta$  highlight a significant variety of mechanisms and functional outcomes. Elucidating the intracellular mechanisms underlying synaptic alterations in early AD represents a keystone to uncover AD pathobiology and to define the associated early behavioral signs and/or therapeutic interventions, able to block factors that fuel the progression of AD and to slow down and, ultimately, even prevent the onset of irreparable intracellular damage leading to synaptic loss and cognitive decline [1]. Indeed, the observed changes in synaptic activity and associated neurotransmission may be at the basis of the onset of psychiatric symptoms during the early phases of the disease (e.g., anxiety, changes in mood) in absence of the usual warning symptoms (e.g., memory loss).

## 2. The effects of A $\beta$ on synaptic vesicle dynamics

Most of presynaptic functions has been reported to directly or indirectly converge on the synaptic vesicle cycle, whose different steps collaborate to allow rapid, regulated and repeated rounds of neurotransmitter release (reviewed by [28]). In recent years, a major goal in neurobiology has been to gain insight into the tightly coordinated membrane-fusion machinery that mediates synaptic vesicle cycle, characterized by sequential steps.

Data from literature showed that A $\beta$  peptides directly interfere with key presynaptic proteins regulating different steps of the synaptic vesicle cycle and, consequently, influencing neurotransmitter release and neurotransmission between functionally related neurons [29, 30]. A $\beta$  has been found to interact with presynaptic proteins mediating synaptic vesicles docking and fusion, necessary for a regulated exocytosis, as well as synaptic vesicles recycling and recovery (illustrated in **Fig. 1**) (reviewed by [31, 32]).

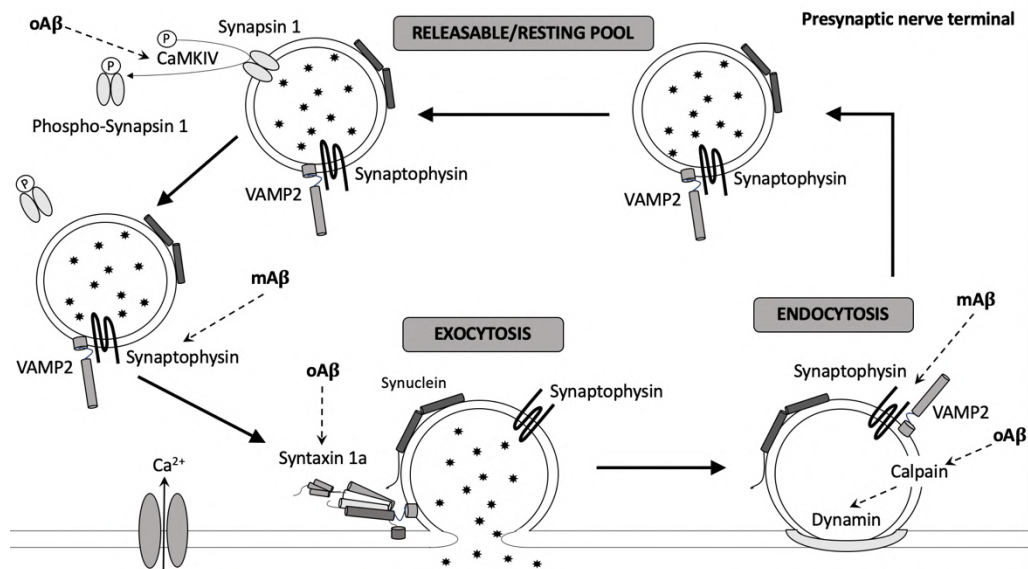


**Fig. 1. A $\beta$  interplay with synaptic vesicle dynamics.** Monomeric A $\beta$  (mA $\beta$ ) directly competes with Synaptobrevin/VAMP2 for binding to Synaptophysin, stimulating the formation of the fusion pore complex, followed by neurotransmitter release. Moreover, oligomeric A $\beta$  (oA $\beta$ ) exerts an inhibitory effect on SNARE-mediated exocytosis by binding to the SNARE motif region (SynH3) of Syntaxin 1a. In addition, oA $\beta$  decreases dynamin-1 levels by increasing its cleavage by calpain, thus impairing endocytosis of synaptic vesicles. mA $\beta$  has been also hypothesized to prevent synaptophysin from triggering synaptic vesicle endocytosis through its interaction with synaptobrevin/VAMP2. Finally, oA $\beta$  enhances the levels of phosphorylated Synapsin I, by activating CaMKIV, thus increasing the availability of synaptic vesicles to dock to the active zone and to allow neurotransmitter release. It should be noted that A $\beta$ , in addition to the direct actions here represented, may affect neurotransmitter release also indirectly through the modulation of various kinases (see text).

In addition, the regulation of synaptic vesicle cycle and, subsequently, of neurotransmitter release by A $\beta$  has been suggested to be, at least in part, mediated by A $\beta$  interactions with specific protein kinases and phosphatases controlling the consequential steps of the synaptic vesicle cycle. It can be postulated that A $\beta$  by influencing the fine-tuning of synaptic vesicle cycling may transiently influence synaptic homeostasis. Such alteration triggered by A $\beta$  may not be restricted to the immediate period. A series of transient modifications by A $\beta$  may generate long-lasting and, then, permanent alterations at synapse, by possibly catalyzing a linear progression from synaptic dysfunction to neuronal degeneration. It is therefore essential to deeper understand A $\beta$  involvement in intraneuronal pathways to identify new drug targets and to set up more precise therapeutic interventions targeting the most relevant molecular mechanisms leading to AD.

In the following sections, we will dissect this remarkably complex scenario in a reductionist fashion, providing an overview of the evidence demonstrating A $\beta$  involvement in synaptic vesicle exocytosis, endocytosis and recycling (illustrated in **Table 1**), focusing on its interplay with key presynaptic proteins and kinases.

Table 1  
Regulation of synaptic vesicle cycle by amyloid- $\beta$

Exocytosis				
Molecular species of A $\beta$	Aggregation status and concentration/time of exposure	Observed effect on synaptic vesicle cycle	<i>In vitro</i> and <i>in vivo</i> model	Reference
A $\beta$	Oligomers (1–20 nM)	Oligomeric form of A $\beta$ has been found to exert an inhibitory effect on SNARE-mediated exocytosis by binding to the SNARE motif region (SynH3) of Syntaxin 1a, thus specifically inhibiting the fusion step between docking and lipid mixing. Instead, the ability of synaptic vesicles to dock to the target membrane has not been affected.	<i>In vitro</i> single-vesicle content-mixing assay	[30]
A $\beta_{42}$	Monomers (50 nM/20 min)	At presynaptic terminals, A $\beta_{42}$ has been demonstrated to directly compete with Synaptobrevin/VAMP2 for binding to Synaptophysin, thus hindering the formation of Synaptophysin/VAMP complex and, subsequently, inducing the formation of the fusion pore complex followed by neurotransmitter release.	Primary cultures of rat CA3-CA1 hippocampal neurons	[29]
Endocytosis				
Molecular species of A $\beta$	Aggregation status and concentration/time of exposure	Observed effect on synaptic vesicle cycle	<i>In vitro</i> and <i>in vivo</i> model	Reference
A $\beta$	Soluble oligomers (2 $\mu$ M)	A $\beta$ oligomers have been found to decrease dynamin-1 levels by increasing its cleavage by calpain, thus impairing endocytosis of synaptic vesicle. Abnormally accumulated amphiphysin at synaptic membrane, following A $\beta$ oligomers application, has also been observed.	Cultured rat hippocampal neurons	[66]
A $\beta_{42}$	Monomers (50 nM/20 min)	At synapse, A $\beta_{42}$ has been shown to compete with synaptobrevin/VAMP2 for binding to synaptophysin, which is known to regulate the retrieval kinetics of VAMP2 during endocytosis. A $\beta_{42}$ has been hypothesized to prevent synaptophysin from triggering synaptic vesicle endocytosis through its interaction with synaptobrevin/VAMP2.	Primary cultures of rat CA3-CA1 hippocampal neurons	[29]
A $\beta$	Monomers and oligomers (200 nM/2h; 200 nM/72h)	Preparation containing both synthetic A $\beta$ oligomers and monomers reduced the efficacy of synaptic vesicle recycling. 72-h treatment with A $\beta$ oligomers induced more severe defects in synaptic vesicle endocytosis. Notably, preparation containing only A $\beta$ monomers did not impaired synaptic vesicle endocytosis.	Rat hippocampal neurons	[69]
A $\beta_{40}$ and A $\beta_{42}$	Increased levels of endogenous	Increased levels of endogenous A $\beta_{42}$ and A $\beta_{40}$ have been found to increase activity-driven recycling of synaptic vesicles in both excitatory and inhibitory synapses, as shown by quantification of synaptotagmin 1 antibody uptake, strongly supporting the involvement of endogenous A $\beta$ peptides in the modulation of basal synaptic vesicle recycling.	Rat cortical and hippocampal neurons	[76]

(Continued)

Table 1  
(Continued)

A $\beta$ <sub>42</sub> and A $\beta$ <sub>40</sub> (1.6- and 1.2-fold compared to controls)/ Synthetic A $\beta$ <sub>42</sub> and A $\beta$ <sub>40</sub> (200 pM/1h; 1 $\mu$ M/1h)		1-h exposure to 200 pM A $\beta$ <sub>40</sub> and A $\beta$ <sub>42</sub> caused an increase in synaptic vesicle recycling.  1-h treatment with 1 $\mu$ M A $\beta$ has been found to decrease it.  The endogenous A $\beta$ -driven modulation of synaptic vesicle recycling has been hypothesized to rely on CDK5 and calcineurin signaling pathway downstream of $\alpha$ 7-nAChR.		
Intra-synaptic trafficking and distribution among vesicle pools				
Molecular species of A $\beta$	Aggregation status and concentration/time of exposure	Observed effect on synaptic vesicle cycle	<i>In vitro</i> and <i>in vivo</i> model	Reference
A $\beta$	Soluble oligomers (200 nM/2h)	A $\beta$ oligomers have been found to alter the recycling/resting pool ratio by expanding the resting fraction at the expense of the recycling fraction, without altering the average total number of synaptic vesicles.  Such A $\beta$ -driven effect on pool size was mediated by the activation of CDK5, the main kinase involved in the regulation of synaptic vesicle pool size (Kim and Ryan, 2010).	Cultured rat hippocampal neurons	[69]
A $\beta$ <sub>42</sub>	Soluble oligomers (300 nM/30 min)	At presynaptic terminals, A $\beta$ <sub>42</sub> enhanced the levels of phosphorylated Synapsin I at Ser <sup>9</sup> , thus increasing the availability of synaptic vesicles to dock to the active zone and to allow glutamate release.	Primary rat hippocampal neurons	[79]
A $\beta$ <sub>42</sub>	Soluble oligomers (200 nM)	A $\beta$ <sub>42</sub> markedly enhanced the levels of phosphorylated Synapsin at Ser <sup>9</sup> by activating CaMKIV. As a result, Synapsin I has been found to disassemble either from synaptic vesicles and actin.	Rat hippocampal neurons	[80]

## 2.1. Regulation of synaptic vesicle exocytosis

Exocytosis of synaptic vesicles is mediated by a conserved array of membrane proteins, commonly known as SNAREs (soluble N-ethylmaleimide-sensitive factor attachment protein (SNAP) receptors) [33]. These proteins include synaptobrevin/VAMP (vesicle-associated membrane protein), which is located on the membrane of synaptic vesicles (v-SNARE), syntaxin 1 and SNAP 25, which are predominantly localized at the synaptic plasma membrane (t-SNARE). In neurons, Synaptobrevin-2/VAMP2 has been found to bind to syntaxin 1a and SNAP-25, located on the presynaptic membrane, thereby assembling a tight stoichiometric complex that catalyzes membrane fusion for exocytosis [34]. Fusion-competent conformations of SNARE proteins are maintained by chaperone complexes composed by CSP $\alpha$  (Cysteine string protein  $\alpha$ ), Hsc70 (Heat shock cognate 70), and SGT (small glutamine-rich tetratricopeptide repeat protein) and by non-enzymatically acting synuclein chaperones. The folding/refolding of SNARE proteins is regulated by several synaptic modulators, such as  $\alpha$ -synuclein ( $\alpha$ -syn) [35]. After fusion, the disassembly of SNARE complexes is mediated by ATPase N-ethylmaleimide-sensitive factor (NSF) and its cofactors SNAPs [36]. Disassembled t-SNAREs are immediately available to participate

in subsequent vesicle docking and fusion reactions, whereas v-SNAREs have to be recycled to the donor membrane before engaging in productive SNARE complex assembly [33].

Sharma *et al.* demonstrated for the first time that, in neurodegenerative diseases including AD, the membrane-fusion machinery is strongly altered [37, 38] and that the level of SNARE complex assembly, necessary for driving synaptic vesicle fusion at the presynaptic active zone, is substantially decreased in postmortem brains of AD patients [39]. The authors suggest a potential involvement of A $\beta$  as hindering of SNARE-mediated fusion of synaptic vesicle. In line with such hypothesis, Yang *et al.* demonstrated by biochemical assay *in vitro* that both A $\beta$ 42 monomers and oligomers are capable to specifically bind to the SNARE motif region (SynH3) of syntaxin 1a [30], which forms a four-helix bundle necessary for membrane fusion [40, 41]. However, only oligomeric form of A $\beta$  (10  $\mu$ M) has been found to exert an inhibitory effect on the SNARE complex assembly and SNARE-mediated exocytosis in A $\beta$ PP-PS1 mice. In particular, oligomeric form of A $\beta$  inhibits the fusion step between docking and lipid mixing by binding to the SNARE motif of syntaxin-1a, without changing the expression of SNARE proteins [30]. This study identifies a potential molecular mechanism by which intracellular A $\beta$  oligomers hinder SNARE-mediated exocytosis, possibly leading to synaptic dysfunctions occurring in AD. Otherwise, A $\beta$  monomers failed to exhibit any inhibitory effects on SNARE complex assembly or SNARE-mediated exocytosis, despite their proved capability to bind to syntaxin-1a. Impairments of synaptic vesicle docking by monomeric and oligomeric form of A $\beta$  have not been observed. Such evidence suggests a differential sensitivity of synaptic vesicle docking and fusion to A $\beta$ . A possible explanation is that the steric hindrance of A $\beta$  oligomers inhibits the “zippering” of SNARE proteins into the *cis*-SNARE complex, but not influences their partial assembly into the *trans*-SNARE complex required for docking. Future investigations are needed to better examine how A $\beta$  differentially influences the docking and fusion of synaptic vesicle at presynaptic terminals. Moreover, another issue to fully elucidate concerns the presence of intraneuronal A $\beta$  accumulations, whose occurrence and relevance in AD have been a matter of controversial scientific debate. First reports showing that A $\beta$  is initially deposited in neurons before occurring in the extracellular space date back roughly 20 years [42]. More recently, intracellular A $\beta$ 42 accumulations have been identified in basal forebrain cholinergic neurons in adult human brain explants and increases in the prevalence of intermediate and large oligomeric assembly states are related to both aging and AD [43]. Such early accumulation of A $\beta$ 42 seems to be a selective feature of basal forebrain cholinergic neurons when compared with cortex, and not due to differences in A $\beta$ PP expression [43]. Accordingly, studies with transgenic animal models of AD have further supported the presence of intraneuronal A $\beta$  before the appearance of extracellular deposits [44, 45]. Observations concerning an intracellular activity of A $\beta$  are

also present in *in vitro* models. Even if data are not at the synaptic level there is evidence that A $\beta$ 40 and A $\beta$ 42 at pM and nM concentrations are able to interfere with the pathways regulating the maintenance of genomic integrity, thus resulting in the comparison of dysfunctional cells [46].

Another interplay between A $\beta$  and a synaptic vesicle-associated protein has been reported by Russel *et al.* This study demonstrated that, in rat CA3-CA1 hippocampal neurons, the acute application of low concentrations (50 nM) of A $\beta$ 42 was followed by its internalization and localization to presynaptic terminals, where the peptide interacted with Synaptophysin-1, a glycoprotein that binds VAMP2 [29]. At the cell soma, the interaction between Synaptophysin-1 and VAMP2 has been found to regulate the transport of this latter from the Golgi to the synapse, whereas, at presynaptic compartment, to control the availability of VAMP2 to participate to the assembly of SNARE complex, necessary for regulated exocytosis [47]. A $\beta$ 42 has been demonstrated to directly compete with VAMP2 for binding Synaptophysin-1 at synaptic contacts and to prevent the formation of Synaptophysin/VAMP2 complex. As a result, A $\beta$ 42 contributed to the formation of the fusion pore complex, resulting in the expansion of the primed synaptic vesicle pool, followed by neurotransmitter release [29]. Consistently, the enhancement of single shock fEPSPs (field excitatory post-synaptic potential) by A $\beta$ 42 at synapses further suggest an increased availability of releasable synaptic vesicles in hippocampal slices [29]. To prove that the enhancement of fEPSPs is not an artefact of the synthetic peptide, hippocampal slices were incubated with cell derived oligomers providing similar results.

Despite these data, a full comprehension of the intracellular mechanism through which A $\beta$  influences the SNARE-mediated priming and fusion of synaptic vesicles and, subsequently, the release of neurotransmitter from presynaptic terminals is still under debate. Data from literature suggest that posttranslational modifications, such as phosphorylation, of SNARE and accessory proteins by protein kinases at specific sites might represent a key regulatory mechanism that tightly modulates the exocytosis of synaptic vesicles and, consequently, neurotransmitter release from presynaptic terminals [41]. Moreover, taking into account that A $\beta$  affects protein kinase transduction machinery [48, 49], it could be hypothesized that A $\beta$  influences the phosphorylation of SNARE and accessory protein and, subsequently, the assembly of SNARE complex by interacting with the transduction machinery of protein kinases. Within this context, experimental results demonstrated that low concentrations of A $\beta$  inhibit the *in vivo* dopamine release in the rat nucleus accumbens (NAc) and counteract *in vitro* the muscarinic receptor-activated dopamine release from dopaminergic terminals by impairing protein kinase C (PKC) transduction machinery [50]. This hypothesis is further supported by *in vitro* results showing that the t-ACPD-induced

PKC-mediated release of DA, elicited by the presynaptic metabotropic glutamate receptors (mGluRs) located on striatal nerve endings, was completely antagonized by A $\beta$ 40 [51]. Such an action has also been demonstrated on signaling cascades downstream mGluRs, where 1  $\mu$ M A $\beta$  has been reported to impair mGluRs regulation of the  $\gamma$ -aminobutyric acid (GABA) transmission by inhibiting PKC transduction machinery in prefrontal cortical neurons [48]. Accordingly, Zhong *et al.* showed that A $\beta$  impairs the muscarinic regulation of GABA transmission in prefrontal cortex, acting on the transduction machinery downstream muscarinic receptors and, particularly, inhibiting PKC [49]. Altogether, all these data point PKC as one of the potential substrates for A $\beta$  inhibitory actions, a view which is also supported by data on a reduced PKC activity/content in tissues derived from AD patients [52, 53]. Interestingly, PKC has been demonstrated to serve a key role in post-translational modifications of SNARE and accessory proteins. The activation of PKC has been observed to enhance the exocytosis of synaptic vesicles by phosphorylating SNARE proteins including SNAP-25, Munc-18, and synaptotagmin [54–56]. In particular, phosphorylation of SNAP-25 at Ser187 in the SNARE domain [57] has been associated to an increased exocytosis of synaptic vesicles [58]. Katayama *et al.* recently demonstrated that knock-in (KI) mice deficient in the phosphorylation by replacing Ser187 of SNAP-25 with Ala exhibit an accumulation of synaptic vesicles in enlarged presynaptic terminals and a decreased efficacy of basal synaptic transmission at hippocampal CA1 synapses [59]. Moreover, Gao *et al.* found that phosphorylation of SNAP-25 by PKC regulates the exocytosis of synaptic vesicles and, consequently, noradrenaline release in PC12 cells, by affecting the SNARE complex assembly [60]. Phosphorylation of SNAP-25 at Ser187 by PKC has been found to increase the amount of bound VAMP-2. Such a finding suggests that Ser187-phosphorylation may either upregulate v-SNARE (VAMP-2) binding to preexisting t-SNARE (SNAP-25) or increase the stability of ternary SNARE complex, thereby promoting SNARE complex assembly and enhancing Ca<sup>2+</sup>-dependent exocytosis. Phosphorylation of SNAP-25 at Ser187 by PKC has also been found to enhance Ca<sup>2+</sup>-dependent release of dopamine and acetylcholine in PC12 cells [57].

Altogether, the involvement of PKC in the regulation of SNARE complex formation and experimental results demonstrating A $\beta$ -induced impairment of PKC transduction machinery support the hypothesis that A $\beta$  may also affect the exocytosis of synaptic vesicle by acting on protein kinases. Notably, Lee *et al.* first demonstrated that A $\beta$  can modulate PKC activity by inhibiting PKC phosphorylation in a dose-dependent manner in cell-free *in vitro* condition [61], thus suggesting a direct interaction between A $\beta$  and PKC. However, further investigations are needed to define A $\beta$ -driven direct and indirect modulatory effects on PKC activity and to reveal the exact action mechanism underlying A $\beta$  regulation of PKC activity.



At a first glance, the emerging role of the direct monomeric A $\beta$  protein interaction with synaptic proteins seems to point to a putative facilitatory role on synaptic release machinery. It is not easy to predict what will be the consequences of a disease associated excessive A $\beta$  production and oligomer formation. It can be postulated that, at preliminary step, synapses will face the upregulation of a reinforcing mechanism, leading to an excess of signaling which may contribute, for example, to excitotoxicity. With time and A $\beta$  oligomer accumulation the picture may change.

## 2.2. Regulation of endocytosis

In neurons, synaptic vesicle endocytosis is controlled by a wide array of regulatory and adaptor proteins including epsin, AP-2 (adaptor protein-2), AP-180 (adaptor protein-180), and dynamin [62]. This latter is a GTPase synaptic protein, highly enriched in presynaptic terminals and involved in synaptic vesicle endocytosis and recovery. It promotes fission, pinching off, and recycling of synaptic vesicles, allowing them to reenter the synaptic vesicle pool to be refilled for future release [63, 64] and its levels and function are regulated by its cleavage by calpain. A decrease in dynamin levels due to its cleavage by calpain has been observed to inhibit synaptic vesicle endocytosis and, subsequently, their refill with neurotransmitters [65]. Interestingly, A $\beta$ 42 has been reported to affect synaptic vesicle recycling acting on dynamin-1. Kelly *et al.* demonstrated that, in rat stimulated hippocampal neurons, high concentration (2  $\mu$ M) of A $\beta$ 42 soluble oligomers impair synaptic vesicle endocytosis and that such disruption was, at least in part, dependent on dynamin-1 depletion induced by calpain activation [66, 67]. However, further investigations are required to examine the specific action mechanism by which A $\beta$  soluble oligomers stimulate calpain activation and to evaluate the functional consequences of A $\beta$ -mediated dynamin-1 depletion in neurons.

Furthermore, A $\beta$ 42 at nanomolar concentrations (50 nM) has been demonstrated to compete with VAMP2 for binding to Synaptophysin-1 at the synapse [29], which is known to regulate the retrieval kinetics of VAMP2 during endocytosis [68]. A $\beta$ 42 has been postulated to hinder the ability of Synaptophysin-1 to initiate synaptic vesicle endocytosis via its interaction with VAMP2 [29]. Such hypothesis implies that A $\beta$  peptides may act as a negative regulator of synaptic vesicle endocytosis after fusion and is consistent with data from literature demonstrating the A $\beta$ -driven disruption of endocytosis and depletion of synaptic vesicles [66, 69].

Among these data, a work by Park *et al.* demonstrated that acute exposure (2 h) of rat stimulated hippocampal neurons to nanomolar concentrations (200 nM) of synthetic A $\beta$

oligomers and monomers transiently reduced the efficacy of synaptic vesicle endocytosis [69]. When A $\beta$  oligomer-containing medium was replaced with control medium after 2 h of exposure, endocytosis recovered to normal levels, indicating that A $\beta$  oligomers-induced effects on endocytosis are transient and not permanent. Prolonged treatment (72 h) of neurons with the same concentration of A $\beta$  oligomers has been shown to induce more severe defects, compared to acute treatment, in synaptic vesicle endocytosis, thus demonstrating that the extent of A $\beta$ -induced endocytic damage also depends on the time of exposure [69]. Interestingly, defects in synaptic vesicle endocytosis were not observed when hippocampal neurons were exposed to the same preparation containing only A $\beta$  monomers. Such result provides evidence that endocytosis was impaired by A $\beta$  oligomers, even at low concentration, and not by monomers, thus suggesting that the aggregation states of A $\beta$  peptides may be a key factor in A $\beta$ -driven effects on synaptic vesicle endocytosis. Notably, PIPkinase- $\gamma$  (phosphatidylinositol-4-phosphate-5-kinase type I- $\gamma$ ) overexpression, which is known to increase PtdIns(4,5)P<sub>2</sub> (phosphatidylinositol-4,5-bisphosphate) levels, completely prevented the A $\beta$ -induced defects in endocytosis in rat stimulated hippocampal neurons [69]. Accordingly, Berman *et al.* found that A $\beta$  oligomers induced a reduction in PtdIns(4,5)P<sub>2</sub> levels via phospholipase C (PLC). In addition, PtdIns(4,5)P<sub>2</sub> has been demonstrated to affect clathrin-mediated endocytic processes by binding several endocytic components, including AP-2, AP-180, dynamin, and epsin, thus playing an key role in recruiting these molecules to sites of endocytosis [70–74]. Collectively, these findings support the hypothesis that PIPkinase- $\gamma$  overexpression compensates for the A $\beta$  oligomers-induced decrease in PtdIns(4,5)P<sub>2</sub> levels, whose abnormally reduced or increased levels have been linked to defects in synaptic vesicle endocytosis [75].

Furthermore, Lazarevic *et al.* tested the effects on synaptic vesicle recycling of increased extracellular concentrations of A $\beta$ 42 and A $\beta$ 40 (1.6- and 1.2-fold, respectively), induced by the inhibition of the A $\beta$ -degrading enzyme neprilysin, in rat cortical and hippocampal neurons cultures [76]. Enhanced levels of A $\beta$ 40 and A $\beta$ 42 have been found to increase the activity-driven synaptic vesicles recycling in both excitatory and inhibitory synapses, as shown by quantification of synaptotagmin 1 antibody uptake. Such effect was completely prevented by chelation of extracellular A $\beta$  using 4G8 antibody, thus confirming that changes in synaptic vesicle recycling rely on the concentrations of the endogenously secreted A $\beta$  peptides. In line with this evidence, treatment either with  $\beta$ -secretase or  $\gamma$ -secretase inhibitors led to a significant decrease in synaptic vesicle recycling, strongly supporting the involvement of endogenous A $\beta$  peptides in the modulation of basal synaptic vesicle recycling. Moreover, 1-h exposure to picomolar (200 pM) concentrations of synthetic A $\beta$ 40 and A $\beta$ 42 induced a significant enhancement in synaptotagmin 1 antibody

uptake; whereas, 1-h treatment with 1  $\mu$ M A $\beta$  has been found to decrease it. Collectively, these experimental results are consistent with the hypothesis of an hormetic effect of A $\beta$  peptides, with low concentration (high picomolar) potentiating synaptic vesicle recycling and high (high nanomolar-low micromolar) exhibiting the opposite effect in the same experimental setting.

Furthermore, the effects on depolarization-driven synaptic vesicle recycling, induced both by inhibition of A $\beta$  degradation and application of 200 pM A $\beta$ 42, have been demonstrated to be fully inhibited by pretreatment with  $\alpha$ -bungarotoxin, thus suggesting the involvement of functional  $\alpha$ 7-nAChR in A $\beta$ -mediated regulation of presynaptic functions [76]. While the effect of 200 pM A $\beta$ 40 and A $\beta$ 42 was completely prevented by pharmacological interference with  $\alpha$ 7-nAChR, the effect of 1  $\mu$ M A $\beta$ 42 was not hindered by the blockage of these receptors, suggesting that, at higher concentrations, A $\beta$ 42 may act through different action mechanisms.

Moreover, the endogenous A $\beta$ -driven modulation of synaptic vesicle recycling has been hypothesized to rely on calpain-cyclin dependent kinase 5 (CDK5) and calcineurin signaling pathway downstream of  $\alpha$ 7-nAChR. A CDK5 and calcineurin activity assay confirmed that cells treated with neprilysin inhibitor and 200 pM A $\beta$ 42 showed significant decrease in CDK5 activity, without changes in total protein levels; on the other hand, a phosphatase activity assay revealed significantly higher calcineurin activity [76]. Such results indicate that balancing the activity of CDK5 and calcineurin may play a role in A $\beta$ -driven modulation of recycling. However, further investigations are needed to better characterize the specific intracellular mechanism through which A $\beta$  regulates this step of synaptic vesicle cycle. To date, only few studies investigated A $\beta$ -driven effects on synaptic vesicle recycling and the potential underlying intracellular mechanism.

Overall, the defects of endocytosis elicited by A $\beta$  oligomers, as well as monomers, may aggravate the synaptic derangement as the disease progresses. The impairment of endocytosis might alter the ability of the synapse to sustain neurotransmitter release, particularly at the level of nerve terminals discharging at high rate, leading to their dysfunction.

### **2.3. Regulation of recycling/resting pool ratio**

The synaptic vesicle pool constitutes a recycling pool, including a ready releasable pool, which is docked at the active zone and ready for immediate release, and a reserve pool, a reservoir to refill vesicles after depletion, and a resting pool that does not normally

participate in the synaptic vesicle recycling. Park *et al.* (2013) observed that the acute treatment (2 h) of cultured rat hippocampal neurons with nanomolar concentrations (200 nM) of soluble A $\beta$  oligomers altered the recycling/resting pool ratio by expanding the resting fraction at the expense of the recycling fraction [69]. The average total number of synaptic vesicles has not been altered. Pretreatment of A $\beta$  oligomers with 6E10 antibody blocked the effect on recycling/resting pool, thus indicating that alteration of the recycling/resting pool ratio relies on A $\beta$  oligomers. In addition, they suggested that the observed effects of A $\beta$  oligomers on pool size are mediated by the activation of CDK5 pathway. Consistently, the CDK5 inhibitor roscovitine and the calpain inhibitor III have been observed to restore the recycling and resting pool near to control levels. Such evidence demonstrates that CDK5 mediates A $\beta$  oligomers-induced alterations of the recycling/resting pool size, an observation consistent with data from literature pointing CDK5 as the main kinase involved in the regulation of synaptic vesicle pool size [76, 77].

Moreover, two independent studies by Marsh *et al.* and Park *et al.* recently proved that soluble A $\beta$ 42 oligomers interfere with Synapsin I, a presynaptic adaptor phosphoprotein, that, under resting conditions, tethers synaptic vesicles to the cytoskeletal network clustering them in the resting pool, by interacting both with synaptic vesicles and the actin cytoskeleton [78–80]. Activity-dependent phosphorylation of Synapsin I at Ser9 within a small N-terminal lipid-binding domain by protein kinase A (PKA) and Ca<sup>2+</sup>/calmodulin-dependent protein kinase IV (CaMKIV) induces its transient disassembly from synaptic vesicles [81] and stimulates the release of synaptic vesicles from the resting pool, enabling their participating in neurotransmitter release. A $\beta$  has been reported to affect the phosphorylation/dephosphorylation dynamics of Synapsin I [79, 80]. Marsh *et al.* demonstrated that the acute exposure (30 min) of primary rat hippocampal neurons to nanomolar concentrations (300 nM) of A $\beta$ 42 oligomers enhanced the levels of phosphorylated Synapsin I at Ser9 after neuronal activity at presynaptic terminals [79]. While in neurons exposed to scrambled A $\beta$ 42 peptide, the enhanced levels of phosphorylated Synapsin I at Ser9 have not been detected, confirming that the effect is mediated by A $\beta$ 42 oligomers. The prolonged phosphorylation of Synapsin I has been found to prevent Synapsin I from tethering synaptic vesicles to the reserve pool after depolarization, thus increasing the availability of synaptic vesicles to dock to the active zone and, consequently, to allow glutamate release from presynaptic terminals [79]. Such hypothesis is consistent with several reports showing that A $\beta$ 42 oligomers affect glutamate release in a concentration and time dependent manner [11, 15, 29, 82]. Interestingly, the levels of phosphorylated Synapsin I at Ser9 are increased in postmortem tissue from AD patients [83]. Accordingly, Park *et al.*, using a live-cell imaging technique to monitor synaptic vesicle trafficking, demonstrated that the exposure of rat hippocampal neurons to

nanomolar concentrations (200 nM) of soluble A $\beta$ 42 oligomers markedly enhances the levels of phosphorylated Synapsin at Ser9 by activating CaMKIV. As a result, Synapsin I has been found to disassemble either from synaptic vesicles and actin, subsequently inhibiting the intersynaptic vesicular trafficking along the axon [80]. However, it is still unclear how soluble A $\beta$ 42 oligomers increase intracellular Ca<sup>2+</sup> that is critical for the phosphorylation-dependent dissociation of Synapsin-synaptic vesicles-actin ternary complex. Recently, soluble A $\beta$ 42 oligomers have been demonstrated to increase intracellular Ca<sup>2+</sup> both enhancing extracellular Ca<sup>2+</sup> influx and Ca<sup>2+</sup> release from mitochondria [84].

### 3. Concluding remarks

Despite the intense effort directed to develop novel therapeutic interventions for the treatment of AD, to date no drugs are yet available to significantly benefit people affected by AD and the few approved drugs so far can only be used for symptomatic treatment of the disease, but not to prevent or reverse it. The main strategy for the development of drugs counteracting AD has been to reduce A $\beta$  accumulation due to its overproduction and/or defective clearance. However, the proved ineffectiveness shown by such approaches, specifically targeting the production or clearance of A $\beta$  peptides, has sparked an intense debate in the scientific community concerning the validity of the amyloid cascade hypothesis. Nevertheless, the neuronal dysfunction caused by A $\beta$  accumulation is still recognized as a significant factor contributing to the progression AD that cannot be discounted [3]. The failure of several clinical trials to meet the desired endpoints highlights the necessity to refocus the experimental approach from frank neurodegeneration on early pathogenic alterations that may cause or contribute to AD. Defective synaptic activity and loss of synapses are the earliest event in AD that precedes the accumulation of A $\beta$  plaques in the brain and clinical outcomes of the disease [5]. In particular, it emerges from the previous paragraphs that during progression of the disease two phenomena may lead the transition from physiology to pathology. At the beginning the increasing concentrations of A $\beta$  monomers may lead to synaptic reinforcement through fusion stimulation and endocytosis inhibition. With further increase of A $\beta$  and the onset of aggregation phenomena the exocytosis inhibition may prevail leading to the impairment of nerve terminals, mainly of those discharging at a high frequency rate, accompanied by an inhibition of the release leading to a more generalized synaptic failure. In all phases, additional intracellular signaling effects exerted through an action of A $\beta$  on kinases may add further complexity in an area-dependent manner. Hence, a deeper understanding of the mechanisms through which A $\beta$  peptides affect synaptic activity and, in particular, synaptic vesicle dynamics orchestrating neurotransmitter release, is needed to elucidate A $\beta$

functions and might be a starting point to understand the early phases and manifestation of the disease as well to design new neurotransmitter/synaptic based strategies to correct these symptoms.

## REFERENCES

- [1] Hardy J, Selkoe DJ (2002) The amyloid hypothesis of Alzheimer's disease: Progress and problems on the road to therapeutics. *Science* 297, 353-356.
- [2] Arendt T (2009) Synaptic degeneration in Alzheimer's disease. *Acta Neuropathol* 118, 167-79.
- [3] Forner S, Baglietto-Vargas D, Martini AC, Trujillo-Estrada L, LaFerla FM (2017) Synaptic impairment in Alzheimer's disease: A dysregulated symphony. *Trends Neurosci* 40, 347-357.
- [4] Glenner GG, Wong CW (1984) Alzheimer's disease: Initial report of the purification and characterization of a novel cerebrovascular amyloid protein. *Biochem Biophys Res Commun* 120, 885-890.
- [5] Lambert MP, Barlow AK, Chromy BA, Edwards C, Freed R, Liosatos M, Morgan TE, Rozovsky I, Trommer B, Viola KL, Wals P, Zhang C, Finch CE, Krafft GA, Klein WL (1998) Diffusible, nonfibrillar ligands derived from Abeta1-42 are potent central nervous system neurotoxins. *Proc Natl Acad Sci U S A* 95, 6448-6453.
- [6] Mucke L, Selkoe DJ (2012) Neurotoxicity of amyloid  $\beta$ - protein: Synaptic and network dysfunction. *Cold Spring Harb Perspect Med* 2, a006338.
- [7] Hartley DM, Walsh DM, Ye CP, Diehl T, Vasquez S, Vassilev PM, Teplow DB, Selkoe DJ (1999) Protofibrillar intermediates of amyloid  $\beta$ -protein induce acute electrophysiological changes and progressive neurotoxicity in cortical neurons. *J Neurosci* 19, 8876-8884.
- [8] Shankar GM, Li S, Mehta TH, Garcia-Munoz A, Shepardson NE, Smith I, Brett FM, Farrell MA, Rowan MJ, Lemere CA, Regan CM, Walsh DM, Sabatini BL, Selkoe DJ (2008) Amyloid- $\beta$  protein dimers isolated directly from Alzheimer's brains impair synaptic plasticity and memory. *Nat Med* 14, 837-842.
- [9] Kamenetz F, Tomita T, Hsieh H, Seabrook G, Borchelt D, Iwatsubo T, Sisodia S, Malinow R (2003) APP processing and synaptic function. *Neuron* 37, 925-937.
- [10] Cirrito JR, Yamada KA, Finn MB, Sloviter RS, Bales KR, May PC, Schoepp DD, Paul SM, Mennerick S, Holtzman DM (2005) Synaptic activity regulates interstitial fluid amyloid- $\beta$  levels *in vivo*. *Neuron* 48, 913-922.
- [11] Abramov E, Dolev I, Fogel H, Ciccotosto GD, Ruff E, Slutsky I (2009) Amyloid- $\beta$  as a positive endogenous regulator of release probability at hippocampal synapses. *Nat Neurosci* 12, 1567-1576.
- [12] Gulisano W, Melone M, Li Puma DD, Tropea MR, Palmeri A, Arancio O, Grassi C, Conti F, Puzzo D (2018) The effect of amyloid- $\beta$  peptide on synaptic plasticity and memory is influenced by different isoforms, concentrations, and aggregation status. *Neurobiol Aging* 71, 51-60.

- [13] Bisceglia F, Natalello A, Serafini MM, Colombo R, Verga L, Lanni C, De Lorenzi E (2018) An integrated strategy to correlate aggregation state, structure and toxicity of A $\beta$  1–42 oligomers. *Talanta* 188, 17-26.
- [14] Puzzo D, Arancio O (2012) Amyloid- $\beta$  peptide: Dr. Jekyll or Mr. Hyde? *J Alzheimers Dis* 33(Suppl 1), S111-S120.
- [15] Puzzo D, Privitera L, Leznik E, Fa M, Staniszewski A, Palmeri A, Arancio O (2008) Picomolar amyloid- $\beta$  positively modulates synaptic plasticity and memory in hippocampus. *J Neurosci* 28, 14537-14545.
- [16] Lanni C, Fagiani F, Racchi M, Preda S, Pascale A, Grilli M, Allegri N, Govoni S (2019) Beta-amyloid short- and long- term synaptic entanglement. *Pharmacol Res* 139, 243-260.
- [17] Gulisano W, Melone M, Ripoli C, Tropea MR, Li Puma DD, Giunta S, Cocco S, Marcotulli D, Origlia N, Palmeri A, Arancio O, Conti F, Grassi C, Puzzo D (2019) Neuromodulatory action of picomolar extracellular A $\beta$ 42 oligomers on presynaptic and postsynaptic mechanisms underlying synaptic function and memory. *J Neurosci* 39, 5986-6000.
- [18] Fogel H, Frere S, Segev O, Bharill S, Shapira I, Gazit N, O'Malley T, Slomowitz E, Berdichevsky Y, Walsh DM, Isacoff EY, Hirsch JA, Slutsky I (2014) APP homodimers transduce an amyloid- $\beta$ -mediated increase in release probability at excitatory synapses. *Cell Rep* 7, 1560-1576.
- [19] Seabrook GR, Smith DW, Bowery BJ, Easter A, Reynolds T, Fitzjohn SM, Morton RA, Zheng H, Dawson GR, Sirinathsinghji DJS, Davies CH, Collingridge GL, Hilla RG (1999) Mechanisms contributing to the deficits in hippocampal synaptic plasticity in mice lacking amyloid precursor protein. *Neuropharmacology* 38, 349-359.
- [20] Saura CA, Choi SY, Beglopoulos V, Malkani S, Zhang D, Rao BSS, Chattarji S, Kelleher RJ, Kandel ER, Duff K, Kirkwood A, Shen J (2004) Loss of presenilin function causes impairments of memory and synaptic plasticity followed by age-dependent neurodegeneration. *Neuron* 42, 23-36.
- [21] Laird FM, Cai H, Savonenko AV, Farah MH, He K, Melnikova T, Wen H, Chiang HC, Xu G, Koliatsos VE, *et al.* (2005) BACE1, a major determinant of selective vulnerability of the brain to amyloid- $\beta$  amyloidogenesis, is essential for cognitive, emotional, and synaptic functions. *J Neurosci* 25, 11693-11709.
- [22] Wang HY, Lee DHS, Davis CB, Shank RP (2000) Amyloid peptide A $\beta$ 1-42 binds selectively and with picomolar affinity to  $\alpha$ 7 nicotinic acetylcholine receptors. *J Neurochem* 75, 1155-1161.
- [23] Dougherty JJ, Wu J, Nichols RA (2003)  $\beta$ -amyloid regulation of presynaptic nicotinic receptors in rat hippocampus and neocortex. *J Neurosci* 23, 6740-6747.
- [24] Wei W, Nguyen LN, Kessels HW, Hagiwara H, Sisodia S, Malinow R (2010) Amyloid beta from axons and dendrites reduces local spine number and plasticity. *Nat Neurosci* 13, 190-196.
- [25] Walsh DM, Klyubin I, Fadeeva J V., Cullen WK, Anwyl R, Wolfe MS, Rowan MJ, Selkoe DJ (2002) Naturally secreted oligomers of amyloid  $\beta$  protein potently inhibit hippocampal long-term potentiation *in vivo*. *Nature* 416, 535-539.
- [26] Hsieh H, Boehm J, Sato C, Iwatsubo T, Tomita T, Sisodia S, Malinow R (2006) AMPAR removal underlies A $\beta$ -induced synaptic depression and dendritic spine loss. *Neuron* 52, 831-843.

- [27] Koppensteiner P, Trinchese F, Fa M, Puzzo D, Gulisano W, Yan S, Poussin A, Liu S, Orozco I, Dale E, Teich AF, Palmeri A, Ninan I, Boehm S, Arancio O (2016) Time-dependent reversal of synaptic plasticity induced by physiological concentrations of oligomeric A $\beta$ 42: An early index of Alzheimer's disease. *Sci Rep* 1, 6-32553.
- [28] Südhof TC (2004) The synaptic vesicle cycle. *Annu Rev Neurosci* 27, 509-547.
- [29] Russell CL, Semerdjieva S, Empson RM, Austen BM, Beesley PW, Alifragis P (2012) Amyloid- $\beta$  acts as a regulator of neurotransmitter release disrupting the interaction between synaptophysin and VAMP2. *PLoS One* 7, e43201.
- [30] Yang Y, Kim J, Kim HY, Ryoo N, Lee S, Kim YS, Rhim H, Shin YK (2015) Amyloid- $\beta$  oligomers may impair SNARE-mediated exocytosis by direct binding to Syntaxin 1a. *Cell Rep* 12, 1244-1251.
- [31] Ovsepian SV, O'Leary VB, Zaborszky L, Ntziachristos V, Dolly JO (2018) Synaptic vesicle cycle and amyloid  $\beta$ : Biting the hand that feeds. *Alzheimers Dement* 14, 502-513.
- [32] Marsh J, Alifragis P (2018) Synaptic dysfunction in Alzheimer's disease: The effects of amyloid beta on synaptic vesicle dynamics as a novel target for therapeutic intervention. *Neural Regen Res* 13, 616-623.
- [33] Südhof TC, Rizo J (2011) Synaptic vesicle exocytosis. *Cold Spring Harb Perspect Biol* 3, a005637.
- [34] Südhof TC, Rothman JE (2009) Membrane fusion: Grasping with SNARE and SM proteins. *Science* 323, 474-477.
- [35] Burre J, Sharma M, Tsetsenis T, Buchman V, Etherton MR, Südhof TC (2010)  $\alpha$ -Synuclein promotes SNARE-complex assembly *in vivo* and *in vitro*. *Science* 329, 1664-1668.
- [36] Söllner T, Bennett MK, Whiteheart SW, Scheller RH, Rothman JE (1993) A protein assembly-disassembly pathway *in vitro* that may correspond to sequential steps of synaptic vesicle docking, activation, and fusion. *Cell* 75, 409-418.
- [37] Garcia-Reitbötrck P, Anichtchik O, Bellucci A, Iovino M, Ballini C, Fineberg E, Ghetti B, Della Corte L, Spano P, Tofaris GK, Goedert M, Spillantini MG (2010) SNARE protein redistribution and synaptic failure in a transgenic mouse model of Parkinson's disease. *Brain* 133(Pt 7), 2032-2044.
- [38] Shen J, Rathore SS, Khandan L, Rothman JE (2010) SNARE bundle and syntaxin N-peptide constitute a minimal complement for Munc18-1 activation of membrane fusion. *J Cell Biol* 190, 55-63.
- [39] Sharma M, Burre J, Südhof TC (2012) Proteasome inhibition alleviates SNARE-dependent neurodegeneration. *Sci Transl Med* 4, 147ra113.
- [40] Poirier MA, Xiao W, Macosko JC, Chan C, Shin YK, Bennett MK (1998) The synaptic SNARE complex is a parallel four-stranded helical bundle. *Nat Struct Biol* 5, 765-769.
- [41] Sutton RB, Fasshauer D, Jahn R, Brunger AT (1998) Crystal structure of a SNARE complex involved in synaptic exocytosis at 2.4 Å resolution. *Nature* 395, 347-353.



- [42] Masters CL, Multhaup G, Simms G, Pottgiesser J, Martins RN, Beyreuther K (1985) Neuronal origin of a cerebral amyloid: Neurofibrillary tangles of Alzheimer's disease contain the same protein as the amyloid of plaque cores and blood vessels. *EMBO J* 4, 2757-2763.
- [43] Baker-Nigh A, Vahedi S, Davis EG, Weintraub S, Bigio EH, Klein WL, Geula C (2015) Neuronal amyloid- $\beta$  accumulation within cholinergic basal forebrain in ageing and Alzheimer's disease. *Brain* 138(Pt 6), 1722-1237.
- [44] LaFerla FM, Green KN, Oddo S (2007) Intracellular amyloid-beta in Alzheimer's disease. *Nat Rev Neurosci* 8, 499-509.
- [45] Li M, Chen L, Lee DHS, Yu LC, Zhang Y (2007) The role of intracellular amyloid  $\beta$  in Alzheimer's disease. *Prog Neurobiol* 83, 131-139.
- [46] Lanni C, Necchi D, Pinto A, Buoso E, Buizza L, Memo M, Uberti D, Govoni S, Racchi M (2013) Zyxin is a novel target for beta-amyloid peptide: Characterization of its role in Alzheimer's pathogenesis. *J Neurochem* 125, 790-799.
- [47] Pennuto M, Bonanomi D, Benfenati FVF (2003) Synaptophysin I controls the targeting of VAMP2/synaptobrevin II to synaptic vesicles. *Mol Biol Cell* 14, 4909-4919.
- [48] Tyszkiewicz JP, Yan Z (2005) Beta-amyloid peptides impair PKC-dependent functions of metabotropic glutamate receptors in prefrontal cortical neurons. *J Neurophysiol* 93, 3102-3111.
- [49] Zhong P, Gu Z, Wang X, Jiang H, Feng J, Yan Z (2003) Impaired modulation of GABAergic transmission by muscarinic receptors in a mouse transgenic model of Alzheimer's disease. *J Biol Chem* 278, 26888-26896.
- [50] Preda S, Govoni S, Lanni C, Racchi M, Mura E, Grilli M, Marchi M (2008) Acute  $\beta$ -amyloid administration disrupts the cholinergic control of dopamine release in the nucleus accumbens. *Neuropsychopharmacology* 33, 1062-1070.
- [51] Mura E, Lanni C, Preda S, Pistoia F, Sara M, Racchi M, Schettini G, Marchi M, Govoni S (2010) Beta-amyloid: A disease target or a synaptic regulator affecting age-related neurotransmitter changes? *Curr Pharm Des* 16, 672-683.
- [52] Govoni S, Bergamaschi S, Racchi M, Battaini F, Binetti G, Bianchetti A, Trabucchi M (1993) Cytosol protein kinase C downregulation in fibroblasts from Alzheimer's disease patients. *Neurology* 43, 2581-2586.
- [53] Battaini F, Pascale A, Lucchi L, Pasinetti GM, Govoni S (1999) Protein kinase C anchoring deficit in postmortem brains of Alzheimer's disease patients. *Exp Neurol* 159, 559-564.
- [54] Nagy G, Reim K, Matti U, Brose N, Binz T, Rettig J, Neher E, Sørensen JB (2004) Regulation of releasable vesicle pool sizes by protein kinase A-dependent phosphorylation of SNAP-25. *Neuron* 41, 417-429.
- [55] Hepp R, Cabaniols JP, Roche PA (2002) Differential phosphorylation of SNAP-25 *in vivo* by protein kinase C and protein kinase A. *FEBS Lett* 532, 52-56.
- [56] Fu J, Naren AP, Gao X, Ahmed GU, Malik AB (2005) Protease-activated receptor-1 activation of endothelial cells induces protein kinase C $\alpha$ -dependent phosphorylation of syntaxin 4 and Munc18c: Role in signaling P-selectin expression. *J Biol Chem* 280, 3178-3184.

- [57] Shimazaki Y, Nishiki TI, Omori A, Sekiguchi M, Kamata Y, Kozaki S, Takahashi M (1996) Phosphorylation of 25-kDa synaptosome-associated protein: Possible involvement in protein kinase C-mediated regulation of neurotransmitter release. *J Biol Chem* 271, 14548-14553.
- [58] Shu Y, Liu X, Yang Y, Takahashi M, Gillis KD (2008) Phosphorylation of SNAP-25 at Ser187 Mediates enhancement of exocytosis by a phorbol ester in INS-1 cells. *J Neurosci* 28, 21-30.
- [59] Katayama N, Yamamori S, Fukaya M, Kobayashi S, Watanabe M, Takahashi M, Manabe T (2017) SNAP-25 phosphorylation at Ser187 regulates synaptic facilitation and short-term plasticity in an age-dependent manner. *Sci Rep* 7, 7996.
- [60] Gao J, Hirata M, Mizokami A, Zhao J, Takahashi I, Takeuchi H, Hirata M (2016) Differential role of SNAP-25 phosphorylation by protein kinases A and C in the regulation of SNARE complex formation and exocytosis in PC12 cells. *Cell Signal* 28, 425-437.
- [61] Lee W, Boo JH, Jung MW, Park SD, Kim YH, Kim SU, Mook-Jung I (2004) Amyloid beta peptide directly inhibits PKC activation. *Mol Cell Neurosci* 26, 222-231.
- [62] Saheki Y, De Camilli P (2012) Synaptic vesicle endocytosis. *Cold Spring Harb Perspect Biol* 4, a005645.
- [63] Daly C, Sugimori M, Moreira JE, Ziff EB, Llinas R (2002) Synaptophysin regulates clathrin-independent endocytosis of synaptic vesicles. *Proc Natl Acad Sci U S A* 97, 6120- 6125.
- [64] Yamashita T, Hige T, Takahashi T (2005) Vesicle endocytosis requires dynamin-dependent GTP hydrolysis at a fast CNS synapse. *Science* 307, 124-127.
- [65] Kelly BL, Vassar R, Ferreira A (2005)  $\beta$ -amyloid-induced dynamin 1 depletion in hippocampal neurons: A potential mechanism for early cognitive decline in Alzheimer disease. *J Biol Chem* 280, 31746-31753.
- [66] Kelly BL, Ferreira A (2007) Beta-amyloid disrupted synaptic vesicle endocytosis in cultured hippocampal neurons. *Neuroscience* 147, 60-70.
- [67] Kelly BL, Ferreira A (2006)  $\beta$ -amyloid-induced dynamin 1 degradation is mediated by N-methyl-D-aspartate receptors in hippocampal neurons. *J Biol Chem* 281, 28079-28089.
- [68] Gordon SL, Leube RE, Cousin MA (2011) Synaptophysin is required for synaptobrevin retrieval during synaptic vesicle endocytosis. *J Neurosci* 31, 14032-14036.
- [69] Park J, Jang M, Chang S (2013) Deleterious effects of soluble amyloid- $\beta$  oligomers on multiple steps of synaptic vesicle trafficking. *Neurobiol Dis* 55, 129-139.
- [70] Itoh T, Erdmann KS, Roux A, Habermann B, Werner H, De Camilli P (2005) Dynamin and the actin cytoskeleton cooperatively regulate plasma membrane invagination by BAR and F-BAR proteins. *Dev Cell* 9, 791-804.
- [71] Praefcke GJK, McMahon HT (2004) The dynamin superfamily: Universal membrane tubulation and fission molecules? *Nat Rev Mol Cell Biol* 5, 133-147.
- [72] Roux A, Uyhazi K, Frost A, De Camilli P (2006) GTP- dependent twisting of dynamin implicates constriction and tension in membrane fission. *Nature* 441, 528-531.

- [73] Takei K, Haucke V (2001) Clathrin-mediated endocytosis: Membrane factors pull the trigger. *Trends Cell Biol* 11, 385-391.
- [74] Takei K, Slepnev VI, Haucke V, De Camilli P (1999) Functional partnership between amphiphysin and dynamin in clathrin-mediated endocytosis. *Nat Cell Biol* 1, 33-39.
- [75] Berman DE, Dall'Armi C, Voronov S V., McIntire LBJ, Zhang H, Moore AZ, Staniszewski A, Arancio O, Kim TW, Di Paolo G (2008) Oligomeric amyloid- $\beta$  peptide disrupts phosphatidylinositol-4,5- bisphosphate metabolism. *Nat Neurosci* 11, 547-554.
- [76] Lazarevic V, Fien'ko S, Andres-Alonso M, Anni D, Ivanova D, Montenegro-Venegas C, Gundelfinger ED, Cousin MAFA (2017) Physiological concentrations of amyloid beta regulate recycling of synaptic vesicles via alpha7 acetylcholine receptor and CDK5/calcineurin signaling. *Front Mol Neurosci* 10, 221.
- [77] Kim SH, Ryan TA (2010) CDK5 serves as a major control point in neurotransmitter release. *Neuron* 67, 797-809.
- [78] Cesca F, Baldelli P, Valtorta F, Benfenati F (2010) The synapsins: Key actors of synapse function and plasticity. *Prog Neurobiol* 91, 313-348.
- [79] Marsh J, Bagol SH, Williams RSB, Dickson G, Alifragis P (2017) Synapsin I phosphorylation is dysregulated by beta-amyloid oligomers and restored by valproic acid. *Neurobiol Dis* 106, 63-75.
- [80] Park D, Na M, Kim JA, Lee U, Cho E, Jang M, Chang S (2017) Activation of CaMKIV by soluble amyloid- $\beta$  1-42 impedes trafficking of axonal vesicles and impairs activity- dependent synaptogenesis. *Sci Signal* 10, doi: eaam8661.
- [81] Jovanovic JN, Sihra TS, Nairn AC, Hemmings HC Jr, Greengard PCA (2001) Opposing changes in phosphorylation of specific sites in synapsin I during  $Ca^{2+}$ -dependent glutamate release in isolated nerve terminals. *J Neurosci* 21, 7944-7953.
- [82] Parodi J, Sepulveda FJ, Roa J, Opazo C, Inestrosa NC, Aguayo LG (2010)  $\beta$ -amyloid causes depletion of synaptic vesicles leading to neurotransmission failure. *J Biol Chem* 285, 2506-2514.
- [83] Parks KM, Sugar JE, Haroutunian V, Bierer L, Perl D, Wallace WC (1991) Reduced *in vitro* phosphorylation of synapsin I (site 1) in Alzheimer's disease postmortem tissues. *Brain Res Mol Brain Res* 9, 125-134.
- [84] Park D, Chang S (2018) Soluble A $\beta$ 1-42 increases the heterogeneity in synaptic vesicle pool size among synapses by suppressing intersynaptic vesicle sharing. *Mol Brain* 11, 10.



---

### PART 3

The following manuscript was published in *European Journal of Medicinal Chemistry* in 2019  
as:

#### **Merging memantine and ferulic acid to probe connections between NMDA receptors, oxidative stress and amyloid- $\beta$ peptide in Alzheimer's disease**

Michela Rosini, Elena Simoni, Roberta Caporaso, Filippo Basagni, Michele Catanzaro,  
Izuddin F. Abu, **Francesca Fagiani**, Federica Fusco, Sara Masuzzo, Diego Albani,  
Cristina Lanni, Ian R. Mellor, Anna Minarini

#### **Abstract**

N-methyl-D-aspartate receptors (NMDAR) are critically involved in the pathogenesis of Alzheimer's disease (AD). Acting as an open-channel blocker, the anti-AD drug memantine preferentially targets NMDAR overactivation, which has been proposed to trigger neurotoxic events mediated by amyloid- $\beta$  peptide ( $A\beta$ ) and oxidative stress. In this study, we applied a multifunctional approach by conjugating memantine to ferulic acid, which is known to protect the brain from  $A\beta$  neurotoxicity and neuronal death caused by ROS. The most interesting compound (**7**) behaved, like memantine, as a voltage-dependent antagonist of NMDAR ( $IC_{50} = 6.9 \mu\text{M}$ ). In addition, at  $10 \mu\text{M}$  concentration, **7** exerted antioxidant properties both directly and indirectly through the activation of the Nrf2 pathway in SH-SY5Y cells. At the same concentration, differently from the parent compounds memantine and ferulic acid alone, it was able to modulate  $A\beta$  production, as revealed by the observed increase of the non-amyloidogenic sAPP $\alpha$  in H4-sw cells. These findings suggest that compound **7** may represent a promising tool for investigating NMDAR-mediated neurotoxic events involving  $A\beta$  burden and oxidative damage.

**Keywords:** memantine; ferulic acid; NMDA receptors; oxidative stress; amyloid- $\beta$  peptide.



Contents lists available at ScienceDirect

European Journal of Medicinal Chemistry

journal homepage: <http://www.elsevier.com/locate/ejmech>

Research paper

## Merging memantine and ferulic acid to probe connections between NMDA receptors, oxidative stress and amyloid- $\beta$ peptide in Alzheimer's disease



Michela Rosini <sup>a,\*</sup>, Elena Simoni <sup>a</sup>, Roberta Caporaso <sup>a</sup>, Filippo Basagni <sup>a</sup>, Michele Catanzaro <sup>b</sup>, Izuddin F. Abu <sup>c,d</sup>, Francesca Fagiani <sup>b,e</sup>, Federica Fusco <sup>f</sup>, Sara Masuzzo <sup>f</sup>, Diego Albani <sup>f</sup>, Cristina Lanni <sup>b</sup>, Ian R. Mellor <sup>c</sup>, Anna Minarini <sup>a,\*\*</sup>

<sup>a</sup> Department of Pharmacy and Biotechnology, Alma Mater Studiorum – University of Bologna, Via Belmeloro 6, 40126, Bologna, Italy

<sup>b</sup> Department of Drug Sciences (Pharmacology Section), University of Pavia, V.le Taramelli 14, 27100, Pavia, Italy

<sup>c</sup> School of Life Sciences, University of Nottingham, University Park, Nottingham, NG7 2RD, UK

<sup>d</sup> Universiti Kuala Lumpur, Institute of Medical Science Technology, A1-1, Jalan TKS1, Taman Kajang Sentral, 43000, Kajang, Selangor, Malaysia

<sup>e</sup> Scuola Universitaria Superiore IUSS Pavia, P.zza Vittoria, 15, 27100, Pavia, Italy

<sup>f</sup> Department of Neuroscience, Istituto di Ricerche Farmacologiche Mario Negri IRCCS, Via Mario Negri 2, 20156, Milan, Italy

### 1. Introduction

Synaptic loss is a major feature in Alzheimer's disease (AD). This chronic neurodegenerative condition, which is currently afflicting about 47 million people worldwide, slowly destroys neurons leading to progressive cognitive disabilities [1]. How synapses are affected in the disease process remains unclear. The mechanistic understanding of synaptic damage represents a challenging goal and may offer new possibilities for the prevention and cure of the disease. N-methyl-D-aspartate receptors (NMDAR) are ionotropic glutamate receptors known to play an important role for synaptic plasticity in the healthy brain [2]. They are primarily involved in neuronal excitatory synaptic transmission that underlies learning and memory but also in excitotoxic damage occurring during acute brain injuries and chronic neurodegenerative conditions. Targeting NMDAR therapeutically is therefore complicated by the dichotomous nature of their downstream signaling. It is the common view that these opposite effects depend on receptor localization: activation of synaptic NMDAR (sNMDAR) may contribute to cell survival and plasticity, while activation of extrasynaptic NMDAR (eNMDAR) may preferentially signal to neuronal death [3,4]. In particular, overactivation of eNMDAR has been associated with glutamate-mediated oxidative damage potentially leading to aberrant, misfolded proteins [5]. The amyloid- $\beta$  peptide ( $A\beta$ ) is a pathogenic feature of AD development. Produced by the sequential cleavage of the amyloid precursor protein (APP) by  $\beta$ - and  $\gamma$ -secretases, as an alternative to the non-amyloidogenic cleavage performed by

$\alpha$ -secretase, A $\beta$  monomers aggregate into soluble oligomeric forms, which are believed to be mainly responsible for amyloid-driven synaptotoxicity [6]. A toxic positive feedback is established between A $\beta$  production and eNMDAR overactivation, which involves cytoplasmic Ca<sup>2+</sup> upregulation and aberrant redox-mediated reactions [7].

Memantine is an anti-AD drug currently in use for the treatment of moderate-to-severe forms of the disease. It is an uncompetitive/fast off-rate NMDAR antagonist. By acting as an open-channel blocker, it preferentially enters the channel's pore in conditions of excessive and prolonged glutamate exposure [8,9]. Its favorable kinetics has been proposed to selectively direct memantine's efficacy toward extrasynaptic/tonically-activated NMDAR over synaptic/phasicly-activated NMDAR [10], accounting for the clinical tolerability of the drug. Further, this peculiar profile seems to play a crucial role in determining memantine's ability to alleviate A $\beta$ -induced synaptic dysfunction and to rescue both neuronal oxidative stress and the transient memory impairment caused by A $\beta$  oligomers [11]. Unfortunately, however, like other available anti-AD drugs, memantine offers only a symptomatic relief to patients and is not able to halt the disease progression.

Based on these premises, we sought to combine in a single molecule memantine, which specifically modulates NMDAR-mediated excitotoxicity, responsible for ROS- and A $\beta$ -mediated neurotoxic events, with the antioxidant ferulic acid (FA), whose well-established biological properties include the ability to protect the brain from A $\beta$  neurotoxicity and neuronal death caused by ROS [12]. Following this rationale, we designed and synthesized memantine-FA conjugates following the two routes shown in **Figure 1**.

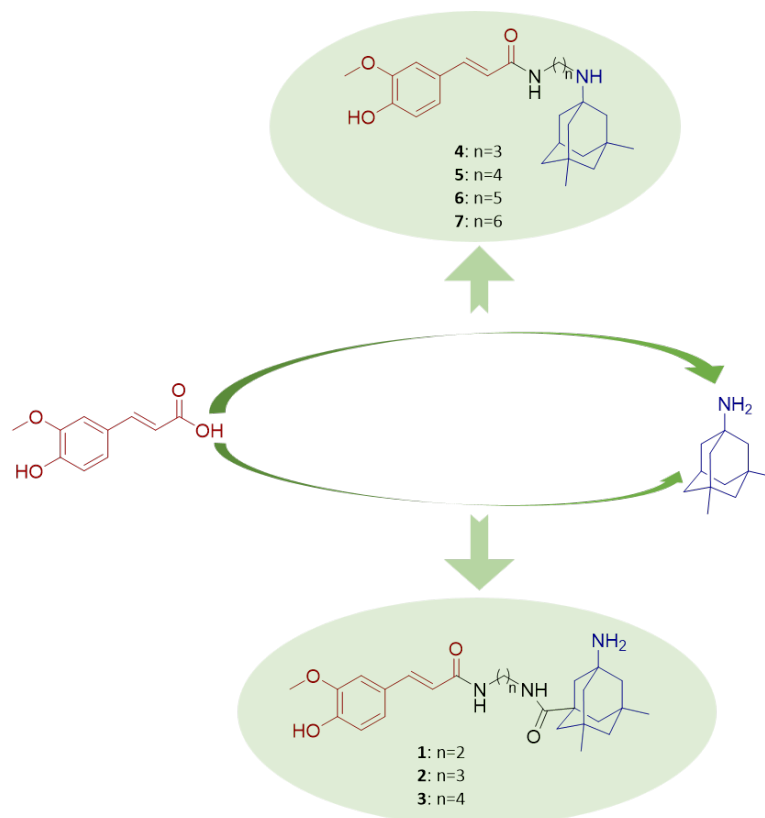


**Figure 1. Drug design of compounds 1-7.**

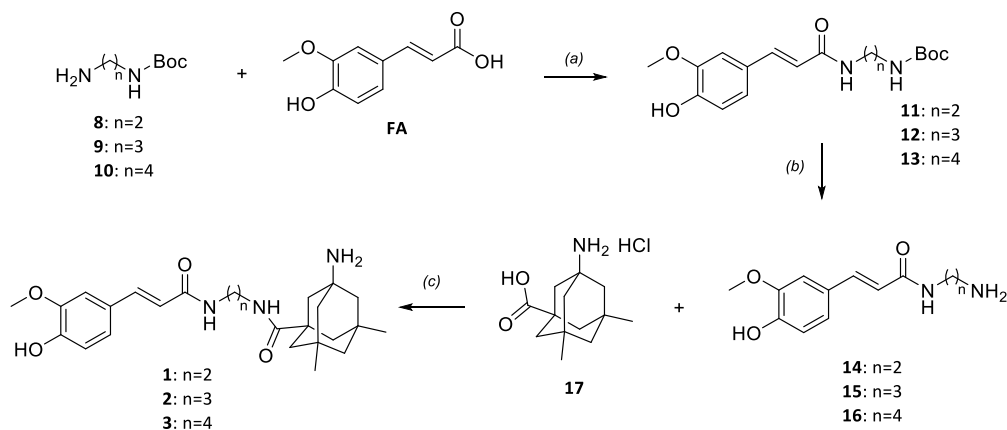
It is well known that memantine's primary amine plays a crucial role in receptor binding [13]. Thus, to preserve this moiety, we functionalized the adamantane nucleus of memantine with a carboxylic function, which acted as the reactive point for FA conjugation, affording compounds 1-3. Further, in compounds 4-7, we explored the possibility to introduce FA appendages on the nitrogen atom of memantine, whose conversion to a secondary amine has previously emerged as a feasible strategy to gain memantine-based NMDAR antagonists [14,15]. Synthesized compounds were first tested against NMDAR. Based on their NMDAR blocking properties, compounds were selected to study their direct and indirect antioxidant efficacy, as well as the ability to modulate the amyloidogenic pathway.



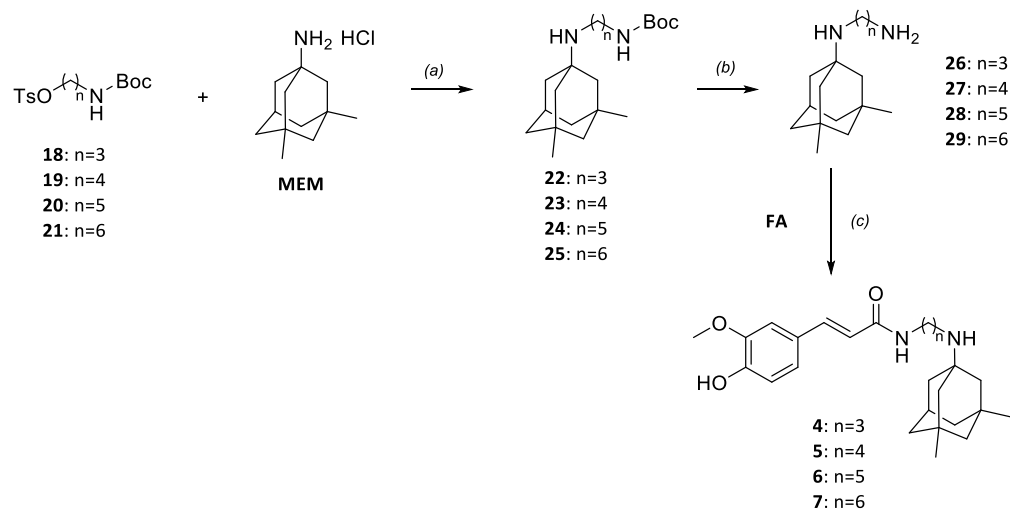
## 2. Results and Discussion

### Chemistry

Memantine-FA hybrids 1-7 were prepared following two different synthetic routes (**Schemes 1** and **2**), depending on the way the two pharmacophores were connected. For the synthesis of compounds 1-3, the appropriate mono Boc-protected diamine (8-10) [16,17] was condensed with FA to give intermediates 11-13. Cleavage of the protecting group in acidic conditions led to compounds 14-16. Conjugation of 14-16 with **17** hydrochloride, which was obtained following a Ritter-type protocol as previously reported by Wanka *et al.* [18], afforded final compounds 1-3 (**Scheme 1**). To gain compounds 4-7, memantine hydrochloride (MEM) was alkylated with the appropriate tosyl-activated alcohol (18-21) under basic conditions to give intermediates 22-25 which, after carbamate deprotection (26-29), were coupled with FA in the presence of EDC and HOBt (**Scheme 2**).



**Scheme 1.** Reagents and conditions: (a) EDC, HOBt, DMF, Et<sub>3</sub>N, N<sub>2</sub>, 12 h, 0°C-rt; (b) HCl 4 M in dioxane, CH<sub>2</sub>Cl<sub>2</sub>, 90°, 0°C-rt; (c) EDC, HOBt, DMF, N<sub>2</sub>, 36 h, 0°C-rt.



**Scheme 2.** Reagents and conditions: (a)  $K_2CO_3$ , KI, DMF,  $140^\circ C$ , 1h, MW; (b) HCl 4 M in dioxane,  $CH_2Cl_2$ ,  $20^\circ$ ,  $0^\circ C$ -rt; (c) EDC, HOBt,  $Et_3N$ , DMF,  $N_2$ , 12 h,  $0^\circ C$ -rt.

### NMDAR blocking activity

All the compounds were initially investigated to assess their effect at NMDAR. In particular, the antagonism of responses to NMDA and glycine were measured by voltage-clamp recordings on GluN1-1a/GluN2A NMDAR expressed in *Xenopus laevis* oocytes at -60 mV, with compounds 1-7 applied in tenfold increments in the range 0.01 to 100  $\mu M$ . Memantine was used as the reference compound. Compounds 1-3, which retain the primary amine function of memantine, demonstrated very low or no potency to block NMDAR (**Figure 2A**). Conversely, employing memantine's amine for connecting FA appendages resulted in significant blocking of NMDA/glycine responses (**Figure 2A**).

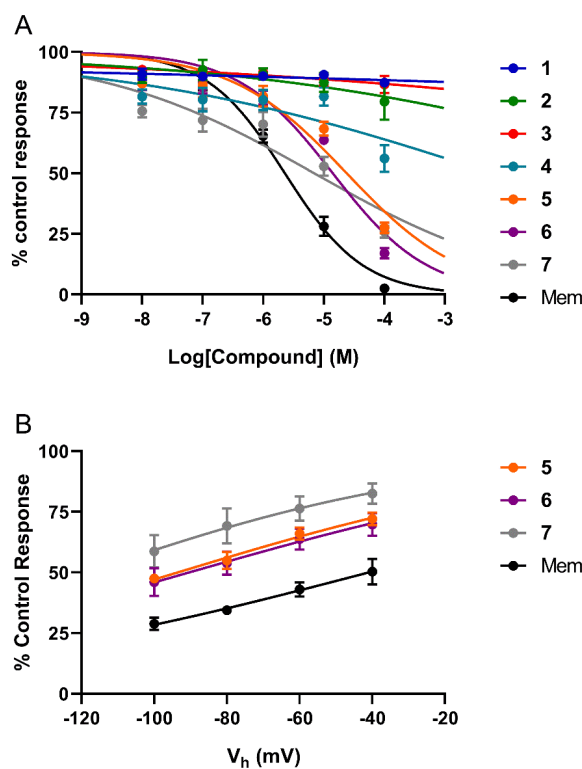


**Figure 2. A)** Concentration-inhibition curves for compounds 1-7 in comparison to memantine (Mem). Data are mean % of control response to 100  $\mu$ M NMDA (+10  $\mu$ M glycine)  $\pm$  SEM (n = 5-7 separate oocytes). The curves are fits to Equation 1 and  $IC_{50}$  values are given in Table 1. **B)** Voltage dependence of inhibition by compounds 5-7 (30  $\mu$ M, 20  $\mu$ M and 10  $\mu$ M respectively) in comparison to memantine (Mem; 3  $\mu$ M). Data are plotted as mean % control response to 100  $\mu$ M NMDA (+10  $\mu$ M glycine)  $\pm$  SEM against the holding potential ( $V_h$ ) (n = 5-6 separate oocytes). The curves are fits of Equation 2 and  $\delta$  values are given in Table 1.

Compounds 5-7 presented a micromolar profile, with  $IC_{50}$  values ranging from 6.9 to 23.9  $\mu$ M, while the shorter compound 4 had an  $IC_{50}$  greater than 100  $\mu$ M, thus suggesting its inefficacy (Table 1). Blocking properties toward NMDAR were influenced by the chain length separating the pharmacophoric functions, with compound 7, carrying a hexamethylene spacer, emerging as the most efficacious. Compounds with considerable blocking properties (5-7) were assessed for voltage dependency. The compounds were diluted to their approximate  $IC_{50}$  concentrations and block of NMDA/glycine responses mediated by GluN1-1a/GluN2A was measured at four different holding potentials (-40, -60, -80 and -100 mV).

Compound	IC <sub>50</sub> [95% CI] $\mu$ M (n)	$\delta \pm$ SE (n)
1	$\gg 100$ (7)	nd
2	$\gg 100$ (6)	nd
3	$\gg 100$ (6)	nd
4	$>100$ (5)	nd
5	23.9 [13.0–49.4] (5)	$0.46 \pm 0.07$ (6)
6	14.1 [8.7–22.6] (5)	$0.43 \pm 0.12$ (6)
7	6.9 [3.0–19.2] (5)	$0.51 \pm 0.17$ (6)
memantine	2.3 [1.7–3.0] (6)	$0.39 \pm 0.08$ (5)

nd = not determined (because inhibition was too weak).

**Table 1.** IC<sub>50</sub> and  $\delta$  values for compounds 1-7 and memantine

Compounds presented a voltage-dependent behavior, acting, like memantine, as open channel blockers of the receptor. Data were fitted with the Woodhull equation to determine their  $\delta$  values, and thus estimate the position of the binding site within the membrane electric field [19,20]. The results of this study showed that three of the new molecules yielded  $\delta$  values comparable to memantine. Compounds 5, 6 and 7 had  $\delta$  values in the range 0.43 to 0.51, which are just slightly higher to that of memantine, 0.39. Based on their  $\delta$  values, we can suggest these compounds may have a binding site midway through the pore, maybe a little deeper but overlapping with that of memantine. This is consistent with binding adjacent to the Q/R/N-site that determines ion selectivity in ionotropic glutamate receptors.

### Cell Toxicity Assay

Compounds 5-7, presenting appreciable NMDAR blocking properties, were selected for deepening their antioxidant profile in SH-SY5Y human neuroblastoma cells. To this aim, we assessed the cytotoxicity of compounds 5-7 to define the concentration range to be used in cellular experimental settings. The antioxidant FA was used for comparison. Cells were exposed to the compounds at concentrations ranging from 1 to 50  $\mu$ M for 24 h and cell viability was determined by MTT assay. As shown in **Figure 3**, all the compounds were devoid of any toxicity at a concentration up to 20  $\mu$ M, while only the shorter derivative 5 retained, like FA, good tolerability up to 50  $\mu$ M. Lack of toxicity was verified also for compound 4, carrying a three-methylene spacer, at all the concentrations investigated (data

not shown), confirming that the spacer length significantly influenced compound tolerability in favor of shorter derivatives.

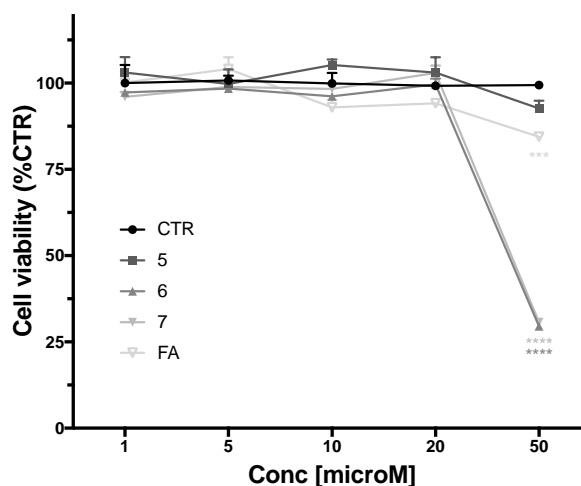


**Figure 3. Cellular toxicity of hybrid compounds (5-7) and Ferulic Acid (FA) on human neuroblastoma SH-SY5Y.** Cells were treated with compounds for 24 h at different concentrations ranging from 1 to 50  $\mu\text{M}$ . Cell viability was assessed by MTT assay. Data are expressed as percentage of cell viability versus CTR;  $***p < 0.001$ , and  $****p < 0.0001$  versus CTR; Dunnett's multiple comparison test,  $n=3$ .

### Protective Effect toward $\text{H}_2\text{O}_2$ -Induced Damage

To determine the antioxidant efficacy of compounds 5-7, we first studied their ROS scavenging activity when coincubated with 300  $\mu\text{M}$   $\text{H}_2\text{O}_2$ , using FA for comparison. The scavenger effect was evaluated in SH-SY5Y cells by using the fluorescent probe dichlorodihydrofluorescein diacetate (DCFH-DA) as a marker for quantitative intracellular ROS formation. The DCFH-fluorescence intensity significantly increased in  $\text{H}_2\text{O}_2$ -treated cells (black line, **Figure 4A**) with respect to untreated cells (dashed grey line, **Figure 4A**). All compounds, at a concentration of 10  $\mu\text{M}$ , were able to markedly reduce  $\text{H}_2\text{O}_2$ -induced intracellular ROS formation, being, however, less effective than FA. To assess if indirect antioxidant effects could accompany radical scavenger properties, further experiments were performed pretreating SH-SY5Y cells with compounds 5-7 (10  $\mu\text{M}$ ) for 24 h before adding 300  $\mu\text{M}$   $\text{H}_2\text{O}_2$  (**Figure 4B**). Again, compounds 5-7 produced a significant reduction in DCHF-fluorescent intensity, albeit an inversion in the trend of efficacy was observed. Indeed, with this experimental setting, compound 7 emerged as the most efficacious,

reaching FA ability to counteract  $\text{H}_2\text{O}_2$ -induced ROS formation. Based on these results, we could speculate that, at least for 7, antioxidant properties might derive from both direct and indirect effects.

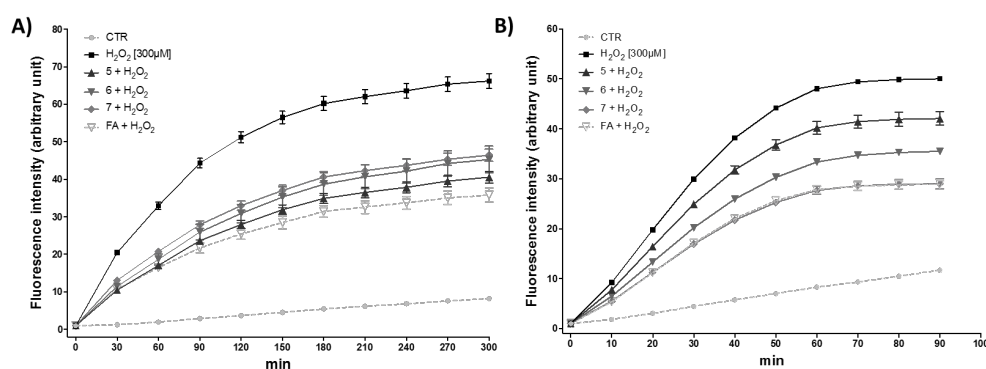


**Figure 4. Hybrid compounds reverse ROS formation induced by  $\text{H}_2\text{O}_2$ .** (A) After the loading with DCFH-DA, SH-SY5Y cells were exposed to 10  $\mu\text{M}$  compounds or FA in combination with 300  $\mu\text{M}$  of  $\text{H}_2\text{O}_2$ . The fluorescence intensity for all compounds tested is significant at any time starting from 60 to 300 min with  $p < 0.0001$  versus  $\text{H}_2\text{O}_2$ . At 30 min the significance versus  $\text{H}_2\text{O}_2$  is  $p < 0.01$  for compound 7,  $p < 0.001$  for compound 6 and  $p < 0.0001$  for compound 5 and FA. Dunnett's multiple comparison test. (B) SH-SY5Y cells were pre-treated with 10  $\mu\text{M}$  of each compound for 24 hours, loaded with DCFH-DA and then exposed to 300  $\mu\text{M}$   $\text{H}_2\text{O}_2$ . Fluorescence intensity for all compounds tested is significant at any time from 30 to 90 min with  $p < 0.0001$  versus  $\text{H}_2\text{O}_2$ . At time 10 min, the fluorescence intensity did not reach statistical significance for compound 5, whereas for 6 the significance is  $p < 0.01$  and for 7 and FA is  $p < 0.0001$  vs  $\text{H}_2\text{O}_2$ . At 20 min, the significance is  $p < 0.001$  for compound 5 and  $p < 0.0001$  for compound 7 and AF vs  $\text{H}_2\text{O}_2$ . Dunnett's multiple comparison test.

### Activation of Nrf2 Pathway in SH-SY5Y Cells

The nuclear factor (erythroid-derived 2)-like 2 (Nrf2) transcriptional pathway is a major player of inducible antioxidant defense [21]. Activation of the Nrf2 pathway, and the subsequent transcription of downstream cytoprotective genes, is triggered by the disruption of interaction and binding of Nrf2 with the cytosolic Nrf2 repressor Kelch-like ECH-associated protein 1 (Keap 1) [22]. A variety of electrophiles from synthetic or natural sources is emerging for their ability to hamper this interaction by targeting key cysteine residues of Keap1, which act as sensors of oxidative insults [23]. In particular, the electrophilic motif recurring in FA and its derivatives, namely the  $\alpha,\beta$ -unsaturated carbonyl group, has already been shown to trigger the Nrf2-driven transcriptional process in a series of hydroxy-cinnamic derivatives for which trapping Keap1 through covalent adduct

formation was proposed to be the initiating event [24,25]. Thus, we studied compounds 5-7 and FA in SH-SY5Y neuroblastoma cells to verify whether they may affect the Nrf2 pathway and indirect mechanisms could therefore contribute to their overall antioxidant profile. To this aim, we first assessed their ability to modulate the mRNA levels of Nrf2 by real-time PCR, using 10  $\mu$ M of each compound incubated for 6 h. Notably, only compound 7 determined a significant increase in Nrf2 mRNA expression (**Figure 5, panel A**), while cells treated with FA or compounds 5 and 6 behaved like untreated cells. Coherently with these results, the same trend was observed when we investigated the ability of compounds to tune the mRNA levels of heme oxygenase-1 (HO-1), a prototypical Nrf2-target gene related to oxidative stress response. Indeed, mRNA levels of the inducible cytoprotective gene raised to about 150% of control following pretreatment with 10  $\mu$ M 7, while no effect was elicited by FA or compounds 5 and 6 (**Figure 5, panel B**).

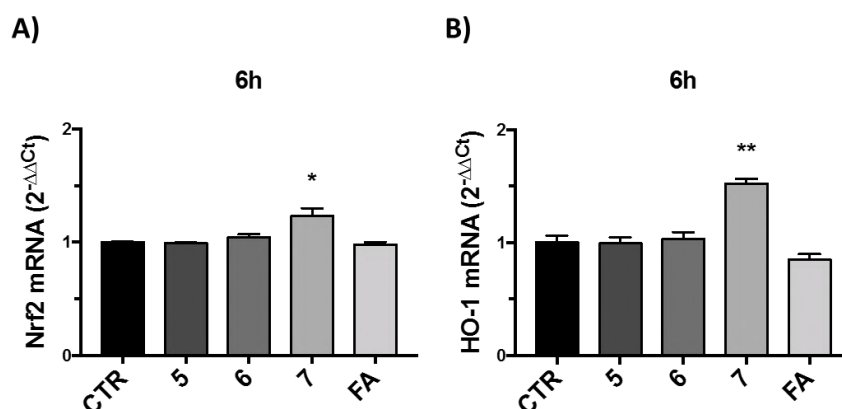


**Figure 5. Hybrid compounds modulate Nrf2 and HO-1 mRNA levels.** RNA was obtained from cellular extracts of SH-SY5Y cells treated for 6 h with compounds 5-7 and FA at 10  $\mu$ M and analyzed for Nrf2 (**A**) and HO-1 (**B**) mRNA expression by RT-PCR. GAPDH was used as housekeeping gene. Results are shown as mean  $\pm$  SEM; \* $p$  < 0.05, \*\* $p$  < 0.01 *versus* CTR; Dunnett's multiple comparison test,  $n=3$ .

Then, we sought to verify whether the increase in HO-1 mRNA expression determined by compound 7 could effectively result in enhanced HO-1 protein levels. To this aim, HO-1 induction was analyzed by means of Western immunoblotting in the same cell line after treatment for 24 h with 7 at 10 or 20  $\mu$ M. Interestingly, compound 7 caused a dose-dependent increase of HO-1 expression, with cells treated with 20  $\mu$ M 7 almost doubling HO-1 protein levels of control (**Figure 6**). These results confirm that compound 7 is a multimodal antioxidant, which combines radical scavenging properties to the ability of potentiating the Nrf2/HO-1 axis. Further, the lack of indirect antioxidant efficacy verified

for compounds 5, 6 and FA, all carrying the  $\alpha,\beta$ -unsaturated carbonyl feature, reveal that an electrophilic moiety is not per se sufficient for activating redox sensor proteins, and shape complementarity may play a pivotal role in this respect. Particularly, we might speculate that compounds 5-7, varying in the linker length, and FA could differently orient their cysteine-reactive group toward nucleophilic traps of Keap1 affecting target recognition and, consequently, a compound's reactivity and specificity.

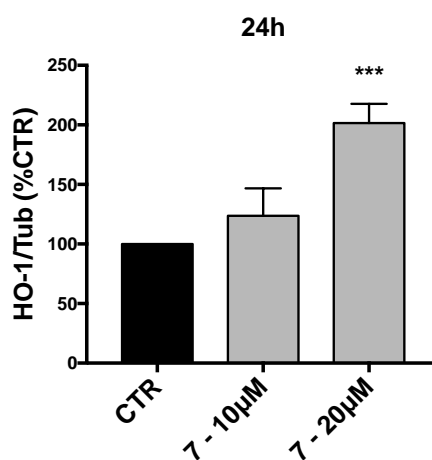


**Figure 6. Effect of compound 7 on HO-1 protein levels.** Cellular extracts of SH-SY5Y cells treated for 24 h with compound 7 at 10 or 20  $\mu$ M were analyzed for HO-1 protein levels by Western Blot. Anti-tubulin was used as protein loading control. Results are shown as ratio (% of CTR)  $\pm$  SEM; \*\*\* $p$  < 0.001 versus CTR; Dunnett's multiple comparison test,  $n=3$ .

### APP processing in H4-SW cells

In AD, a direct link exists between eNMDAR overactivation and increased neuronal  $A\beta$  production [26]. NMDAR have been proposed to modulate  $\alpha$ -secretase activity, shifting APP metabolism towards a non-amyloidogenic pathway. Memantine has been shown to lower  $A\beta$  synthesis in a number of studies [27,28]. Mechanisms potentially involved in memantine-driven  $A\beta$  modulation are not completely clear, and both NMDAR-mediated and NMDAR-independent mechanisms have been proposed [29]. In this context, we sought to investigate whether the most promising compounds 5-7 could affect the APP processing favoring the production of the non-amyloidogenic soluble amyloid precursor protein  $\alpha$  (sAPP $\alpha$ ). Current research suggests that sAPP $\alpha$  plays a role in synaptic growth and plasticity, featuring neuroprotective and neurotrophic properties [30]. Thus, we studied



the effect of the compounds on sAPP $\alpha$  levels in the human H4 cell line expressing the Swedish mutant form of APP (H4-SW), after 24 h treatment. Compounds 5-7 were tested at 10  $\mu$ M concentration, which had no impact on cell viability, as confirmed by a dose-response curve where memantine, FA and compounds 5-7 had no toxic effect up to 20  $\mu$ M concentration (data not shown). Memantine and FA alone were used for comparison. The Western blot analysis reported in **Figure 7** shows that compound 7, but not compounds 5 and 6, significantly increased sAPP $\alpha$  levels (**Figure 7, panel A**).

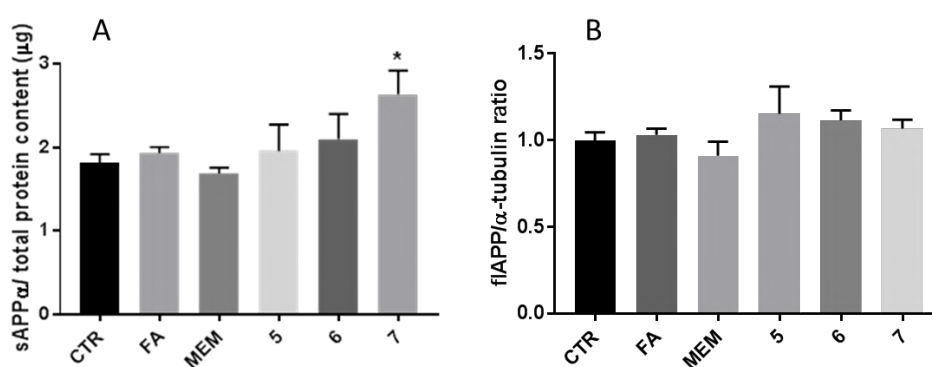


**Figure 7. Assessment of the effect of compounds 5-7, MEM and FA on amyloid precursor protein (APP) proteolytic processing in H4-SW cells. (A) Determination of sAPP $\alpha$  levels.** Cells were treated with 10  $\mu$ M of each compound and after 24 h conditioned media were collected and sAPP $\alpha$  content assessed by Western blotting. The graph shows the densitometric quantification of the Western blotting bands, normalized to the total protein content of plated cells. \*  $p < 0.05$ , one-way ANOVA and *post-hoc* test. **(B) Determination of full-length amyloid precursor protein (flAPP) expression.** Cells were treated with 10  $\mu$ M of each compound. After 24 h, H4-SW were lysed and flAPP expression assessed by Western blotting. The graph shows the densitometric quantification of the Western blotting bands, normalized to  $\alpha$ -tubulin as internal reference.

Notably, compounds 5-7 were not able to affect full-length APP (fl-APP) expression levels, which was determined in the same cells to evaluate the effect of the compounds on total intracellular APP (**Figure 7, panel B**). By enhancing sAPP $\alpha$  levels without affecting the levels of total intracellular APP, compound 7 seems to stimulate APP processing towards the  $\alpha$ -secretase (non-amyloidogenic) pathway, which should result in decreased A $\beta$  production. Noteworthy, at the same concentration, memantine and FA alone showed no effect on APP processing, strengthening the value of the design of a hybrid molecule. The lack of efficacy of memantine, whose potency as NMDAR antagonist is 3-fold higher than that of 7, suggests that the effect of 7 on APP processing we observed in this experimental setting seems to be not principally mediated by NMDAR. Interestingly, lengthening of the linker between the pharmacophoric functions up to six methylenes switched on the efficacy

toward both APP processing and Nrf2 activation, pointing to 7 as the most promising molecule of the series.

### 3. Conclusions

NMDAR play a crucial role in the pathophysiology of AD. Excessive activation of NMDAR can compromise synapse function by triggering neurotoxic events, which involve A $\beta$  peptide and oxidative stress. By preferentially blocking extrasynaptic rather than synaptic currents, the anti-AD drug memantine limits neurotoxicity mediated by excessive NMDAR activity while relatively sparing physiological neurotransmission. This peculiar NMDAR profile prompted us to conjugate memantine with the bioactive payload FA, aiming to synergistically modulate the critical partnership occurring between oxidative damage, A $\beta$  burden, and hyperfunctioning NMDAR. For compounds 4-7, which exploit memantine's nitrogen for FA connection, chain lengthening positively influenced NMDAR blocking properties. The longer derivative 7, carrying a hexamethylene spacer between the pharmacophoric functions, presented a micromolar profile as NMDAR antagonist ( $IC_{50}$ =6.9  $\mu$ M), being only three times less effective than the parent compound memantine ( $IC_{50}$ = 2.3  $\mu$ M). Further, compound 7 also shares with memantine the binding site midway through the pore and a voltage-dependent behavior, suggesting that conjugation with FA produced only a modest perturbation of memantine's NMDAR binding mode. Compounds with appreciable NMDAR blocking properties were studied in SH-SY5Y cells to assess their antioxidant properties. All compounds tested showed notable free radical scavenging effects. Conversely, only 7 was able to significantly potentiate the expression of Nrf2 and its downstream protective gene HO-1 at the concentration of 10  $\mu$ M, therefore emerging as a multimodal antioxidant. Notably, the lack of indirect antioxidant efficacy observed for 5 and 6, varying in the linker length, and FA, suggests the importance of target recognition as a pre-requisite for electrophile reactivity, excluding an indiscriminate effect driven by the  $\alpha,\beta$ -unsaturated carbonyl group. At the same concentration (10  $\mu$ M), compound 7, and not shorter derivatives 5 and 6, significantly enhanced sAPP $\alpha$  levels in H4-SW cells, suggesting that it may stimulate APP processing in favor of the  $\alpha$ -secretase (non-amyloidogenic) pathway and consequently limit A $\beta$  formation. Thus, the most potent NMDAR antagonist 7 was also able to activate inducible protective pathways which play a crucial role in contrasting the neurotoxic cascade driven by eNMDAR overactivation. The multimodal profile of compound 7 was well balanced, in the micromolar-range, and not accompanied by any cytotoxicity in both SH-SY5Y and H4-SW cells up to the concentration of 20  $\mu$ M. Based on these findings, compound 7 emerges as a promising pharmacologic tool for deepening our insight on the significance of NMDAR-mediated neurotoxic events involving ROS formation and A $\beta$  damage.

## 4. Experimental section

### Chemistry

Chemical reagents were purchased from Sigma-Aldrich, Fluka and Lancaster (Italy) and used without further purification. Chromatographic separations were performed on silica gel columns (Kieselgel 40, 0.040-0.063 mm, Merck) by chromatography. Reactions were followed by TLC on Merck (0.25 mm) glass-packed precoated silica gel plates (60 F254), then visualized with an UV lamp, bromocresol green or  $\text{KMnO}_4$ . Melting points were measured in glass capillary tubes on a Büchi SMP-20 apparatus and are uncorrected. Microwave assisted synthesis was performed by using CEM Discover<sup>®</sup> SP apparatus (2.45 GHz, maximum power of 300W). NMR spectra were recorded at 400 MHz for  $^1\text{H}$  and 100 MHz for  $^{13}\text{C}$  on Varian VXR 400 spectrometer. Chemical shifts ( $\delta$ ) are reported in parts per millions (ppm) relative to tetramethylsilane (TMS), and spin multiplicities are given as s (singlet), br s (broad singlet), d (doublet), t (triplet), q (quartet), or m (multiplet). Direct infusion ESI-MS mass spectra were recorded on a Waters ZQ 4000 apparatus. Final compounds 1-7 were >95% pure as determined by HPLC analyses. The analyses were performed under reversed-phase conditions on a Phenomenex Jupiter C18 (150 × 4.6 mm I.D.) column, using a binary mixture of 0.1% TFA in  $\text{H}_2\text{O}$ /acetonitrile (70/30, v/v for 5; 65/35, v/v for 3, 4, 6, 7; 80/20, v/v for 1, 2) as the mobile phase, UV detection at  $\lambda = 302$  nm and a flow rate of 1 mL/min. Analyses were performed on a liquid chromatograph model PU-2089Plus UV equipped with a 20  $\mu\text{L}$  loop valve (Jasco Europe, Italy). Compounds were named relying on the naming algorithm developed by CambridgeSoft Corporation and used in Chem-BioDrawUltra 15.1.

*General procedure for the intermediates 11-13.* To an ice-cooled solution of ferulic acid (FA, 1 equiv) in dry DMF (3-4 mL) were added HOBt (1.3 equiv) and EDC (1.3 equiv). The reaction mixture was stirred for 10 min, followed by addition of  $\text{Et}_3\text{N}$  (1.3 equiv) and the appropriate mono-protected diamine (8-10) (1 equiv). Stirring was then continued at room temperature overnight, and the solvent evaporated under *vacuum*. The crude was purified by flash chromatography on silica gel using dichloromethane/methanol (9.5:0.5) as mobile phase.

*tert-butyl (E)-(2-(3-(4-hydroxy-3-methoxyphenyl)acrylamido)ethyl)carbamate (11).* Synthesized from FA (400 mg, 2.06 mmol) and 8 [17] (330 mg, 2.06 mmol) to afford 11 as waxy solid: 200 mg (30%);  $^1\text{H}$  NMR (400 MHz,  $\text{CDCl}_3$ )  $\delta$  7.50 (d,  $J = 15.6$  Hz, 1H), 6.99 (d,  $J = 8$  Hz, 1H), 6.94 (s, 1H), 6.88 (d,  $J = 8.4$  Hz, 1H), 6.60 (br s, 1H), 6.26 (d,  $J = 15.6$  Hz, 1H), 5.33 (br s, 1H), 3.85 (s, 3H), 3.50-3.46 (m, 2H), 3.33-3.30 (m, 2H), 1.42 (s, 9H).

*tert-butyl (E) - (3 - (3 - (4 - hydroxy - 3 - methoxyphenyl) acrylamido) propyl) carbamate (12)*. Synthesized from FA (100 mg, 0.51 mmol) and 9 [16](174 mg, 0.51 mmol) to afford 12 as waxy solid: 100 mg (56%); <sup>1</sup>H NMR (400 MHz, CDCl<sub>3</sub>) δ 7.55 (d, *J* = 15.2 Hz, 1H), 7.05 (d, *J* = 8 Hz, 1H), 7.01 (s, 1H), 6.90 (d, *J* = 8 Hz, 1H), 6.50 (br s, 1H), 6.30 (d, *J* = 15.2 Hz, 1H), 4.96 (br s, 1H), 3.92 (s, 3H), 3.44-3.40 (m, 2H), 3.23-3.19 (m, 2H), 1.67-1.61 (m, 2H), 1.45 (s, 9H).

*tert-butyl (E)-(4-(3-(4-hydroxy-3-methoxyphenyl)acrylamido)butyl)carbamate (13)*. Synthesized from FA (400 mg, 2.06 mmol) and 10 [31](188 mg, 2.06 mmol) to afford 13 as waxy green solid: 230 mg (33%); <sup>1</sup>H NMR (400 MHz, CDCl<sub>3</sub>) δ 7.52 (d, *J* = 15.2 Hz, 1H), 7.03 (d, *J* = 8.4 Hz, 1H), 6.98 (s, 1H), 6.88 (d, *J* = 8 Hz, 1H), 6.25 (d, *J* = 15.2 Hz, 1H), 6.01 (br s, 1H), 4.64 (br s, 1H), 3.89 (s, 3H), 3.39-3.38 (m, 2H), 3.17-3.13 (m, 2H), 1.60-1.55 (m, 4H), 1.43 (s, 9H).

*General procedure for the intermediates 14-16*. To an ice-cooled solution of the appropriate Boc-protected intermediate (11-13, 1 equiv) in CH<sub>2</sub>Cl<sub>2</sub> (2-3 mL) was added HCl 4 M in dioxane (2-3 mL) and the reaction mixture was stirred at 0 °C for 90 min. The solvent was evaporated, and the crude purified by flash chromatography on silica gel using dichloromethane/methanol/aqueous ammonia 33% (8:2:0.2) affording desired intermediates as free bases.

*(E) - N - (2-aminoethyl) - 3 - (4-hydroxy-3-methoxyphenyl) acrylamide (14)*. Synthesized from 11 (200 mg, 0.60 mmol) to afford 14 as pale yellow solid: 120 mg (86%); <sup>1</sup>H NMR (400 MHz, DMSO-*d*<sub>6</sub>) δ 8.34 (t, *J* = 5.4 Hz, 1H), 7.72 (d, *J* = 15.6 Hz, 1H), 7.53 (s, 1H), 7.41-7.38 (m, 1H), 7.20 (d, *J* = 7.6 Hz, 1H), 6.86 (d, *J* = 15.6 Hz, 1H), 4.21 (s, 3H), 3.59-3.55 (m, 2H), 3.04-3.00 (m, 2H), 2.92 (br s, 2H).

*(E) - N - (3-aminopropyl) - 3 - (4-hydroxy-3-methoxyphenyl) acrylamide (15)*. Synthesized from 12 (100 mg, 0.30 mmol) to afford 15 as pale green solid: 71 mg (99%); <sup>1</sup>H NMR (400 MHz, CD<sub>3</sub>OD) δ 7.40 (d, *J* = 15.6 Hz, 1H), 7.10 (s, 1H), 7.00-6.98 (m, 1H), 6.77 (d, *J* = 8.4 Hz, 1H), 6.48 (d, *J* = 15.6 Hz, 1H), 3.84 (s, 3H), 3.38 (t, *J* = 6.4 Hz, 2H), 2.96 (t, *J* = 7.2 Hz, 2H), 1.95-1.88 (m, 2H).

*(E) - N - (4-aminobutyl) - 3 - (4-hydroxy-3-methoxyphenyl) acrylamide (16)*. Synthesized from 13 (230 mg, 0.63 mmol) to afford 16 as pale green solid: 160 mg (96%); <sup>1</sup>H NMR (400 MHz, CD<sub>3</sub>OD) δ 7.39 (d, *J* = 15.6 Hz, 1H), 7.05 (s, 1H), 6.96 (d, *J* = 7.6 Hz, 1H), 6.73 (d, *J* = 8.4 Hz, 1H), 6.40 (d, *J* = 15.6 Hz, 1H), 3.82 (s, 3H), 3.31-3.23 (m, 2H), 2.80-2.78 (m, 2H), 1.59-1.58 (m, 4H).

*General procedure for compounds 1-3.* To an ice-cooled solution of the hydrochloride salt 17 [18](1 equiv) in dry DMF (3 mL) were added HOBt (1.3 equiv) and EDC (1.3 equiv) under N<sub>2</sub> atmosphere. The reaction mixture was stirred for 10 min, followed by addition of the appropriate intermediates (14-16) (2 equiv). Stirring was continued at room temperature for 36-48 h, and then the solvent evaporated under *vacuum*. The crude was purified by column chromatography on silica gel using dichloromethane /methanol/aqueous ammonia 33% (8.5:1.5:0.15) as mobile phase.

*(1r,3s,5R,7S)-3-amino-N-(2-((E)-3-(4-hydroxy-3-methoxyphenyl) acrylamido) ethyl)-5,7-dimethyladamantane-1-carboxamide (1).* Synthesized from 17 (64 mg, 0.24 mmol) and 14 (115 mg, 0.48 mmol) to afford 1 as green solid: 80 mg (74%); mp 122-124 °C; <sup>1</sup>H NMR (400 MHz, DMSO-*d*<sub>6</sub>) δ 7.99 (br s, 1H), 7.46 (br s, 1H), 7.32 (d, *J* = 15.6 Hz, 1H), 7.11 (s, 1H), 6.99-6.97 (m, 1H), 6.80 (d, *J* = 8.4 Hz, 1H), 6.40 (d, *J* = 15.6 Hz, 1H), 3.80 (s, 3H), 3.20-3.17 (m, 2H), 3.15-3.12 (m, 2H), 1.40 (s, 2H), 1.29-1.23 (m, 4H), 1.16-1.12 (m, 4H), 1.01 (s, 2H), 0.82 (s, 6H). <sup>13</sup>C NMR (100 MHz, DMSO-*d*<sub>6</sub>) δ 176.77, 166.17, 148.84, 148.27, 139.54, 126.70, 121.97, 119.25, 116.10, 111.23, 55.96, 51.30, 49.90, 49.79, 49.03, 46.18, 44.55, 44.10, 38.90, 32.95, 30.19. MS [ESI+] *m/z* 442 [M+1]<sup>+</sup>.

*(1r,3s,5R,7S)-3-amino-N-(3-((E)-3-(4-hydroxy-3-methoxyphenyl) acrylamido) propyl)-5,7-dimethyladamantane-1-carboxamide (2).* Synthesized from 17 (37 mg, 0.14 mmol) and 15 (71 mg, 0.28 mmol) to afford 2 as green solid: 31 mg (52%); mp 118-119 °C; <sup>1</sup>H NMR (400 MHz, CD<sub>3</sub>OD) δ 7.43 (d, *J* = 16 Hz, 1H), 7.11 (s, 1H), 7.03-7.00 (m, 1H), 6.78 (d, *J* = 8 Hz, 1H), 6.41 (d, *J* = 16 Hz, 1H), 3.87 (s, 3H), 3.29 (t, *J* = 8 Hz, 2H), 3.22 (t, *J* = 8 Hz, 2H), 1.73-1.66 (m, 2H), 1.63 (s, 2H), 1.44 (s, 4H), 1.32-1.26 (m, 4H), 1.14 (s, 2H), 0.92 (s, 6H). <sup>13</sup>C NMR (100 MHz, CD<sub>3</sub>OD) δ 177.79, 168.00, 148.87, 148.00, 140.82, 126.55, 121.91, 117.08, 115.16, 110.09, 54.95, 50.48, 48.96, 48.41, 48.28, 44.09, 43.78, 43.43, 36.40, 36.37, 32.47, 28.98, 28.60. MS [ESI+] *m/z* 455 [M+1]<sup>+</sup>.

*(1r,3s,5R,7S)-3-amino-N-(4-((E)-3-(4-hydroxy-3-methoxyphenyl) acrylamido) butyl)-5,7-dimethyladamantane-1-carboxamide (3).* Synthesized from 17 (89 mg, 0.30 mmol) and 16 (160 mg, 0.61 mmol) to afford 3 as green solid: 68 mg (48%); mp 116-117 °C; <sup>1</sup>H NMR (400 MHz, CD<sub>3</sub>OD) δ 7.40 (d, *J* = 15.6 Hz, 1H), 7.05 (s, 1H), 6.98-6.95 (m, 1H), 6.73 (d, *J* = 8 Hz, 1H), 6.37 (d, *J* = 15.6 Hz, 1H), 3.82 (s, 3H), 3.27-3.24 (m, 2H), 3.18-3.15 (m, 2H), 1.54-1.49 (m, 6H), 1.38-1.36 (m, 4H), 1.24 (s, 4H), 1.07 (s, 2H), 0.86 (s, 6H). <sup>13</sup>C NMR (100 MHz, CD<sub>3</sub>OD) δ 177.94, 167.83, 149.83, 148.29, 140.76, 126.04, 122.02, 116.86, 115.46, 110.03, 54.92, 49.76, 49.12, 49.09, 48.47, 44.22, 44.09, 43.91, 38.77, 38.63, 32.46, 28.76, 26.53, 26.44. MS [ESI+] *m/z* 470 [M+1]<sup>+</sup>.

General procedure for the intermediates 22-25. A mixture of memantine hydrochloride (MEM, 1 equiv), K<sub>2</sub>CO<sub>3</sub> (2 equiv), KI (1 equiv) and the appropriate intermediate (18-21, 1 equiv) in dry DMF (2-5 ml) was placed in a microwave (140°C, 250 Psi, 100 W) and left stirring for 1 h. The solvent was removed under reduced pressure and the crude purified by chromatography on silica gel using dichloromethane/methanol/aqueous ammonia 33% (9:1:0.2) as mobile phase.

*tert-butyl (3-(((1*r*,3*R*,5*S*,7*r*)-3,5-dimethyladamantan-1-yl) amino) propyl) carbamate (22)*. Synthesized from 18 [14](0.4 g, 1.2 mmol) to afford 22 as a pale oil: 0.24 g (59%); <sup>1</sup>H NMR (400 MHz, CDCl<sub>3</sub>) δ 5.34 (br s, 1H), 3.16-3.14 (m, 2H), 2.65 (t, *J* = 6.6 Hz, 2H), 2.09-2.07 (m, 1H), 1.67-1.64 (m, 2H), 1.49 (s, 2H), 1.38 (s, 9H), 1.32-1.23 (m, 8H), 1.06-1.05 (m, 2H), 0.78 (s, 6H).

*tert-butyl (4-(((1*r*,3*R*,5*S*,7*r*)-3,5-dimethyladamantan-1-yl) amino) butyl) carbamate (23)*. Synthesized from 19 [32](0.4 g, 1.5 mmol) to afford 23 as a pale oil: 0.35 g (87%); <sup>1</sup>H NMR (400 MHz, CDCl<sub>3</sub>) δ 5.32 (br s, 1H), 3.00-2.99 (m, 2H), 2.63 (t, *J* = 7.2 Hz, 2H), 2.06-2.04 (m, 1H), 1.59-1.55 (m, 4H), 1.48-1.43 (m, 2H), 1.37-1.28 (m, 13H), 1.24-1.13 (m, 4H), 1.02-1.01 (m, 2H), 0.73 (s, 6H).

*tert-butyl (5-(((1*r*,3*R*,5*S*,7*r*)-3,5-dimethyladamantan-1-yl) amino) pentyl) carbamate (24)*. Synthesized from 20 [33](0.4 g, 1 mmol) to afford 24 as a pale oil: 0.22 g (55%); <sup>1</sup>H NMR (400 MHz, CDCl<sub>3</sub>) δ 5.31 (br s, 1H), 3.11-3.09 (m, 2H), 2.59 (t, *J* = 7.4 Hz, 2H), 2.15-2.13 (m, 1H), 1.54-1.42 (m, 15H), 1.40-1.25 (m, 10H), 1.16-1.11 (m, 2H), 0.85 (s, 6H).

*tert-butyl (6-(((1*r*,3*R*,5*S*,7*r*)-3,5-dimethyladamantan-1-yl) amino) hexyl) carbamate (25)*. Synthesized from 21 [34](0.6 g, 1.6 mmol) to afford 25 as a pale oil: 0.4 g (79%); <sup>1</sup>H NMR (400 MHz, CDCl<sub>3</sub>) δ 4.61 (br s, 1H), 2.99-2.97 (m, 2H), 2.48 (t, *J* = 7.4 Hz, 2H), 2.03-2.02 (m, 1H), 1.41-1.32 (m, 15H), 1.24-1.15 (m, 12H), 1.01-1.00 (m, 2H), 0.73 (s, 6H).

General procedure for the intermediates 26-29. To an ice-cooled appropriate Boc-protected intermediate (22-25, 1 equiv) was added HCl 4 M in dioxane (4 mL) and the reaction mixture was stirred at 0°C for 15-20 min under N<sub>2</sub> atmosphere. The solvent was evaporated, and the crude purified by flash chromatography on silica gel using dichloromethane/methanol/aqueous ammonia 33% (8:2:0.4) affording desired intermediates as free bases.

*N<sup>1</sup>-(((1*r*,3*R*,5*S*,7*r*)-3,5-dimethyladamantan-1-yl)propane-1,3-diamine (26)*. Synthesized from 22 (0.24 g, 0.7 mmol) to afford 26 as a pale oil: 0.09 g (54%); <sup>1</sup>H NMR (400 MHz, DMSO-*d*<sub>6</sub>)

$\delta$  3.94 (br s, 3H), 2.74-2.73 (m, 2H) 2.59 (t,  $J$  = 6.8 Hz, 2H), 2.06-2.04 (m, 1H), 1.57- 1.50 (m, 2H), 1.42-1.41 (m, 2H), 1.26-1.18 (m, 8H), 1.09-1.00 (m, 2H), 0.78 (s, 6H).

*N*<sup>1</sup>-(((1*r*,3*R*,5*S*,7*r*)-3,5-dimethyladamantan-1-yl)butane-1,4-diamine (27). Synthesized from 23 (0.35 g, 1 mmol) to afford 27 as a pale oil: 0.18 g (72%); <sup>1</sup>H NMR (400 MHz, CDCl<sub>3</sub>)  $\delta$  2.66-2.62 (m, 5H), 2.53 (t,  $J$  = 6.8 Hz, 2H), 2.06-2.03 (m, 1H), 1.48-1.40 (m, 6H), 1.26-1.17 (m, 8H), 1.05-0.98 (m, 2H), 0.74 (s, 6H).

*N*<sup>1</sup>-(((1*r*,3*R*,5*S*,7*r*)-3,5-dimethyladamantan-1-yl)pentane-1,5-diamine (28). Synthesized from 24 (0.22 g, 0.6 mmol) to afford 28 as a pale oil: 0.11 g (70%); <sup>1</sup>H NMR (400 MHz, CDCl<sub>3</sub>)  $\delta$  2.63 (t,  $J$  = 7.1 Hz, 2H), 2.52 (t,  $J$  = 7.1 Hz, 2H), 2.07-2.06 (m, 1H), 1.59 (br s, 3H), 1.42-1.38 (m, 6H), 1.31-1.17 (m, 10H), 1.05-1.04 (m, 2H), 0.78 (s, 6H).

*N*<sup>1</sup>-(((1*r*,3*R*,5*S*,7*r*)-3,5-dimethyladamantan-1-yl)hexane-1,6-diamine (29). Synthesized from 25 (0.4 g, 1.06 mmol) to afford 29 as a pale oil: 0.16 g (54%); <sup>1</sup>H NMR (400 MHz, CDCl<sub>3</sub>)  $\delta$  2.63 (t,  $J$  = 7.2 Hz, 2H), 2.52 (t,  $J$  = 7.2 Hz, 2H), 2.38 (br s, 3H), 2.08-2.07 (m, 1H), 1.44-1.38 (m, 6H), 1.30-1.19 (m, 12H), 1.06-1.05 (m, 2H), 0.78 (s, 6H).

*General procedure for compounds 4-7.* To an ice-cooled solution of FA (1 equiv) in dry DMF (3-4 mL) was added HOBt (1.3 equiv) and EDC (1.3 equiv) under N<sub>2</sub> atmosphere. The reaction mixture was stirred for 10 min at 0°C, followed by addition of Et<sub>3</sub>N (1.3 equiv) and the appropriate amine (26-29) (1 equiv). Stirring was then continued at room temperature overnight, then the solvent was evaporated under reduced pressure and the crude purified by chromatography on silica gel.

(*E*) - *N* - (3-(((1*r*,3*R*,5*S*,7*r*)-3,5-dimethyladamantan-1-yl) amino) propyl) - 3 - (4-hydroxy -3-methoxyphenyl) acrylamide (4). Synthesized from 26 (90 mg, 0.38 mmol), purified by chromatography on silica gel using petroleum ether/dichloromethane/methanol/aqueous ammonia 33% (2:6.5:1.5:0.16) as mobile phase to afford 4 as a yellow solid: 61.5 mg (39%); mp 213-215 °C; <sup>1</sup>H NMR (400 MHz, CDCl<sub>3</sub>)  $\delta$  7.66 (br s, 1H), 7.49 (d,  $J$  = 15.6 Hz, 1H), 7.09 (s, 1H), 7.08-7.04 (m, 1H), 6.88 (d,  $J$  = 8 Hz, 1H), 6.64 (d,  $J$  = 15.6 Hz, 1H), 3.90 (s, 3H), 3.57-3.52 (m, 2H), 2.94-2.91 (m, 2H), 2.24 (m, 3H), 1.89-1.88 (m, 2H), 1.72-1.63 (m, 4H), 1.43-1.32 (m, 4H), 1.20 (s, 2H), 0.85 (s, 6H). <sup>13</sup>C NMR (100 MHz, CDCl<sub>3</sub>)  $\delta$  167.60, 147.53, 147.02, 140.33, 127.35, 122.15, 119.07, 114.87, 110.05, 59.04, 56.03, 49.88, 44.16, 41.92, 39.60, 38.59, 37.00, 32.57, 29.67, 26.77, 24.06. MS [ESI+]  $m/z$  413 [M+1]<sup>+</sup>.

(*E*) - *N* - (4-(((1*r*,3*R*,5*S*,7*r*)-3,5-dimethyladamantan-1-yl) amino) butyl) - 3 - (4-hydroxy-3-methoxyphenyl) acrylamide (5). Synthesized from 27 (72.5 mg, 0.28 mmol), purified by

chromatography on silica gel using petroleum ether/dichloromethane/methanol/aqueous ammonia 33% (2:6.5:1.5:0.07) as mobile phase to afford 5 as a yellow solid: 39.6 mg (32%); mp 174-175 °C; <sup>1</sup>H NMR (400 MHz, CDCl<sub>3</sub>) δ 7.83 (br s, 1H), 7.41 (d, *J* = 15.6 Hz, 1H), 7.04 (s, 1H), 6.95 (d, *J* = 8.2 Hz, 1H), 6.86 (d, *J* = 8.2 Hz, 1H), 6.70 (d, *J* = 15.6 Hz, 1H), 3.81 (s, 3H), 3.33-3.32 (m, 2H), 2.82 (t, *J* = 7.4 Hz, 2H), 2.17 (s, 1H), 1.89-1.88 (m, 4H), 1.71-1.62 (m, 4H), 1.37-1.23 (m, 6H), 1.14 (s, 2H), 0.84 (s, 6H). <sup>13</sup>C NMR (100 MHz, CDCl<sub>3</sub>) δ 167.60, 147.53, 147.02, 140.33, 127.35, 122.15, 119.07, 114.87, 110.05, 59.04, 56.03, 49.88, 44.16, 41.92, 39.60, 38.59, 37.00, 32.57, 29.67, 26.77, 24.06. MS [ESI+] *m/z* 427 [M+1]<sup>+</sup>.

(*E*) – *N* – (5-(((1*r*,3*R*,5*S*,7*r*)-3,5-dimethyladamantan-1-yl) amino) pentyl) – 3 – (4-hydroxy-3-methoxyphenyl) acrylamide (6). Synthesized from 28 (54 mg, 0.2 mmol), purified by chromatography on silica gel using petroleum ether/dichloromethane/methanol/aqueous ammonia 33% (2:6.5:1.5:0.09) as mobile phase to afford 6 as a yellow solid: 27.7 mg (31%); mp 200-202 °C; <sup>1</sup>H NMR (400 MHz, CDCl<sub>3</sub>) δ 7.51 (d, *J* = 15.6 Hz, 1H), 7.03 (d, *J* = 7.6 Hz, 1H), 6.96 (s, 1H), 6.86 (d, *J* = 7.6 Hz, 1H), 6.31 (d, *J* = 15.6 Hz, 1H), 5.82 (br s, 1H), 3.86 (s, 3H), 3.37-3.33 (m, 2H), 2.61 (t, *J* = 7.2 Hz, 2H), 2.13-2.11 (m, 1H), 1.58-1.53 (m, 4H), 1.36-1.24 (m, 12H), 1.10-1.09 (m, 2H), 0.82 (s, 6H). <sup>13</sup>C NMR (100 MHz, CDCl<sub>3</sub>) δ 166.21, 147.43, 146.81, 140.72, 127.33, 121.93, 118.40, 114.84, 109.72, 55.86, 50.83, 48.43, 42.89, 40.83, 40.37, 39.52, 32.37, 30.24, 30.19, 29.45, 24.78. MS [ESI+] *m/z* 441 [M+1]<sup>+</sup>.

(*E*) – *N* – (6-(((1*r*,3*R*,5*S*,7*r*)-3,5-dimethyladamantan-1-yl) amino) hexyl) – 3 – (4-hydroxy-3-methoxyphenyl) acrylamide (7). Synthesized from 29 (0.1 g, 0.36 mmol), purified by chromatography on silica gel using petroleum ether/dichloromethane/methanol/aqueous ammonia 33% (2:6.5:1.5:0.1) as mobile phase to afford 7 as a yellow solid: 95.9 mg (59%); mp 203-204 °C; <sup>1</sup>H NMR (400 MHz, CDCl<sub>3</sub>) δ 7.51 (d, *J* = 15.2 Hz, 1H), 7.03 (d, *J* = 8.4 Hz, 1H), 6.97 (s, 1H), 6.86 (d, *J* = 8.4 Hz, 1H), 6.25 (d, *J* = 15.2 Hz, 1H), 5.73 (br s, 1H), 3.88 (s, 3H), 3.36-3.31 (m, 2H), 2.57 (t, *J* = 7.4 Hz, 2H), 2.12-2.09 (m, 1H), 1.54-1.45 (m, 6H), 1.33-1.23 (12H), 1.13-1.05 (m, 2H), 0.82 (s, 6H). <sup>13</sup>C NMR (100 MHz, CDCl<sub>3</sub>) δ 166.20, 147.57, 146.90, 140.74, 127.26, 121.96, 118.35, 114.90, 109.75, 55.85, 50.85, 48.42, 42.90, 40.79, 40.45, 39.54, 32.37, 30.24, 30.20, 29.50, 27.03, 26.73. MS [ESI+] *m/z* 455 [M+1]<sup>+</sup>.

### Electrophysiological assays

Inhibition of NMDARs by compounds 1-7 and memantine was assessed by the expression of GluN1-1a and GluN2A subunits in *Xenopus* oocytes followed by voltage clamp recording. Oocytes were obtained from the European *Xenopus* Resource Centre (University



of Portsmouth, UK) directly following their removal from mature female *Xenopus laevis* according to UK Home Office guidelines. Sections of the ovary were cut into smaller pieces and treated with 1 mg/mL collagenase type 1A (Sigma-Aldrich) in Ca<sup>2+</sup>-free modified Barth's media containing 96 mM NaCl, 2 mM KCl, 1 mM MgCl<sub>2</sub>, 5 mM HEPES, 2.5 mM pyruvic acid, 0.5 mM theophylline, 0.05 mg/mL gentamicin, pH 7.5, with shaking at 18°C for 40-60 minutes, in order to separate them into individual defolliculated oocytes. The oocytes were then rinsed in Ca<sup>2+</sup>-free modified Barth's media multiple times until the solution was clear and stored in modified Barth's media (as per Ca<sup>2+</sup>-free but including 1.8 mM CaCl<sub>2</sub>). Oocytes were injected with 50 nL of cRNA encoding both the GluN1-1a and GluN2A subunits (1:1 by weight ratio; total 250 ng/μL). The cRNA was synthesized from linearized plasmid DNA (pRK7) containing the GluN-encoding genes using an mMessage mMachine kit (Invitrogen). Following injection, oocytes were kept in modified Barth's media at 18 °C for 3-4 days before electrophysiological testing. Voltage-clamp recording was conducted using an Axoclamp-2A voltage-clamp amplifier (Axon Instruments, USA). Microelectrodes were pulled from borosilicate glass capillaries (TW150F-4, World Precision Instruments) using a Sutter P-97 programmable micropipette puller to have a resistance of 0.5-2 MΩ when filled with 3 M KCl. Oocytes were placed in a perfusion chamber and constantly perfused (~5 mL/min) with solution containing 96 mM NaCl, 2 mM KCl, 1.8 mM CaCl<sub>2</sub>, 10 mM HEPES, pH 7.5, and voltage-clamped at holding potentials (V<sub>h</sub>) between -40 and -100 mV. NMDAR currents were initiated by application of 100 μM NMDA + 10 μM glycine. Once the current had reached a steady state (~30 s) the test compounds were introduced at concentrations ranging from 0.01 to 100 μM until a new plateau (inhibited current) was achieved. All agonists and test compounds were applied using an Automate Valvelink 8 perfusion system. Analogue output from the amplifier was digitized by a CED 1401 plus A/D converter at 100 Hz and recorded on a windows PC using WinEDR software (Dr John Dempster, University of Strathclyde, UK). NMDA/glycine-evoked current in the presence of test compound was normalized to that in its absence just before test compound addition (% control response) and plotted against concentration. Concentration-inhibition data were fit by:

$$\% \text{ control response} = \frac{100}{1 + 10^{((\log_{10} IC_{50} - X) \times HillSlope)}} \quad \text{Equation 1}$$

to obtain IC<sub>50</sub> values, where X = Log<sub>10</sub>[compound]; using Graphpad Prism 7. All points were means of at least 5 separate oocytes. For voltage dependence studies the test compounds were applied at a single (~IC<sub>50</sub>) concentration but at four V<sub>h</sub>s in the range -40 to -100 mV. Data were normalized as above and fit by:

$$\% \text{ control response} = \frac{100}{(1 + [B]/K_D)e^{z\delta(FE/RT)}} \quad \text{Equation 2}$$

to obtain  $\delta$  values (fraction of the membrane electric field crossed by the blocking compound), where  $[B]$  is the concentration of the blocker,  $K_D$  is the dissociation constant at 0 mV,  $z$  is the charge valence of the blocker,  $F$  is Faraday's constant,  $E$  is the membrane potential,  $R$  is the universal gas constant and  $T$  is absolute temperature; using Graphpad Prism 7. All points were means of at least 5 separate oocytes.

### Reagents for cellular experiments (SH-SY5Y cells)

All hybrid compounds were solubilized in DMSO (at stock concentrations) and frozen ( $-20^\circ\text{C}$ ) in aliquots that were diluted immediately prior to use. For each experimental setting, one stock aliquot was thawed out and diluted to minimize compound damage due to repeated freeze and thaw cycles. The final concentration of DMSO in culture medium was  $<0.1\%$ . Ferulic Acid was purchased from Sigma Aldrich (Merck KGaA, Darmstadt, Germany). Rabbit polyclonal anti-human HO-1 (NBP1-31341) antibody was purchased from Novus (Biotechnne, Minneapolis USA). Mouse monoclonal anti- $\beta$ -tubulin (T0198) was purchased from by Sigma Aldrich (Merck KGaA, Darmstadt, Germany).

### Cell cultures

All culture media, supplements and Foetal Bovine Serum (FBS) were purchased from Sigma Aldrich (Merck KGaA, Darmstadt, Germany). Human neuroblastoma SH-SY5Y cells from the European Collection of Cell Cultures (ECACC No. 94030304) were cultured in a medium with equal amounts of Eagle's minimum essential medium and Nutrient Mixture Ham's F-12, supplemented with 10% heat-inactivated FBS, 2 mM glutamine, 0.1 mg/mL streptomycin, 100 IU/mL penicillin and non-essential aminoacids at  $37^\circ\text{C}$  in 5%  $\text{CO}_2$  and 95% air atmosphere. H4-SW cells were cultured in D-MEM medium (Invitrogen, Carlsbad, CA) supplemented with 10% fetal bovine serum (FBS), 100 U/mL penicillin, 100  $\mu\text{g}/\text{mL}$  streptomycin and 2 mM L-glutamine. Hygromycin B and Blasticidin S were used as selection antibiotics for SW mutation maintenance.

### Cell Viability

The mitochondrial dehydrogenase activity that reduces 3-(4,5-dimethylthiazol-2-yl)-2,5-diphenyl-tetrazolium bromide (MTT, Sigma Aldrich, Merck KGaA, Darmstadt, Germany) was used to determine cellular viability, in a quantitative colorimetric assay. At day 0, SH-

SY5Y cells were plated at a density of  $2.5 \times 10^4$  viable cells per well in 96-well plates. After treatment, according to the experimental setting, cells were exposed to an MTT solution in complete medium (1 mg/mL). Following 4 h incubation with MTT and treatment with sodium dodecyl sulfate (SDS) for 24 h, cell viability reduction was quantified by using a Synergy HT multidetection microplate reader (Bio-Tek).

### **Measurement of Intracellular ROS**

DCFH-DA (Sigma Aldrich, Merck KGaA, Darmstadt, Germany) was used to estimate intracellular ROS following two different experimental settings described in each figure legend. In each setting, cells were loaded with 25  $\mu$ M DCFH-DA for 45 min. After centrifugation DCFH-DA was removed, and the results were visualized using Synergy HT multidetection microplate reader (BioTek) with excitation and emission wavelengths of 485 and 530 nm, respectively.

### **Real-time PCR (RT-PCR)**

For RNA extraction,  $2 \times 10^6$  cells were used. Total RNA was extracted using a Direct-zol™ RNA MiniPrep (Zymo Research, Irvine, USA) following the manufacturer's instructions. QuantiTect reversion transcription kit and QuantiTect Sybr Green PCR kit (Qiagen, Valencia, CA, USA) were used for cDNA synthesis and gene expression analysis, following the manufacturer's specifications. Nrf2, HO-1, and GAPDH primers were provided by Qiagen. GAPDH was used as an endogenous reference.

### **Immunodetection of HO-1, flAPP and sAPP $\alpha$**

The expression of HO-1 in whole cell lysates was assessed by Western blot analysis. After treatment, cell monolayers were washed twice with ice-cold PBS, lysed on the culture dish by the addition of ice-cold homogenization buffer (50 mM Tris-HCl pH 7.4, 150 mM NaCl, 5 mM EDTA, 0.5% Triton X-100 and protease inhibitor mix) and an aliquot was used for protein quantification, whereas the remainder was prepared for western blot by mixing the cell lysate with 2X sample buffer (125 mM Tris-HCl pH 6.8, 4% SDS, 20% glycerol, 6%  $\beta$ -mercaptoethanol, 0.1% bromophenol blue) and then denaturing at 95°C for 5 min. Equivalent amounts of extracted proteins were loaded into a SDS-PAGE gel, electrophoresed under reducing conditions, transferred to a PVDF membrane (Sigma Aldrich, Merck KGaA, Darmstadt, Germany) and then blocked for 1 h with 5% w/v BSA in Tris-buffered saline containing 0.1% Tween 20 (TBS-T). The proteins were visualized using primary antibodies for HO-1, full length (fl) APP or soluble APP alpha (sAPP $\alpha$ ) and

$\alpha$ - or  $\beta$ -tubulin (1:1000) followed by secondary horseradish peroxidase conjugated antibody (1:5000) diluted in 5% w/v BSA in TBS-T. Tubulins were performed as a control for gel loading. Signal development was carried out using an enhanced chemiluminescent method (Pierce, Rockford, IL, USA).

### Densitometry and statistics

All experiments, unless specified, were performed at least three times with representative results being shown. Data are expressed as mean  $\pm$  SEM. The relative densities of the acquired images of Western blotting bands were analyzed with ImageJ software. Statistical analyses were performed using Prism software version 7.0 (GraphPad Software, La Jolla, CA, USA). Statistical differences were determined by analysis of variance (ANOVA) followed, when significant, by an appropriate *post hoc* test as indicated in figure legends. A *p* value of <0.05 was considered statistically significant.

### REFERENCES

- [1] Niu H, Álvarez-Álvarez I, Guillén-Grima F, Aguinaga-Ontoso I. Prevalence and incidence of Alzheimer's disease in Europe: A meta-analysis. *Neurologia*, 32(8), 523-532 (2017).
- [2] Traynelis SF, Wollmuth LP, McBain CJ *et al.* Glutamate receptor ion channels: structure, regulation, and function. *Pharmacol Rev*, 62(3), 405-496 (2010).
- [3] Müller MK, Jacobi E, Sakimura K, Malinow R, von Engelhardt J. NMDA receptors mediate synaptic depression, but not spine loss in the dentate gyrus of adult amyloid Beta ( $A\beta$ ) overexpressing mice. *Acta Neuropathol Commun*, 6(1), 110 (2018).
- [4] Hardingham GE, Fukunaga Y, Bading H. Extrasynaptic NMDARs oppose synaptic NMDARs by triggering CREB shut-off and cell death pathways. *Nat Neurosci*, 5(5), 405-414 (2002).
- [5] Lipton SA. NMDA receptor activity regulates transcription of antioxidant pathways. *Nat Neurosci*, 11(4), 381-382 (2008).
- [6] Lanni C, Fagiani F, Racchi M *et al.* Beta-amyloid short- and long-term synaptic entanglement. *Pharmacol Res*, 139, 243-260 (2019).
- [7] Tu S, Okamoto S, Lipton SA, Xu H. Oligomeric  $A\beta$ -induced synaptic dysfunction in Alzheimer's disease. *Mol Neurodegener*, 9, 48 (2014).
- [8] Xia P, Chen HS, Zhang D, Lipton SA. Memantine preferentially blocks extrasynaptic over synaptic NMDA receptor currents in hippocampal autapses. *J Neurosci*, 30(33), 11246-11250 (2010).
- [9] Song X, Jensen M, Jogini V *et al.* Mechanism of NMDA receptor channel block by MK-801 and memantine. *Nature*, 556(7702), 515-519 (2018).

- [10] Takahashi H, Xia P, Cui J *et al.* Pharmacologically targeted NMDA receptor antagonism by NitroMemantine for cerebrovascular disease. *Sci Rep*, 5, 14781 (2015).
- [11] Figueiredo CP, Clarke JR, Ledo JH *et al.* Memantine rescues transient cognitive impairment caused by high-molecular-weight  $\alpha\beta$  oligomers but not the persistent impairment induced by low-molecular-weight oligomers. *J Neurosci*, 33(23), 9626-9634 (2013).
- [12] Benchekroun M, Romero A, Egea J *et al.* The Antioxidant Additive Approach for Alzheimer's Disease Therapy: New Ferulic (Lipoic) Acid Plus Melatonin Modified Tacrines as Cholinesterases Inhibitors, Direct Antioxidants, and Nuclear Factor (Erythroid-Derived 2)-Like 2 Activators. *J Med Chem*, 59(21), 9967-9973 (2016).
- [13] Lipton SA. Paradigm shift in neuroprotection by NMDA receptor blockade: memantine and beyond. *Nat Rev Drug Discov*, 5(2), 160-170 (2006).
- [14] Simoni E, Daniele S, Bottegoni G *et al.* Combining galantamine and memantine in multitargeted, new chemical entities potentially useful in Alzheimer's disease. *J Med Chem*, 55(22), 9708-9721 (2012).
- [15] Reggiani AM, Simoni E, Caporaso R *et al.* *In Vivo* Characterization of ARN14140, a Memantine/Galantamine-Based Multi-Target Compound for Alzheimer's Disease. *Sci Rep*, 6, 33172 (2016).
- [16] Minniti E, Byl JAW, Riccardi L *et al.* Novel xanthone-polyamine conjugates as catalytic inhibitors of human topoisomerase II $\alpha$ . *Bioorg Med Chem Lett*, 27(20), 4687-4693 (2017).
- [17] Riva E, Comi D, Borrelli S *et al.* Synthesis and biological evaluation of new camptothecin derivatives obtained by modification of position 20. *Bioorg Med Chem*, 18(24), 8660-8668 (2010).
- [18] Wanka L, Cabrele C, Vanejews M, Schreiner P. gamma-aminoadamantanecarboxylic acids through direct C-H bond amidations. *European Journal of Organic Chemistry*, (9), 1474-1490 (2007).
- [19] Sobolevsky A, Koshelev S, Khodorov B. Probing of NMDA channels with fast blockers. *Journal of Neuroscience*, 19(24), 10611-10626 (1999).
- [20] Woodhull AM. Ionic blockage of sodium channels in nerve. *J Gen Physiol*, 61(6), 687-708 (1973).
- [21] Cuadrado A, Rojo AI, Wells G *et al.* Therapeutic targeting of the NRF2 and KEAP1 partnership in chronic diseases. *Nat Rev Drug Discov*, 18(4), 295-317 (2019).
- [22] Dinkova-Kostova AT, Kostov RV, Canning P. Keap1, the cysteine-based mammalian intracellular sensor for electrophiles and oxidants. *Arch Biochem Biophys*, 617, 84-93 (2017).
- [23] Basagni F, Lanni C, Minarini A, Rosini M. Lights and shadows of electrophile signaling: focus on the Nrf2-Keap1 pathway. *Future Med Chem*, 11(7), 707-721 (2019).
- [24] Simoni E, Serafini MM, Caporaso R *et al.* Targeting the Nrf2/Amyloid-Beta Liaison in Alzheimer's Disease: A Rational Approach. *ACS Chem Neurosci*, 8(7), 1618-1627 (2017).

- 
- [25] Simoni E, Bergamini C, Fato R *et al.* Polyamine conjugation of curcumin analogues toward the discovery of mitochondria-directed neuroprotective agents. *J Med Chem*, 53(19), 7264-7268 (2010).
- [26] Bordji K, Becerril-Ortega J, Nicole O, Buisson A. Activation of extrasynaptic, but not synaptic, NMDA receptors modifies amyloid precursor protein expression pattern and increases amyloid- $\beta$  production. *J Neurosci*, 30(47), 15927-15942 (2010).
- [27] Folch J, Busquets O, Ettcheto M *et al.* Memantine for the Treatment of Dementia: A Review on its Current and Future Applications. *J Alzheimers Dis*, 62(3), 1223-1240 (2018).
- [28] Alley GM, Bailey JA, Chen D *et al.* Memantine lowers amyloid-beta peptide levels in neuronal cultures and in APP/PS1 transgenic mice. *J Neurosci Res*, 88(1), 143-154 (2010).
- [29] Bordji K, Becerril-Ortega J, Buisson A. Synapses, NMDA receptor activity and neuronal A $\beta$  production in Alzheimer's disease. *Rev Neurosci*, 22(3), 285-294 (2011).
- [30] Habib A, Sawmiller D, Tan J. Restoring Soluble Amyloid Precursor Protein  $\alpha$  Functions as a Potential Treatment for Alzheimer's Disease. *J Neurosci Res*, 95(4), 973-991 (2017).
- [31] Palermo G, Minniti E, Greco M *et al.* An optimized polyamine moiety boosts the potency of human type II topoisomerase poisons as quantified by comparative analysis centered on the clinical candidate F14512. *Chemical Communications*, 51(76), 14310-14313 (2015).
- [32] Nguyen C, Ruda GF, Schipani A *et al.* Acyclic nucleoside analogues as inhibitors of *Plasmodium falciparum* dUTPase. *J Med Chem*, 49(14), 4183-4195 (2006).
- [33] Lamanna G, Smulski C, Chekkat N *et al.* Multimerization of an Apoptogenic TRAIL-Mimicking Peptide by Using Adamantane-Based Dendrons. *Chemistry-a European Journal*, 19(5), 1762-1768 (2013).
- [34] Zanicelli V, Bazzoni M, Arduini A *et al.* Redox-Switchable Calix[6]arene-Based Isomeric Rotaxanes. *Chemistry*, 24(47), 12370-12382 (2018).

---

**PART 4**

The following manuscript was published in *Alzheimer's & Dementia (N Y)* in 2020 as:

**Targeting dementias through cancer kinases inhibition**

**Francesca Fagiani, Cristina Lanni, Marco Racchi, and Stefano Govoni**

**Abstract**

The failures in Alzheimer's disease (AD) therapy strongly suggest the importance of reconsidering the research strategies analyzing other mechanisms that may take place in AD as well as, in general, in other neurodegenerative dementias. Taking into account that in AD a variety of defects result in neurotransmitter activity and signaling efficiency imbalance, neuronal cell degeneration and defects in damage/repair systems, aberrant and abortive cell cycle, glial dysfunction, and neuroinflammation, a target may be represented by the intracellular signaling machinery provided by the kinome. In particular, based on the observations of a relationship between cancer and AD, we focused on cancer kinases for targeting neurodegeneration, highlighting the importance of targeting the intracellular pathways at the intersection between cell metabolism control/duplication, the inhibition of which may stop a progression in neurodegeneration.

**Keywords:** Alzheimer's disease, c-Abl, c-kit, cancer kinases, dementia, Fyn, GSK-3 $\beta$ , kinase inhibitors, neurodegeneration, p38 MAPK.

**PERSPECTIVE**

## Targeting dementias through cancer kinases inhibition

**Francesca Fagiani<sup>1,2</sup> | Cristina Lanni<sup>1</sup> | Marco Racchi<sup>1</sup> | Stefano Govoni<sup>1</sup>**<sup>1</sup> Department of Drug Sciences (Pharmacology Section), University of Pavia, Pavia, Italy<sup>2</sup> Scuola Universitaria Superiore IUSS Pavia, Pavia, Italy

### 1. Objective

The present review aims to dissect the burgeoning landscape of druggable kinases in Alzheimer's disease (AD), focusing on selected cancer kinases currently under investigation in clinical trials as therapeutic targets. The present review intends to: (1) examine the dysregulation of intracellular signaling pathways, regulated by protein kinases, involved in the activation/inhibition of either pro-survival or cell death pathways, playing a central role both in cancer and neurodegeneration; (2) pinpoint the most relevant druggable kinases to counteract neurodegeneration in AD, with strong implications also in other dementias; (3) discuss cancer kinases inhibition as a therapeutic approach for AD treatment, repurposing existing anti-cancer drugs for non-oncological indications; and (4) summarize current challenges and discuss future limitations of such a rapidly evolving field. Groundbreaking understating of kinase signaling networks at molecular level may lead to major advances in repurposing existing drugs for new targets or disease indications.

### 2. Background

The current knowledge on the pathogenesis of AD, as well as the existing models of etiology, have been unable to provide an effective therapeutic option for the treatment of AD. As an example, therapeutic approaches targeting amyloid beta (A $\beta$ ), on which a great effort has been spent by the scientific and clinical communities, have so far largely failed to reach a significant clinical outcome. Several thousands of patients have been treated with anti-A $\beta$  drugs, ranging from strategies targeting the levels of A $\beta$  peptides, either by interfering with A $\beta$  production (eg,  $\beta$ - and  $\gamma$ -secretase inhibitors), by promoting A $\beta$  clearance, or neutralizing it with humanized monoclonal antibodies. However, although, using the latter, plaques may be cleared, so far, no convincing and significant clinical



advantages in affecting the ongoing degenerative processes have been reported. Notably, results from trials involving anti-A $\beta$  antibodies, such as gantenerumab, solanezumab, and aducanumab, suggested that to appreciate cognitive improvements in AD patients the treatment should probably be started at the very early stages of the disease<sup>1</sup>. Accordingly, to avoid the challenges associated with prevention trials design in late-onset sporadic AD, the pioneering DIAN-TU (Dominantly Inherited Alzheimer Network Trials Unit) was launched. DIAN-TU is phase 2/3 trial based on a primary prevention of the autosomal dominant form of AD, which has been shown to be linked to A $\beta$  dysfunction and to cause cognitive impairment at a younger and predictable age<sup>1</sup>. Unfortunately, a topline analysis of the trial reported that both of the investigational anti-amyloid drugs, Roche's gantenerumab and Lilly's solanezumab, missed the primary endpoint, consisting of a composite of four cognitive tests (ie, DIAN-Multivariate Cognitive Endpoint). Several considerations (small sample size, heterogeneity of the disease stage, secondary outcomes still under scrutiny) suggest caution in interpreting these preliminary disappointing data. Some encouragement derives from the application in October 2019 to the U.S. Food and Drug Administration (FDA) for the marketing approval of aducanumab<sup>2</sup> after that the reanalysis of the phase 3 studies, originally discontinued after a futility analysis showing no clinical advantage of the treatment, revealed some significant results<sup>2</sup>. The discouraging results observed in AD therapy emphasize the need to redirect the research strategies by better rethinking the biological mechanisms and intracellular signaling machinery involved in AD, as well as, more in general, in other neurodegenerative dementias. Even if the pathological profile of neurodegenerative disorders is different, common biological traits are present including neuronal cell degeneration, defects in damage/repair systems, aberrant and abortive cell cycle events, and neuroinflammation. The further observations of a relationship between cancer and neurodegenerative disorders, such as AD and Parkinson's disease (PD)<sup>3</sup>, may direct to cancer kinases for targeting neurodegeneration. The field of cancer kinase inhibition for non-oncological indications, such as AD, is emerging as a challenging area to develop disease-modifying therapies. Indeed, tyrosine kinase inhibition provides a double-edged sword by manipulating autophagy to inhibit cell division and tumor growth in cancer, and by inducing toxic protein degradation as well as neuronal survival in neurodegeneration on the other hand.

### 3. New or updated hypothesis

Over the past decades, kinases have emerged as one of the most intensively investigated drug targets in current pharmacological research, due to their pivotal roles in modulating a wide array of cellular processes. A great effort has been directed toward the development of molecules specifically targeting the human kinome.<sup>4</sup> To date, the majority of molecules

show a spectrum of kinase inhibitors, with >250 currently in clinical trials and 48 approved by U.S. FDA, mostly to treat malignancies.<sup>5</sup> The therapeutic potential of kinase manipulation, as well as the functions of kinases as tumor biomarkers for diagnosis, prognosis, and treatment, have widely been characterized in oncology. Several kinase inhibitors have revolutionized the treatment of malignancies driven by a single oncogenic kinase, such as chronic myeloid leukemia and gastrointestinal stromal tumors. Initially focused on cancer therapy, kinase drug discovery has recently broadened its focus to include an expanded range of therapeutic areas, such as autoimmune and inflammatory diseases, as well as neurodegenerative disorders (reviewed by Ferguson and Gray<sup>6</sup>), including AD. However, the contribution of the dysregulation of human kinome to neurodegeneration has not been clarified so far and the field of kinase-directed therapies is still immature compared to their application in cancer therapy. The neuronal functions of many kinases are still largely uncharacterized, with a sparse indication of how these targets influence the major signaling pathways involved in AD. Further investigations on human brains are needed to profile the changes in protein kinase activity in the different brain areas during aging and the progression of neurodegeneration.

Unlike cancer, for which the identification of the specific kinase target led to the development of successful treatments, such lack of knowledge complicates the identification of single or clusters of specific kinases as drug target to counteract AD. The recognition of AD complexity suggests that addressing more than one target might be needed to set up a successful AD treatment. Accordingly, the complex and multifactorial pathophysiology of AD would suggest a multi-pharmacological approach rather than single target therapy, also in the context of kinase-directed drug discovery. Therefore, targeting multiple kinases rather than inhibiting any single kinase, by using either single drugs binding multiple proteins or cocktails of highly selective inhibitors, might be a promising strategy. In particular, some of the investigated protein kinase inhibitors show a “target promiscuity” profile. Owing to the fact that all kinases share a high degree of sequence conservation as well as common substrate recognition motifs, profiling the kinome selectivity of these inhibitors represents a fundamental step to attain the selectivity necessary for pharmacological target validation, as well as to predict and avoid off-target adverse effects. Such aspects may also present positive implications by allowing the identification of novel drug targets for already approved drugs and their repurposing for new targets or clinical indications. However, such wide diversity of interaction patterns shows a number of limitations. For instance, Karaman *et al.* screened 38 kinase inhibitors against a panel of 317 distinct human kinases, by using an *in vitro* competition binding assay, and identified a total of 3175 potential binding interactions,<sup>7</sup> with several kinase inhibitors showing higher affinity for their secondary targets rather than for their primary recognized targets. Such

wide diversity of interaction patterns strongly suggests the importance of fully characterizing the target spectrum of kinase inhibitors to better interpret their biological activity observed in preclinical and clinical studies. Furthermore, some kinase inhibitors exhibit a paradoxical effect, thus resulting in the activation of the same target kinase or different kinases. As an example, c-Raf (rapidly accelerated fibrosarcoma) inhibitors have been reported to trigger a reactivation of c-Raf, without affecting other targets involved in the same signaling pathway, such as MKK1 (mitogen-activated protein kinase 1) or p42 MAPK (mitogen-activated protein kinase)/ERK2 (extracellular signal-regulated kinase 2).<sup>8</sup> In addition, some Bcr (break point cluster)-Abl (Abelson) inhibitors possess off-target activity against Raf and stimulate paradoxical activation of BRAF and CRAF in a Ras-dependent manner.<sup>9</sup>

Based on these observations, in the following sections, we will focus on some selected kinase inhibitors, repurposed in AD and other dementias, that are currently under investigation in clinical trials as therapeutic tools (**Table 1**), highlighting the strength and weakness of their use.

**TABLE 1** Clinical trials of cancer kinase inhibitors in Alzheimer's Disease

Agent	Mechanism of action	Therapeutic purpose	Clinicaltrials.gov ID	Phase/status	Sponsor
Saracatinib (AZD0530)	Selective Src tyrosine kinase inhibitor	Effect on cerebral metabolic rate for glucose	NCT02167256	Phase 2 Completed	Yale University
Masitinib (AB1010)	Tyrosine kinase inhibitor targeting c-Kit, platelet-derived growth factor receptors, and, a lesser extent, Lyn, Fyn, and the FAK pathway	Activity on mast cells, modulation of inflammatory processes	NCT01872598	Phase 3 Active, not recruiting	AB Science
			NCT00976118	Phase 2 Completed	AB Science
Neflamapimod (VX-745)	Selective p38 MAPK inhibitor	Affects multiple cellular processes including inflammation and cellular plasticity; reduces amyloid plaque burden (DMT)	NCT03402659	Phase 2 Completed	EIP Pharma Inc, VU University
			NCT03435861	Phase 2 Recruiting	EIP Pharma Inc, Toulouse University, Foundation Plan Alzheimer
Nilotinib (AMN107)	Abl Tyrosine kinase inhibitor	Reduce amyloid and tau phosphorylation (DMT)	NCT02947893	Phase 2 Active, not recruiting	Georgetown University
DNL747	RIPK1 inhibitor	Reduce cytokines and other inflammatory factors (DMT)	NCT03757325	Phase 1 Active, not recruiting	Denali Therapeutics Inc
Tideglusib (NP031112)	GSK inhibitor	Reduce tau phosphorylation	NCT00948259	Phase 1 and 2 Completed	Noscira SA
			NCT01350362	Phase 2 Completed	Noscira SA

## 4. Kinase inhibitors to counteract tau and A $\beta$ -driven neurotoxicity

### 4.1 Saracatinib

Saracatinib (also known as AZD0530), a Fyn kinase inhibitor, has been largely investigated for its inhibitory effect on cell growth. Originally developed by AstraZeneca as a therapy for solid tumors to counteract tumor cell adhesion, migration, invasion, and cell proliferation,<sup>10</sup> saracatinib was deprioritized due to its limited benefits as a single agent for oncological conditions and is currently being investigated in clinical and preclinical programs for a variety of non-oncological conditions, including AD, pain, and psychosis. In particular, it has been repurposed as a disease-modifying therapy in AD, as Fyn modulates both A $\beta$ -induced synaptic dysfunctions and neurotoxicity, as well as tau phosphorylation. In particular, the capability of extracellular oligomeric A $\beta$  to bind with nanomolar affinity to cellular prion protein (PrP<sup>C</sup>) on neuronal cell surface and to activate the downstream signaling pathway involving Fyn kinase has been demonstrated (**Figure 1**).<sup>11,12</sup> Notably, A $\beta$  binding to PrP<sup>C</sup> has been shown to be highly specific for the soluble oligomeric form, with low or no affinity for fibrillary or monomeric A $\beta$  peptides.<sup>13</sup> Such connection between oligomeric A $\beta$ -PrP<sup>C</sup> complexes at the cell surface and intracellular Fyn kinase has been found to require the participation of the metabotropic glutamate receptor 5 (mGluR5).<sup>14</sup> Fyn activation by oligomeric A $\beta$ -PrP<sup>C</sup> has been reported to activate N-methyl-D-aspartate receptors (NMDA-R) by phosphorylating the intracellular segment of the NR2B subunit at Y-1472<sup>11,15</sup> and to induce dendritic spine loss.<sup>11</sup> In addition, Fyn kinase has been demonstrated to induce the downstream phosphorylation of tau. Accordingly, Fyn has been found to directly associate with tau and to phosphorylate tyrosine residues near the amino terminus.<sup>16-18</sup>

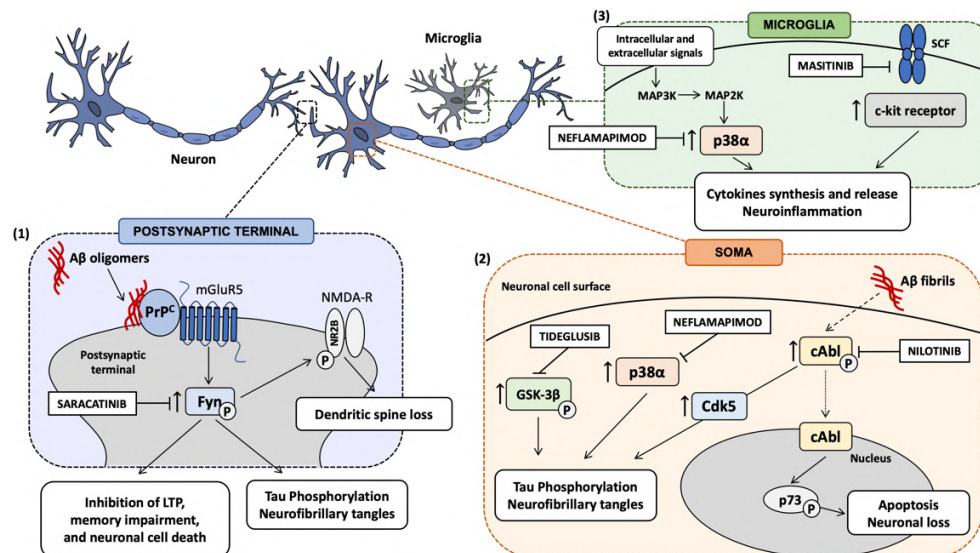


**FIGURE 1. Targeting cancer kinases with inhibitors in dementias.** (1) The intracellular pathway involving Fyn kinase has been demonstrated to be altered in Alzheimer's disease (AD), in which Fyn modulates both amyloid beta ( $A\beta$ )-driven synaptic dysfunction and neurotoxicity. At postsynaptic terminal, the extracellular soluble  $A\beta$  oligomers bind with nanomolar affinity to cellular prion protein (PrPC) on neuronal cell surface, thus triggering the activation of the downstream intracellular signaling pathway involving Fyn kinase. This activation of Fyn kinase by oligomeric  $A\beta$ -PrPC, which requires the participation of mGluR5, leads to the activation of N-methyl-D-aspartate receptors (NMDA-Rs) by phosphorylating their intracellular segment NR2B subunit, inducing dendritic spine loss. In addition, Fyn triggers the downstream phosphorylation of tau, by possibly contributing to neurofibrillary tangles formation. Saracatinib, a Fyn inhibitor, has been repurposed as disease-modifying therapy in AD. (2) At neuronal cell surface,  $A\beta$  fibrils increase c-Abl kinase activity, thus stimulating the nuclear translocation of c-Abl and inducing apoptosis and neuronal loss through c-Abl-mediated p73 phosphorylation. Furthermore, the activation of c-Abl kinase by  $A\beta$  fibrils promotes tau phosphorylation, both directly and indirectly, by activating the tau kinase Cdk5. c-Abl has been found to be hyperactivated in human AD and PD brains, as well as in Lewy body dementia (LBD), and its inhibitor nilotinib has been repurposed for PD, LBD, and AD. Moreover, in neurons, the overactivation of GSK-3 $\beta$  and p38 $\alpha$  contributes to tau phosphorylation. Tideglusib, a GSK-3 inhibitor, and neflamapimod, a p38 $\alpha$  inhibitor, have been repurposed in AD as potential disease-modifying therapies. Moreover, the U.S. Food and Drug Administration recently granted fast-track designation to neflamapimod for the treatment of LBD. (3) In microglia, several extracellular and intracellular signals trigger the consequential activation of MAPK3, MAPK2, and p38 $\alpha$ , stimulating the synthesis and release of pro-inflammatory cytokines, thus promoting neuroinflammatory processes. Neflamapimod has been investigated as therapeutic approach to counteract neuroinflammation in AD. Finally, the activation of the stem cell factor (SCF)/c-kit pathway mediates neuroinflammatory responses and the c-kit inhibitor, masitinib, has been tested in clinical trials for the treatment of rheumatoid arthritis, asthma, and as add-on therapy to riluzole in amyotrophic lateral sclerosis.

Taken together, these data prompted intense investigations on targeting Fyn kinase for the treatment of AD. Accordingly, Kaufman *et al.* demonstrated that AZD0530 at a dose of 5 mg/kg/d for 4 weeks fully rescued both spatial learning and memory deficits in 11/12-

month-old APP/PS1 transgenic mice.<sup>19</sup> In addition, after 6 weeks of AZD0530 or vehicle treatment, the AZD0530-treated APP/PS1 mice exhibited performance equal to wild type mice in novel object recognition,<sup>19</sup> demonstrating that AZD0530 was capable of reversing the age-dependent memory impairment produced by the transgene. Moreover, AZD0530 at a dose of 5 mg/kg/day for 5 weeks decreased total tau and phosphorylated tau in 11-month-old APP/PS1/Tau transgenic mice.<sup>19</sup> However, a recent multicenter randomized clinical trial (NCT02167256) of 159 participants with mild AD, whose primary outcome was the reduction in relative CMRgl (cerebral metabolic rate for glucose) measured by 18F-fluorodeoxyglucose (18F-FDG) PET (positron emission tomography), reported non-statistically significant effects of AZD0530 treatment on the relative cerebral metabolic rate for glucose or on secondary clinical or biomarker measures.<sup>20</sup> AZD0530 treatment did not slow cerebral metabolic decline and did not improve cognitive function, compared to placebo. In particular, the treatment groups did not significantly differ in secondary clinical outcomes, such as rates of change in ADAS-Cog11 (Alzheimer's Disease Assessment Scale–Cognitive Subscale), ADCS-ADL (Alzheimer's Disease Cooperative Study–Activities of Daily Living), CDR-SB (Clinical Dementia Rating–Sum of Boxes), NPI (Neuropsychiatric Inventory), or MMSE (Mini-Mental State Examination) scores.<sup>20</sup> Moreover, in patients receiving saracatinib, consistent trends in worsening cognitive, functional, as well as clinical global outcome, have been observed compared to placebo as measured by ADAS-Cog, ADCS-ADL, CDR-SB, respectively.<sup>20</sup> It is likely that such negative trends did not reach statistical significance due to the limited sample size. In addition, almost two-fold number of dropouts in the group receiving saracatinib ( $n = 21$ ) has been reported, compared to placebo group ( $n = 12$ ), mostly due to adverse events.<sup>20</sup> In detail, 73 participants (92.4%) treated with saracatinib and 65 participants (81.2%) receiving placebo have been reported to experience at least one adverse event.<sup>20</sup> In particular, the most frequent adverse events were diarrhea and other gastrointestinal disorders that occurred in 38 participants (48.1%) receiving saracatinib and 23 participants (28.8%) receiving placebo.<sup>20</sup> On the other hand, trends for slowing the decrease in hippocampal volume and entorhinal thickness were observed.<sup>20</sup>

Therefore, although such results are discouraging, Fyn kinase cannot be excluded as a potential therapeutic target in AD. First of all, further optimization of selective Fyn inhibition is required to achieve a complete target engagement that can give us clues on Fyn kinase as a target of disease modification in AD. Moreover, given the well-established effect of saracatinib on glutamatergic transmission, it can be speculated that the drug does not modify the cognitive ability, but it may affect other behavioral disturbances. Notably, the inhibition of Fyn kinase may be addressed to specific subpopulations of AD patients. The identification of kinase-based molecular signatures in AD patients may allow us to

identify patients more prone to respond to the therapy. In particular, AD patients carrying a specific Tyr<sub>682</sub> APP phosphorylation might be more likely to respond to Fyn kinase inhibitor therapy. This hypothesis arises from literature data showing that Fyn binds to amyloid- $\beta$  precursor protein (APP) on the <sub>682</sub>YENPTY<sub>687</sub> domain in human AD neurons and mediates APP phosphorylation on the Tyr<sub>682</sub> residue, in turn altering APP trafficking and sorting<sup>21,22</sup> and these effects are completely prevented by the Src tyrosine kinase inhibitor PP2.<sup>21</sup> Specific investigation of saracatinib on AD subpopulations carrying Tyr<sub>682</sub> APP phosphorylation may solve this problem and help to better select the responsive patients. Notably, the identification of specific molecular signatures and biomarkers may be useful to better select and stratify subpopulations of AD patients for an appropriate drug treatment. However, this approach, yet theoretical, has to be investigated to practically translate it from the bench to the bedside and, to date, no clinical data are available to substantiate this hypothesis.

#### 4.2. Nilotinib

Nilotinib (Tasigna, AMN107, Novartis, Switzerland), a Bcr-Abl tyrosine kinase inhibitor, was approved by EMA in 2007 and by the U.S. FDA in 2010 and authorized for the treatment of adults with Philadelphia chromosome positive chronic myeloid leukemia.<sup>23</sup> Nilotinib has been recently repurposed in a number of neurodegenerative diseases, such as PD, Lewy body dementia (LBD), and AD. The rationale for c-Abl inhibition as treatment for neurodegenerative diseases relies on the hyperactivation of such kinase in human AD and PD brains, as well as in a variety of tauopathies.<sup>24–27</sup> Accordingly, Schlatterer *et al.* reported an increased activation of the tyrosine kinase c-Abl both in *in vivo* and *in vitro* transgenic AD models.<sup>28</sup> Notably, the activation of c-Abl signaling has been reported as a crucial event mediating the synaptic damage induced by A $\beta$ .<sup>29</sup> The exposure of rat hippocampal neurons to 5  $\mu$ M A $\beta$  fibrils has been found to increase c-Abl activity, thus inducing apoptosis through c-Abl-mediated p73 phosphorylation (**Figure 1**).<sup>30</sup> The neuronal death of hippocampal neurons exposed to A $\beta$  fibrils was prevented by the treatment with the c-Abl inhibitor STI571 (imatinib mesylate, Gleevec). Moreover, the intraperitoneal administration of STI571 has been shown to reduce rat cognitive impairment on spatial memory performance, induced by the bilateral hippocampal injection of 5  $\mu$ M A $\beta$  fibrils, and to ameliorate spatial learning and memory impairment in 11-month-old APP/PS1 transgenic mice.<sup>31</sup> Furthermore, the activation of c-Abl by A $\beta$  has been found not only to stimulate proapoptotic signaling pathway through p73, but also to promote tau phosphorylation,<sup>29</sup> by activating the tau kinase Cdk5 (cyclin-dependent kinase 5) and by directly phosphorylating tau at tyrosine 394.<sup>29,32</sup> Notably, tau phosphorylated at tyrosine 394 has been shown to be present in pre-tangle neurons in AD brains, supporting

the hypothesis that c-Abl may contribute to neurofibrillary tangle formation and to their associated cognitive deficits.<sup>26,32</sup> It can be speculated that nilotinib, via c-Abl inhibition, may prevent A $\beta$ -driven apoptosis and neurodegeneration by reducing both the activation of c-Abl/p73 proapoptotic signaling pathway and c-Abl/Cdk5-mediated tau phosphorylation, possibly preventing neurofibrillary tangle formation. However, A $\beta$ -driven effects on c-Abl activity and its downstream intracellular pathways require further investigations.

Taken together, these findings suggest that c-Abl abnormal activation may contribute to neuronal dysfunction and support the use of cAbl inhibitors as potential AD treatments.

On the basis of preclinical data, nilotinib has been considered for a clinical application. A randomized, double-blind, and placebocontrolled phase 2 study (NCT02947893) is currently evaluating the impact of low doses of nilotinib in 42 patients with mild to moderate AD and ended in February 2020. Safety has been assessed as primary endpoint based on the number of participants who experienced adverse effects or had abnormal laboratory values after 12 months of treatment, whereas cerebrospinal fluid (CSF) biomarkers (eg, levels of A $\beta$  and tau), clinical outcomes, as well as target engagement and proof of mechanism (c-Abl inhibition) have been evaluated as secondary endpoints. Despite the strong limitations related to the study design, some preliminary results came from Pagan et al. open label pilot study, enrolling only 12 participants, that evaluated the safety and tolerability of nilotinib in patients with advanced PD with dementia or LBD, exposed to once daily oral dose of nilotinib for 6 months.<sup>33</sup> Nilotinib has been reported to be safe and well tolerated, to penetrate the blood brain barrier (BBB), as well as to significantly reduce CSF total tau and p-tau.<sup>33</sup> Moreover, positive trends for cognitive improvement, measured by MMSE and the Scales for Outcomes in Parkinson's Disease-Cognition, were observed.<sup>33</sup> In addition, c-Abl target engagement was demonstrated, with an observed 30% reduction in c-Abl activation.<sup>33</sup> Such decrease in c-Abl phosphorylation may account, at least in part, for the observed reduction in CSF p-tau. Beyond c-Abl inhibition, however, nilotinib showed the capability to interfere with other signaling pathways. In particular, in a variety of lines expressing oncogenic RAS, nilotinib has been found to possess the spectrum of weak RAF inhibitor, and to lead to the formation of BRAF: CRAF dimers, thus stimulating paradoxical activation of the pathway.<sup>9</sup> Moreover, in a recent phase 2 placebo-controlled randomized clinical trial testing the safety and tolerability of nilotinib in 75 patients with PD, doses of 150 or 300 mg nilotinib have been found reasonably safe, although serious adverse effects (eg, cardiovascular, gastrointestinal, renal, neurological, pulmonary) have been observed in 24% and 48% of the nilotinib-150 mg and nilotinib-300 mg groups, respectively, compared to 16% of the placebo group.<sup>34</sup> However, further larger and long-term studies are required to assess the



safety and tolerability of nilotinib in PD patients. In addition, nilotinib-150 mg, but not nilotinib-300 mg, treatment has been shown to significantly reduce the levels of oligomeric  $\alpha$ -synuclein, with no change of CSF total  $\alpha$ -synuclein at 12 months.<sup>34</sup> This result is consistent with previous findings reporting a higher reduction of  $\alpha$ -synuclein levels upon treatment with lower dose of nilotinib (1 mg/kg) compared to higher dose (10 mg/kg) in animal models of  $\alpha$ -synucleinopathies.<sup>35</sup>

## 5. Tideglusib

Tideglusib (NP-12, NP031112), a selective non-ATP competitive GSK3 inhibitor, is repurposed for the treatment of AD. GSK-3 represents a therapeutic node at the intersection of multiple disorders, ranging from cancer to neurodegenerative disorders. According to “the GSK3 hypothesis” of AD postulated by Hooper *et al.*, the overactivation of GSK-3 $\beta$  accounts for cognitive impairment, tau hyperphosphorylation, increased A $\beta$  production, and neuronal death in AD.<sup>36</sup> Tideglusib has been reported to reduce a range of disease markers (**Figure 1**), including tau hyperphosphorylation, amyloid deposition, neuron loss, and gliosis in mouse entorhinal cortex and hippocampus, and to reverse a spatial memory deficit in AD transgenic mice.<sup>37–39</sup> Furthermore, GSK3 $\beta$  inhibition has been shown to reduce A $\beta$  production and to ameliorate the AD-like neuropathology and behavioral deficits in the water maze in hAPP transgenic mice.<sup>40</sup>

A pilot, double-blind, randomized phase II trial (NCT00948259) evaluated the safety and efficacy of tideglusib in 30 patients with mild to moderate AD, reporting good tolerability and positive trends for cognitive benefits in MMSE, ADAS-cog, GDS (Geriatric Depression Scale), and GCA (Global Clinical Assessment).<sup>41</sup> A subsequent doubleblind, randomized, placebo-controlled phase II trial (NCT01350362), testing the efficacy of tideglusib in a cohort of 306 mild to moderate AD patients, reported to have missed its primary cognitive endpoint.<sup>42</sup> Recently, Matsunaga *et al.* proposed a systematic review and metaanalysis of randomized controlled trials testing the efficacy and safety of GSK-3 inhibitors in mild cognitive impairment and AD patients.<sup>43</sup> Among the five trials included in study, no significant differences in cognitive function scores between GSK-3 inhibitors and placebo groups were observed, further corroborating data demonstrating the ineffectiveness of such a therapeutic approach.<sup>43</sup> A better focused analysis might be useful to understand whether a marker, a subgroup of patients, and/or other different parameters may refine the effectiveness of such a therapeutic approach.

## 6. Kinase inhibitors to counteract neuroinflammation

## 6.1 Neflamapimod

Neflamapimod (previously code-named VX-745) is an oral selective small molecule initially tested for rheumatoid arthritis and then repurposed as a disease-modifying drug for AD.<sup>44</sup> It is classified as an inhibitor of the intracellular signal transduction enzyme p38 MAPK $\alpha$  (p38 $\alpha$ ), a key modulator of microglia regulation and neuroinflammation (**Figure 1**).<sup>45</sup> Indeed, p38 $\alpha$  is expressed in microglia where it mediates inflammatory responses stimulating the release of pro-inflammatory cytokines such as tumor necrosis factor  $\alpha$  (TNF $\alpha$ ) and Interleukin1 $\beta$  (IL-1 $\beta$ )<sup>46</sup>, and in neurons where it modulates memory formation through effects on long-term potentiation (LTP)/depression.<sup>47</sup> Moreover, neuronal p38 $\alpha$  has been implicated in tau phosphorylation<sup>48</sup> and in A $\beta$  oligomer-induced neurotoxicity,<sup>49</sup> and its role has been investigated as a therapeutic target for neuroinflammatory conditions, including AD.<sup>50</sup> In AD transgenic models, p38 $\alpha$  inhibition has been found to reverse A $\beta$  induced synaptic dysfunction and loss,<sup>51,52</sup> and p38 $\alpha$  gene knockout improves synaptic function and memory as well as reduces A $\beta$  production in AD transgenic mice.<sup>53,54</sup>

Preclinical studies demonstrated that neflamapimod improved performance in the Morris water maze test and significantly reduced hippocampal IL-1 $\beta$  protein levels in cognitively impaired aged (20 to 22 months) rats.<sup>55</sup> Such effects appear to be independent because the behavioral improvement in the Morris water maze was evident at a lower dose than that required to reduce IL-1 $\beta$ .<sup>55</sup> A blinded and placebo-controlled Phase 2b study (REVERSE-SD), enrolling 161 people with mild AD, compared a 6-month course of neflamapimod group with placebo on change in total and delayed recall on the Hopkins Verbal Learning Test, Revised (HVLTR).<sup>56</sup> The REVERSE-SD trial failed to meet its primary endpoint of improving episodic memory at the end of the study period, as measured by HVLTR and, secondarily, by the Wechsler Memory Scale (WMS) immediate and delayed recall (<https://www.prnewswire.com/news-releases/eip-pharmaannounces-clinical-trial-results-of-reverse-sd-a-phase-2b-study-ofneflamapimod-in-early-stage-alzheimers-disease-300953422.html>). Notably, a pharmacokinetics-pharmacodynamic analysis showed positive trends toward improvement in the HVLTR and WMS in patients with the highest plasma drug concentrations, suggesting that the clinical outcome may be dose-dependent. Thus, the observed effects of neflamapimod on CSF biomarkers, associated with those on episodic memory in patients with the highest blood concentrations, highlight the need to further investigate neflamapimod at higher doses and for long-term exposure. Such promising results are currently under investigation. In the REVERSE-SD trial, neflamapimod met its secondary objectives of target engagement and proof-of-mechanism, demonstrating statistically significant reductions in the CSF biomarkers phospho-tau and total tau. Moreover, the CSF levels of the postsynaptic protein neurogranin have been

measured as biomarker of AD correlating with cognitive decline<sup>57</sup>, and a trend toward reduced CSF neurogranin has been reported.<sup>56</sup> Notably, the observed reduction in CSF phospho-tau and total tau by neflamapimod provides the rationale for the extended application of neflamapimod to tauopathies, such as LBD. Consistently, the FDA recently granted fast track designation for the treatment of LBD to neflamapimod, which is currently being studied in separate Phase 2 trials in patients with LBD.

Another Phase 2 study (NCT03435861), enrolling 40 people with prodromal AD and with cerebral amyloidopathy (as measured by CSF analysis or amyloid PET), is currently monitoring brain inflammation in response to a 12-week course of treatment with neflamapimod or placebo, by using the microglial activation tracer DPA-714. Three DPA714 SUV (standard uptake value) measures accounting for microglia activation and neuroinflammation represent the primary outcome. Secondary outcomes span 35 different parameters ranging from neuropsychological assessments to blood and CSF markers of inflammation. The trial is expected to run until January 2021.

## 6.2 Masitinib

Originally approved for veterinary therapeutics for the treatment of mast cell tumors in dogs<sup>58,59</sup>, masitinib (also known as AB1010) is a tyrosine kinase inhibitor with a wide spectrum of targets, among which are c-kit; platelet-derived growth factor receptors; and, to a lesser extent, lymphocyte-specific kinase (Lck), Lck/Yes-related protein (Lyn), Fyn, and FAK (focal adhesion kinase) pathways.<sup>58</sup> By combined targeting of c-Kit and Lyn, masitinib is particularly efficient in controlling the survival, differentiation, and degranulation of mast cells, thus indirectly controlling the release of proinflammatory and vasoactive mediators.<sup>58</sup> Promising results come from human clinical trials testing masitinib for the treatment of mastocytosis,<sup>60</sup> rheumatoid arthritis,<sup>61</sup> and asthma,<sup>62</sup> and as add-on therapy to riluzole in patients with amyotrophic lateral sclerosis.<sup>63</sup> Recently, the potential clinical application of masitinib in neurodegenerative diseases, such as AD, has emerged due to the involvement of the stem cell factor (SCF, the c-kit natural agonist) receptor/c-kit in mast cells-mediated neuroinflammation (**Figure 1**). A randomized, placebo-controlled, phase 2 study (NCT00976118) was performed in patients with mild to moderate AD, receiving masitinib as an adjunct to cholinesterase inhibitor and/or memantine.<sup>64</sup> Compared to placebo, masitinib administration as an adjunct to standard treatments slowed the rate of cognitive decline at 24 weeks, as evident from the sustained and statistically significant response in ADAS-Cog.<sup>64</sup> Moreover, significant improvement in cognitive function and functional capacity was evident through the mean change in ADAS-Cog, MMSE, and ADCS-ADL values relative to baseline.<sup>64</sup> However, the weaknesses of this

study concern the small sample size, with only 34 participants, and the high rate of discontinuation, with 17 dropouts (65.4%) in the group receiving masitinib versus 2 dropouts in the placebo group (25.0%). Moreover, the effective penetration of the BBB by masitinib was not assessed and, consequently, the mechanism underlying the positive cognitive outcome remains to be fully elucidated. One can speculate that, in the event that masitinib passes through BBB and accumulates to a sufficient high therapeutic concentration, it can reduce neuroinflammation by directly modulating microglial activity via disruption of SCF/c-Kit signaling pathway.<sup>58</sup> Moreover, masitinib may also reduce tau phosphorylation via targeting Fyn and FAK intracellular pathway, thus providing a dual benefit in AD.

Currently, masitinib is under phase 3 clinical trial (NCT01872598) to test its efficacy and safety as add-on therapy in patients with mild to moderate AD treated for a minimum of 6 months with a stable dose of cholinesterase inhibitor and/or memantine. As reported by the investor communication, the interim results showed positive trends of masitinib efficacy at one of the doses tested. However, the status of the trial is currently unknown.

## **7. Concluding remarks**

Among the drug discovery programs currently testing disease modifying strategies in AD, the field of protein kinase inhibition is emerging as a challenging area, with several molecules originally developed for oncological indications recently repurposed for the treatment of neurodegenerative diseases (Table 1). Notably, protein kinases represent key nodes at the intersection of multiple intracellular pathways, also acting as critical regulators of divergent signaling cascades. As well as in cancer, where mutated cells have to be counteracted, in neurodegenerative diseases the target is represented by dysfunctional cells. In both conditions, a common dysfunctional process is represented by an imbalance in the intracellular pathways regulating cell metabolism control and duplication, the inhibition of which may hence contribute to stop the disease progression (**Figure 2**). Therefore, kinases may represent modulable druggable targets in neurodegenerative diseases (**Figure 1**).

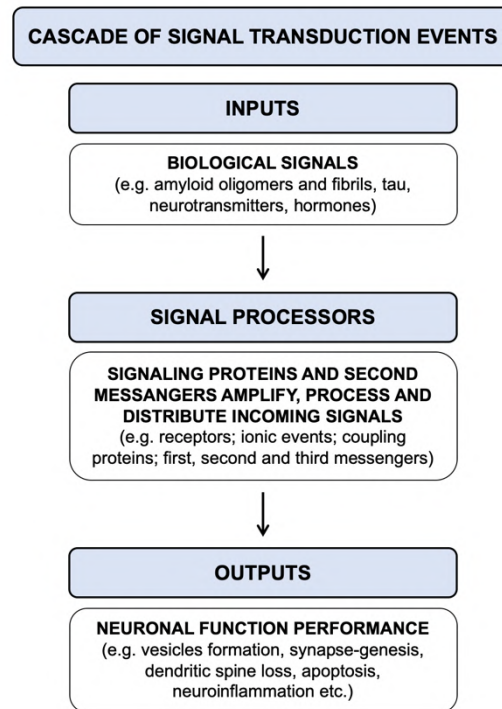


**FIGURE 2. Cascade of signal transduction events: a schematic representation.** Several biological signals, such as amyloid oligomers and fibrils, tau, neurotransmitters as well as hormones, trigger the activation of signaling proteins and cellular messengers that amplify, process, and distribute the incoming signals. The activation of intracellular signal processors induces neuronal responses, including vesicles trafficking, synapse-genesis, dendritic spine loss, apoptosis, and neuroinflammation, as outputs affecting neuronal performance.

However, despite promising preclinical results obtained in animal models, all the clinical trials testing kinase inhibitors in AD have ended in failure, with only few potential and still unconfirmed positive trends, further indicating that animal models cannot completely recapitulate the complexity of human biology and this is especially evident in the context of neurodegenerative diseases. The discouraging results may be justified by the fact that still few attempts have been made and few therapeutic strategies have been so far explored. In particular, addressing a single target and its related signaling pathway may not be an appropriate therapeutic strategy for AD, whose etiology is complex and multifactorial. The recognition of AD complexity suggests that using either single drugs binding multiple protein kinases or cocktails of highly selective inhibitors might be more effective, pending the assessment of their tolerability by frail elderly patients (**Box 1**). The toxicity burden associated to kinase inhibitors and, in particular, substantial side effects due to off-target effects (eg, cardiovascular, gastrointestinal, and hematologic toxicity) cannot be neglected.<sup>65</sup>

**BOX 1** Emerging key questions while studying cancer kinase role in neurodegenerative diseases

**QUESTION BOX**

How do different disease-associated biological signals (eg, amyloid oligomers, tau, neurotransmitters, and/or other signals) trigger the cascade of signal transduction events within the neurons?

Where do such biological signals activate the described intracellular pathways within the neurons? Is the activation of these cascades related to a specific portion (eg, soma, synaptic terminal) of the neuron?

Are there different receptors for each type of signal or is a given receptor involved in diverse signal derangements?

Are the cascades of intracellular events the same or different for each signal? If different, how do such intracellular pathways crosstalk?

How do protein kinase expression and activity change in different brain areas during aging and neurodegenerative processes?

Which are the most relevant signaling pathways to target?

What would be the best: targeting a hierarchically organized pathway or multiple parallel pathways?

Moreover, another major weakness related to the field of kinase inhibition in AD is that most of the preclinical studies testing kinase inhibitors in AD-like models investigated their impact on A $\beta$ -centered pathways. However, this vision is too limited and, considering the failures of the anti-amyloid strategies, including the DIANTU trial on familial cases, may not be optimal in addition to be limited to AD among the neurodegenerative diseases (<sup>1</sup>; <https://www.reuters.com/article/us-roche-alzheimers/roche-lilly-drugsfail-to-halt-gene-driven-alzheimers-disease-idUSKBN2040JQ>).

However, as well as in cancer, in neurodegeneration it is important to target the drug to the dysfunctional cells and to differentiate them from the healthy ones. A differential mapping of the kinases is fundamental to selectively identify the right target in the affected tissue depending on the disease to be treated. To date, it cannot be discounted that we still have

a partial knowledge regarding the functions of protein kinases in the major signaling pathways in neurodegenerative processes and several key questions have yet to be addressed (Box 1). In particular, an accurate profile of degenerative modifications of protein kinase expression and activity in different brain areas, associated with aging and neurodegenerative processes, is still lacking. To this end, the recent advancements in proteomic technologies will facilitate a detailed profiling of the human brain kinome.

## REFERECES

- [1] Bateman RJ, Benzinger TL, Berry S, *et al.* The DIAN-TU next generation Alzheimer's prevention trial: adaptive design and disease progression model. *Alzheimer's Dement.* 2017;13:8-19.
- [2] Schneider L. A resurrection of aducanumab for Alzheimer's disease. *Lancet Neurol.* 2020;19:111-112.
- [3] Houck AL, Seddighi S, Driver JA. At the crossroads between neurodegeneration and cancer: a review of overlapping biology and its implications. *Curr Aging Sci.* 2018;11:77-89.
- [4] Klaeger S, Heinzlmeir S, Wilhelm M, *et al.* The target landscape of clinical kinase drugs. *Science.* 2017;358(6367):eaan4368.
- [5] Wu P, Nielsen TE, Clausen MH. FDA-approved small-molecule kinase inhibitors. *Trends Pharmacol Sci.* 2015;36:422-439.
- [6] Ferguson FM, Gray NS. Kinase inhibitors: the road ahead. *Nat Rev Drug Discov.* 2018;17:353-377.
- [7] Karaman MW, Herrgard S, Treiber DK, *et al.* A quantitative analysis of kinase inhibitor selectivity. *Nat Biotechnol.* 2008;26:127-132.
- [8] Hall-Jackson CA, Eyers PA, Cohen P, *et al.* Paradoxical activation of Raf by a novel Raf inhibitor. *Chem Biol.* 1999;6:559-568.
- [9] Packer LM, Rana S, Hayward R, *et al.* Nilotinib and MEK inhibitors induce synthetic lethality through paradoxical activation of RAF in drug-resistant chronic myeloid leukemia. *Cancer Cell.* 2011;20:715-727.
- [10] Hennequin LF, Allen J, Breed J, *et al.* N-(5-chloro-1,3-benzodioxol-4-yl)-7-[2-(4-methylpiperazin-1-yl)ethoxy]-5-(tetrahydro-2H-pyran-4-yloxy)quinazolin-4-amine, a novel, highly selective, orally available, dual-specific c-Src/Abl kinase inhibitor. *J Med Chem.* 2006;49:6465-6488.
- [11] Um JW, Nygaard HB, Heiss JK, *et al.* Alzheimer amyloid-beta oligomer bound to postsynaptic prion protein activates Fyn to impair neurons. *Nat Neurosci.* 2012;15:1227-1235.
- [12] Larson M, Sherman MA, Amar F, *et al.* The complex PrPc-Fyn couples human oligomeric A $\beta$  with pathological tau changes in Alzheimer's disease. *J Neurosci.* 2012;32:16857-16871.

- [13] Chen S, Yadav SP, Surewicz WK. Interaction between human prion protein and amyloid- $\beta$  ( $A\beta$ ) oligomers: role of N-terminal residues. *J Biol Chem*. 2010;285:26377-26383.
- [14] Um JW, Kaufman AC, Kostylev M, *et al*. Metabotropic glutamate receptor 5 is a coreceptor for alzheimer  $A\beta$  oligomer bound to cellular prion protein. *Neuron*. 2013;79:887-902.
- [15] Salter MW, Kalia L V. Src kinases: a hub for NMDA receptor regulation. *Nat Rev Neurosci*. 2004;5:317-328.
- [16] Bhaskar K, Hobbs GA, Yen SH, Lee G. Tyrosine phosphorylation of tau accompanies disease progression in transgenic mouse models of tauopathy. *Neuropathol Appl Neurobiol*. 2010;36:462-477.
- [17] Bhaskar K, Yen SH, Lee G. Disease-related modifications in tau affect the interaction between Fyn and tau. *J Biol Chem*. 2005;280:3511935125.
- [18] Lee G, Thangavel R, Sharma VM, *et al*. Phosphorylation of tau by Fyn: implications for Alzheimer's disease. *J Neurosci*. 2004;24:2304-2312.
- [19] Kaufman AC, Salazar S V, Haas LT, *et al*. Fyn inhibition rescues established memory and synapse loss in Alzheimer mice. *Ann Neurol*. 2015;77:953-971.
- [20] Van Dyck CH, Nygaard HB, Chen K, *et al*. Effect of AZD0530 on cerebral metabolic decline in Alzheimer disease. *JAMA Neurol*. 2019;76:1219-1229.
- [21] Poulsen ET, Iannuzzi F, Rasmussen HF, *et al*. An aberrant phosphorylation of amyloid precursor protein tyrosine regulates its trafficking and the binding to the clathrin endocytic complex in neural stem cells of Alzheimer's disease patients. *Front Mol Neurosci*. 2017;10:59.
- [22] Hoe HS, Minami SS, Makarova A, *et al*. Fyn modulation of Dab1 effects on amyloid precursor protein and apoe receptor 2 processing. *J Biol Chem*. 2008;283:6288-6299.
- [23] Deremer DL, Ustun C, Natarajan K. Nilotinib: a second-generation tyrosine kinase inhibitor for the treatment of chronic myelogenous leukemia. *Clin Ther*. 2008;30(11):1956-75.
- [24] Jing Z, Caltagarone J, Bowser R. Altered subcellular distribution of cAbl in Alzheimer's disease. *J Alzheimer's Dis*. 2009;17:409-422.
- [25] Ko HS, Lee Y, Shin JH, *et al*. Phosphorylation by the c-Abl protein tyrosine kinase inhibits parkin's ubiquitination and protective function. *Proc Natl Acad Sci U S A*. 2010;107:16691-16696.
- [26] Tremblay MA, Acker CM, Davies P. Tau phosphorylated at tyrosine 394 is found in Alzheimer's disease tangles and can be a product of the Abl-related kinase, Arg. *Arg J Alzheimer's Dis*. 2010;19:721733.
- [27] Imam SZ, Zhou Q, Yamamoto A, *et al*. Novel regulation of Parkin function through c-Abl-Mediated tyrosine phosphorylation: implications for Parkinson's disease. *J Neurosci*. 2011;31:157-163.
- [28] Schlatterer SD, Acker CM, Davies P. C-Abl in neurodegenerative disease. *J Mol Neurosci*. 2011;45:445-452.



- [29] Cancino GI, Perez de Arce K, Castro PU, Toledo EM, von Bernhardt R, Alvarez AR. C-Abl tyrosine kinase modulates tau pathology and Cdk5 phosphorylation in AD transgenic mice. *Neurobiol Aging*. 2011;32:1249-1261.
- [30] Alvarez AR, Sandoval PC, Leal NR, Castro PU, Kosik KS. Activation of the neuronal c-Abl tyrosine kinase by amyloid-beta-peptide and reactive oxygen species. *Neurobiol Dis*. 2004;17:326-336.
- [31] Cancino GI, Toledo EM, Leal NR, *et al*. STI571 prevents apoptosis, tau phosphorylation and behavioural impairments induced by Alzheimer's beta-amyloid deposits. *Brain*. 2008;131:2425-2442.
- [32] Derkinderen P, Scales TME, Hanger DP, *et al*. Tyrosine 394 is phosphorylated in Alzheimer's paired helical filament tau and in fetal tau with c-abl as the candidate tyrosine kinase. *J Neurosci*. 2005;25:65846593.
- [33] Pagan F, Hebron M, Valadez EH, *et al*. Nilotinib effects in Parkinson's disease and dementia with Lewy bodies. *J Parkinsons Dis*. 2016;6:503517.
- [34] Pagan FL, Hebron ML, Wilmarth B, *et al*. Nilotinib effects on safety, tolerability, and potential biomarkers in Parkinson disease. *JAMA Neurol*. 2019;77:309-317.
- [35] Hebron ML, Irina L, Paul O, Selby ST, Fernando P, Moussa CE-H. Tyrosine kinase inhibition regulates early systemic immune changes and modulates the neuroimmune response in  $\alpha$ -Synucleinopathy. *J Clin Cell Immunol*. 2014;30:259.
- [36] Hooper C, Killick R, Lovestone S. The GSK3 hypothesis of Alzheimer's disease. *J Neurochem*. 2008;104:1433-1439.
- [37] Serenó L, Coma M, Rodríguez M, *et al*. A novel GSK-3 $\beta$  inhibitor reduces Alzheimer's pathology and rescues neuronal loss *in vivo*. *Neurobiol Dis*. 2009;35:359-367.
- [38] Morales-García JA, Luna-Medina R, Alonso-Gil S, *et al*. Glycogen synthase kinase 3 inhibition promotes adult hippocampal neurogenesis *in vitro* and *in vivo*. *ACS Chem Neurosci*. 2012;3:963-971.
- [39] Wang H, Huang S, Yan K, *et al*. Tideglusib, a chemical inhibitor of GSK3 $\beta$ , attenuates hypoxic-ischemic brain injury in neonatal mice. *Biochim Biophys Acta - Gen Subj*. 2016;1860:2076-2085.
- [40] Rockenstein E, Torrance M, Adame A, *et al*. Neuroprotective effects of regulators of the glycogen synthase kinase-3 $\beta$  signaling pathway in a transgenic model of Alzheimer's disease are associated with reduced amyloid precursor protein phosphorylation. *J Neurosci*. 2007;27:19811991.
- [41] Del Ser T, Steinwachs KC, Gertz HJ, *et al*. Treatment of Alzheimer's disease with the GSK-3 inhibitor tideglusib: a pilot study. *J Alzheimer's Dis*. 2013;33:205-215.
- [42] Lovestone S, Boada M, Dubois B, *et al*. A phase II trial of tideglusib in Alzheimer's disease. *J Alzheimer's Dis*. 2015;45:75-88.
- [43] Matsunaga S, Fujishiro H, Takechi H. Efficacy and safety of glycogen synthase kinase 3 inhibitors for Alzheimer's disease: a systematic review and meta-analysis. *J Alzheimer's Dis*. 2019;69:1031-1039.

- [44] Duffy JP, Harrington EM, Salituro FG, *et al.* The discovery of VX745: a novel and selective p38 $\alpha$  kinase inhibitor. *ACS Med Chem Lett.* 2011;2:758-763.
- [45] Bachstetter AD, Xing B, de Almeida L, Dimayuga ER, Watterson DM, Van Eldik LJ. Microglial p38 $\alpha$  MAPK is a key regulator of proinflammatory cytokine up-regulation induced by toll-like receptor (TLR) ligands or beta-amyloid (A $\beta$ ). *J Neuroinflammation.* 2011;8:79.
- [46] Bachstetter AD, Van Eldik LJ. The p38 MAP kinase family as regulators of proinflammatory cytokine production in degenerative diseases of the CNS. *Aging Dis.* 2010;1:199-211
- [47] Barrientos RM, Frank MG, Watkins LR, Maier SF. Aging-related changes in neuroimmune-endocrine function: implications for hippocampal-dependent cognition. *Horm Behav.* 2012;62:219-227.
- [48] Li Y, Liu L, Barger SW, Griffin WST. Interleukin-1 mediates pathological effects of microglia on tau phosphorylation and on synaptophysin synthesis in cortical neurons through a p38-MAPK pathway. *J Neurosci.* 2003;23:1605-1611.
- [49] Li S, Jin M, Koeglsperger T, Shepardson NE, Shankar GM, Selkoe DJ. Soluble A $\beta$  oligomers inhibit long-term potentiation through a mechanism involving excessive activation of extrasynaptic NR2B-containing NMDA receptors. *J Neurosci.* 2011;31:6627-6638.
- [50] Corrêa SAL, Eales KL. The role of p38 MAPK and its substrates in neuronal plasticity and neurodegenerative disease. *J Signal Transduct.* 2012;2012:649079.
- [51] Watterson DM, Grum-Tokars VL, Roy SM, *et al.* Development of novel *in vivo* chemical probes to address CNS protein kinase involvement in synaptic dysfunction. *PLoS One.* 2013;8:e66226.
- [52] Munoz L, Ranaivo H, Roy SM, *et al.* A novel p38 $\alpha$  MAPK inhibitor suppresses brain proinflammatory cytokine up-regulation and attenuates synaptic dysfunction and behavioral deficits in an Alzheimer's disease mouse model. *J Neuroinflammation.* 2007;4:21.
- [53] Colié S, Sarroca S, Palenzuela R, *et al.* Neuronal p38 $\alpha$  mediates synaptic and cognitive dysfunction in an Alzheimer's mouse model by controlling  $\beta$ -amyloid production. *Sci Rep.* 2017;7:45306.
- [54] Schnöder L, Hao W, Qin Y, *et al.* Deficiency of neuronal p38 $\alpha$  MAPK attenuates amyloid pathology in Alzheimer disease mouse and cell models through facilitating lysosomal degradation of BACE1. *J Biol Chem.* 2016;291:2067-2079.
- [55] Alam JJ. Selective brain-targeted antagonism of p38 MAPK $\beta$  reduces hippocampal IL-1 $\beta$  levels and improves morris water maze performance in aged rats. *J Alzheimer's Dis.* 2015;48:219-227.
- [56] Alam J, Blackburn K, Patrick D. Neflamapimod: clinical phase 2b-Ready oral small molecule inhibitor of p38 $\alpha$  to reverse synaptic dysfunction in early Alzheimer's disease. *J Prev Alzheimer's Dis.* 2017;4:273-278.
- [57] Wang L. Association of cerebrospinal fluid neurogranin with Alzheimer's disease. *Aging Clin Exp Res.* 2019;31:185-191.
- [58] Dubreuil P, Letard S, Ciufolini M, *et al.* Masitinib (AB1010), a potent and selective tyrosine kinase inhibitor targeting KIT. *PLoS One.* 2009;4:e7258.

- 
- [59] Marech I, Patrino R, Zizzo N, *et al.* Masitinib (AB1010), from canine tumor model to human clinical development: where we are?. *Crit Rev Oncol Hematol.* 2014;91:98-111.
- [60] Lortholary O, Chandesris MO, Livideanu CB, *et al.* Masitinib for treatment of severely symptomatic indolent systemic mastocytosis: a randomised, placebo-controlled, phase 3 study. *Lancet.* 2017;389:612-620.
- [61] Tebib J, Mariette X, Bourgeois P, *et al.* Masitinib in the treatment of active rheumatoid arthritis: results of a multicentre, open-label, doseranging, phase 2a study. *Arthritis Res Ther.* 2009;11:R95.
- [62] Humbert M, De Blay F, Garcia G, *et al.* Masitinib, a c-kit/PDGF receptor tyrosine kinase inhibitor, improves disease control in severe corticosteroid-dependent asthmatics. *Allergy Eur J Allergy Clin Immunol.* 2009;64:1194-1201.
- [63] Mora JS, Genge A, Chio A, *et al.* Masitinib as an add-on therapy to riluzole in patients with amyotrophic lateral sclerosis: a randomized clinical trial. *Amyotroph Lateral Scler Front Degener.* 2019;7:1-10.
- [64] Piette F, Belmin J, Vincent H, *et al.* Masitinib as an adjunct therapy for mild-to-moderate Alzheimer's disease: a randomised, placebocontrolled phase 2 trial. *Alzheimer's Res Ther.* 2011;3:16.
- [65] Caldemeyer L, Dugan M, Edwards J, Akard L. Long-term side effects of tyrosine kinase inhibitors in chronic myeloid leukemia. *Curr Hematol Malig Rep.* 2016;11:71-79.



---

## PART 5

The following manuscript was published in *Molecular Neurobiology* in 2020 as:

### **The peptidyl-prolyl isomerase Pin1 in neuronal signaling: from neurodevelopment to neurodegeneration**

**Francesca Fagiani**, Stefano Govoni, Marco Racchi, and Cristina Lanni

#### **Abstract**

The peptidyl-prolyl isomerase Pin1 is a unique enzyme catalyzing the isomerization of the peptide bond between phosphorylated serine-proline or threonine-proline motifs in proteins, thereby regulating a wide spectrum of protein functions, including folding, intracellular signaling, transcription, cell cycle progression and apoptosis. Pin1 has been reported to act as a key molecular switch inducing cell-type specific effects, critically depending on the different phosphorylation patterns of its targets within different biological contexts. While its implication in proliferating cells, and, in particular, in the field of cancer, has been widely characterized, less is known about Pin1 biological functions in terminally differentiated and post-mitotic neurons. Notably, Pin1 is widely expressed in the central and peripheral nervous system, where it regulates a variety of neuronal processes, including neuronal development, apoptosis, and synaptic activity. However, despite studies reporting the interaction of Pin1 with neuronal substrates or its involvement in specific signaling pathways, a more comprehensive understanding of its biological functions at neuronal level is still lacking. Besides its implication in physiological processes, a growing body of evidence suggests the crucial involvement of Pin1 in aging and age-related and neurodegenerative diseases, including Alzheimer's disease, Parkinson disease, Frontotemporal dementias, Huntington disease, and Amyotrophic lateral sclerosis, where it mediates profoundly different effects, ranging from neuroprotective to neurotoxic. Therefore, a more detailed understanding of Pin1 neuronal functions may provide relevant information on the consequences of Pin1 deregulation in age-related and neurodegenerative disorders.

**Keywords:** Pin1; neurodevelopment; neurodegeneration; neuronal apoptosis; Alzheimer's disease.



## The Peptidyl-prolyl Isomerase Pin1 in Neuronal Signaling: from Neurodevelopment to Neurodegeneration

Francesca Fagiani<sup>1,2</sup> · Stefano Govoni<sup>1</sup> · Marco Racchi<sup>1</sup> · Cristina Lanni<sup>1</sup>

### Background

#### The peptidyl-prolyl isomerase Pin1

Discovered in 1996 as a protein associating with NIMA (never in mitosis) regulating mitosis [1], the peptidyl-prolyl isomerase Pin1 (protein interacting with NIMA-1) is an ubiquitously expressed *cis/trans* isomerase targeting the phosphorylated serine-proline (pSer-Pro) or threonine-proline (pThr-Pro) motifs [1], belonging to the evolutionarily conserved family of PPIase (peptidyl-prolyl *cis/trans* isomerase). The WW domain on the N-terminus specifically interacts with pSer-Pro or pThr-Pro motifs [2], while the PPIase domain on the C-terminus is responsible for its catalytic activity [3]. Substrate recognition by Pin1 requires phosphorylation of Ser-Pro and Thr-Pro motifs by proline-directed kinase family, including cyclin-dependent kinases (CDKs), mitogen-activated protein kinases (MAPKs), and dual-specificity tyrosine-phosphorylation regulated protein kinase (DYRK). Moreover, Pin1 activity is controlled by protein kinase phosphorylation, as demonstrated by Pin1 phosphorylation in the WW domain, responsible for its increased or decreased binding to the pSer/pThr-Pro motif in substrates [4, 5].

The ensuing conformational changes induced by Pin1 on its protein substrates, as consequence of prolyl-isomerization, produce a variety of functional effects (e.g. substrate stability, catalytic activity, protein-protein interaction, and subcellular localization), thus impinging on several cellular processes, including cell cycle, transcription, and cell fate commitment [6, 7]. In cells, Pin1 has been widely investigated as mitotic regulator, with a fundamental role in checkpoint mechanisms in the cell cycle [8]. However, besides its role in cell cycle progression, Pin1 has been found to interact and regulate also non-nuclear targets with roles in apoptosis, endocytosis, protein translation, maintenance of the cytoskeleton, and neuronal function [6]. Given the role of Pin1 as regulator of cell function by fine-tuning cellular pathways downstream to phosphorylation signaling, perturbation in

---

intracellular pathways and/or deregulation of Pin1 expression/activity, albeit in different directions, have been reported to be implicated in several pathological conditions, such as cancer and neurodegenerative diseases [9].

### **Main Text**

By controlling the change of the backbones of several cellular substrates, Pin1 acts as key fine-tuner and amplifier of multiple signaling pathways, thereby inducing many functional consequences both in physiological and pathological conditions. In this review, we will critically discuss the highly pleiotropic and context-dependent nature of Pin1 functional activity, which emerges to be strictly related to the phosphorylation patterns of its cellular substrates. In particular, we will specifically focus on Pin1 functions in neurons, starting from its implication in neurodevelopment to its role in cellular homeostasis in adult neurons (**Figure 1**). Moreover, we will discuss evidence from the literature supporting the notion of a differential role of Pin1 within the different neurodegenerative diseases (**Table 1**).

### PIN1 PHYSIOLOGICAL FUNCTIONS IN NERVOUS SYSTEM

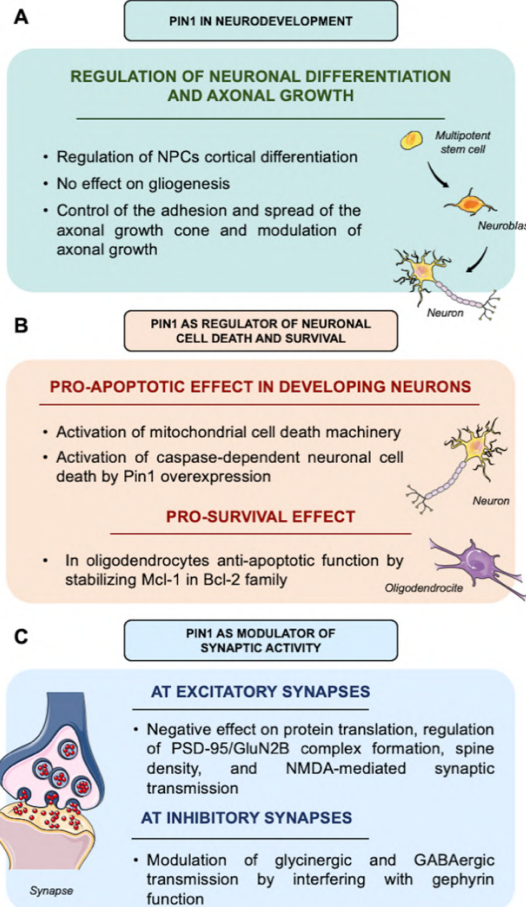


**Fig. 1. The physiological functions of Pin1 in the nervous system. (A)** Pin1 is implicated in neurodevelopment, where it tightly regulates neuronal differentiation and axonal growth. In particular, Pin1 is highly expressed during neurodevelopmental stages, where it controls cortical differentiation of neuron progenitor cells (NPCs), by acting on  $\beta$ -catenin pathway, without affecting gliogenesis. Moreover, Pin1 is required for the development of the central nervous system for axonal growth during embryonic development and for establishing a proper axonal connectivity, by controlling the adhesion and spread of the axonal growth cone. **(B)** Pin1 acts also as modulator of synaptic activity. At glutamatergic synapses, Pin1 is catalytically present in dendrites, where, under basal conditions, it inhibits protein translation, required for late LTP maintenance, and negatively regulates PSD95/GluN2B complex formation, as well as spine density, and NMDA-mediated synaptic transmission. At glycinergic synapses, Pin1 interacts with gephyrin and alters its overall conformation, thereby affecting the function of glycine receptors. At GABAergic synapses, it inhibits the ability of neuroligin 2 to interact with the scaffolding protein gephyrin. **(C)** Pin1 is a key context-dependent signal transducer of neuronal cell death and survival signals. In developing neurons, Pin1 binds and stabilizes JNK-phosphorylated



forms of BIM<sub>EL</sub>, protecting it from proteasomal degradation and thereby activating the mitochondrial cell death machinery via c-Jun. In addition, Pin1 overexpression overrides NGF-derived survival signals and triggers caspase-dependent neuronal cell death. Besides such pro-apoptotic action, Pin1 also mediates pro-survival effects: as shown by various observation, as reported in the text, and in *in vitro* experiments on oligodendrocytes, where Pin1 exerts an anti-apoptotic function by binding and stabilizing the anti-apoptotic Bcl-2 family protein Mcl-1, a pro-survival member of the Bcl-2 family, in the cytosol.

**Table 1. Summary of Pin1 changes in neurodegenerative diseases.**

Neurodegenerative disease	Pin 1 changes observed in human samples	Pin 1 putative role	References
Alzheimer's disease	Pin1 has been reported to be oxidatively modified, with consequent reduced activity and expression in hippocampus from MCI and AD patients compared to age-matched controls.	Protective role against age-associated neurodegeneration	[10, 11]
	Change in Pin1 neuronal localization, with a shift from nucleus to cytoplasm, have been found in <i>postmortem</i> human brains from AD patients compared to age-matched controls.		[12–14]
	Loss of Pin1 within the synapses of human frontal tissues from AD patients compared to age-matched control brains.		[12]
	Pin1 co-localized with deposits of aggregated tau.		[15]
Frontotemporal dementias	Overall reduction of Pin1 and redirection of the predominantly nuclear Pin1 into the neuronal cytoplasm in FTD <i>postmortem</i> brains compared to normal brains.	Protective role against age-associated neurodegeneration	[16]
	A trend for downregulation of Pin1 in human non-motor cortex and in the spinal cord derived from patients with FTD-U.		[17]
Parkinson disease	Pin1 has been reported to accumulate in the Lewy Bodies of human PD brains and to co-localize with $\alpha$ -synuclein inclusions.	Neurotoxic action by promoting with $\alpha$ -synuclein inclusions	[18]
	Increased levels of Pin1 have been observed in pigmented dopaminergic neurons in <i>postmortem</i> human brains from PD patients.		[19]
Huntington disease	No data on human samples are available, but only <i>in vitro</i> and <i>in vivo</i> preclinical results.	Neurotoxic action by promoting p53-dependent neuronal apoptosis induced by mutant huntingtin	[20]
Amyotrophic lateral sclerosis	Downregulation of Pin1 expression in the spinal cord and non-motor cortex of a cohort of ALS patients.	Protective role against neurofilament-H hyperphosphorylation and its perikaryal accumulation in <i>in vitro</i> models	[17, 21]

## Pin1 in neurons

Pin1 is widely expressed in human tissues including the central and peripheral nervous system [22]. In particular, it is highly expressed in terminally differentiated and post-mitotic neurons, specifically enriched at mitochondrial membranes [23], but also present in neuronal cytosol, dendrites [24, 25], and distal axons [26]. Consistently with its neuronal localization, Pin1 has been reported to regulate a variety of neuronal processes, such as neurodevelopment, neuronal differentiation [27], dendritic protein synthesis [25], and axonal growth and guidance [26] (**Fig. 1**). However, while the role of Pin1 in proliferating cells and, in particular, in the field of cancer, has been widely characterized, less is known about the functions of Pin1 during the development of the nervous system and in post-mitotic adult neurons. In fact, despite studies reporting the effects of Pin1 on its neuronal substrates or specific intracellular signaling pathways, as detailed below, a more comprehensive understanding of its biological role at neuronal level is still lacking.

## The Physiological Role of Pin1 in Neurodevelopment

Pin1 has been found highly expressed during neurodevelopmental stages, playing a key role in regulating cortical differentiation of neuron progenitor cells (NPCs). Pin1 knockdown in mice has been observed to reduce NPC differentiation, while Pin1 overexpression has been reported to enhance it, without affecting gliogenesis, thus suggesting that Pin1 may specifically promote neuronal but not glial differentiation of NPCs [27]. In accordance with the pattern of Pin1 expression in developing brains, Pin1 knockdown inhibited NPC differentiation into migrating immature neurons at E15.5, without affecting NPCs expansion phase [27]. In addition, Pin1 knockdown specifically inhibited the birth of upper layer neurons, but not that of the lower layers in the cerebral cortex. Such reduction in the upper layer neurons, induced by Pin1 knockdown, was also confirmed in mice motor cortex at late embryonic stages and in the neonatal stage, where mice displayed a severe impairment in neonatal motor activity [27]. The molecular mechanism by which Pin1 has been reported to regulate NPC differentiation seems to rely on its interplay with  $\beta$ -catenin, identified as Pin1 major substrate in NPCs by proteomic approach [27]. Pin has been demonstrated to bind and stabilize  $\beta$ -catenin conformation at late stage during mouse brain development [27]. Consistently, Pin1 knockout reduced  $\beta$ -catenin in NPCs at late stages during brain development [27].

Moreover, conformational changes induced by Pin1 represent an important regulatory mechanism also in axonal growth during embryonic development [26]. Pin1 has been shown to bind and stabilize CDK5-phosphorylated CRMP2A (collapsin response mediator protein 2 A) [26]. The kinase-mediated phosphorylation of CRMP2 reduces its affinity to tubulin, thus promoting microtubule disassembly. Notably, Pin1 knockout, knockdown, and inhibition reduced CRMP2A levels, specifically in distal axons, and inhibited axon growth, fully rescued by Pin1 overexpression [26]. Noteworthy, in Pin1 knockout mouse embryos, defects in developmental axon growth both in the peripheral and central nervous system have been observed at E12.5, with cranial and spinal nerves displaying stunted and less branched neurite processes [26]. Moreover, entorhinal hippocampal perforant projections were significantly shorter in Pin1 knockout embryos at E15.5 compared to wild-type mice [26]. Interestingly, in newborn and adult Pin1 knockout mice, the entorhino-hippocampal projections were detected in the stratum lacunosum-moleculare as in Pin1 wild-type mice, thus indicating that the previously mentioned defects in Pin1 knockout embryos were later corrected [26].

Among the functions of Pin1 in the developing brain, Pin1 has been also recently implicated in the regulation of the axonal growth cone motility [28]. In particular, in embryonic rat brain, Pin1 has been found to directly interact and regulate the dephosphorylation of the myristoylated alanine-rich C kinase substrate (MARCKS), a

protein enriched in the developing brain, modulating neuronal spreading and migration, and stabilizing the adhesion complex at the growth cone [28]. Pin1 seems to be required for the normal development of the central nervous system for establishing a proper axonal connectivity, by controlling adhesion and spread of the axonal growth cone. Accordingly, in Pin1 knockout mice, Sosa *et al.* described the presence of morphological alterations in the corpus callosum and cerebral cortex fibers [28]. In particular, a thinner corpus callosum in the midline, along with a reduction in the amount of fibers crossing over, has been observed in Pin1 null mice compared to control mice, indicating a defective connection between the two cortical hemispheres [28].

Taken together, such evidence indicating the correlation between Pin1 deregulation and morphological and functional modifications during brain development strongly points the critical involvement of Pin1 in embryogenesis and neurodevelopment.

### **Pin1 as regulator of neuronal apoptosis**

Data from literature suggest that, in the nervous system, the regulation of neuronal cell death and survival by the prolyl isomerase Pin1 critically depends on the tissue context and the developmental stage, with Pin1 capable to trigger both pro-survival [29] and pro-apoptotic pathways [24, 30]. Accordingly, Pin1 has been shown to promote cell survival by maintaining the normal mitochondrial homeostasis. Consistently, Pin1 has been reported to exert an anti-apoptotic function in adult mouse oligodendrocytes by binding and stabilizing the anti-apoptotic protein Mcl-1 (myeloid cell leukemia sequence-1), a pro-survival member of the Bcl-2 family, in the cytosol [29]. In a mouse model of spinal cord injury, obtained by hemisection at thoracic level, JNK3 (c-Jun N-terminal kinase-3) has been demonstrated to perturb the interaction between Pin1 and Mcl-1 by phosphorylating the latter at Ser121, thereby inducing proteasome-mediated degradation of Mcl-1 and, ultimately, leading to cytochrome c release from mitochondria [29], a fundamental step to activate caspase pathways triggering apoptotic process. According to Pin1 anti-apoptotic function, in Pin1<sup>-/-</sup> mice, Mcl-1 levels were reduced, cytochrome c release is constitutive in the absence of injury, and apoptosis significantly increased after injury [29]. Noteworthy, given the relevance of mitochondrial dysfunction in the pathophysiology of several neurodegenerative diseases, further investigations are required to investigate the JNK3-mediated perturbation of Pin1/Mcl-1 interaction, necessary for maintaining mitochondrial homeostasis, also in the central nervous system.

In contrast with these findings reporting Pin1 pro-survival effects in the nervous system, Pin1 has been also demonstrated to act as positive regulator of programmed cell death

specifically in developing neurons [24, 30]. Consistently, Becker and Bonni provided evidence showing Pin1 implication in the regulation of neuronal apoptosis [24]. In post-natal cerebellar granule neurons, Pin1 has been shown to mediate the activation of the mitochondrial cell death machinery following trophic factor deprivation [24]. In particular, Pin1 has been reported to specifically bind and stabilize JNK-phosphorylated at Ser65 forms of BIMEL (Bcl-2-interacting mediator of cell death) via its WW domain, protecting BIMEL from proteasomal degradation and thereby activating the mitochondrial cell death machinery via c-Jun [24]. Notably, a significant proportion of Pin1 in neural cells is tethered to the mitochondrial membrane, where it engages in a physical complex with the JNK scaffold protein JIP3. Later, Barone *et al.* confirmed that, in primary cultures of sympathetic neurons from superior cervical ganglia of newborn (post-natal day 0–1) mice, the overexpression of catalytically active Pin1 was capable to override NGF (nerve growth factor)-derived survival signals and to trigger caspase-dependent cell death of neurons, which was accompanied by the accumulation of Ser63-phosphorylated c-Jun in neuronal nuclei [30]. In contrast, the downregulation of Pin1 expression suppressed the accumulation of phosphorylated c-Jun, as well as the consequent release of cytochrome c from mitochondria and delayed cell death [30]. Moreover, ectopic Pin1-induced cell death was prevented by the expression of dominant-negative c-Jun [30].

Overall, these findings suggest that Pin1 may participate to the regulation of neuronal cell death specifically in developing neurons, but it promotes neuronal survival in adult neurons. However, future studies are required to define Pin1 role as pro-apoptotic and/or pro-survival regulator within neurons at different stages of neuronal development and to investigate its potential interaction with other apoptotic and metabolic regulators residing at mitochondria. In addition, as widely reported in cancer cell lines [31], Pin1 intimately interacts with the tumor suppressor protein p53 sculpting the active pro-apoptotic shape of p53, thus promoting its activity as inducer of cellular death [32]. However, data concerning Pin1/p53 interplay in neuronal context and its implication in the regulation of cell fate are still lacking. In this regard, although several cellular components of the cell death machinery are shared by both post-mitotic neurons and proliferating cells, their functions in apoptotic processes can be profoundly different. As an example, while the phosphorylation of BIM<sub>EL</sub>, induced by specific stimuli, triggers neuronal cell death, the same event in non-neuronal cells promotes survival [23].

### **Pin1 as modulator of synaptic activity**

By performing immune-electron microscopy, Westmark and collaborators demonstrated that Pin1 is highly expressed and catalytically active in dendritic shafts and spines in rodent

cortex and hippocampus, with a preferential post-synaptic localization, where, under basal conditions, it inhibits protein translation [25]. In particular, Pin1 has been reported to be associated with Shank proteins at dendritic rafts and with post-synaptic density protein-95 (PSD-95), indicating its potential involvement both in regulating signal transduction at dendritic rafts and signal processing at the PSD [12, 33]. Notably, at excitatory synapses, Pin1 has been described to negatively regulate PSD-95/GluN2B complex formation, as well as spine density, and NMDA (N-methyl D-aspartate)-mediated synaptic transmission [33]. In parallel, Pin1 has been also reported to be involved in the regulation of inhibitory transmission, by modulating neuroligin 2 (NL2)/gephyrin interaction at inhibitory GABAergic synapses [34, 35]. Therefore, an emerging role of Pin1 as modulator of synaptic activity has been proposed. However, despite sparse information about Pin1 involvement in synaptic activity, as discussed in the following sections, the balance of Pin1 effects on excitatory and inhibitory transmission, under basal conditions, remains to be unveiled.

### **Pin1 in excitatory transmission**

Westmark *et al.* demonstrated that Pin1 is present and catalytically active at dendrites of glutamatergic synapses, where it inhibits protein synthesis under basal conditions [25]. Notably, protein synthesis is essential for the formation of long-term memory and the maintenance of long-term forms of synaptic plasticity, such as late LTP (long-term potentiation). Interestingly, while basal synaptic transmission, as measured by the field excitatory post-synaptic potential (fEPSP) slope versus voltage, did not differ in hippocampal slices from Pin<sup>-/-</sup> mice compared to wild-type controls, paired-pulse facilitation, a form of short-term synaptic plasticity, was increased in Pin<sup>-/-</sup> mice, thus suggesting that Pin1 may affect neurotransmitter release [25]. Furthermore, during a protocol designed to stimulate late LTP (four high-frequency trains of stimuli), hippocampal slices from Pin<sup>-/-</sup> mice displayed normal early LTP, but significantly enhanced protein synthesis – dependent late LTP, compared to wild-type slices [25]. Such increase was prevented by protein synthesis inhibitors [25].

Moreover, at post-synaptic terminal, Pin1 has been demonstrated to directly interact with PSD-95, a membrane-associated guanylate kinase acting as scaffold protein at excitatory post-synaptic densities and anchoring NMDA receptor via GluN2-type receptor subunit [33]. In particular, Pin1 has been reported to interact with PSD-95 at specific Ser/Thr-Pro consensus motifs localized in the linker region connecting PDZ2 and PDZ3 domains [33]. Upon binding, Pin1 induces structural modifications in PSD-95, thereby inhibiting its ability to interact with NMDA receptors. Notably, electrophysiological experiments showed that, in hippocampal slices from Pin1<sup>-/-</sup> mice, larger NMDA-mediated synaptic

currents, evoked in CA1 principal cells by Schaffer collateral stimulation, were detected [33]. Such effect was also observed in cultured hippocampal cells expressing a PSD-95 mutant, unable to undergo prolyl-isomerization, further corroborating the hypothesis that Pin1 isomerase activity on PSD-95 is pivotal. Moreover, a significant increase in spine density, due to a selective gain in mushroom spines, was observed in Pin1<sup>-/-</sup> pyramidal neurons [33].

Overall, these data suggest that, under basal conditions, Pin1 negatively regulates the induction of dendritic translation, required for late LTP maintenance, as well as PSD-95/GluN2B complex formation, spine density, and NMDA-mediated synaptic transmission at excitatory synapses [25, 33]. However, despite such sparse information concerning Pin1 interplay with excitatory transmission, a comprehensive understanding of Pin1 synaptic effects has still to be unveiled. In this regard, behavioral tests in germ-line Pin1 knockout mice would be useful to assess whether potential Pin1-related changes not only in LTP but also in LTD (long-term depression) are accompanied by modifications in spatial memory, contextual fear memory, and social behavior.

Noteworthy, Tang *et al.* recently demonstrated that Pin1 directly interacts with NR2A- and NR2B-containing NMDA receptors, but not AMPA ( $\alpha$ -amino-3-hydroxy-5-methyl-4-isoxazole propionic acid) receptors in the hippocampus of epileptic mouse models and suggested the implication of Pin1/NMDA receptors complex in epileptic seizures [36]. Notably, Tang *et al.* reported a reduction in Pin1 protein levels in the neocortex of patients with temporal lobe epilepsy compared to controls, a decrease observed also in the hippocampus and cortex of chronic pilocarpine epileptic mouse model [36]. These findings suggest that epileptic seizures may downregulate Pin1 expression. However, further studies are needed to clarify whether dysregulation of such Pin1-based mechanism may participate to epileptogenesis.

### **Pin1 in Inhibitory Transmission**

At inhibitory synapses, Pin1 was found to interact with gephyrin, the functional homolog of PSD-95, and to alter its overall conformation, thereby affecting the function of glycine receptors [34]. Later, Antonelli *et al.* showed a mechanism by which Pin1 may affect the efficacy of GABAergic transmission by modulating NL2/gephyrin interaction at inhibitory GABAergic synapses [35]. In particular, NL2 has been reported to undergo proline-directed phosphorylation at Ser714-Pro consensus site and, subsequently, Pin1-mediated *cis/trans* isomerization [35]. Such post-phosphorylation prolyl-isomerization by Pin1 has been found to inhibit the ability of NL2, a cell adhesion molecule of the neuroligin family,

enriched at GABAergic synapses, to interact with the scaffolding protein gephyrin [35]. Accordingly, immunocytochemical analysis demonstrated that NL2/gephyrin complexes were enriched at GABAergic post-synaptic sites in the hippocampus of Pin1-knockout mice (Pin1<sup>-/-</sup>) [35]. This enrichment was accompanied by an enhanced synaptic recruitment of GABAA receptors and by a concomitant increase in the amplitude, but not in frequency, of spontaneous GABAA-mediated post-synaptic currents. Thus, Pin1-mediated modulation of NL2/gephyrin interaction represents a novel mechanism by which Pin1 may impinge on GABAergic transmission, thus possibly playing a key role in remodeling GABAergic synapses.

### **Pin1 in Aging and Neurodegenerative Diseases**

Data from the literature indicates that Pin1 plays a central role in regulating aging process *in vivo*. Accordingly, Pin1-knockout mice are viable and, despite transitory changes observed in the neurodevelopmental studies reported above and that are later corrected, they develop with a normal phenotype for an extended period of time [37]. However, adult Pin1-deficient mice display a range of abnormalities, including reduced body size, changes in skeletal or muscular structure (e.g., osteoporosis, lordokyphosis), retinal degeneration, and widespread signs of premature aging and neurodegeneration, such as acceleration of telomere shortening, massive tau phosphorylation and deposition in typical paired helical filaments, increased production of  $\beta$ -amyloid 42 (A $\beta$ 42), loss of motor coordination and behavioral defects, neuronal loss, and degeneration [38]. Hence, ablation of Pin1 gene results in a phenotype that recapitulates the phenomena associated with aging and some neurodegenerative conditions, in the absence of defective transgenes such as mutant human APP (amyloid precursor protein) or tau [39]. Accordingly, a growing body of evidence suggests that Pin1 plays a crucial role in the pathophysiology of several neurodegenerative diseases. In the context of Alzheimer's disease (AD), the *cis/trans* isomerase Pin1 has been proposed to protect against age-dependent neurodegeneration, by directly restoring the conformation and function of phosphorylated tau [13], as well as by promoting the non-amyloidogenic processing of APP and, consequently, reducing A $\beta$  production [40]. Notably, in AD brains, changes in Pin1 neuronal localization, with a shift from nucleus to cytoplasm, have been observed in postmortem human brains, with a significant overall reduction of Pin1 compared to age-matched controls [29]. Such redirection of Pin1 has been also reported in brains of patients with Frontotemporal dementias. In contrast with Pin1 neuroprotective role in AD, Pin1 has been found to accumulate in the Lewy bodies of human PD (Parkinson disease) brains and to contribute to the formation of  $\alpha$ -synuclein inclusions [31]. Moreover, increased levels of Pin1 compared to age-matched controls [13]. Such redirection of Pin1 has been also reported in

brains of patients with frontotemporal dementias. In contrast with Pin1 neuroprotective role in AD, Pin1 has been found to accumulate in the Lewy bodies of human PD (Parkinson disease) brains and to contribute to the formation of  $\alpha$ -synuclein inclusions [18]. Moreover, increased levels of Pin1 have been reported in pigmented dopaminergic neurons in PD human brains, where it mediated a neurotoxic action contributing to dopaminergic neurodegeneration [19]. Furthermore, in Huntington disease (HD), Pin1 has been found to promote p53-dependent neuronal apoptosis, induced by mutant huntingtin [20]. In addition, inhibition of Pin1 has been shown to reduce neurofilament (NFT)-H hyperphosphorylation and its pathological perikaryal accumulation in *in vitro* models of amyotrophic lateral sclerosis (ALS) [21]. In contrast, in mice intracerebrally infected with RLM (Rocky Mountain Laboratory) prion strain – a mouse-adapted scrapie prions resembling the pathological features occurring in prion protein diseases – neither total depletion nor reduced levels of Pin1 have been found to affect the process of prion protein misfolding or to alter the typical clinical and neuropathological features of the disease both in hemizygous Pin1<sup>+/-</sup> and knockout Pin1<sup>-/-</sup> mice [41]. Therefore, a differential role of Pin1 within the different neurodegenerative diseases clearly emerges (**Table 1**) and it is still subject of scientific debate. Such diverse implication of Pin1 in neurodegeneration may rely, at least in part, on the different phosphorylation patterns of Pin1 targets in the different cellular and pathological context.

### **Pin1 in Alzheimer's Disease**

The first evidence of Pin1 involvement in neurodegenerative disorders, such as AD, dates back to 1999, when elevated levels of Pin1 binding to NFT-rich cytoplasm of AD neurons were reported [13]. Later, Pin1 has been reported to be oxidatively modified, with consequent reduced activity and expression in hippocampus from MCI (mild cognitive impairment) and AD patients compared to age-matched controls [10, 11]. Moreover, using light microscopy, change in Pin1 intracellular localization – predominantly nuclear – has been also observed in neurons from AD patients, where Pin1 was localized to neuronal cytoplasm and perikaryal NFTs [13]. Notably, after the application of exogenous recombinant Pin1 to AD brain sections, it has been observed that recombinant Pin1 was bound to the phosphorylated Thr231 residue of tau and it was sequestered within tangles, thereby reducing the amount of soluble Pin1 protein [13]. In addition, Pin1 activity has been reported to directly restore the conformation and function of phosphorylated tau by indirectly promoting its dephosphorylation [13]. In particular, Pin1 has been found to bind to tau at phosphorylated Thr231-Pro, thereby stimulating PP2A-driven dephosphorylation and restoring its microtubule-binding functions [13, 42]. However, the hypothesis that aggregated tau sequesters and depletes soluble Pin1 reserve is controversial. In fact, Dakson



and collaborators, by analyzing the content of Pin1 in hippocampal and cortical neurons of brains from AD patients, demonstrated an increase in Pin1 immunoreactive granules within the hippocampal regions of CA2, CA1, subiculum, and presubiculum, whereas minimal occurrence or complete absence have been reported in cortical areas with prominent NFT pathology, such as the entorhinal and temporal cortices [43]. Thus, the incidence of Pin1 immunoreactive granules seems not to correlate with the frequency and distribution of NFT pathology, as well as with the presence or absence of A $\beta$  [43]. In young brains, absent or mild Pin1 immunoreactivity has been observed [43].

Besides Pin1 correlation to tau, Pastorino *et al.* demonstrated that Pin1 also regulates APP processing and A $\beta$  production [40], by binding to the phosphorylated Thr668-Pro motif of APP and accelerating its intracellular domain isomerization [40]. In particular, they reported that the cis phosphorylated Thr668-Pro conformation promoted the amyloidogenic processing of APP, whereas the trans conformation the non-amyloidogenic pathway. By catalyzing such conversion, Pin1 has been demonstrated to promote the non-amyloidogenic processing of APP [40]. In mice, Pin1 knockout, alone or in combination with overexpression of mutant APP, has been linked to increased amyloidogenic APP processing, with a selective enhancement in insoluble A $\beta$ 42 levels in an age-dependent manner [40]. These data are intriguing since they suggest that the Pin1 mutation is sufficient alone to induce an age-dependent brain amyloidosis. In particular, while, in Pin1<sup>-/-</sup> mice at 2–6 months of age, no change in the levels of A $\beta$ 42 was detected, at 15 months, a significant increase in insoluble A $\beta$ 42 content was observed compared to Pin1<sup>+/+</sup> mice [40]. Such increase in insoluble A $\beta$ 42 levels was accelerated by APP overexpression in Pin1<sup>-/-</sup> transgenic mice (Tg2576), where enhanced insoluble A $\beta$ 42 by 46% was detected at 6 months compared to Pin1<sup>+/+</sup> littermates [40].

Recently, Xu *et al.* demonstrated a pathological loss of Pin1 within the synapses of human frontal tissues from AD patients compared to age-matched control brains [12]. In particular, total synaptic Pin1 protein content was significantly reduced by 39% in human AD patient frontal cortical tissues compared to controls [12]. In C57/BL6 cortical neurons, the pharmacological inhibition of Pin1 catalytic activity with PiB (diethyl-1,3,6,8-tetrahydro-1,3,6,8-tetraoxobenzol-phenanthroline-2,7-diacetate) or Pin1 siRNA-mediated knockout induced an increase in ubiquitin-regulated modification of PSD proteins and a reduction in Shank3 protein levels [12], an observation consistent with Shank3 protein loss and enhanced ubiquitination described in AD brains [44, 45]. Such effects induced by Pin1 loss may possibly contribute to pathological changes in PSD structures and synaptic damage [12]. Based on evidence reporting a reduced activity of Pin1 in the early stage of the disease, as observed in MCI, loss of Pin1 may represent an early event participating to

the pathological alterations of synaptic proteins and, ultimately, leading to synaptic loss or alternatively the consequence of a reduced number of synapses. Notably, since Pin1 has been found downregulated and oxidatively modified in MCI patients [10, 11], it might be further investigated as potential biomarker to detect neurodegenerative processes occurring early in the progression of AD [46].

The emerging picture is that of a neuroprotective role for Pin, the loss of which, observed both in MCI and AD brains, may accelerate both neurofibrillary tangles and senile plaques formation and impair synaptic homeostasis. Consistently, a functional polymorphism, rs2287839, in Pin1 promoter has been reported to associate with a 3-year delay in the average age-at-onset of late-onset AD in a Chinese population [47]. Specifically, this polymorphism, located within the consensus motif for the brain-selective transcription factor AP4, almost completely prevented AP4 binding to Pin1 promoter and, consequently, Pin1 expression was unresponsive to the repressive effect of AP4 [47]. In contrast, other polymorphisms in the promoter region of PIN1 gene have been related to an increased risk of AD. As an example, a study by Segat *et al.* identified two single nucleotide polymorphisms at positions – 842 and – 667 in the promoter region of PIN1 gene and reported a significantly higher percentage of – 842C allele carriers in AD subjects compared to controls, suggesting that the inheritance of such allele may alter Pin1 expression and, consequently, enhance the risk of developing AD [48].

### **Pin1 in Frontotemporal dementia**

As observed in AD brains, tau hyperphosphorylation in the NFTs is accompanied by the redirection of the predominantly nuclear Pin1 into the neuronal cytoplasm, as well as by Pin1 deficits throughout subcellular compartments. Intriguingly, a similar redistribution and reduction of Pin1 have been observed in a range of frontotemporal dementias (FTDs), both with tau pathology (FTD with tau mutation, Pick disease, corticobasal degeneration) and without tau pathology (frontotemporal lobar degeneration with motor neuron-type inclusions, and neuronal intermediate filament inclusion disease) [16]. Accordingly, in neurons derived from the middle frontal gyrus of control and FTD postmortem brains, Thorpe and collaborators found a redistribution of Pin1 from the nucleus to the cytoplasm in all the FTD cases, compared to normal brains, which conversely displayed a prevalent nuclear localization of Pin1 [16]. This observed redirection of the mitotic regulator Pin1 from neuronal nucleus to cytoplasm is likely to depend on the presence of p-tau, as well as on the increased amount of its other target phosphoproteins in neuronal cytoplasm, such as mitotic phosphoepitopes and cell cycle-related proteins [49–52]. Accumulation of these proteins has been observed in different pathological contexts (e.g., AD, FTDP-17,

progressive supranuclear palsy, corticobasal degeneration) [53] and described as manifestations of interrupted mitotic process leading to cytoskeletal abnormalities and neuronal apoptosis [16]. However, further investigations are necessary to evaluate whether Pin1 redirection to the cytoplasm represents an early event occurring and mediating the neurodegenerative processes or the result of it.

Notably, Iridoy *et al.* recently analyzed the pattern of Pin1 expression by using a proteomic approach, demonstrating a trend for downregulation of Pin1 in human non-motor cortex and in the spinal cord derived from patients with ubiquitin frontotemporal lobar degeneration (FTLD-U), the most common form of FTD [17].

### **Pin1 in Parkinson Disease**

The prolyl isomerase Pin1 has been also implicated in the pathogenesis of PD. Ryo and collaborators demonstrated that Pin1 accumulated in the Lewy bodies of human PD brains and colocalized with  $\alpha$ -synuclein inclusions [18]. In particular, Pin1 overexpression has been observed to facilitate the formation of  $\alpha$ -synuclein inclusions in 293T cells transfected with  $\alpha$ -synuclein, while dominant-negative Pin1 abrogated it [18]. Specifically, Pin1 overexpression has been reported to enhance the half-life and insolubility of  $\alpha$ -synuclein, as well as to bind to synphilin-1, an  $\alpha$ -synuclein partner, thereby promoting its interaction with  $\alpha$ -synuclein and the formation of  $\alpha$ -synuclein cytoplasmic inclusions [18]. Later, Ghosh *et al.* provided evidence regarding the upregulation of Pin1 due to neurotoxic stress and its role as pro-apoptotic factor contributing to dopaminergic neuronal degeneration [19]. Indeed, Pin1 has been reported to be significantly upregulated in postmortem human midbrain of PD patients in comparison with aged-matched controls [19], as well as in vitro in dopaminergic MN9D neurons, treated with 1-methyl-4-phenylpyridinium (MPP<sup>+</sup>), and in the substantia nigra of the 1-methyl-4-phenyl-1,2,3,6-tetra-hydropyridine (MPTP)-induced PD mouse model [19]. Notably, siRNA-mediated knockdown of Pin1 has been observed to prevent MPP<sup>+</sup>-induced caspase-3 activation and DNA fragmentation, thus suggesting that Pin1 may induce apoptosis in dopaminergic neurons [19]. Accordingly, different pharmacological Pin1 inhibitors, such as juglone, reduced MPP<sup>+</sup>-driven Pin1 upregulation,  $\alpha$ -synuclein aggregation, caspase-3 activation, and neuronal death [19]. Furthermore, juglone treatment in the MPTP mouse model of PD suppressed Pin1 levels and ameliorated functional locomotor deficits, dopamine depletion, and nigral dopaminergic neuronal loss [19]. Noteworthy, the Pin1 inhibitor PiB reduced  $\alpha$ -synuclein protein aggregation, induced by MPP<sup>+</sup>, in the N27 dopaminergic cell models, thereby indicating that upregulation of Pin1, driven by neurotoxic pulse, might contribute to  $\alpha$ -synuclein protein misfolding and aggregation [19]. However, the precise intracellular

mechanism of Pin1 upregulation in  $\alpha$ -synuclein misfolding and aggregation has to be unveiled.

Taken together, such results provide evidence of a potential pro-apoptotic role of Pin in dopaminergic neurons, indicating that its upregulation may represent a critical neurotoxic event in the pathogenesis of PD.

### **Pin1 in Huntington disease**

HD is a dominantly inherited neurodegenerative disorder, caused by CAG repeat expansion in the gene codifying for huntingtin protein and characterized by massive loss of medium spiny neurons in the striatum [54]. Among the different mechanisms by which mutated huntingtin triggers striatal neurodegeneration, DNA damage and neuronal apoptosis have been proposed as key mechanisms. In this regard, the tumor suppressor p53 has been found to mediate toxic effects of mutated huntingtin with expanded polyglutamine [20, 55]. Mutated huntingtin has been reported to bind to p53 and to increase p53 levels in whole tissue lysates of postmortem cerebral cortex and striatum of HD patients, as well as to induce its transcriptional activity [55]. Later, Grison *et al.* demonstrated that, in postmortem brains of HD patients, the expression of mutated huntingtin evoked a canonical DNA damage response and was correlated to an enhanced phosphorylation of p53 at Ser46 [20]. Such phosphorylation generated a target site for Pin1, thereby promoting p53 interaction with Pin1 and the dissociation of p53 from the apoptosis inhibitor iASPP in *in vitro* models, thereby inducing the expression of its apoptotic target genes [20]. Noteworthy, Ser46 phosphorylation, triggered by severe or persistent stress, has been reported to be the major event in shifting p53 response from cell cycle arrest to apoptosis and the isomerization by Pin1 as a key step to stimulate the apoptotic potential of p53. Furthermore, a toxic feedback loop has been demonstrated, where mutated huntingtin promotes Pin1-mediated activation of p53 that, in turn, induces the expression of mutated huntingtin [56]. Therefore, such results provide evidence of a potential mechanism through which Pin1/p53 pathways participate to the induction of neuronal apoptosis in response to mutated huntingtin.

### **Pin1 in Amyotrophic Lateral Sclerosis**

ALS is a neurodegenerative disorder that affects the upper and lower motor neurons, leading to paralysis of voluntary muscles, dysphagia, dysarthria, and respiratory failure [57]. Recently, by using a proteomic approach, Iridoy and collaborators demonstrated a significant downregulation of Pin1 expression in the spinal cord and non-motor cortex of

a small cohort of patients with ALS [17], indicating Pin1 expression as a potential marker of neurodegeneration. However, the current knowledge about the expression profile of Pin1 in ALS is extremely limited, as well as its involvement in the pathophysiology of this disease. Evidence from the literature suggests that it may promote the abnormal accumulations of phosphorylated neurofilament proteins in the perikaryon, a major hallmark of ALS, as well as of other neurodegenerative diseases [21, 58]. Accordingly, Pin1 has been reported to associate with phosphorylated NF-H in neurons and to co-localize in ALS-affected spinal cord neuronal inclusions [21]. In rat dorsal root ganglion cultures subjected to excitotoxic stress to evoke the accumulation of phosphorylated NF-H within the cell body in order to mimic neurodegeneration, glutamate-induced toxicity has been demonstrated to increase phosphorylated NF-H in perikaryal accumulations that co-localized with Pin1 and induced neuronal apoptosis [21]. Such effects were reduced by pharmacological inhibition or siRNA-mediated downregulation of Pin1 [21], thus suggesting that, upon neurotoxic pulse, Pin1 may promote cell death by stimulating the perikaryal aggregation of phosphorylated NF-H.

## Conclusions

### **Pin1 as a crucial signal transducer acting in a context-dependent manner**

By inducing the isomerization of the *cis/trans* configuration of its cellular substrates, Pin1 acts as key fine-tuner and amplifier of multiple signaling pathways, thereby displaying a variety of functional consequences both in physiological and pathological conditions. As discussed in this review, a highly pleiotropic and context-dependent nature of Pin1 functional activity, strictly dependent on the phosphorylation patterns of its cellular targets, clearly emerges. Noteworthy, in the nervous system, Pin1 is fundamental both for embryonic development and cellular homeostasis in adult neurons, due to its role as regulator of cell death and survival. In particular, in developing neurons, it seems to participate to the induction of neuronal cell death, whereas in adult neurons, to promote neuronal survival. Notably, while accumulating evidence has characterized Pin1 role in the regulation of cell fates in cancer, Pin1 functional activity on neuronal homeostasis and, specifically, Pin1 role as pro-apoptotic and/or pro-survival regulator within neurons, at different stages of neuronal development, has still to be unveiled. Moreover, despite sparse evidence supporting Pin1 regulation of protein translation at dendrites and its interaction with specific synaptic substrates at excitatory and inhibitory synapses, the overall balance of its activity at synapses, under physiological conditions, is unknown. However, a comprehensive understanding of Pin1 physiological functions in neurons and, specifically, at synapses is critical to define whether and how an imbalance in of Pin1 activity and/or

expression may impact on neuronal homeostasis and, ultimately, contribute to pathological mechanisms. In this regard, our knowledge of Pin1 physiological activity in neurons is extremely limited and some inconsistencies complicate the scenario. As an example, multiple lines of evidence report that in human AD brains, Pin1 activity and protein content are markedly reduced [10, 11] and that in Tg2576 mice, germ-line Pin1 knockout significantly accelerates AD pathology, as discussed above [15]. However, data from literature paradoxically demonstrate that hippocampal slices derived from germ-line Pin1 knockout mice showed enhanced, rather than decreased, LTP [25], as well as increased, rather than reduced, hippocampal spine density [33]. Notably, these phenotypes are opposite to those expected from the pathology commonly observed in human AD brains and murine AD models. In this regard, it is tempting to speculate that such discrepancies between spine density and LTP in germ-line Pin1 knockout and AD mouse models depend upon the model used, one based on the lifelong lack of Pin1 versus the progressive loss of it over time. Accordingly, while germ-line knockout mice harboring a null allele provide appropriate genetic models of inherited disease, conditional gene inactivation seems to be a more appropriate approach to assess the post-development effects of Pin1 loss in adult organisms and to achieve gene inactivation in selected cell types [59]. Hence, depending on the model used, it is possible to differentiate distinct functions of Pin1 in dendritic spine development and spine maintenance. As proof of concept, Stalling *et al.* recently demonstrated that in Pin1 floxed mice and derived neuronal cultures, postnatal Pin1 loss induced a significant decrease in spine density, rescued by the application of exogenous Pin1, thus suggesting that Pin1 is required for dendritic spine maintenance in mature neurons [60]. Therefore, further investigations should consider this aspect to select more suitable models to assess Pin1 role in age-related pathologies, where Pin1 loss occurs late in the lifespan.

In conclusion, while under physiological conditions, Pin1 activity ensures a homeostatic equilibrium by fine-tuning the ability of cells to transduce a variety of stimuli and to elicit integrated biological responses, in pathological contexts, an imbalance in Pin1 activity and/or expression may exacerbate diseases by hijacking cellular processes regulated by Pin1 to sustain pathological mechanisms [61]. In line with this hypothesis, Pin1 has been reported to play a key role in acute neurological conditions associated with subsequent neurodegeneration, such as ischemic stroke [62], where it promotes neuronal death by acting on Notch1 signaling pathway [62]. Pin1-deficiency has been found to prevent stroke-induced brain damage and neurological deficits in Pin1<sup>-/-</sup> mice [62]. Such evidence supports the notion that Pin1 is a key molecular switch regulating neuronal cell fates also in pathological conditions. Indeed, profoundly different roles of Pin1, ranging from

neuroprotective to neurotoxic, have been observed within different pathological contexts (**Table 1**), further indicating the context-dependent nature of Pin1 functional activity.

Therefore, Pin1 clearly emerges as a crucial signal transducer that, under normal conditions, regulates the activation of multiple signaling pathways, thereby inducing biological outcomes downstream to a plethora of stimuli, but, when imbalanced, may participate to pathological mechanisms, thus providing a promising therapeutic target in a wide array of pathological conditions. Its chameleonic role increases the difficulties associated with drug interventions targeting it in absence of biomarkers allowing to decide whether a certain status will benefit from Pin 1 agonism or antagonism. Further investigations are needed to explore the potential role of Pin1 as biomarker of neurodegeneration, in particular in the early stages of the disease. Based on the hypothesis that peripheral cells may allow to study in vitro the dynamic alterations of metabolic and biochemical processes that may reflect events occurring in the brain, future studies may help elucidating the possibility to measure Pin1 expression in easily accessible cells, such as peripheral tissues. In this regard, Ferri *et al.* reported a lower gene expression of Pin1 with a higher DNA methylation in three CpG sites at Pin1 gene promoter in FTD subjects, while a higher Pin1 gene expression with a lower DNA methylation in late-onset AD patients and controls, corroborating the hypothesis of a diverse involvement of Pin1 in different types of dementia [63].

## REFERENCES

1. Lu KP, Hanes SD, Hunter T (1996) A human peptidyl-prolyl isomerase essential for regulation of mitosis. *Nature* 380:544-547. <https://doi.org/10.1038/380544a0>
2. Lu PJ, Zhou XZ, Shen M, Lu KP (1999) Function of WW domains as phosphoserine- or phosphothreonine-binding modules. *Science* 283:1325-1328. <https://doi.org/10.1126/science.283.5406.1325>
3. Ranganathan R, Lu KP, Hunter T, Noel JP (1997) Structural and functional analysis of the mitotic rotamase Pin1 suggests substrate recognition is phosphorylation dependent. *Cell* 89:875-886. [https://doi.org/10.1016/S0092-8674\(00\)80273-1](https://doi.org/10.1016/S0092-8674(00)80273-1)
4. Lu PJ, Zhou XZ, Liou YC, Noel JP, Lu KP (2002) Critical role of WW domain phosphorylation in regulating phosphoserine binding activity and Pin1 function. *J Biol Chem* 277:2381-2384. <https://doi.org/10.1074/jbc.C100228200>
5. Kim G, Khanal P, Kim JY, Yun HJ, Lim SC, Shim JH, Choi HS (2015) COT phosphorylates prolyl-isomerase Pin1 to promote tumorigenesis in breast cancer. *Mol Carcinog* 54:440-448. <https://doi.org/10.1002/mc.22112>
6. Lu KP, Zhou XZ (2007) The prolyl isomerase PIN1: a pivotal new twist in phosphorylation signalling and disease. *Nat Rev Mol Cell Biol* 8:904-916. <https://doi.org/10.1038/nrm2261>

7. Hu X, Chen LF (2020) Pinning down the transcription: a role for peptidyl-prolyl cis-trans isomerase Pin1 in gene expression. *Front Cell Dev Biol* 8:179. <https://doi.org/10.3389/fcell.2020.00179>
8. Winkler KE, Swenson KI, Kornbluth S, Means AR (2000) Requirement of the prolyl isomerase Pin1 for the replication checkpoint. *Science* 287:1644-1647. <https://doi.org/10.1126/science.287.5458.1644>
9. Lanni C, Masi M, Racchi M, Govoni S (2020) Cancer and Alzheimer's disease inverse relationship: an age-associated diverging derailment of shared pathways. *Mol Psychiatry*. <https://doi.org/10.1038/s41380-020-0760-2>
10. Sultana R, Boyd-Kimball D, Poon HF, Cai J, Pierce WM, Klein JB, Markesbery WR, Zhou XZ *et al* (2006) Oxidative modification and down-regulation of Pin1 in Alzheimer's disease hippocampus: a redox proteomics analysis. *Neurobiol Aging* 27:918-925. <https://doi.org/10.1016/j.neurobiolaging.2005.05.005>
11. Butterfield DA, Poon HF, St. Clair D, Keller JN, Pierce WM, Klein JB, Markesbery WR (2006) Redox proteomics identification of oxidatively modified hippocampal proteins in mild cognitive impairment: insights into the development of Alzheimer's disease. *Neurobiol Dis* 22:223-232. <https://doi.org/10.1016/j.nbd.2005.11.002>
12. Xu L, Ren Z, Chow FE, Tsai R, Liu T, Rizzolio F, Boffo S, Xu Y *et al* (2017) Pathological role of peptidyl-prolyl isomerase Pin1 in the disruption of synaptic plasticity in Alzheimer's disease. *Neural Plast* 2017:32707. <https://doi.org/10.1155/2017/3270725>
13. Lu PJ, Wulf G, Zhou XZ, Davies P, Lu KP (1999) The prolyl isomerase Pin1 restores the function of Alzheimer-associated phosphorylated tau protein. *Nature* 399:784-788. <https://doi.org/10.1038/21650>
14. Thorpe JR, Morley SJ, Rulten SL (2001) Utilizing the peptidyl-prolyl cis-trans isomerase Pin1 as a probe of its phosphorylated target proteins: examples of binding to nuclear proteins in a human kidney cell line and to tau in Alzheimer's diseased brain. *J Histochem Cytochem* 49:97-108. <https://doi.org/10.1177/002215540104900110>
15. Liou YC, Sun A, Ryo A, Zhou XZ, Yu ZX, Huang HK, Uchida T, Bronson R *et al* (2003) Role of the prolyl isomerase Pin1 in protecting against age-dependent neurodegeneration. *Nature* 424:556-561. <https://doi.org/10.1038/nature01832>
16. Thorpe JR, Mosaheb S, Hashemzadeh-Bonehi L, Cairns NJ, Kay JE, Morley SJ, Rulten SL (2004) Shortfalls in the peptidyl-prolyl cis-trans isomerase protein Pin1 in neurons are associated with frontotemporal dementias. *Neurobiol Dis* 17:237-249. <https://doi.org/10.1016/j.nbd.2004.07.008>
17. Iridoy MO, Zubiri I, Zelaya MV, Martinez L, AusiÃn K, Lachen-Montes M, SantamariÃa E, Fernandez-Irigoyen J *et al* (2019) Neuroanatomical quantitative proteomics reveals common pathogenic biological routes between amyotrophic lateral sclerosis (ALS) and frontotemporal dementia (FTD). *Int J Mol Sci* 20. <https://doi.org/10.3390/ijms20010004>
18. Ryo A, Togo T, Nakai T, Hirai A, Nishi M, Yamaguchi A, Suzuki K, Hirayasu Y *et al* (2006) Prolyl-isomerase Pin1 accumulates in Lewy bodies of Parkinson disease and facilitates formation of  $\alpha$ -synuclein inclusions. *J Biol Chem* 281:4117-4125. <https://doi.org/10.1074/jbc.M507026200>



19. Ghosh A, Saminathan H, Kanthasamy A, Anantharam V, Jin H, Sondarva G, Harischandra DS, Qian Z *et al* (2013) The peptidyl-prolyl isomerase Pin1 up-regulation and proapoptotic function in dopaminergic neurons: relevance to the pathogenesis of parkinson disease. *J Biol Chem* 288:21955-21971. <https://doi.org/10.1074/jbc.M112.444224>
20. Grison A, Mantovani F, Comel A, Agostoni E, Gustincich S, Persichetti F, del Sal G (2011) Ser46 phosphorylation and prolyl-isomerase Pin1-mediated isomerization of p53 are key events in p53-dependent apoptosis induced by mutant huntingtin. *Proc Natl Acad Sci U S A* 108:17979-17984. <https://doi.org/10.1073/pnas.1106198108>
21. Kesavapany S, Patel V, Zheng YL *et al* (2007) Inhibition of Pin1 reduces glutamate-induced perikaryal accumulation of phosphorylated neurofilament-H in neurons. *Mol Biol Cell* 18:3645-3655. <https://doi.org/10.1091/mbc.E07-03-0237>
22. Becker EBE, Bonni A (2007) Pin1 in neuronal apoptosis. *Cell Cycle* 6:1332-1335. <https://doi.org/10.4161/cc.6.11.4316>
23. Sorrentino G, Comel A, Mantovani F, Del Sal G (2014) Regulation of mitochondrial apoptosis by Pin1 in cancer and neurodegeneration. *Mitochondrion* 19:88-96. <https://doi.org/10.1016/j.mito.2014.08.003>
24. Becker EBE, Bonni A (2006) Pin1 mediates neural-specific activation of the mitochondrial apoptotic machinery. *Neuron* 49:655-662. <https://doi.org/10.1016/j.neuron.2006.01.034>
25. Westmark PR, Westmark CJ, Wang SQ *et al* (2010) Pin1 and PKMCE  $\delta$  sequentially control dendritic protein synthesis. *Sci Signal* 3:ra18. <https://doi.org/10.1126/scisignal.2000451>
26. Balastik M, Zhou XZ, Alberich-Jorda M, Weissova R, ZÅaiak J, Pazyra-Murphy MF, Cosker KE, Machonova O *et al* (2015) Prolyl isomerase Pin1 regulates axon guidance by stabilizing CRMP2A selectively in distal axons. *Cell Rep* 13:812-828. <https://doi.org/10.1016/j.celrep.2015.09.026>
27. Nakamura K, Kosugi I, Lee DY, Hafner A, Sinclair DA, Ryo A, Lu KP (2012) Prolyl isomerase Pin1 regulates neuronal differentiation via  $\beta$ -catenin. *Mol Cell Biol* 32:2966-2978. <https://doi.org/10.1128/mcb.05688-11>
28. Sosa L, Malter J, Hu J *et al* (2016) Protein interacting with NIMA (never in mitosis A)-1 regulates axonal growth cone adhesion and spreading through myristoylated alanine-rich C kinase substrate isomerization. *J Neurochem* 137:744-755. <https://doi.org/10.1111/jnc.13612>
29. Qi ML, Tep C, Yune TY *et al* (2007) Opposite regulation of oligodendrocyte apoptosis by JNK3 and Pin1 after spinal cord injury. *J Neurosci* 27:8395-8404. <https://doi.org/10.1523/JNEUROSCI.2478-07.2007>
30. Barone MC, Desouzaf LA, Freeman RS (2008) Pin 1 promotes cell death in NGF-dependent neurons through a mechanism requiring c-jun activity. *J Neurochem* 106:734-745. <https://doi.org/10.1111/j.1471-4159.2008.05427.x>
31. Mantovani F, Tocco F, Girardini J, Smith P, Gasco M, Lu X, Crook T, Sal GD (2007) The prolyl isomerase Pin1 orchestrates p53 acetylation and dissociation from the apoptosis inhibitor iASPP. *Nat Struct Mol Biol* 14:912-920. <https://doi.org/10.1038/nsmb1306>

32. Zheng H, You H, Zhou XZ, Murray SA, Uchida T, Wulf G, Gu L, Tang X *et al* (2002) The prolyl isomerase Pin1 is a regulator of p53 in genotoxic response. *Nature* 419:849-853. <https://doi.org/10.1038/nature01116>
33. Antonelli R, de Filippo R, Middei S, Stancheva S, Pastore B, Ammassari-Teule M, Barberis A, Cherubini E *et al* (2016) Pin1 modulates the synaptic content of NMDA receptors via prolyl-isomerization of PSD-95. *J Neurosci* 36:5437-5447. <https://doi.org/10.1523/JNEUROSCI.3124-15.2016>
34. Moretto Zita M, Marchionni I, Bottos E, Righi M, del Sal G, Cherubini E, Zacchi P (2007) Post-phosphorylation prolyl isomerisation of gephyrin represents a mechanism to modulate glycine receptors function. *EMBO J* 26:1761-1771. <https://doi.org/10.1038/sj.emboj.7601625>
35. Antonelli R, Pizzarelli R, Pedroni A, Fritschy JM, del Sal G, Cherubini E, Zacchi P (2014) Pin1-dependent signalling negatively affects GABAergic transmission by modulating neuroligin2/gephyrin interaction. *Nat Commun* 5:5066. <https://doi.org/10.1038/ncomms6066>
36. Tang L, Zhang Y, Chen G, Xiong Y, Wang X, Zhu B (2017) Down-regulation of Pin1 in temporal lobe epilepsy patients and mouse model. *Neurochem Res* 42:1211-1218. <https://doi.org/10.1007/s11064-016-2158-8>
37. Fujimori F, Takahashi K, Uchida C, Uchida T (1999) Mice lacking Pin1 develop normally, but are defective in entering cell cycle from G0 arrest. *Biochem Biophys Res Commun* 265:658-663. <https://doi.org/10.1006/bbrc.1999.1736>
38. Liou YC, Ryo A, Huang HK, Lu PJ, Bronson R, Fujimori F, Uchida T, Hunter T *et al* (2002) Loss of Pin1 function in the mouse causes phenotypes resembling cyclin D1-null phenotypes. *Proc Natl Acad Sci U S A* 99:1335-1340. <https://doi.org/10.1073/pnas.032404099>
39. Lee TH, Pastorino L, Lu KP (2011) Peptidyl-prolyl cis-trans isomerase Pin1 in ageing, cancer and Alzheimer disease. *Expert Rev Mol Med* 13:e21. <https://doi.org/10.1017/S1462399411001906>
40. Pastorino L, Sun A, Lu PJ, Zhou XZ, Balastik M, Finn G, Wulf G, Lim J *et al* (2006) The prolyl isomerase Pin1 regulates amyloid precursor protein processing and amyloid- $\beta$  production. *Nature* 440:528-534. <https://doi.org/10.1038/nature04543>
41. Legname G, Virgilio T, Bistaffa E, de Luca CMG, Catania M, Zago P, Isopi E, Campagnani I *et al* (2018) Effects of peptidyl-prolyl isomerase 1 depletion in animal models of prion diseases. *Prion* 12:127-137. <https://doi.org/10.1080/19336896.2018.1464367>
42. Zhou XZ, Kops O, Werner A, Lu PJ, Shen M, Stoller G, KuÅallertz G, Stark M *et al* (2000) Pin1-dependent prolyl isomerization regulates dephosphorylation of Cdc25C and Tau proteins. *Mol Cell* 6:873-883. [https://doi.org/10.1016/S1097-2765\(05\)00083-3](https://doi.org/10.1016/S1097-2765(05)00083-3)
43. Dakson A, Yokota O, Esiri M, Bigio EH, Horan M, Pendleton N, Richardson A, Neary D *et al* (2011) Granular expression of prolyl-peptidyl isomerase PIN1 is a constant and specific feature of Alzheimer's disease pathology and is independent of tau, A $\beta$  and TDP-43 pathology. *Acta Neuropathol* 121:635-649. <https://doi.org/10.1007/s00401-011-0798-y>
44. Gong Y, Lippa CF, Zhu J, Lin Q, Rosso AL (2009) Disruption of glutamate receptors at Shank-postsynaptic platform in Alzheimer's disease. *Brain Res* 1292:191-198. <https://doi.org/10.1016/j.brainres.2009.07.056>

45. Pham E, Crews L, Ubhi K, Hansen L, Adame A, Cartier A, Salmon D, Galasko D *et al* (2010) Progressive accumulation of amyloid- $\beta$  oligomers in Alzheimer's disease and in amyloid precursor protein transgenic mice is accompanied by selective alterations in synaptic scaffold proteins. *FEBS J* 277:3051-3067. <https://doi.org/10.1111/j.1742-4658.2010.07719.x>
46. Keeney JTR, Swomley AM, Harris JL, Fiorini A, Mitov MI, Perluigi M, Sultana R, Butterfield DA (2012) Cell cycle proteins in brain in mild cognitive impairment: Insights into progression to Alzheimer disease. *Neurotox Res* 22:220-230. <https://doi.org/10.1007/s12640-011-9287-2>
47. Ma SL, Tang NLS, Tam CWC, Lui VWC, Lam LCW, Chiu HFK, Driver JA, Pastorino L *et al* (2012) A PIN1 polymorphism that prevents its suppression by AP4 associates with delayed onset of Alzheimer's disease. *Neurobiol Aging* 33:804-813. <https://doi.org/10.1016/j.neurobiolaging.2010.05.018>
48. Segat L, Pontillo A, Annoni G, Trabattoni D, Vergani C, Clerici M, Arosio B, Crovella S (2007) PIN1 promoter polymorphisms are associated with Alzheimer's disease. *Neurobiol Aging* 28:69-74. <https://doi.org/10.1016/j.neurobiolaging.2005.11.009>
49. Arendt T, Holzer M, GaÛrtner U, BruÛckner MK (1998) Aberrancies in signal transduction and cell cycle related events in Alzheimer's disease. *J Neural Transm Suppl* 54:147-158. [https://doi.org/10.1007/978-3-7091-7508-8\\_14](https://doi.org/10.1007/978-3-7091-7508-8_14)
50. Arendt T, Holzer M, Stobe A *et al* (2000) Activated mitogenic signaling induces a process of dedifferentiation in Alzheimer's disease that eventually results in cell death. *Ann N Y Acad Sci* 920: 249-255. <https://doi.org/10.1111/j.1749-6632.2000.tb06931.x>
51. Busser J, Geldmacher DS, Herrup K (1998) Ectopic cell cycle proteins predict the sites of neuronal cell death in Alzheimer's disease brain. *J Neurosci* 18:2801-2807. <https://doi.org/10.1523/JNEUROSCI.18-08-02801.1998>
52. Cataldo AM, Peterhoff CM, Troncoso JC, Gomez-Isla T, Hyman BT, Nixon RA (2000) Endocytic pathway abnormalities precede amyloid  $\beta$  deposition in sporadic Alzheimer's disease and Down syndrome: Differential effects of APOE genotype and presenilin mutations. *Am J Pathol* 157:277-286. [https://doi.org/10.1016/S0002-9440\(10\)64538-5](https://doi.org/10.1016/S0002-9440(10)64538-5)
53. Husseman JW, Nochlin D, Vincent I (2000) Mitotic activation: a convergent mechanism for a cohort of neurodegenerative diseases. *Neurobiol Aging* 21:815-828. [https://doi.org/10.1016/S0197-4580\(00\)00221-9](https://doi.org/10.1016/S0197-4580(00)00221-9)
54. Ehrlich ME (2012) Huntington's disease and the striatal medium spiny neuron: cell-autonomous and non-cell-autonomous mechanisms of disease. *Neurotherapeutics* 9:270-284. <https://doi.org/10.1007/s13311-012-0112-2>
55. Bae BI, Xu H, Igarashi S *et al* (2005) p53 mediates cellular dysfunction and behavioral abnormalities in Huntington's disease. *Neuron* 47:29-41. <https://doi.org/10.1016/j.neuron.2005.06.005>
56. Feng Z, Jin S, Zupnick A, Hoh J, de Stanchina E, Lowe S, Prives C, Levine AJ (2006) p53 tumor suppressor protein regulates the levels of huntingtin gene expression. *Oncogene* 25:1-7. <https://doi.org/10.1038/sj.onc.1209021>

- 
57. Wijesekera LC, Leigh PN (2009) Amyotrophic lateral sclerosis. *Orphanet J Rare Dis* 4:3. <https://doi.org/10.1186/1750-1172-4-3>
58. Itoh T, Sobue G, Ken E, Mitsuma T, Takahashi A, Trojanowski JQ (1992) Phosphorylated high molecular weight neurofilament protein in the peripheral motor, sensory and sympathetic neuronal perikarya: system-dependent normal variations and changes in amyotrophic lateral sclerosis and multiple system atrophy. *Acta Neuropathol* 83:240-245. <https://doi.org/10.1007/BF00296785>
59. Friedel RH, Wurst W, Wefers B, Kühn R (2011) Generating conditional knockout mice. *Methods Mol Biol* 693:205-231. [https://doi.org/10.1007/978-1-60761-974-1\\_12](https://doi.org/10.1007/978-1-60761-974-1_12)
60. Stallings NR, O'Neal MA, Hu J, Kavalali ET, Bezprozvanny I, Malter JS (2018) Pin1 mediates ACE $\leq$ 42-induced dendritic spine loss. *Sci Signal* 11:eaap8734. <https://doi.org/10.1126/scisignal.aap8734>
61. Zannini A, Rustighi A, Campaner E, Del Sal G (2019) Oncogenic hijacking of the PIN1 signaling network. *Front Oncol* 9:94. <https://doi.org/10.3389/fonc.2019.00094>
62. Baik SH, Fane M, Park JH, Cheng YL, Yang-Wei Fann D, Yun UJ, Choi Y, Park JS *et al* (2015) Pin1 promotes neuronal death in stroke by stabilizing notch intracellular domain. *Ann Neurol* 77:504-516. <https://doi.org/10.1002/ana.24347>
63. Ferri E, Arosio B, D'Addario C *et al* (2016) Gene promoter methylation and expression of Pin1 differ between patients with frontotemporal dementia and Alzheimer's disease. *J Neurol Sci* 362:283-286. <https://doi.org/10.1016/j.jns.2016.02.004>

---

## **CHAPTER II**

Targeting Nrf2 and NF- $\kappa$ B signaling pathways to counteract  
oxidative stress and inflammation



## PART 1

The following manuscript was published in *Frontiers in Pharmacology* in 2020 as:

### **Modulation of Keap1/Nrf2/ARE signaling pathway by curcuma- and garlic-derived hybrids**

Melania Maria Serafini†, Michele Catanzaro†, **Francesca Fagiani**, Elena Simoni, Roberta Caporaso, Marco Dacrema, Irene Romanoni, Stefano Govoni, Marco Racchi, Maria Daglia, Michela Rosini and Cristina Lanni

(† these authors have contributed equally to this work)

#### **Abstract**

Nrf2 is a basic leucine zipper transcription factor that binds to the promoter region of the antioxidant response element (ARE), inducing the coordinated up-regulation of antioxidant and detoxification genes. We recently synthesized a set of new molecules by combining the functional moieties of curcumin and diallyl sulfide, both known to induce the expression of antioxidant phase II enzymes by activating Nrf2 pathway. The aim of the study is to investigate the ability of such compounds to activate Keap1/Nrf2/ARE cytoprotective pathway, in comparison with two reference Nrf2-activators: curcumin and dimethyl fumarate, a drug approved for the treatment of relapsing-remitting multiple sclerosis. Furthermore, since Nrf2 pathway is known to be regulated also by epigenetic modifications, including key modifications in microRNA (miRNA) expression, the effects of the hybrids on the expression levels of selected miRNAs, associated with Nrf2 signaling pathway have also been investigated. The results show that compounds exert antioxidant effect by activating Nrf2 signaling pathway and inducing the ARE-regulated expression of its downstream target genes, such as HO-1 and NQO1, with two hybrids to a higher extent than curcumin. In addition, some molecules induce changes in the expression levels of miR-125b-5p, even if to a lesser extent than curcumin. However, no changes have been observed in the expression levels of mRNA coding for glutathione synthetase, suggesting that the modulation of this mRNA is not strictly under the control of miR-125b-5p, which could be influenced by other miRNAs.

**Keywords:** curcumin, Nrf2, Keap1, NQO1, HO-1, dimethyl fumarate, miRNAs.



## Modulation of Keap1/Nrf2/ARE Signaling Pathway by Curcuma- and Garlic-Derived Hybrids

Melania Maria Serafini<sup>1,2†</sup>, Michele Catanzaro<sup>1†</sup>, Francesca Fagiani<sup>1,2</sup>, Elena Simoni<sup>3</sup>, Roberta Caporaso<sup>3</sup>, Marco Dacrema<sup>4</sup>, Irene Romanoni<sup>1</sup>, Stefano Govoni<sup>1</sup>, Marco Racchi<sup>1</sup>, Maria Daglia<sup>4</sup>, Michela Rosini<sup>3</sup> and Cristina Lanni<sup>1\*</sup>

### OPEN ACCESS

**Edited by:**  
Filippo Caraci,  
University of Catania, Italy

<sup>1</sup> Department of Drug Sciences, University of Pavia, Pavia, Italy, <sup>2</sup> Scuola Universitaria Superiore IUSS, Pavia, Italy, <sup>3</sup> Department of Pharmacy and Biotechnology, University of Bologna, Bologna, Italy, <sup>4</sup> Department of Pharmacy, University of Napoli Federico II, Naples, Italy

## INTRODUCTION

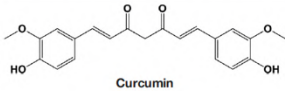
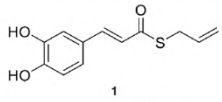
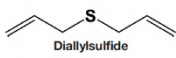
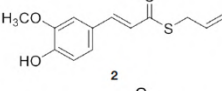
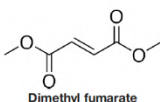
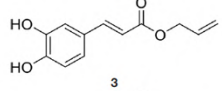
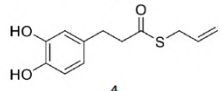
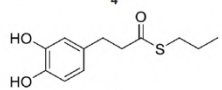
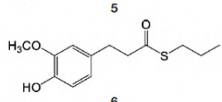
Nrf2 (NF-E2-related factor 2), a member of the Cap'n'collar (CNC) transcription factor family, is a redox-sensitive transcription factor that plays a key role in adaptation to cellular stress. Under normal homeostatic conditions, Keap1 anchors the Nrf2 transcription factor within the cytoplasm targeting it for ubiquitination and degradation by 26S proteasomes (Niture *et al.*, 2014). Under stress conditions, phosphorylation and/or redox modification of critical cysteines residues in Keap1 inhibits the enzymatic activity of the Keap1-Cul3-Rbx1 E3 ubiquitin ligase complex (Tebay *et al.*, 2015). Consequently, free Nrf2 translocates to the nucleus, where it dimerizes with Maf proteins (musculoaponeurotic fibrosarcoma) and binds to the antioxidant response element (ARE), also called electrophile response element (EpRE), a cis-acting enhancer sequence located in the promoter region of a battery of downstream genes encoding cyto-protective, antioxidant, and phase II detoxifying enzymes or proteins, such as NAD(P)H: quinone reductase-1 (NQO1), heme oxygenase-1 (HO-1), and glutathione synthetase (GSS) (Tebay *et al.*, 2015). The Nrf2/Keap1/ARE signaling pathway can be activated by various exogenous and endogenous small molecules (Baird and Dinkova-Kostova, 2011; Paunkov *et al.*, 2019) and controls also the expression of genes involved in the regulation of cell proliferation and survival (Malhotra *et al.*, 2010).

Natural products have emerged as a great source of bioactive compounds with health beneficial impact. One example are polyphenols, phenolic compounds that act on biological systems exerting protective effects not only by direct antioxidant capacity, but



also by interacting with signal-transduction pathways that regulate transcription factors and, consequently, the expression of genes and proteins (Auclair *et al.*, 2009; Spencer, 2010; Camargo *et al.*, 2010). Among the variety of pathways, it has been demonstrated that polyphenols such as curcumin, hydroxytyrosol contained in olive oil, resveratrol, and epigallocatechin-3-gallate extracted from green tea could modulate the transcription factor Nrf2, via translocation into the cell nucleus and induction of the expression of its target genes (Scapagnini *et al.*, 2011; Xicota *et al.*, 2017; Martínez-Huélamo *et al.*, 2017).

In our previous papers, we described and characterized the ability of a set of new curcuma- and garlic-derived compounds to inhibit A $\beta$  oligomerization and fibrilization (Simoni *et al.*, 2016; Simoni *et al.*, 2017). The main structure of these hybrids combines the diallyl sulfide (DAS), which represents the mercaptan moiety of garlic-derived organosulfur compounds, and the hydroxycinnamoyl group, a recurring chemical function of polyphenols, such as curcumin, rosmarinic acid, and coumarin (Ho *et al.*, 2012; Witaicenis *et al.*, 2014; Nabavi *et al.*, 2015a). Our data demonstrated the ability of these molecules to act as scavenger agents in presence of oxidant stressors (Simoni *et al.*, 2016; Simoni *et al.*, 2017). In particular, we identified a catechol derivative (compound 1, see **Table 1**), with remarkable anti-aggregating ability and antioxidant properties (Simoni *et al.*, 2016). Starting from the results obtained with compound 1, which is considered the lead compound, its structure was systematically modified by focusing on the aryl substitution pattern, the thioester function, and the aliphatic skeleton with the aim of strategically tuning the pharmacological profile (Simoni *et al.*, 2017). Herein, to investigate the structure-dependent activation of intracellular defensive pathways, we focused on a selection of these hybrids (compounds 1–6, **Table 1**). Two reference molecules, known to activate Nrf2 pathway, were used for comparison: curcumin (CURC) and dimethyl fumarate (DMF), whose structure are also reported in **Table 1**. CURC has been extensively studied in different pathological contexts and, while to date there are no confirmed applications in humans due to the failure of clinical trials, its antioxidant properties are well-known and confirmed by a plethora of publications (Darvesh *et al.*, 2012; Shen *et al.*, 2013; Vera-Ramirez *et al.*, 2013; Nabavi *et al.*, 2015b; Serafini *et al.*, 2017; Catanzaro *et al.*, 2018). DMF has been approved by the Food and Drug Administration (FDA) for the treatment of relapsing-remitting multiple sclerosis and its anti-inflammatory and antioxidant properties are widely reported in literature (for an extensive review see Suneetha and Raja Rajeswari, 2016; Saidu *et al.*, 2019).

Combined compounds		Derived hybrid compounds	
		Structure	Functional groups
	Curcumin		<ul style="list-style-type: none"> <li>• Michael acceptor</li> <li>• Catechol moiety</li> <li>• Thioester</li> <li>• Terminal double bond</li> </ul>
	Diallylsulfide		<ul style="list-style-type: none"> <li>• Michael acceptor</li> <li>• Thioester</li> <li>• Terminal double bond</li> </ul>
	Dimethyl fumarate		<ul style="list-style-type: none"> <li>• Michael acceptor</li> <li>• Catechol moiety</li> <li>• Terminal double bond</li> </ul>
	Reference compound		<ul style="list-style-type: none"> <li>• Catechol moiety</li> <li>• Thioester</li> <li>• Terminal double bond</li> </ul>
			<ul style="list-style-type: none"> <li>• Catechol moiety</li> <li>• Thioester</li> </ul>
			<ul style="list-style-type: none"> <li>• Thioester</li> </ul>

Compound 1: S-allyl (E)-3-(3,4-dihydroxyphenyl)prop-2-enethioate;  
 Compound 2: S-allyl (E)-3-(4-hydroxy-3-methoxyphenyl)prop-2-enethioate;  
 Compound 3: allyl (E)-3-(3,4-dihydroxyphenyl)acrylate;  
 Compound 4: S-allyl 3-(3,4-dihydroxyphenyl)propanethioate;  
 Compound 5: S-propyl 3-(3,4-dihydroxyphenyl)propanethioate;  
 Compound 6: S-propyl 3-(4-hydroxy-3-methoxyphenyl)propanethioate

**Table 1. Design strategy of curcuma- and garlic-derived compounds.**

To investigate the potential interplay of compounds 1–6 with the Nrf2 cellular pathway, we first evaluated their ability to modulate the expression of the Nrf2 transcription factor and its negative regulator Kelch-like ECH-associated protein 1 (Keap1), as well as its nuclear translocation and the activation of Nrf2 downstream target genes in human neuroblastoma SH-SY5Y cells, a cell line commonly used to perform preliminary molecules screening and to dissect the underlying molecular mechanism (Narasimhan *et al.*, 2012; Park *et al.*, 2014; de Oliveira *et al.*, 2019). In addition, a growing body of evidence demonstrated that several natural products, such as polyphenols, exert their protective effect through the induction of different epigenetic changes, including key modifications in microRNAs (miRNAs) expression (Howell *et al.*, 2013; Curti *et al.*, 2014; Boyanapalli and Kong, 2015; Liang and Xi, 2016; Curti *et al.*, 2017; Pandima Devi *et al.*, 2017). MiRNAs are small non-coding RNA molecules of ~22 nucleotides in length, which are endogenously expressed and play a key role in RNA-silencing and post-transcriptional regulation of gene expression. Indeed, those noncoding RNAs modulate gene expression by suppressing translation

and/or reducing the stability of their target mRNAs and consequently their target proteins. In fact, their binding to the target mRNAs, usually at the 3'-UTR, induces the recruitment of the RNA-induced silencing complex (RISC) that represses the translation of target mRNAs or enhances their cleavage (Bartel, 2004). MiRNAs can target in a combinatorial fashion a great variety of genes, which, in turn, indirectly modulate the expression of thousands of genes.

Recent studies revealed important roles of miRNAs in the control of Nrf2 activity. In addition, Nrf2 itself has been identified as a regulator of miRNAs, suggesting a loop system of mechanisms (Kurinna and Werner, 2015). In particular, miRNAs could directly target the Nrf2 mRNA and the mRNAs encoding for proteins that control the level and activity of Nrf2. As a transcription factor, Nrf2 can regulate not only the expression of protein coding parts of the genome, but also protein non-coding parts of the genome which, in turn, contains the majority of functional Nrf2-binding sites (Hirotsu *et al.*, 2012). In silico analysis by Papp and colleagues predicted 85 Nrf2-miRNA interactions, with 63 miRNAs able to directly or indirectly regulate Nrf2 (Papp *et al.*, 2012).

In line with these premises, the investigation of miRNA modulation could potentially be important in providing novel insights for a better understanding of the antioxidant activities of natural products and hybrids. Hence, we further investigated whether compounds are capable to exert epigenetic effects by modulating specific miRNAs associated with Nrf2 signaling pathway.

## MATERIAL AND METHODS

### Reagents

Compounds were synthesized according to previous procedures (Simoni *et al.*, 2016; Simoni *et al.*, 2017). Final compounds were >98% pure as determined by High Performance Liquid Chromatography (HPLC) analyses. The analyses were performed under reversed-phase conditions on a Phenomenex Jupiter C18 (150 × 4.6 mm I.D.) column, using a binary mixture of H<sub>2</sub>O/acetonitrile (60/40, v/v for 1, 2; 65/35, v/v for 3; 50/50, v/v for 4, 5, 6) as the mobile phase, UV detection at  $\lambda = 302$  nm (for 1, 2, 3) or 254 nm (for 4, 5, 6), and a flow rate of 0.7 ml/min. Analyses were performed on a liquid chromatograph model PU-1585 UV equipped with a 20 ml loop valve (Jasco Europe, Italy). CURC (CAS number 08511) and DMF (CAS number 242926) were  $\geq 98\%$  and  $\geq 97\%$  pure respectively, and were purchased by Sigma-Aldrich (Merck KGaA, Darmstadt, Germany). All compounds were solubilized in DMSO at stock concentrations of 10 mM, frozen ( $-20^{\circ}\text{C}$ ) in aliquots and

diluted in culture medium immediately prior to use. For each experimental setting, a stock aliquot was thawed and diluted to minimize repeated freeze and thaw damage. The final concentration of DMSO in culture medium was less than 0.1%. Cell culture media and all supplements were purchased from Sigma-Aldrich (Merck KGaA, Darmstadt, Germany). Rabbit polyclonal anti-human Nrf2 (NBP1-32822), mouse monoclonal anti-human NQO1 (NB200-209), and rabbit polyclonal anti-human HO-1 (NBP1-31341) antibodies were purchased from Novus (Biotechnne, Minneapolis, USA). Mouse monoclonal anti-human Keap1 antibody (MAB3024) was purchased from R&D Systems (Biotechnne, Minneapolis, USA). Mouse monoclonal anti-human  $\beta$ -actin (612656) and mouse anti-human lamin A/C (612162) antibodies were purchased from BD Biosciences (Franklin Lakes, NJ, USA). Finally, mouse anti-human  $\alpha$ -tubulin (sc-5286) and mouse anti-human GSS (sc-166882) antibodies were purchased from Santa Cruz Biotechnology (Dallas, Texas, USA).

### **SH-SY5Y Cell Cultures**

Human neuroblastoma SH-SY5Y cells from the European Collection of Cell Cultures (ECACC No. 94030304) were cultured in a medium with equal amounts of Eagle's minimum essential medium and Nutrient Mixture Ham's F-12, supplemented with 10% heat-inactivated fetal bovine serum (FBS), 2 mM glutamine, 0.1 mg/ml streptomycin, 100 IU·ml penicillin and non-essential amino acids at 37°C in 5% CO<sub>2</sub>-containing, and 95% air atmosphere. All culture media, supplements and FBS were purchased from Sigma-Aldrich (Merck KGaA, Darmstadt, Germany).

### **Cell Viability**

The mitochondrial dehydrogenase activity that reduces 3-(4,5-dimethylthiazol-2-yl)-2,5-diphenyl-tetrazolium bromide (MTT, Sigma-Aldrich, Merck KGaA, Darmstadt, Germany) was used to determine cell viability using a quantitative colorimetric assay (van Meerloo *et al.*, 2011; Kumar *et al.*, 2018). At day 0, SH-SY5Y cells were plated in 96-well plates at a density of  $2.5 \times 10^4$  viable cells per well, respectively. After treatment, according to the experimental setting, cells were exposed to an MTT solution (1 mg/ml) in complete medium. After 4 hours of incubation with MTT, we lysed cells with sodium dodecyl sulfate (SDS) for 24 hours and cell viability was quantified by reading absorbance at 570 nm wavelength, using a Synergy HT multi-detection micro-plate reader (Bio-Tek).

### **Subcellular Fractionation for Nrf2 Nuclear Translocation**

The expression of Nrf2 in nuclear SH-SY5Y cell lysates was assessed by Western blot analysis. Cell monolayers were washed twice with ice-cold PBS, harvested, and subsequently homogenized 20 times using a glass-glass homogenizer in ice-cold fractionation buffer (20 mM Tris/HCl pH 7.4, 2 mM EDTA, 0.5 mM EGTA, 0.32 M sucrose, 50 mM  $\beta$ -mercaptoethanol). The homogenate was centrifuged at 300g for 5 minutes to obtain the nuclear fraction. An aliquot of the nuclear extract was used for protein quantification by Bradford method, whereas the remaining was boiled at 95°C for 10 minutes after dilution with 2 $\times$  sample buffer (125 mM Tris-HCl pH 6.8, 4% SDS, 20% glycerol, 6%  $\beta$ -mercaptoethanol, 0.1% bromophenol blue). Equivalent amount of nuclear extracted proteins (30  $\mu$ g) were subjected to polyacrylamide gel electrophoresis and immunoblotting as described below.

### **Immunodetection of Nrf2, Keap1, NQO1, and HO-1**

The expression of Nrf2, Keap1, NQO1, and HO-1 in whole cell lysates or nuclear extracts was assessed by Western blot analysis. After treatment, cell monolayers were washed twice with ice-cold PBS, lysed on the culture dish by the addition of ice-cold homogenization buffer (50 mM Tris-HCl pH 7.5, 150 mM NaCl, 5 mM EDTA, 0.5% Triton X-100, and protease inhibitor mix). Samples were sonicated and centrifuged at 13,000g for 10 seconds at 4°C. The resulting supernatants were transferred into new tubes, and protein content was determined by Bradford method. For Western blot analysis, equivalent amounts of both total and nuclear extracts (30  $\mu$ g) were electrophoresed in 10% acrylamide gel, under reducing conditions, then, electroblotted into PVDF membranes (Merck KGaA, Darmstadt, Germany), blocked for 1 hour with 5% w/v bovine serum albumin (BSA) in TBS-T (0.1 M Tris-HCl, pH 7.4, 0.15 M NaCl, and 0.1% Tween 20), and incubated overnight at 4°C with primary antibodies diluted in 5% w/v BSA in TBS-T. The proteins were visualized using primary antibodies for Nrf2 (1:2,000), Keap1 (1:1,000), NQO1 (1:2,000), or HO-1 (1:2,000). Detection was carried out by incubation with secondary horseradish peroxidase-conjugated antibodies (1:5,000) diluted in 5% w/v BSA in TBS-T for 1 hour at room temperature. Membranes were subsequently washed three times with TBS-T and proteins of interest were visualized using an enhanced chemiluminescent reagent (Pierce, Rockford, IL, USA).  $\beta$ -Actin,  $\alpha$ -tubulin, and lamin A/C were performed as control for gel loading.

### **Real-Time PCR (RT-qPCR)**

Total RNA was extracted from SH-SY5Y cells by using a RNeasy Plus Mini Kit (Qiagen, Valencia, CA, USA) following the manufacturer's instructions. QuantiTect reversion transcription kit and QuantiTect SYBR Green PCR kit (Qiagen, Valencia, CA, USA) were used for cDNA synthesis and gene expression analysis, following the manufacturer's specifications. Nrf2, Keap1, NQO1, HO-1, GSS, and GAPDH primers (genome wide bioinformatically validated primers sets) were provided by Qiagen (QuantiTect Primer Assays; Qiagen, Valencia, CA, USA). GAPDH was used as an endogenous reference.

### **MicroRNA Analysis**

After the extraction procedure, the RNA quantification was assessed using a spectrophotometric method with FLUOstar® Omega (BMG LABTECH, Ortenberg, Germany) and the LVIS plate, following the operating manual instructions. RNA purity was assessed by calculating the 260/280 absorbance ratio. After quantification, a RTII Retrotranscription Kit (Qiagen) was used to promote the retrotranscription of exclusively mature miRNA following the manufacturer's instructions. The cDNA was diluted with RNase-free water prior to start the RT-qPCR procedure. To verify the expression of miRNA targets, a miScript® miRNA PCR Array (Qiagen) was used, following the manufacturer's instructions. We performed the RT-qPCR using StepOnePlus RT-qPCR (Applied Biosystem, Foster City, California, USA). The primers were purchased from Qiagen, with specific forward primers contained in the miScript® miRNA PCR Array and with reverse primers contained in the in miScript SYBR® Green PCR Array. For each plate the amplification conditions were set as follows: 95°C for 15 minutes, 94°C for 15 seconds, 55°C for 30 seconds, and 70°C for 30 seconds. The last three steps were repeated for 45 cycles. SNORD61 and RNU6-6P were used as endogenous controls.

### **Densitometry and Statistics**

All experiments were performed at least three times. Data are expressed as mean  $\pm$  SEM. The acquisition of the Western blotting images was done through a scanner and the relative densities of the bands were analyzed with ImageJ software. Statistical analyses were performed using GraphPad Software version 7.0 (La Jolla, CA, USA). Statistical differences were determined by analysis of variance (ANOVA) followed, when significant, by an appropriate post hoc test as indicated in figure legends. For miRNA expression, we used linear mixed models, including treatments as fixed terms and plates as random effects, which allowed for different intercepts for each run. In miRNA figures, the points indicate

the mean value while the bars represent the SEM. In all reported statistical analyses, effects were designated as significant with a p-value < 0.05. Statistical analyses were performed using R software version 3.4.1 (R Core Team, 2018).

## RESULTS

### Cellular Toxicity of Curcuma- and Garlic- Derived Compounds

The cytotoxicity of compounds 1–6 has been assessed by MTT assay in SH-SY5Y human neuroblastoma cells, in comparison with CURC and DMF. Cells were exposed to the compounds and CURC at concentrations ranging from 1 to 12.5  $\mu\text{M}$  for 24 hours. The concentrations for DMF were chosen basing on literature data (Brennan *et al.*, 2015; Campolo *et al.*, 2018) and a range of concentrations starting from 1  $\mu\text{M}$  to 50  $\mu\text{M}$  has been analyzed.

As shown in **Figure 1**, all the compounds were well tolerated (reduction of cell viability of about 10%) at a concentration up to 5  $\mu\text{M}$ , with the exception of the prototype 1, that at 5  $\mu\text{M}$  induced a slight decrease (about 20%) in cell viability, consistent with our previous data (Simoni *et al.*, 2017).

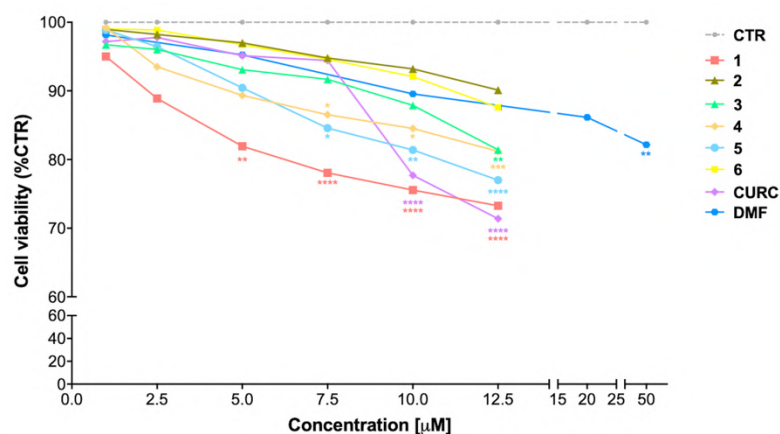


**Figure 1.** Cellular toxicity of hybrid compounds (1–6), curcumin (CURC), and dimethyl fumarate (DMF) on human neuroblastoma SH-SY5Y. Cells were treated with compounds 1–6 and CURC for 24 hours at different concentrations ranging from 1 to 12.5  $\mu\text{M}$ . DMF was used in a range of concentrations starting from 0.5  $\mu\text{M}$  till to 50  $\mu\text{M}$ . Cell viability was assessed by MTT assay. Data are expressed as percentage of cell viability *versus* CTR; \* $p$  < 0.05, \*\* $p$  < 0.01 and \*\*\*\* $p$  < 0.0001 *versus* CTR; Dunnett's multiple comparison test ( $n \geq 5$ ).

### Modulation of Nrf2 and Its Negative Regulator Keap1

To understand the molecular mechanisms underlying the antioxidant activity of compounds 1–6, we decided to investigate the Nrf2 pathway, which plays a key role in orchestrating cellular antioxidant defenses and in maintaining cellular redox homeostasis. To analyze the modulation of the Nrf2-mediated detoxification pathway, we performed RT-qPCR and Western immunoblotting in SH-SY5Y human neuroblastoma cells exposed to compounds 1–6 and CURC at the concentration of 5  $\mu$ M or to DMF at the concentration of 20  $\mu$ M for 24 hours (**Figure 2**). All compounds tested did not affect the mRNA levels of Nrf2 (**Figure 2A**) and Keap1 (**Figure 2B**), neither Keap1 protein amount (**Figure 2D**). In contrast, a strong increase in Nrf2 protein expression (**Figure 2C**) is induced by all compounds, with the exception of compound 6. DMF treatment did not produce statistically significant results in our experimental setting, although an increase trend could be assumed. Altogether, these results show that all compounds tested, with the exception of compound 6, modulate Nrf2 protein levels, but do not act at the transcriptional level.

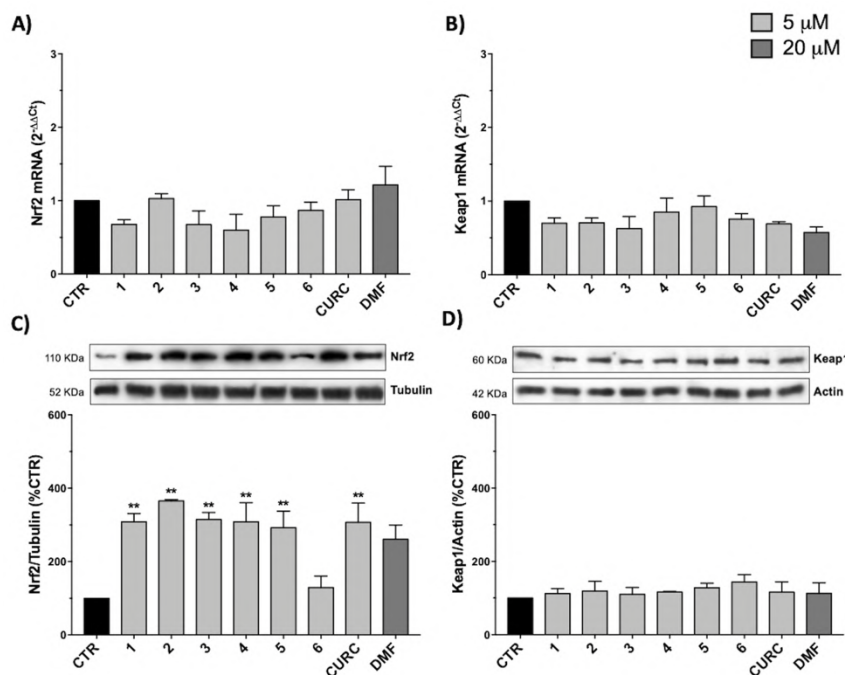


**Figure 2.** Modulation of Nrf2 and Keap1 mRNA and protein levels by compounds 1–6, curcumin (CURC), and dimethyl fumarate (DMF). (A–B) RNA from total cellular extracts of SH-SY5Y cells treated for 24 hours with 5  $\mu$ M compounds or 20  $\mu$ M DMF were analyzed for Nrf2 (A) and Keap1 (B) mRNA



expression by RTqPCR. GAPDH was used as housekeeping gene. Results are shown as mean  $\pm$  SEM; no statistically significant data with Dunnett's multiple comparison test (A, n = 3, F ratio = 1.249; B, n = 3, F ratio = 1.671). **(C–D)** Cellular extracts of SH-SY5Y cells treated for 24 hours with compounds at 5  $\mu$ M or 20  $\mu$ M DMF were analyzed for Nrf2 **(C)** and Keap1 **(D)** protein levels by Western blot. Anti-tubulin was used as protein loading control. Results are shown as ratio (% of CTR)  $\pm$  SEM; \*\* $p$  < 0.01, *versus* CTR; Dunnett's multiple comparison test (C, n  $\geq$  5, F ratio = 3.981; D, n = 3, F ratio = 0.4049).

### Nuclear Translocation of the Nrf2 Transcription Factor

Since Nrf2 nuclear translocation is an essential step for the complete activation of its pathway, we further examined the ability of the hybrids to induce the nuclear localization of Nrf2 in SH-SY5Y, by comparing their effects with CURC and DMF.

Data from literature suggest that a pro-electrophilic moiety (catechol) and/or an electrophilic moiety (the Michael acceptor  $\alpha,\beta$ -unsaturated carbonyl group) are important structural functions for Nrf2 induction (Tanigawa *et al.*, 2007; Satoh *et al.*, 2013). The tested compounds were selected to delineate the structural requirements responsible for the activation of the transcription factor and its downstream signaling pathway. The six hybrids investigated in this study differ from each other by the presence or absence of the mentioned key functional groups (**Table 1**). Indeed, the compounds 1 and 3 provide the catechol moiety as well as the Michael acceptor group. The compounds 4 and 5 lack the Michael acceptor function but have the catechol moiety, whereas 2 shows only the Michael acceptor. The compound 6 was chosen as negative control, lacking for both Michael acceptor and catechol function. Moreover, the effects of CURC and DMF as positive controls have also been investigated.

SH-SY5Y cells were treated with the compounds at different concentrations: 5  $\mu$ M, 500 nM, and 50 nM of 1–6 and CURC or 20  $\mu$ M, 10  $\mu$ M, and 5  $\mu$ M of DMF. As indicated in **Figure 3A**, all tested hybrids, except 6, lacking for both electrophilic features, are capable to significantly induce Nrf2 nuclear translocation at their highest concentration. This result indicates that Nrf2 nuclear translocation may rely on the presence of both the  $\alpha,\beta$ -unsaturated carbonyl function and the catechol group, either alone or in combination, thus suggesting that nucleophilic addition of Keap1 cysteine residues to (pro)- electrophilic portions of the molecule might activate the Nrf2 pathway. Moreover, 1 and 5 significantly induce Nrf2 nuclear localization at the intermediate concentration of 500 nM, whereas 1 also at a concentration of 50 nM. None of the molecules, with the exception of 1, were found to act on the Nrf2 pathway at the lowest concentrations investigated (i.e., 50 nM).

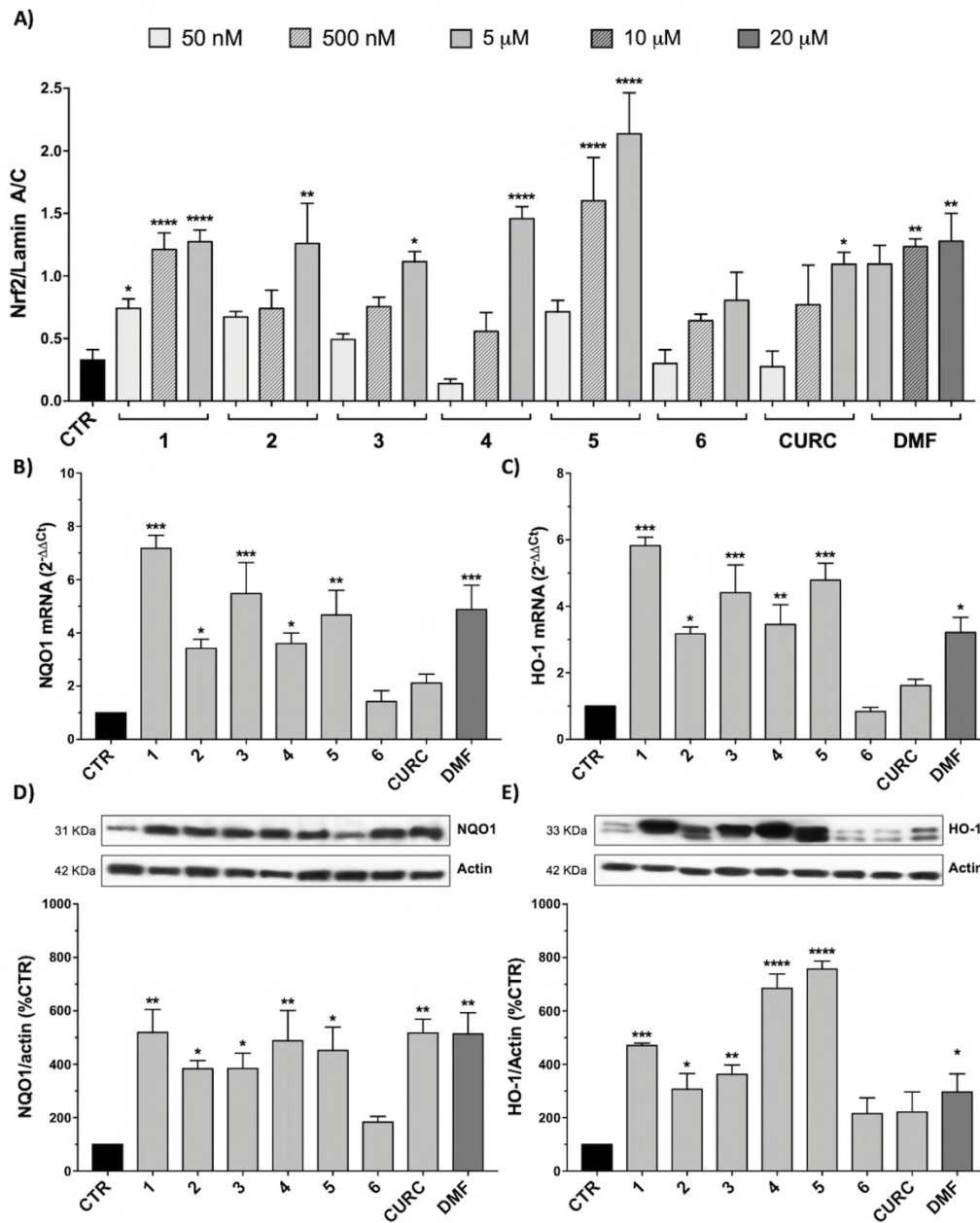


**Figure 3. Nrf2-pathway activation by hybrids: nuclear translocation and targets induction.** (A) Nuclear cellular extracts of SH-SY5Y cells were treated for 3 hours with compounds at 5  $\mu$ M, 500 nM, and 50 nM or with 20, 10, and 5  $\mu$ M dimethyl fumarate (DMF). Nrf2 protein content in the nucleus was determined by Western blot. Anti-lamin A/C was used as a protein loading control. Results are shown as ratio Nrf2/lamin

A/C  $\pm$  SEM; \* $p$  < 0.05, \*\* $p$  < 0.01 and \*\*\*\* $p$  < 0.0001 *versus* CTR; Dunnett's multiple comparison test (F ratio = 6.797,  $n \geq 3$ ). **(B–C)** RNA from total cellular extracts of SH-SY5Y cells, treated for 24 hours with 5  $\mu$ M compounds or 20  $\mu$ M DMF, were analyzed for NQO1 **(B)** and HO-1 **(C)** mRNA expression by RT-qPCR. GAPDH was used as housekeeping gene. Results are shown as mean  $\pm$  SEM; \* $p$  < 0.05, \*\* $p$  < 0.01, and \*\*\* $p$  < 0.001 *versus* CTR; Dunnett's multiple comparison test (B,  $n \geq 3$ , F ratio = 10.44; C,  $n \geq 3$ , F ratio = 13.95). **(D–E)** Cellular extracts of SH-SY5Y cells treated for 24 hours with compounds at 5  $\mu$ M or 20  $\mu$ M DMF were analyzed for NQO1 **(D)** and HO-1 **(E)** protein levels by Western blot. Anti-actin was used as protein loading control. Results are shown as ratio (% of CTR)  $\pm$  SEM; \* $p$  < 0.05, \*\* $p$  < 0.01, \*\*\* $p$  < 0.001, and \*\*\*\* $p$  < 0.0001 *versus* CTR; Dunnett's multiple comparison test (D,  $n \geq 3$ , F ratio = 5.144; E,  $n \geq 3$ , F ratio = 17.26).

### Activation of the Nrf2 Target Genes

To demonstrate the complete activation of Nrf2 pathway by the synthesized hybrids, the expression of two Nrf2 target genes has also been evaluated. Indeed, once in the nucleus, Nrf2 binds to the ARE sequences in the promoter region of its target genes, inducing the expression of phase II cyto-protective genes related to cellular stress response, such as those codifying for NQO1 and HO-1. The mRNA expression and protein levels of these two genes were evaluated by RT-qPCR and Western blot in SH-SY5Y, treated with compounds 1–6 and CURC at the concentration of 5  $\mu$ M and with 20  $\mu$ M DMF for 24 hours. As shown in **Figure 3**, all compounds, with the exception of 6 and CURC, induced an increase in NQO1 mRNA levels (**Figure 3B**), followed by an increase in NQO1 protein with the exception of 6 (**Figure 3D**). In a similar way, the mRNA (**Figure 3C**) and protein (**Figure 3E**) levels of HO-1 are positively modulated by all hybrids except 6, and CURC. The increase in transcription and translation of two Nrf2 target genes demonstrates the complete activation of the Nrf2 pathway.

To explain the discrepancy between the obtained data showing the loss of efficacy of CURC on Nrf2 target gene activation, we further evaluated whether such result may rely on the timing of the treatment. Thus, we performed a time course using CURC and compound 1, as an example of the most active hybrid compound. SH-SY5Y cells were treated with compound 1 or CURC at the concentration of 5  $\mu$ M for 3, 6, 9, 16, and 24 hours. NQO1 (**Figures 4A, B**) and HO-1 (**Figures 4C, D**) mRNAs levels were differently regulated in time, with NQO1 slowly increasing and HO-1 being boosted for 3 hours and, then, decreasing with time. Treatment with compound 1 induced a significant increase in relative NQO1 mRNA levels from 6 hours to 16 hours (**Figure 4A**), whereas CURC treatment induced an increase at 6 hours, which reached a peak at 9 hours and then lost statistical significance by 16 hours (**Figure 4B**). Treatment with compound 1 induced a strong increase in HO-1 mRNA levels, already statistically significant at 3 hours, then decreasing with time (**Figure 4C**). Here, the effect of curcumin was similar to that induced

by hybrid 1, though the increase in the HO-1 mRNA levels was smaller (**Figure 4C**). Taken together, these data demonstrate that CURC induces a significant increase in NQO1 and HO-1 mRNA and protein levels at different times of treatment compared to compound 1. These results suggest that compounds may affect the Nrf2 pathway through different temporal kinetics.

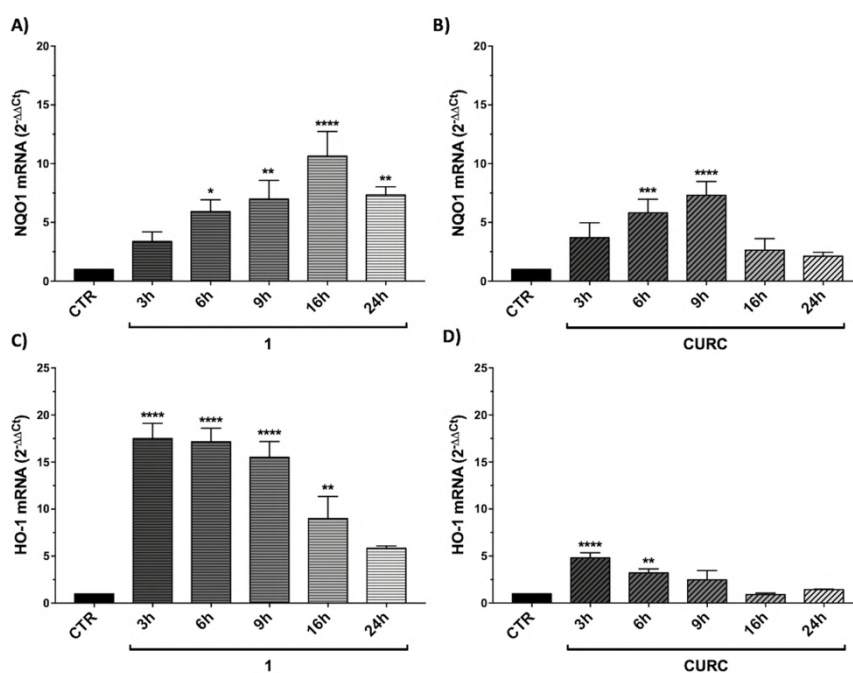


**Figure 4. Time-dependent modulation of Nrf2 targets by compound 1 and curcumin.** RNA from total cellular extracts of SH-SY5Y cells, treated for 3, 6, 9, 16, and 24 hours with 5 μM compounds 1 and curcumin (CURC), were analyzed for NQO1 (**A-B**) or HO-1 (**C-D**) relative mRNA expression by RT-qPCR. GAPDH was used as housekeeping gene. Results are shown as mean ± SEM; \**p* < 0.05, \*\**p* < 0.01, \*\*\**p* < 0.001, and \*\*\*\**p* < 0.0001 *versus* CTR; Dunnett's multiple comparison test (A, *n* ≥ 3, *F* ratio = 9.346; B, *n* ≥ 3, *F* ratio = 10.44; C, *n* ≥ 3, *F* ratio = 18.02; D, *n* ≥ 3, *F* ratio = 13.87).

### Modulation of miRNAs Related to the Nrf2 Signaling Pathway

To deepen the understanding of the mechanism through which the selected hybrids exert their antioxidant activities, in comparison to CURC, we determined the expression levels of different miRNAs in SH-SY5Y cell cultures. MiRNAs were chosen on the basis of their predicted targets with the aid of miRTarBase (<http://miRTarBase.mbc.nctu.edu.tw/>) an open access database which provides information about experimentally validated miRNA-

target interactions (Chou *et al.*, 2018). One single miRNA could have multiple targets, thus we focused our attention on miRNAs, which could modulate the mRNA, and consequently the protein amount, of genes involved in the Nrf2 signaling pathway, such as those codifying for HO-1 (hsa-miR-196a-5p), GSS (hsa-miR-125b-5p), and SOD2 (hsa-miR-222-3p, hsa-miR-17-3p).

SH-SY5Y human neuroblastoma cells were treated with compounds 1–6 and CURC at different concentrations (5  $\mu$ M, 500 nM, and 50 nM) for 24 hours. Total RNA was extracted from treated and control cell cultures, as according to the Material and Methods section, and RT-qPCR assays were performed.

Among all the miRNAs analyzed, only hsa-miR-125b-5p results to be modulated with a statistically significant p-value. Data from literature indicate that hsa-miR-125b-5p is involved in oxidative stress, since it has mRNA coding for GSS as target (Chou *et al.*, 2016). As far as hsa-miR-125b-5p is concerned, the results obtained following statistical analysis suggest that the expression level of this miRNA is downregulated after treatment with CURC at all concentrations (**Figure 5**). In addition, significant differences in miRNA expression levels were registered between the control and the following treatments: 5  $\mu$ M and 500 nM of 2, 5  $\mu$ M of 3, 50 nM of 4, 50 nM and 500 nM of 5, and 50 nM and 500 nM of 6. The decrease in miR-125b-5p after treatment with compounds 2–6 and CURC at different concentrations confirms that they have the capacity to modulate miRNAs involved in protection against oxidative stress. Nevertheless, the compounds tested did not significantly modulate the expression of mRNA coding for GSS, even if CURC at all concentrations shows an increased trend in line with the reduction of miR-125b-5p (**Table 2**). These data suggest that the process of GSS synthesis is regulated by other molecular mechanisms and the modulation of this mRNA is not strictly under the control of miR-125b-5p.

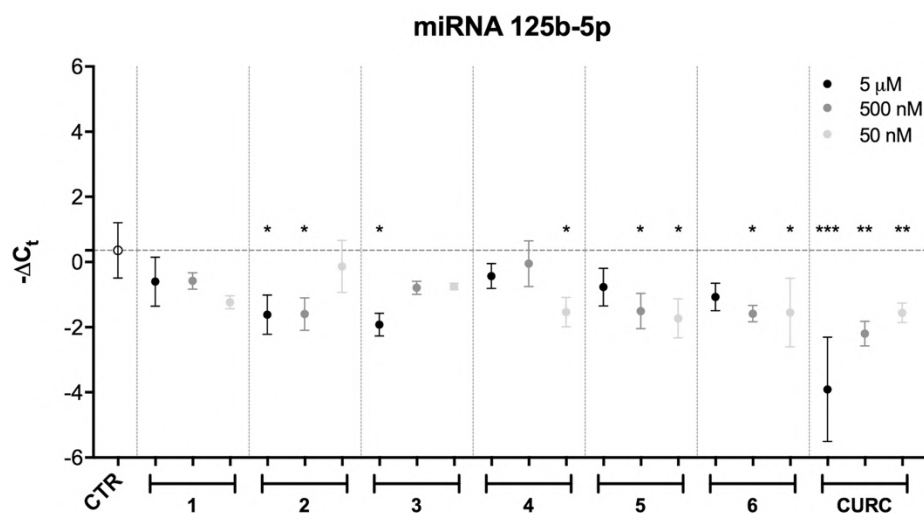


**Figure 5. miRNA modulation by hybrids and curcumin.** Expression levels (-Delta Ct) of hsa-miR-125b-5p in SH-SY5Y cells treated with different newly synthesized compounds at different concentrations (50 and 500 nM). Results are shown as mean  $\pm$  SEM; \* $p$  < 0.05, \*\* $p$  < 0.01, and \*\*\* $p$  < 0.001 *versus* CTR; Dunnett's multiple comparison test ( $n = 3$ , F ratio = 4.584).

Compound	GSS mRNA ( $2^{-\Delta\Delta Ct}$ )		
	Concentration		
	5 $\mu$ M	500 nM	50 nM
1	0.83 $\pm$ 0.25	1.16 $\pm$ 0.12	0.61 $\pm$ 0.10
2	1.07 $\pm$ 0.14	1.04 $\pm$ 0.35	1.14 $\pm$ 0.05
3	1.17 $\pm$ 0.03	0.96 $\pm$ 0.02	1.08 $\pm$ 0.24
4	1.25 $\pm$ 0.22	1.31 $\pm$ 0.25	1.10 $\pm$ 0.10
5	1.42 $\pm$ 0.29	0.97 $\pm$ 0.25	1.90 $\pm$ 0.44
6	1.18 $\pm$ 0.21	1.22 $\pm$ 0.42	1.19 $\pm$ 0.23
<b>CURC</b>	1.81 $\pm$ 0.25	1.93 $\pm$ 0.45	2.24 $\pm$ 0.61

**Table 2. GSS mRNA levels modulation.** RNA from total cellular extracts of SHSY5Y cells treated for 24 hours at different concentrations (50, 500 nM, and 5  $\mu$ M) of compounds were analyzed for GSS mRNA expression by RT-qPCR. GAPDH was used as housekeeping gene. Results are shown as mean  $\pm$  SEM.

## DISCUSSION

Nrf2 is a redox-sensitive transcription factor that has been described to play a critical role in adaptation to cellular stress and affords cellular defense by initiating transcription of antioxidant phase II and detoxification genes (Tebay *et al.*, 2015). The hybrids here tested have been demonstrated to modulate in an *in vitro* model the activation of Nrf2-pathway and the ARE-controlled expression of its target genes codifying cyto-protective enzymes (i.e., NQO1 and HO-1).

The mechanism at the basis of the effects exerted by the compounds has been shown not to be related to the modulation in the transcription levels of Nrf2 and Keap1 (**Figures 2A, B**), as well as in the protein levels of Keap1 (**Figure 2D**), thus suggesting that in our experimental setting the increase in Nrf2 (**Figure 2C**) protein expression is not due to a decreased transcription or translation of the negative regulator Keap1. We hypothesize that compounds may directly interact with Keap1, preventing its binding to Nrf2 and, consequently, the ubiquitination process, by possibly modifying the sulfhydryl groups of cysteine residues on Keap1 and inhibiting Keap1-Nrf2 protein-protein interaction.

Subsequently, free Nrf2 in the cytoplasm could escape proteasome-targeted degradation and migrate into the nucleus to carry out its activities as a transcription factor. A proof of the hypothesis of an electrophile-based modulation of the Nrf2- pathway [consistently with what reviewed by (Basagni *et al.*, 2019)] is the lack of efficacy in activating Nrf2 observed for compound 6, which, lacking a (pro)electrophile feature is not able to engage covalent bond with cysteine residues of Keap-1 (**Figure 3**). Combining virtual screening/molecular docking with focused exploration of structure-activity relationships (SAR) of our compounds could significantly contribute to investigate the mode of action of the hybrid compounds at a molecular level, opening prospects for further investigation. Beyond the activation of the Nrf2 pathway in a Keap1-dependent manner, data from literature further indicate that polyphenols, such as CURC, and DMF are capable to activate Nrf2 by other pathways or alternative mechanisms, including glutathione (GSH) depletion (Schmidt *et al.*, 2007; Satoh *et al.*, 2013; Brennan *et al.*, 2015). GSH is known to play an important role in cellular defense against various stressors and its depletion has been also suggested to be protective against inflammation and neurodegeneration (Ewing and Maines, 1993; Aschner, 2000). Electrophiles such as curcumin and DMF have been found to induce severe side effects, due to their non-specific interaction with cysteine thiols of GSH, consequently reducing GSH levels (Satoh *et al.*, 2013; Brennan *et al.*, 2015). In our hand, we found that, unlike CURC, the curcuma- and garlic- inspired compounds seem not to affect the expression of GSS (**Table 2**), thus suggesting a lack of modulation in glutathione levels. This hypothesis is also supported by the results that only CURC at all the concentrations tested induces epigenetic changes through modifications in miR-125b-5p expression

(**Figure 5**), in turn modulating the expression levels of mRNA coding for glutathione synthetase. Taking into account that electrophiles have complex time- and dose-dependent relationships with cellular GSH (Jobbagy *et al.*, 2019), whether this different effect on the regulation of glutathione levels is specific only for CURC and not for our hybrids requires further investigation.

In conclusion, we have characterized, by using *in vitro* techniques, a pathway by our hybrids, which emerge as promising pharmacological tools. However, we are conscious that to translate these positive outcomes in a potential therapeutic benefit, the obtained results require to be validated in *in vivo* models. Indeed, also curcumin, whose antioxidant properties are well recognized by a plethora of publications (Darvesh *et al.*, 2012; Shen *et al.*, 2013; Vera-Ramirez *et al.*, 2013; Nabavi *et al.*, 2015b; Serafini *et al.*, 2017; Catanzaro *et al.*, 2018), to date does not show confirmed applications in humans due to the failure of clinical trials. Some considerations can be made on this point. A direct antioxidant effect *in vivo* may be limited by several factors, such as bioavailability, metabolic reactions, and modification of intracellular concentrations (Crespo *et al.*, 2015). Furthermore, recent data highlight attention when referring to the use of antioxidants for supplement practice. Not only positive effects, but also negative outcomes have been observed when analyzing large numbers of studies (Visioli, 2015). As an example, the use of antioxidant mixtures (a combination of vitamins A, C, E, beta-carotene, selenium, and zinc) in the cardiovascular disease prevention has been found in several studies not to show benefits, but to result in an increase in all-cause mortality (Jenkins *et al.*, 2018). Hence, a careful evaluation also concerning the lifestyle or other dietary factors adopted by supplement users requires multiple assessments over time.

Based on these considerations, we believe that the results here exposed evaluating the activity of hybrids 1–6 in *in vitro* studies, are promising. However, whether these profiles might result in better translational outcomes require further *in vivo* investigations to verify bioavailability issues and to test their potential in pathological models characterized by deficit in the redox system.

## REFERENCES

- Aschner, M. (2000). Neuron-astrocyte interactions: implications for cellular energetics and antioxidant levels. *Neurotoxicology* 21, 1101–1107.
- Auclair, S., Milenkovic, D., Besson, C., Chauvet, S., Gueux, E., Morand, C., *et al.* (2009). Catechin reduces atherosclerotic lesion development in apo E-deficient mice: a transcriptomic study. *Atherosclerosis* 204 (2), e21–e27. doi: 10.1016/j.atherosclerosis.2008.12.007



- Baird, L., and Dinkova-Kostova, A. T. (2011). The cytoprotective role of the Keap1–Nrf2 pathway. *Arch. Toxicol.* 85, 241–272. doi: 10.1007/s00204-011-0674-5
- Bartel, D. P. (2004). MicroRNAs: genomics, biogenesis, mechanism, and function. *Cell* 116 (2), 281–297. doi: 10.1016/s0092-8674(04)00045-5
- Basagni, F., Lanni, C., Minarini, A., and Rosini, M. (2019). Lights and shadows of electrophile signaling: focus on the Nrf2-Keap1 pathway. *Future Med. Chem.* 11, 707–721. doi: 10.4155/fmc-2018-0423
- Boyanapalli, S. S. S., and Kong, A. N. T. (2015). “Curcumin, the King of Spices”: epigenetic regulatory mechanisms in the prevention of cancer, neurological, and inflammatory diseases. *Curr. Pharmacol. Rep.* 1, 129–139. doi: 10.1007/s40495-015-0018-x
- Brennan, M. S., Matos, M. F., Li, B., Hronowski, X., Gao, B., Juhasz, P., *et al.* (2015). Dimethyl fumarate and monoethyl fumarate exhibit differential effects on KEAP1, NRF2 activation, and glutathione depletion In Vitro. *PLoS One* 10, e0120254. doi: 10.1371/journal.pone.0120254
- Camargo, A., Ruano, J., Fernandez, J. M., Parnell, L. D., Jimenez, A., Santos-Gonzalez, M., *et al.* (2010). Gene expression changes in mononuclear cells in patients with metabolic syndrome after acute intake of phenol-rich virgin olive oil. *BMC Genomics* 11, 253. doi: 10.1186/1471-2164-11-253
- Campolo, M., Casili, G., Lanza, M., Filippone, A., Paterniti, I., Cuzzocrea, S., *et al.* (2018). Multiple mechanisms of dimethyl fumarate in amyloid b-induced neurotoxicity in human neuronal cells. *J. Cell Mol. Med.* 22 (2), 1081–1094. doi: 10.1111/jcmm.13358
- Catanzaro, M., Corsini, E., Rosini, M., Racchi, M., and Lanni, C. (2018). Immunomodulators inspired by nature: a review on curcumin and echinacea. *Mol. Basel Switz.* 23 (11), 2778. doi: 10.3390/molecules23112778
- Chou, C.-H., Chang, N.-W., Shrestha, S., Hsu, S.-D., Lin, Y.-L., Lee, W.-H., *et al.* (2016). miRTarBase 2016: updates to the experimentally validated miRNA-target interactions database. *Nucleic Acids Res.* 44, D239–D247. doi: 10.1093/nar/gkv1258
- Chou, C. H., Shrestha, S., Yang, C. D., Chang, N. W., Lin, Y. L., Liao, K. W., *et al.* (2018). miRTarBase update 2018: a resource for experimentally validated microRNA-target interactions. *Nucleic Acids Res.* 46 (D1), D296–D302. doi: 10.1093/nar/gkx1067
- Crespo, M. C., Tomé-Carneiro, J., Burgos-Ramos, E., Loria Kohen, V., Espinosa, M. I., Herranz, J., *et al.* (2015). One-week administration of hydroxytyrosol to humans does not activate Phase II enzymes. *Pharmacol. Res.* 95–96, 132–137. doi: 10.1016/j.phrs.2015.03.018
- Curti, V., Capelli, E., Boschi, F., Nabavi, S. F., Bongiorno, A. I., Habtemariam, S., *et al.* (2014). Modulation of human miR-17-3p expression by methyl 3-O-methyl gallate as explanation of its in vivo protective activities. *Mol. Nutr. Food Res.* 58, 1776–1784. doi: 10.1002/mnfr.201400007
- Curti, V., Di Lorenzo, A., Rossi, D., Martino, E., Capelli, E., Collina, S., *et al.* (2017). Enantioselective modulatory effects of naringenin enantiomers on the expression levels of miR-17-3p involved in endogenous antioxidant defenses. *Nutrients* 9, 215. doi: 10.3390/nu9030215

Darvesh, A. S., Carroll, R. T., Bishayee, A., Novotny, N. A., Geldenhuys, W. J., and Van der Schyf, C. J. (2012). Curcumin and neurodegenerative diseases: a perspective. *Expert Opin. Investig. Drugs* 21, 1123–1140. doi: 10.1517/13543784.2012.693479

de Oliveira, M. R., Custódio de Souza, I. C., and Fürstenau, C. R. (2019). Promotion of mitochondrial protection by naringenin in methylglyoxal-treated SH-SY5Y cells: involvement of the Nrf2/GSH axis. *Chem. Biol. Interact.* 310, 108728. doi: 10.1016/j.cbi.2019.108728

Ewing, J. F., and Maines, M. D. (1993). Glutathione depletion induces heme oxygenase-1 (HSP32) mRNA and protein in rat brain. *J. Neurochem.* 60, 1512–1519. doi: 10.1111/j.1471-4159.1993.tb03315.x

Hirotsu, Y., Katsuoka, F., Funayama, R., Nagashima, T., Nishida, Y., Nakayama, K., *et al.* (2012). Nrf2-MafG heterodimers contribute globally to antioxidant and metabolic networks. *Nucleic Acids Res.* 40 (20), 10228–10239. doi: 10.1093/nar/gks827

Ho, C.-Y., Cheng, Y.-T., Chau, C.-F., and Yen, G.-C. (2012). Effect of diallyl sulfide on in vitro and in vivo Nrf2-mediated pulmonary antioxidant enzyme expression via Activation ERK/p38 Signaling Pathway. *J. Agric. Food Chem.* 60, 100–107. doi: 10.1021/jf203800d

Howell, J. C., Chun, E., Farrell, A. N., Hur, E. Y., Caroti, C. M., Iuvone, P. M., *et al.* (2013). Global microRNA expression profiling: curcumin (diferuloylmethane) alters oxidative stress-responsive microRNAs in human ARPE-19 cells. *Mol. Vis.* 19, 544–560.

Jenkins, D. J. A., Spence, J. D., Giovannucci, E. L., Kim, Y.-I., Josse, R., Vieth, R., *et al.* (2018). Supplemental vitamins and minerals for CVD prevention and treatment. *J. Am. Coll. Cardiol.* 71, 2570–2584. doi: 10.1016/j.jacc.2018.04.020

Jobby, S., Vitturi, D. A., Salvatore, S. R., Turell, L., Pires, M. F., Kansanen, E., *et al.* (2019). Electrophiles modulate glutathione reductase activity via alkylation and upregulation of glutathione biosynthesis. *Redox Biol.* 21, 101050. doi: 10.1016/j.redox.2018.11.008

Kumar, P., Nagarajan, A., and Uchil, P. D. (2018). Analysis of cell viability by the MTT assay. *Cold Spring Harb. Protoc.* 2018 (6). doi: 10.1101/pdb.prot095505

Kurinna, S., and Werner, S. (2015). NRF2 and microRNAs: new but awaited relations. *Biochem. Soc. Trans.* 43 (4), 595–601. doi: 10.1042/BST20140317

Liang, Z., and Xi, Y. (2016). MicroRNAs mediate therapeutic and preventive effects of natural agents in breast cancer. *Chin. J. Nat. Med.* 14, 881–887. doi: 10.1016/S1875-5364(17)30012-2

Malhotra, D., Portales-Casamar, E., Singh, A., Srivastava, S., Arenillas, D., Happel, C., *et al.* (2010). Global mapping of binding sites for Nrf2 identifies novel targets in cell survival response through ChIP-Seq profiling and network analysis. *Nucleic Acids Res.* 38 (17), 5718–5734. doi: 10.1093/nar/gkq212

Martínez-Huélamo, M., Rodríguez-Morató, J., Boronat, A., and De La Torre, R. (2017). Modulation of Nrf2 by flive oil and wine polyphenols and neuroprotection. *Antioxidants (Basel)* 6 (4), E73. doi: 10.3390/antiox6040073

- Nabavi, S. F., Tenore, G. C., Daglia, M., Tundis, R., Loizzo, M. R., and Nabavi, S. M. (2015a). The cellular protective effects of rosmarinic acid: from bench to bedside. *Curr. Neurovasc. Res.* 12, 98–105. doi: 10.2174/1567202612666150109113638
- Nabavi, S. F., Thiagarajan, R., Rastrelli, L., Daglia, M., Sobarzo-Sánchez, E., Alinezhad, H., *et al.* (2015b). Curcumin: a natural product for diabetes and its complications. *Curr. Top. Med. Chem.* 15, 2445–2455. doi: 10.2174/1568026615666150619142519
- Narasimhan, M., Patel, D., Vedpathak, D., Rathinam, M., Henderson, G., and Mahimainathan, L. (2012). Identification of novel microRNAs in post-transcriptional control of Nrf2 expression and redox homeostasis in neuronal, SH-SY5Y cells. *PloS One* 7, e51111. doi: 10.1371/journal.pone.0051111
- Niture, S. K., Khatri, R., and Jaiswal, A. K. (2014). Regulation of Nrf2—an update. *Free Radic. Biol. Med.* 66, 36–44. doi: 10.1016/j.freeradbiomed.2013.02.008
- Pandima Devi, K., Rajavel, T., Daglia, M., Nabavi, S. F., Bishayee, A., and Nabavi, S. M. (2017). Targeting miRNAs by polyphenols: novel therapeutic strategy for cancer. *Semin. Cancer Biol.* 46, 146–157. doi: 10.1016/j.semcancer.2017.02.001
- Papp, D., Lenti, K., Módos, D., Fazekas, D., Dúl, Z., Túrei, D., *et al.* (2012). The NRF2-related interactome and regulome contain multifunctional proteins and fine-tuned autoregulatory loops. *FEBS Lett.* 586 (13), 1795–1802. doi: 10.1016/j.febslet.2012.05.016
- Park, S. Y., Kim, D. Y., Kang, J.-K., Park, G., and Choi, Y.-W. (2014). Involvement of activation of the Nrf2/ARE pathway in protection against 6-OHDA-induced SH-SY5Y cell death by a-iso-cubebenol. *Neurotoxicology* 44, 160–168. doi: 10.1016/j.neuro.2014.06.011
- Paunkov, A., Chartoumpakis, D. V., Ziros, P. G., and Sykiotis, G. P. (2019). A Bibliometric Review of the Keap1/Nrf2 Pathway and its Related Antioxidant Compounds. *Antioxidants* 8 (9), E353. doi: 10.3390/antiox8090353
- R Core Team (2018). R: A Language and Environment for Statistical Computing. R Foundation for Statistical Computing (Vienna).
- Saidu, N. E. B., Kaviani, N., Leroy, K., Jacob, C., Nicco, C., Batteux, F., *et al.* (2019). Dimethyl fumarate, a two-edged drug: current status and future directions. *Med. Res. Rev.* 39 (5), 1923–1952. doi: 10.1002/med.21567
- Satoh, T., McKercher, S. R., and Lipton, S. A. (2013). Nrf2/ARE-mediated antioxidant actions of pro-electrophilic drugs. *Free Radic. Biol. Med.* 65, 645–657. doi: 10.1016/j.freeradbiomed.2013.07.022
- Scapagnini, G., Sonya, V., Abraham, N. G., Calogero, C., Zella, D., and Fabio, G. (2011). Modulation of Nrf2/ARE pathway by food polyphenols: a nutritional neuroprotective strategy for cognitive and neurodegenerative disorders. *Mol. Neurobiol.* 44, 192–201. doi: 10.1007/s12035-011-8181-5
- Schmidt, T. J., Ak, M., and Mrowietz, U. (2007). Reactivity of dimethyl fumarate and methylhydrogen fumarate towards glutathione and N-acetyl-L-cysteine—preparation of S-substituted thiosuccinic acid esters. *Bioorg. Med. Chem.* 15, 333–342. doi: 10.1016/j.bmc.2006.09.053

- Serafini, M. M., Catanzaro, M., Rosini, M., Racchi, M., and Lanni, C. (2017). Curcumin in Alzheimer's disease: Can we think to new strategies and perspectives for this molecule? *Pharmacol. Res.* 124, 146–155. doi: 10.1016/j.phrs.2017.08.004
- Shen, L.-R., Parnell, L. D., Ordovas, J. M., and Lai, C.-Q. (2013). Curcumin and aging. *BioFactors* 39, 133–140. doi: 10.1002/biof.1086
- Simoni, E., Serafini, M. M., Bartolini, M., Caporaso, R., Pinto, A., Necchi, D., *et al.* (2016). Nature-inspired multifunctional ligands: focusing on amyloid-based molecular mechanisms of alzheimer's disease. *ChemMedChem* 11, 1309–1317. doi: 10.1002/cmdc.201500422
- Simoni, E., Serafini, M. M., Caporaso, R., Marchetti, C., Racchi, M., Minarini, A., *et al.* (2017). Targeting the Nrf2/Amyloid-Beta Liaison in Alzheimer's Disease: a rational approach. *ACS Chem. Neurosci.* 8, 1618–1627. doi: 10.1021/acschemneuro.7b00100
- Spencer, J. P. (2010). Beyond antioxidants: the cellular and molecular interactions of flavonoids and how these underpin their actions on the brain. *Proc. Nutr. Soc.* 69 (2), 244–260. doi: 10.1017/S0029665110000054
- Suneetha, A., and Raja Rajeswari, K. (2016). Role of dimethyl fumarate in oxidative stress of multiple sclerosis: a review. *J. Chromatogr. B.* 1019, 15–20. doi: 10.1016/j.jchromb.2016.02.010
- Tanigawa, S., Fujii, M., and Hou, D.-X. (2007). Action of Nrf2 and Keap1 in ARE-mediated NQO1 expression by quercetin. *Free Radic. Biol. Med.* 42, 1690–1703. doi: 10.1016/j.freeradbiomed.2007.02.017
- Tebay, L. E., Robertson, H., Durant, S. T., Vitale, S. R., Penning, T. M., Dinkova-Kostova, A. T., *et al.* (2015). Mechanisms of activation of the transcription factor Nrf2 by redox stressors, nutrient cues, and energy status and the pathways through which it attenuates degenerative disease. *Free Radic. Biol. Med.* 88 (Pt B), 108–146. doi: 10.1016/j.freeradbiomed.2015.06.021
- van Meerloo, J., Kaspers, G. J., and Cloos, J. (2011). Cell sensitivity assays: the MTT assay. *Methods Mol. Biol.* 731, 237–245. doi: 10.1007/978-1-61779-080-5\_20
- Vera-Ramirez, L., Pérez-Lopez, P., Varela-Lopez, A., Ramirez-Tortosa, M., Battino, M., and Quiles, J. L. (2013). Curcumin and liver disease. *BioFactors* 39, 88–100. doi: 10.1002/biof.1057
- Visioli, F. (2015). Xenobiotics and human health: a new view of their pharmanutritional role. *PharmaNutrition* 3 (2), 60–64. doi: 10.1016/j.phanu.2015.04.001
- Witaicenis, A., Seito, L. N., da Silveira Chagas, A., de Almeida, L. D., Luchini, A. C., Rodrigues-Orsi, P., *et al.* (2014). Antioxidant and intestinal anti-inflammatory effects of plant-derived coumarin derivatives. *Phytomedicine* 21, 240–246. doi: 10.1016/j.phymed.2013.09.001
- Xicota, L., Rodriguez-Morato, J., Dierssen, M., and De La Torre, R. (2017). Potential Role of (–)-epigallocatechin-3-gallate (EGCG) in the secondary prevention of Alzheimer disease. *Curr. Drug Targets* 18, 174–195. doi: 10.2174/1389450116666150825113655

## PART 2

The following manuscript was published in *Frontiers in Pharmacology* in 2020 as:

### **Targeting cytokine release through the differential modulation of Nrf2 and NF- $\kappa$ B pathways by electrophilic/non-electrophilic compounds**

**Fagiani Francesca**, Catanzaro Michele, Buoso Erica, Basagni Filippo, Di Marino Daniele, Raniolo Stefano, Amadio Marialaura, Frost Eric, Corsini Emanuela, Racchi Marco, Fulop Tamas, Govoni Stefano, Rosini Michela, Lanni Cristina

#### **Abstract**

The transcription factor Nrf2 coordinates a multifaceted response to various forms of stress and to inflammatory processes, maintaining a homeostatic intracellular environment. Nrf2 anti-inflammatory activity has been related to the crosstalk with the transcription factor NF- $\kappa$ B, a pivotal mediator of inflammatory responses and of multiple aspects of innate and adaptive immune functions. However, the underlying molecular basis has not been completely clarified. By combining into new chemical entities, the hydroxycinnamoyl motif from curcumin and the allyl mercaptan moiety of garlic organosulfur compounds, we tested a set of molecules, carrying (pro)electrophilic features responsible for the activation of the Nrf2 pathway, as valuable pharmacologic tools to dissect the mechanistic connection between Nrf2 and NF- $\kappa$ B. We investigated whether the activation of the Nrf2 pathway by (pro)electrophilic compounds may interfere with the secretion of pro-inflammatory cytokines, during immune stimulation, in a human immortalized monocytic cell line (THP-1). The capability of compounds to affect the NF- $\kappa$ B pathway was also evaluated. We assessed the compounds-mediated regulation of cytokine and chemokine release by using Luminex X-MAP<sup>®</sup> technology in human primary peripheral blood mononuclear cells (PBMCs) upon LPS stimulation. We found that all compounds, also in the absence of electrophilic moieties, significantly suppressed the LPS-evoked secretion of pro-inflammatory cytokines such as TNF $\alpha$  and IL-1 $\beta$ , but not of IL-8, in THP-1 cells. A reduction in the release of pro-inflammatory mediators similar to that induced by the compounds was also observed after siRNA mediated-Nrf2 knockdown, thus indicating that the attenuation of cytokine secretion cannot be directly ascribed to the activation of Nrf2 signaling pathway. Moreover, all compounds, with the exception of compound 1, attenuated the LPS-induced activation of the NF- $\kappa$ B pathway, by reducing the upstream phosphorylation of I $\kappa$ B, the NF- $\kappa$ B nuclear translocation, as well as the activation of NF- $\kappa$ B promoter. In human PBMCs, compound 4 and CURC attenuated TNF $\alpha$  release as

observed in THP-1 cells, and all compounds acting as Nrf2 inducers significantly decreased the levels of MCP-1/CCL2, as well as the release of the proinflammatory cytokine IL-12. Altogether, the compounds induced a differential modulation of innate immune cytokine release, by differently regulating Nrf2 and NF- $\kappa$ B intracellular signaling pathways.

**Keywords:** Nrf2, NF- $\kappa$ B, curcumin, antioxidant, inflammation, cytokine release, TNF $\alpha$ , MCP-1.



# Targeting Cytokine Release Through the Differential Modulation of Nrf2 and NF- $\kappa$ B Pathways by Electrophilic/Non-Electrophilic Compounds

Francesca Fagiani<sup>1,2†</sup>, Michele Catanzaro<sup>1†</sup>, Erica Buoso<sup>1</sup>, Filippo Basagni<sup>3</sup>, Daniele Di Marino<sup>4</sup>, Stefano Raniolo<sup>5</sup>, Marialaura Amadio<sup>1</sup>, Eric H. Frost<sup>6</sup>, Emanuela Corsini<sup>7</sup>, Marco Racchi<sup>1</sup>, Tamas Fulop<sup>8</sup>, Stefano Govoni<sup>1</sup>, Michela Rosini<sup>3\*</sup> and Cristina Lanni<sup>1\*</sup>

## OPEN ACCESS

**Edited by:**  
Filippo Caraci,  
University of Catania, Italy

**Reviewed by:**  
Rosalia Crupi,  
University of Messina, Italy  
Raffaella Gozzelino,  
New University of Lisbon, Portugal

<sup>1</sup> Department of Drug Sciences, Pharmacology Section, University of Pavia, Pavia, Italy, <sup>2</sup> Scuola Universitaria Superiore IUSS Pavia, Pavia, Italy, <sup>3</sup> Department of Pharmacy and Biotechnology, University of Bologna, Bologna, Italy, <sup>4</sup> Department of Life and Environmental Sciences, New York-Marche Structural Biology Center (NY-MaSBIC), Polytechnic University of Marche, Ancona, Italy, <sup>5</sup> Università della Svizzera Italiana (USI), Faculty of Biomedical Sciences, Institute of Computational Science—Center for Computational Medicine in Cardiology, CH-Lugano, Switzerland, <sup>6</sup> Department of Microbiology and Infectiology, Centre de Recherches Cliniques, Faculty of Medicine and Health Sciences, University of Sherbrooke, Sherbrooke, QC, Canada, <sup>7</sup> Department of Environmental Science and Policy, Università degli Studi di Milano, Milan, Italy, <sup>8</sup> Geriatric Division, Department of Medicine, Faculty of Medicine and Health Sciences, Research Center on Aging, University of Sherbrooke, Sherbrooke, QC, Canada

## INTRODUCTION

Nuclear factor (erythroid-derived 2)-like 2 (Nrf2) is a transcription factor regulating the expression of about 250 genes encoding a network of cooperating enzymes involved in endobiotic and xenobiotic biotransformation reactions, antioxidant metabolism, protein degradation and regulation of inflammation (Hayes and Dinkova-Kostova, 2014). By governing such complex transcriptional networks, Nrf2 coordinates a multifaceted response to various forms of stress, maintaining a homeostatic intracellular environment. Several studies demonstrate that Nrf2 plays also a key role in the resolution of inflammatory processes. Consistently, Nrf2 is abundant in monocytes and granulocytes, proving its crucial involvement in immune response driven by these cell types. Data from the literature demonstrate that genetic or pharmacological activation of Nrf2 strongly suppresses the production of proinflammatory cytokines (Innamorato *et al.*, 2008; Knatko *et al.*, 2015; Kobayashi *et al.*, 2016; Quinti *et al.*, 2017) and Nrf2-deficiency induces an exacerbation of inflammation in a variety of murine models such as sepsis, pleurisy, and emphysema (Iizuka

*et al.*, 2005; Ishii *et al.*, 2005; Thimmulappa *et al.*, 2006). However, while the contribution of Nrf2 in inflammatory processes has been widely recognized, the underlying molecular basis has not been completely clarified. Its anti-inflammatory activity has been related to several mechanisms, including crosstalk with the transcription factor nuclear factor- $\kappa$ B (NF- $\kappa$ B), the modulation of redox balance, and the direct downregulation of some antioxidant response element (ARE)-dependent expression of pro-inflammatory cytokines, such as IL-6 and IL-1 $\beta$  (Kobayashi *et al.*, 2016). Among them, the crosstalk between Nrf2 and NF- $\kappa$ B relies on both transcriptional and post-transcriptional mechanisms, allowing fine-tuning of dynamic responses to ever-changing environmental cues. NF- $\kappa$ B is a key transcription factor governing the expression of a plethora of genes involved in diverse biological processes, including immune and inflammatory responses, cell proliferation, death, angiogenesis, cell survival, and oncogenesis (Häcker and Karin, 2006; Perkins, 2007). In particular, NF- $\kappa$ B controls the transcription of genes encoding pro-inflammatory cytokines, such as TNF $\alpha$  and IL-1 $\beta$ . In the absence of a stimulant, NF- $\kappa$ B remains inactive and sequestered in the cytoplasm by binding to an inhibitory protein, I $\kappa$ B. The exposure of cells to pro-inflammatory stimuli, such as cytokines and infectious agents, triggers the activation of the I $\kappa$ B kinase (IKK) complex that phosphorylates I $\kappa$ B protein on two serine residues. Phosphorylated I $\kappa$ B is ubiquitinated and, subsequently, degraded via proteasome (Hayden *et al.*, 2006; Perkins, 2007). The degradation of I $\kappa$ B allows NF- $\kappa$ B translocation into the nucleus to drive the expression of target genes; within the nucleus it interacts with other transcription factors and transcriptional co-factors to regulate expression of an array of genes, many of which are involved in inflammatory signaling (e.g. cytokines, chemokines, adhesion molecules, and acute phase proteins) (Baeuerle and Baltimore, 1996). Notably, several pharmacological and genetic studies suggest a functional crosstalk between Nrf2 and NF- $\kappa$ B transcription factors, with a range of complex molecular interactions depending on the cell type and tissue context (Wardyn *et al.*, 2015). A strong activity in both NF- $\kappa$ B and Nrf2 has been found fundamental for well-coordinated responses to counteract a cellular inflammatory status (Fusco *et al.*, 2017; D'amico *et al.*, 2019). Indeed, an imbalance between Nrf2 and NF- $\kappa$ B pathways has been associated with a variety of diseases ranging from neurodegeneration, cardiovascular and autoimmune disorders.

The transcriptional factor Nrf2, with its redox sensitive repressor Keap1 (Kelch-like ECH-associated protein 1), orchestrates adaptive responses to diverse forms of stress through regulatory cysteine switches. Thus, precise electrophilic addition is emerging as a valuable opportunity to shed light on previously untapped roles of this redox sensing system (Basagni *et al.*, 2019). By combining into new chemical entities the hydroxycinnamoyl motif derived from curcumin and the allyl mercaptan moiety of garlic organosulfur compounds, we previously synthesized a set of molecules (compounds 1-3), carrying, with the exception



of compound 3, a catechol moiety and/or an  $\alpha,\beta$ -unsaturated carbonyl group (**Table 1**). These (pro)electrophilic features were shown to be responsible for the activation of the Nrf2 pathway and the subsequent induction of ARE-dependent target genes, possibly by covalent conjugation with Keap1 cysteine sensors (Simoni *et al.*, 2017; Serafini *et al.*, 2019). Notably, alkylation of functionally significant cysteines of NF- $\kappa$ B was also shown to play a prominent role in the inhibition of pro-inflammatory transcriptional pathways (Kastrati *et al.*, 2016), albeit alternative mechanisms have been proposed, such as the inhibition of IKK $\beta$ , or promotion of RelA polyubiquitination and proteasomal degradation (Woodcock *et al.*, 2018).

Herein, we considered the abovementioned compounds as valuable pharmacologic tools to explore the mechanistic connection between Nrf2 and NF- $\kappa$ B. To exclude possible oxidative activation of the methoxyphenol ring of compound 3 into reactive metabolites such as quinone methide, which could provide an additional electrophilic site (Luis *et al.*, 2018), an additional new compound 4 was synthesized (**Table 1**).

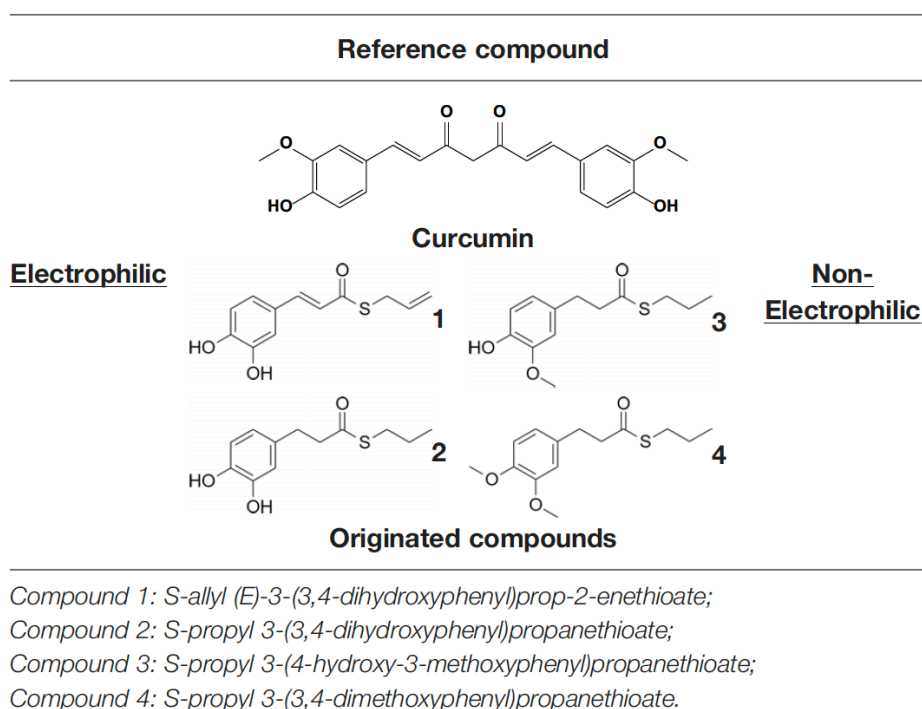


**Table 1.** Design strategy of electrophilic and non-electrophilic compounds.

In the present work, we investigated whether the modulation in Nrf2 pathway activation by our molecules was able to interfere with the LPS-induced secretion of pro-inflammatory cytokines, during immune stimulation, in a human immortalized monocyte-like cell line (THP-1), a well-established cell model for the immune modulation approach (Chanput *et al.*, 2014), using curcumin (CURC) as a reference compound. Moreover, the capability of compounds to affect the NF- $\kappa$ B intracellular pathway, a pivotal mediator of inflammatory responses and critical regulator of multiple aspects of both innate and adaptive immune functions, was also investigated. To validate the results obtained in THP-1 cells in a human primary cellular model, we assessed the regulation of cytokine and chemokine (e.g. IFN $\gamma$ , IL-1 $\beta$ , IL-4, IL-6, IL-8, IL-12 (p40), IL-12 (p70), IL-13, IL-27, MCP-1, MCP-3, TNF $\alpha$ ) release by the described compounds, upon immune LPS stimulation, in human peripheral blood mononuclear cells (PBMCs), obtained from venous whole blood of healthy patients, by using Luminex X-MAP<sup>®</sup> technology.

Altogether, we demonstrated that compounds modulated the innate immune cytokine release, by differently regulating Nrf2 and NF- $\kappa$ B intracellular signaling pathways.

## MATERIALS AND METHODS

### Compounds Synthesis

Compounds 1–3 were synthesized according to procedures reported in (Simoni *et al.*, 2016; Simoni *et al.*, 2017); details on the newly synthesized compound 4 are reported here below.

### Synthesis of S-Propyl 3-(3,4-Dimethoxyphenyl)propanethioate (Compound 4)

To a solution of compound 2 (110 mg, 0.46 mmol) in 1.80 mL of DMF potassium carbonate (222.5 mg, 1.61 mmol) and methyl iodide dropwise (0.10 mL, 1.61 mmol) were added. The reaction mixture was left stirring at room temperature overnight. The reaction was quenched by adding 3 mL of water and the mixture obtained was further extracted with diethyl ether (2 x 5 mL). Organic phases were collected, reunited, dried with anhydrous sodium sulphate and solvent was evaporated under vacuum. The crude oil was purified by column chromatography on silica gel using petroleum ether/ethyl acetate (8/2) as mobile phase. 4 was obtained as colorless oil (110 mg, 89%). <sup>1</sup>H NMR (400 MHz, CDCl<sub>3</sub>)  $\delta$  6.74 (d, J = 8 Hz, 1H), 6.69–6.67 (m, 2H), 3.82 (s, 3H), 3.80 (s, 3H), 2.89 (t, J = 8 Hz, 2H), 2.83–2.77 (m, 4H), 1.59–1.50 (m, 2H), 0.91 (t, J = 8 Hz, 3H). <sup>13</sup>C NMR (100 MHz, CDCl<sub>3</sub>)  $\delta$  198.79, 148.98, 147.61, 132.83, 120.27, 111.77, 111.41, 55.98, 55.89, 45.88, 31.23, 30.87, 23.06, 13.39. MS [ESI<sup>+</sup>] m/z 291.10 + [M+Na]<sup>+</sup>.

Chromatographic separations were performed on silica gel columns (Kieselgel 40, 0.040–0.063 mm, Merck). Reactions were followed by TLC on Merck (0.25 mm) glass-packed precoated silica gel plates (60 F254), then visualized with a UV lamp. NMR spectra were recorded at 400 MHz for <sup>1</sup>H and 100 MHz for <sup>13</sup>C on a Varian VXR 400 spectrometer (**Supplementary Figure 1**). Chemical shifts (δ) are reported in parts per million (ppm) relative to tetramethylsilane (TMS), and spin multiplicities are given as s (singlet), br s (broad singlet), d (doublet), t (triplet), q (quartet), or m (multiplet). Direct infusion ESI-MS mass spectra were recorded on a Waters ZQ 4000 and Xevo G2-XS QToF apparatus. Final compounds were >95% pure as determined by High Performance Liquid Chromatography (HPLC) analyses. The analyses were performed under reversed-phase conditions on a Phenomenex Jupiter C18 (150 × 4.6 mm I.D.) column, using a binary mixture of H<sub>2</sub>O/acetonitrile (60/40, v/v for 1; 50/50, v/v for 2 and 3; 40/60, v/v for 4) as the mobile phase, UV detection at λ=302 nm (for1) or 254 nm (for2–4), and a flow rate of 0.7 mL/min. Analyses were performed on a liquid chromatograph model PU-1587 UV equipped with a 20 μL loop valve (Jasco Europe, Italy).

All compounds were solubilized in DMSO (dimethyl sulfoxide) at stock concentrations of 10 mM, frozen (−20°C) in aliquots and diluted in culture medium immediately prior to use. For each experimental setting, a stock aliquot was thawed and diluted to minimize repeated freeze and thaw damage. The final concentration of DMSO in culture medium was less than 0.1%.

## Reagents

CURC (#08511) was ≥98% pure (HPLC) and purchased by Sigma-Aldrich (Merck KGaA, Darmstadt, Germany). Cell culture media and all supplements were purchased from Sigma Aldrich (Merck KGaA, Darmstadt, Germany). Rabbit polyclonal anti-human Nrf2 (NBP1-32822) and anti-human HO-1 (NBP1-31341) antibodies were purchased from Novus (Biotechnie, Minneapolis USA). Mouse monoclonal anti-human IκBα (#4814T), mouse monoclonal anti-human phospho-IκBα (Ser32/36) (#9246T), and rabbit monoclonal anti-human NF-κB p65 (D14E12) XP® (#8242) were purchased from Cell Signaling (Cell Signaling Technology, Danvers, MA, USA). Mouse monoclonal anti-human lamin A/C (612162) antibody was purchased from BD Biosciences (Franklin Lakes, NJ, USA). Mouse anti-human α-tubulin (sc-5286) was purchased from Sigma-Aldrich (Merck KGaA, Darmstadt, Germany). Peroxidase conjugate-goat anti-mouse (A4416) was purchased from Sigma-Aldrich (Merck KGaA, Darmstadt, Germany). Anti-rabbit peroxidase-linked antibody (#7074) was purchased from Cell Signaling (Cell Signaling Technology, Danvers, MA, USA). Lipopolysaccharide (LPS) from *Escherichia coli* O111:B4 (L2630) was purchased

from Sigma-Aldrich (Merck KGaA, Darmstadt, Germany). The proteasome inhibitor MG132 (474790) was purchased from Calbiochem (San Diego, CA).

### **Cell Culture and Treatments**

Human THP-1 cells were purchased from the European Collection of Authenticated Cell Cultures (ECACC, Salisbury, UK) and diluted to 106 cells/mL in RPMI 1640 medium supplemented with 10% heat-inactivated Fetal Bovine Serum (FBS), 2 mM glutamine, 0.1 mg/mL streptomycin, 100 IU·mL penicillin, and 0.05 mM 2-mercaptoethanol (complete medium) and maintained at 37°C in 5% CO<sub>2</sub>-containing and 95% air atmosphere. The experiments were carried out on passages 5–15. Cells were treated as reported in figure legends. Control cells were exposed only to solvent (DMSO).

### **Cell Viability**

The mitochondrial dehydrogenase activity that reduces 3-(4,5- dimethylthiazol-2-yl)-2,5-diphenyl-tetrazolium bromide (MTT, Sigma Aldrich, Merck KGaA, Darmstadt, Germany) was used to determine cell viability using a quantitative colorimetric assay (Kumar *et al.*, 2018). At day 0, THP-1 cells were plated in 96-well plates at a density of 50 x 10<sup>3</sup> viable cells per well. After treatment, according to the experimental setting, cells were exposed to an MTT solution (1 mg/mL) in complete medium. After 4 h of incubation with MTT, cells were lysed with sodium dodecyl sulfate (SDS) for 24 h and cell viability was quantified by reading absorbance at 570 nm wavelength, using Synergy HT multi-detection microplate reader (Bio-Tek, Winooski, VT, USA).

### **Subcellular Fractionation for Nrf2 and NF- $\kappa$ B Nuclear Translocation**

The expression of Nrf2 and NF- $\kappa$ B in nuclear THP-1 lysates was assessed by Western blot analysis. Suspended cells were collected, centrifugated, and washed twice with ice-cold PBS (phosphate buffered saline), and, subsequently, homogenized 20 times using a glass-glass homogenizer in ice-cold fractionation buffer (20 mM Tris/HCl pH 7.4, 2 mM EDTA, 0.5 mM EGTA, 0.32 M sucrose, 50 mM  $\beta$ -mercaptoethanol). The homogenate was centrifuged at 300  $\times$  g for 5 min to obtain the nuclear fraction. An aliquot of the nuclear extract was used for protein quantification by the Bradford method, whereas the remaining sample was boiled at 95°C for 5 min after dilution with 2X sample buffer (125 mM Tris-HCl pH 6.8, 4% SDS, 20% glycerol, 6%  $\beta$ -mercaptoethanol, 0.1% bromophenol blue). Equivalent amounts of nuclear extracted proteins (30 mg) were subjected to polyacrylamide gel electrophoresis and immunoblotting, as described below.

### **Immunodetection of Nrf2, HO-1, p-I $\kappa$ B $\alpha$ , I $\kappa$ B $\alpha$ , and NF- $\kappa$ B**

The expression of Nrf2, HO-1, p-I $\kappa$ B $\alpha$ , I $\kappa$ B $\alpha$ , and NF- $\kappa$ B in whole cell lysates or nuclear extracts was assessed by Western blot analysis. After treatments, suspended cells were collected, centrifuged, and washed twice with ice-cold PBS, lysed by the addition of ice-cold homogenization buffer (50 mM Tris-HCl pH 7.5, 150 mM NaCl, 5 mM EDTA, 0.5% Triton X-100 and protease- phosphatase inhibitors mix). Samples were sonicated and centrifuged at 13,000  $\times g$  for 10 s at 4°C. The resulting supernatants were transferred into new tubes, and protein content was determined by Bradford method. After that, the samples were boiled at 95°C for 5 min after dilution with 5X sample buffer. For Western blot analysis, equivalent amounts of both total and nuclear extracts (30 mg) were electrophoresed in 10% acrylamide gel, under reducing conditions, then, electroblotted into PVDF membranes (Sigma Aldrich, Merck KGaA, Darmstadt, Germany), blocked for 1 h with 5% w/v bovine serum albumin (BSA) in TBS-T (0.1 M Tris-HCl pH 7.4, 0.15 M NaCl, and 0.1% Tween 20), and incubated overnight at 4°C with primary antibodies diluted in 5% w/v BSA in TBS-T. The proteins were visualized using primary antibodies for Nrf2 (1:1000), HO-1 (1:1000), I $\kappa$ B $\alpha$  (1:1000), p-I $\kappa$ B $\alpha$  (1:1000), or NF- $\kappa$ B (1:1000). Detection was carried out by incubation with secondary horseradish peroxidase-conjugated antibodies (1:5000) diluted in 5% w/v BSA in TBS-T for 1 h at room temperature. Membranes were subsequently washed three times with TBS-T and proteins of interest were visualized using an enhanced chemiluminescent reagent (Pierce, Rockford, IL, USA). A  $\alpha$ -tubulin and lamin A/C were performed as controls for gel loading.

### **Small Interference RNA (siRNA) for Nrf2**

Nrf2 siRNA designed for the human gene Nrf2 was purchased from Sigma Aldrich, Merck KGaA (Darmstadt, Germany). A scrambled siRNA, without known homology with any gene, was used as negative control (Sigma Aldrich, Merck KGaA, Darmstadt, Germany). RNA interference experiments in THP-1 cells were performed by transient transfection for 24 h, using RNAiMAX Lipofectamine (Invitrogen, Thermo Fisher Scientific, Waltham, MA, USA), according to manufacturer's protocol. To confirm Nrf2 silencing, the proteasome inhibitor MG132 (Calbiochem) was added to the medium of selected plates at a final concentration of 5  $\mu$ M. After 24 h, cells were analyzed for Nrf2 expression by Western blot analysis.

### **Enzyme-Linked Immunosorbent Assay (ELISA) Determination of TNF $\alpha$ , IL-8, and IL-1 $\beta$**

THP-1 cells were treated with compounds 1–4 and CURC at a concentration of 5  $\mu$ M for 24 h, and then stimulated with LPS for 3 h, as described in the legends to figures. TNF $\alpha$ , IL-8, and IL-1 $\beta$  released from THP-1 cells were measured in cell-free supernatants obtained by centrifugation at 250 x g for 5 min and immediately processed for ELISA, according to the manufacturer's protocol. TNF $\alpha$ , IL-8 and IL-1 $\beta$  production was assessed by specific sandwich ELISA (Invitrogen, Thermo Fisher Scientific, Waltham, MA, USA; Immunotools GmbH, Friesoythe, Germany). Results were expressed as stimulation index. The limit of detection under optimal conditions was 4 pg/mL for TNF $\alpha$ , 2.6 pg/mL for IL-8, and 18 pg/mL for IL-1 $\beta$ .

### **Plasmid DNA Preparation, Transient Transfections, and Luciferase Assay**

Plasmids for transfections were purified with the HiSpeed<sup>®</sup> Plasmid Midi Kit (Qiagen, Valencia, CA). DNA was quantified and assayed for purity using Quantus<sup>™</sup> Fluorometer (Promega, Madison, WI). Transient transfections were performed in 12- multiwell culture plates; for each well 5 x 10<sup>5</sup> cells were seeded in RPMI 1640 complete medium. Transfections were carried out using Lipofectamin 2000 Transfection Reagent (Invitrogen, Thermo Fisher Scientific, Waltham, MA, USA), according to manufacturer's instructions. pGL4.32 vector (E8491, Promega, Madison, WI) luciferase-reporter construct plasmid DNA was co-transfected with pRL-TK Renilla (E2241, Promega, Madison, WI) luciferase expressing vector to measure transfection efficiency, as described in Buoso *et al.* (2019). During transfection THP-1 cells were incubated at 37°C in 5% CO<sub>2</sub> overnight and, then, treated with 5  $\mu$ M compounds and CURC for 24 h and, then, stimulated with 10 ng/mL LPS for 6 h. At the end of the treatments, cells were lysed with Passive Lysis Buffer provided by Dual-Luciferase<sup>®</sup> Reporter Assay System, following manufacturer's instructions (Promega, Madison, WI). The luminescent signals were measured using a 20/20 Luminometer with 10 s of integration (Turner BioSystems, Sunnyvale, CA).

### **PBMCs Purification and Culture**

Human peripheral blood mononuclear cells (PBMCs) were obtained from the blood of five (5) healthy individuals (mean age  $\pm$  SD: 71  $\pm$  5.22 years; gender: 3 females and 2 males) satisfying the SENIEUR standard protocol for immuno-gerontological studies (Pawelec *et al.*, 2001). Subjects having a history or physical signs of atherosclerosis or inflammation were excluded. All subjects gave written informed consent in accordance with the Declaration of Helsinki (Ethical Committee Project approval: Fulop\_2019-2877). Heparinized blood was subjected to density gradient centrifugation over Ficoll-Paque Plus medium (GE Healthcare Life Sciences, Marlborough, MA, USA) as described in (Le Page

*et al.*, 2017). Briefly, PBS-diluted blood was carefully layered onto the Ficoll- Paque density gradient and centrifuged for 20 min at 400 x g at slow acceleration and with the brake off at room temperature. After centrifugation, the PBMCs layer, consisting of monocytes, T and B lymphocytes, was collected and washed three times with fresh PBS. Cell viability, assessed by Trypan blue exclusion, was more than 95%. For experiments, PBMCs were resuspended at a density of 1x10<sup>6</sup> cells/mL in complete culture medium consisting of RPMI 1640 supplemented with 10% heat-inactivated FBS, 2 mM glutamine, 0.1 mg/mL streptomycin and 100 IU mL penicillin and maintained at 37°C in 5% CO<sub>2</sub> and 95% air atmosphere.

### **Luminex X-MAP® Assay**

Human cytokine MILLIPLEX® MAP Kit (customized for IFN $\gamma$ , IL-1 $\beta$ , IL-4, IL-6, IL-8, IL-12 (p40), IL-12 (p70), IL-13, IL-27, MCP-1, MCP-3, TNF $\alpha$ ) was purchased from Millipore-Sigma (Merck KGaA). The assay was performed in a 96-well plate and all reagents were prepared according to the manufacturer's instructions. Each well was cleaned and pre-wet with 200 mL of wash buffer on plate at 450 rpm during 10 min at RT. Wash buffer was removed by inverting the plate. Assay buffer, matrix solution or culture medium was used as a blank, each standard from a range of concentrations (different for each analyte), quality controls and samples were added to the appropriate wells. The mixed magnetic microbead solution was sonicated and vortexed prior to adding 25 mL into each well. The plates were sealed and incubated with agitation on a plate shaker at 750 rpm overnight at 4°C in a darkroom. Plates were put on the magnetic support to retain microbeads, then fluid was removed by inverting the plate to avoid touching the beads. Each well was washed three times with 200 mL of wash buffer with a plate shaker at 450 rpm for 30 s at RT. 25 mL of biotinylated detection antibodies were added per well, and plates were incubated in dark room at RT on a plate shaker at 750 rpm for 1 h. Then, 25 mL of streptavidin-phycoerythrin solution were added to each well, and plates were incubated on a plate shaker at 750 rpm for 30 min at RT and protected from light. Plates were washed three times with 200 mL of wash buffer. Microbeads were resuspended in 150 mL/well of sheath fluid on a plate shaker at 450 rpm for 5 min at RT. Data were acquired on a Luminex® 200™ System using the Luminex xPonent® software. An acquisition gate of between 8,000 and 15,000 was set to discriminate against any doublet events and ensure that only single microbeads were measured. Fifty beads/assay were collected and median fluorescence intensities (MFIs) were measured. Sensitivity limits (in pg/mL) were 0.86 for IFN $\gamma$ ; 0.52 for IL-1 $\beta$ ; 0.2 for IL-4; 0.14 for IL-6; 0.52 for IL-8; 2.24 for IL-12 (p40); 0.88 for IL-12 (p70); 2.58 for IL-13; 50.78 for IL-27; 3.05 for MCP-1; 8.61 for MCP-3 and 5.39 for TNF $\alpha$ .

MFIs were converted to concentrations using the equation of standard range of the appropriate cytokine using Milliplex<sup>®</sup> Analyst 5.1 Software.

### Densitometry and Statistics

All the experiments were performed at least three times with representative results being shown. Data are expressed as mean  $\pm$  SEM. The relative densities of the acquired images of Western blotting bands were analyzed with ImageJ software. Statistical analyses were performed using Prism software (GraphPad software, San Diego, CA, USA; version 8.0). Statistical differences were determined by analysis of variance (ANOVA) followed, when significant, by an appropriate post hoc test, as indicated in the figure legends. In all reported statistical analyses, effects were designated as non-significant for  $p > 0.05$ , significant (\*) for  $p < 0.05$  or less as indicated.

### Quantum Mechanics Calculations

The study for the conformational freedom of compounds 1–4 was conducted with the software Gaussian 09 (Gaussian Inc., Wallingford, CT, USA; Revision A.02). Each molecule underwent a protocol of geometrical optimization, involving an increasing level of precision of basis sets [i.e., from 3-21 (Binkley *et al.*, 1980) to 6-31G\* (Petersson and Al-Laham, 1991)], with the Hartree-Fock (HF) method (Kohn and Sham, 1965). The “Scan” functionality was used to estimate the barrier hindering conformational variability in the compounds for two different dihedral angles (**Supplementary Figure 2**). During this step, a Møller-Plesset correlation energy correction truncated at the second order (MP2) (Møller and Plesset, 1934) was added to the HF method and the torsions were rotated by intervals of 5 degrees until they completed the 360-degree turn. For each of these steps, the dihedral angle under study was fixed and the energy of the structure was computed after few steps of minimization.

## RESULTS

### Cellular Toxicity of Compounds

The cytotoxicity of compounds 1–4 was assessed by MTT assay in THP-1 cells, in comparison with CURC, as a reference compound. Cells were exposed to compounds 1–4 and CURC at concentrations of 1  $\mu$ M, 2.5  $\mu$ M, 5  $\mu$ M, and 10  $\mu$ M for 24 h. Consistently with our previous data on a different cellular model (Simoni *et al.*, 2016; Simoni *et al.*, 2017; Serafini *et al.*, 2019; Catanzaro *et al.*, 2020), all the compounds were well-tolerated, with a



slight reduction of cell viability of about 10% observed for compounds 3 and 4 (**Figure 1**). Based on these results and according to our previous investigations (Simoni *et al.*, 2017; Serafini *et al.*, 2019; Catanzaro *et al.*, 2020), all further experiments were conducted using the concentration of 5  $\mu$ M.

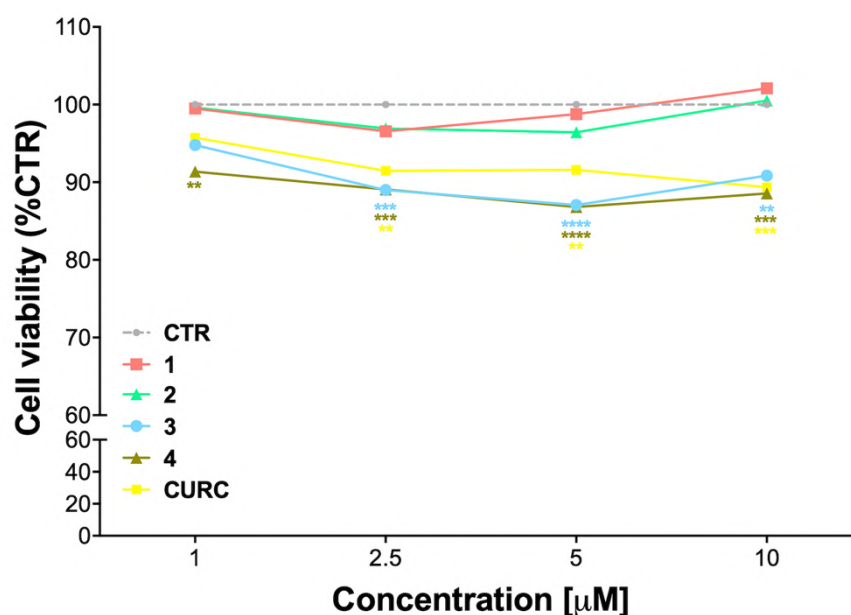


**Figure 1.** Cell viability in undifferentiated THP-1 exposed to compounds and CURC. THP-1 cells were treated with compounds 1–4 and CURC at the indicated concentrations for 24 h. Cell viability was assessed by MTT assay. Data are expressed as means of percentage of cell viability  $\pm$  SEM. Dunnett's multiple comparison test; \*\* $p < 0.01$ ; \*\*\* $p < 0.001$  and \*\*\*\* $p < 0.0001$  versus CTR;  $n = 4$ .

### Modulation of Nrf2 Nuclear Translocation and HO-1 Target by Compounds

Nrf2 is a redox-sensitive transcription factor orchestrating the expression and coordinated induction of a wide battery of genes encoding phase II and detoxifying enzymes. Under unstressed conditions, Nrf2 is retained in the cytoplasm by its negative repressor Keap1 and rapidly subjected to ubiquitination and proteasomal degradation, mediated by the binding of Keap1 to the Cul3/Rbx1 E1 ubiquitin ligase complex (Niture *et al.*, 2014). After exposure to oxidative and/or electrophilic stimuli, Nrf2 is released from structurally modified Keap1 and translocates into the nucleus, forms a heterodimer with one of the small musculoaponeurotic fibrosarcoma (Maf) proteins, and activates the ARE-mediated expression of cytoprotective genes. Since Nrf2 nuclear translocation is a fundamental step for the complete activation of its pathway, we tested the ability of compounds to induce

the nuclear translocation of Nrf2 in THP-1 cells, by comparing their effects to CURC, used as a positive control.

Notably, evidence from the literature demonstrates that pro-electrophilic (catechol) and/or electrophilic moieties (the Michael acceptor  $\alpha,\beta$ -unsaturated carbonyl group) are important structural functions necessary for the induction of the Nrf2 pathway (Tanigawa *et al.*, 2007; Satoh *et al.*, 2013). Compounds were synthesized and screened to identify the structural moieties responsible for the activation of Nrf2 and its downstream signaling pathway. The four compounds investigated in this study differ from each other by the presence or absence of the mentioned key functional groups (as shown in **Table 1**). Indeed, while compound 1 provides the catechol moiety, as well as the Michael acceptor group, 2 displays only the catechol moiety. Conversely, compounds 3 and 4 lack for both the Michael acceptor group and the catechol function.

Thus, THP-1 cells were treated with DMSO as vehicle control, compounds 1–4 and CURC at a concentration of 5  $\mu$ M for 3 h. After treatment, Nrf2 nuclear content was assessed by Western blot analysis. As shown in **Figure 2A**, compounds 1, 2, as well as CURC, significantly induced Nrf2 nuclear translocation, whereas compounds 3 and 4 did not increase Nrf2 nuclear content (**Figure 2A**). Such results are consistent with our previous work (Simoni *et al.*, 2017; Serafini *et al.*, 2019; Catanzaro *et al.*, 2020), where the ability of compounds 1 and 2, but not 3, to activate the Nrf2 pathway in SH-SY5Y and ARPE-19 cells suggested that the addition of Keap1 nucleophilic cysteines to (pro)electrophilic portions of the molecule could represent the initiating event. The finding that the newly synthesized molecule, compound 4, was also unable to induce Nrf2 nuclear translocation corroborates this hypothesis.

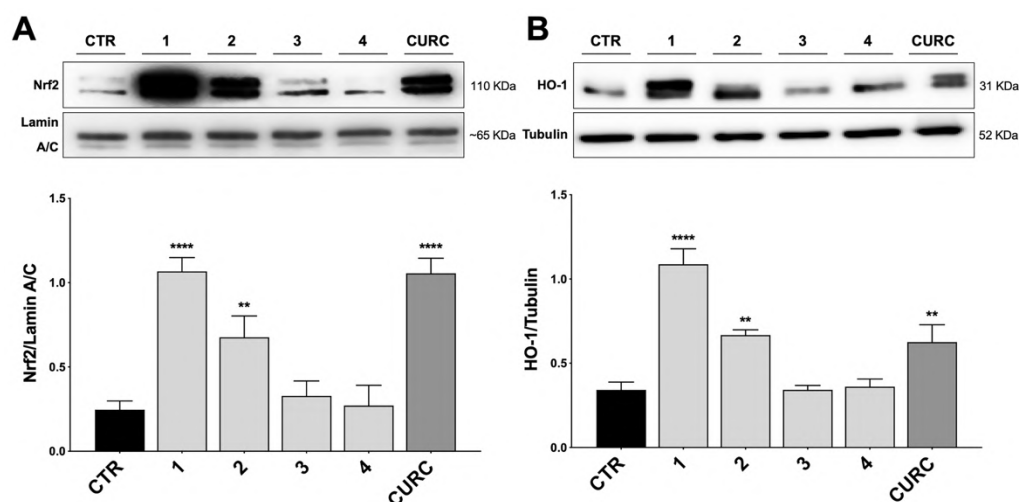


**Figure 2. Nrf2 nuclear translocation and modulation of HO-1 protein content in THP-1 cells. (A)** THP-1 cells were treated with compounds 1–4 and CURC at a concentration of 5  $\mu$ M for 3 h. After isolation, nuclear extracts were examined by Western blot analysis and Nrf2 expression was determined using an anti-Nrf2 antibody. Anti-lamin A/C was used as protein loading control. Results are shown as means of Nrf2/lamin A/C ratio  $\pm$  SEM. Dunnett's multiple comparison test; \*\* $p$  < 0.01 and \*\*\*\* $p$  < 0.0001 *versus* CTR;  $n$  = 5–7. **(B)** Total protein extracts of THP-1 cells, treated with compounds 1–4 and CURC at the concentration of 5  $\mu$ M for 24 h, were analyzed for HO-1 protein content by Western blot analysis. Anti-tubulin was used as protein loading control. Results are shown as means of HO-1/Tubulin ratio  $\pm$  SEM. Dunnett's multiple comparison test; \*\* $p$  < 0.01 and \*\*\*\* $p$  < 0.0001 *versus* CTR;  $n$  = 7.

To demonstrate the downstream activation of the Nrf2 signaling pathway, the protein amount of HO-1, one of the main targets of Nrf2, was evaluated by Western blot analysis. THP-1 cells were treated with DMSO as vehicle control, compounds 1–4 and CURC at a concentration of 5  $\mu$ M for 24 h. As shown in **Figure 2B**, compounds 1, 2 and CURC positively modulated HO-1 protein levels, confirming the activation of the Nrf2 pathway. In contrast, compounds 3 and 4 did not affect the protein amount of HO-1 in THP-1 whole cell lysates, confirming their inability to promote Nrf2 pathway activation.

### Compounds Attenuate TNF $\alpha$ and IL-1 $\beta$ , but Not IL-8 Release, in LPS-Stimulated THP-1 Cells

To investigate the immunomodulatory potential of compounds acting as Nrf2 inducers, we exposed THP-1 cells to LPS from *E. coli*, resulting in enhanced production and secretion of pro-inflammatory mediators (**Supplementary Figure 3** and **Figure 4A**). Thus, THP-1 cells were treated with DMSO as vehicle control, compounds 1–4 and CURC at a concentration of 5  $\mu$ M for 24 h and, then, exposed to 10 ng/mL LPS for 3 h in order to

evoke the inflammatory response (**Figure 3**). TNF $\alpha$  (**Figure 3A**) and IL-8 protein release (**Figure 3B**) were measured by ELISA in the supernatants of LPS-stimulated THP-1 cells. Notably, all compounds, independently from their ability to act as Nrf2 inducers, significantly reduced TNF $\alpha$  protein release into cell culture medium (**Figure 3A**). In contrast, in the same experimental setting, all compounds, as well as CURC, did not affect IL-8 protein release into cell culture medium (**Figure 3B**).

We further investigated the effects of compounds 1–4 and CURC on the release of the pro-inflammatory mediator IL-1 $\beta$  upon stimulation. Unlike TNF $\alpha$  and IL-8, no increase in IL-1 $\beta$  protein release was observed in THP-1 cells exposed to 10 ng/mL LPS, but only after stimulation with 1 mg/mL LPS for 3 h, as reported in **Figure 4A**. Then, THP-1 cells were treated with DMSO as vehicle control, compounds 1–4 and CURC at a concentration of 5  $\mu$ M for 24 h, exposed to 1 mg/mL LPS for 3 h to promote the inflammatory response, and tested for IL-1 $\beta$  release by ELISA (**Figure 4B**). All the compounds, as well as CURC, significantly reduced IL-1 $\beta$  protein release into cell culture medium. As observed for TNF $\alpha$ , both compounds acting as Nrf2 inducers (1 and 2) and those inactive on the Nrf2 pathway (3 and 4) counteracted the LPS-driven inflammatory response, thus suggesting the involvement of different intracellular pathways.

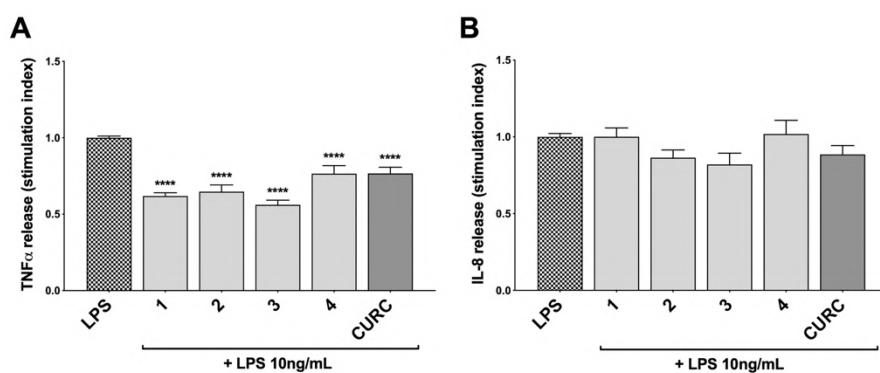


**Figure 3. Modulation of TNF $\alpha$  and IL-8 release in LPS-stimulated THP-1 cells exposed to compounds.** THP-1 cells were treated with compounds 1–4 and CURC at a concentration of 5  $\mu$ M for 24 h, and then stimulated with 10 ng/mL LPS for 3 h. TNF $\alpha$  (**A**) and IL-8 (**B**) protein release was measured in THP-1 supernatants by ELISA. Data are presented as means of stimulation index  $\pm$  SEM. Dunnett's multiple comparison test; \*\*\*\* $p$  < 0.0001 versus CTR; n = 5.

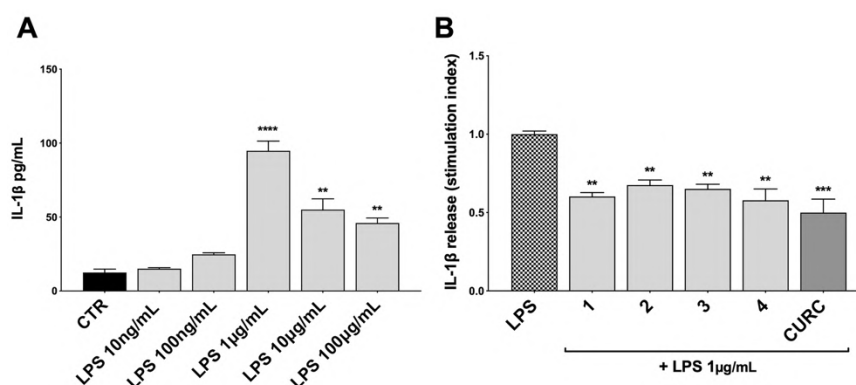


**Figure 4. Modulation of IL-1 $\beta$  release in LPS-stimulated THP-1 cells.** (A) IL-1 $\beta$  protein secretion was measured in THP-1 cell supernatants stimulated with LPS at the indicated concentrations for 3 h. At the end of the treatment, IL-1 $\beta$  protein release was assessed by ELISA. Data are presented as means of released picograms per mL (pg/mL)  $\pm$  SEM. Dunnett's multiple comparison test; \*\* $p$  < 0.01 and \*\*\*\* $p$  < 0.0001 *versus* CTR; n = 3. (B) IL-1 $\beta$  protein release was measured in THP-1 cells supernatants, treated for 24 h with compounds 1–4 and CURC at a concentration of 5  $\mu$ M and then stimulated with 1 mg/mL LPS for 3 h. The level of IL-1 $\beta$  was assessed by ELISA. Data are presented as means of stimulation index  $\pm$  SEM. Dunnett's multiple comparison test; \*\* $p$  < 0.01 and \*\*\* $p$  < 0.001 *versus* CTR; n = 3.

### siRNA Mediated Nrf2 Knockdown Does Not Affect TNF $\alpha$ Release in LPS-Stimulated THP-1 Cells

Based on the effect elicited by compounds 3 and 4 on cytokine release, the Nrf2 gene was knocked down by siRNA in THP-1 cells with the aim to evaluate the weight of the Nrf2 pathway in pro-inflammatory cytokine modulation upon LPS stimulation. Accordingly, cells were transfected with scrambled (siRNA<sub>CTR</sub>) and Nrf2 siRNA (siRNA<sub>Nrf2</sub>) for 24 h and the proteasome inhibitor MG132 (5  $\mu$ M) was added 4 h before the end of the experiment to the medium of selected plates in order to assess Nrf2 silencing. Nrf2 shows a short half-life, with a rapid ubiquitin-proteasome-mediated degradation (Kobayashi and Yamamoto, 2006). Thus, to properly appreciate Nrf2 silencing, we blocked Nrf2 degradation using the proteasome inhibitor MG132. After treatments, the Nrf2 protein content was measured in whole cell lysates by Western blot analysis. As reported in **Figure 5A**, the proteasome inhibitor MG132 induced an increase in Nrf2 protein levels in comparison with control. No statistically significant difference in Nrf2 protein levels between wild type (WT) and scrambled treated cells, treated with MG132, was found, whereas a marked decrease in Nrf2 protein content between WT and siRNA<sub>Nrf2</sub>-treated cells was observed (**Figure 5A**). Then, WT and siRNA<sub>Nrf2</sub> cells were treated for 24 h with 5  $\mu$ M of selected compounds (the Nrf2 inducer 1, and the inactive 3 and 4), stimulated with 10 ng/mL LPS for 3 h to evoke the inflammatory response, and analysed for TNF $\alpha$  release

by ELISA. Notably, all the selected compounds significantly suppressed LPS-induced release of TNF $\alpha$  both in WT and siRNA<sub>Nrf2</sub> cells (**Figure 5B**), indicating that the observed reduction in pro-inflammatory cytokines release upon LPS stimulation, cannot be explained on the basis of the activation of Nrf2 pathway.

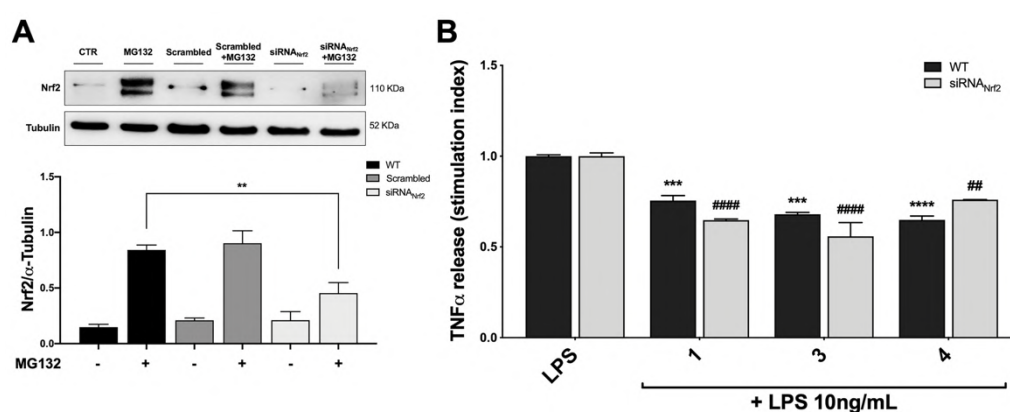


**Figure 5. Optimization of Nrf2-silenced THP-1 model (A) and effect of Nrf2-knockdown on modulation of TNF $\alpha$  release by compounds 1, 3 and 4, upon LPS stimulation (B).** (A) THP-1 cells were treated either with vehicle (WT), scrambled or siRNA<sub>Nrf2</sub> for 24 h. Where indicated MG132 was added 4 h before the end of the experiment to block the proteasomal degradation of Nrf2. After treatments, Nrf2 expression was determined in total protein extracts by Western blot analysis using an anti-Nrf2 antibody. Anti- $\alpha$ -tubulin was used as protein loading control. Results are shown as means of Nrf2/a-Tubulin ratio  $\pm$  SEM. Unpaired Student t-test;  $*p < 0.01$ ;  $n = 3$ . (B) TNF $\alpha$  amount was measured in the supernatants of THP-1 Nrf2-knockdown cells, treated with compounds 1, 3, and 4 at a concentration of 5  $\mu$ M for 24 h and then stimulated with 10 ng/mL LPS for 3 h. The protein secretion of TNF $\alpha$  was determined by ELISA. Data are shown as means of stimulation index  $\pm$  SEM. Dunnett's multiple comparison test;  $***p < 0.001$  and  $****p < 0.0001$  versus WT LPS;  $##p < 0.01$  and  $####p < 0.0001$  versus siRNA<sub>Nrf2</sub> LPS;  $n = 3$ .

### Modulation of the NF- $\kappa$ B Cellular Pathway by Compounds

To better understand the mechanism of action underlying the reduction of cytokines induced by compounds, we investigated their potential effect on the NF- $\kappa$ B pathway. Exposure of THP-1 cells to LPS from *E. coli* resulted in activation of the NF- $\kappa$ B transcription factor (Gomes *et al.*, 2015; Sakai *et al.*, 2017). To assess the effect of compounds on the NF- $\kappa$ B signaling pathway, we investigated the modulation of the upstream signaling molecule I $\kappa$ B $\alpha$ . In our experimental setting, THP-1 cells were treated with DMSO as vehicle control, compounds 1–4 and CURC at a concentration of 5  $\mu$ M and, then, stimulated for 45 min with 10 ng/mL LPS. The phosphorylation of I $\kappa$ B $\alpha$  was measured in whole cell lysates by Western blot analysis. As shown in **Figure 6A**, LPS stimulation markedly increased the level of p-I $\kappa$ B $\alpha$  compared to controls, whereas

treatments with compounds 2, 3, 4, and CURC significantly prevented I $\kappa$ B $\alpha$  phosphorylation, thus indicating that they might hinder the activation of the NF- $\kappa$ B pathway by preventing I $\kappa$ B $\alpha$  phosphorylation. Compound 1 did not produce statistically significant results in our experimental setting, although a slight trend to decrease in I $\kappa$ B $\alpha$  phosphorylation could be observed (**Figure 6A**).

To further evaluate the capability of compounds to influence NF- $\kappa$ B nuclear translocation, THP-1 cells were treated with vehicle, 5  $\mu$ M compounds 1–4 and CURC and, then, stimulated for 1 h and 30 min with 10 ng/mL LPS, as inflammatory stimulus promoting NF- $\kappa$ B nuclear translocation. Compounds 3 and 4, and CURC markedly suppressed NF- $\kappa$ B nuclear translocation, whereas compound 2 acted to a lower extent (**Figure 6B**). Compound 1 did not produce statistically significant results in our experimental setting, although a slight trend to decrease could be observed (**Figure 6B**).

Finally, we investigated the activation of the NF- $\kappa$ B promoter by luciferase assay. To evaluate whether compounds may exert a basal activity on NF- $\kappa$ B promoter, THP-1 cells were transiently transfected with pGL4.32 luciferase reporter construct, containing NF- $\kappa$ B-response elements (RE), and treated with vehicle, 5  $\mu$ M compounds 1–4 and CURC for 24 h and, then, analyzed for NF- $\kappa$ B luciferase. No difference in NF- $\kappa$ B luciferase activity between untreated and treated cells was observed, thus suggesting that compounds did not basally influence NF- $\kappa$ B pathways (**Figure 6C**). THP-1 cells were then stimulated with 10 ng/mL LPS for 6 h after treatment with vehicle and 5  $\mu$ M compounds 1–4 and CURC for 24 h. As reported in **Figure 6D**, upon LPS stimulation, NF- $\kappa$ B luciferase activity significantly increased, as expected, and treatments with compounds 2, 3, 4, and CURC significantly reduced it. In accordance with the slight effect on I $\kappa$ B $\alpha$  phosphorylation and NF- $\kappa$ B nuclear translocation, compound 1 did not hinder the activation of the NF- $\kappa$ B promoter, thus suggesting that the modulation of cytokine release by this molecule seems not to be driven by NF- $\kappa$ B signaling pathway (**Figure 6D**).

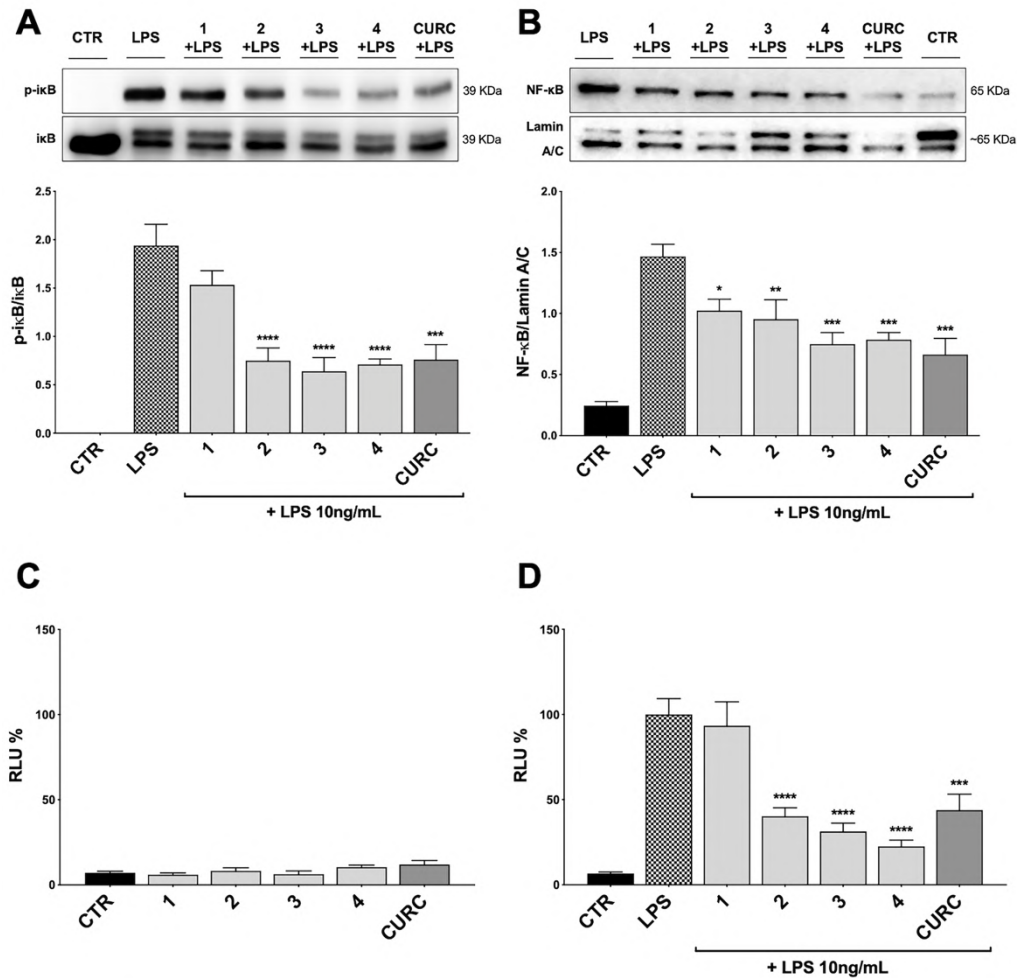


**Figure 6. Modulation of NF- $\kappa$ B pathway by compounds and CURC in LPS-stimulated THP-1 cells.** (A) THP-1 cells were treated with 5  $\mu$ M compounds 1–4 and CURC for 24 h and then stimulated with 10 ng/mL LPS for 45 min. After stimulation, p-I $\kappa$ B $\alpha$  expression was determined in total protein extracts by Western blot analysis, using an anti-p-I $\kappa$ B $\alpha$  antibody. Anti-I $\kappa$ B $\alpha$  (total) was used to normalize the data. Results are shown as means of p-I $\kappa$ B $\alpha$ /I $\kappa$ B $\alpha$  ratio  $\pm$  SEM. Dunnett's multiple comparison test; \*\*\* $p$  < 0.001 and \*\*\*\* $p$  < 0.0001 versus LPS;  $n$  = 5. (B) THP-1 cells were treated for 24 h with compounds 1–4 and CURC at a concentration of 5  $\mu$ M and then stimulated with 10 ng/mL LPS for 90 min. After isolation, nuclear extracts were examined by Western blot analysis and NF- $\kappa$ B expression was determined using an anti-NF- $\kappa$ B antibody. Anti-lamin A/C was used as protein loading control. Results are shown as means of NF- $\kappa$ B/Lamin A/C ratio  $\pm$  SEM. Dunnett's multiple comparison test; \* $p$  < 0.05, \*\* $p$  < 0.01 and \*\*\* $p$  < 0.001 versus LPS;  $n$  = 5. (C, D) THP-1 cells were transiently transfected with pGL4.32 [luc2P/NF- $\kappa$ B-RE/Hygro] Vector reporter construct, and subsequently treated with compounds 1–4 and CURC at a concentration of 5  $\mu$ M for 24 h. After treatments, the cells were stimulated (D) or not (C) with 10 ng/mL LPS for 6 h. For each condition, luciferase activity was expressed as RLU% and compared to CTR values assumed at 100%. Results are shown as means  $\pm$  SEM. Dunnett's multiple comparison test; \*\*\* $p$  < 0.001 and \*\*\*\* $p$  < 0.0001 versus LPS;  $n$  = 3.



### Differential Regulation of Innate Immune Cytokine Release in Human PBMCs From Healthy Donors

To further study the differential capability of compounds in modulating cytokine and chemokine release, we moved from THP-1 cells to human primary PBMCs from healthy donors. Human PBMCs were stimulated with 10 ng/mL LPS for 3 h after having been treated with vehicle and 5  $\mu$ M compounds 1–4 and CURC for 24 h. The release of a panel of the most common cytokines and chemokines [e.g. IFN $\gamma$ , IL-1 $\beta$ , IL-4, IL-6, IL-8, IL-12 (p40), IL-12 (p70), IL-13, IL-27, MCP-1, MCP-3, TNF $\alpha$ ] was measured in culture medium by Luminex X-MAP<sup>®</sup> technology. Protein release of IFN $\gamma$ , IL-4, IL-12 (p70), IL-13 and IL-27 was undetectable both in untreated and LPS-stimulated PBMCs from healthy donors, while, exposure of human PBMCs to LPS significantly increased protein release of IL-6, IL-8, IL-12 (p40), MCP-1, and TNF $\alpha$  compared to controls (**Table 2**). A differential regulation of cytokine and chemokine release by compounds was observed during immune stimulation. In particular, compounds 1 and CURC, significantly reduced the release of the pro-inflammatory cytokine IL-6 in LPS-stimulated human PBMCs. In accordance with preliminary results obtained in THP-1 cells, no effect on IL-8 release was observed for 1–4 and CURC, further indicating that all compounds, as well as CURC, did not influence the intracellular pathways regulating IL-8 release. In addition, compounds 1 and 2 significantly decreased IL-12 (p40) release in human PBMCs upon LPS stimulation (**Table 2**). No differences in IL-1 $\beta$  and MCP-3 release were observed between PBMCs that were stimulated by LPS, untreated, or treated with compounds or CURC PBMCs (**Table 2**). Interestingly, compounds 1, 2, and CURC were capable to significantly attenuate the release of the chemokine MCP-1 in LPS-stimulated PBMCs from healthy patients. In contrast, compounds 3 and 4 did not affect MCP-1 release, revealing the same activity trend observed for Nrf2 induction (**Table 2**). Notably, such results are consistent with evidence from literature reporting that, after innate immune stimulation, treatment of human PBMCs with Nrf2 activators, such as the Nrf2 agonist CDDO-Me (bardoxolone methyl), markedly reduced LPS-evoked MCP-1/ CCL2 production and that this effect was not specific to LPS- induced immune responses, as Nrf2 activation also reduced MCP-1/CCL2 production after stimulation with IL-6 (Eitas *et al.*, 2017). Furthermore, compound 4 and CURC confirmed their capability to significantly reduce TNF $\alpha$  release in LPS-stimulated PBMCs, as previously observed in the THP-1 cell line (**Table 2**).

	CTR	LPS10 ng/mL	Luminex xMAP® Technology				CURC+ LPS
			1+ LPS	2+ LPS	3+ LPS	4+ LPS	
IFN $\gamma$	Nd	Nd	Nd	Nd	Nd	nd	nd
IL-1 $\beta$	2.76 $\pm$ 0.56	2.43 $\pm$ 0.49	1.36 $\pm$ 0.14	1.58 $\pm$ 0.16	1.85 $\pm$ 0.30	2.59 $\pm$ 0.56	1.31 $\pm$ 0.17
IL-4	Nd	Nd	nd	Nd	Nd	nd	nd
IL-6	33.20 $\pm$ 6.38****	164.4 $\pm$ 12.1	129.2 $\pm$ 7.68*	139.9 $\pm$ 8.32	147.1 $\pm$ 10.5	156.0 $\pm$ 11.4	99.65 $\pm$ 6.71****
IL-8	1659 $\pm$ 178****	3349 $\pm$ 292	4012 $\pm$ 141	3272 $\pm$ 224	2794 $\pm$ 124	3026 $\pm$ 333	2665 $\pm$ 221
IL-12 (p40)	2.44 $\pm$ 0.14**	5.56 $\pm$ 0.57	2.40 $\pm$ 0.12**	3.28 $\pm$ 0.27*	4.82 $\pm$ 0.87	5.30 $\pm$ 0.90	3.61 $\pm$ 0.70
IL-12 (p70)	nd	Nd	nd	nd	Nd	nd	nd
IL-13	nd	Nd	nd	nd	Nd	nd	nd
IL-27	nd	Nd	nd	nd	nd	nd	nd
MCP-1	1149 $\pm$ 89.2*	1627 $\pm$ 139	899 $\pm$ 163**	819 $\pm$ 89.5****	1243 $\pm$ 125	1198 $\pm$ 105	625 $\pm$ 76.9****
MCP-3	38.9 $\pm$ 8.2	50.6 $\pm$ 8.9	36.7 $\pm$ 6.0	35.11 $\pm$ 5.7	43.0 $\pm$ 8.3	42.1 $\pm$ 6.9	25.3 $\pm$ 3.3
TNF $\alpha$	13.75 $\pm$ 2.76****	350.2 $\pm$ 18.6	264.8 $\pm$ 6.74	295.2 $\pm$ 18.7	328.3 $\pm$ 16.3	220.8 $\pm$ 31.1**	252.8 $\pm$ 38.6*

PBMCs were treated with compounds 1–4 and CURC at a concentration of 5  $\mu$ M for 24 h, and then stimulated with 10 ng/mL LPS for 3 h. IFN $\gamma$ , IL-1 $\beta$ , IL-4, IL-6, IL-8, IL-12 (p40), IL-12 (p70), IL-13, IL-27, MCP-1, MCP-3, TNF $\alpha$  protein release was measured in PBMC supernatants by Luminex xMAP® Technology. Data are presented as means of released picograms per mL (pg/mL)  $\pm$  SEM. Dunnett's multiple comparison test; \*p < 0.05; \*\*p < 0.01; \*\*\*p < 0.001 and \*\*\*\*p < 0.0001 versus LPS; n = 5.

**Table 2. Differential regulation of innate immune cytokine release in human PBMCs from healthy donors.**

## DISCUSSION

The transcription factor Nrf2 regulates a complex network of cellular responses to oxidative stress and inflammation. Cysteine residues of its repressor Keap1 act as sensor sites for Nrf2 electrophilic activators. Thus, we studied a set of previously synthesized compounds (1, 2, and 3), for which the ability to induce the Nrf2 pathway was strictly related to the (pro)-electrophilic character of the molecule in THP-1 cells, a widely used cellular model for the immune modulation approach (Chanput *et al.*, 2014). In agreement with previous results (Simoni *et al.*, 2017; Serafini *et al.*, 2019; Catanzaro *et al.*, 2020), a significant effect was detected for the Nrf2 inducers 1 and 2, carrying a catechol moiety and/or an  $\alpha,\beta$ -unsaturated carbonyl group, while no effect was observed for compound 3, lacking both (pro)-electrophilic features (Table 1). The same lack of effect was observed for compound 4, which was included in the study to exclude possible oxidative activation into electrophilic metabolites such as quinone methide, which could provide an additional site for adduct formation.

Based on these results, we investigated the potential effects of the compounds on the secretion of pro-inflammatory cytokines upon immune stimulation (e.g. LPS from *E. coli*) in the same cellular model. We found that both compounds which induced Nrf2 (1 and 2) as well as compounds inactive on the Nrf2 pathway (3 and 4) were capable to attenuate the release of the pro-inflammatory cytokines TNF $\alpha$  (Figure 3A) and IL-1 $\beta$  (Figure 4B), but not IL-8 secretion (Figure 3B), thus suggesting that the reduction of cytokine release by compounds could not be directly ascribed to the activation of Nrf2 pathway. Accordingly, the ability of compounds to attenuate the secretion of TNF $\alpha$ , upon immune stimulation,

was also observed after siRNA mediated Nrf2 knockdown (**Figure 5**). To further dissect the molecular mechanism underlying the reduction of cytokine release induced by compounds 1–4, we investigated their potential interplay with other signaling cascades, specifically focusing on the NF- $\kappa$ B pathway, a pivotal mediator of inflammatory responses and critical regulator of multiple aspects of innate and adaptive immune functions (Häcker and Karin, 2006; Perkins, 2007). All compounds, with the exception of compound 1, significantly attenuated the LPS-induced activation of the NF- $\kappa$ B canonical pathway, by impairing the upstream phosphorylation of I $\kappa$ B $\alpha$ , NF- $\kappa$ B nuclear translocation, as well as the activation of the NF- $\kappa$ B promoter (**Figure 5**). As a consequence, the ability of compounds 2, 3, and 4 to reduce the activation of NF- $\kappa$ B pathway may account, at least in part, for their observed effect on pro-inflammatory cytokine release. Notably, both Nrf2 and NF- $\kappa$ B offer unique patterns of thiol modifications, indicating electrophilic signaling mediators as a valuable instrument to control their redox-sensitive transcriptional regulatory function. However, while a (pro)-electrophilic feature is required for Nrf2 induction, suggesting covalent adduction as the triggering event, both (pro)- electrophile 2 and non-electrophilic compounds 3 and 4 were able to inhibit NF- $\kappa$ B activation, revealing a different mode of interaction (**Figure 7**).

### Nrf2 activation

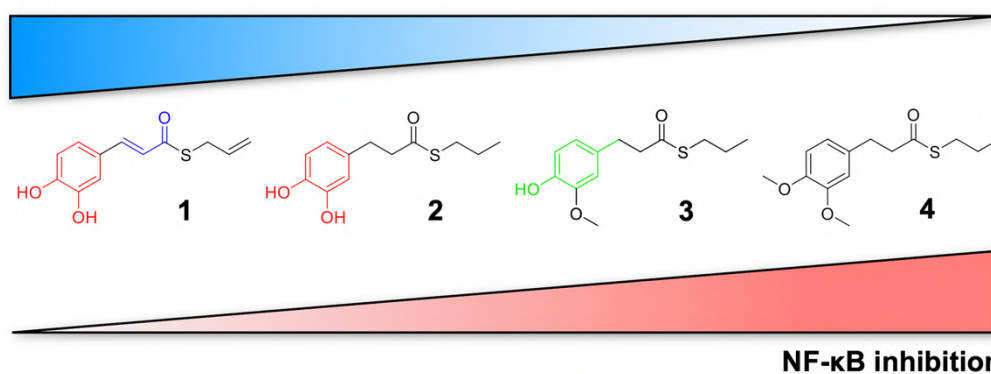


**Figure 7. Differential modulation of Nrf2 and NF- $\kappa$ B intracellular signaling pathways by compounds.** Electrophile 1, carrying both the catechol moiety (red) and the  $\alpha,\beta$ -unsaturated carbonyl group (blue), is the most active Nrf2 inducer, while being devoid of activity on NF- $\kappa$ B pathway. Conversely, the non-electrophilic compound 4, synthesized to exclude eventual oxidative transformation of the methoxyphenol ring (green) of 3 into reactive metabolites, is the most potent NF- $\kappa$ B inhibitor, with no impact on Nrf2 activation.

Noteworthy, compound 1, carrying both the catechol moiety and the  $\alpha,\beta$ -unsaturated carbonyl group, was unable to significantly modulate the NF- $\kappa$ B pathway. The modulation of cytokine release by this molecule might be, at least in part, related to anti-inflammatory

effect mediated by the induction of Nrf2 targets, such as HO-1 (Roach *et al.*, 2009). Accordingly, HO-1 expression has been demonstrated to decrease the LPS-stimulated secretion of cytokines and chemokines such as MCP-1, IL-6, IL-10, and TNF $\alpha$  in murine and human macrophages (Roach *et al.*, 2009). Altogether, these results indicate that an electrophilic moiety is neither necessary nor per se sufficient to guarantee inhibition of the pro-inflammatory transcriptional activity of NF- $\kappa$ B, with shape complementarity emerging as a plausible feature of target recognition. The different biological behavior of electrophiles 1 and 2, which only varies in the presence or absence of two double bonds, might indeed reflect the more constrained conformation assumed by compound 1 with respect to flexible compound 2. The conjugation extended throughout most of the backbone stabilized compound 1 in a planar conformation, as opposed to the sp<sup>3</sup> counterparts which manifested a maximum in energy for the same state (**Supplementary Figure 2**). Moreover, the possibility for compounds 2-4 to populate several conformations due to lower energy barriers might indicate that a conformational selection or induced fit effect in the ligand is necessary to execute the desired activity. The overall effects of compounds 1–4 on Nrf2 and NF- $\kappa$ B intracellular pathways were summarized in **Figure 8**.

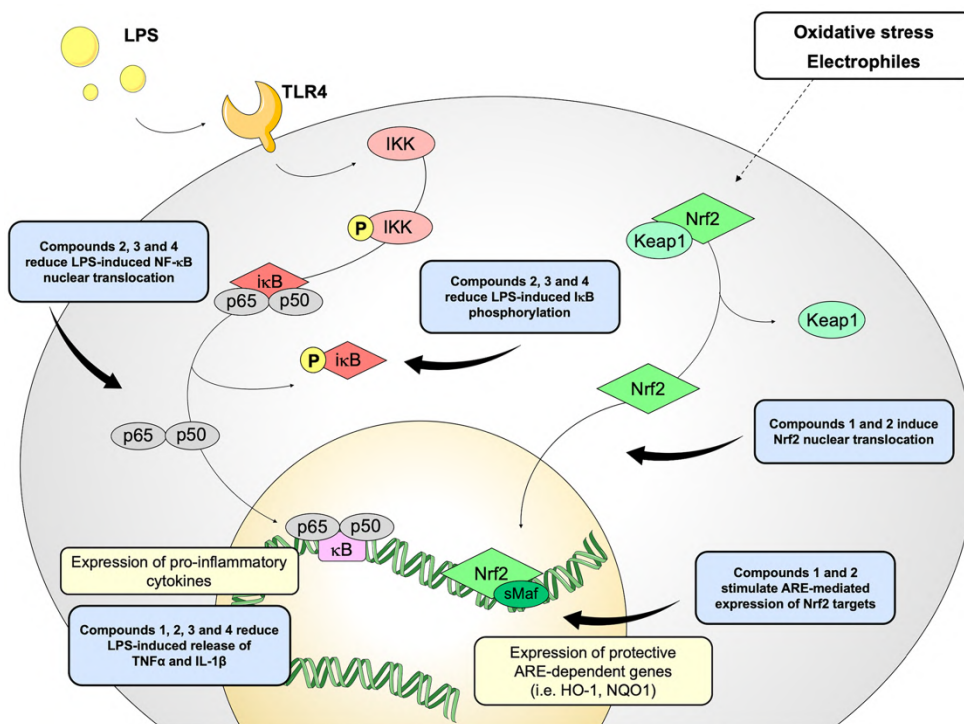


**Figure 8.** Schematic representation of the effects induced by compounds 1–4 on Nrf2 and NF- $\kappa$ B pathways.

When moving in a human primary model, by Luminex X- MAP<sup>®</sup> technology, we screened the effects of compounds on a panel of cytokines and chemokines (e.g. IFN $\gamma$ , IL-1 $\beta$ , IL-4, IL-6, IL-8, IL-12 (p40), IL-12 (p70), IL-13, IL-27, MCP-1, MCP-3, TNF $\alpha$ ) in order to unveil their potential modulatory effect on other inflammatory mediators (**Table 2**). Compared to data observed in THP-1 cells, we found a differential regulation of innate immune cytokine production by compounds, in line with previous data (Schildberger *et al.*, 2013). In particular, compounds 1 and CURC significantly reduced the secretion of the pro-inflammatory cytokine IL-6 in LPS-stimulated human PBMCs, while compound 4 and CURC attenuated TNF $\alpha$  release (**Table 2**). Furthermore, compounds acting as Nrf2 inducers (1 and 2) also suppressed the secretion of IL-12 (p40), corroborating the hypothesis that inhibition of IL-12 expression may be mediated by Nrf2 activation, as suggested by Macoch *et al.* (2015). Consistently, tert-butylhydroquinone, a well-known Nrf2 inducer, has been reported to activate Nrf2 and to inhibit the induction of IL-12 expression by LPS (Macoch *et al.*, 2015). However, further investigations are required to unravel the molecular mechanism by which Nrf2 represses IL-12 production and secretion.

In human PBMCs, we further found that only compounds acting as Nrf2 inducers (1 and 2) significantly suppressed the release of MCP-1, after LPS stimulation (**Table 2**). In accordance with data from the literature (Eitas *et al.*, 2017), this result indicates that MCP-1 production may rely on activation of the transcription factor Nrf2. Thus, the effect of Nrf2 inducers on MCP-1/CCL2 suggests a novel aspect of Nrf2 pharmacological activation as a regulator of key immunomodulatory functions. This finding represents a potentially generalizable aspect of pharmacological Nrf2 activation occurring with different stimuli (e.g. LPS, IL-6) and consistent across more than 60 individual human samples, as reported by Eitas *et al.* (2017). Thus, contrary to the prevalent view that Nrf2 represses inflammatory processes through redox control, we demonstrated that Nrf2 activation also directly counteracts the production of a key chemokine, by possibly regulating the expression of its encoding gene. Such hypothesis is consistent with data reporting Nrf2-mediated downregulation of proinflammatory mediator gene expression (Kobayashi *et al.*, 2016). However, the precise molecular mechanism underlying Nrf2 and MCP-1 crosstalk is still elusive. Interestingly, by regulating the production of the chemokine MCP-1, Nrf2 can be considered an upstream regulator of MCP-1 production, thereby providing a molecular basis for a Nrf2-mediated anti-inflammatory approach. In this regard, elevated systemic MCP-1 system levels have been linked to worse outcomes in patients with cardiovascular disease (Martín-Ventura *et al.*, 2009), and pulmonary accumulation of MCP-1 has been reported in patients with acute respiratory distress syndrome (Rosseau *et al.*, 2000). Hence, targeting transcriptional accumulation of MCP-1 through pharmacological Nrf2 activation may represent a promising therapeutic approach.

Although the THP-1 and human PBMCs response can hint to potential responses that may occur *in vivo*, these results need to be validated in *in vivo* studies to draw more definite conclusions. Moreover, further mechanistic investigations are required to unravel the biological connection among Nrf2 activation, innate immune cytokine production, and the regulation of the NF- $\kappa$ B pathway.

#### **SUPPLEMENTARY MATERIAL**

The Supplementary Material for this article can be found online at: <https://www.frontiersin.org/articles/10.3389/fphar.2020.01256/full#supplementary-material>.

#### **REFERENCES**

- Baeuerle, P. A., and Baltimore, D. (1996). NF-kappa B: ten years after. *Cell* 87, 13– 20. doi: 10.1016/s0092-8674(00)81318-5
- Basagni, F., Lanni, C., Minarini, A., and Rosini, M. (2019). Lights and shadows of electrophile signaling: focus on the Nrf2-Keap1 pathway. *Future Med. Chem.* 11, 707–721. doi: 10.4155/fmc-2018-0423
- Binkley, J. S., Pople, J. A., and Hehre, W. J. (1980). Self-consistent molecular orbital methods. 21. Small split-valence basis sets for first-row elements. *J. Am. Chem. Soc.* 102, 939–947. doi: 10.1021/ja00523a008
- Buoso, E., Ronfani, M., Galasso, M., Ventura, D., Corsini, E., and Racchi, M. (2019). Cortisol-induced SRSF3 expression promotes GR splicing, RACK1 expression and breast cancer cells migration. *Pharmacol. Res.* 143, 17–26. doi: 10.1016/j.phrs.2019.03.008
- Catanzaro, M., Lanni, C., Basagni, F., Rosini, M., Govoni, S., and Amadio, M. (2020). Eye-Light on Age-Related Macular Degeneration: Targeting Nrf2-Pathway as a Novel Therapeutic Strategy for Retinal Pigment Epithelium. *Front. Pharmacol.* 11, 844. doi: 10.3389/fphar.2020.00844
- Chanput, W., Mes, J. J., and Wichers, H. J. (2014). THP-1 cell line: an *in vitro* cell model for immune modulation approach. *Int. Immunopharmacol.* 23, 37–45. doi: 10.1016/j.intimp.2014.08.002
- D'amico, R., Fusco, R., Gugliandolo, E., Cordaro, M., Siracusa, R., Impellizzeri, D., *et al.* (2019). Effects of a new compound containing Palmitoylethanolamide and Baicalein in myocardial ischaemia/reperfusion injury *in vivo*. *Phytomed. Int. J. Phytother. Phytopharm.* 54, 27–42. doi: 10.1016/j.phymed.2018.09.191
- Eitas, T. K., Stepp, W. H., Sjeklocha, L., Long, C. V., Riley, C., Callahan, J., *et al.* (2017). Differential regulation of innate immune cytokine production through pharmacological activation of Nuclear Factor-Erythroid-2-Related Factor 2 (NRF2) in burn patient immune cells and monocytes. *PLoS One* 12, e0184164. doi: 10.1371/journal.pone.0184164
- Fusco, R., Gugliandolo, E., Biundo, F., Campolo, M., Di Paola, R., and Cuzzocrea, S. (2017). Inhibition of inflammasome activation improves lung acute injury induced by carrageenan in a mouse model of pleurisy. *FASEB J.* 31, 3497– 3511. doi: 10.1096/fj.201601349R
- Gomes, A., Capela, J. P., Ribeiro, D., Freitas, M., Silva, A. M. S., Pinto, D. C. G. A., *et al.* (2015). Inhibition of NF- $\kappa$ B activation and cytokines production in THP-1 monocytes by 2-styrylchromones. *Med. Chem. Shariqah United Arab Emir.* 11, 560–566. doi: 10.2174/1573406411666150209114702
- Häcker, H., and Karin, M. (2006). Regulation and function of IKK and IKK-related kinases. *Sci. STKE Signal Transduction Knowl. Environ.* 2006, re13. doi: 10.1126/stke.3572006re13
- Hayden, M. S., West, A. P., and Ghosh, S. (2006). NF- $\kappa$ B and the immune response. *Oncogene* 25, 6758–6780. doi: 10.1038/sj.onc.1209943

- Hayes, J. D., and Dinkova-Kostova, A. T. (2014). The Nrf2 regulatory network provides an interface between redox and intermediary metabolism. *Trends Biochem. Sci.* 39, 199–218. doi: 10.1016/j.tibs.2014.02.002
- Iizuka, T., Ishii, Y., Itoh, K., Kiwamoto, T., Kimura, T., Matsuno, Y., *et al.* (2005). Nrf2-deficient mice are highly susceptible to cigarette smoke-induced emphysema. *Genes Cells Devoted Mol. Cell. Mech.* 10, 1113–1125. doi: 10.1111/ j.1365-2443.2005.00905.x
- Innamorato, N. G., Rojo, A.II, García -Yaguë, A. J., Yamamoto, M., de Ceballos, M. L., and Cuadrado, A. (2008). The transcription factor Nrf2 is a therapeutic target against brain inflammation. *J. Immunol. Baltim. Md* 1950 181, 680–689. doi: 10.4049/jimmunol.181.1.680
- Ishii, Y., Itoh, K., Morishima, Y., Kimura, T., Kiwamoto, T., Iizuka, T., *et al.* (2005). Transcription factor Nrf2 plays a pivotal role in protection against elastase- induced pulmonary inflammation and emphysema. *J. Immunol. Baltim. Md* 1950 175, 6968–6975. doi: 10.4049/jimmunol.175.10.6968
- Kastrati, I., Siklos, M.II, Calderon-Gierszal, E. L., El-Shennawy, L., Georgieva, G., Thayer, E. N., *et al.* (2016). Dimethyl Fumarate Inhibits the Nuclear Factor  $\kappa$ B Pathway in Breast Cancer Cells by Covalent Modification of p65 Protein. *J. Biol. Chem.* 291, 3639–3647. doi: 10.1074/jbc.M115.679704
- Knatko, E. V., Ibbotson, S. H., Zhang, Y., Higgins, M., Fahey, J. W., Talalay, P., *et al.* (2015). Nrf2 Activation Protects against Solar-Simulated Ultraviolet Radiation in Mice and Humans. *Cancer Prev. Res. Phila. Pa* 8, 475–486. doi: 10.1158/1940-6207.CAPR-14-0362
- Kobayashi, M., and Yamamoto, M. (2006). Nrf2-Keap1 regulation of cellular defense mechanisms against electrophiles and reactive oxygen species. *Adv. Enzyme Regul.* 46, 113–140. doi: 10.1016/j.advenzreg.2006.01.007
- Kobayashi, E. H., Suzuki, T., Funayama, R., Nagashima, T., Hayashi, M., Sekine, H., *et al.* (2016). Nrf2 suppresses macrophage inflammatory response by blocking proinflammatory cytokine transcription. *Nat. Commun.* 7:11624. doi: 10.1038/ ncomms11624
- Kohn, W., and Sham, L. J. (1965). Self-Consistent Equations Including Exchange and Correlation Effects. *Phys. Rev.* 140, A1133–A1138. doi: 10.1103/PhysRev.140.A1133
- Kumar, P., Nagarajan, A., and Uchil, P. D. (2018). Analysis of Cell Viability by the MTT Assay. *Cold Spring Harb. Protoc.* 2018. doi: 10.1101/pdb.prot095505
- Le Page, A., Garneau, H., Dupuis, G., Frost, E. H., Larbi, A., Witkowski, J. M., *et al.* (2017). Differential Phenotypes of Myeloid-Derived Suppressor and T Regulatory Cells and Cytokine Levels in Amnestic Mild Cognitive Impairment Subjects Compared to Mild Alzheimer Diseased Patients. *Front. Immunol.* 8:783. doi: 10.3389/fimmu.2017.00783
- Luis, P. B., Boeglin, W. E., and Schneider, C. (2018). Thiol Reactivity of Curcumin and Its Oxidation Products. *Chem. Res. Toxicol.* 31, 269–276. doi: 10.1021/ acs.chemrestox.7b00326



- Macoch, M., Morzadec, C., Génard, R., Pallardy, M., Kerdine-Römer, S., Fardel, O., *et al.* (2015). Nrf2-dependent repression of interleukin-12 expression in human dendritic cells exposed to inorganic arsenic. *Free Radic. Biol. Med.* 88, 381–390. doi: 10.1016/j.freeradbiomed.2015.02.003
- Martín-Ventura, J.L., Blanco-Colio, L.M., Tuñón, J., Muñoz-García, B., Madrigal-Matute, J., Moreno, J. A., *et al.* (2009). Biomarkers in cardiovascular medicine. *Rev. Esp. Cardiol.* 62, 677–688. doi: 10.1016/s1885-5857(09)72232-7
- Møller, C., and Plesset, M. S. (1934). Note on an Approximation Treatment for Many-Electron Systems. *Phys. Rev.* 46, 618–622. doi: 10.1103/PhysRev.46.618
- Niture, S. K., Khatri, R., and Jaiswal, A. K. (2014). Regulation of Nrf2—an update. *Free Radic. Biol. Med.* 66, 36–44. doi: 10.1016/j.freeradbiomed.2013.02.008
- Pawelec, G., Ferguson, F. G., and Wikby, A. (2001). The SENIEUR protocol after 16 years. *Mech. Ageing Dev.* 122, 132–134. doi: 10.1016/s0047-6374(00)00240-2
- Perkins, N. D. (2007). Integrating cell-signalling pathways with NF-kappaB and IKK function. *Nat. Rev. Mol. Cell Biol.* 8, 49–62. doi: 10.1038/nrm2083
- Petersson, G. A., and Al-Laham, M. A. (1991). A complete basis set model chemistry. II. Open-shell systems and the total energies of the first-row atoms. *J. Chem. Phys.* 94, 6081–6090. doi: 10.1063/1.460447
- Quinti, L., Dayalan Naidu, S., Träger, U., Chen, X., Kegel-Gleason, K., Llères, D., *et al.* (2017). KEAP1-modifying small molecule reveals muted NRF2 signaling responses in neural stem cells from Huntington's disease patients. *Proc. Natl. Acad. Sci. U. S. A.* 114, E4676–E4685. doi: 10.1073/pnas.1614943114
- Roach, J. P., Moore, E. E., Partrick, D. A., Damle, S. S., Silliman, C. C., McIntyre, R. C., *et al.* (2009). Heme oxygenase-1 induction in macrophages by a hemoglobin-based oxygen carrier reduces endotoxin-stimulated cytokine secretion. *Shock Augusta Ga* 31, 251–257. doi: 10.1097/SHK.0b013e3181834115
- Rosseau, S., Hammerl, P., Maus, U., Walmrath, H. D., Schütte, H., Grimminger, F., *et al.* (2000). Phenotypic characterization of alveolar monocyte recruitment in acute respiratory distress syndrome. *Am. J. Physiol. Lung Cell. Mol. Physiol.* 279, L25–L35. doi: 10.1152/ajplung.2000.279.1.L25
- Sakai, J., Cammarota, E., Wright, J. A., Cicuta, P., Gottschalk, R. A., Li, N., *et al.* (2017). Lipopolysaccharide-induced NF- $\kappa$ B nuclear translocation is primarily dependent on MyD88, but TNF $\alpha$  expression requires TRIF and MyD88. *Sci. Rep.* 7, 1428. doi: 10.1038/s41598-017-01600-y
- Satoh, T., McKercher, S. R., and Lipton, S. A. (2013). Nrf2/ARE-mediated antioxidant actions of pro-electrophilic drugs. *Free Radic. Biol. Med.* 65, 645–657. doi: 10.1016/j.freeradbiomed.2013.07.022

Schildberger, A., Rossmannith, E., Eichhorn, T., Strassl, K., and Weber, V. (2013). Monocytes, peripheral blood mononuclear cells, and THP-1 cells exhibit different cytokine expression patterns following stimulation with lipopolysaccharide. *Mediators Inflamm.* 2013, 697972. doi: 10.1155/2013/697972

Serafini, M. M., Catanzaro, M., Fagiani, F., Simoni, E., Caporaso, R., Dacrema, M., *et al.* (2019). Modulation of Keap1/Nrf2/ARE Signaling Pathway by Curcuma- and Garlic-Derived Hybrids. *Front. Pharmacol.* 10, 1597. doi: 10.3389/fphar.2019.01597

Simoni, E., Serafini, M. M., Bartolini, M., Caporaso, R., Pinto, A., Necchi, D., *et al.* (2016). Nature-Inspired Multifunctional Ligands: Focusing on Amyloid-Based Molecular Mechanisms of Alzheimer's Disease. *ChemMedChem* 11, 1309–1317. doi: 10.1002/cmde.201500422

Simoni, E., Serafini, M.M., Caporaso, R., Marchetti, C., Racchi, M., Minarini, A., *et al.* (2017). Targeting the Nrf2/Amyloid-Beta Liaison in Alzheimer's Disease: A Rational Approach. *ACS Chem. Neurosci.* 8, 1618–1627. doi: 10.1021/acschemneuro.7b00100

Tanigawa, S., Fujii, M., and Hou, D.-X. (2007). Action of Nrf2 and Keap1 in ARE- mediated NQO1 expression by quercetin. *Free Radic. Biol. Med.* 42, 1690–1703. doi: 10.1016/j.freeradbiomed.2007.02.017

Thimmulappa, R. K., Lee, H., Rangasamy, T., Reddy, S. P., Yamamoto, M., Kensler, T. W., *et al.* (2006). Nrf2 is a critical regulator of the innate immune response and survival during experimental sepsis. *J. Clin. Invest.* 116, 984–995. doi: 10.1172/JCI25790

Wardyn, J. D., Ponsford, A. H., and Sanderson, C. M. (2015). Dissecting molecular crosstalk between Nrf2 and NF- $\kappa$ B response pathways. *Biochem. Soc Trans.* 43, 621–626. doi: 10.1042/BST20150014

Woodcock, C.-S. C., Huang, Y., Woodcock, S. R., Salvatore, S. R., Singh, B., Golin- Bisello, F., *et al.* (2018). Nitro-fatty acid inhibition of triple-negative breast cancer cell viability, migration, invasion, and tumor growth. *J. Biol. Chem.* 293, 1120–1137. doi: 10.1074/jbc.M117.814368

---

**CHAPTER III**

Study of gene environment interactions contributing  
to autism spectrum disorders



## PART 1

The following manuscript is currently under review in *Environmental Health Perspectives* as:

### **Gene environment interactions in developmental neurotoxicity - a case study of synergy between chlorpyrifos and CHD8 knockout in human BrainSpheres**

Sergio Modafferi, Xiali Zhong, Andre Kleensang, Yohei Murata, **Francesca Fagiani**, David Pamies, Helena T. Hogberg, Vittorio Calabres, Herbert Lachman, Thomas Hartung and Lena Smirnova

#### **Abstract**

**Background:** Autism spectrum disorder (ASD) is a major public health concern caused by complex genetic and environmental components. The reliable and sensitive biomarkers for early detection, diagnosis of ASD and biomarkers of chemical exposure are still controversial. Using induced pluripotent stem cells (iPSC) from patients or CRISPR/Cas9 generated mutations in candidate genes for neurodevelopmental disorders, provide an opportunity to study gene-environment interactions (GxE).

**Objectives:** To identify a potential synergy between mutation in high-risk autism gene encoding chromodomain helicase DNA binding protein 8 (*CHD8*) and environmental exposure to organophosphate pesticide (chlorpyrifos) in iPSC-derived human 3D brain model.

**Methods:** This study pioneers GxE using human iPSC-derived BrainSpheres with a CRISPR/Cas9-introduced inactivating mutation in *CHD8*, exposed to chlorpyrifos (CPF)/its oxon-metabolite (CPO), and validation against metabolic derangements in human data. Neural differentiation, viability, oxidative stress, neurite outgrowth, level of main neurotransmitters and selected metabolites were assessed.

**Results:** CHD8 protein was significantly reduced in *CHD8* heterozygous knockout (*CHD8*<sup>+/-</sup>) BrainSpheres compared to *CHD8*<sup>+/+</sup> derived BrainSpheres and in response to CPF/CPO treatment. Neurite outgrowth was also perturbed. The toxicity of CPF/CPO and their synergy with *CHD8*<sup>+/-</sup> extended to a number of mechanistic aspects, which are considered key elements in the rather incomplete adverse outcome pathway (AOP) of ASD. Metabolic perturbations reported in patients were in part reflected in *CHD8*<sup>+/-</sup> spheroids: lower GABA, dopamine, stronger decrease in choline, and increase in SAM, SAH, tryptophan, kynurenic acid, lactic acid, and α-hydroxyglutaric acid upon treatment with CPF/CPO.

**Discussion:** This strategy enables biomonitoring and environmental risk assessment for ASD. A novel approach for validation of the model has been chosen. From literature we identified a panel of metabolic biomarkers in patients and assessed them by targeted metabolomics *in vitro*. Some synergistic effects of genetic background and exposure stress the validity of this model.

**Keywords:** Gene-environment interactions (GxE), autism spectrum disorders, organotypic cell culture, validation, metabolomics

## Introduction

ASD includes a cluster of neurodevelopmental conditions characterized by variable deficits in social communication and interaction, as well as restricted, stereotyped, and repetitive interests and behaviors (Lai *et al.* 2014; Mandy and Lai 2016). Individuals with ASD may show a broad range of comorbidities: epilepsy, attention deficits, intellectual disability, gastrointestinal problems, and diverse motor cognitive and mood impairments – all of which contribute to clinical heterogeneity (Courchesne *et al.* 2019). ASD is a major public health concern, as its prevalence is currently estimated at ~1.5% in developed countries (Baxter *et al.* 2015; Lyall *et al.* 2017).

Genome-wide association and large-scale sequencing studies have identified hundreds of ASD risk loci with common and/or rare risk variants, highlighting the heterogeneity of ASD genetic architecture (Rubeis *et al.* 2014; Sanders 2015; Sanders *et al.* 2015; Satterstrom *et al.* 2020; Vorstman *et al.* 2017; Willsey *et al.* 2013). High-confidence genes were identified and predicted to be involved in pathways affected in ASD (Ayhan and Konopka 2019). However, it was established that overall genetic effects account for ~59% of the etiological contribution to ASD, leaving a substantial role for environment-mediated effects (Gaugler *et al.* 2014). It is now generally believed that diverse (epi)genetic factors, environmental factors, and gene-environment interaction (GxE) increase autism risk (Chaste *et al.* 2012; Dietert *et al.* 2011; Karimi *et al.* 2017; Kim *et al.* 2019; Koufaris and Sismani 2015; LaSalle 2013; Lyall *et al.* 2017; Modabbernia *et al.* 2017; Peter *et al.* 2015; Rossignol *et al.* 2014). How environmental factors and genetic susceptibilities can interplay to increase ASD risk remains mostly unknown.

For many years, autism research relied on animal models. Rodent and human brain development, however, differ significantly (Lancaster *et al.* 2013). Animal-based models have shown low predictivity for human health (Halladay *et al.* 2009; Hartung 2013, 2017). The emerging 3D human organoid-based culture systems (especially those derived from induced pluripotent stem cells (iPSC)) promise the possibility of GxE testing at a cellular and molecular level in human-relevant models (Yang and Shcheglovitov 2020). The CRISPR/Cas9 genome-editing of iPSC further strengthens these models by enabling the generation of gain- and loss-of-function mutation in the risk genes, which greatly facilitates interpretation of the effects of risk alleles on neuronal function (Wang *et al.* 2017).

ASD susceptibility genes converge during certain period of the development and on certain specific biological pathways, including transcription/chromatin remodeling complexes, and synaptic function (Modabbernia *et al.* 2017). Some environmental chemicals can

interact with these pathways (Stamou *et al.* 2013). Loss-of-function mutations in such regulator genes can initiate developmental network dysregulations, causing ASD (Ayhan and Konopka 2019). The *CHD8* gene is an example of high risk ASD gene (Cotney *et al.* 2015; Neale *et al.* 2012; Stolerman *et al.* 2016). CHD8 is an ATP-dependent protein that represses transcription by altering nucleosome positioning and regulates a network of genes critical for early neurodevelopment (Bernier *et al.* 2014). Studies in cell and animal models demonstrated that *CHD8* mutations modulate other genes involved in ASD, affecting global developmental, neural differentiation, and brain volume (Bernier *et al.* 2014; Cotney *et al.* 2015; Sugathan *et al.* 2014; Wang *et al.* 2015). Cerebral organoids derived from iPSCs with a *CHD8* null mutation, for example, showed that CHD8 affects GABAergic interneuron development consistent with abnormalities in cortical GABA interneuron function found in a subgroup of ASD (Wang *et al.* 2017).

Organophosphorus pesticides (OP) such as chlorpyrifos (CPF) are widely used, but there is increasing concern about their adverse effects on the developing nervous system (Juberg *et al.* 2019; Mie *et al.* 2018; Rauh *et al.* 2006; Stamou *et al.* 2013). Several studies have suggested that chronic exposure to low levels of OP cause behavioral and cognitive deficits in children, and OP residues have been found in blood and urine of most children sampled in the U.S. (Barr *et al.* 2005). Exposure to OP, especially during the second and third trimester of pregnancy, was associated with an increased risk of ASD in offspring (Shelton *et al.* 2014). Although the mechanism underlying the risk of ASD upon OP exposure is unknown, it has been suggested that OP might affect expression and function of ASD risk genes to derail normal neurodevelopment. Whether there exists a particularly vulnerable subpopulation at greater risk for pesticide exposure remains to be clarified using GxE studies (Stamou *et al.* 2013).

Here, we aimed to address the GxE hypothesis in ASD by using an iPSC-derived brain organoid model (BrainSpheres) with a CRISPR/Cas9 engineered *CHD8* heterozygous knockout, and exposure to CPF. To account for limiting xenobiotic metabolism *in vitro*, active metabolite chlorpyrifos-oxon (CPO) was also included. A literature survey identified adverse outcome pathways (AOPs) and an array of putative biomarkers of metabolic perturbation in individuals with ASD. Which of these perturbations, we asked, can be reproduced with either a prominent ASD-risk genetic alteration, or environmental exposure, as well as their combination? Though a broad alignment of metabolic perturbation cannot be expected when using just one genetic and one chemical exposure agent, the actual usefulness of such models in a testing strategy depends on the fidelity of their representation of relevant human pathophysiology and its biomarkers.



## Methods

### BrainSphere differentiation

*CHD8*<sup>+/+</sup> and *CHD8*<sup>+/-</sup> neural progenitor cells (NPC) were generated previously from the *iPS-2C1* and *iPS-2C4G1C4* lines, respectively, authenticated and characterized (Wang *et al.* 2015). NPC were mycoplasma-negative upon receipt at CAAT laboratory. NPC were expanded in poly-L-ornithine and laminin-coated 175 cm<sup>2</sup> flask in NPC medium (KO DMEM/F12 medium, 5% Pen/Strep, 1x Stempro, 2 x glutamax, 0.02 µg/ml FGF and 0.02 µg/ml EGF (all reagents from ThermoFisher Scientific). Half of the medium was changed every day.

For BrainSpheres, 2x10<sup>6</sup> NPC were plated per-well in non-coated 6-well plates and cultured under constant gyratory shaking (88 rpm, 19 mm orbit) in NPC medium. After 48 hours, medium was changed to differentiation medium (Neurobasal<sup>®</sup> electro Medium (ThermoFisher Scientific), 5% Pen/Strep, 2 x glutamax, 1 x B-27 electro (ThermoFisher Scientific), 0.02 µg/ml GDNF (Gemini) and 0.02 µg/ml BDNF (Gemini)). Cultures were maintained under constant gyratory shaking for up to 8 weeks. Differentiation medium was changed every second day. See (Pamies *et al.* 2017) for details and characterization of the BrainSpheres.

### Chlorpyrifos and clorpyrifos-oxon treatment, cytotoxicity assay

For all experiments, BrainSpheres were exposed to 100 µM CPF or CPO (Sigma-Aldrich) for 24 hours at 4 weeks of differentiation. For viability, 8-week time point was included, as well as a concentration of 47 µM. DMSO (<0.01%) was used as vehicle controls. For viability measurements, BrainSpheres were plated in a 24-well plate for exposure. Four and 8-week spheroids were exposed to vehicle, 47 and 100 µM CPF or its oxon (CPO). After 24 h exposure, resazurin reduction assay was performed (Harris *et al.* 2017). Viability was measured in three independent experiments with three technical replicates per run.

### Measurement of mitochondria membrane potential (MMP) and reactive oxygen species (ROS)

MMP was assessed using Mitotracker<sup>®</sup> Red CMXRos<sup>™</sup> (ThermoFisher Scientific) and images were taken with ECHO laboratories Revolve microscope with 4/0.13 magnification objective and quantified with ImageJ (<https://fiji.sc/#>), as previously described in details (Harris *et al.* 2017). MMP was assessed in at least seven spheroids per condition in three

independent experiments. ROS were assessed by CellROX™ Green Reagent (ThermoFisher Scientific) and quantified with flow cytometry. Briefly, BrainSpheres were treated with 5  $\mu$ M CellROX™ Green Reagent for 30 min. Spheroids were washed three times with Hibernate E medium (Gibco) and dissociated with Collagenase IV/Papain/DNase to a single cell suspension as described in (Fan *et al.* 2018). Levels of ROS were measured on BD LSRII flow cytometer using Diva software. Unstained cells were used for gating. Data from three independent experiments was analyzed with FlowJo and presented as Mean  $\pm$  SEM.

### RNA extraction and Real-Time PCR

Total RNA was extracted using Trizol (ThermoFisher Scientific) and concentrated using RNA clean and concentrator kit (Zymo Research). RNA quantity and purity were determined using NanoDrop 2000c. 500 ng of RNA was reverse-transcribed using the M-MLV Reverse Transcriptase and Random Hexamer primers (Promega) according to the manufacturer's instructions. The expression of genes was evaluated using TaqMan gene expression assay (Applied Biosystems) or SYBRGreen assay listed in **Tables S1, S2**. Real-Time qPCR was performed using a 7500 Fast Real-Time system machine (Applied Biosystems). GAPDH or 18S were used as housekeeping genes. To demonstrate gene expression levels during differentiation, RT-PCR results were presented as  $2^{-\Delta C_t}$ . Fold changes were calculated using the  $2^{-\Delta\Delta C_t}$  method, if gene expression was compared between treated and control samples and between cell lines. All  $2^{-\Delta\Delta C_t}$  values were normalized to vehicle treated controls of the *CHD8*<sup>+/+</sup> cell line. Mean  $\pm$  SEM from at least three independent experiments were calculated.

### Immunofluorescence staining of the BrainSpheres

BrainSpheres were stained with primary antibodies (**Table S3**) for 48 hours and with secondary antibodies (**Table S4**) for 24 hours as described in (Harris *et al.* 2017). Nuclei were stained with Hoechst 33342. BrainSpheres were mounted on the glass slides. Images were taken using a Zeiss UV-LSM 700 confocal microscope with 20x and 63x magnification objectives and Zeiss Zen software.

### Measurement of acetylcholinesterase activity

Acetylcholinesterase (AChE) assay (Abcam, ab138873) was performed according to manufacturer's instructions. Briefly, spheroids were lysed in Lysis Buffer (0.3 g NaCl, 1 mL of 1 M Tris, PH 7.5, 1 mL 10% NP-40, 0.2 mL of 0.5 M EDTA, PH 8.0, 17.8 mL dd

H<sub>2</sub>O), centrifuged at 600 *g* for 5 min. 50  $\mu$ L of supernatant was combined with 50  $\mu$ L of assay buffer in 96-well plate, incubated for 20 min in the dark; reaction was stopped with stop buffer. The fluorescence was measured at 540 nm using multi-well fluorometric reader CytoFluor series 4000 (Perspective Biosystems). AChE activity was measured in three independent experiments.

### Neurite outgrowth

The detailed protocol of neurite outgrowth was previously published (Harris *et al.* 2018; Zhong *et al.* 2020). Briefly, spheroids were plated in Martrigel-coated 24-well black, glass-bottom plates (Cellvis), and incubated without shaking for 24-48 h to allow outgrowth of neurites. Then, spheroids were immunostained with  $\beta$ -III-tubulin antibody. Spheroids were imaged with Zeiss LSM 500 confocal microscope with 10x magnification objective (**Figure 3, S5, S6**) or with ECHO laboratories Revolve microscope with 4/0.13 magnification objective (**Figure S7**). Neurite density and length was quantified using ImageJ Sholl plugin for each individual spheroid. The ratio was calculated for each shell (number of intersections/distance from center of the spheroid) and plotted. Area under the curve (AUC) was calculated for each spheroid and then averaged from 8 to 13 spheroids per condition. The experiment was repeated three times showing the same CPF effects between the experiments. To attenuate the CPF effect on neurite outgrowth, BrainSpheres were co-treated with 100  $\mu$ M tocopherol, with treatment started two hours prior CPF exposure.

### Western blot analysis

Western blot was performed as described by (Zhong *et al.* 2020). Briefly, spheroids were lysed with RIPA lysis buffer (Sigma-Aldrich). Protein concentration was quantified with NanoDrop 2000c. Lysates were separated on 4%-15% gradient SDS-polyacrylamide gel with 100 V for 120 min and transferred to a polyvinylidene difluoride membrane by electroblotting for 120 min at 200 mA at 4°C. After 1 h blocking with blocking solution (PBS, 0.5% Tween-20, pH 7.4, containing 5% non-fat dry milk), membrane was incubated with primary antibodies (CHD8, 1:1000; GAPDH, 1:1000) overnight at 4°C, followed by washing and secondary antibody incubation for 1 h (anti-mouse, 1:3000, BIO-RAD; anti-rabbit 1:2000). Protein of interest was detected by chemiluminescence reagent and exposed to film. Quantification was performed using Image-J software. Data were normalized on samples from vehicle-treated *CHD8*<sup>+/+</sup> cell line and presented as Mean  $\pm$  SEM (n=5).

### LC-MS mass spectrometry (LC-MS/MS)

For LC-MS mass spectrometry, BrainSpheres were lysed in 100% methanol/0.1% formic acid, and sonicated. Lysates were centrifuged at 16,000 *g* for 30 min at 4°C. Supernatant was transferred to a new tube, 10 µL aliquots were taken for protein quantification using an BCA kit (ThermoFisher Scientific). Samples were dried for at least 6 h in a SpeedVac at 35°C and reconstituted in 0.1% formic acid in water/acetonitrile, 50:50.

LC-MS/MS was run on an Agilent 6490A triple stage quadrupole mass spectrometer equipped with a Jet Stream ESI ion source and a 1260 HPLC system. The analytes were separated at 35°C on a Sigma Discovery HS F5 column in reverse phase (150\*2.1 mm, 3 µm) or an Agilent Poroshell 120 HILIC-Z, PEEK-lined (150\*2.1 mm, 2.7 µm) in normal phase dependent on retention time of the metabolite. The mobile phase consisting of 0.1% formic acid in water (Solvent A) and 98% acetonitrile plus 0.1% formic acid (Solvent B) and was used with a gradient elution: For reverse-phase 0–3 min, 0% B; 23 min, 100% B at a flowrate of 0.3 mL/min. For normal phase HILIC 0–3 min, 92% B; 23 min, 61% B at a flowrate of 0.25 mL/min. All metabolites were identified, and the measurements optimized as spike-in reference metabolites (Sigma-Aldrich) in a QC-mixture of various study samples from the same study. Each measurement run also consisted of two sample spike-in reference metabolites in a QC-mixture to address possible retention time drifts.

It was necessary to use benzoyl chloride derivatization for some of the metabolites to increase sensitivity and stability of metabolite detection. Briefly, samples were dried and resuspended in freshly prepared reaction buffer consisting of 1 vol% benzoyl chloride, 50 vol% sodium tetraborate buffer and 49 vol% acetonitrile. After incubation at 50°C for 30 min, reaction was stopped by adding formic acid to a final concentration of 0.7 vol%. Metabolomics quality assurance followed (Beger *et al.* 2019; Bouhifd *et al.* 2015).

Peaks were integrated with Agilent MassHunter Workstation Quantitative Analysis software version 10.1. All peaks were manually checked, and integration was corrected if necessary. Area under the curve for each peak was normalized on protein content in each sample and spike-in control (IS – 3,4-dihydroxybenzylamine, when included). The Glutamate/GABA and SAM/SAH ratios were calculated as follows:  $AUC(\text{glutamate})/AUC(\text{GABA})$  and  $AUC(\text{SAM})/AUC(\text{SAH})$ , respectively. A few obvious outliers (due to technical errors) were identified and replaced by an average of the technical replicates from the same experiment. The experiment was repeated three times with 12 technical replicates in total. All metabolites were then normalized to vehicle-treated *CHD8*<sup>+/+</sup> samples.

### Statistical analysis

Detailed description of statistical analysis is provided in figure legends. Briefly, all assays were conducted in at least three independent experiments. If not specified otherwise, the data is presented as Tukey's box-and-whiskers plots showing quartiles with outliers. For viability, to compare different treatment groups between the cell lines multiple unpaired t-test with Benjamini, Krieger and Yekutieli FDR (5%) correction was used. For Mitotracker and CellRox assays Kruskal-Wallis test, corrected for multiple comparison (Dunn's test) was applied. Gene expression and mass spectrometry data were analyzed either with unpaired t-test (when compared cell lines without treatment) or with one-way ANNOVA with Holm-Sidak's multiple comparison test (for experiments, treated with CPF/CPO). A level of  $P < 0.05$  was considered significantly different. For mass spectrometry-based metabolite analysis, a level of  $P < 0.01$  was considered significantly different.

## Results

### Comparable efficiency of BrainSphere differentiation from *CHD8*<sup>+/+</sup> and *CHD8*<sup>+/-</sup> NPC

Control iPSC line (*CHD8*<sup>+/+</sup>) and the iPSC line carrying a CRISPR/Cas9-induced heterozygous knockout mutation in *CHD8* gene (*CHD8*<sup>+/-</sup>) used in this study were generated from the same donor, differentiated into NPC, and fully characterized previously (Wang *et al.* 2015). The *CHD8*<sup>+/-</sup> line is heterozygous for a two-base pair deletion, which leads to a frameshift mutation and premature stop signal in exon 1. Reduced expression of CHD8 protein in *CHD8*<sup>+/-</sup> neuroprogenitors is shown in **Figure 1A**. **Figure 1B** shows immunostaining of control and *CHD8*<sup>+/-</sup> NPCs with neuroprogenitor markers Sox2 and Nestin. Both NPC cell lines were differentiated to generate 3D BrainSphere cultures, as described in **Figure 1C** and (Pamies *et al.* 2017). We were not able to generate BrainSpheres from a homozygous *CHD8* knockout line (*CHD8*<sup>-/-</sup>). The differentiation efficiency was compared between two cell lines by immunostaining (**Figure S1**) and RT-PCR (**Figure S2**) and showed similar efficiency of BrainSphere differentiation in both cell lines (supplemental material). This allowed further comparison of the response of both lines to exposure to CPF and CPO. To be noted, *CHD8*<sup>+/-</sup> spheroids were slightly bigger in diameter than *CHD8*<sup>+/+</sup> (data not shown).

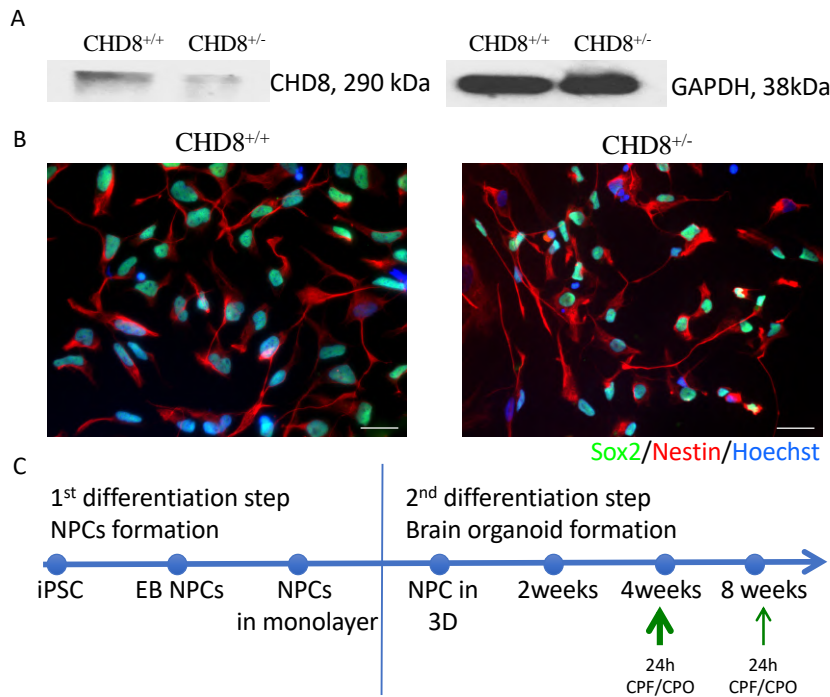


**Figure 1. CHD8<sup>+/+</sup> and CHD8<sup>+/-</sup> NPC and BrainSpheres.** (A) Reduced expression of CHD8 protein in CHD8<sup>+/-</sup> vs. CHD8<sup>+/+</sup> NPC. (B) Expression of NPC marker Sox2 (green) and Nestin (red) in CHD8<sup>+/+</sup> and CHD8<sup>+/-</sup> NPC cultures. The nuclei were visualized with Hoechst 33342. Scale bars are 50  $\mu$ m. (C) Differentiation and toxicant treatment scheme. EB – Embryoid Bodies, NPC – Neural Progenitor Cells, CPF – chlorpyrifos, CPO – chlorpyrifos-oxon.

### **CPO treatment reduces acetylcholinesterase (AChE) activity in CHD8<sup>+/+</sup> and CHD8<sup>+/-</sup> BrainSpheres. CHD8<sup>+/-</sup> BrainSpheres have higher levels of ROS**

We tested the sensitivity of both control and CHD8<sup>+/-</sup> BrainSpheres to the CPF and its active metabolite CPO. CPO is mainly responsible for acetylcholinesterase (AChE) inhibition—the supposed primary acute mode of action of OP pesticides. We treated the spheroids at 4 and 8 weeks of differentiation with 47 and 100  $\mu$ M CPF or CPO for 24 h. The high concentrations and short-term exposures employed do not imply a risk to humans in the real world, but were rather used as a model exposure, making use of the substance's well-established DNT hazard. Both concentrations were subtoxic, as measured by resazurin reduction assay. CHD8<sup>+/-</sup> BrainSpheres, however, were slightly more sensitive to CPF and CPO at eight weeks (Figure 2A, B). For the next experiments, we selected

100  $\mu$ M CPF and CPO concentrations and 4 weeks of differentiation as an intermediate and immature stage of the differentiation process.

It has been previously shown that CPF induces oxidative stress in neuronal cultures (Slotkin and Seidler 2010). Thus, we analyzed the level of reactive oxygen species (ROS) and mitochondrial membrane potential (MMP). There were no significant changes observed in MMP besides a slight reduction of MMP upon treatment of  $CHD8^{+/+}$  with CPO (**Figure S3A**). We observed higher levels of ROS in  $CHD8^{+/-}$  than in  $CHD8^{+/+}$ . No changes in ROS level upon CPF/CPO treatment were found (**Figure S3B**).

Since AChE is the main target of CPF acutely, its enzymatic activity was quantified (**Figure 2C**). As expected, CPO had stronger inhibitory effect on AChE than CPF in both cell lines. No significant difference was observed between the two cell lines. Consequently, the level of AChE substrate—acetylcholine, measured intracellularly by mass spectrometry—was increased after CPO treatment in both cell lines (**Figure 2D**). The basal level of acetylcholine was higher in  $CHD8^{+/+}$  than in  $CHD8^{+/-}$  samples. Although the peak of acetylcholine in  $CHD8^{+/+}$  BrainSpheres treated with CPO was higher than in  $CHD8^{+/-}$ , the magnitude of induction was greater in  $CHD8^{+/-}$  BrainSpheres: 18-fold change vs. 9-fold change in the  $CHD8^{+/+}$  group of samples. We observed a slight, but not significant, increase of acetylcholine in CPF-treated samples in both cell lines. This finding, supported by a significant reduction of AChE activity, may rely on the presence of low levels of CPO in CPF-treated samples (**Figure S4**), thus suggesting that BrainSpheres have the capacity to metabolize CPF to CPO. In accordance with these results, the level of choline was already lower in the mutant cell line than in the control, and was further reduced by CPO (**Figure 2E**). These results demonstrate that based on resazurin assay,  $CHD8^{+/-}$  is slightly more sensitive to CPO insult in general, and CPO exposure leads to greater accumulation of acetylcholine and reduction of choline in  $CHD8^{+/-}$  BrainSpheres.

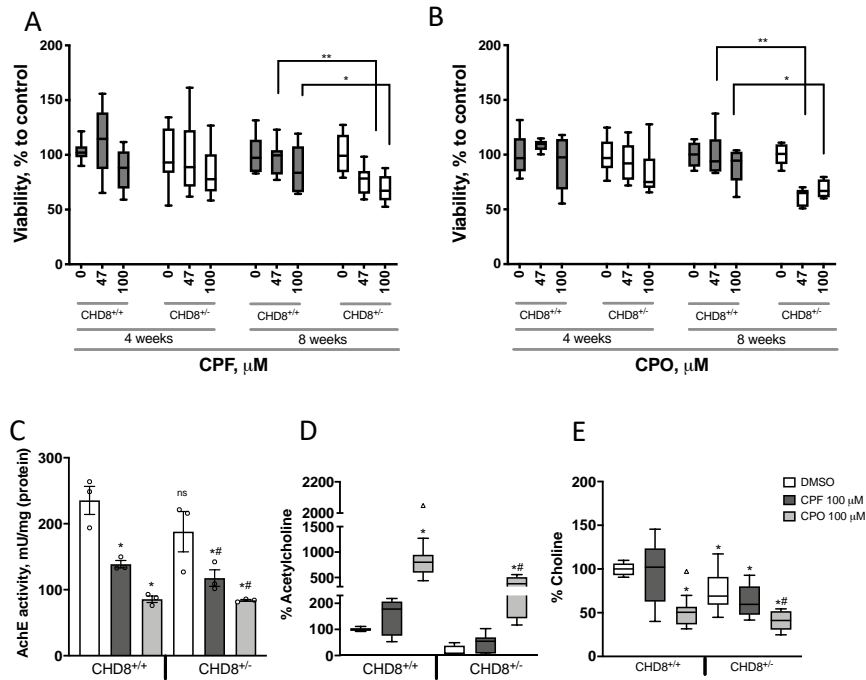


**Figure 2. Cell viability and AChE activity after exposure CPF and CPO.** Resazurin reduction assay in 47 and 100  $\mu$ M CPF (**A**) and CPO (**B**) treated *CHD8*<sup>+/+</sup> (grey) and *CHD8*<sup>+/-</sup> (white) BrainSpheres for 24 hours at 4 and 8 weeks of differentiation. The data represents 3 independent experiments with 3 technical replicates per run (n=9) normalized to vehicle treated controls. \* P < 0.05, \*\* P < 0.01, multiple unpaired t-test with Benjamini, Krieger and Yekutieli FDR (5%) correction. AChE activity (**C**), intracellular levels of acetylcholine (**D**) and choline (**E**) measured at 4 weeks of differentiation in *CHD8*<sup>+/+</sup> and *CHD8*<sup>+/-</sup> spheroids after exposure to 100  $\mu$ M CPF (dark grey) and 100  $\mu$ M CPO (light grey). Vehicle-treated controls are depicted in white. The data represent the AChE activity normalized to protein amount in each sample (mean  $\pm$  SEM, n=3). Acetylcholine and choline were measured by LC-MS/MS in three independent experiments with a total of 12 technical replicates. Data normalized to vehicle treated *CHD8*<sup>+/+</sup> control. \* P < 0.05 (compared to *CHD8*<sup>+/+</sup> DMSO), # P < 0.05 (compared to *CHD8*<sup>+/-</sup> DMSO), one-way ANOVA with Holm-Sidak's post-test.

### CPF and CPO reduce neurite outgrowth

Since AChE is an essential factor regulating neurite outgrowth, we analyzed this process as a functional endpoint (**Figure 3, Figures S5-7**). The CPF/CPO exposure significantly reduced neurite length in both cell lines. Pre-treatment of spheroids with the antioxidant – tocopherol - attenuated the CPF effect, suggesting that the CPF effect on neurite outgrowth can be due to oxidative stress, even though we were unable to detect increased ROS production in CPF-treated samples at the timepoint of measurement. Although in



one of three experiments there was a difference in neurite outgrowth between the untreated cell lines, the data was difficult to interpret due to differences in spheroid size between two cell lines. The magnitude of CPF and CPO effect was, however, similar in both cell lines in all three experiments, as indicated by AUC measurements (**Figure 3B**).

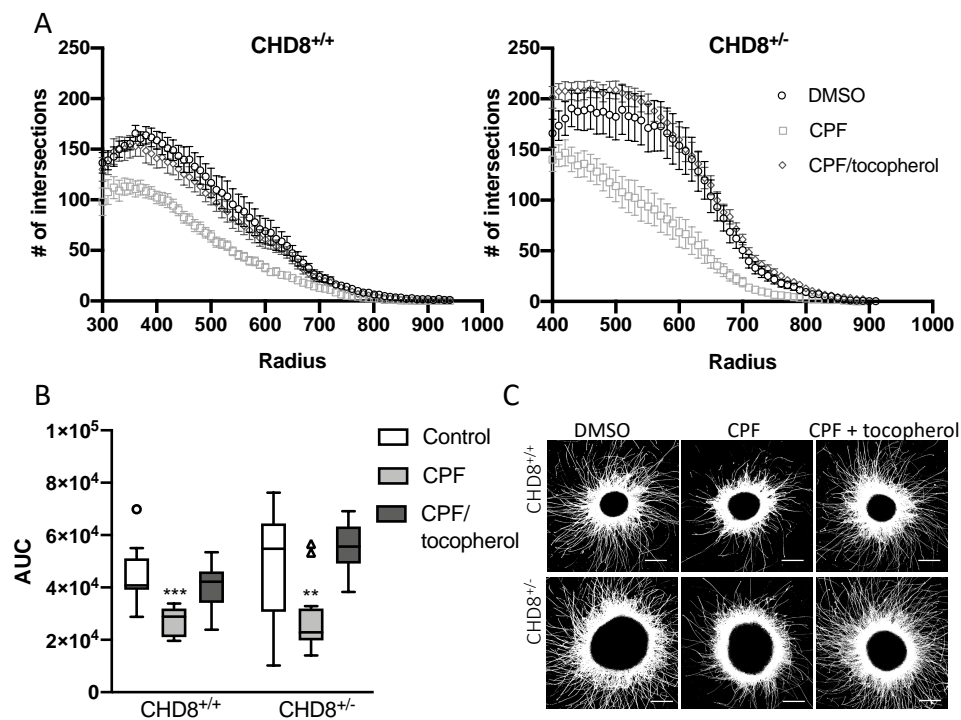


**Figure 3. Neurite outgrowth upon 100  $\mu$ M CPF treatment and co-treatment with 100  $\mu$ M tocopherol.** (A) Sholl analysis of neurite outgrowth in *CHD8<sup>+/+</sup>* (left) and *CHD8<sup>+/-</sup>* (right) showing number of intersections (neurite density) starting from the edge of the spheroid. Each curve represents mean  $\pm$  SEM from 8 to 12 spheroids. (B) Area under the curve (AUC), calculated for each condition in (A). \*\* $P < 0.01$  and \*\*\* $P < 0.001$ , one-way ANOVA with Holm-Sidak's post-test. (C) Representative images for each treatment. Scale bar is 200  $\mu$ m.

### Lower level of CHD8 due to CPF/CPO exposure

The next question addressed was whether CPF/CPO exposure may influence the level of CHD8 in BrainSpheres. In agreement with previous studies, we did not observe significant differences in *CHD8* mRNA expression between *CHD8<sup>+/+</sup>* and *CHD8<sup>+/-</sup>* BrainSpheres

(**Figure 4A** (Wang *et al.* 2017)). The expression pattern of *CHD8* reached its peak at 4 weeks of differentiation and was reduced thereafter, which correlates with *CHD8* expression in human brain (where it is induced earlier in development (9-16 postconceptional weeks) and decreases during fetal and postnatal development (Bernier *et al.* 2014). CPF/CPO treatment did not significantly alter *CHD8* mRNA expression at 4 weeks of differentiation (**Figure 4B**). We observed, however, significant downregulation of CHD8 protein levels—not only due to mutation, but also after treatment with CPF or CPO (**Figure 4C,D**). These results suggest that CPF and CPO may directly or indirectly disrupt CHD8 translation and possibly have the same downstream effects as *CHD8* inactivating mutation.

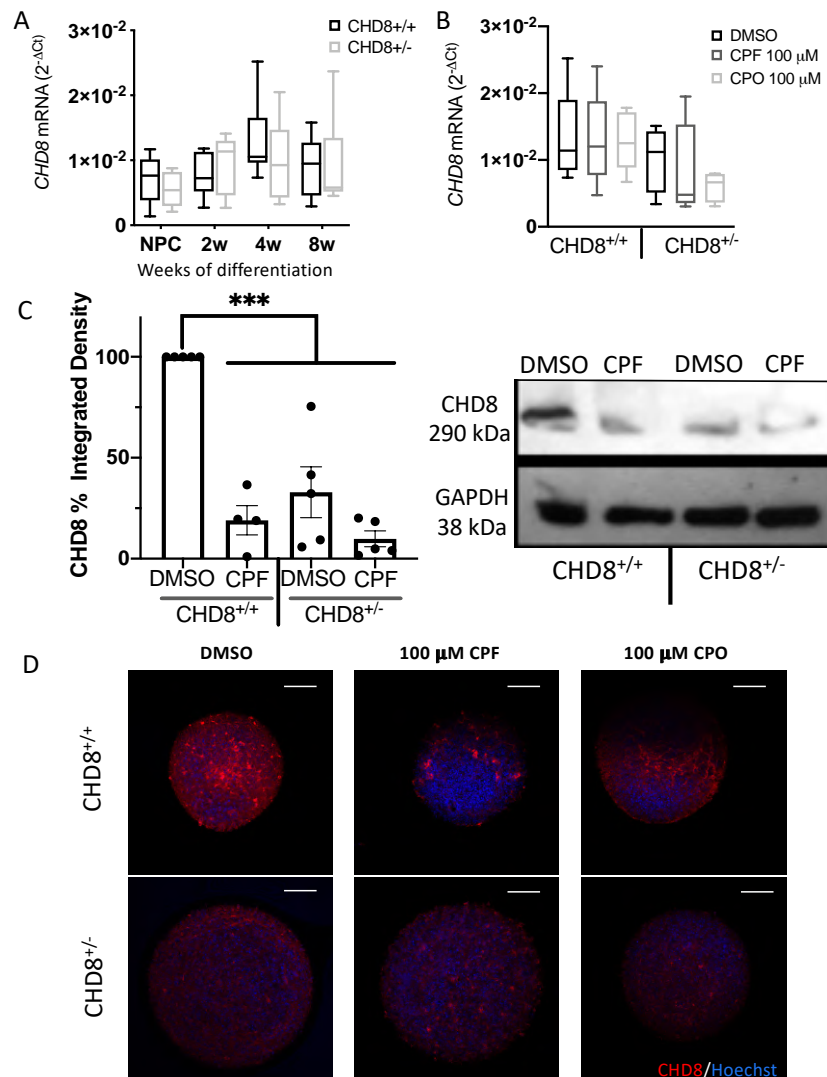


**Figure 4. CHD8 expression upon CPF/CPO treatment.** (A) *CHD8* expression in course of differentiation. (B) *CHD8* expression in *CHD8*<sup>+/+</sup> and *CHD8*<sup>+/-</sup> exposed to CPF/CPO. (C) Western Blot quantification of CHD8 protein in *CHD8*<sup>+/+</sup> and *CHD8*<sup>+/-</sup> BrainSpheres treated with CPF. CHD8 protein level was normalized to GAPDH and is expressed as % of *CHD8*<sup>+/+</sup> vehicle treated control. Dendrogram is shown as mean  $\pm$  SEM ( $n = 5$ ). Statistical significance was calculated by one-way ANOVA with Holm-Sidak's post-test. Representative blot is shown to the right. (D) Immunostaining of *CHD8*<sup>+/+</sup> and *CHD8*<sup>+/-</sup> BrainSpheres with CHD8 antibody (red) after CPF and CPO exposure. Nuclei are stained with Hoechst 33342 (blue). Scale bar 100  $\mu$ m.

Taken together, the data indicate that *CHD8*<sup>+/-</sup> and CPF/CPO can both impair neurodevelopment, as increased ROS production and impaired neurite outgrowth are key events of DNT AOP.

### **Identification of ASD metabolic biomarkers from literature**

The key question was how to possibly validate this data with clinical findings. We decided to use an exposomics approach (Sillé *et al.* 2020), where population findings of biomarkers in biofluids are compared to changes in the mechanistic model (i.e., BrainSpheres). A comprehensive review of the literature identified a panel of pathways and metabolites perturbed in ASD patients (e.g. amino acids, fatty acid metabolism, one carbon metabolism, energy metabolism, oxidative stress, and neurotransmitters). We have selected a list of representative metabolites and neurotransmitters and compared the levels of those in the *CHD8*<sup>+/+</sup> and *CHD8*<sup>+/-</sup> BrainSpheres after treatment with CPF/CPO with human data (**Table 1** and references therein). Noteworthy, the direction of change was sometimes controversial, with some studies reporting increases and others decreases. This might be due to the biological compartment for sampling, e.g., tissue or blood/urine or stage of the disease. We were therefore primarily interested in whether we could observe perturbations in these biomarkers as an indication of a perturbation of the linked pathways, and not necessarily in direction of changes.

Metabolite/KEGG ID	BrainSpheres			Literature		
	<i>CHD8</i> <sup>-/-</sup>	CPF/CPO	<i>CHD8</i> <sup>-/-</sup> CPF/CPO	Brain	Blood	Urine
L-Glutamic acid, C00025	-	-	↑	- 22,36,39	- 9,47,58	↓ 17,18,34,35
				↑ 37,38,39,52	↑ 6,11,15,26-31,33,37	
				↓ 40,42,55	↓ 32.59	
GABA, C00025	↓	-	-	- 22,44,54,55	- 12.58	↑ 51
				↓ 36, 41-44	↑ 23.30	
L-Tyrosine, C00025	↓	-	-		- 9.12	↑ 2.25
					↑ 15	↓ 34
					↓ 6,28,29,58	
L-Dopa, C00355	↑	-	-			
Dopamine, C03758	↓	-	-	↓ 49	↑ 48,46	↓ 48,14
Choline, C00114	↓	↓	↓	↓ 24.53	- 9	
Acetylcholine, C01996	↓	↑	-			
L-Tryptophan, C00078	-	↑ (CHD8+/-)	-	-	- 9	↑ 18
					↓ 6,12,13,28,50	
Kynurenic acid, C01717	↑	-	↑		↓ 13.50	
Kynurenine, C00328	-	↑ (CHD8+/-)	-			↓ 2
D-Lactic acid, C00256	-	-	↑		- 9.19	↓ 18
					↑ 4.61	
					↓ 11.45	
Creatine, C00300	↓	-	-	↓ 53		↑ 18
						↓ 20.21
L-Arginine, C00062	-	↑(CHD8+/+)	-		- 9,12,28,58	↑ 56
					↑ 45	
Ornithine, C01602	↓	↑(CHD8+/+)	-		- 12,58,60,	
					↑ 9	
α-Hydroxyglutaric acid, C01087	-	↑(CHD8+/-)	↑			↑ 3
Folic acid, C00504	-	↑	-		- 57	
SAM, C00019	↑	↑	↑		↓ 7.8	↓ 1
SAH, C00021	↑	-	↑		↑ 7.8	↑ 1
L-Cysteine, C00097	-	-	↑		- 12	↓ 1
					↓ 5,7,8,58	
GSH, C00051	-	↓(CHD8+/+)	-		↓ 4,5,8	
Cystathionine, C02291	↓	↓(CHD8+/+)	-		↑ 8	↓ 1
					↓ 7	
Cystine, C00491	-	↑(CHD8+/+)	-		↑ 10	
					↓ 11	
Carnosine, C00386	↑	-	-			↓ 16.56

**Table 1. Metabolites, significantly ( $P < 0.01$ ) perturbed by (i) *CHD8* mutation, (ii) CPF/CPO treatment or by (iii) *CHD8* mutation and CPF/CPO treatment and existing knowledge on association of those metabolites with ASD. *CHD8* mutation: metabolites that were altered in *CHD8*<sup>-/-</sup> BrainSpheres when compared to *CHD8*<sup>+/+</sup> control line by unpaired t-test. CPF/CPO: metabolites, which were changed due to CPF (blue), CPO (green) or both (red) treatments, when compared to corresponding DMSO control in each cell line (one-way ANOVA with Holm-Sidak's post-test). *CHD8*<sup>-/-</sup> plus CPF/CPO: metabolites, which were not different between *CHD8*<sup>+/+</sup> and *CHD8*<sup>-/-</sup> vehicle treated samples, but were significantly altered due to CPF/CPO treatment in *CHD8*<sup>-/-</sup> BrainSpheres compared to control BrainSpheres (*CHD8*<sup>+/+</sup> vehicle control)**

or the effects of *CHD8* mutation were enhanced with the treatment, when compared to *CHD8*<sup>+/+</sup> vehicle control (one-way ANOVA with Holm-Sidak's post-test). **References in the table:** 1(Geier *et al.* 2009), 2 (Gevi *et al.* 2016), 3 (Kalužna-Czaplińska *et al.* 2014), 4 (El-Ansary *et al.* 2017), 5 (Han *et al.* 2015), 6 (Tu *et al.* 2012), 7 (James *et al.* 2004), 8 (James *et al.* 2006), 9 (Orozco *et al.* 2019), 10 (Melnik *et al.* 2012), 11 (West *et al.* 2014), 12 (Saleem *et al.* 2020), 13 (Ormstad *et al.* 2018), 14 (Martineau *et al.* 1992), 15 (Aldred *et al.* 2003), 16 (Ming *et al.* 2012), 17 (Yap *et al.* 2010), 18 (Lussu *et al.* 2017), 19 (Khemakhem *et al.* 2017), 20 (Bitar *et al.* 2018), 21 (Mavel *et al.* 2013), 22 (Kolodny *et al.* 2020), 23 (Dhossche *et al.* 2002), 24 (Corrigan *et al.* 2013), 25 (Noto *et al.* 2014), 26 (Moreno-Fuenmayor *et al.* 1996), 27 (Shimmura *et al.* 2011), 28 (Tirouvanziam *et al.* 2012), 29 (Naushad *et al.* 2013), 30 (El-Ansary and Al-Ayadhi 2014), 31 (Cai *et al.* 2016), 32 (El-Ansary 2016), 33 (Shinohe *et al.* 2006), 34 (Evans *et al.* 2013), 35 (Nadal-Desbarats *et al.* 2014), 36 (Cochran *et al.* 2015), 37 (Hassan *et al.* 2013), 38 (Brown *et al.* 2013), 39 (Joshi *et al.* 2013), 40 (Elst *et al.* 2014), 41 (Gaetz *et al.* 2014), 42 (Kubas *et al.* 2012), 43 (Rojas *et al.* 2014), 44 (Harada *et al.* 2011), 45 (Kuwabara *et al.* 2013), 46 (Hérault *et al.* 1993), 47 (Arnold *et al.* 2003), 48 (Martin'eau *et al.* 1994), 49 (Ernst *et al.* 1997), 50 (Bryn *et al.* 2018), 51 (Cohen 2002), 52 (Drenthen *et al.* 2016), 53 (Ford and Crewther 2016), 54 (Brix *et al.* 2015), 55 (Horder *et al.* 2018), 56 (Liu *et al.* 2019), 57 (Schaevitz and Berger-Sweeney 2012), 58 (ElBaz *et al.* 2014), 59 (Delaye *et al.* 2018), 60 (Smith *et al.* 2018), 61 (Hassan *et al.* 2019).

### Effects of *CHD8* mutation and CPF/CPO on energy metabolism, one carbon metabolism, and selected neurotransmitters

We analyzed the intracellular levels of the 29 selected metabolites by mass spectrometry and compared them between *CHD8*<sup>+/+</sup> and *CHD8*<sup>+/-</sup> BrainSpheres, with and without CPF and CPO treatment. (Table S5). 23 metabolites, which were significantly different ( $P < 0.01$ ) in at least one condition, are shown in **Table 1**. We found perturbations in ASD metabolic biomarkers under either genetic alteration (13 metabolites), chemical treatment, or its combination. Since selected CPF and CPO concentrations were subtoxic, and the fact that some perturbations were seen in untreated *CHD8*<sup>+/-</sup> BrainSpheres compared to *CHD8*<sup>+/+</sup>, it argues against a global derangement of metabolism; but as no-effect data are difficult to obtain from the literature, the specificity of effects cannot be assessed.

Folate-dependent, one-carbon metabolism is a central hub in the cellular pathways, and is essential for production of methyl groups for all methylation reactions. One-carbon metabolism plays a critical role in autism (James 2013; Orozco *et al.* 2019; Schaevitz and Berger-Sweeney 2012). S-adenosylmethionine (SAM) was increased after treatment with CPF and CPO only in *CHD8*<sup>+/-</sup> BrainSpheres. The basal level of S-adenosylhomocysteine (SAH) was higher in *CHD8*<sup>+/-</sup>. The SAM/SAH ratio was higher in CPO-treated samples in both cell lines compared to corresponding DMSO-treated controls (**Figure 5A**). Although SAH was elevated in urine and blood of ASD patients, SAM was reduced (**Table 1**). Folic acid was increased following CPF and CPO treatment in both cell lines (**Figure 5A**). Methionine and GSSG remained unchanged and GSH was lower only in CPF-treated *CHD8*<sup>+/+</sup> samples. Cystathionine, which was found to be lower in blood and urine of ASD

patients, was low in the mutant samples and reduced by CPO only in *CHD8*<sup>+/+</sup> samples (**Table 1**).

Energy cycle metabolites (TCA) is perturbed in ASD patients (Orozco *et al.* 2019). In our experimental set-up, creatine was slightly lower in the mutant cell line, which correlates with lower levels observed in the brains of ASD patients. Lactic acid was induced by CPF and CPO only in *CHD8*<sup>+/-</sup> BrainSpheres, suggesting a synergetic effect of CPF/CPO exposure and *CHD8* mutation on the TCA cycle (**Table 1** and **Figure 5B**). Another potential synergy between *CHD8* mutation and CPF/CPO treatment was observed in the levels of L-tryptophan and its metabolite kynurenic acid (KA). Both were elevated following CPF/CPO treatment only in the mutant cell line. KA was slightly higher in the mutant cell line and further increased due to CPO treatment (**Table 1** and **Figure 5C**). In ASD, elevated levels of L-tryptophan have been found in urine, while both, L-tryptophan and KA were lower in the blood (**Table 1**). The  $\alpha$ -Hydroxyglutaric acid was significantly increased due to CPO treatment only in the mutant line (**Figure 5D**), which is in line with elevated levels in urine in ASD individuals (Kaluźna-Czaplińska *et al.* 2014).

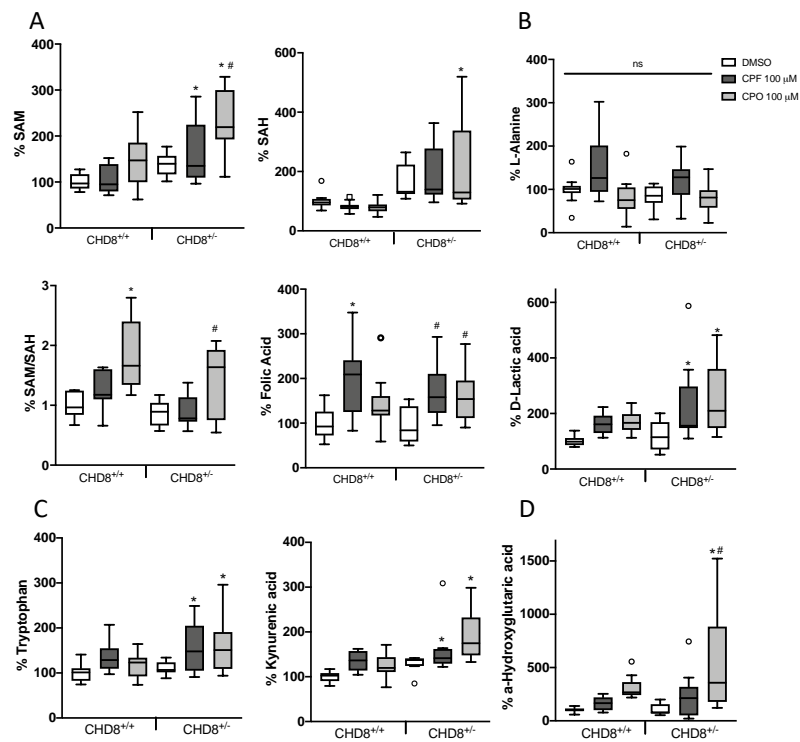


**Figure 5. Effects of *CHD8* mutation and CPF/CPO exposure on key Adverse Outcome Pathways of ASD.** (A) methyl donor system: SAM, SAH and folic acid; (B) lactic acid and alanine; (C) Tryptophan and KA, (D)  $\alpha$ -Hydroxyglutaric acid levels were measured by LC-MS/MS in three independent experiments with total of 12 technical replicates. Vehicle-treated controls are depicted in white, CPF-treated in dark grey and CPO in light grey. Data is normalized to vehicle treated *CHD8*<sup>+/+</sup> control. \*  $P < 0.01$  (compared to *CHD8*<sup>+/+</sup> DMSO), #  $P < 0.01$  (compared to *CHD8*<sup>+/-</sup> DMSO), one-way ANOVA with Holm-Sidak's post-test. SAM – S-Adenosylmethionine SAH – S-Adenosylhomocysteine, KA – Kynurenic Acid.

Taken together, alterations of metabolites associated with ASD are also affected by the combination of *CHD8* mutation and CPF, and/or CPO treatment.

### Imbalance of excitatory and inhibitory systems in *CHD8*<sup>+/-</sup> BrainSpheres

The imbalance of excitatory/inhibitory neuronal systems is known to be associated with ASD. Consequently, we measured the levels of intracellular GABA and glutamate neurotransmitters. *CHD8*<sup>+/-</sup> BrainSpheres had lower basal levels of GABA in comparison to *CHD8*<sup>+/+</sup>, with a higher ratio of glutamate *vs.* GABA *CHD8*<sup>+/-</sup> (Figure 6). Exposure to CPF and CPO did not change the glutamate/GABA ratio, but CPO treatment led to



significant increase of glutamate in *CHD8*<sup>+/-</sup> BrainSpheres. Abnormalities in arginine/ornithine/aspartate (urea) cycle in ASD patients has also been reported (Liu *et al.* 2019). Since glutamate and ornithine are linked, alterations in the urea cycle can play a role in the excitatory/inhibitory imbalance. Arginine was significantly increased by CPF treatment in *CHD8*<sup>+/+</sup> BrainSpheres. Ornithine was significantly lower in mutant BrainSpheres compared to *CHD8*<sup>+/+</sup> and increased following CPF/CPO treatment in the latter (**Table 1**). Increased ornithine and arginine levels have been reported in blood and urine in ASD patients (**Table 1**). Increases in the excitatory amino acids due to CPF/CPO treatment and lower levels of GABA in *CHD8*<sup>+/-</sup> samples suggest an excitatory/inhibitory imbalance.

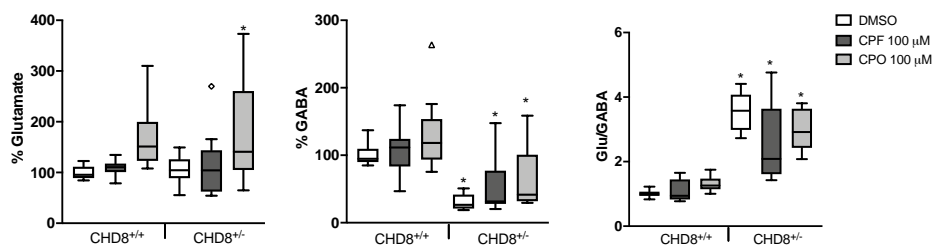


**Figure 6. Excitatory/inhibitory neurotransmitters detection in *CHD8*<sup>+/+</sup> and *CHD8*<sup>+/-</sup> after CPF/CPO exposure.** Glutamate and GABA levels and their ratio in *CHD8*<sup>+/-</sup> *vs.* *CHD8*<sup>+/+</sup> BrainSpheres treated with CPF (dark grey)/CPO (light grey)/vehicle (white) were assessed by LC-MS/MS. Data from three independent experiments (12 technical replicates in total) normalized to vehicle treated *CHD8*<sup>+/+</sup> control is shown. \*P < 0.01 (compared to *CHD8*<sup>+/+</sup> DMSO), one-way ANOVA with Holm-Sidak's post-test.

### Perturbation of the dopaminergic system by *CHD8* and CPF/CPO

CPF has been found to affect dopaminergic neurons *in vivo* (Aldridge *et al.* 2005; Torres-Altora *et al.* 2011; Zhang *et al.* 2015). Imbalanced levels of dopamine have been reported in ASD, but the observations were not consistent undefined. Because of these inconsistent findings, we analyzed several parameters of dopaminergic metabolism in our system. We observed no statistically significant changes in the levels of phenylalanine and tyrosine, an increase in L-DOPA, and a decrease of dopamine in *CHD8*<sup>+/-</sup> with no changes due to treatment (**Figure 7A**). Gene expression of tyrosine hydroxylase (*TH*), an enzyme responsible for conversion of tyrosine to L-DOPA, was increased due to CPF treatment (**Figure 7B**), slightly higher but not significantly in *CHD8*<sup>+/-</sup> *vs.* *CHD8*<sup>+/+</sup> at 4 weeks, and significantly higher at 8 weeks of differentiation (**Figure S2**, last panel). *COMT* (catechol-O-methyltransferase) expression was elevated in *CHD8*<sup>+/-</sup> samples compared to *CHD8*<sup>+/+</sup> (**Figure 7B**), which correlates with lower levels of dopamine, as *COMT* initiates

catecholamine degradation by transferring a methyl group from S-adenosylmethionine (SAM) to catecholamines. In line with this, levels of SAM were also higher in the *CHD8*<sup>+/-</sup> group than in the control group (**Figure 5A**). Finally, we assessed the presence of TH<sup>+</sup> dopaminergic neurons in the cultures and observed higher numbers of dopaminergic neurons in *CHD8*<sup>+/-</sup> than in *CHD8*<sup>+/+</sup> (**Figure 7C**). Exposure to CPO increased the number of TH<sup>+</sup> positive neurons in *CHD8*<sup>+/+</sup> BrainSpheres. Two different morphologies of the TH<sup>+</sup> signal were observed. Flat, non-neuronal-like cells were predominantly found in *CHD8*<sup>+/+</sup> BrainSpheres (marked with blue arrowhead), and TH<sup>+</sup> cells with distinctive neuronal morphology (marked with white arrowhead) predominantly found in *CHD8*<sup>+/-</sup> BrainSpheres. These findings suggest that both exposure to CPF/CPO and *CHD8* mutation alter the dopamine neurotransmitter system.

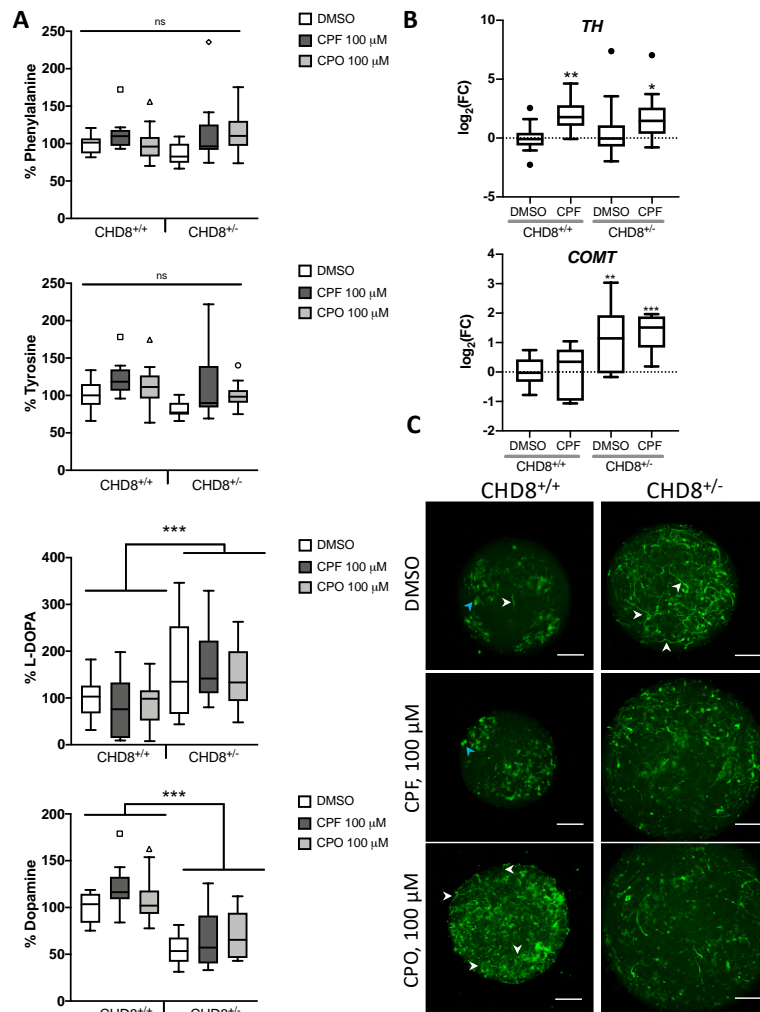


**Figure 7. Perturbations of dopaminergic system in CHD8<sup>+/-</sup> vs. CHD8<sup>+/+</sup> BrainSpheres after CPF/CPO treatment. (A)** Levels of methionine, tyrosine, L-DOPA and dopamine measured by LC-MS/MS. Data from three independent experiments (12 technical replicates in total) normalized to vehicle-treated CHD8<sup>+/+</sup> control is shown. \*\*\* P < 0.001 (compared all CHD8<sup>+/+</sup> samples vs. CHD8<sup>+/-</sup> group) by unpaired t-test. **(B)** RT-PCR of tyrosine hydroxylase (TH) and catechol-O-methyltransferase (COMT) in both cell lines treated with CPF. Data represents  $\log_2(2^{-\Delta\Delta C_t})$  of five independent experiments. \*P < 0.05, one-way ANOVA with Holm-Sidak's post-test. **(C)** Immunohistochemistry with anti-TH-specific antibody (green) of CHD8<sup>+/+</sup> and CHD8<sup>+/-</sup> BrainSpheres treated with CPF/CPO. White arrow heads indicate neuronal-shaped cells, blue arrows indicate flat clusters of cells. Nuclei were stained with Hoechst 33342 (blue). Scale bar 100  $\mu$ m.

## Discussion

ASD is genetically and symptomatically heterogeneous condition, which makes it difficult to identify confounders that trigger the disease and influence the severity of symptoms. Although genetics has a substantial impact (Persico and Napolioni 2013), environmental factors also appear to play a role (Landrigan *et al.* 2012; Rylaarsdam and Guemez-Gamboa 2019; Sandin *et al.* 2014). Earlier studies have shown that valproic acid, thalidomide, misoprostol, lead, and organophosphates contribute to ASD risk (Geier *et al.* 2009; Kuwagata *et al.* 2009; Landrigan 2010). However, there is limited understanding of the mechanisms by which environment contributes. It is key to determine whether GxE contributes to the etiology and severity of ASD. We suggest that a strong genetic background (e.g., mutation in a high-risk autism gene that alone can trigger the disease) can still synergize with environmental cofactors, thereby worsening symptoms and severity. Similarly, individuals with similar genetic variants can have significantly different symptoms and degrees of disease progression, including being on different levels of the ASD spectrum, leaving substantial room for the contribution of environmental factors (Rylaarsdam and Guemez-Gamboa 2019). Approximately 65 high-autism-risk genes caused by *de novo* mutations, which can be clustered into two large groups: genes expressed early in development (during first and second trimesters of pregnancy) and genes expressed later in pregnancy and after birth. The first group includes transcription factors and chromatin remodelers, while the second group consists mainly of genes involved in synaptogenesis (Sanders 2015; Sanders *et al.* 2015). *CHD8* – a focus of this proof-of-principle study – is one of the nine high-confidence autism genes (Willsey *et al.* 2013) that can also regulate the expression of other autism-related genes (Cotney *et al.* 2015).

Traditional validation of the findings with animal studies are not only cost-prohibitive, but animal findings on the effects of chlorpyrifos are also controversial. Rat is the standard species used for neurotoxicity and developmental neurotoxicity tests (according to OECD test guidelines 424, 426, and 443 (Smirnova *et al.* 2014)). *Chd8* KO rats are not available, and although there is a *Chd8* mouse model (Platt *et al.* 2017; Suetterlin *et al.* 2018) that shows ASD features, the mouse is not a standard model organism for neurotoxicity testing. Thus, GxE analyses focusing on neurotoxicity are best carried out using human neural cultures, with brain organotypic cultures providing more complex cellular architecture and interactions than traditional monolayer culture settings. In addition, using human neural models provides an opportunity to compare *in vitro* findings with clinical data from patients. Finally, the established adverse outcome pathways (AOP) for developmental neurotoxicity (Bal-Price *et al.* 2015, 2017; Li *et al.* 2019) allowed us to focus on specific key events associated with neurotoxicity and developmental neurotoxicity AOPs.

A key use scenario of our model is for regulatory testing of chemicals for possible effects on neurodevelopment. This requires formal validation (Hartung *et al.* 2004; leist *et al.* 2012) of the model. However, not enough chemicals have been tested in the respective animal guideline tests. We suggested earlier the validation of a model by mechanistic validation (Hartung *et al.* 2013), i.e. by demonstrating that relevant mechanisms are reflected instead of the mere correlation of findings from animal studies. This would ideally be done on the basis of agreed AOP, but in this case, the AOP of DNT have not been sufficiently developed and accepted yet.

Nevertheless, there is a substantial body of clinical and epidemiological findings on autism pathophysiology, metabolic biomarkers, and associations with the environment. These lend themselves to correlation with findings obtained with model systems, as suggested in a human exposome approach (Sillé *et al.* 2020). Here, we attempted to correlate the metabolic perturbations observed in a human brain model carrying a high-risk autism mutation in *CHD8* gene, exposed to a model environmental toxicant – chlorpyrifos – with findings in epidemiological and clinical studies. We established a synergy between the risk gene and the risk exposure. An important finding was that exposure to CPF and CPO reduced the level of CHD8 protein, but not mRNA, suggesting (i) a post-transcriptional mechanism and (ii) possible further interactions of CPF and CPO with CHD8's downstream targets that may be crucial for neural development and disease progression. Further research is needed to address the effects of CPF and CPO on CHD8 molecular networks during development.

Dysfunction of cholinergic activity in individuals with ASD has been linked to social and behavioral abnormalities, including sensory processing and attention re-orienting behavior (Ford and Crewther 2016; Orekhova and Stroganova 2014). Choline levels are lower in ASD patients (**Table 1**), as mirrored by *CHD8* mutation in our model. Synergistically, acetylcholine, and choline were perturbed by CPO to the greater extent in *CHD8*<sup>+/-</sup> – demonstrating an increased susceptibility of mutant BrainSpheres to CPF/CPO toxic effects with respect to cholinergic dysfunction (**Figure 2C - E**).

Folate-dependent, one-carbon metabolism and transsulfuration pathways can be perturbed in ASD (Orozco *et al.* 2019). In our system, we detected a synergy between *CHD8* mutation and CPO in elevated levels of both SAM and SAH, where the SAM/SAH ratio was higher in CPO-treated samples of both lines, suggesting hypermethylation (**Figure 5A**) (although reduced levels of SAM and increased SAH have been found in biofluids of ASD patients) (**Table 1**). Increased expression of the methyltransferase COMT (**Figure 7B**) and elevated SAM would suggest hypermethylation in *CHD8*<sup>+/-</sup>, but in this case, decreased SAH levels

would be expected (as was the case in control BrainSpheres treated with CPO, but not in mutant BrainSpheres). More detailed analyses is required to clarify mechanisms, but the findings indicate a perturbation of this pathway by both mutation and exposure.

Elevated plasma alanine and lactate in ASD patients suggest peripheral mitochondrial dysfunction associated with this disorder (Aldred *et al.* 2003; El-Ansary *et al.* 2017; Orozco *et al.* 2019). Although we were not able to see any significant changes in MMP in our system, lactic acid levels were increased by both CPF and CPO in *CHD8*<sup>+/-</sup> only (**Figure 5B**). These results suggest that although the presence of *CHD8* mutation and the exposure to CPF/CPO are not sufficient to induce a profound mitochondrial dysfunction independently, they might act synergistically to increase levels of metabolites involved in mitochondrial function and respiration.

Plasma levels of tryptophan and its metabolite KA were reported to be attenuated in ASD (**Table 1**). Animal models and studies on postmortem brain revealed increased levels of KA, which was associated with cognitive, behavioral, and learning impairments in ASD, ADHD, and schizophrenia (Iaccarino *et al.* 2013; Murakami *et al.* 2019; Scharfman *et al.* 2000; Vohra *et al.* 2018; Yerys *et al.* 2009). In agreement with that, levels of tryptophan, kynurenine, and KA were increased by exposure to CPF and/or CPO exclusively in the *CHD8*<sup>+/-</sup> line in our study (**Figure 5C**). Tryptophan enters the kynurenine pathway leading to the production of several neuroactive compounds, including KA. KA can interact with NMDA, nicotinic, and GPR35 receptors, modulating the release of glutamate, dopamine, acetylcholine, and GABA. Furthermore, KA functions as scavenger of ROS, thereby playing a role in redox homeostasis (Ramos-Chávez *et al.* 2018). Higher level of oxidative stress is a known feature of ASD (Chauhan and Chauhan 2006). Thus, compensatory elevated KA may be a result of higher oxidative stress observed in *CHD8*<sup>+/-</sup> BrainSpheres (**Figure S3B**).

The physiological functions of  $\alpha$ -Hydroxyglutaric acid remain widely unknown, but its accumulation is toxic to the mammalian brain (Schafingen *et al.* 2009). L-2- and D-2-hydroxyglutaric aciduria in urine, plasma, and cerebrospinal fluid are associated with diverse neurologic deficits (Zafeiriou *et al.* 2008). Interestingly, L-2-hydroxyglutaric aciduria has been observed in a few ASD case reports (Zafeiriou *et al.* 2008). Furthermore, L-2-hydroxyglutaric acid has been shown to inhibit mitochondrial creatine kinase and to induce oxidative stress in the cerebellum (Schafingen *et al.* 2009). Our metabolomic analysis revealed increased levels of 2-hydroxyglutaric acid in BrainSpheres exposed to CPO when compared to both *CHD8*<sup>+/+</sup> and *CHD8*<sup>+/-</sup> DMSO controls (**Figure 5D**). The difference was statistically significant only in the mutant cell line, suggesting that the elevation of 2-

hydroxyglutaric acid levels might be due to the synergistic effect of *CHD8* mutation and exposure to CPO. It is difficult, however, to speculate about mechanism behind this finding. Further analysis is needed to distinguish between  $\alpha$  and  $\beta$  forms.

We observed one of the main ASD features: an imbalance in excitatory and inhibitory neurotransmitters in *CHD8*<sup>+/-</sup> BrainSpheres (**Figure 6**). About 80% of neurons in the cerebral cortex are excitatory undefined, and the remaining 20% are inhibitory (represented primarily by GABAergic interneurons). In some studies, lower levels of GABA and numbers of GABAergic interneurons were found (Belmonte *et al.* 2004; Gogolla *et al.* 2009; Rippon *et al.* 2007; Rubenstein and Merzenich 2003), which is also consistent with a higher incidence of epilepsy (Lewine *et al.* 1999). The lower level of GABA neurotransmission in sound processing and motor control regions may be the cause of hypersensitivity of autistic patients to loud sounds and motor impairment (Gaetz *et al.* 2014). In other studies, an increase GABAergic interneurons was observed (Lawrence *et al.* 2010; Mariani *et al.* 2015). This discrepancy may be due to different brain regions analyzed, underlying genetic perturbations in different autistic patients, and differences occurring during the lifespan in reported studies. In our system, *CHD8* heterozygous KO resulted in lower levels of GABA, which did not significantly change following CPF/CPO treatment. Interestingly, expression of the GABAergic transcription factor *DLX1*, which regulates Glutamic Acid Decarboxylase 1 (*GAD1*) expression (among many other genes), was higher in *CHD8*<sup>+/-</sup>, such that an increased level of GABA might be expected. But neither *GAD1* nor GABA levels were increased. Here, more experiments are needed to understand and validate the exact mechanism of this circuit. Excessive and unbalanced excitatory glutamatergic signaling is associated with the high epilepsy rates in ASD (Zheng *et al.* 2016). Glutamate was significantly increased upon exposure to CPO of both *CHD8*<sup>+/+</sup> and *CHD8*<sup>+/-</sup> BrainSpheres. A recent meta-analysis by Zheng *et al.* established overall higher blood glutamate levels in ASD than in typically developing individuals, with a positive correlation between increased glutamate levels in ASD blood and brain samples (Zheng *et al.* 2016). Thus, further investigations are needed to elucidate whether CPO is specifically correlated with an increased risk of developing forms of ASD associated with epilepsy, which is present in about 20% of ASD patients (Besag 2018).

The dopamine synthesis pathway was perturbed in our experimental model system (**Figure 7**). Interestingly, we observed slightly reduced level of tyrosine, higher levels of L-DOPA along with lower level of dopamine in *CHD8*<sup>+/-</sup> BrainSpheres, but no changes due to CPF/CPO treatment. Moreover, *TH* and *COMT* expression were increased due to both mutation and treatment. Although there is some controversy in the literature reporting both elevated and reduced levels of dopamine in ASD, the perturbation of catecholamine

synthesis in ASD has been established (Ernst *et al.* 1997; Kaluzna-Czaplinska *et al.* 2010). *COMT* gene variations have been associated with ASD, anxiety, and bipolar disorder (James *et al.* 2006; Lachman 2008; Lachman *et al.* 1996; Schmidt *et al.* 2011). Elevated *COMT* activity due to functional polymorphism (Val158) was associated with lower levels of dopamine, poorer cognitive performance, and increased predisposition for psychiatric disorders (Kamath *et al.* 2012; Simpson *et al.* 2014), which was similarly attenuated in our model. Increased expression of *COMT* and decreased levels of dopamine suggests that dopamine is metabolized more rapidly in *CHD8*<sup>+/-</sup> BrainSpheres – even if these cells produce more L-DOPA.

Overall, our findings are consistent with an imbalance in the synthesis and function of glutamate, GABA, catecholamines, and acetylcholine neurotransmitter systems observed in ASD, as summarized by (Cetin *et al.* 2015; Marotta *et al.* 2020). Here, we recapitulated some of the key findings from the literature and demonstrated that both genetic background and/or exposure to environmental factors may contribute to the imbalance in neurotransmission. Although the changes in biofluids and in our model, as well as in aforementioned animal models, were sometimes contradictory (such as tryptophan and SAM/SAH), we interpret them as perturbations in the same pathway. Alternatively, the differences could be due to analysis of intracellular metabolites, while the clinical findings are mainly in blood and urine. Additional quantification of these metabolites and neurotransmitters in the medium supernatant, to model clinical biofluid findings, could contribute to a better understanding of the perturbation of these pathways.

As a direct outcome of perturbations in energy metabolism and acetylcholine degradation, the highly energy-dependent process of neurite outgrowth was assessed (**Figure 3, Figure S7**). As expected, both CPF and CPO significantly reduced neurite outgrowth. This effect could be rescued by pre-treatment with tocopherol, confirming perturbation in energy metabolism and oxidative stress. We have not observed an increase in ROS in response to CPF or CPO (**Figure 3B**) or changes in oxidized/reduced glutathione (data not shown), likely due to the 24-hour-exposure selected. Because of the different spheroid sizes, we were unable to draw a conclusion about synergy effects on neurite outgrowth between exposure and *CHD8* mutation. Axonal growth was shown to be perturbed by OPs in the developing nervous system. In neural cell lines, CPF has been shown to inhibit neurite outgrowth, while axonal growth was perturbed by CPF in rat primary neurons (Howard *et al.* 2005; Yang *et al.* 2008).

In conclusion, this study demonstrated how a known genetic ASD risk factor and the exposure to an environmental chemical can synergize via perturbing metabolic pathways



and neurotransmitter systems implicated in ASD. Remarkably, common targets for both *CHD8* mutation and CPF/CPO exposure suggest that CPF can mimic some effects of *CHD8*<sup>+/-</sup> and *vice versa*. This suggests that in patients with *CHD8* mutations, severity of symptoms might be exacerbated if exposed to these toxicants. Although only two cell lines were used in this study (control and mutant), the findings point to potential targets and AOPs to evaluate when performing GxE studies. Extension of these findings to more cell lines, as well as to patient-derived iPSC, is needed to validate the findings presented here. The identification of selected GxE factors converging on common metabolic pathways could then foster the development of treatments tailored to specific clusters of patients. These types of GxE in organotypic models (Marx *et al.* 2016, 2020) represent a way forward to study the interplay of genetic and environmental components of autism and other neurodevelopmental disorders. The mechanistic validation through consensus AOP, and especially the corroboration with biomarker identification and correlation between epidemiological and mechanistic studies, opens new approaches for establishing the relevance of such findings.

## REFERENCES

- Aldred S, Moore KM, Fitzgerald M, Waring RH. 2003. Plasma Amino Acid Levels in Children with Autism and Their Families. *Journal of Autism and Developmental Disorders* 33:93–97; doi:10.1023/a:1022238706604.
- Aldridge JE, Meyer A, Seidler FJ, Slotkin TA. 2005. Alterations in Central Nervous System Serotonergic and Dopaminergic Synaptic Activity in Adulthood after Prenatal or Neonatal Chlorpyrifos Exposure. *Environ Health Persp* 113:1027–1031; doi:10.1289/ehp.7968.
- Arnold GL, Hyman SL, Mooney RA, Kirby RS. 2003. Plasma Amino Acids Profiles in Children with Autism: Potential Risk of Nutritional Deficiencies. *J Autism Dev Disord* 33:449–454; doi:10.1023/a:1025071014191.
- Ayhan F, Konopka G. 2019. Regulatory genes and pathways disrupted in autism spectrum disorders. *Progress in neuro-psychopharmacology & biological psychiatry* 89:57–64; doi:10.1016/j.pnpbp.2018.08.017.
- Bal-Price A, Crofton KM, Leist M, Allen S, Arand M, Buetler T, *et al.* 2015. International STakeholder NETwork (ISTNET): creating a developmental neurotoxicity (DNT) testing road map for regulatory purposes. *Archives of Toxicology* 89:269–287; doi:10.1007/s00204-015-1464-2.
- Bal-Price A, Lein PJ, Keil KP, Sethi S, Shafer T, Barenys M, *et al.* 2017. Developing and applying the adverse outcome pathway concept for understanding and predicting neurotoxicity. *Neurotoxicology* 59:240–255; doi:10.1016/j.neuro.2016.05.010.
- Barr DB, Allen R, Olsson AO, Bravo R, Caltabiano LM, Montesano A, *et al.* 2005. Concentrations of selective metabolites of organophosphorus pesticides in the United States population. *Environmental research* 99:314–326; doi:10.1016/j.envres.2005.03.012.

- Baxter AJ, Brugha TS, Erskine HE, Scheurer RW, Vos T, Scott JG. 2015. The epidemiology and global burden of autism spectrum disorders. *Psychological medicine* 45:601–613; doi:10.1017/s003329171400172x.
- Beger RD, Dunn WB, Bandukwala A, Bethan B, Broadhurst D, Clish CB, *et al.* 2019. Towards quality assurance and quality control in untargeted metabolomics studies. *Metabolomics* 15:4; doi:10.1007/s11306-018-1460-7.
- Belmonte MK, Cook EH, Anderson GM, Rubenstein JLR, Greenough WT, Beckel-Mitchener A, *et al.* 2004. Autism as a disorder of neural information processing: directions for research and targets for therapy. *Molecular Psychiatry* 9:646–663; doi:10.1038/sj.mp.4001499.
- Bernier R, Golzio C, Xiong B, Stessman HA, Coe BP, Penn O, *et al.* 2014. Disruptive CHD8 mutations define a subtype of autism early in development. *Cell* 158:263–276; doi:10.1016/j.cell.2014.06.017.
- Besag FM. 2018. Epilepsy in patients with autism: links, risks and treatment challenges. *Neuropsychiatric disease and treatment* 14:1–10; doi:10.2147/ndt.s120509.
- Bitar T, Mavel S, Emond P, Nadal-Desbarats L, Lefèvre A, Mattar H, *et al.* 2018. Identification of metabolic pathway disturbances using multimodal metabolomics in autistic disorders in a Middle Eastern population. *J Pharmaceut Biomed* 152:57–65; doi:10.1016/j.jpba.2018.01.007.
- Bouhifd M, Beger R, Flynn T, Guo L, Harris G, Hogberg H, *et al.* 2015. Quality assurance of metabolomics. *Altex* 32:319–326; doi:10.14573/altex.1509161.
- Brix MK, Erslund L, Hugdahl K, Grüner R, Posserud M-B, Hammar Å, *et al.* 2015. “Brain MR spectroscopy in autism spectrum disorder—the GABA excitatory/inhibitory imbalance theory revisited.” *Front Hum Neurosci* 9:365; doi:10.3389/fnhum.2015.00365.
- Brown MS, Singel D, Hepburn S, Rojas DC. 2013. Increased Glutamate Concentration in the Auditory Cortex of Persons With Autism and First-Degree Relatives: A 1H-MRS Study. *Autism Res* 6:1–10; doi:10.1002/aur.1260.
- Bryn V, Verkerk R, Skjeldal OH, Saugstad OD, Ormstad H. 2018. Kynurenine Pathway in Autism Spectrum Disorders in Children. *Neuropsychobiology* 76:82–88; doi:10.1159/000488157.
- Cai J, Ding L, Zhang J-S, Xue J, Wang L-Z. 2016. Elevated plasma levels of glutamate in children with autism spectrum disorders. *Neuroreport* 27:272–276; doi:10.1097/wnr.0000000000000532.
- Cetin FH, Tunca H, Güney E, Iseri E. 2015. Neurotransmitter Systems in Autism Spectrum Disorder. *Autism Spectrum Disorder - Recent Advances*. InTech.
- Chaste P, Chaste P, Leboyer M, Leboyer M. 2012. Autism risk factors: genes, environment, and gene-environment interactions. *Dialogues in clinical neuroscience* 14: 281–292.
- Chauhan A, Chauhan V. 2006. Oxidative stress in autism. *Pathophysiology* 13:171–181; doi:10.1016/j.pathophys.2006.05.007.
- Cochran DM, Sikoglu EM, Hodge SM, Edden RAE, Foley A, Kennedy DN, *et al.* 2015. Relationship among Glutamine,  $\gamma$ -Aminobutyric Acid, and Social Cognition in Autism Spectrum Disorders. *J Child Adol Psychop* 25:314–322; doi:10.1089/cap.2014.0112.

- Cohen BI. 2002. The significance of ammonia/gamma-aminobutyric acid (GABA) ratio for normality and liver disorders. *Med Hypotheses* 59:757–758; doi:10.1016/s0306-9877(02)00325-0.
- Corrigan NM, Shaw DWW, Estes AM, Richards TL, Munson J, Friedman SD, *et al.* 2013. Atypical Developmental Patterns of Brain Chemistry in Children With Autism Spectrum Disorder. *Jama Psychiat* 70:964–974; doi:10.1001/jamapsychiatry.2013.1388.
- Cotney J, Muhle RA, Sanders SJ, Liu L, Willsey AJ, Niu W, *et al.* 2015. The autism-associated chromatin modifier CHD8 regulates other autism risk genes during human neurodevelopment. *Nature Communications* 6:6404; doi:10.1038/ncomms7404.
- Courchesne E, Pramparo T, Gazestani VH, Lombardo MV, Pierce K, Lewis NE. 2019. The ASD Living Biology: from cell proliferation to clinical phenotype. *Molecular psychiatry* 24:88–107; doi:10.1038/s41380-018-0056-y.
- Delaye J-B, Patin F, Lagrue E, Tilly OL, Bruno C, Vuillaume M-L, *et al.* 2018. Post hoc analysis of plasma amino acid profiles: towards a specific pattern in autism spectrum disorder and intellectual disability. *Ann Clin Biochem* 55:543–552; doi:10.1177/0004563218760351.
- Dhossche D, Applegate H, Abraham A, Maertens P, Bland L, Bencsath A, *et al.* 2002. Elevated plasma gamma-aminobutyric acid (GABA) levels in autistic youngsters: stimulus for a GABA hypothesis of autism. *Medical Sci Monit Int Medical J Exp Clin Res* 8: PR1-6.
- Dietert RR, Dietert JM, Dewitt JC. 2011. Environmental risk factors for autism. *Emerging health threats journal* 4:7111; doi:10.3402/ehj.v4i0.7111.
- Drenthen GS, Barendse EM, Aldenkamp AP, Veenendaal TM van, Puts NAJ, Edden RAE, *et al.* 2016. Altered neurotransmitter metabolism in adolescents with high-functioning autism. *Psychiatry Res Neuroimaging* 256:44–49; doi:10.1016/j.psychresns.2016.09.007.
- El-Ansary A. 2016. Data of multiple regressions analysis between selected biomarkers related to glutamate excitotoxicity and oxidative stress in Saudi autistic patients. *Data Brief* 7:111–116; doi:10.1016/j.dib.2016.02.025.
- El-Ansary A, Al-Ayadhi L. 2014. GABAergic/glutamatergic imbalance relative to excessive neuroinflammation in autism spectrum disorders. *J Neuroinflamm* 11:189; doi:10.1186/s12974-014-0189-0.
- El-Ansary A, Bjørklund G, Chirumbolo S, Alnakhli OM. 2017. Predictive value of selected biomarkers related to metabolism and oxidative stress in children with autism spectrum disorder. *Metab Brain Dis* 32:1209–1221; doi:10.1007/s11011-017-0029-x.
- ElBaz FM, Zaki MM, Youssef AM, ElDorry GF, Elalfy DY. 2014. Study of plasma amino acid levels in children with autism: An Egyptian sample. *Egypt J Medical Hum Genetics* 15:181–186; doi:10.1016/j.ejmhg.2014.02.002.
- Elst LT van, Maier S, Fangmeier T, Endres D, Mueller GT, Nickel K, *et al.* 2014. Disturbed cingulate glutamate metabolism in adults with high-functioning autism spectrum disorder: evidence in support of the excitatory/inhibitory imbalance hypothesis. *Mol Psychiatr* 19:1314–1325; doi:10.1038/mp.2014.62.

- Ernst M, Zametkin AJ, Matochik JA, Pascualvaca D, Cohen RM. 1997. Low medial prefrontal dopaminergic activity in autistic children. *Lancet* 350:638; doi:10.1016/s0140-6736(05)63326-0.
- Evans C, Dunstan HR, Rothkirch T, Roberts TK, Reichelt KL, Cosford R, *et al.* 2013. Altered amino acid excretion in children with autism. *Nutr Neurosci* 11:9–17; doi:10.1179/147683008x301360.
- Fan X, Dong J, Zhong S, Wei Y, Wu Q, Yan L, *et al.* 2018. Spatial transcriptomic survey of human embryonic cerebral cortex by single-cell RNA-seq analysis. *Cell research* 28:730–745; doi:10.1038/s41422-018-0053-3.
- Ford TC, Crewther DP. 2016. A Comprehensive Review of the 1H-MRS Metabolite Spectrum in Autism Spectrum Disorder. *Front Mol Neurosci* 9:14; doi:10.3389/fnmol.2016.00014.
- Gaetz W, Bloy L, Wang DJ, Port RG, Blaskey L, Levy SE, *et al.* 2014. GABA estimation in the brains of children on the autism spectrum: measurement precision and regional cortical variation. *NeuroImage* 86:1–9; doi:10.1016/j.neuroimage.2013.05.068.
- Gaugler T, Klei L, Sanders SJ, Bodea CA, Goldberg AP, Lee AB, *et al.* 2014. Most genetic risk for autism resides with common variation. *Nature Genetics* 46:881–885; doi:10.1038/ng.3039.
- Geier DA, Kern JK, Garver CR, Adams JB, Audhya T, Nataf R, *et al.* 2009. Biomarkers of environmental toxicity and susceptibility in autism. *Journal of the Neurological Sciences* 280:101–108; doi:10.1016/j.jns.2008.08.021.
- Gevi F, Zolla L, Gabriele S, Persico AM. 2016. Urinary metabolomics of young Italian autistic children supports abnormal tryptophan and purine metabolism. *Mol Autism* 7:47; doi:10.1186/s13229-016-0109-5.
- Gogolla N, Leblanc JJ, Quast KB, Südhof TC, Fagiolini M, Hensch TK. 2009. Common circuit defect of excitatory-inhibitory balance in mouse models of autism. *Journal of neurodevelopmental disorders* 1:172–181; doi:10.1007/s11689-009-9023-x.
- Halladay AK, Amaral D, Aschner M, Bolivar VJ, Bowman A, DiCicco-Bloom E, *et al.* 2009. Animal models of autism spectrum disorders: Information for neurotoxicologists. *Neurotoxicology* 30:811–821; doi:10.1016/j.neuro.2009.07.002.
- Han Y, Xi Q, Dai W, Yang S, Gao L, Su Y, *et al.* 2015. Abnormal transsulfuration metabolism and reduced antioxidant capacity in Chinese children with autism spectrum disorders. *Int J Dev Neurosci* 46:27–32; doi:10.1016/j.ijdevneu.2015.06.006.
- Harada M, Taki MM, Nose A, Kubo H, Mori K, Nishitani H, *et al.* 2011. Non-Invasive Evaluation of the GABAergic/Glutamatergic System in Autistic Patients Observed by MEGA-Editing Proton MR Spectroscopy Using a Clinical 3 Tesla Instrument. *J Autism Dev Disord* 41:447–454; doi:10.1007/s10803-010-1065-0.
- Harris G, Eschment M, Orozco SP, McCaffery JM, MacLennan R, Severin D, *et al.* 2018. Toxicity, recovery, and resilience in a 3D dopaminergic neuronal in vitro model exposed to rotenone. *Archives of Toxicology* 31:441–20; doi:10.1007/s00204-018-2250-8.
- Harris G, Hogberg H, Hartung T, Smirnova L. 2017. 3D Differentiation of LUHMES Cell Line to Study Recovery and Delayed Neurotoxic Effects. *Current protocols in toxicology* / editorial board, Mahin D Maines (editor-in-chief) . [*et al*] 73:11.23.1-11.23.28; doi:10.1002/cptx.29.

- Hartung T. 2017. Evolution of toxicological science: the need for change. *International Journal of Risk Assessment and Management* 20:21; doi:10.1504/ijram.2017.082570.
- Hartung T. 2013. Look back in anger - what clinical studies tell us about preclinical work. *Altex* 30:275–291; doi:10.14573/altex.2013.3.275.
- Hartung T, Bremer S, Casati S, Coecke S, Corvi R, Fortaner S, *et al.* 2004. A Modular Approach to the ECVAM Principles on Test Validity. *Altern Laboratory Animals* 32:467–472; doi:10.1177/026119290403200503.
- Hartung T, Hoffmann S, Stephens M. 2013. Mechanistic validation. *Altex* 30: 119–130.
- Hassan MH, Desoky T, Sakhr HM, Gabra RH, Bakri AH. 2019. Possible Metabolic Alterations among Autistic Male Children: Clinical and Biochemical Approaches. *J Mol Neurosci* 67:204–216; doi:10.1007/s12031-018-1225-9.
- Hassan TH, Abdelrahman HM, Fattah NRA, El-Masry NM, Hashim HM, El-Gerby KM, *et al.* 2013. Blood and brain glutamate levels in children with autistic disorder. *Res Autism Spect Dis* 7:541–548; doi:10.1016/j.rasd.2012.12.005.
- Hérault J, Martineau J, Perrot-Beaugerie A, Jouve J, Tournade H, Barthelemy C, *et al.* 1993. Investigation of whole blood and urine monoamines in autism. *Eur Child Adoles Psy* 2:211–220; doi:10.1007/bf02098580.
- Horder J, Petrinovic MM, Mendez MA, Bruns A, Takumi T, Spooren W, *et al.* 2018. Glutamate and GABA in autism spectrum disorder—a translational magnetic resonance spectroscopy study in man and rodent models. *Transl Psychiat* 8:106; doi:10.1038/s41398-018-0155-1.
- HOWARD A, Bucelli R, JETT D, Bruun D, Yang D, LEIN P. 2005. Chlorpyrifos exerts opposing effects on axonal and dendritic growth in primary neuronal cultures. *Toxicology and Applied Pharmacology* 207:112–124; doi:10.1016/j.taap.2004.12.008.
- Iaccarino HF, Suckow RF, Xie S, Bucci DJ. 2013. The effect of transient increases in kynurenic acid and quinolinic acid levels early in life on behavior in adulthood: Implications for schizophrenia. *Schizophrenia research* 150:392–397; doi:10.1016/j.schres.2013.09.004.
- James SJ. 2013. Autism and Folate-dependent One-carbon Metabolism: Serendipity and Critical Branch-point Decisions in Science. *Global advances in health and medicine* 2:48–51; doi:10.7453/gahmj.2013.088.
- James SJ, Cutler P, Melnyk S, Jernigan S, Janak L, Gaylor DW, *et al.* 2004. Metabolic biomarkers of increased oxidative stress and impaired methylation capacity in children with autism. *The American journal of clinical nutrition* 80: 1611–1617.
- James SJ, Melnyk S, Jernigan S, Cleves MA, Halsted CH, Wong DH, *et al.* 2006. Metabolic endophenotype and related genotypes are associated with oxidative stress in children with autism. *American Journal of Medical Genetics Part B: Neuropsychiatric Genetics* 141B:947–956; doi:10.1002/ajmg.b.30366.
- Joshi G, Biederman J, Wozniak J, Goldin RL, Crowley D, Furtak S, *et al.* 2013. Magnetic resonance spectroscopy study of the glutamatergic system in adolescent males with high-functioning autistic disorder: a pilot study at 4T. *Eur Arch Psy Clin N* 263:379–384; doi:10.1007/s00406-012-0369-9.

- Juberg DR, Hoberman AM, Marty S, Picut CA, Stump DG. 2019. Letter to the editor regarding “safety of safety evaluation of pesticides: developmental neurotoxicity of chlorpyrifos and chlorpyrifos-methyl” by Mie *et al.* (environmental health. 2018. 17:77). *Environmental health : a global access science source* 18:21–6; doi:10.1186/s12940-019-0454-x.
- Kaluzna-Czaplińska J, Socha E, Rynkowski J. 2010. Determination of homovanillic acid and vanillylmandelic acid in urine of autistic children by gas chromatography/mass spectrometry. *Medical Science Monitor* 16: CR445–CR450.
- Kaluźna-Czaplińska J, Żurawicz E, Struck W, Markuszewski M. 2014. Identification of organic acids as potential biomarkers in the urine of autistic children using gas chromatography/mass spectrometry. *Journal of Chromatography B* 966:70–76; doi:10.1016/j.jchromb.2014.01.041.
- Kamath V, Moberg PJ, Gur RE, Doty RL, Turetsky BI. 2012. Effects of the Val(158)Met catechol-O-methyltransferase Gene Polymorphism on Olfactory Processing in Schizophrenia. *Behav Neurosci* 126:209–215; doi:10.1037/a0026466.
- Karimi P, Kamali E, Mousavi SM, Karahmadi M. 2017. Environmental factors influencing the risk of autism. *Journal of research in medical sciences : the official journal of Isfahan University of Medical Sciences* 22:27; doi:10.4103/1735-1995.200272.
- Khemakhem AM, Frye RE, El-Ansary A, Al-Ayadhi L, Bacha AB. 2017. Novel biomarkers of metabolic dysfunction in autism spectrum disorder: potential for biological diagnostic markers. *Metab Brain Dis* 32:1983–1997; doi:10.1007/s11011-017-0085-2.
- Kim JY, Son MJ, Son CY, Radua J, Eisenhut M, Gressier F, *et al.* 2019. Environmental risk factors and biomarkers for autism spectrum disorder: an umbrella review of the evidence. *The lancet Psychiatry* 6:590–600; doi:10.1016/s2215-0366(19)30181-6.
- Kolodny T, Schallmo M, Gerds J, Edden RAE, Bernier RA, Murray SO. 2020. Concentrations of Cortical GABA and Glutamate in Young Adults With Autism Spectrum Disorder. *Autism Res* 13:1111–1129; doi:10.1002/aur.2300.
- Koufaris C, Sismani C. 2015. Modulation of the Genome and Epigenome of Individuals Susceptible to Autism by Environmental Risk Factors. *International Journal of Molecular Sciences* 16:8699–8718; doi:10.3390/ijms16048699.
- Kubas B, Kulak W, Sobaniec W, Tarasow E, Lebkowska U, Walecki J. 2012. Metabolite alterations in autistic children: a 1H MR spectroscopy study. *Adv Med Sci* 57:152–156; doi:10.2478/v10039-012-0014-x.
- Kuwabara H, Yamasue H, Koike S, Inoue H, Kawakubo Y, Kuroda M, *et al.* 2013. Altered Metabolites in the Plasma of Autism Spectrum Disorder: A Capillary Electrophoresis Time-of-Flight Mass Spectroscopy Study. *Plos One* 8:e73814; doi:10.1371/journal.pone.0073814.
- Kuwagata M, Ogawa T, Shioda S, Nagata T. 2009. Observation of fetal brain in a rat valproate-induced autism model: a developmental neurotoxicity study. *International journal of developmental neuroscience : the official journal of the International Society for Developmental Neuroscience* 27:399–405; doi:10.1016/j.ijdevneu.2009.01.006.

- Lachman HM. 2008. Perspective: Does COMT val158met Affect Behavioral Phenotypes: Yes, No, Maybe? *Neuropsychopharmacol* 33:3027–3029; doi:10.1038/npp.2008.189.
- Lachman HM, Papolos DF, Saito T, Yu Y-M, Szumlanski CL, Weinshilboum RM. 1996. Human catechol-O-methyltransferase pharmacogenetics: description of a functional polymorphism and its potential application to neuropsychiatric disorders. *Pharmacogenetics* 6:243–250; doi:10.1097/00008571-199606000-00007.
- Lai M-C, Lombardo MV, Baron-Cohen S. 2014. Autism. *Lancet* 383:896–910; doi:10.1016/s0140-6736(13)61539-1.
- Lancaster MA, Renner M, Martin C-A, Wenzel D, Bicknell LS, Hurles ME, *et al.* 2013. Cerebral organoids model human brain development and microcephaly. *Nature* 501:373–379; doi:10.1038/nature12517.
- Landrigan PJ. 2010. What causes autism? Exploring the environmental contribution. *Current opinion in pediatrics* 22:219–225; doi:10.1097/mop.0b013e328336eb9a.
- Landrigan PJ, Lambertini L, Birnbaum LS. 2012. A research strategy to discover the environmental causes of autism and neurodevelopmental disabilities. *Environ Health Perspect* 120:a258–a260; doi:10.1289/ehp.1104285.
- LaSalle JM. 2013. Epigenomic strategies at the interface of genetic and environmental risk factors for autism. *Journal of human genetics* 58:396–401; doi:10.1038/jhg.2013.49.
- Lawrence YA, Kemper TL, Bauman ML, Blatt GJ. 2010. Parvalbumin-, calbindin-, and calretinin-immunoreactive hippocampal interneuron density in autism. *Acta neurologica Scandinavica* 121:99–108; doi:10.1111/j.1600-0404.2009.01234.x.
- leist M, Hasiwa N, Daneshian M, Hartung T. 2012. Validation and quality control of replacement alternatives – current status and future challenges. *Toxicol Res* 1:8–22; doi:10.1039/c2tx20011b.
- Lewine JD, Andrews R, Chez M, Patil AA, Devinsky O, Smith M, *et al.* 1999. Magnetoencephalographic patterns of epileptiform activity in children with regressive autism spectrum disorders. *Pediatrics* 104:405–418; doi:10.1542/peds.104.3.405.
- Li J, Settivari R, LeBaron MJ, Marty MS. 2019. An industry perspective: a streamlined screening strategy using alternative models for chemical assessment of developmental neurotoxicity. *Neurotoxicology* 73:17–30; doi:10.1016/j.neuro.2019.02.010.
- Liu A, Zhou W, Qu L, He F, Wang H, Wang Y, *et al.* 2019. Altered Urinary Amino Acids in Children With Autism Spectrum Disorders. *Frontiers in Cellular Neuroscience* 13:7; doi:10.3389/fncel.2019.00007.
- Lussu M, Noto A, Masili A, Rinaldi AC, Dessì A, Angelis MD, *et al.* 2017. The urinary 1H-NMR metabolomics profile of an Italian autistic children population and their unaffected siblings. *Autism Res* 10:1058–1066; doi:10.1002/aur.1748.
- Lyall K, Croen L, Daniels J, Fallin MD, Ladd-Acosta C, Lee BK, *et al.* 2017. The Changing Epidemiology of Autism Spectrum Disorders. *Annual review of public health* 38:81–102; doi:10.1146/annurev-publhealth-031816-044318.

Mandy W, Lai M-C. 2016. Annual Research Review: The role of the environment in the developmental psychopathology of autism spectrum condition. *Journal of child psychology and psychiatry, and allied disciplines* 57:271–292; doi:10.1111/jcpp.12501.

Mariani J, Coppola G, Zhang P, Abyzov A, Provini L, Tomasini L, *et al.* 2015. FOXP1-Dependent Dysregulation of GABA/ Glutamate Neuron Differentiation in Autism Spectrum Disorders. *Cell* 162:375–390; doi:10.1016/j.cell.2015.06.034.

Marotta R, Risoleo MC, Messina G, Parisi L, Carotenuto M, Vetri L, *et al.* 2020. The Neurochemistry of Autism. *Brain Sciences* 10:163; doi:10.3390/brainsci10030163.

Martineau J, Barthélémy C, Jouve J, Muh J, LeLord G. 1992. Monoamines (serotonin and catecholamines) and their derivatives in infantile autism: age-related changes and drug effects. *Dev Medicine Child Neurology* 34:593–603; doi:10.1111/j.1469-8749.1992.tb11490.x.

Martin'eau J, Héroult J, Petit E, Guérin P, Hameury L, Perrot A, *et al.* 1994. Catecholaminergic metabolism and autism. *Dev Medicine Child Neurology* 36:688–697; doi:10.1111/j.1469-8749.1994.tb11911.x.

Marx U, Akabane T, Andersson TB, Baker E, Beilmann M, Beken S, *et al.* 2020. Biology-inspired microphysiological systems to advance patient benefit and animal welfare in drug development. *Altex*; doi:10.14573/altex.2001241.

Marx U, Andersson TB, Bahinski A, Beilmann M, Beken S, Cassee FR, *et al.* 2016. Biology-inspired microphysiological system approaches to solve the prediction dilemma of substance testing. *Altex* 33:272–321; doi:10.14573/altex.1603161.

Mavel S, Nadal-Desbarats L, Blasco H, Bonnet-Brilhaut F, Barthélémy C, Montigny F, *et al.* 2013. <sup>1</sup>H–<sup>13</sup>C NMR-based urine metabolic profiling in autism spectrum disorders. *Talanta* 114:95–102; doi:10.1016/j.talanta.2013.03.064.

Melnik S, Fuchs GJ, Schulz E, Lopez M, Kahler SG, Fussell JJ, *et al.* 2012. Metabolic Imbalance Associated with Methylation Dysregulation and Oxidative Damage in Children with Autism. *J Autism Dev Disord* 42:367–377; doi:10.1007/s10803-011-1260-7.

Mie A, Rudén C, Grandjean P. 2018. Safety of Safety Evaluation of Pesticides: developmental neurotoxicity of chlorpyrifos and chlorpyrifos-methyl. *Environmental health: a global access science source* 17:77–5; doi:10.1186/s12940-018-0421-y.

Ming X, Stein TP, Barnes V, Rhodes N, Guo L. 2012. Metabolic Perturbance in Autism Spectrum Disorders: A Metabolomics Study. *J Proteome Res* 11:5856–5862; doi:10.1021/pr300910n.

Modabbernia A, Velthorst E, Reichenberg A. 2017. Environmental risk factors for autism: an evidence-based review of systematic reviews and meta-analyses. *Molecular Autism* 8:13–16; doi:10.1186/s13229-017-0121-4.

Moreno-Fuenmayor H, Borjas L, Arrieta A, Valera V, Socorro-Candanoza L. 1996. Plasma excitatory amino acids in autism. *Investigación Clínica* 37: 113–28.

Murakami Y, Imamura Y, Saito K, Sakai D, Motoyama J. 2019. Altered kynurenine pathway metabolites in a mouse model of human attention-deficit hyperactivity/autism spectrum disorders:



A potential new biological diagnostic marker. *Scientific reports* 9:13182–15; doi:10.1038/s41598-019-49781-y.

Nadal-Desbarats L, Aidoud N, Emond P, Blasco H, Filipiak I, Sarda P, *et al.* 2014. Combined <sup>1</sup>H-NMR and <sup>1</sup>H–<sup>13</sup>C HSQC-NMR to improve urinary screening in autism spectrum disorders. *Analyst* 139:3460–3468; doi:10.1039/c4an00552j.

Naushad SM, Jain JMN, Prasad CK, Naik U, Akella RRD. 2013. Autistic children exhibit distinct plasma amino acid profile. *Indian J Biochem Bio* 50: 474–8.

Neale BM, Kou Y, Liu L, Ma'ayan A, Samocha KE, Sabo A, *et al.* 2012. Patterns and rates of exonic de novo mutations in autism spectrum disorders. *Nature* 485:242–245; doi:10.1038/nature11011.

Noto A, Fanos V, Barberini L, Grapov D, Fattuoni C, Zaffanello M, *et al.* 2014. The urinary metabolomics profile of an Italian autistic children population and their unaffected siblings. *J Maternal-fetal Neonatal Medicine* 27:46–52; doi:10.3109/14767058.2014.954784.

Orekhova EV, Stroganova TA. 2014. Arousal and attention re-orienting in autism spectrum disorders: evidence from auditory event-related potentials. *Front Hum Neurosci* 8:34; doi:10.3389/fnhum.2014.00034.

Ormstad H, Bryn V, Verkerk R, Skjeldal OH, Halvorsen B, Saugstad OD, *et al.* 2018. Serum tryptophan, tryptophan catabolites and brain-derived neurotrophic factor in subgroups of youngsters with autism spectrum disorders. *Cns Neurological Disord - Drug Targets* 17; doi:10.2174/1871527317666180720163221.

Orozco JS, Hertz-Picciotto I, Abbeduto L, Slupsky CM. 2019. Metabolomics analysis of children with autism, idiopathic-developmental delays, and Down syndrome. *Translational psychiatry* 9:243–15; doi:10.1038/s41398-019-0578-3.

Pamies D, Barreras P, Block K, Makri G, Kumar A, Wiersma D, *et al.* 2017. A human brain microphysiological system derived from induced pluripotent stem cells to study neurological diseases and toxicity. *Altex* 34:362–376; doi:10.14573/altex.1609122.

Persico AM, Napolioni V. 2013. Autism genetics. *Behavioural Brain Research* 251:95–112; doi:10.1016/j.bbr.2013.06.012.

Peter CJ, Reichenberg A, Akbarian S. 2015. Epigenetic Regulation in Autism. *The Molecular Basis of Autism*. Springer New York. 67–92.

Platt RJ, Zhou Y, Slaymaker IM, Shetty AS, Weisbach NR, Kim J-A, *et al.* 2017. Chd8 Mutation Leads to Autistic-like Behaviors and Impaired Striatal Circuits. *Cell reports* 19:335–350; doi:10.1016/j.celrep.2017.03.052.

Ramos-Chávez LA, Huitrón RL, Esquivel DG, Pineda B, Ríos C, Silva-Adaya D, *et al.* 2018. Relevance of Alternative Routes of Kynurenic Acid Production in the Brain. *Oxidative medicine and cellular longevity* 2018:5272741–14; doi:10.1155/2018/5272741.

Rauh VA, Garfinkel R, Perera FP, Andrews HF, Hoepner L, Barr DB, *et al.* 2006. Impact of prenatal chlorpyrifos exposure on neurodevelopment in the first 3 years of life among inner-city children. *Pediatrics* 118:e1845-59; doi:10.1542/peds.2006-0338.

- Rippon G, Brock J, Brown C, Boucher J. 2007. Disordered connectivity in the autistic brain: challenges for the “new psychophysiology”. *International journal of psychophysiology: official journal of the International Organization of Psychophysiology* 63:164–172; doi:10.1016/j.ijpsycho.2006.03.012.
- Rojas DC, Singel D, Steinmetz S, Hepburn S, Brown MS. 2014. Decreased left perisylvian GABA concentration in children with autism and unaffected siblings. *Neuroimage* 86:28–34; doi:10.1016/j.neuroimage.2013.01.045.
- Rossignol DA, Genuis SJ, Frye RE. 2014. Environmental toxicants and autism spectrum disorders: a systematic review. *Transl Psychiat* 4:e360–e360; doi:10.1038/tp.2014.4.
- Rubeis SD, He X, Goldberg AP, Poultney CS, Samocha K, Cicek AE, *et al.* 2014. Synaptic, transcriptional and chromatin genes disrupted in autism. *Nature*; doi:10.1038/nature13772.
- Rubenstein JLR, Merzenich MM. 2003. Model of autism: increased ratio of excitation/inhibition in key neural systems. *Genes, Brain and Behavior* 2:255–267; doi:10.1034/j.1601-183x.2003.00037.x.
- Rylaarsdam L, Guemez-Gamboa A. 2019. Genetic Causes and Modifiers of Autism Spectrum Disorder. *Frontiers in Cellular Neuroscience* 13:385; doi:10.3389/fncel.2019.00385.
- Saleem TH, Shehata GA, Toghian R, Sakhr HM, Bakri AH, Desoky T, *et al.* 2020. Assessments of Amino Acids, Ammonia and Oxidative Stress Among Cohort of Egyptian Autistic Children: Correlations with Electroencephalogram and Disease Severity. *Neuropsych Dis Treat* 16:11–24; doi:10.2147/ndt.s233105.
- Sanders SJ. 2015. First glimpses of the neurobiology of autism spectrum disorder. *Current Opinion in Genetics & Development* 33:80–92; doi:10.1016/j.gde.2015.10.002.
- Sanders SJ, He X, Willsey AJ, Ercan-Sencicek AG, Samocha KE, Cicek AE, *et al.* 2015. Insights into Autism Spectrum Disorder Genomic Architecture and Biology from 71 Risk Loci. *Neuron* 87:1215–1233; doi:10.1016/j.neuron.2015.09.016.
- Sandin S, Lichtenstein P, Kuja-Halkola R, Larsson H, Hultman CM, Reichenberg A. 2014. The familial risk of autism. *JAMA* 311:1770–1777; doi:10.1001/jama.2014.4144.
- Satterstrom FK, Kosmicki JA, Wang J, Breen MS, Rubeis SD, An J-Y, *et al.* 2020. Large-Scale Exome Sequencing Study Implicates Both Developmental and Functional Changes in the Neurobiology of Autism. *Cell* 180:568–584.e23; doi:10.1016/j.cell.2019.12.036.
- Schaevitz LR, Berger-Sweeney JE. 2012. Gene-environment interactions and epigenetic pathways in autism: the importance of one-carbon metabolism. *ILAR journal* 53:322–340; doi:10.1093/ilar.53.3-4.322.
- Schafingen EV, Rzem R, Veiga-da-Cunha M. 2009. L: -2-Hydroxyglutaric aciduria, a disorder of metabolite repair. *Journal of inherited metabolic disease* 32:135–142; doi:10.1007/s10545-008-1042-3.
- Scharfman HE, Goodman JH, Schwarcz R. 2000. Electrophysiological effects of exogenous and endogenous kynurenic acid in the rat brain: studies in vivo and in vitro. *Amino acids* 19:283–297; doi:10.1007/s007260070060.

- Schmidt RJ, Hansen RL, Hartiala J, Allayee H, Schmidt LC, Tancredi DJ, *et al.* 2011. Prenatal vitamins, one-carbon metabolism gene variants, and risk for autism. *Epidemiology (Cambridge, Mass)* 22:476–485; doi:10.1097/ede.0b013e31821d0e30.
- Shelton JF, Geraghty EM, Tancredi DJ, Delwiche LD, Schmidt RJ, Ritz B, *et al.* 2014. Neurodevelopmental disorders and prenatal residential proximity to agricultural pesticides: the CHARGE study. *Environ Health Perspect* 122:1103–1109; doi:10.1289/ehp.1307044.
- Shimmura C, Suda S, Tsuchiya KJ, Hashimoto K, Ohno K, Matsuzaki H, *et al.* 2011. Alteration of Plasma Glutamate and Glutamine Levels in Children with High-Functioning Autism. *Plos One* 6:e25340; doi:10.1371/journal.pone.0025340.
- Shinohe A, Hashimoto K, Nakamura K, Tsujii M, Iwata Y, Tsuchiya KJ, *et al.* 2006. Increased serum levels of glutamate in adult patients with autism. *Prog Neuro-psychopharmacology Biological Psychiatry* 30:1472–1477; doi:10.1016/j.pnpbp.2006.06.013.
- Sillé FCM, Karakitsios S, Kleensang A, Koehler K, Maertens A, Miller GW, *et al.* 2020. The exposome - a new approach for risk assessment. *Altex* 37:3–23; doi:10.14573/altex.2001051.
- Simpson EH, Morud J, Winiger V, Biezonski D, Zhu JP, Bach ME, *et al.* 2014. Genetic variation in COMT activity impacts learning and dopamine release capacity in the striatum. *Learn Memory* 21:205–214; doi:10.1101/lm.032094.113.
- Slotkin TA, Seidler FJ. 2010. Oxidative stress from diverse developmental neurotoxicants: antioxidants protect against lipid peroxidation without preventing cell loss. *Neurotoxicology and Teratology* 32:124–131; doi:10.1016/j.ntt.2009.12.001.
- Smirnova L, Hogberg HT, leist M, Hartung T. 2014. Developmental neurotoxicity - challenges in the 21st century and in vitro opportunities. *Altex* 31:129–156; doi:10.14573/altex.1403271.
- Smith AM, King JJ, West PR, Ludwig MA, Donley ELR, Burrier RE, *et al.* 2018. Amino Acid Dysregulation Metabotypes: Potential Biomarkers for Diagnosis and Individualized Treatment for Subtypes of Autism Spectrum Disorder. *Biol Psychiat* 85:345–354; doi:10.1016/j.biopsych.2018.08.016.
- Stamou M, Streifel KM, Goines PE, Lein PJ. 2013. Neuronal connectivity as a convergent target of gene × environment interactions that confer risk for Autism Spectrum Disorders. *Neurotoxicology and Teratology* 36:3–16; doi:10.1016/j.ntt.2012.12.001.
- Stolerman ES, Smith B, Chaubey A, Jones JR. 2016. CHD8 intragenic deletion associated with autism spectrum disorder. *European Journal of Medical Genetics* 59:189–194; doi:10.1016/j.ejmg.2016.02.010.
- Suetterlin P, Hurley S, Mohan C, Riegman KLH, Pagani M, Caruso A, *et al.* 2018. Altered Neocortical Gene Expression, Brain Overgrowth and Functional Over-Connectivity in Chd8 Haploinsufficient Mice. *Cerebral cortex (New York, NY : 1991)* 28:2192–2206; doi:10.1093/cercor/bhy058.
- Sugathan A, Biagioli M, Golzio C, Erdin S, Blumenthal I, Manavalan P, *et al.* 2014. CHD8 regulates neurodevelopmental pathways associated with autism spectrum disorder in neural progenitors. *Proceedings of the National Academy of Sciences of the United States of America* 111:E4468–E4477; doi:10.1073/pnas.1405266111.

Tirouvanziam R, Obukhanych TV, Laval J, Aronov PA, Libove R, Banerjee AG, *et al.* 2012. Distinct Plasma Profile of Polar Neutral Amino Acids, Leucine, and Glutamate in Children with Autism Spectrum Disorders. *J Autism Dev Disord* 42:827–836; doi:10.1007/s10803-011-1314-x.

Torres-Altora MI, Mathur BN, Drerup JM, Thomas R, Lovinger DM, O'Callaghan JP, *et al.* 2011. Organophosphates dysregulate dopamine signaling, glutamatergic neurotransmission, and induce neuronal injury markers in striatum. *J Neurochem* 119:303–313; doi:10.1111/j.1471-4159.2011.07428.x.

Tu W-J, Chen H, He J. 2012. Application of LC-MS/MS analysis of plasma amino acids profiles in children with autism. *J Clin Biochem Nutr* 51:248–249; doi:10.3164/jcbn.12-45.

Vohra M, Lemieux GA, Lin L, Ashrafi K. 2018. Kynurenic acid accumulation underlies learning and memory impairment associated with aging. *Genes & Development* 32:14–19; doi:10.1101/gad.307918.117.

Vorstman JAS, Parr JR, Moreno-De-Luca D, Anney RJL, Nurnberger JI, Hallmayer JF. 2017. Autism genetics: opportunities and challenges for clinical translation. *Nature Reviews Genetics* 18:362–376; doi:10.1038/nrg.2017.4.

Wang P, Lin M, Pedrosa E, Hrabovsky A, Zhang Z, Guo W, *et al.* 2015. CRISPR/Cas9-mediated heterozygous knockout of the autism gene CHD8 and characterization of its transcriptional networks in neurodevelopment. *Molecular Autism* 6:1; doi:10.1186/s13229-015-0048-6.

Wang P, Mokhtari R, Pedrosa E, Kirschenbaum M, Bayrak C, Zheng D, *et al.* 2017. CRISPR/Cas9-mediated heterozygous knockout of the autism gene CHD8 and characterization of its transcriptional networks in cerebral organoids derived from iPS cells. *Molecular Autism* 8:11; doi:10.1186/s13229-017-0124-1.

West PR, Amaral DG, Bais P, Smith AM, Egnash LA, Ross ME, *et al.* 2014. Metabolomics as a tool for discovery of biomarkers of autism spectrum disorder in the blood plasma of children. S. Sanyal, ed *PLoS ONE* 9:e112445; doi:10.1371/journal.pone.0112445.

Willsey AJ, Sanders SJ, Li M, Dong S, Tebbenkamp AT, Muhle RA, *et al.* 2013. Coexpression networks implicate human midfetal deep cortical projection neurons in the pathogenesis of autism. *Cell* 155:997–1007; doi:10.1016/j.cell.2013.10.020.

Yang D, Howard A, Bruun D, Ajua-Alemanj M, Pickart C, Lein PJ. 2008. Chlorpyrifos and chlorpyrifos-oxon inhibit axonal growth by interfering with the morphogenic activity of acetylcholinesterase. *Toxicology and Applied Pharmacology* 228:32–41; doi:10.1016/j.taap.2007.11.005.

Yang G, Shcheglovitov A. 2020. Probing disrupted neurodevelopment in autism using human stem cell-derived neurons and organoids: An outlook into future diagnostics and drug development. *Developmental Dynamics* 249:6–33; doi:10.1002/dvdy.100.

Yap IKS, Angley M, Veselkov KA, Holmes E, Lindon JC, Nicholson JK. 2010. Urinary Metabolic Phenotyping Differentiates Children with Autism from Their Unaffected Siblings and Age-Matched Controls. *J Proteome Res* 9:2996–3004; doi:10.1021/pr901188e.

Yerys BE, Wallace GL, Harrison B, Celano MJ, Giedd JN, Kenworthy LE. 2009. Set-shifting in children with autism spectrum disorders: reversal shifting deficits on the

Intradimensional/Extradimensional Shift Test correlate with repetitive behaviors. *Autism: the international journal of research and practice* 13:523–538; doi:10.1177/1362361309335716.

Zafeiriou DI, Ververi A, Salomons GS, Vargiami E, Haas D, Papadopoulou V, *et al.* 2008. 1-2-Hydroxyglutaric aciduria presenting with severe autistic features. *Brain and Development* 30:305–307; doi:10.1016/j.braindev.2007.09.005.

Zhang J, Dai H, Deng Y, Tian J, Zhang C, Hu Z, *et al.* 2015. Neonatal chlorpyrifos exposure induces loss of dopaminergic neurons in young adult rats. *Toxicology* 336:17–25; doi:10.1016/j.tox.2015.07.014.

Zheng Z, Zhu T, Qu Y, Mu D. 2016. Blood Glutamate Levels in Autism Spectrum Disorder: A Systematic Review and Meta-Analysis. K. Hashimoto, ed *PLoS ONE* 11:e0158688; doi:10.1371/journal.pone.0158688.

Zhong X, Harris G, Smirnova L, Zufferey V, Sá R de C da S e, Russo FB, *et al.* 2020. Antidepressant Paroxetine Exerts Developmental Neurotoxicity in an iPSC-Derived 3D Human Brain Model. *Frontiers in Cellular Neuroscience* 14:493; doi:10.3389/fncel.2020.00025.

## SUPPLEMENTAL MATERIAL

### SUPPLEMENTAL RESULTS

#### Comparable differentiation efficiency of *CHD8*<sup>+/+</sup> and *CHD8*<sup>+/-</sup> BrainSpheres

The differentiation was monitored by immunocytochemistry and RT-PCR. The BrainSpheres were efficiently generated from both cell lines and contained NPC (Nestin<sup>+</sup>, Ki-67<sup>+</sup>), neurons (β-III-Tubulin<sup>+</sup>, NF-200<sup>+</sup>, MAP2<sup>+</sup>), astrocytes (GFAP<sup>+</sup>), and oligodendrocytes (Olig1<sup>+</sup>, MPB<sup>+</sup>). Co-immunostaining of neurons (β-III-Tubulin<sup>+</sup>, MAP2<sup>+</sup>) with neuroprogenitors (Nestin<sup>+</sup>, Ki-67<sup>+</sup>) at 2, 4, and 8 weeks of differentiation showed progressive increase of β-III-Tubulin<sup>+</sup> and MAP2<sup>+</sup> and decrease of Nestin<sup>+</sup> and Ki-67<sup>+</sup> cells (**Figure S1A, B**), demonstrating neuronal maturation. GFAP<sup>+</sup> astroglia, as well as Olig1<sup>+</sup> and MBP<sup>+</sup> oligodendroglia, were identified. Oligodendrocyte-specific markers were first expressed at high levels at eight weeks of differentiation (**Figure S1C, D**).

At the gene expression level, a panel of neural genes—along with a set of autism risk genes and *CHD8* targets—were analyzed by RT-PCR. RT-PCR confirmed the similar efficiency of neural differentiation in both cell lines. Strong reduction in expression of progenitor marker genes (*Pax6*, *Sox2* and *Ki-67*) and induction of neuronal (*β-III-Tubulin*, *NeuN*, *Synapsin1*, *ACbE*, *GABRA1*, *RNXN2*, *SHANK3*) and glial (*GFAP*) genes were observed in the course of differentiation of both cell lines (**Figure S2**).

Several genes, however, showed different expression level between *CHD8*<sup>+/-</sup> and *CHD8*<sup>+/+</sup> BrainSpheres. In agreement with previous studies (Wang *et al.* 2015, 2017), we observed an overexpression of genes involved in GABAergic neuronal fate. *DLX1*, a transcription factor known to regulate GABAergic interneuron development, was strongly upregulated in *CHD8*<sup>+/-</sup> BrainSpheres. The *GAD1*<sup>+</sup> was higher in *CHD8*<sup>+/-</sup> NPC cultures (not significant). *GABRA1*, a

marker for GABAergic neurons, was low expressed in two- and four-week BrainSpheres and was strongly upregulated at eight weeks of differentiation and with higher expression in *CHD8*<sup>+/-</sup> BrainSpheres in comparison to the control cell line. *FOXP1*, another transcription factor responsible for GABAergic neuronal differentiation and telencephalon development, was, however, expressed at the similar level in both cell lines.

*CHD8* target *Pax6* was expressed at higher levels in *CHD8*<sup>+/-</sup> vs. *CHD8*<sup>+/+</sup> BrainSpheres at four weeks of differentiation. Autism risk gene *SCN2A*, involved in generation and propagation of action potential, was downregulated in *CHD8*<sup>+/-</sup> BrainSpheres at two and four weeks of differentiation. Postsynaptic *Neurologin 3 (NLGN3)* was upregulated at 8 weeks in *CHD8*<sup>+/-</sup> BrainSpheres and presynaptic *NRXN2* was significantly higher at NPC stage only, while post-synaptic protein *SHANK3* was not significantly changed. Two other *CHD8* targets and autism risk genes, *AUTS2* and *POGZ*, were deregulated in *CHD8*<sup>+/-</sup> BrainSpheres. *AUTS2* was downregulated in NPC but upregulated in BrainSpheres. *POGZ* was downregulated at 4 weeks of differentiation in *CHD8*<sup>+/-</sup> in comparison to the control BrainSpheres. We did not observe any statistically significant differences in expression of autism risk genes *TCA*, *RELN*, and *PTEN* at any stage of neural differentiation. However, *PTEN* and *RELN* were significantly downregulated at NPC stage (data not shown). Neuronal marker NeuN was expressed at lower level, while dopaminergic marker *Tyrosine Hydroxylase (TH)* was upregulated in eight-week-old *CHD8*<sup>+/-</sup> BrainSpheres. Thus, these results demonstrate similar efficiency of differentiation in both cell systems, with differences in expression of some autism and/or *CHD8* targets (as previously reported by others).

## SUPPLEMENTAL TABLES

**Table S1. Primer sequences used in SYBRGreen Expression Assay.**

Gene name	Primer sequence	
	Forward sequence	Reverse sequence
<i>CHD8</i>	CTGCTGTTTCAGCGCATTTGT	CCAGGTGATGCGGTTTCGAT
	ACCATGAGTAACCCTCCAG	
<i>SCN2A</i>	ACT	CCAGGTCCACAAACTCTGTAC
	AGGAACITGCCTCCATTCG	
<i>SHANK3</i>	G	AATGAGCTAATCTCGGCGGG
<i>POGZ</i>	TGGGCACCTCTCTACATCCA	ATGAGTGGCTGTCCACCTTG
<i>DLX1</i>	TACCCCTACGTCAACAGGT	CCACCCTGCTTCACAGCTT
	GAGGTGCAATGTGGGGAG	
<i>FOXP1</i>	AA	TTCTCAAGGTCTGCGTCCAC
	TCCCATGTTTGACAAATACC	
<i>AUTS2</i>	CTA	AGGATCTGTCAACTTCGGCTG

<i>NRXN2</i>	GAGGTGGGCTGCGACTG	CTCCTTGCCCTCCATGGGG
	CTTGGCCTGGAGGCGATAT	
<i>NLGN3</i>	G	CAGGTGCCCAGCAATGTAGA
<i>GAPDH</i>	TGACAACAGCCTCAAGAT	GAGTCCTTCCACGATACC

**Table S2. Primers sequences used in TaqMan® Gene Expression Assays.**

Gene name	Assay Type	Catalog number
<i>Ki67</i>	TaqMan® Gene Expression Assay	Mm01278617_m1
<i>Pax6</i>	TaqMan® Gene Expression Assay	Hs01088112
<i>TUBB3</i>	TaqMan® Gene Expression Assay	Hs00801390_s1
<i>SYN1</i>	TaqMan® Gene Expression Assay	Hs00199577_m1
<i>NeuN</i>	TaqMan® Gene Expression Assay	Hs01370654_m1
<i>GFAP</i>	TaqMan® Gene Expression Assay	Hs00909233
<i>ACbE</i>	TaqMan® Gene Expression Assay	Hs01085739_g1
<i>SOX2</i>	TaqMan® Gene Expression Assay	Hs1053049_s1
<i>TH</i>	TaqMan® Gene Expression Assay	Hs00165941
<i>GABRA1</i>	TaqMan® Gene Expression Assay	Hs00971228
<i>GAD1</i>	TaqMan® Gene Expression Assay	Hs01065893
<i>18S</i>	TaqMan® Gene Expression Assay	Hs99999901

**Table S3. The list of primary antibodies.**

Primary antibody	Property	Company	Dilution
CHD8	anti-rabbit, polyclonal	CST	1:200
SOX2	anti-mouse, monoclonal	Santa Cruz	1:200
Nestin	anti-rabbit, polyclonal	Sigma	1:200
$\beta$ -III-tubulin	anti-mouse, monoclonal	Sigma	1:1500
NF200	anti-rabbit, monoclonal	Sigma	1:200
Ki67	anti-rabbit, polyclonal	abcam	1:100

MAP2	anti-mouse, monoclonal	Chemicon	1:200
Olig1	anti-mouse, monoclonal	Millipore	1:200
GFAP	anti-rabbit, polyclonal	Dako	1:500
MBP	anti-mouse, monoclonal	COVANCE	1:200
TH	anti-mouse, monoclonal	Millipore	1:200

Table S4. The list of secondary antibodies.

Secondary antibody	Property	Catalog number	Company	Dilution
Alexa Fluor 488	Goat-anti mouse, IgG	A-11004	Thermo Fisher	1:500
Alexa Fluor 568	Goat-anti rabbit, IgG	A-11036	Thermo Fisher	1:600

Supplemental table 5. Optimized triple stage quadrupole mass spectrometer measurement parameters. CE denotes collision energy in Volt on an Agilent 6490A mass spectrometer; Bz benzoylated, DiBz – derivatization procedure.

Name	METLINID	Formula	Monoisotopic Mass	Polarity	Precursor	Transition 1	CE 1	Transition 2	CE 2	Detected
(+)Epinephrine	62	C9H13NO3	183.089543	+	184.10	166.1	9	77.1	41	-
3,4-Dihydroxybenzylamine	62817	C7H9NO2	139.063330	-	138.05	122.0	17	92.9	17	+
5-HIAA / 5-Hydroxy-3-indoleacetic acid	2975	C10H9NO3	191.058243	+	192.07	146.1	17	91.2	45	-
$\alpha$ -Hydroxyglutaric acid	63268	C5H8O5	148.037173	-	147.03	129.0	9	57.0	17	+
Acetylcholine	57	C7H15NO2	146.118104	+	147.13	86.9	13	43.2	29	+
BZL-Phenylalanine	na	C16H15NO3	269.105200	+	270.12	104.8	17	77.1	45	+
Carnosine	38	C9H14N4O3	226.106590	+	227.12	156.0	13	110.1	25	+
Choline	56	C5H14NO	104.107539	+	104.11	60.1	21	45.2	25	+
Creatine	7	C4H9N3O2	131.069480	+	132.08	90.1	9	72.1	29	+
D-Lactic acid	63094	C3H6O3	90.031694	-	89.02	43.1	9	41.0	29	+
DiBz-L-Tyrosine	na	C23H19NO5	389.126300	+	390.14	239.9	13	105.1	29	+
Dopamine	64	C8H11NO2	153.078979	+	154.09	137.1	5	91.1	21	-
Folic acid	246	C19H19N7O6	441.139681	+	442.15	295.1	10	176.0	41	+
GABA / gamma-Aminobutyric acid	279	C4H9NO2	103.063329	+	104.07	87.0	9	45.1	21	+
GSH / Glutathione	44	C10H17N3O6S	307.083806	+	308.09	178.9	9	76.0	29	+
GSSG / L-Glutathione (oxidized)	45	C20H32N6O12S2	612.151962	+	613.16	484.1	17	355.1	21	+
Homovanillic acid	971	C9H10O4	182.057909	-	181.05	137.0	9	122.0	9	-
Kynurenic acid	5683	C10H9NO3	189.042593	+	190.05	144.2	21	116.1	33	+
Kynurenine	72	C10H12N2O3	208.084792	+	209.09	192.2	5	94.0	9	+
L-Alanine	11	C3H7NO2	89.047678	+	90.06	44.1	13	na	na	+
L-Asparagine	4195	C10H16N4O3	240.122240	+	241.13	108.9	21	96.0	45	-
L-Arginine	13	C6H14N4O2	174.111676	+	175.12	70.1	21	60.1	17	+
L-Ascorbic acid	249	C6H8O6	176.032088	+	177.04	140.9	5	95.0	9	-
L-Cystathionine	39	C7H14N2O4S	222.067428	+	223.08	134.0	13	88.2	29	+
L-Cysteine	63299	C3H7NO2S	121.019749	+	122.02	76.0	5	59.0	21	+
L-Cystine	17	C6H12N2O4S2	240.023648	+	241.03	151.9	9	74.0	29	+
L-DOPA_neg	42	C9H11NO4	197.068810	-	196.10	178.8	9	134.8	17	+
L-DOPA_pos	42	C9H11NO4	197.068810	+	198.08	152.2	9	107.2	29	+
L-Glutamic Acid	19	C5H9NO4	147.053160	+	148.06	84.0	17	56.0	33	+
L-Histidine	21	C6H9N3O2	155.069477	+	156.08	109.9	13	56.0	41	+
L-Homocysteine	3256	C4H9NO2S	135.035399	+	136.05	90.0	9	55.9	17	+
L-Methionine	26	C5H11NO2S	149.051049	+	150.06	61.0	21	56.2	17	+
L-Phenylalanine	28	C9H11NO2	165.078979	+	166.09	120.0	5	103.1	29	+
L-Tryptophan	33	C11H12N2O2	204.089878	+	205.10	188.1	5	146.1	13	+
L-Tyrosine	34	C9H11NO3	181.073893	+	182.08	136.1	9	91.2	33	+
N-Acetylaspartate	3769	C6H9NO5	175.048072	+	176.07	88.0	9	74.0	21	+
Norepinephrine	63	C8H11NO3	169.073890	-	168.06	150.1	9	123.0	13	-
Oxithione	27	C5H11N2O2	132.089878	+	133.10	116.0	9	69.9	21	+
S-Adenosylmethionine	3289	C15H23NO5S	399.145064	+	399.15	250.2	13	136.0	33	+
SAH / S-Adenosyl-L-homocysteine	296	C14H20NO5S	384.121589	+	385.13	136.2	21	87.8	41	+
Serotonin	74	C10H12N2O	176.094963	+	177.10	160.1	5	115.1	33	-
$\beta$ -Alanine	36	C3H7NO2	89.047678	+	90.06	72.0	5	45.0	41	-
TriBz-3,4-Dihydroxybenzylamine	na	C28H21NO5	451.142000	+	452.15	105.0	25	77.0	45	+
TriBz-Dopamine	na	C29H23NO5	465.157600	+	466.17	104.9	25	76.8	45	+
TriBz-L-DOPA	na	C30H23NO7	509.147500	+	510.16	388.1	9	360.2	13	+



## SUPPLEMENTAL FIGURES

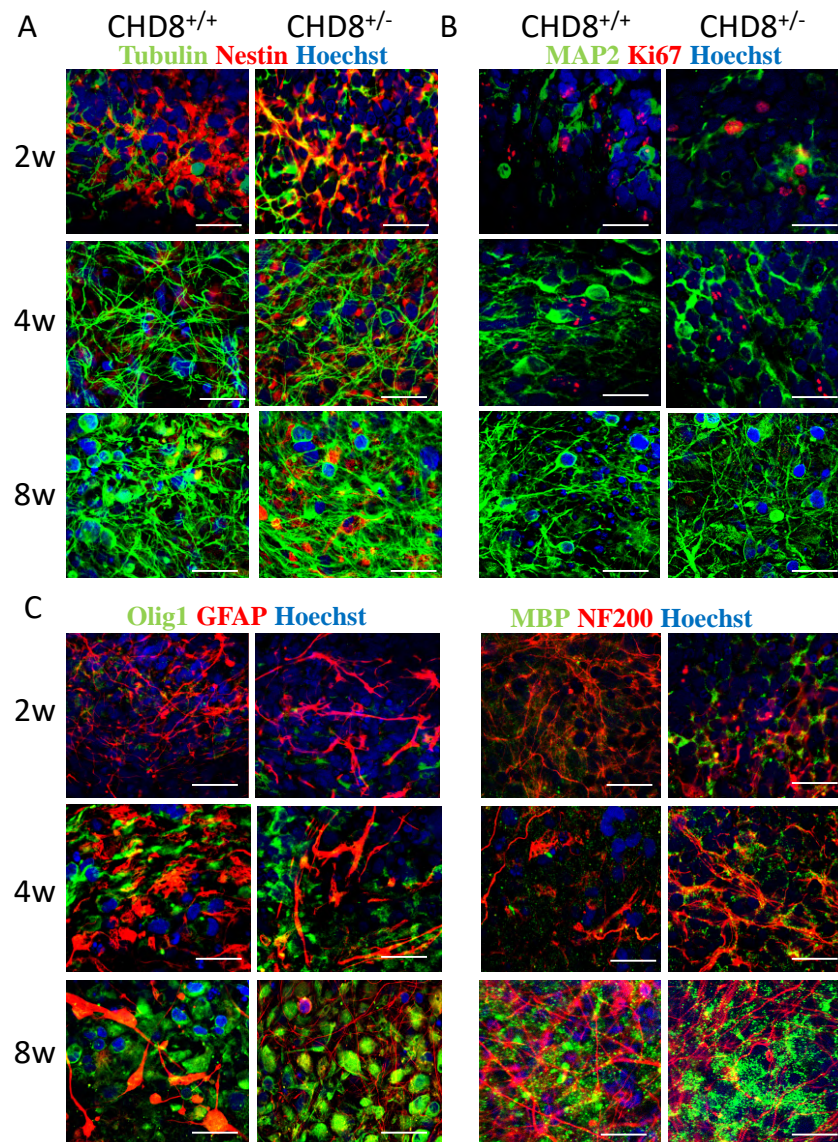


**Figure S1.** Expression of neural markers in *CHD8*<sup>+/+</sup> and *CHD8*<sup>+/-</sup> BrainSpheres at 2, 4 and 8 weeks after induction of neural differentiation in 3D. **(A)** and **(B)**: co-immunostaining of neurons ( $\beta$ -III-Tubulin<sup>+</sup>, MAP2<sup>+</sup>, green) with neuroprogenitors (Nestin<sup>+</sup>, Ki-67<sup>+</sup>, red) shows maturation of BrainSpheres. **(C)** the presence of GFAP<sup>+</sup> astroglia (red) and Olig1<sup>+</sup> oligodendroglia (green). **(D)** accumulation of myelin basic protein (MBP<sup>+</sup>, green) at 8 weeks of differentiation and expression of axonal marker neurofilament 200 (NF200<sup>+</sup>, red). The nuclei were visualized with Hoechst 33342 staining. Scale bars are 50  $\mu$ m.

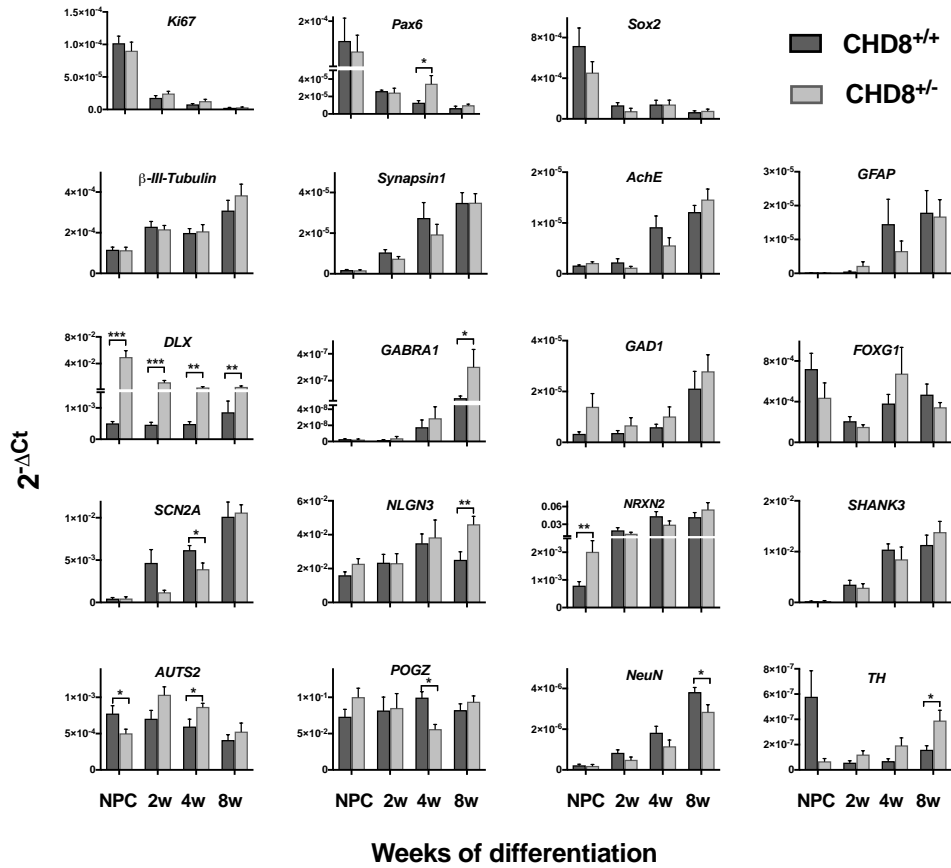


**Figure S2. Neural gene marker expression measured by RT-PCR in *CHD8*<sup>+/+</sup> and *CHD8*<sup>+/-</sup> NPC, and after two, four and eight weeks of differentiation in 3D.** The data represent Mean  $\pm$  SEM of expression values ( $2^{-\Delta Ct}$ ) from four independent experiments. \* P < 0.05, \*\* P < 0.01, \*\*\* P < 0.001, unpaired student t-test. Pax6 – paired box protein 6, Sox2 – (sex determining region Y)-box 2, AChE – Acetylcholinesterase, GFAP – Glial Fibrillary Acidic Protein, DLX1 - Distal-Less Homeobox 1, GABRA1 - Gamma-Aminobutyric Acid Receptor Subunit Alpha-1, GAD1 - Glutamate Decarboxylase 1, FOXP1 - Forkhead Box G1, SCN2A - Sodium voltage-gated channel alpha subunit 2, NLGN3 - Neuroligin 3, NRXN2 – Neurexin 2, SHANK3 - SH3 and multiple ankyrin repeat domains 3, AUTS2 - Autism Susceptibility Gene 2, POGZ - Pogo Transposable Element Derived With ZNF Domain, NeuN - RNA binding fox-1 homolog 3, TH - Tyrosine Hydroxylase.

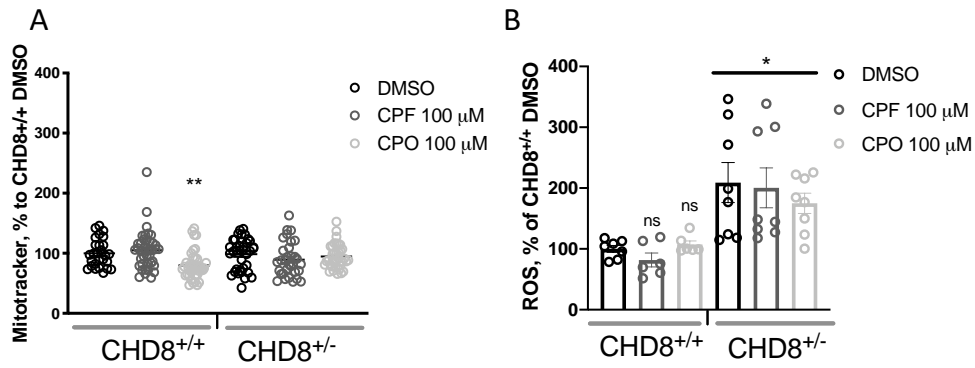


**Figure S3. Mitochondrial membrane potential and ROS production in *CHD8*<sup>+/-</sup> vs. *CHD8*<sup>+/+</sup> BrainSpheres with and without CPF/CPO treatment.** (A) Mitochondrial membrane potential and (B) ROS production was measured in both cell lines treated with 100 μM CPF or CPO for 24 h. The data represents Mean (%) ± SEM from three independent experiments normalized to vehicle treated *CHD8*<sup>+/+</sup> control. \* P < 0.05, \*\*\* P < 0.001, Kruskal-Wallis test with Dunn's multiple comparisons test.

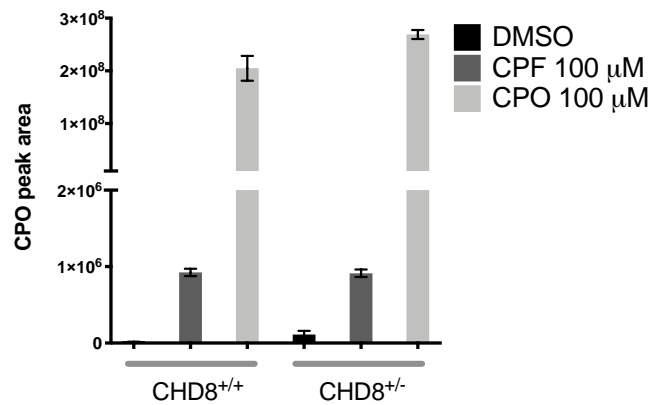


**Figure S4. CPF and CPO detection in the *CHD8*<sup>+/+</sup> and *CHD8*<sup>+/-</sup> BrainSpheres treated with CPF and CPO by LC MS/MS.** Low levels of CPO were detected in both cell lines treated with CPF (n=3).

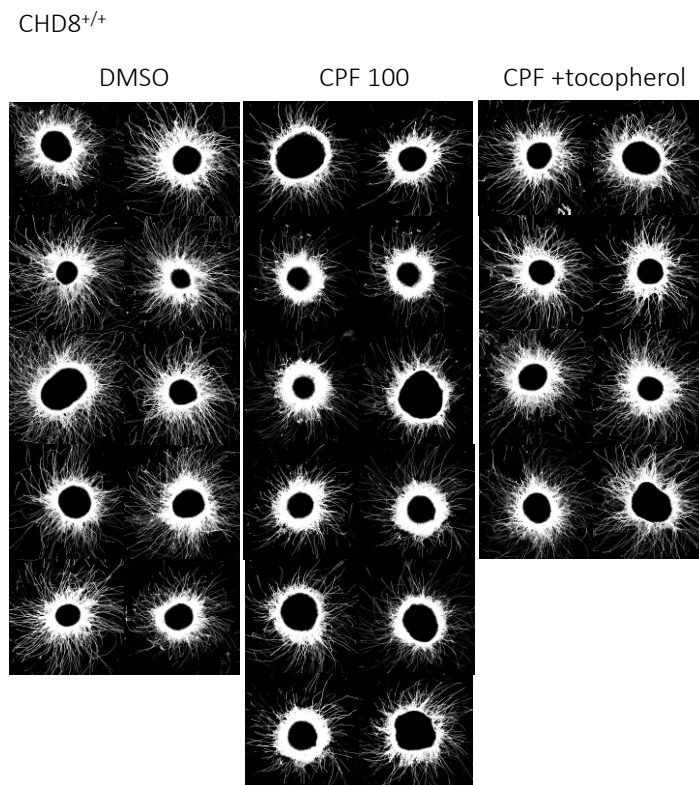
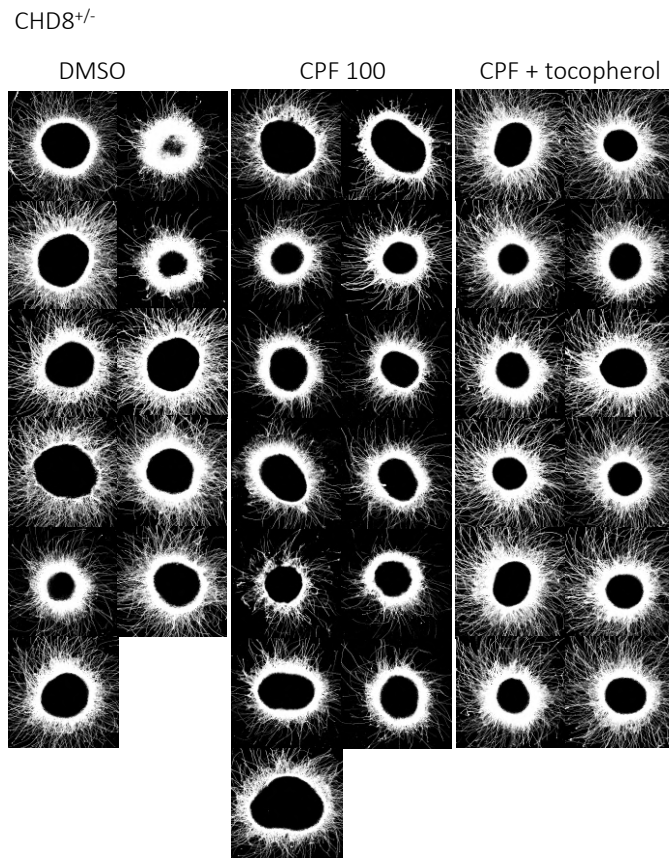
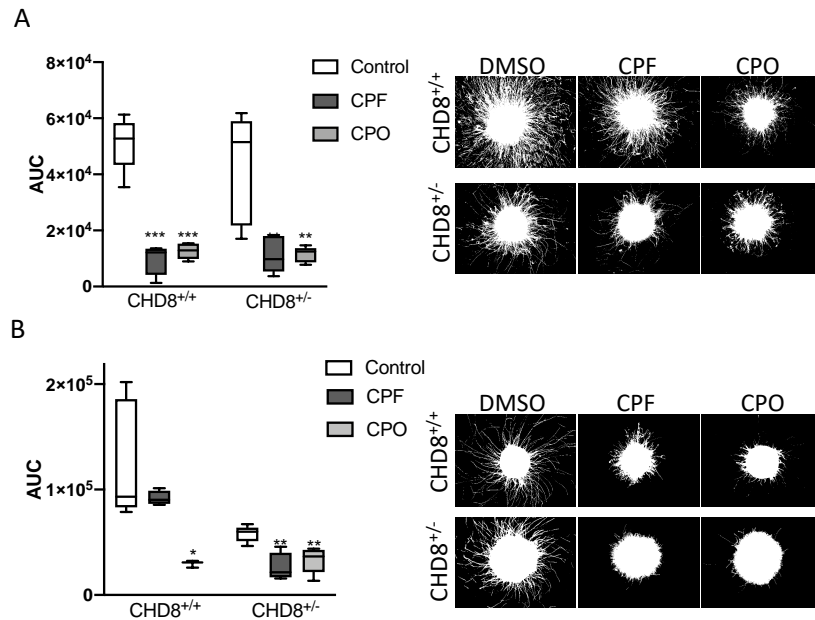


Figure S5. Individual images, which were used for quantification of the neurite outgrowth with Sholl analysis for *CHD8*<sup>+/+</sup> cell line treated with CPF and CPF+tocopherol. Quantification results and representative images are shown in Figure 3. Magnification of microscope images 10x.



**Figure S6.** Individual images which were used for quantification of the neurite outgrowth with Sholl analysis for *CHD8*<sup>+/-</sup> cell line treated with CPF and CPF+tocopherol. Quantification results and representative images are shown in Figure 3. Magnification of microscope images 10x.



**Figure S7. Two additional experiments showing the significant reduction of neurite outgrowth in both cell lines upon treatment with CPF and CPO.** Area under the curve and representative images are shown. Magnification of microscope images 10x.

## REFERENCES

Wang P, Lin M, Pedrosa E, Hrabovsky A, Zhang Z, Guo W, *et al.* 2015. CRISPR/Cas9-mediated heterozygous knockout of the autism gene CHD8 and characterization of its transcriptional networks in neurodevelopment. *Molecular Autism* 6:1; doi:10.1186/s13229-015-0048-6.

Wang P, Mokhtari R, Pedrosa E, Kirschenbaum M, Bayrak C, Zheng D, *et al.* 2017. CRISPR/Cas9-mediated heterozygous knockout of the autism gene CHD8 and characterization of its transcriptional networks in cerebral organoids derived from iPS cells. *Molecular Autism* 8:11; doi:10.1186/s13229-017-0124-1.

## **CHAPTER IV**

---

The COVID-19 pandemic outbreak: a critical discussion of the major pharmacological challenges





## PART 1

The following manuscript was published in *Signal Transduction and Targeted Therapy* in 2020  
as:

### **Immune response in COVID-19: addressing a pharmacological challenge by targeting pathways triggered by SARS-CoV-2**

Michele Catanzaro, **Francesca Fagiani (co-first author)**, Marco Racchi, Emanuela Corsini, Stefano Govoni and Cristina Lanni

#### **Abstract**

To date, no vaccines or effective drugs have been approved to prevent or treat COVID-19 and the current standard care relies on supportive treatments. Therefore, based on the fast and global spread of the virus, urgent investigations are warranted in order to develop preventive and therapeutic drugs. In this regard, treatments addressing the immunopathology of SARS-CoV-2 infection have become a major focus. Notably, while a rapid and well-coordinated immune response represents the first line of defense against viral infection, excessive inflammatory innate response and impaired adaptive host immune defense may lead to tissue damage both at the site of virus entry and at systemic level. Several studies highlight relevant changes occurring both in innate and adaptive immune system in COVID-19 patients. In particular, the massive cytokine and chemokine release, the so-called “cytokine storm”, clearly reflects a widespread uncontrolled dysregulation of the host immune defense. Although the prospective of counteracting cytokine storm is compelling, a major limitation relies on the limited understanding of the immune signaling pathways triggered by SARS-CoV-2 infection. The identification of signaling pathways altered during viral infections may help to unravel the most relevant molecular cascades implicated in biological processes mediating viral infections and to unveil key molecular players that may be targeted. Thus, given the key role of the immune system in COVID-19, a deeper understanding of the mechanism behind the immune dysregulation might give us clues for the clinical management of the severe cases and for preventing the transition from mild to severe stages.

**Keywords:** SARS-CoV-2; inflammation; immune signaling; NF- $\kappa$ B; JAK/STAT; sphingosine-1-phosphate.

REVIEW ARTICLE **OPEN**

# Immune response in COVID-19: addressing a pharmacological challenge by targeting pathways triggered by SARS-CoV-2

Michele Catanzaro<sup>1</sup>, Francesca Fagiani<sup>1,2</sup>, Marco Racchi<sup>1</sup>, Emanuela Corsini<sup>3</sup>, Stefano Govoni<sup>1</sup> and Cristina Lanni<sup>1</sup>

<sup>1</sup>Department of Drug Sciences (Pharmacology Section), University of Pavia, V.le Taramelli 14, 27100 Pavia, Italy; <sup>2</sup>Scuola Universitaria Superiore IUSS Pavia, P.zza Vittoria, 15, 27100 Pavia, Italy and <sup>3</sup>Laboratory of Toxicology, Department of Environmental and Political Sciences, Università Degli Studi di Milano, Via Balzaretti 9, 20133 Milano, Italy  
Correspondence: Cristina Lanni (cristina.lanni@unipv.it)  
These authors contributed equally: Michele Catanzaro, Francesca Fagiani

## 1. Introduction

The outbreak of the novel coronavirus disease 2019 (COVID-19), induced by severe acute respiratory syndrome coronavirus 2 (SARS-CoV-2), originated in Wuhan, in the Hubei province of China, in December 2019, has rapidly spread worldwide, becoming a global public health emergency. On 11th March 2020, the World Health Organization (WHO) declared COVID-19 a pandemic. As of April 28, 2020, WHO reports more than 2,8 million confirmed cases and 198 842 deaths worldwide (WHO, 2020, <https://covid19.who.int>). After the isolation of SARS-CoV-2, the viral genome was sequenced, thus facilitating diagnostic testing, epidemiologic tracking, as well as investigations on potential preventive and therapeutic strategies in the management of COVID-19. To date, despite the intense scientific effort demonstrated by more than 600 clinical trials currently underway (typing SARS-CoV-2 on [clinicaltrials.gov](https://clinicaltrials.gov)), no vaccines or effective drugs have been approved to prevent or treat COVID-19 and the current standard care is supportive treatment. Therefore, based on the fast and global spread of the virus, urgent investigations are warranted in order to develop effective therapies. Within this context, treatments addressing the immunopathology of the infection have become a major focus.

## 2. Virology and host-pathogen interaction

The new human-infecting severe acute respiratory syndrome coronavirus 2 (SARS-CoV-2) is a positive-sense single-stranded RNA-enveloped virus belonging to CoV family.<sup>1</sup> Among the six CoVs pathogenic to humans, four of them have been associated with mild respiratory symptoms,<sup>2</sup> while two SARS-CoV and the Middle East respiratory syndrome (MERS) CoV (MERS-CoV), whose epidemic outbreaks took place in 2002 and 2012

respectively, caused severe respiratory diseases in affected individuals.<sup>2</sup> SARS-CoV-2 is the seventh identified CoV and, after SARS-CoV and MERS-CoV, the third zoonotic virus of CoVs that has been transmitted from animals to humans via an intermediate mammalian host.<sup>3,4</sup> In particular, based on genetic analysis, Chinese horseshoe bats have been proposed to serve as natural reservoir hosts for SARS-CoV-2, similar to SARS-CoV and MERS-CoV.<sup>4-6</sup> Moreover, genomic analysis indicates that SARS-CoV-2 is in the same beta-CoV clade as SARS-CoV and MERS-CoV.<sup>1</sup> In particular, SARS-CoV-2 has been observed to share almost 80% of the genome with SARS-CoV<sup>1,6,7</sup> and almost all encoded proteins of SARS-CoV-2 are homologous to SARS-CoV proteins.<sup>1</sup> In contrast, SARS-CoV-2 has been found to be more distant from MERS-CoV, with only 50% identity.<sup>1</sup> Moreover, the entry of SARS-CoV-2 into human host cells has been found to rely on the same receptor as SARS-CoV: the surface angiotensin-converting enzyme 2 (ACE2), which is expressed in the type II surfactant-secreting alveolar cells of the lungs.<sup>8,9</sup> Consistently, despite amino acid variations at specific key residues, homology modelling revealed a structural similarity between the receptor-binding domains of SARS-CoV and SARS-CoV-2.<sup>1</sup> However, further studies are necessary to compare SARS-CoV and SARS-CoV-2 affinities to ACE2 receptor that might explain the increased transmissibility and greater virulence of SARS-CoV-2 compared to SARS-CoV.<sup>8</sup>

Two independent groups provided key insights into the first step of SARS-CoV2 infection, by demonstrating that ACE2 host receptor is required for host cell entry of SARS-CoV-2.<sup>8,10</sup> Noteworthy, the expression of ACE2 receptors is not only restricted to the lung, and extrapulmonary spread of SARS-CoV in ACE-expressing tissues has been demonstrated.<sup>11-13</sup> Hence the same pattern may be expected for SARS-CoV-2, with most of human tissues, such as oral mucosa and gastrointestinal tract, kidney, heart, blood vessels expressing ACE2 receptors, particularly prone to SARS-CoV-2 infection.<sup>14,15</sup> The viral entry of SARS-CoV-2 has been further found to be prevented by a clinically proven inhibitor of the cellular host type 2 transmembrane serine protease TMPRSS2 (camostat mesylate).<sup>8</sup> Priming of the envelope-located trimeric spike (S) protein by host proteases, which cleave at the S1/S2 and the S2' sites, has been described as a fundamental step for viral entry, and the host protease TMPRSS2 emerged as a key cellular factor necessary for the priming of S protein and for the consequent membrane fusion and viral internalization by endocytosis in the pulmonary epithelium.<sup>8</sup> Hence, TMPRSS2 has been proposed as a potential target for clinical intervention<sup>6,8</sup> and its inhibitor camostat mesylate, approved for human use in Japan to treat pancreatic inflammation, has attracted the attention of the scientific community. Currently, a randomized, placebo-controlled, phase IIa trial is investigating the use of camostat mesylate (NCT04321096) and is expected to run until December 2020, whereas another independent trial will start in June 2020 to evaluate the efficacy of camostat

mesilate in combination with hydroxychloroquine in hospitalized patients with moderate coronavirus disease 2019 (COVID-19) infection (NCT04338906).

A detailed analysis of additional mechanisms of cellular viral infection for SARS-CoV-2 is still missing and would be fundamental to identify further potential biological substrates to target.

## **2. Immunopathology of COVID-19**

The majority of COVID-19 cases (about 80%) is asymptomatic or exhibits mild to moderate symptoms, but approximately the 15% progresses to severe pneumonia and about 5% eventually develops acute respiratory distress syndrome (ARDS), septic shock and/or multiple organ failure.<sup>16,17</sup> As for SARS and MERS, the most common symptoms of COVID-19 are fever, fatigue, and respiratory symptoms, including cough, sore throat and shortness of breath.<sup>16,18</sup>

Notably, SARS-CoV-2 infection activates innate and adaptive immune response, thus sustaining the resolution of COVID-19. While a rapid and well-coordinated immune response represents the first line of defense against viral infection, excessive inflammatory innate response and dysregulated adaptive host immune defense may cause harmful tissue damage at both at the site of virus entry and at systemic level. The excessive pro-inflammatory host response has been hypothesized to induce an immune pathology resulting in the rapid course of acute lung injury (ALI) and ARDS occurring in SARS-CoV-2 infected patients.<sup>16–18</sup> For example, the massive cytokine and chemokine release, the so-called “cytokine storm”, clearly reflects a widespread uncontrolled dysregulation of host immune defense. Thus, given the key role of the immune system in COVID-19, a deeper understanding of the mechanism behind the immune dysregulation, as well as of SARS-CoV-2 immune-escape mechanisms might give us clues for the clinical management of the severe cases and for preventing the transition from mild to severe stages. Moreover, although no within the goal of the present review, future investigations concerning the systemic effects of uncontrolled immune system on other physiological systems, such as the gastrointestinal tract, neuroendocrine, renal and cardiovascular are urgent.

### **2.1. Immune response to SARS-CoV-2**

Several studies highlight relevant changes occurring both in innate and adaptive immune system in COVID-19 patients. In particular, lymphocytopenia and a modulation in total neutrophils are common hallmarks and seem to be directly correlated with disease severity

and death.<sup>6,18</sup> In patients with severe COVID-19, a marked decrease in the levels of absolute number of circulating CD4<sup>+</sup> cells, CD8<sup>+</sup> cells, B cells and natural killers (NK) cells,<sup>16,17,19</sup> as well as a decrease in monocytes, eosinophils and basophils has been reported.<sup>19–21</sup> In addition, most of patients with severe COVID-19 displayed significantly increased serum levels of pro-inflammatory cytokines (e.g. IL-6, IL-1 $\beta$ , IL-2, IL-8, IL-17, G-CSF, GM-CSF, IP-10, MCP-1, CCL3, and TNF $\alpha$ ).<sup>20,22</sup> Although no direct evidence for pro-inflammatory cytokines and chemokines involvement in lung pathology in COVID-19 has been reported, an increase in serum cytokine and chemokine levels, as well as in neutrophil-lymphocyte-ratio (NLR) in SARS-CoV-2 infected patients has been correlated with the severity of the disease and adverse outcomes, suggesting a possible role for hyper-inflammatory responses in COVID-19 pathogenesis.<sup>20</sup> Moreover, a recent multicenter retrospective cohort study analyzing data from the Early Risk Stratification of Novel Coronavirus Pneumonia (ERS-COVID-19) study (ChiCTR2000030494) showed that patients with COVID-19 had elevated high-sensitivity C-reactive protein (Hs-CRP) and procalcitonin serum levels, two major inflammation markers associated with high risks of mortality and organ injury.<sup>23</sup>

Noteworthy, MERS-CoV has been demonstrated to infect THP-1 cells, human peripheral blood monocyte-derived macrophages and dendritic cells, and SARS-CoV to directly infect macrophages and T cells,<sup>24</sup> thereby inducing delayed but elevated levels of pro-inflammatory cytokines and chemokines.<sup>25,26</sup> However, ACE2 receptor is only minimally expressed in monocytes, macrophages, and T cells in the lung, hence, the mechanism by which SARS-CoV directly infects immune cells is still unknown.<sup>27</sup> Taking into account the similarities between SARS-CoV and SARS-CoV-2, it is likely that also this latter may infect monocytes and macrophages by a mechanism that has to be still unveiled. In this regard, it is possible that the virus may be capable to bind other specific receptors and/or other mechanisms of viral entry mode can be exploited by the virus.

As far as concerns the adaptive immunity, the novel SARS-CoV-2 has been demonstrated to mainly affect lymphocyte counting and balance. In particular, Li et al. reported that, compared to survivors, dead COVID-19 patients showed lower percentage and count in CD3<sup>+</sup>, CD4<sup>+</sup>, and CD8<sup>+</sup> lymphocytes populations, strong predictive values for in-hospital mortality, organ injury, and severe pneumonia.<sup>23</sup>

In a retrospective, single-center study enrolling a cohort of 452 patients with COVID-19 in Wuhan, patients with severe COVID-19 displayed a significantly lower number of total T cells, both helper T cells and suppressor T cells.<sup>20</sup> In particular, among helper T cells, a decrease in regulatory T cells, with a more pronounced reduction according to the severity

of the cases, and in memory T cells has been observed, whereas the percentage of naïve T cells was found increased.<sup>20</sup> Notably, naïve and memory T cells are essential immune components, whose balance is crucial for maintaining a highly efficient defensive response. Naïve T cells enable the defenses against new and previously unrecognized infection by a massive and tightly coordinated release of cytokines, whereas memory T cells mediate antigen-specific immune response. A dysregulation in their balance, favoring naïve T cells activity compared to regulatory T cells, could highly contribute to hyperinflammation. A reduction in memory T cells on the other hand could be implicated in COVID-19 relapse, since a number of recurrences has been reported in recovered cases of COVID-19.<sup>6,28</sup> These data are consistent with results reported by Tan et al.<sup>29</sup> Overall, the lymphopenia observed in COVID-19 patients may depend on the fact that SARS-CoV-2 may directly infect lymphocytes minimally expressing ACE2, leading to lymphocyte death or, alternatively, may directly damage lymphatic organs since they express ACE2 receptors.<sup>29</sup> However, to date no data are available on lymph nodes and spleen shrinking and lymphocytes functionalities, hence such speculations need to be further investigated to confirm these hypotheses.

As far as concerns B cells, by using single-cell RNA sequencing to characterize the transcriptome landscape of blood immune cell subsets during the recovery stage of COVID-19, Wen et al. found significant changes in B cells.<sup>30</sup> In particular, while the naïve B cells have been reported to be decreased, the plasma cells have been found remarkably increased in peripheral blood mononuclear cells.<sup>30</sup> Moreover, several new B cell-receptor changes have been identified (e.g. IGHV3-23 and IGHV3-7).<sup>30</sup> In addition, isotypes, including IGHV3-15, IGHV3-30, and IGKV3-11, previously used for virus vaccine development have been confirmed.<sup>30</sup> The strongest pairing frequencies, IGHV3-23-IGHJ4, has been suggested to indicate a monoclonal state associated with SARS-CoV-2 specificity.<sup>30</sup> Moreover, given the pivotal role of B cells in the control of infections, tracking the antibody seroconversion response is an important process for the clinical evaluation of infections. In COVID-19 patients, while serum samples from patients with COVID-19 showed no cross-binding to the S1 subunit of the SARS-CoV spike antigen, some cross-reactivity of serum samples has been observed from patients with COVID-19 to nucleocapsid antigens of SARS-CoV.<sup>31</sup> Interestingly, this study reports that 96.8% of tested patients achieved seroconversion of IgG or IgM within 20 days after symptom onset with a titer plateaued within 6 days after seroconversion.<sup>31</sup> Moreover, 100% of patients had positive virus-specific IgG approximately 17-19 days after symptom onset.<sup>31</sup> Instead, 94.1% patients showed positive virus-specific IgM approximately 20-22 days after symptom onset.<sup>31</sup>

In addition to these observations about immunity, a critical aspect has to be raised concerning the ability to escape from anti-viral host defenses. Viral evasion of host immune response is in fact believed to play a major role in disease severity.<sup>32</sup> As an example, SARS-CoV and MERS-CoV escape and suppress the signaling pathways mediated by type I Interferon (IFN), a key cytokine secreted by virus-infected cells to enroll nearby cells to heighten their anti-viral immune defenses.<sup>33</sup> Based on genomic sequence comparison and on partial identity of SARS-CoV-2 with SARS-CoV, it is speculative that SARS-CoV-2 can adopt similar strategies to modulate the host innate immune response, thus evading immune detection and dampening human defenses.

## **2.2. Inflammatory cytokine storm and lung damage**

Mounting clinical evidence from severe COVID-19 patients suggests that extensive changes in the serum levels of several cytokines play a pivotal role in the pathogenesis of COVID-19.<sup>22,34,35</sup> Such hypercytokinemia, the so-called “cytokine storm”, has been proposed as one of the key leading factors that trigger the pathological processes leading to plasma leakage, vascular permeability, and disseminated vascular coagulation, observed in COVID-19 patients, and accounting for life-threatening respiratory symptoms.<sup>17</sup> Huang et al. found that plasma concentrations of IL1B, IL1RA, IL7, IL8, IL9, IL10, basic FGF, GCSF, GMCSF, IFN $\gamma$ , IP10, MCP1, MIP1A, MIP1B, PDGF, TNF $\alpha$ , and VEGF were higher in both ICU (intensive care unit) patients and non-ICU patients than in healthy adults.<sup>16</sup> Moreover, when comparing ICU and non-ICU patients, plasma concentrations of IL2, IL7, IL10, GCSF, IP10, MCP1, MIP1A, and TNF $\alpha$  were higher in ICU patients than non-ICU patients, thus indicating that the cytokine storm might be correlated with disease severity.<sup>16</sup> Another study on a small set of patients with severe COVID-19 pneumonia, found 15 cytokines (IFN- $\alpha$ 2, IFN- $\gamma$ , IL1ra, IL2, 4, 7, 10, 12 and 17, chemokine IP-10, as well as G-CSF and M-CSF) associated with lung injury based on Murray score.<sup>35</sup> Evidence from literature indicates that the cytokine storm observed in COVID-19 resembles that occurring in Cytokines Release Syndrome (CRS), a form of systemic inflammatory response syndrome, and in secondary haemophagocytic lymphohistiocytosis (sHLH), an hyperinflammatory syndrome characterized by fulminant and fatal hypercytokinemia with multiorgan failure, mainly induced by viral infections.<sup>22,36</sup> Therefore, as detailed below, existing pharmaceutical modulators of cytokines might be repurposed as therapeutic strategy to attenuate the hypercytokinemia in COVID-19 patients.

Interestingly, Gou et al. recently reported that the disruption of gut microbiome features by host and environmental factors may predispose healthy individuals to abnormal inflammatory response observed in COVID-19.<sup>37</sup> In particular, the authors constructed a

blood proteomic risk score for the prediction of COVID-19 progression to clinically severe phase and observed that core gut microbiota features were significantly correlated with proinflammatory cytokines in a set of 366 individuals, using a machine learning model.<sup>37</sup> Specifically, *Bacteroides* genus, *Streptococcus* genus and *Clostridiales* order have been negatively correlated with most of the tested inflammatory cytokines, whereas *Ruminococcus* genus, *Blautia* genus and *Lactobacillus* genus have been positively associated.<sup>37</sup> Moreover, fecal metabolomics analysis indicated some potential amino acid-related pathways (e.g. aminoacyl-tRNA biosynthesis pathway, arginine biosynthesis pathway, and valine, leucine and isoleucine biosynthesis pathway) that correlate core microbial features with host inflammation among 987 participants.<sup>37</sup> Thus, the core intestinal microbiological characteristics, along with its related metabolites, should be further investigated as potential predictors for the individual susceptibility to COVID-19 progression and severity and might represent potential targets for the prevention of susceptible populations, as well as for the development of therapeutic approaches to manage COVID-19.

### 3 Putative signaling pathways triggered by SARS-CoV-2

It is well-established that, upon binding of the viral spike protein to the host cells by the entry receptor ACE2, the viral RNAs, as pathogen-associated molecular patterns (PAMPs), are detected by the pattern recognition receptors, which include the family of Toll-like receptors (TLRs). In particular, for RNA virus such as CoVs, viral genomic RNA or the intermediates during viral replication, including dsRNA, are recognized by either the endosomal RNA receptors, TLR3 and TLR7/8, and the cytosolic RNA sensor, retinoic acid-inducible gene (RIG-I)/MDA5.<sup>38</sup> Consistently, such TLRs have been found to activate different signaling pathways in human CD14<sup>+</sup> monocytes, correlating with differential type I IFN and cytokine secretion involved in CD4<sup>+</sup> T cells polarization.<sup>38</sup> As a result of virus recognition, downstream transduction pathways, crucial for proper antiviral response, such as IRF3 (IFN regulatory factor-3), nuclear factor  $\kappa$ B (NF- $\kappa$ B), JAK (Janus kinase)/STAT (signal transducer and activator of transcription) signaling pathways, are activated.<sup>39</sup> The identification of the most relevant intracellular signaling pathways involved in the modulation of host immune systems may give important hints on how to overcome the infectious disease driven by SARS-CoV-2. In particular, taking into account the structural similarities of SARS-CoV-2 as well as the analogies in the infection mechanisms with pathogenic SARS-CoV, it is tempting to speculate that the viral infection may induce the activation of shared intracellular pathways, in particular of those mainly involved in the innate immune response. However, to date, it has to be demonstrated whether such sequence similarities between SARS-CoV and SARS-CoV-2 can be directly translated into similar biological outcomes. Taking into account such limitation, the identification of



signaling pathways altered during viral infections may help to unravel the most relevant molecular cascades implicated in biological processes mediating viral infections and to unveil key molecular players that may be targeted. The advantage of targeting intracellular molecules rather than viral proteins is that their effect is not likely to be negated by mutations in the virus genome. In fact, antiviral drugs inhibiting virus replication may select for mutational escape, thus rendering the therapy ineffective. Thus, the modulation of the host immune response shows the potential advantage of exerting less-selective pressure on viral populations.<sup>40</sup> Repurposing of existing drugs targeting specific signal transducers will be discussed as potential treatment options for the management of COVID-19, as schematized in **Figure 1**.

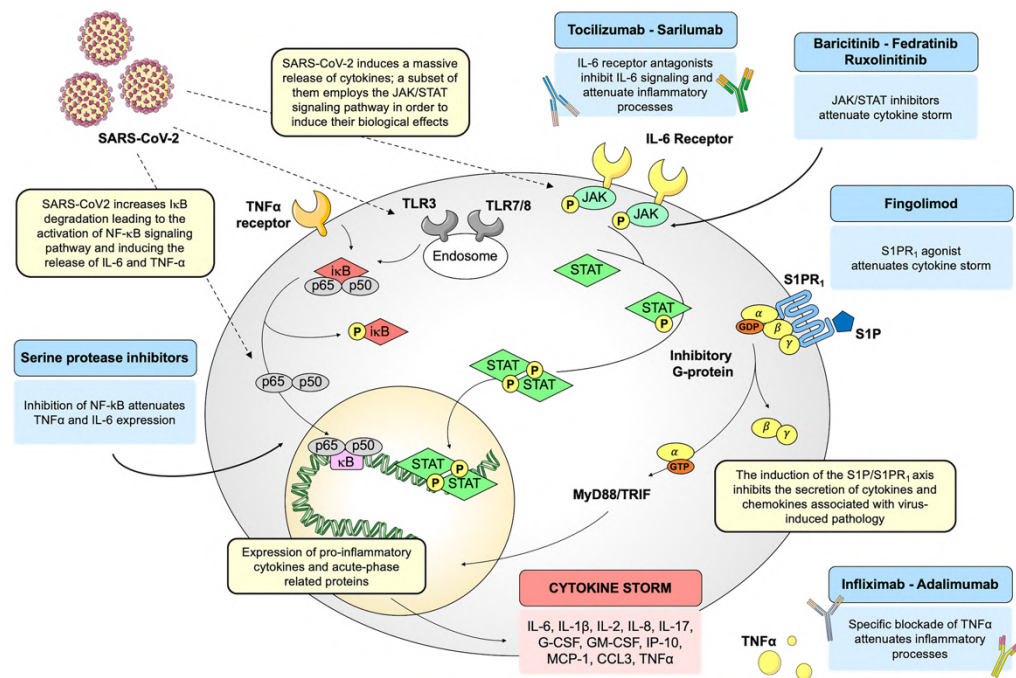


**Figure 1. Schematic representation of SARS-CoV-2-driven signaling pathways and potential drug targets. Schematic representation of host intracellular signaling pathways induced by SARS-CoV-2 infection.** Selected drugs, acting on these pathways, are repurposed to manage the cytokine storm induced by the viral infection. SARS-CoV-2, severe acute respiratory syndrome coronavirus 2; I $\kappa$ B, inhibitor of nuclear factor  $\kappa$ B; NF- $\kappa$ B, p65-p50, nuclear factor  $\kappa$ B; IL-6, interleukin 6; IL-1 $\beta$ , interleukin 1 $\beta$ ; IL-2, interleukin 2; IL-8, interleukin 8; IL-17, interleukin 17; G-CSF, granulocyte-colony stimulating factor; GM-CSF, granulocyte macrophage-colony stimulating factor; IP-10, IFN- $\gamma$ -induced protein 10; MCP-1, monocyte chemoattractant protein 1; CCL3, chemokine (C-C motif) ligand 3; TNF $\alpha$ , Tumor necrosis factor  $\alpha$ ; JAK, Janus kinase; STAT, signal transducer and activator of transcription; S1P, sphingosine-1-phosphate; S1PR $_1$ , sphingosine-1-

phosphate receptor 1; MyD88, myeloid differentiation primary response gene 88; TRIF, TIR-domain-containing adapter-inducing IFN- $\beta$ .

### 3.1 The NF- $\kappa$ B/TNF $\alpha$ signaling pathway

The transcription factor NF- $\kappa$ B is a critical regulator of both innate and adaptive immunity.<sup>41</sup> Under basal conditions, NF- $\kappa$ B is retained in the cytoplasm by the inhibitory proteins (I $\kappa$ Bs). A variety of cellular stimuli, including pathogens, induce I $\kappa$ B phosphorylation, ubiquitination and degradation by the proteasome, thereby promoting NF- $\kappa$ B nuclear translocation.<sup>41</sup> In the nucleus, NF- $\kappa$ B induces the transcription of a wide spectrum of genes encoding pro-inflammatory cytokines and chemokines, stress-response proteins, and anti-apoptotic proteins. NF- $\kappa$ B activity is essential for survival and activation, and for initiating and propagating optimal immune responses.<sup>42</sup> By contrast, the constitutive activation of the NF- $\kappa$ B pathway is often associated with inflammatory diseases, such as rheumatoid arthritis and asthma. Notably, the exacerbation of NF- $\kappa$ B activation has been reported to be implicated in lung inflammatory immunopathology induced by respiratory viruses, including SARS-CoV.<sup>43,44</sup> Moreover, Wang and collaborators demonstrated that, in murine macrophages cell line (RAW264.7), the exposure to recombinant SARS-CoV spike protein induced a massive protein release of IL-6 and TNF $\alpha$  in a time- and concentration-dependent manner in the supernatants and that such increase in IL-6 and TNF $\alpha$  secretion relies on the activation of NF- $\kappa$ B signaling pathway.<sup>45</sup> In fact, SARS-CoV spike protein has been associated with an increase in I $\kappa$ B $\alpha$  degradation, an essential step required for the activation of NF- $\kappa$ B signaling pathway.<sup>45</sup> Accordingly, transfection with dominant-negative NIK, which inhibits NF- $\kappa$ B activation, produced a strong reduction in spike protein IL-6 and TNF $\alpha$  release in RAW264.7 cells, thus demonstrating that NF- $\kappa$ B is required for the induction of IL-6 and TNF $\alpha$  by SARS-CoV spike protein.<sup>45</sup> Such *in vitro* data were consistent with results obtained *in vivo*, where treatments with drugs inhibiting NF- $\kappa$ B activation (such as caffeic acid phenethyl ester (CAPE), Bay11-7082, and parthenolide) reduced inflammation by suppressing the mRNA expression of TNF $\alpha$ , CXCL2, and MCP-1 in the lung of SARS-CoV-infected mice. Moreover, pharmacological inhibition of NF- $\kappa$ B protected against pulmonary pathology and enhanced mice survival after SARS-CoV infection.<sup>43</sup>

In line with these findings, Smits et al. demonstrated that SARS-CoV-infected aged macaques show in the lungs an increase in NF- $\kappa$ B nuclear translocation, as a result of NF- $\kappa$ B activation, and developed a stronger host response to virus infection compared to young adult macaques, with a significant increase in the expression of pro-inflammatory genes mainly regulated by NF- $\kappa$ B.<sup>44</sup>

Taken together these data suggest that NF- $\kappa$ B inhibition might be an effective strategy to counteract pathogenic SARS-CoV. However, targeting NF- $\kappa$ B is an approach strongly limited by intrinsic pathways complexity. Molecules blocking NF- $\kappa$ B lack for specificity and interfere with NF- $\kappa$ B physiological roles in cellular homeostasis, resulting in increased risk of undesired side effects, such as a broad suppression of innate immunity.<sup>46</sup> Moreover, within the context of viral infection, a major limitation of targeting NF- $\kappa$ B signaling depends on the ability of viruses to efficiently escape, by encoding proteins specifically blocking this pathway.<sup>46</sup> Thus, a promising strategy may rely on directly targeting the downstream effectors of the pathway, such as TNF $\alpha$ , whose expression is mainly controlled by NF- $\kappa$ B transcriptional activity. While TNF $\alpha$  is known to play a key role in the coordination and development of the inflammatory response, especially in the acute phase, long-lasting and excessive production of TNF $\alpha$  may become less effective by possibly altering TNF/TNF receptor signaling threshold which, after an initial wave of NF- $\kappa$ B activation, favors sustained basal NF- $\kappa$ B activity.<sup>47</sup> In addition, despite many other pro-inflammatory cytokines and mediators are involved in the cytokine storm, specific blockade of TNF $\alpha$  has been reported to be clinically effective in several pathological conditions. Accordingly, TNF $\alpha$  blockers, such as infliximab and adalimumab, have been successfully used for the treatment of several immune-mediated disorders, such as psoriasis, rheumatoid arthritis, inflammatory bowel diseases and ankylosing spondylitis.<sup>48,49</sup> Hence, anti-TNF $\alpha$  monoclonal antibodies are likely to attenuate inflammatory processes occurring in COVID-19, reducing the release of other inflammatory-exacerbating mediators. Indeed, when an anti-TNF $\alpha$  is administrated in patients with active rheumatoid arthritis, it has been demonstrated to induce a rapid decrease of a broad spectrum of cytokines (e.g. IL-6 and IL-1), as well as of others acute-phase related proteins and vascular permeability factor.<sup>50-</sup>

52

Furthermore, the envelope viral spike protein of SARS-CoV has been found to promote the activity of TNF $\alpha$ -converting enzyme (TACE)-dependent shedding of ACE2 receptor, which is a fundamental step for virus entry into the cell.<sup>53</sup> Thus, TNF $\alpha$  blockers represent effective therapeutic tools to counteract SARS-CoV infection by exerting a dual mechanism of action: attenuation of inflammation and inhibition of viral infection.<sup>45</sup> However, warnings about the potential increased risk of bacterial and fungal superinfections due to anti-TNF $\alpha$  therapy have to be taken into account.<sup>54</sup> Taking into account the sequence similarities between SARS-CoV and SARS-CoV-2 and the strong limitation in directly inhibiting NF- $\kappa$ B, to date, a clinical trial investigating adalimumab for the management of COVID-19 has been registered in the Chinese Clinical Trial Registry (ChiCTR2000030089) and is expected to run until August 2020. However, further investigations concerning the use and safety of TNF $\alpha$ -blockers in COVID-19 patients are urgently needed.

In addition, concerning a potential intervention on NF- $\kappa$ B signaling pathway, serine protease inhibitors of trypsin-like serine proteases (e.g. camostat mesylate, nafamostat mesylate, gabexate mesylate, ulinastatin), used for the treatment of pancreatitis, disseminated intravascular coagulation, and anticoagulant for hemodialysis,<sup>55,56</sup> have been found to inhibit viral replication<sup>57,58</sup> and to attenuate inflammatory processes in different pathological contexts, such as asthma, chronic allergic pulmonary inflammation, and inflammatory myocardial injury.<sup>59–62</sup> For instance, nafamostat mesylate and gabexate mesylate have been demonstrated to attenuate allergen-induced airway inflammation and eosinophilia in mouse model of allergic asthma,<sup>61</sup> thus reducing mast cell activation, eosinophils infiltrations in the lung, and *Dermatophagoides pteronyssinus*-driven IL-4 and TNF $\alpha$  production in bronchoalveolar lavage fluid.<sup>61</sup> Furthermore, treatment with nafamostat mesylate downregulated the expression of IL-1 $\beta$ , TNF $\alpha$ , IL-6, eotaxin, inducible NO synthase (iNOS), CD86, and NF- $\kappa$ B activation, but enhanced the expression of IL-12 and IL-10 in *Dermatophagoides pteronyssinus*-driven IL-4 and TNF $\alpha$  production in bronchoalveolar lavage fluid.<sup>61</sup> Moreover, gabexate mesylate has been found to inhibit LPS-induced TNF $\alpha$  production in human monocytes by blocking both NF- $\kappa$ B and mitogen-activated protein kinase activation.<sup>63</sup> Thus, the pharmacological profile of serine protease inhibitors, as inhibitors of complement pathways and broad-spectrum anti-inflammatory agents, provide a strong rationale for their use in the management of COVID-19. However, the specific mechanism of action through which serine protease inhibitors induce their anti-inflammatory effects is still unknown.

### 3.2 The IL-6/JAK/STAT signaling pathway

First discovered as the primary mediator of intracellular signaling induced by IFN in hematopoietic and immune cells, the JAK/STAT signaling is a key pathway transducing extracellular signals transmitted by a large number of cytokines, lymphokines and growth factors. In particular, a subset of cytokines employs the JAK/STAT signaling pathway in order to induce their biological effects. Notably, one of the major activators of JAK/STAT signaling is the cytokine IL-6, which has been reported to be dramatically increased in COVID-19 patients,<sup>20,22</sup> with a strong implication in acute inflammation and cytokine storm. In particular, IL-6 has been reported to activate numerous cell types expressing the glycoprotein (gp130) receptor and the membrane-bound IL-6 receptor, as well as a soluble form of IL-6 receptor interacting with gp130, thereby promoting the downstream activation of JAK/STAT signaling.<sup>64</sup> In turn, the activation of JAK/STAT pathway has been reported to stimulate the production of IL-6.<sup>65</sup> Such signaling pathway has been reported to be aberrantly activated in patients with chronic inflammation conditions, such as arthritis rheumatoid, and it is likely that its excessive overactivation may also occur in

COVID-19 patients, thereby exacerbating the host inflammatory response. Noteworthy, chronic elevation of circulating IL-6 has been widely recognized as a predictor for increased risk of cardiovascular events.<sup>66,67</sup> Consistently, IL-6 is produced from several tissues, including activated macrophages and endothelial and smooth muscle cells, where it promotes the secretion of other cytokines and, among others, it stimulates MCP1 secretion from macrophages to promote atherogenesis,<sup>68</sup> increases the expression of cell adhesion molecules,<sup>69,70</sup> and stimulates the proliferation and migration of vascular smooth muscle cells.<sup>71</sup> Thus, the abnormal increase in IL-6 levels may be implicated, at least in part, in the occurrence cardiovascular diseases (e.g. coronary atherosclerosis, inflammation in the vascular system resulting in diffuse microangiopathy with thrombosis) observed in COVID-19 patients.<sup>72</sup> Accordingly, the synthesis and secretion of IL-6 has been demonstrated to be induced by angiotensin II, which is locally produced by the inflamed vessels in a JAK/STAT-dependent manner.<sup>73</sup> In particular, angiotensin II binding to Angiotensin II receptor type 1 (AT<sub>1</sub> receptor) has been found to activate JAK/STAT pathway and to promote the downstream production of IL-6.<sup>73,74</sup> Increased angiotensin II enhances IL-6 production in AT<sub>1</sub>/JAK/STAT dependent manner, thus establishing a positive inflammatory feedback loop. Interestingly, the spike protein of SARS-CoV has been demonstrated to downregulate ACE2 expression, thus resulting in over-production of angiotensin II by the related enzyme ACE.<sup>75,76</sup> In a similar way, it could be hypothesized that SARS-CoV-2 may downregulate ACE2 receptors, thus leading to an over-production of angiotensin II, in turn enhancing IL-6 production in AT<sub>1</sub>/JAK/STAT dependent manner, and ultimately driving to vascular inflammation and lung injury, clinical signatures of COVID-19 (**Figure 2**). Moreover, the angiotensin II/AT<sub>1</sub> receptor axis has been reported to also activate both NF- $\kappa$ B and ADAM17.<sup>77</sup> Notably, an important substrate for ADAM17 is ACE2, whose cleavage by ADAM17 has been reported to inactivate it, enhancing angiotensin II retention, thus leading to hypertension, cardiovascular remodeling, and other types of pathophysiology associated with enhancement of the renin-angiotensin system.<sup>77</sup> Beside its implication in the shedding of ACE2 receptor, fundamental for virus entry,<sup>53</sup> ADAM17 induction has been found to process the membrane form of IL-6R $\alpha$  to the soluble form (sIL-6R $\alpha$ ), followed by the gp130-mediated activation of STAT3 via the sIL-6R $\alpha$ -IL-6 complex in a variety of IL-6R $\alpha$ -negative non-immune cells.<sup>78</sup> The activation of STAT3 has been reported to be required for the complete induction of NF- $\kappa$ B pathway.<sup>78</sup> Thus, SARS-CoV-2 infection may activate both NF- $\kappa$ B and STAT3 signaling, which in turn can promote the IL-6 amplifier mechanism, required for the hyper-activation of NF- $\kappa$ B by STAT3, thereby inducing multiple inflammatory and autoimmune diseases.<sup>78</sup> The IL-6 amplifier promotes the production and secretion of several pro-inflammatory cytokines and chemokines, such as IL-6, and the recruitment of lymphoid

and myeloid cells, sustaining the IL-6 amplifier-driven positive feedback loop (as proposed by Hirano and Murakami)<sup>79</sup> (**Figure 2**). Furthermore, the metalloprotease ADAM17 has been found to mediate angiotensin II-induced EGFR (epidermal growth factor receptor) transactivation by generating the mature form of heparin-binding EGF-like growth factor in vascular smooth muscle cells, thus leading to vascular remodeling.<sup>77</sup> Notably, EGFR transactivation is critical for angiotensin II-mediated cardiovascular complications.<sup>77</sup> In this regard, the EGFR kinase inhibitor Erlotinib has been recently repurposed for the treatment of COVID-19, based on its capability to reduce the infectivity of a wide range of viruses.<sup>80–82</sup> Beside its antiviral activity, the implication of EGFR transactivation in cardiovascular complications represent another theoretical foundation for the use of erlotinib in the management of COVID-19 patients.

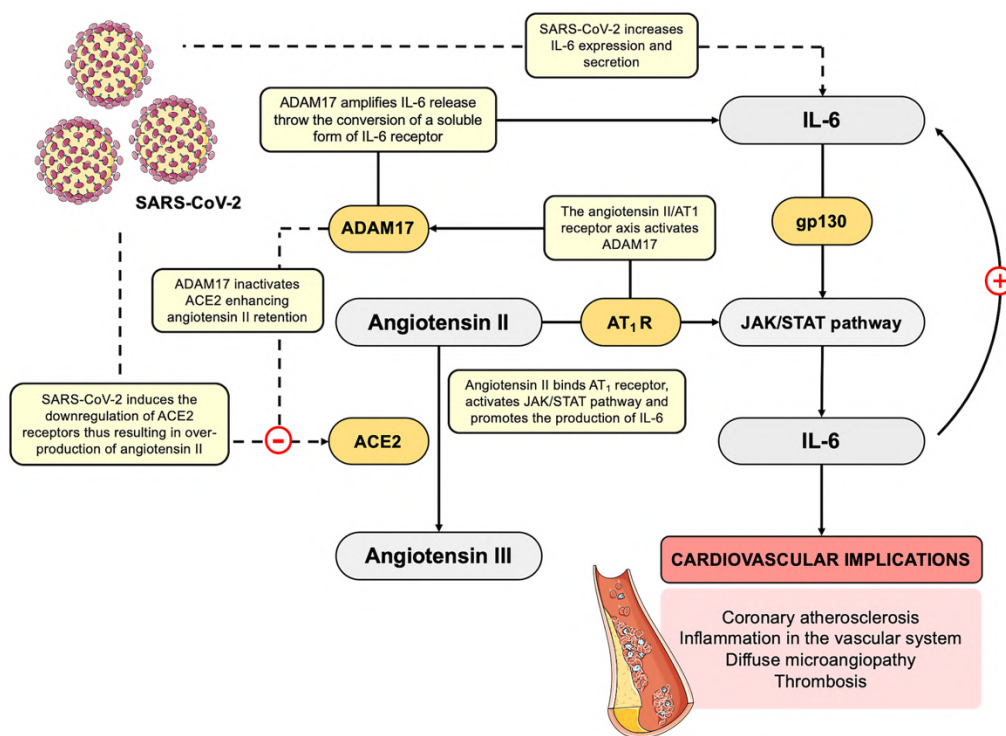


**Figure 2. Hypothetical mechanism by SARS-CoV-2 in establishing an inflammatory feedback loop between IL-6 and angiotensin II.** Cytokine IL-6 has been found increased in COVID-19 patients, thus suggesting a direct role of SARS-CoV-2 in a massive cytokine release. IL-6 is able to activate a soluble form of IL-6 receptor interacting with gp130, thereby promoting the downstream activation of JAK/STAT signaling, and thereby production of IL-6. Moreover, SARS-CoV-2 has been directly related with the occurrence of cardiovascular implications, such as coronary atherosclerosis, inflammation in the vascular system and diffuse microangiopathy with thrombosis. Synthesis and secretion of IL-6 are directly implicated in cardiovascular

damages. Indeed, IL-6 production is also induced by angiotensin II in AT<sub>1</sub>/JAK/STAT-dependent manner. As observed in SARS-CoV, also SARS-CoV-2 may be hypothesized to downregulate ACE2 expression, thus resulting in over-production of angiotensin II by the related enzyme ACE. In turn, increased angiotensin II enhances IL-6 production via JAK/STAT pathway, thus establishing a positive inflammatory feedback loop, ultimately resulting in the exacerbation of vascular and lung injuries. Moreover, the angiotensin II/AT<sub>1</sub> receptor axis activates ADAM17 that cleavages and inactivates ACE2, enhancing angiotensin II retention. In addition, ADAM17 induction has been found to process the membrane form of IL-6R $\alpha$  to the soluble form (sIL-6R $\alpha$ ), followed by the gp130-mediated activation of STAT3 via the sIL-6R $\alpha$ -IL-6 complex in a variety of IL-6R $\alpha$ -negative non-immune cells. The IL-6 amplifier promotes the production and secretion of several pro-inflammatory cytokines and chemokines, such as IL-6, sustaining the IL-6 amplifier-driven positive feedback. SARS-CoV-2, severe acute respiratory syndrome coronavirus 2; IL-6, interleukin 6; ACE2, angiotensin-converting enzyme 2; AT<sub>1</sub>, angiotensin II receptor type 1; JAK, Janus Kinase; STAT, Signal Transducer and Activator of Transcription; ADAM17, A Disintegrin And Metalloproteinase domain-containing protein 17.

Moreover, given the importance of angiotensin II/AT<sub>1</sub> receptor axis, the attempt to use angiotensin II-receptor blockers as a therapeutic benefit in COVID-19 by targeting the host response to the virus has been made.<sup>83</sup> However, their use needs to be deepened, since ACE inhibitors and angiotensin II-receptor blockers have been suggested to further increase the risk of COVID-19 infection by up-regulating ACE2.<sup>84</sup> Whether patients affected by COVID-19 and hypertension, taking an ACE inhibitors or angiotensin II-receptor blockers, should switch to another antihypertensive drug is still a matter of debate, and further evidence is required.

Since IL-6 appears a key driver of cytokine storm and of its consequent detrimental effects, monoclonal antibodies against IL-6, such as tocilizumab and sarilumab, have been also proposed to dampen this process. Tocilizumab, a monoclonal antibody IL-6 receptor antagonist, approved for the treatment of rheumatoid arthritis and CRS, has been used in clinical practice in order to manage severe cases of COVID-19 and it has been included in the current Chinese national treatment guidelines (<https://www.chinalawtranslate.com/wp-content/uploads/2020/03/Who-translation.pdf>). To date, 40 clinical trials (typing COVID-19 and tocilizumab on [clinicaltrials.gov](https://clinicaltrials.gov) and [clinicaltrialsregister.eu](https://clinicaltrialsregister.eu)) are underway to test tocilizumab, alone or in combination, in patients with COVID-19. Moreover, 18 clinical trials (typing COVID-19 and tocilizumab on [clinicaltrials.gov](https://clinicaltrials.gov) and [clinicaltrialsregister.eu](https://clinicaltrialsregister.eu)) will study the efficacy and safety of another IL-6 receptor antagonist, sarilumab, approved for the treatment of rheumatoid arthritis in patients with COVID-19.

Beside monoclonal antibodies specifically targeting IL-6, approved drugs inhibiting IL-6/JAK/STAT signaling may represent a valuable tool. In particular, JAK signaling inhibitors, such as baricitinib, fedratinib, and ruxolitinib – approved for indications such as rheumatoid arthritis and myelofibrosis – have been reported to attenuate the host

inflammatory response associated with massive pro-inflammatory cytokine and chemokine release.<sup>85</sup> Based on this anti-inflammatory effect, they are likely to be effective against the consequences of the elevated levels of cytokines typically observed in patients with COVID-19.<sup>80</sup> Among them, baricitinib, a selective inhibitor of JAK 1 and 2, has been predicted by crystallographic studies to inhibit two members of the numb-associated kinase family, such as AP2-associated protein kinase 1 (AAK1) and cyclin G-associated kinase (GAK), thus hindering viral endocytosis into lung cells, at the concentration approved for the treatment of arthritis rheumatoid.<sup>86</sup> However, despite such undeniable advantages, the repurposing of baricitinib and, in general, of JAK inhibitors for the management of COVID-19 is debated. In particular, concerns arise mainly from evidence reporting that the activation of JAK/STAT pathway, mediated by IFNs, is required for the induction of many IFN-regulated genes, playing a pivotal role as innate early defense system against viral infections. The defensive role of JAK/STAT pathway is corroborated by evidence demonstrating that the majority of virus have developed escaping strategies, such as the production of viral-encoded factors blocking this pathway, which are recognized as crucial determinants of virulence.<sup>87</sup> Therefore, inhibition of JAK/STAT signaling is likely to produce an impairment of IFN-related antiviral response, exacerbating SARS-CoV-2 infection. However, since several benefits, such as the blockage of virus entry and the attenuation of host excessive inflammatory response, as well as vascular and lung damage, provide a strong rationale for the use of baricitinib in the management of COVID-19 patients, the balance between positive and negative aspects of JAK/STAT signaling inhibition has to be still drawn up.

To date, several clinical trials are testing the efficacy and safety JAK inhibitors in COVID-19 patients (typing COVID-19 and JAK inhibitors on [clinicaltrials.gov](https://clinicaltrials.gov) and [clinicaltrialsregister.eu](https://clinicaltrialsregister.eu)).

### **3.3 The sphingosine-1-phosphate receptor 1 pathway**

The sphingosine-1-phosphate (S1P) 1 has emerged as a crucial signaling lipid regulator of inflammation and immune response, including lymphocyte trafficking, vascular integrity, and cytokine and chemokine production.<sup>88</sup> Beside S1P role of second messenger during inflammation, most of S1P effects on innate and adaptive immunity are mediated by its binding to five G-protein-coupled receptors (S1PR<sub>s1-5</sub>), which are differentially expressed in tissues.<sup>88</sup> Among them, S1P<sub>1</sub> receptor is ubiquitously expressed and coupled with a G inhibitory protein.<sup>89</sup> The activation of S1P<sub>1</sub> receptor is associated with Ras/ERK,



PI3K/Akt/eNOS, and PLC/Ca<sup>2+</sup> downstream pathways.<sup>89</sup> Notably, under physiological and pathological conditions, the S1P/S1PR<sub>1</sub> axis has been demonstrated to regulate the trafficking and migration of numerous types of immune cells, including T and B lymphocytes, NK cells, dendritic cells.<sup>88</sup> Moreover, the S1P<sub>1</sub> receptor signaling pathways have been reported to inhibit the pathological damage induced by the host innate and adaptive immune responses, thus attenuating the cytokine storm observed in influenza virus infection.<sup>40</sup> In particular, Teijaro et al. demonstrated that, in mice infected with A/Wisconsin/WSN/34939/09 influenza virus, S1P<sub>1</sub> receptor subtype regulates a crucial signaling loop fundamental for the initiation of cytokine storm in respiratory endothelial cells.<sup>40</sup> The administration of S1P<sub>1</sub> agonist blunted cytokine storm, by significantly inhibiting secretion of cytokines and chemokines associated with influenza virus-induced pathology, such as IFN- $\alpha$ , CCL2, IL-6, TNF $\alpha$ , and IFN- $\gamma$ .<sup>40</sup> Notably, in endothelial cells, suppression of early innate immune responses through S1P<sub>1</sub> signaling has been found to decrease mortality during influenza virus infection in mice.<sup>40</sup> Interestingly, in a later work by the same group, activation of S1P<sub>1</sub> signaling has been demonstrated to block cytokine and chemokine production, as well as immune cell activation and recruitment in the lungs of mice infected with the H1N1 WSN strain of influenza virus.<sup>90</sup> Moreover, S1P<sub>1</sub> agonism has been found to reduce cytokine storm independently of TLR3 and TLR7 signaling, as well as of multiple endosome and cytosolic innate pathogen-sensing pathways.<sup>90</sup> In contrast, S1P<sub>1</sub>R agonism has been found to suppress cytokine and chemokine production by targeting MyD88 (myeloid differentiation primary response gene 88)/TRIF (TIR-domain-containing adapter-inducing IFN- $\beta$ ) signaling, two common actors with NF- $\kappa$ B pathway.<sup>90</sup> However, S1P<sub>1</sub>R agonism is likely to modulate other signaling pathways that have not yet identified.

Thus, based on the effects of S1P receptor signaling on multiple immunological processes indicating such pathway a promising for the modulation of harmful inflammatory responses, the application of therapies targeting S1P and S1P signaling may be repurposed for immune-mediated disorders and inflammatory conditions, such as COVID-19. For instance, S1P agonists, approved for multiple sclerosis, such as fingolimod, might be used as therapeutic tools to dampen cytokine and chemokine responses in those patients displaying excessive immune responses. To date, only one non-randomized phase II clinical trial is underway to establish the efficacy of fingolimod in the treatment of COVID-19 (NCT04280588) (typing COVID-19 and fingolimod on [clinicaltrials.gov](https://clinicaltrials.gov)).

#### **4 Concluding remarks: a glimpse into the future**

The COVID-19 pandemic, induced by the novel SARS-CoV-2, represents one of the greatest global public health emergencies since the pandemic influenza outbreak of 1918 and provides an unprecedented challenge for the identification of both preventive and therapeutic drugs. In particular, vaccines and effective therapeutics to tackle this novel virus are urgently needed. Fortunately, in the last decade vaccine technology has significantly evolved, with the development of several RNA and DNA vaccine candidates, licensed vectored vaccines, recombinant proteins and cell-culture based vaccines for many indications.<sup>91</sup> Moreover, given the similarities of SARS-CoV-2 with SARS-CoV, the ideal target for the vaccine, the spike S protein on the surface of the virus required for viral entry, has been quickly identified, providing a target antigen to incorporate into advanced vaccine platforms. Thus, antibodies specifically targeting the S protein can block the binding of SARS-CoV-2 to the host ACE2 receptor, thus neutralizing the virus. However, given the lesson learned from SARS and MERS, the development of the vaccine against SARS-CoV-2 is likely to be an uphill road with several obstacles. In fact, several vaccines for SARS-CoV, including recombinant S protein-based vaccines, have been already developed and tested in animal models, but many did not produce sterilizing immunity in animal models and/or induced severe side effects, such as lung and liver damage.<sup>92,93</sup> To date, no human CoV vaccines have been approved so far. Moreover, to complicate this scenario, it has to be still unveiled whether infection with CoVs induces long-lived antibody response protecting against the risk of relapsing infections. Thus, scientific community has to overcome several issues for the development of an effective and safe SARS-CoV-2 vaccine. In this regard, Ling et al. recently detected SARS-CoV-2-specific humoral and cellular immunity in 8 COVID-19 patients, recently become virus-free and consequently discharged.<sup>94</sup> In addition, the neutralizing antibody titers have been significantly correlated with the numbers of nucleocapsid protein-specific T cells.<sup>94</sup> Such evidence indicates that both B and T cells cooperate to protect the host from viral infection. Notably, despite the small sample size, this study laid a theoretical foundation for the diagnosis of infectious diseases, the tracing of past infections, as well as the development of therapeutic antibody drugs and the design of an effective vaccine. Consistently, Long et al. reported acute antibody responses to SARS-CoV-2 in a cohort of 285 patients with COVID-19.<sup>31</sup> In particular, 19 days after symptom onset, 100% of patients have been tested positive for antiviral IgG and seroconversion for IgG and IgM have been reported to occur simultaneously or sequentially.<sup>31</sup> Thus, serological testing might be useful to identify suspected patients with negative RT-PCR results as well as asymptomatic infections.<sup>31</sup>

However, the speed at which SARS-CoV-2 is spreading has emphasized the urgent need to identify alternative therapeutic strategies in order to contain viral infection and to attenuate the excessive host immune response during the lag of vaccine availability,

especially in a scenario where the virus may become endemic and recurrent seasonal epidemics may occur. In this regard, several antiviral drugs, such as remdesivir, lopinavir and ritonavir, are currently tested in several clinical trials, either alone or in combination, and compassionate use of these drugs has already been reported for SARS-CoV-2.<sup>95,96</sup> However, antiviral drugs might select for mutational escape, thus rendering this therapeutic approach ineffective. Moreover, still unconfirmed reports indicate sufficient pre-clinical rationale and evidence regarding the use of chloroquine and hydroxychloroquine as prophylactic agent,<sup>97</sup> with evidence of safety from long-time use in clinical practice for the treatment of malaria and autoimmune diseases.<sup>98</sup> However, their use needs further evidence and clinical evaluation. Chloroquine and hydroxychloroquine are known to potentially cause heart rhythm problems, that may be exacerbated whether combined with other drugs with similar effects on the heart, and induce adverse liver, kidney and cerebral effects.<sup>99</sup> Thus, as discussed in this review, treatments addressing the immunopathology of the infection, such as immunomodulatory drugs approved for different clinical indications, have become a major focus. Such approaches show the advantage to override viral mutational escape and to exert less-selective pressure on viral population. Although the prospective of counteracting cytokine storm is compelling, a major limitation relies on the limited understanding of the immune signaling pathways triggering such process. Hence, future dissection of immune signaling pathways triggered by SARS-CoV-2 will provide novel insight on the effects of the virus on human immune system and may reveal relevant biological players that can be targeted to blunt cytokine storm. Notably, since it is well established that innate immune responses trigger the activation of multiple and redundant signaling pathways, an effective therapy may require to acting, at the same time, on multiple signaling pathways. In this regard, cocktails of immunomodulatory drugs, such as monoclonal antibody targeting a specific cytokine (e.g. TNF- inhibitors, IL-1-inhibitors, IL-6 inhibitors), corticosteroids (e.g., prednisone, methylprednisolone and dexamethasone), and S1PR<sub>1</sub> agonists (e.g. fingolimod), rather than a single drug, might be more effective in the management of COVID-19, by exerting either synergic or additive effects. In this regard, it would be of key importance to assess whether patients with immune-mediated disorders treated with immunomodulatory drugs, such as cytokine blockers, are more resistant to the excessive immune response observed in COVID-19 patients and more protected against SARS-CoV-2-driven pneumonia. However, to date, no evidence reporting either decreased or increased risk of SARS-CoV-driven pneumonia has been documented in this patients and further investigations are required to verify this hypothesis.

Furthermore, another aspect to better investigate concerns the possibility that the uncontrolled immune response to viral infection may cause detrimental systemic effects on

several physiological systems, such as the nervous, endocrine, renal and cardiovascular systems. Accordingly, it is likely that the massive cytokine and chemokine release may critically impact on these physiological systems, thereby inducing both short- and long-term detrimental effects. As an example, the neuro-invasive potential of SARS-CoV and MERS-CoV has been previously reported.<sup>100</sup> Thus, given the high similarity between SARS-CoV and SARS-CoV-2, it is likely that this latter displays a similar potential.<sup>101–103</sup> As a matter of fact, a study carried out in 214 COVID-19 patients reported that about 88% of severe COVID-19 cases showed neurologic manifestations, such as acute cerebrovascular diseases and impaired consciousness.<sup>104</sup>

Finally, beside the putative long-term effects directly induced by SARS-CoV-2 infection, another key issue to address concerns the long-term effects of empirical and experimental treatments in COVID-19 patients. In this regard, a study carried out in 25 recovered SARS patients, recruited 12 years after the viral infection, reported significant differences in the serum metabolomes in recovered SARS patients compared to controls.<sup>105</sup> In particular, a significant metabolic alteration – increased levels of phosphatidylinositol and lysophosphatidylinositol – has been found to coincide with the effect of methylprednisolone administration,<sup>105</sup> thus suggesting that high-dose pulses of steroid treatment may induce long-term systemic damage associated with serum metabolic alterations.<sup>105</sup>

Therefore, all the challenges discussed above highlight some of the major gaps in our knowledge of COVID-19 clinical spectrum, underlying immune signaling pathways, systemic effects, and long-term pathological signatures, which need to be urgently fulfilled by future investigations.

## REFERENCES

1. Lu, R. *et al.* Genomic characterisation and epidemiology of 2019 novel coronavirus: implications for virus origins and receptor binding. *Lancet Lond. Engl.* 395, 565–574 (2020).
2. Corman, V. M., Lienau, J. & Witzentrath, M. [Coronaviruses as the cause of respiratory infections]. *Internist* 60, 1136–1145 (2019).
3. Chan, J. F. W. *et al.* Middle East respiratory syndrome coronavirus: another zoonotic betacoronavirus causing SARS-like disease. *Clin. Microbiol. Rev.* 28, 465–522 (2015).
4. Mackenzie, J. S. & Smith, D. W. COVID-19: a novel zoonotic disease caused by a coronavirus from China: what we know and what we don't. *Microbiol. Aust.* MA20013 (2020) doi:10.1071/MA20013.

5. Lau, S. K. P. *et al.* Severe acute respiratory syndrome coronavirus-like virus in Chinese horseshoe bats. *Proc. Natl. Acad. Sci. U. S. A.* 102, 14040–14045 (2005).
6. Zhou, L., Liu, K. & Liu, H. G. [Cause analysis and treatment strategies of ‘recurrence’ with novel coronavirus pneumonia (covid-19) patients after discharge from hospital]. *Zhonghua Jie He He Hu Xi Za Zhi Zhonghua Jie He Huxi Zazhi Chin. J. Tuberc. Respir. Dis.* 43, E028 (2020).
7. Chan, J. F.-W. *et al.* Genomic characterization of the 2019 novel human-pathogenic coronavirus isolated from a patient with atypical pneumonia after visiting Wuhan. *Emerg. Microbes Infect.* 9, 221–236 (2020).
8. Hoffmann, M. *et al.* SARS-CoV-2 Cell Entry Depends on ACE2 and TMPRSS2 and Is Blocked by a Clinically Proven Protease Inhibitor. *Cell* 181, 271-280.e8 (2020).
9. Wan, Y., Shang, J., Graham, R., Baric, R. S. & Li, F. Receptor Recognition by the Novel Coronavirus from Wuhan: an Analysis Based on Decade-Long Structural Studies of SARS Coronavirus. *J. Virol.* 94, (2020).
10. Ou, X. *et al.* Characterization of spike glycoprotein of SARS-CoV-2 on virus entry and its immune cross-reactivity with SARS-CoV. *Nat. Commun.* 11, 1620 (2020).
11. Ding, Y. *et al.* Organ distribution of severe acute respiratory syndrome (SARS) associated coronavirus (SARS-CoV) in SARS patients: implications for pathogenesis and virus transmission pathways. *J. Pathol.* 203, 622–630 (2004).
12. Gu, J. *et al.* Multiple organ infection and the pathogenesis of SARS. *J. Exp. Med.* 202, 415–424 (2005).
13. Hamming, I. *et al.* Tissue distribution of ACE2 protein, the functional receptor for SARS coronavirus. A first step in understanding SARS pathogenesis. *J. Pathol.* 203, 631–637 (2004).
14. Xu, H. *et al.* High expression of ACE2 receptor of 2019-nCoV on the epithelial cells of oral mucosa. *Int. J. Oral Sci.* 12, 8 (2020).
15. Zhao, Y. *et al.* Single-cell RNA expression profiling of ACE2, the putative receptor of Wuhan 2019-nCoV. *Biorxiv* 2020(1):26.919985, (2020).
16. Huang, C. *et al.* Clinical features of patients infected with 2019 novel coronavirus in Wuhan, China. *Lancet Lond. Engl.* 395, 497–506 (2020).
17. Xu, Z. *et al.* Pathological findings of COVID-19 associated with acute respiratory distress syndrome. *Lancet Respir. Med.* 8, 420–422 (2020).
18. Wu, F. *et al.* A new coronavirus associated with human respiratory disease in China. *Nature* 579, 265–269 (2020).

19. Shi, Y. *et al.* Immunopathological characteristics of coronavirus disease 2019 cases in Guangzhou, China. *medRxiv* 2020.03.12.20034736 (2020) doi:10.1101/2020.03.12.20034736.
20. Qin, C. *et al.* Dysregulation of immune response in patients with COVID-19 in Wuhan, China. *Clin. Infect. Dis. Off. Publ. Infect. Dis. Soc. Am.* (2020) doi:10.1093/cid/ciaa248.
21. Zhang, B. *et al.* Immune phenotyping based on neutrophil-to-lymphocyte ratio and IgG predicts disease severity and outcome for patients with COVID-19. *medRxiv* 2020.03.12.20035048 (2020) doi:10.1101/2020.03.12.20035048.
22. Mehta, P. *et al.* COVID-19: consider cytokine storm syndromes and immunosuppression. *Lancet Lond. Engl.* 395, 1033–1034 (2020).
23. Li, D. *et al.* Immune dysfunction leads to mortality and organ injury in patients with COVID-19 in China: insights from ERS-COVID-19 study. *Signal Transduct. Target. Ther.* 5, 62 (2020).
24. Perlman, S. & Dandekar, A. A. Immunopathogenesis of coronavirus infections: implications for SARS. *Nat. Rev. Immunol.* 5, 917–927 (2005).
25. Tynell, J. *et al.* Middle East respiratory syndrome coronavirus shows poor replication but significant induction of antiviral responses in human monocyte-derived macrophages and dendritic cells. *J. Gen. Virol.* 97, 344–355 (2016).
26. Zhou, J. *et al.* Active replication of Middle East respiratory syndrome coronavirus and aberrant induction of inflammatory cytokines and chemokines in human macrophages: implications for pathogenesis. *J. Infect. Dis.* 209, 1331–1342 (2014).
27. Zhu, N. *et al.* A Novel Coronavirus from Patients with Pneumonia in China, 2019. *N. Engl. J. Med.* 382, 727–733 (2020).
28. Chen, D. *et al.* Recurrence of positive SARS-CoV-2 RNA in COVID-19: A case report. *Int. J. Infect. Dis. IJID Off. Publ. Int. Soc. Infect. Dis.* 93, 297–299 (2020).
29. Tan, L. *et al.* Lymphopenia predicts disease severity of COVID-19: a descriptive and predictive study. *Signal Transduct. Target. Ther.* 5, 33 (2020).
30. Wen, W. *et al.* Immune Cell Profiling of COVID-19 Patients in the Recovery Stage by Single-Cell Sequencing. *medRxiv* 2020.03.23.20039362 (2020) doi:10.1101/2020.03.23.20039362.
31. Long, Q.-X. *et al.* Antibody responses to SARS-CoV-2 in patients with COVID-19. *Nat. Med.* (2020) doi:10.1038/s41591-020-0897-1.
32. Alcami, A. & Koszinowski, U. H. Viral mechanisms of immune evasion. *Immunol. Today* 21, 447–455 (2000).
33. de Wit, E., van Doremalen, N., Falzarano, D. & Munster, V. J. SARS and MERS: recent insights into emerging coronaviruses. *Nat. Rev. Microbiol.* 14, 523–534 (2016).

34. Wan, S. *et al.* Characteristics of lymphocyte subsets and cytokines in peripheral blood of 123 hospitalized patients with 2019 novel coronavirus pneumonia (NCP). *medRxiv* 2020.02.10.20021832 (2020) doi:10.1101/2020.02.10.20021832.
35. Liu, Y. *et al.* Elevated plasma level of selective cytokines in COVID-19 patients reflect viral load and lung injury. *Natl. Sci. Rev.* (2020) doi:10.1093/nsr/nwaa037.
36. Favalli, E. G. *et al.* COVID-19 infection and rheumatoid arthritis: Faraway, so close! *Autoimmun. Rev.* 19, 102523 (2020).
37. Gou, W. *et al.* Gut microbiota may underlie the predisposition of healthy individuals to COVID-19. *medRxiv* 2020.04.22.20076091 (2020) doi:10.1101/2020.04.22.20076091.
38. de Marcken, M., Dhaliwal, K., Danielsen, A. C., Gautron, A. S. & Dominguez-Villar, M. TLR7 and TLR8 activate distinct pathways in monocytes during RNA virus infection. *Sci. Signal.* 12, (2019).
39. Olejnik, J., Hume, A. J. & Mühlberger, E. Toll-like receptor 4 in acute viral infection: Too much of a good thing. *PLoS Pathog.* 14, e1007390 (2018).
40. Teijaro, J. R. *et al.* Endothelial cells are central orchestrators of cytokine amplification during influenza virus infection. *Cell* 146, 980–991 (2011).
41. Li, Q. & Verma, I. M. NF-kappaB regulation in the immune system. *Nat. Rev. Immunol.* 2, 725–734 (2002).
42. Hayden, M. S., West, A. P. & Ghosh, S. NF- $\kappa$ B and the immune response. *Oncogene* 25, 6758–6780 (2006).
43. DeDiego, M. L. *et al.* Inhibition of NF- $\kappa$ B-Mediated Inflammation in Severe Acute Respiratory Syndrome Coronavirus-Infected Mice Increases Survival. *J. Virol.* 88, 913 (2014).
44. Smits, S. L. *et al.* Exacerbated innate host response to SARS-CoV in aged non-human primates. *PLoS Pathog.* 6, e1000756 (2010).
45. Wang, W. *et al.* Up-regulation of IL-6 and TNF-alpha induced by SARS-coronavirus spike protein in murine macrophages via NF-kappaB pathway. *Virus Res.* 128, 1–8 (2007).
46. Hiscott, J., Nguyen, T.-L. A., Arguello, M., Nakhaei, P. & Paz, S. Manipulation of the nuclear factor-kappaB pathway and the innate immune response by viruses. *Oncogene* 25, 6844–6867 (2006).
47. Clark, J., Vagenas, P., Panesar, M. & Cope, A. P. What does tumour necrosis factor excess do to the immune system long term? *Ann. Rheum. Dis.* 64 Suppl 4, iv70-76 (2005).
48. Silva, L. C. R., Ortigosa, L. C. M. & Benard, G. Anti-TNF- $\alpha$  agents in the treatment of immune-mediated inflammatory diseases: mechanisms of action and pitfalls. *Immunotherapy* 2, 817–833 (2010).
49. Lapadula, G. *et al.* Adalimumab in the treatment of immune-mediated diseases. *Int. J. Immunopathol. Pharmacol.* 27, 33–48 (2014).

50. Charles, P. *et al.* Regulation of cytokines, cytokine inhibitors, and acute-phase proteins following anti-TNF-alpha therapy in rheumatoid arthritis. *J. Immunol. Baltim. Md 1950* 163, 1521–1528 (1999).
51. Feldmann, M. & Maini, R. N. Anti-TNF alpha therapy of rheumatoid arthritis: what have we learned? *Annu. Rev. Immunol.* 19, 163–196 (2001).
52. Dvorak, H. F., Brown, L. F., Detmar, M. & Dvorak, A. M. Vascular permeability factor/vascular endothelial growth factor, microvascular hyperpermeability, and angiogenesis. *Am. J. Pathol.* 146, 1029–1039 (1995).
53. Haga, S. *et al.* Modulation of TNF-alpha-converting enzyme by the spike protein of SARS-CoV and ACE2 induces TNF-alpha production and facilitates viral entry. *Proc. Natl. Acad. Sci. U. S. A.* 105, 7809–7814 (2008).
54. Galloway, J. B. *et al.* Anti-TNF therapy is associated with an increased risk of serious infections in patients with rheumatoid arthritis especially in the first 6 months of treatment: updated results from the British Society for Rheumatology Biologics Register with special emphasis on risks in the elderly. *Rheumatol. Oxf. Engl.* 50, 124–131 (2011).
55. Hirano, T. Pancreatic injuries in rats with fecal peritonitis: protective effect of a new synthetic protease inhibitor, sepinostat mesilate (FUT-187). *J. Surg. Res.* 61, 301–306 (1996).
56. Takahashi, H. *et al.* Combined treatment with nafamostat mesilate and aspirin prevents heparin-induced thrombocytopenia in a hemodialysis patient. *Clin. Nephrol.* 59, 458–462 (2003).
57. Zhirmov, O. P., Klenk, H. D. & Wright, P. F. Aprotinin and similar protease inhibitors as drugs against influenza. *Antiviral Res.* 92, 27–36 (2011).
58. Yamaya, M. *et al.* The serine protease inhibitor camostat inhibits influenza virus replication and cytokine production in primary cultures of human tracheal epithelial cells. *Pulm. Pharmacol. Ther.* 33, 66–74 (2015).
59. Ishizaki, M. *et al.* Nafamostat mesilate, a potent serine protease inhibitor, inhibits airway eosinophilic inflammation and airway epithelial remodeling in a murine model of allergic asthma. *J. Pharmacol. Sci.* 108, 355–363 (2008).
60. Florencio, A. C. *et al.* Effects of the serine protease inhibitor rBmTI-A in an experimental mouse model of chronic allergic pulmonary inflammation. *Sci. Rep.* 9, 12624 (2019).
61. Chen, C.-L. *et al.* Serine protease inhibitors nafamostat mesilate and gabexate mesilate attenuate allergen-induced airway inflammation and eosinophilia in a murine model of asthma. *J. Allergy Clin. Immunol.* 118, 105–112 (2006).
62. Lin, C.-C. *et al.* The Effect of Serine Protease Inhibitors on Airway Inflammation in a Chronic Allergen-Induced Asthma Mouse Model. *Mediators Inflamm.* 2014, 879326 (2014).



63. Yuksel, M., Okajima, K., Uchiba, M. & Okabe, H. Gabexate mesilate, a synthetic protease inhibitor, inhibits lipopolysaccharide-induced tumor necrosis factor- $\alpha$  production by inhibiting activation of both nuclear factor- $\kappa$ B and activator protein-1 in human monocytes. *J. Pharmacol. Exp. Ther.* 305, 298–305 (2003).
64. Zhang, C., Wu, Z., Li, J.-W., Zhao, H. & Wang, G.-Q. The cytokine release syndrome (CRS) of severe COVID-19 and Interleukin-6 receptor (IL-6R) antagonist Tocilizumab may be the key to reduce the mortality. *Int. J. Antimicrob. Agents* 105954 (2020) doi:10.1016/j.ijantimicag.2020.105954.
65. Lee, C. *et al.* Janus kinase-signal transducer and activator of transcription mediates phosphatidic acid-induced interleukin (IL)-1 $\beta$  and IL-6 production. *Mol. Pharmacol.* 69, 1041–1047 (2006).
66. Wainstein, M. V. *et al.* Elevated serum interleukin-6 is predictive of coronary artery disease in intermediate risk overweight patients referred for coronary angiography. *Diabetol. Metab. Syndr.* 9, 67 (2017).
67. Zhang, B., Li, X.-L., Zhao, C.-R., Pan, C.-L. & Zhang, Z. Interleukin-6 as a Predictor of the Risk of Cardiovascular Disease: A Meta-Analysis of Prospective Epidemiological Studies. *Immunol. Invest.* 47, 689–699 (2018).
68. Biswas, P. *et al.* Interleukin-6 induces monocyte chemotactic protein-1 in peripheral blood mononuclear cells and in the U937 cell line. *Blood* 91, 258–265 (1998).
69. McLoughlin, R. M. *et al.* Differential Regulation of Neutrophil-Activating Chemokines by IL-6 and Its Soluble Receptor Isoforms. *J. Immunol.* 172, 5676 (2004).
70. van der Meer Irene M. *et al.* Inflammatory Mediators and Cell Adhesion Molecules as Indicators of Severity of Atherosclerosis. *Arterioscler. Thromb. Vasc. Biol.* 22, 838–842 (2002).
71. Xiang, S. *et al.* Inhibitory effects of suppressor of cytokine signaling 3 on inflammatory cytokine expression and migration and proliferation of IL-6/IFN- $\gamma$ -induced vascular smooth muscle cells. *J. Huazhong Univ. Sci. Technol. Med. Sci. Hua Zhong Ke Ji Xue Xue Bao Yi Xue Ying Wen Ban Huazhong Keji Daxue Xuebao Yixue Yingdewen Ban* 33, 615–622 (2013).
72. Qu, D., Liu, J., Lau, C. W. & Huang, Y. IL-6 in diabetes and cardiovascular complications. *Br. J. Pharmacol.* 171, 3595–3603 (2014).
73. Schieffer, B. *et al.* Role of NAD(P)H oxidase in angiotensin II-induced JAK/STAT signaling and cytokine induction. *Circ. Res.* 87, 1195–1201 (2000).
74. Marrero, M. B. *et al.* Direct stimulation of Jak/STAT pathway by the angiotensin II AT1 receptor. *Nature* 375, 247–250 (1995).
75. Kuba, K. *et al.* A crucial role of angiotensin converting enzyme 2 (ACE2) in SARS coronavirus-induced lung injury. *Nat. Med.* 11, 875–879 (2005).

76. Glowacka, I. *et al.* Differential downregulation of ACE2 by the spike proteins of severe acute respiratory syndrome coronavirus and human coronavirus NL63. *J. Virol.* 84, 1198–1205 (2010).
77. Eguchi, S., Kawai, T., Scalia, R. & Rizzo, V. Understanding Angiotensin II Type 1 Receptor Signaling in Vascular Pathophysiology. *Hypertens. Dallas Tex 1979* 71, 804–810 (2018).
78. Murakami, M., Kamimura, D. & Hirano, T. Pleiotropy and Specificity: Insights from the Interleukin 6 Family of Cytokines. *Immunity* 50, 812–831 (2019).
79. Hirano, T. & Murakami, M. COVID-19: A New Virus, but a Familiar Receptor and Cytokine Release Syndrome. *Immunity* (2020) doi:10.1016/j.immuni.2020.04.003.
80. Stebbing, J. *et al.* COVID-19: combining antiviral and anti-inflammatory treatments. *Lancet Infect. Dis.* 20, 400–402 (2020).
81. Bekerman, E. *et al.* Anticancer kinase inhibitors impair intracellular viral trafficking and exert broad-spectrum antiviral effects. *J. Clin. Invest.* 127, 1338–1352 (2017).
82. Pu, S.-Y. *et al.* Feasibility and biological rationale of repurposing sunitinib and erlotinib for dengue treatment. *Antiviral Res.* 155, 67–75 (2018).
83. Gurwitz, D. Angiotensin receptor blockers as tentative SARS-CoV-2 therapeutics. *Drug Dev. Res.* (2020) doi:10.1002/ddr.21656.
84. Zheng, Y.-Y., Ma, Y.-T., Zhang, J.-Y. & Xie, X. COVID-19 and the cardiovascular system. *Nat. Rev. Cardiol.* 17, 259–260 (2020).
85. Sanchez, G. A. M. *et al.* JAK1/2 inhibition with baricitinib in the treatment of autoinflammatory interferonopathies. *J. Clin. Invest.* 128, 3041–3052 (2018).
86. Sorrell, F. J., Szklarz, M., Abdul Azeez, K. R., Elkins, J. M. & Knapp, S. Family-wide Structural Analysis of Human Numb-Associated Protein Kinases. *Struct. Lond. Engl. 1993* 24, 401–411 (2016).
87. Fleming, S. B. Viral Inhibition of the IFN-Induced JAK/STAT Signalling Pathway: Development of Live Attenuated Vaccines by Mutation of Viral-Encoded IFN-Antagonists. *Vaccines* 4, (2016).
88. Spiegel, S. & Milstien, S. The outs and the ins of sphingosine-1-phosphate in immunity. *Nat. Rev. Immunol.* 11, 403–415 (2011).
89. Bryan, A. M. & Del Poeta, M. Sphingosine-1-phosphate receptors and innate immunity. *Cell. Microbiol.* 20, e12836 (2018).
90. Teijaro, J. R., Walsh, K. B., Rice, S., Rosen, H. & Oldstone, M. B. A. Mapping the innate signaling cascade essential for cytokine storm during influenza virus infection. *Proc. Natl. Acad. Sci. U. S. A.* 111, 3799–3804 (2014).
91. Amanat, F. & Krammer, F. SARS-CoV-2 Vaccines: Status Report. *Immunity* 52, 583–589 (2020).

92. Bolles, M. *et al.* A double-inactivated severe acute respiratory syndrome coronavirus vaccine provides incomplete protection in mice and induces increased eosinophilic proinflammatory pulmonary response upon challenge. *J. Virol.* 85, 12201–12215 (2011).
93. Tseng, C.-T. *et al.* Immunization with SARS coronavirus vaccines leads to pulmonary immunopathology on challenge with the SARS virus. *PLoS One* 7, e35421 (2012).
94. Ni, L. *et al.* Detection of SARS-CoV-2-specific humoral and cellular immunity in COVID-19 convalescent individuals. *Immunity* (2020) doi:10.1016/j.immuni.2020.04.023.
95. Holshue, M. L. *et al.* First Case of 2019 Novel Coronavirus in the United States. *N. Engl. J. Med.* 382, 929–936 (2020).
96. Lim, J. *et al.* Case of the Index Patient Who Caused Tertiary Transmission of COVID-19 Infection in Korea: the Application of Lopinavir/Ritonavir for the Treatment of COVID-19 Infected Pneumonia Monitored by Quantitative RT-PCR. *J. Korean Med. Sci.* 35, e79 (2020).
97. Cortegiani, A., Ingoglia, G., Ippolito, M., Giarratano, A. & Einav, S. A systematic review on the efficacy and safety of chloroquine for the treatment of COVID-19. *J. Crit. Care* (2020) doi:10.1016/j.jcrc.2020.03.005.
98. Lee, S.-J., Silverman, E. & Bargman, J. M. The role of antimalarial agents in the treatment of SLE and lupus nephritis. *Nat. Rev. Nephrol.* 7, 718–729 (2011).
99. Touret, F. & de Lamballerie, X. Of chloroquine and COVID-19. *Antiviral Res.* 177, 104762 (2020).
100. Xu, J. *et al.* Detection of severe acute respiratory syndrome coronavirus in the brain: potential role of the chemokine mig in pathogenesis. *Clin. Infect. Dis. Off. Publ. Infect. Dis. Soc. Am.* 41, 1089–1096 (2005).
101. Netland, J., Meyerholz, D. K., Moore, S., Cassell, M. & Perlman, S. Severe acute respiratory syndrome coronavirus infection causes neuronal death in the absence of encephalitis in mice transgenic for human ACE2. *J. Virol.* 82, 7264–7275 (2008).
102. Li, K. *et al.* Middle East Respiratory Syndrome Coronavirus Causes Multiple Organ Damage and Lethal Disease in Mice Transgenic for Human Dipeptidyl Peptidase 4. *J. Infect. Dis.* 213, 712–722 (2016).
103. Li, Y.-C., Bai, W.-Z. & Hashikawa, T. The neuroinvasive potential of SARS-CoV2 may play a role in the respiratory failure of COVID-19 patients. *J. Med. Virol.* (2020) doi:10.1002/jmv.25728.
104. Mao, L. *et al.* Neurological Manifestations of Hospitalized Patients with COVID-19 in Wuhan, China: a retrospective case series study. *medRxiv* 2020.02.22.20026500 (2020) doi:10.1101/2020.02.22.20026500.

105. Wu, Q. *et al.* Altered Lipid Metabolism in Recovered SARS Patients Twelve Years after Infection. *Sci. Rep.* 7, 9110 (2017).

**PART 2**

The following manuscript was published in *Signal Transduction and Targeted Therapy* in 2020  
as:

**Molecular features of IGHV3-53-encoded antibodies elicited by  
SARS-CoV-2**

**Francesca Fagiani, Michele Catanzaro, and Cristina Lanni**



## RESEARCH HIGHLIGHT OPEN

## Molecular features of IGHV3-53-encoded antibodies elicited by SARS-CoV-2

Francesca Fagiani<sup>1,2</sup>, Michele Catanzaro<sup>1</sup> and Cristina Lanni *Signal Transduction and Targeted Therapy* (2020)5:170; <https://doi.org/10.1038/s41392-020-00287-4>

<sup>1</sup>Department of Drug Sciences (Pharmacology Section), University of Pavia, V.le Taramelli 14, 27100 Pavia, Italy and <sup>2</sup>Scuola Universitaria Superiore IUSS Pavia, P.zza Vittoria, 15, 27100 Pavia, Italy

Correspondence: Cristina Lanni ([cristina.lanni@unipv.it](mailto:cristina.lanni@unipv.it))

These authors contributed equally: Francesca Fagiani, Michele Catanzaro

An elegant paper by Yuan *et al.*, recently published in *Science*, provides novel insights into the molecular features of neutralizing antibody responses to the severe acute respiratory syndrome coronavirus 2 (SARS-CoV-2).<sup>1</sup>

According to the principles of the “reverse vaccinology 2.0” postulated by Burton *et al.*,<sup>2</sup> the authors explore the interactions between potent neutralizing antibodies from naturally infected donors and their target epitopes, providing key information about structural motifs and binding mode that may facilitate the design of vaccine antigens capable to elicit the immune response against SARS-CoV-2. The vast majority of anti-CoV neutralizing antibodies have been found to specifically target the receptor-binding domain (RBD) of the viral spike (S) protein, thus hindering SARS-CoV-2 binding to the host angiotensin converting enzyme 2 (ACE2) receptor and viral entry.<sup>3</sup>

Yuan and collaborators analyzed 294 anti-SARS-CoV-2 antibodies from COVID-19 patients and demonstrated that among these antibodies the immunoglobulin heavy variable 3-53 (IGHV3-53) represents the most frequently used IGHV gene, with 10% encoded by IGHV3-53. In the cohort investigated by Yuan *et al.*, IGHV3-53 antibodies have been reported to be more potent compared to other germ lines, as well as to display lower somatic mutation rates. The authors determined the crystal structures of two antibodies, CC12.1 and CC12.3, encoded by a common IGHV353 gene, but belonging to different clonotypes, in order to define the structural features, and to add favorable properties for RBD recognition to IGHV3-53. Notably, among the antibodies tested against live replicating SARS-CoV-2 and pseudovirus, CC12.1 and CC12.3 ( $IC_{50} \sim 20$  ng/mL), isolated from COVID-19 patients, are among the top four highly potent neutralizing antibodies, with a binding affinity ( $K_d$ ) of Fabs CC12.1 and CC12.3 to SARS-CoV-2 RBD of 17 and 14 nM, respectively.<sup>1,4</sup> By performing competitions experiments, Yuan *et al.* demonstrated that both CC12.1 and CC12.3 bind to the ACE2 binding site on SARS-CoV-2 RBD with an identical

angle of approach. Among 17 ACE2 binding residues on RBD, 15 and 11 are within the epitopes of CC12.1 and CC12.3, respectively. Remarkably, several epitope residues are not conserved between SARS-CoV-2 and SARS-CoV, thus explaining, at least in part, the absence of antibody cross-reactivity between these two CoVs.<sup>5</sup> Such evidence is consistent with data, reported by Ju *et al*, showing the lack of antibody cross-reactivity with RBDs not only from SARS-CoV, but also from middle east respiratory syndrome coronavirus (MERS-CoV), thus suggesting that SARSCoV, SARS-CoV-2, and MERS-CoV are immunologically distinct.<sup>5</sup> As an example, despite SARS-CoV-2 and SARS-CoV display both sequential and structural similarities, diverse viral species-specific responses have been observed in patients.<sup>5</sup> Such evidence justifies the failures of the attempts to neutralize SARS-CoV-2 by using previously isolated SARS-CoV antibodies.<sup>5</sup>

Moreover, the authors provided evidence that CC12.1 presents immunoglobulin kappa variable1-9 (IGKV1-9) and CCL12.3 IGKV320, thereby suggesting that IGHV3-53 can pair with different light chains. Such finding indicates that the identity of the heavy chain, instead of that of the light-chain, might be critical for targeting ACE2 binding site in SARS-CoV-2 RBD.

Furthermore, the complementarity-determining regions (CDRs) of IGHV3-53 were structurally analyzed. Based on structural analysis, the presence of two structural motifs, the NY motif in the CDR H1 and an SGGs motif in the CDR H2, as well as the short length of CDR H3, appear fundamental for the binding to the RBD. CDR H1 and H2 of CC12.1 and CC12.3 antibodies have been found to stabilize the CDR conformation with the surrounding framework and to establish hydrogen bonds with the carbonyl backbone of key amino acids in the RBD. While high similarity in the interaction modes between SARS-CoV-2 RBD and CDR H1 and H2 loops has been found, significant differences in the CDR H3 sequence and conformations have been observed when comparing two antibodies. As an example, while CDR H3 of CC12.2 has been found to establish a hydrogen bond with RBD Y453, CDR H3 of CC12.3 has been observed not to form it. Notably, an interesting feature of CDR H3 region of IGHV3-53-encoded antibodies is its short length. Accordingly, CC12.1 and CC12.3 have a CDR H3 consisting of nine amino acids in lengths. This structural feature may rely on the fact that the epitopes of IGHV3-53 antibodies are relatively flat and present a small pocket to insert the CDR H3 loop. Hence, longer CDR H3 regions might not be accommodated in IGHV3-53-encoded antibodies.

In sum, based on this structural characterization, Yuan and collaborators shed lights on some key molecular features (illustrated in **Fig. 1**) contributing to an effective antibody

response against SARS-CoV-2 infection, demonstrating that IGHV3-53 provides a versatile framework to target the ACE2 binding site in SARS-CoV-2 RBD.

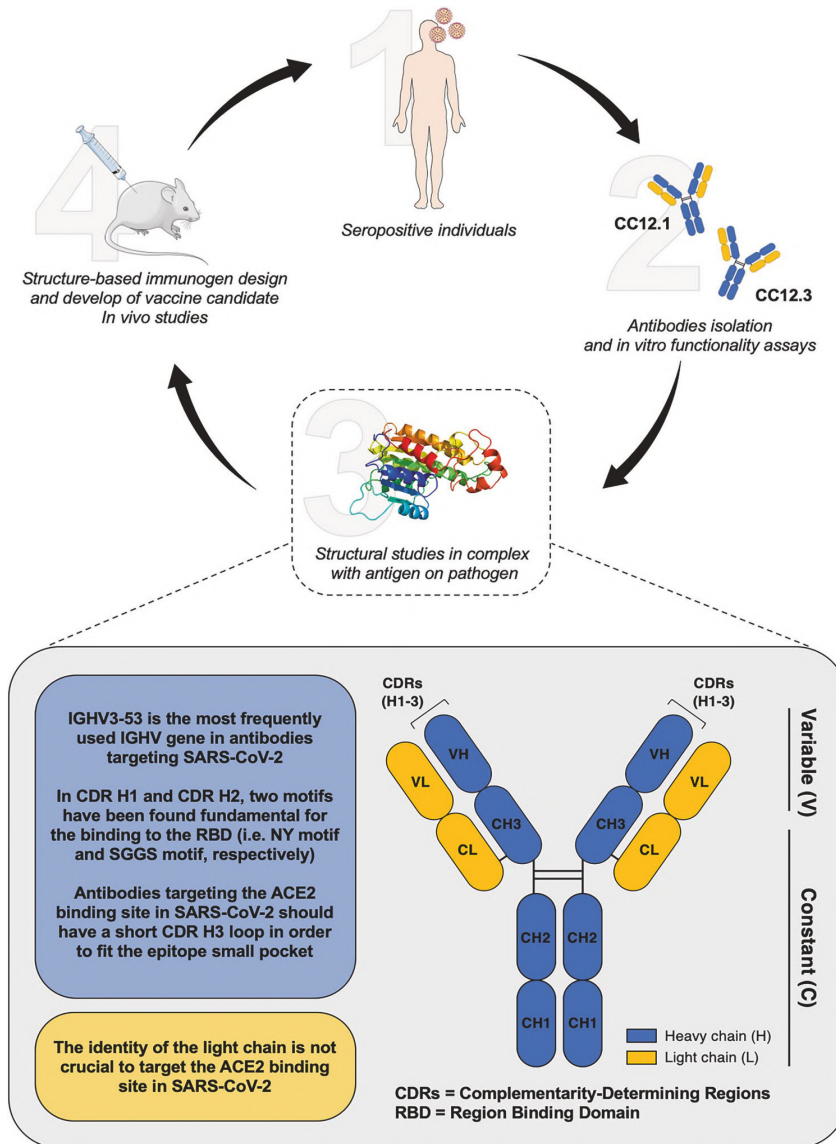


**Fig. 1. Representation of “reverse vaccinology 2.0” theory: focus on the molecular features of IGHV3-53-encoded antibodies.** Monoclonal antibodies are obtained from seropositive subjects, isolated and structurally characterized. Based on the molecular features, a structure-based immunogen is designed and then tested in appropriate animal models.



In conclusion, understanding of IGHV3-53-encoded antibodies and, in general, of anti-SARS-CoV-2 neutralizing antibodies, produced by infected donors, is required to generate immunogens that optimally present neutralizing epitopes to the immune system. Such approach may further open new horizons toward the identification of multiple functional antibodies, derived from several donors and directed toward single epitopes regions in order to combine sites of different shapes recognizing the critical regions, thereby capturing the biological diversity of antibody response.<sup>2</sup>The characterization by Yuan *et al.* may also allow to create anti-SARS-CoV-2 antibody templates for immunogens design, thus greatly improving the sophistication in the design of immunogens and in immunization strategies.

### ACKNOWLEDGEMENTS

This work has been supported by the University of Pavia (Grants from FR&G 2019, Fondo Ricerca & Giovani, to C.L.).

### REFERENCES

- [1] Yuan, M. et al. Structural basis of a shared antibody response to SARS-CoV-2. *Science* <https://doi.org/10.1126/science.abd2321> (2020).
- [2] Burton, D. R. What are the most powerful immunogen design vaccine strategies? Reverse vaccinology 2.0 shows great promise. *Cold Spring Harb. Perspect. Biol.* 9, a030262 (2017).
- [3] Hoffmann, M. et al. SARS-CoV-2 cell entry depends on ACE2 and TMPRSS2 and is blocked by a clinically proven protease inhibitor. *Cell* 181, 271–280.e8(2020).
- [4] Rogers, T. F. et al. Isolation of potent SARS-CoV-2 neutralizing antibodies and protection from disease in a small animal model. *Science* <https://doi.org/10.1126/science.abc7520> (2020).
- [5] Ju, B. et al. Human neutralizing antibodies elicited by SARS-CoV-2 infection. *Nature* <https://doi.org/10.1038/s41586-020-2380-z> (2020).



---

**CHAPTER V**

Other collaborative activities



## PART 1

The following manuscript was published in *Marine Drugs* in 2020 as:

### **Dual-Functioning Scaffolds for the Treatment of Spinal Cord Injury: Alginate Nanofibers Loaded with the Sigma 1 Receptor (S1R) Agonist RC-33 in Chitosan Films**

Barbara Vigani, Silvia Rossi, Giuseppina Sandri, Maria Cristina Bonferoni, Marta Rui, Simona Collina, **Francesca Fagiani**, Cristina Lanni, and Franca Ferrari

#### **Abstract**

The present work proposed a novel therapeutic platform with both neuroprotective and neuroregenerative potential to be used in the treatment of spinal cord injury (SCI). A dual-functioning scaffold for the delivery of the neuroprotective S1R agonist, RC-33, to be locally implanted at the site of SCI, was developed. RC-33-loaded fibers, containing alginate (ALG) and a mixture of two different grades of poly(ethylene oxide) (PEO), were prepared by electrospinning. After ionotropic cross-linking, fibers were incorporated in chitosan (CS) films to obtain a drug delivery system more flexible, easier to handle, and characterized by a controlled degradation rate. Dialysis equilibrium studies demonstrated that ALG was able to form an interaction product with the cationic RC-33 and to control RC-33 release in the physiological medium. Fibers loaded with RC-33 at the concentration corresponding to 10% of ALG maximum binding capacity were incorporated in films based on CS at two different molecular weights - low (CSL) and medium (CSM) - solubilized in acetic (AA) or glutamic (GA) acid. CSL - based scaffolds were subjected to a degradation test in order to investigate if the different CSL salification could affect the film behavior when in contact with media that mimic SCI environment. CSL AA exhibited a slower biodegradation and a good compatibility towards human neuroblastoma cell line.

**Keywords:** spinal cord injury; S1R agonist; chitosan; alginate; RC-33/ALG interaction product; electrospinning; film casting; mechanical properties; biodegradation; human neuroblastoma cells.



## PART 2

The following manuscript has been accepted for publication in *Oncogenesis* as:

### **OXER1 and RACK1 associated pathway: a promising drug target for breast cancer progression**

Mirco Masi, Enrico Garattini, Marco Bolis, Daniele di Marino, Luisa Maraccani, Elena Morelli, Ambra Grolla, **Francesca Fagiani**, Emanuela Corsini, Cristina Travelli, Stefano Govoni, Marco Racchi, and Erica Buoso

#### **Abstract**

Recent data indicate that Receptor for Activated C Kinase 1 (RACK1) is a putative prognostic marker and drug target in breast cancer (BC). High RACK1 expression is negatively associated with overall survival, as it seems to promote BC progression. In tumors, RACK1 expression is controlled by a complex balance between glucocorticoids and androgens. Given the fact that androgens and androgenic derivatives can inhibit BC cell proliferation and migration, the role of androgen signaling in regulating RACK1 transcription in mammary tumors is of pivotal interest. Here, we provide evidence that nandrolone (19-nortosterone) inhibits BC cell proliferation and migration by antagonizing the PI3K/Akt/NF- $\kappa$ B signaling pathway, which eventually results in RACK1 down-regulation. We also show that nandrolone impairs the PI3K/Akt/NF- $\kappa$ B signaling pathway and decreases RACK1 expression via binding to the membrane-bound receptor, Oxoeicosanoid Receptor 1 (OXER1). High levels of OXER1 are observed in several BC cell lines and correlate with RACK1 expression and poor prognosis. Our data provide evidence on the role played by the OXER1-dependent intracellular pathway in BC progression and shed light on the mechanisms underlying membrane-dependent androgen effects on RACK1 regulation. Besides the mechanistic relevance, the results of the study are of interest from a translational prospective. In fact, they identify a new and actionable pathway to be used for the design of innovative and rational therapeutic strategies in the context of the personalized treatment of BC. In addition, they draw attention on nandrolone-based compounds that lack hormonal activity as potential anti-tumor agents.

**Keywords:** OXER1, RACK1, invasion, migration, breast cancer, androgen





**LIST OF PUBLICATIONS**

(from 2019 to 2020)

- [1] Lanni, C., **Fagiani, F.**, Racchi, M., Preda, S., Pascale, A., Grilli, M., Allegri, N., Govoni, S. [2019] "Beta-amyloid short- and long-term synaptic entanglement", *Pharmacol Res*, Vol. 139, pp. 243-260. doi:10.1016/j.phrs.2018.11.018.
- [2] Rosini, M., Simoni, E., Caporaso, R., Basagni, F., Catanzaro, M., Abu, I.F., **Fagiani, F.**, Fusco, F., Masuzzo, S., Albani, D., Lanni, C., Mellor, I.R., Minarini, A. [2019] "Merging memantine and ferulic acid to probe connections between NMDA receptors, oxidative stress and amyloid- $\beta$  peptide in Alzheimer's disease", *Eur J Med Chem*, Vol. 180, pp. 111-120. doi:10.1016/j.ejmech.2019.07.011
- [3] **Fagiani, F.\***, Lanni, C.\*, Racchi, M., Pascale, A., Govoni, S. [2019] "Amyloid- $\beta$  and Synaptic Vesicle Dynamics: A Cacophonous Orchestra", *J Alzheimers Dis*, Vol. 72, No. 1, pp. 1-14. doi:10.3233/JAD-190771. \*both authors equally contributed
- [4] Vigani, B., Rossi, S., Sandri, G., Bonferoni, M.C., Rui, M., Collina, S., **Fagiani, F.**, Lanni, C., Ferrari, F. [2019] "Dual-Functioning Scaffolds for the Treatment of Spinal Cord Injury: Alginate Nanofibers Loaded with the Sigma 1 Receptor (S1R) Agonist RC-33 in Chitosan Films", *Mar Drugs*, Vol. 18, No. 1, pp. 21. doi:10.3390/md18010021.
- [5] Serafini, M.M.\*, Catanzaro, M.\*, **Fagiani, F.**, Simoni, E., Caporaso, R., Dacrema, M., Romanoni, I., Govoni, S., Racchi, M., Daglia, M., Rosini, M., Lanni, C. [2020] "Modulation of Keap1/Nrf2/ARE Signaling Pathway by Curcuma- and Garlic-Derived Hybrids", *Front Pharmacol*, 10:1597. doi:10.3389/fphar.2019.01597. \*both authors equally contributed
- [6] Catanzaro, M.\*, **Fagiani, F.\***, Racchi, M., Corsini, E., Govoni, S., Lanni, C. [2020] "Immune response in COVID-19: addressing a pharmacological challenge by targeting pathways triggered by SARS-CoV-2", *Signal Transduct Target Ther*, Vol. 5, No. 1, pp. 84. doi:10.1038/s41392-020-0191-1. \*both authors equally contributed
- [7] **Fagiani, F.\***, Lanni, C.\*, Racchi, M., Govoni, S. [2020] "Targeting dementias through cancer kinases inhibition", *Alzheimers Dement (NY)*, 6(1):e12044. doi:10.1002/trc2.12044. \*both authors equally contributed

- [8] **Fagiani, F.\***, Catanzaro, M.\*, Buoso, E., Basagni, F., Di Marino, D., Raniolo, S., Amadio, M., Frost, E.H., Corsini, E., Racchi, M., Fulop, T., Govoni, S., Rosini, M., Lanni, C. [2020] “Targeting cytokine release through the differential modulation of Nrf2 and NF- $\kappa$ B pathways by electrophilic/non-electrophilic compounds”, *Front. Pharmacol*, doi: 10.3389/fphar.2020.01256. \*both authors equally contributed
- [9] **Fagiani, F.\***, Catanzaro, M.\*, Lanni, C. [2020] “Molecular features of IGHV3-53-encoded antibodies elicited by SARS-CoV-2”, *Signal Transduct Target Ther*, Vol. 5, No. 1, pp. 170. doi:10.1038/s41392-020-00287-4. \*both authors equally contributed
- [10] **Fagiani, F.\***, Govoni, S.\*, Racchi, M., Lanni, C. [2020] “The peptidyl-prolyl isomerase Pin1 in neuronal signaling at the crossroad between cell death and survival”, *Molecular Neurobiology*. doi:10.1007/s12035-020-02179-8. \*both authors equally contributed
- [11] Masi, M., Garattini, E., Bolis, M., Di Marino, D., Maraccani, L., Morelli, E., Grolla, A., **Fagiani, F.**, Corsini, E., Travelli, C., Govoni, S., Racchi, M., and Buoso, E. [2020] “OXER1 and RACK1-associated pathway: a promising drug target for breast cancer progression”, accepted for publication in *Oncogenesis*.
- [12] Modafferi, S., Zhong, X., Kleensang, A., Murata, Y., **Fagiani, F.**, Pamies, D., Hogberg, H., Calabrese, V., Lachman, H., Hartung, T., Smirnova, L. [2020] “Synergistic developmental neurotoxicity of chlorpyrifos and CHD8 knockout in human BrainSpheres”, currently under review in *Environmental Health Perspectives*.